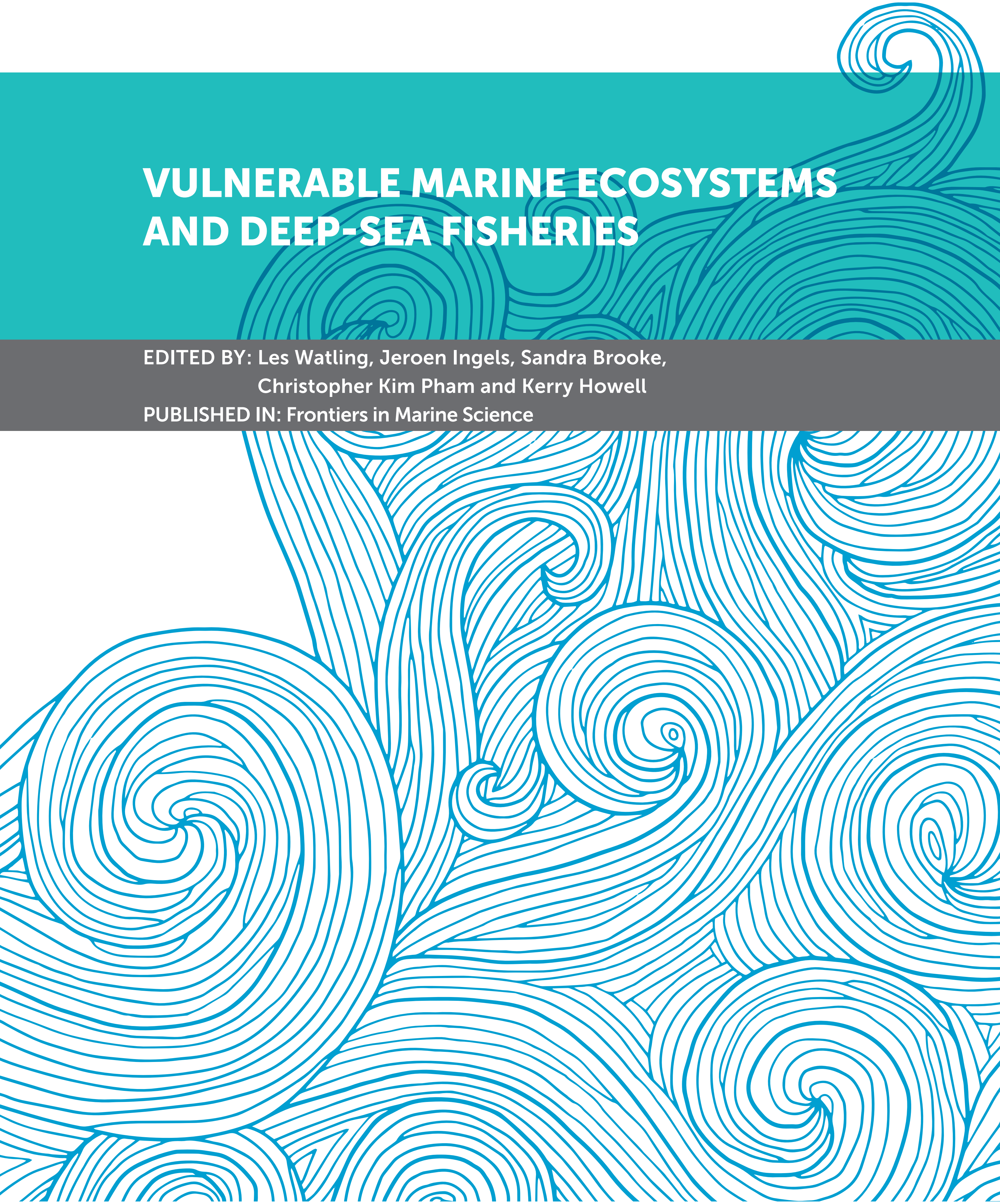

VULNERABLE MARINE ECOSYSTEMS AND DEEP-SEA FISHERIES

EDITED BY: Les Watling, Jeroen Ingels, Sandra Brooke,
Christopher Kim Pham and Kerry Howell

PUBLISHED IN: Frontiers in Marine Science

frontiers Research Topics

ISSN 1664-8714
ISBN 978-2-88974-165-6
DOI 10.3389/978-2-88974-165-6

About Frontiers

Frontiers is more than just an open-access publisher of scholarly articles: it is a pioneering approach to the world of academia, radically improving the way scholarly research is managed. The grand vision of Frontiers is a world where all people have an equal opportunity to seek, share and generate knowledge. Frontiers provides immediate and permanent online open access to all its publications, but this alone is not enough to realize our grand goals.

Frontiers Journal Series

The Frontiers Journal Series is a multi-tier and interdisciplinary set of open-access, online journals, promising a paradigm shift from the current review, selection and dissemination processes in academic publishing. All Frontiers journals are driven by researchers for researchers; therefore, they constitute a service to the scholarly community. At the same time, the Frontiers Journal Series operates on a revolutionary invention, the tiered publishing system, initially addressing specific communities of scholars, and gradually climbing up to broader public understanding, thus serving the interests of the lay society, too.

Dedication to Quality

Each Frontiers article is a landmark of the highest quality, thanks to genuinely collaborative interactions between authors and review editors, who include some of the world's best academicians. Research must be certified by peers before entering a stream of knowledge that may eventually reach the public - and shape society; therefore, Frontiers only applies the most rigorous and unbiased reviews.
Frontiers revolutionizes research publishing by freely delivering the most outstanding research, evaluated with no bias from both the academic and social point of view. By applying the most advanced information technologies, Frontiers is catapulting scholarly publishing into a new generation.

What are Frontiers Research Topics?

Frontiers Research Topics are very popular trademarks of the Frontiers Journals Series: they are collections of at least ten articles, all centered on a particular subject. With their unique mix of varied contributions from Original Research to Review Articles, Frontiers Research Topics unify the most influential researchers, the latest key findings and historical advances in a hot research area! Find out more on how to host your own Frontiers Research Topic or contribute to one as an author by contacting the Frontiers Editorial Office: frontiersin.org/about/contact

VULNERABLE MARINE ECOSYSTEMS AND DEEP-SEA FISHERIES

Topic Editors:
Les Watling, University of Hawaii at Manoa, United States
Jeroen Ingels, Florida State University, United States
Sandra Brooke, Florida State University, United States
Christopher Kim Pham, University of the Azores, Portugal
Kerry Howell, University of Plymouth, United Kingdom

Citation: Watling, L., Ingels, J., Brooke, S., Pham, C. K., Howell, K., eds. (2022). Vulnerable Marine Ecosystems and Deep-Sea Fisheries. Lausanne: Frontiers Media SA. doi: 10.3389/978-2-88974-165-6

Table of Contents

frontiers in Marine Science

ORIGINAL RESEARCH
published: 02 July 2019
doi: 10.3389/fmars.2019.00374

Small-Scale Patterns in the Distribution and Condition of Bamboo Coral, *Keratoisis grayi*, in Submarine Canyons on the Grand Banks, Newfoundland

Krista D. Baker[1,2]*, Paul V. R. Snelgrove[3], David A. Fifield[4], Evan N. Edinger[5], Vonda E. Wareham[1], Richard L. Haedrich[2†] and Kent D. Gilkinson[1]

[1] Fisheries and Oceans Canada, Northwest Atlantic Fisheries Centre, St. John's, NL, Canada, [2] Department of Biology, Memorial University of Newfoundland and Labrador, St. John's, NL, Canada, [3] Department of Ocean Sciences and Biology, Memorial University of Newfoundland and Labrador, St. John's, NL, Canada, [4] Environment and Climate Change Canada, Mount Pearl, NL, Canada, [5] Departments of Geography, Biology, and Earth Sciences, Memorial University of Newfoundland and Labrador, St. John's, NL, Canada

Edited by:
*Les Watling,
University of Hawai'i at Mānoa,
United States*

Reviewed by:
*Jaime Selina Davies,
University of Plymouth,
United Kingdom
Rhian G. Waller,
University of Gothenburg, Sweden*

***Correspondence:**
*Krista D. Baker
Krista.Baker@dfo-mpo.gc.ca*

†Deceased

Specialty section:
*This article was submitted to
Deep-Sea Environments and Ecology,
a section of the journal
Frontiers in Marine Science*

Received: *04 April 2019*
Accepted: *17 June 2019*
Published: *02 July 2019*

Citation:
Baker KD, Snelgrove PVR, Fifield DA, Edinger EN, Wareham VE, Haedrich RL and Gilkinson KD (2019) Small-Scale Patterns in the Distribution and Condition of Bamboo Coral, Keratoisis grayi, in Submarine Canyons on the Grand Banks, Newfoundland. Front. Mar. Sci. 6:374. doi: 10.3389/fmars.2019.00374

Keratoisis grayi is one of the most abundant large gorgonian corals found off Newfoundland and Labrador, yet we know little regarding the factors influencing its distribution, abundance, and condition. We employed remotely operated vehicle (ROV) transect data collected in three canyons off the Grand Banks, Newfoundland to quantitatively examine the influence of depth, bottom type, canyon, and trawling intensity on *K. grayi* abundance, height, and condition at small spatial scales. While surveying 105 km of seafloor with a ROV, we observed 5770 *K. grayi* colonies and 167 trawl marks. We found that *K. grayi* were significantly more likely to occur in boulder areas than in cobble or gravel. Bottom depth related positively and significantly with colony height and our models predict that the largest bamboo coral colonies occur in boulders in Halibut Channel, and in boulders and cobble in Haddock Channel. The majority of colonies observed were alive and undamaged, but tipped, broken, dead and partially dead colonies were also recorded. *K. grayi* were more likely to occur in trawled areas, but these colonies were more likely to be damaged, broken, smaller in size, and less abundant than colonies outside trawled areas. These results demonstrate a negative impact of bottom trawling on *K. grayi* colonies off Newfoundland and Labrador and that fishers may specifically target areas where these corals occur.

Keywords: gorgonian coral, trawling, fishing effects, deep-sea, cold-water coral

INTRODUCTION

Deep-sea octocorals have garnered world-wide attention because of their potential longevity (Sherwood and Edinger, 2009), importance for biodiversity and life-history of other taxa (Buhl-Mortensen et al., 2010; Baillon et al., 2012), fragility to fishing damage (Edinger et al., 2007; Yoklavich et al., 2018), and vulnerability to other anthropogenic disturbances such as oil and gas exploration and ocean acidification (Dayton et al., 1995; Gass, 2003; Roberts and Hirshfield, 2004). Deep-sea octocoral conservation concerns underscore the growing need to better understand the factors influencing their distributions at a range of spatial scales.

Previous studies related deep-sea octocoral distributional patterns to temperature (Bryan and Metaxas, 2006; Mortensen et al., 2006), substrate (Baker et al., 2012a), salinity (Mortensen et al., 2006), slope, oxygen (Yesson et al., 2012), and other environmental factors. For example, Paragorgiidae along the Atlantic continental margin occurred primarily between 300 and 500 m, in areas with slopes between 1.1° and 1.4°, temperatures $> 5°$C, currents between 10 and 30 cm s^{-1}, and low chlorophyll *a* concentrations (Bryan and Metaxas, 2006). Watanabe et al. (2009) reported a strong negative correlation between *Primnoa resedaeformis* abundance and depth and a positive correlation with cobble and/or boulders in the Northeast Channel, off Nova Scotia, Canada.

Given the known vulnerability of cold-water corals to trawling damage, distributional patterns could relate to current and past fishing intensity (Roberts et al., 2009). The majority of research related to this topic has focused on scleractinian corals. For example, an estimated 5–52% of the total area covered by *Lophelia pertusa* in Norwegian waters was damaged by fishing activities (Fossa et al., 2002), and researchers attributed destruction of all but 10% of *Oculina* spp. in a Florida reserve to illegal trawling activity (Koenig et al., 2005). However, trawl survey data, showed highest abundances of gorgonians (and deep-water corals, in general) in areas with little to no past trawling along the eastern Grand Banks and Flemish Cap (Murillo et al., 2010). Althaus et al. (2009) also reported reduced density of scleratinians, antipatharians, and alcyonaceans (combined) on trawled seamounts, compared to untrawled seamounts off Australia.

The octocoral colonies that remain in previously trawled areas may be heavily damaged. In Alaskan waters, only 31 *Primnoa* spp. colonies remained in a trawl path visited 7 years after the removal of 1 t of corals; five large colonies were missing 95–99% of their branches and 80% of the polyps were missing from two smaller colonies (Krieger, 2001). Nearly 50% of the bamboo coral colonies observed in an area subjected to heavy trawling off California and Oregon were damaged or disturbed (Yoklavich et al., 2018).

Keratoisis grayi, a long-lived bamboo coral found throughout the North Atlantic and Mediterranean Sea (Appeltans et al., 2012), is among the most common large gorgonians off Newfoundland and Labrador, Canada (Wareham and Edinger, 2007; Baker et al., 2012a). Using fisheries observer and Fisheries and Oceans Canada survey data from that region, Wareham and Edinger (2007) reported *K. grayi* (synonym: *K. ornata*: Deichmann, 1936; van der Land, 1994) in depths from 195 to 1,262 m. Baker et al. (2012a) reported *K. grayi* often co-occurred with *Acanthogorgia armata* and *Anthomastus* spp. at relatively shallow depths with boulders and cobbles. *K. grayi* was associated with steep topography and semi-consolidated mudstone in a submarine canyon off Nova Scotia (Mortensen and Buhl-Mortensen, 2005). Large gorgonians (including *K. grayi*) were recorded as bycatch in multiple fisheries spanning trawl sets (*Pandalus borealis*, *Reinhardtius hippoglossoides*, and *Sebastes* spp. fisheries), crab pots, longlines (*R. hippoglossoides* and *Hippoglossus hippoglossus* fisheries), and gillnets (*R. hippoglossoides* and *Sebastes* spp. fisheries) off Newfoundland between 2004 and 2005 (Edinger et al., 2007), illustrating the vulnerability of *K. grayi* to fishing disturbances.

We employed remotely operated vehicle (ROV) transect data collected in three canyons off the Grand Banks to examine quantitatively the influence of depth, bottom type, canyon, and trawling intensity on *K. grayi* abundance, height, and condition at small spatial scales.

MATERIALS AND METHODS

Video Surveys

We explored three submarine canyons on the slopes of the Grand Banks south of Newfoundland: Halibut Channel, Haddock Channel, and Desbarres Canyon (**Figure 1**) with the ROV, Remotely Operated Platform for Ocean Science (ROPOS) (CSSF, 2010). The southerly flowing, cold Labrador Current and the northerly flowing, warm Gulf Stream both influence the three canyons. Fishers frequently target the areas using trawlers directed at *Sebastes* spp. and various flatfish, usually at depths shallower than 1000 m (Kulka and Pitcher, 2001; Edinger et al., 2007; Koen-Alonso et al., 2018). Trawl surveys in these areas indicate the presence of abundant and diverse cold-water coral taxa (Edinger et al., 2007).

Remotely Operated Platform for Ocean Science performed video surveys from *CCGS Hudson* during seven dives between July 16 and 24, 2007 (see Baker et al., 2012a,b, for details). The ROV was equipped with lasers placed 10 cm apart to indicate scale. Depth, date, time, altitude (distance above bottom), temperature, and position were logged at 1-s intervals (though sporadic problems with the logger resulted in several long periods with no temperature data).

Based on known distributions of corals in relation to bathymetry, we planned 1-km transects at 200-m depth intervals along depth contours between 2200 and 600 m and along contours every 100 m in waters shallower than 500 m (Baker et al., 2012a,b). We standardized transects by maintaining the ROV as close to the bottom as possible, at a constant slow speed (approx. 0.2–0.5 m s^{-1}) while tilting the camera down slightly on a wide-angle view in order to image the seafloor and water column directly above. Between pre-selected transects, we explored the area with ROPOS, capturing still images and video of interesting features, and collecting voucher specimens to validate visual identification.

Video Processing

Using the program ClassAct Mapper (Benjamin, 2007), we recorded continuous geo-referenced data describing bottom type, ROV mode, trawl marks, and corals. We identified all corals to the lowest possible taxonomic level (typically species) and measured colony height and diameter of *K. grayi* to the nearest 5 cm using the lasers for scale. Whenever possible, we quantified the general condition of colonies using two descriptors: proportion of colony dead and overall status. We estimated the proportion of each colony that appeared dead to the nearest 5%, using the lasers for scale. The overall status of each *K. grayi* colony was scored as "normal" (the colony appeared

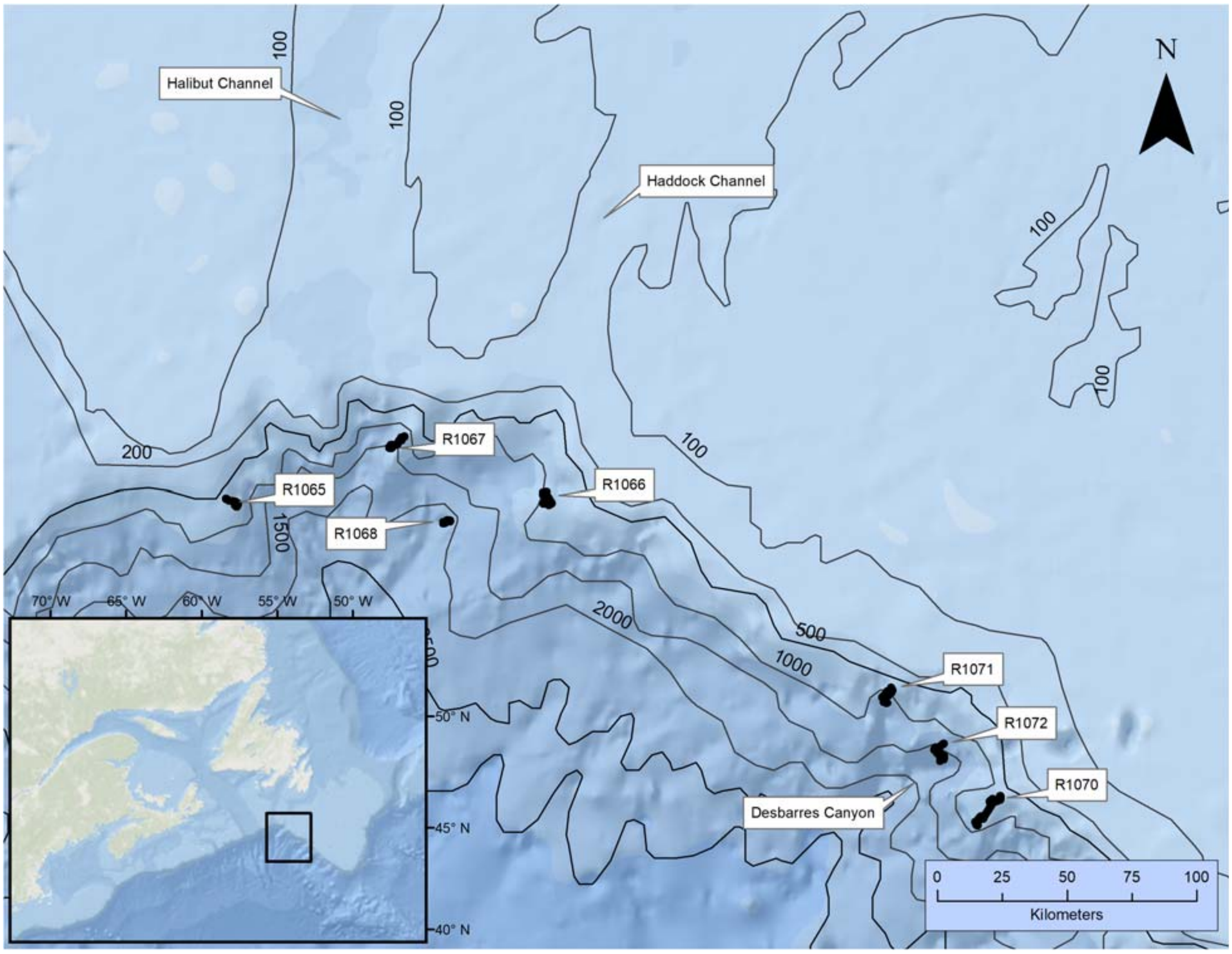

FIGURE 1 | Locations surveyed using the remotely operated vehicle, ROPOS. Individual dive numbers and canyons of interest are identified.

upright), "broken" (the colony or pieces of the colony appeared detached), or "tipped" (the colony was tilted and laying against another object, such as the substrate). If a colony was both broken and tipped, we classified it as broken.

We characterized bottom type every second by primary (most abundant) substrate and secondary (next most abundant) substrate, with optional additional comments. Bottom types included (1) outcrop (vertically exposed bedrock and consolidated Quaternary sediment), (2) boulder (>25 cm), (3) cobble (5–25 cm), (4) gravel (0.2–5 cm), or (5) mud-sand (fine-grain) sediments (Thrush et al., 2001).

We defined "transect-mode" as any portion of the video when the ROV followed the prescribed methodology for transects (described above), regardless of whether the transect was planned. All other ROV behaviors were combined as "Other" (Baker et al., 2012a,b).

Data Analysis

Flatfish and *Sebastes* spp. in the area are typically fished using bottom trawls. Commercial trawl-doors off Newfoundland spread approximately 116 m for flatfish trawlers and 95 m for *Sebastes* spp. trawlers. Therefore, using ArcGIS 9.3 (ESRI, 2008), we created circular 100-m buffers around each observed trawl mark location. We then calculated the frequency with which each second of video coincided with a buffer to determine the potential trawling intensity at each second (∼location).

Our analysis considered the effect of average temperature, bottom type, depth, canyon, trawl intensity (Trawl), and their interactions. However, because of strong collinearity in average temperature and depth, we removed average temperature from consideration (furthermore, 72% of the colonies had no associated temperature records). When necessary, we $\log_{10}$-transformed Trawl in our models to adjust for non-linearity (logTrawl), and chose all final models through backward selection using likelihood ratio tests to remove insignificant terms.

Abundance

We examined patterns in *K. grayi* colony abundance observed when the ROV was in transect-mode by splitting transects into 10-m segments (=sample unit) and summing the number of live

K. grayi colonies (<100% dead) in each segment. Regardless of abundance, large, hard substrates likely influence *K. grayi* distribution (Baker et al., 2012a). Therefore, we used the largest size category in each 10-m segment to classify bottom type in that segment. We used mean depth of each 10-m segment as "depth" and maximum number of trawl mark buffers coinciding with any point in the segment as the Trawl value for that segment. Given low sample sizes, we chose to remove the 10-m segments in mud-sand, outcrops, or depths > 1000 m. Because the data were zero-inflated we chose a hurdle (zero-altered) model. A hurdle model consists of two parts: a binomial generalized linear model (GLM) to model presence/absence, combined with a count model for values greater than zero (Zuur et al., 2009). Because our count data were overdispersed, we implemented a truncated negative binomial GLM count model using the *Pscl* package (Jackman et al., 2011) in *R* (RDevCoreTeam., 2012).

Height

We used all video (regardless of ROV mode) to examine patterns in *K. grayi* colony height, treating each *K. grayi* colony as a sample unit. Low sample size led us to remove Desbarres Canyon and mud-sand data. A gamma GLM with identity link produced the best explanatory model for patterns in height of *K. grayi*.

Condition

We examined all video for patterns in *K. grayi* condition, again removing Desbarres Canyon and mud-sand data because of low sample size, and assessed status using two approaches: proportion dead and overall status (normal, broken, or tipped).

Values of zero (n = 5037) and 1 (n = 317) strongly skewed the proportion dead, and common transformations used for proportional data (e.g., arcsine and logit) therefore did not improve our ability to meet model assumptions. As a result, we categorized all colonies with any dead portions as "dead/partially dead," thereby creating a binary response variable: dead/partially dead (1) or alive (0). We used a binomial GLM to examine patterns in live versus dead/partially dead colonies, and a multinomial logit model to examine overall status (normal, broken, or tipped).

RESULTS

We surveyed approximately 105 km (90 h) of seafloor, and recorded a total of 5031 10-m segments using all dives and depth categories (see Baker et al., 2012a,b). We observed 5770 *K. grayi* colonies, most in Halibut Channel (n = 4341) and Haddock Channel (n = 1427), and only two colonies in Desbarres Canyon (**Table 1**).

We recorded 167 trawl marks (**Table 2**), spanning all canyons and depths from 377 to 821 m. A total of 1086 *K. grayi* colonies occurred within at least one 100-m trawl buffer zone; the greatest number of buffers coinciding with a *K. grayi* colony was 13 (n = 8).

Abundance

Overall, we enumerated 3765 live *K. grayi* colonies while the ROV was in transect mode, 2820 of which occurred in 10-m segments. Of the 1422 10-m segments used in our model, a total of 440 segments contained *K. grayi*. The median of counts greater than zero in a 10-m segment was 3 and the maximum of 43 occurred at 573 m within segments with boulders in Halibut Channel (Dive R1067).

TABLE 1 | Number of *Keratoisis grayi* colonies and status observed during ROV surveys off the Grand Banks, Newfoundland in 2007.

Canyon	Dive	# Observed	# Normal	# Broken	# Tipped	# Dead/Partially Dead	# Alive
Halibut Channel	R1065	192	154	19	9	19	150
Haddock Channel	R1066	1427	1090	184	57	213	1117
Halibut Channel	R1067	4149	3738	140	131	164	3773
Haddock Channel	R1068	–	–	–	–	–	–
Desbarres Canyon	R1070	2	1	1	0	1	1
Desbarres Canyon	R1071	–	–	–	–	–	–
Desbarres Canyon	R1072	–	–	–	–	–	–
	Total	5770	4983	344	197	397	5041

TABLE 2 | Number of trawl marks observed by depth and dive during ROV surveys off the Grand Banks, Newfoundland in 2007.

Dive	300–400 m	400–500 m	500–600 m	600–700 m	700–800 m	800–900 m
R1065	–	–	–	5	4	1
R1066	–	1	26	52	–	1
R1067	–	2	–	–	–	–
R1068	–	–	–	–	–	–
R1070	3	6	33	18	–	–
R1071	1	2	11	1	–	–
R1072	–	–	–	–	–	–
Total	4	11	70	76	4	2

Bottom type ($p < 0.0001$), Trawl ($p = 0.018$), and the interaction of Depth and Canyon ($p < 0.0001$) were significant predictors of *K. grayi* presence within a 10-m segment (**Table 3**). *K. grayi* colonies were significantly more likely to be present as Trawl increased (**Figure 2**). The probability of *K. grayi* presence in habitats with boulders was significantly greater than in cobble ($p < 0.0001$) and gravel ($p < 0.0001$), but cobble and gravel habitats did not differ significantly from each other ($p = 0.053$).

The interaction of Depth and Bottom type was a significant predictor of *K. grayi* counts greater than zero ($p = 0.004$) (**Table 3**), and as trawl intensity (logTrawl) increased counts of *K. grayi* decreased ($p < 0.0001$). Trawling intensity appeared to have the greatest negative influence on *K. grayi* counts during the first trawl (**Figure 3**). Depth greatly influenced counts in habitats with cobble, which was less obvious in habitats with boulders and gravel (**Figure 3**).

Height

We determined height (median = 30 cm) confidently for 4654 *K. grayi* colonies. The tallest colony (215 cm) occurred in a segment with cobble in the absence of trawling at 776 m in Halibut Channel.

Depth ($p < 0.0001$), logTrawl ($p < 0.0001$), and the interaction of Canyon and Bottom type ($p < 0.0001$) were significant predictors of *K. grayi* height (**Table 3**). We found a significant negative relationship between *K. grayi* colony height and logTrawl, and a significant positive relationship between height and depth. The predicted height of *K. grayi* increased by 0.07 m for each 1 m increase in depth. In Halibut Channel, the largest colonies occurred in habitats with boulders, in contrast with Haddock Channel where the largest colonies occurred in habitats with cobble and boulders (**Figure 4**).

Condition

Over 75% of the *K. grayi* colonies we recorded appeared healthy (**Table 1**).

LogTrawl ($p = 0.0001$) and the interaction of Canyon and Depth ($p < 0.0001$) were significant predictors of a *K. grayi* colony with dead portions ($n = 5428$) (**Table 3**). As logTrawl increased, so did the probability of recording a colony with dead portions (**Figure 5**). Depth strongly influenced the probability of dead portions in *K. grayi* in Haddock Channel, but not Halibut Channel. The probability of dead portions in a *K. grayi* colony in Haddock Channel was highest in the shallowest depths (**Figure 5**).

Canyon ($p < 0.0001$), Depth ($p = 0.004$), and logTrawl ($p < 0.0001$) were significant predictors of *K. grayi* overall status ($n = 5513$) (**Table 3**). As trawl intensity increased, the probability of a healthy *K. grayi* colony decreased (**Figure 6**) and the probability of a broken colony increased ($p < 0.0001$) (**Figure 6**). We found no significant relationship between logTrawl and probability of a tipped colony ($p = 0.848$). Healthy *K. grayi* were more likely and broken coral less likely in Halibut Channel ($p < 0.0001$) compared to Haddock Channel. We found no significant difference between canyons when comparing the probability of a tipped colony ($p = 0.313$). As depth increased, the probability of a tipped *K. grayi* colony decreased ($p = 0.003$) (**Figure 6**). We found no significant relationship between the probability of a broken colony and depth ($p = 0.155$).

TABLE 3 | Significant terms in models predicting abundance, height, and status of *Keratoisis grayi* colonies from ROV surveys off the Grand Banks, Newfoundland.

Response	Model terms	*p*-value
Abundance: presence/absence	Bottom type	<0.0001
	Trawl	0.0178
	Depth × Canyon	<0.0001
Abundance: counts	$\log_{10}$Trawl	<0.0001
	Depth × Bottom type	0.0036
Height	$\log_{10}$Trawl	<0.0001
	Depth	<0.0001
	Canyon × Bottom type	<0.0001
Probability of having dead portions	Canyon × Depth	<0.0001
	$\log_{10}$Trawl	0.0001
Overall status	Canyon	<0.0001
	Depth	0.0037
	$\log_{10}$Trawl	<0.0001

DISCUSSION

Abundance

Keratoisis grayi colonies were significantly more likely to occur in boulder areas, than cobble or gravel. This species requires hard substrate for attachment, therefore, boulders presumably create more available stable habitat for attachment than smaller substrata, such as gravel or cobble. In The Gully, off Nova Scotia, *K. grayi* also associate with large, hard substrate (consolidated mudstone) (Mortensen and Buhl-Mortensen, 2005), and off California and Oregon bamboo corals were only observed on rock substrate (Yoklavich et al., 2018).

We found significant interactions when modeling both presence and counts of *K. grayi*. The significant Depth × Canyon interaction in predicting counts and presence of *K. grayi* indicates a between canyon difference in *K. grayi* presence and abundance at a given depth, implying that while depth is important, other environmental factors that differ between canyons likely also influence *K. grayi* distributional patterns. Other factors that co-vary with depth may account for differences in *K. grayi* between bottom types. For example, current regime may change with depth and contribute to bottom type. Multiple environmental factors, such as current velocity, temperature, sedimentation rates, slope, and food availability that likely influence presence and abundance (but not measured in the present study) may differ between depths and/or canyons and therefore help to explain these interactions (Roberts et al., 2009; Watanabe et al., 2009). Future ROV studies could include additional methodologies and sampling (e.g., Digital Terrain Modeling, CTD samples, and planktonic samples) to examine other likely contributors to coral health and abundance.

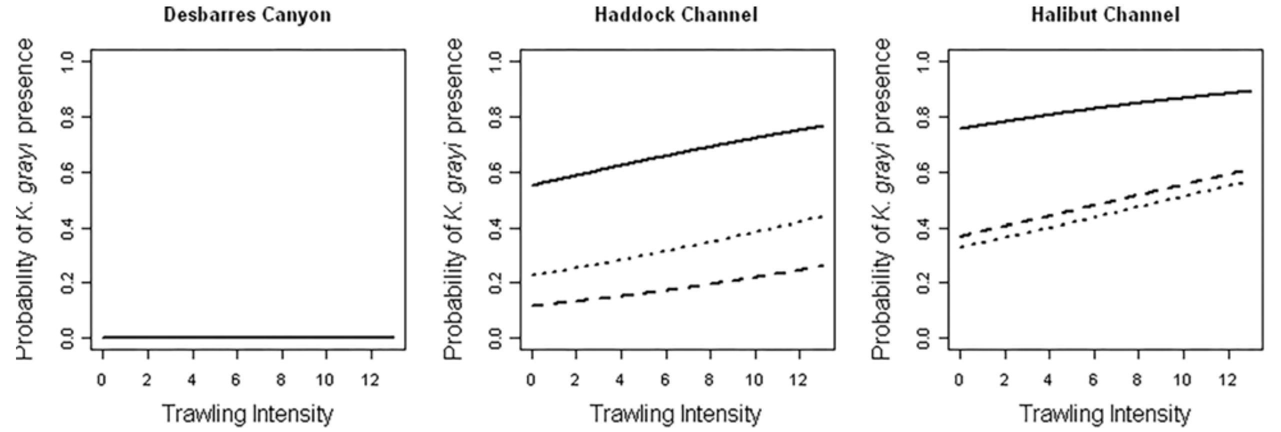

FIGURE 2 | Model predictions of the influence of trawl intensity on the probability of *Keratoisis grayi* presence in boulders (solid), cobble (dotted), and gravel (dashed) within each canyon. Depth was held constant at the mean depth in each canyon in all models.

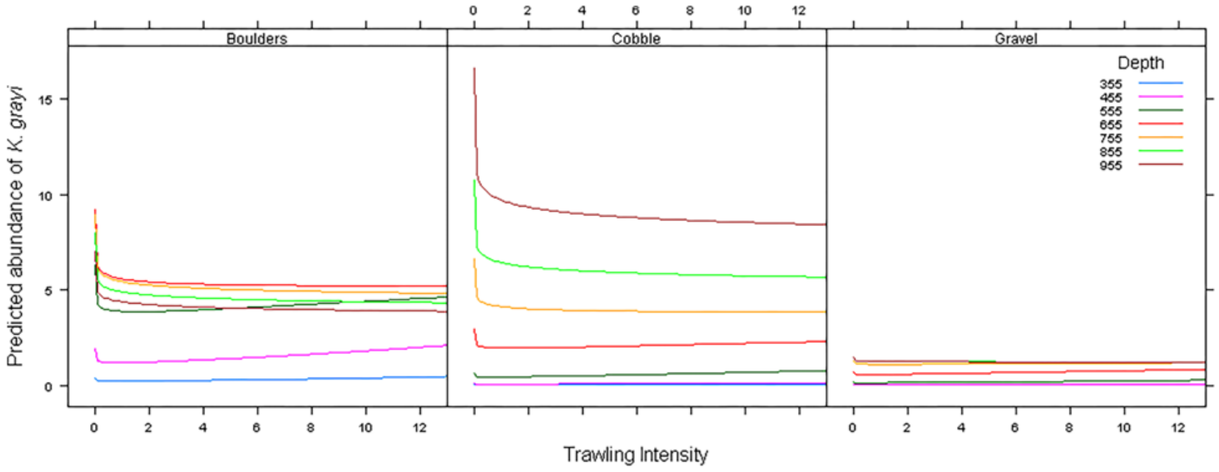

FIGURE 3 | Model predictions of the influence of trawling intensity on *Keratoisis grayi* counts in boulders, cobble, and gravel at various depths in Haddock Channel.

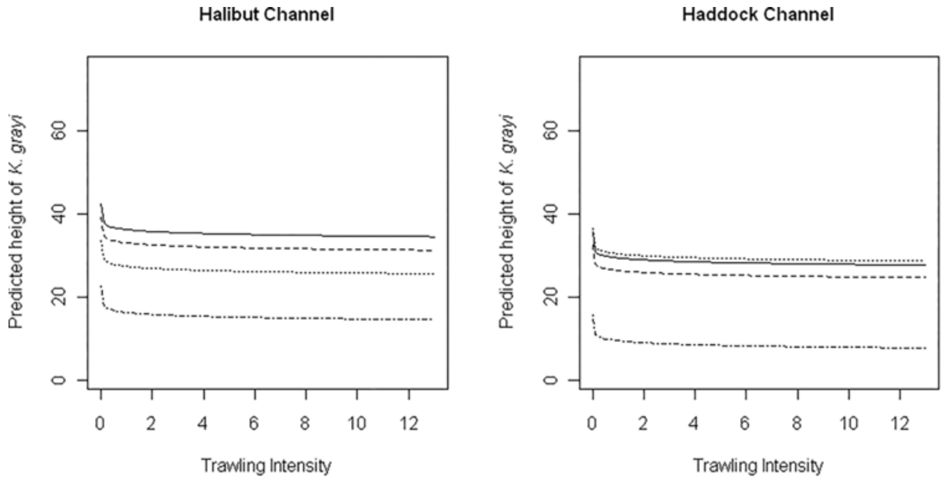

FIGURE 4 | Model predictions of the influence of trawling intensity on *Keratoisis grayi* height in Halibut and Haddock Channels in boulders (solid), cobble (dotted), gravel (dashed), and outcrops (dot/dash) at mean depth (650 m).

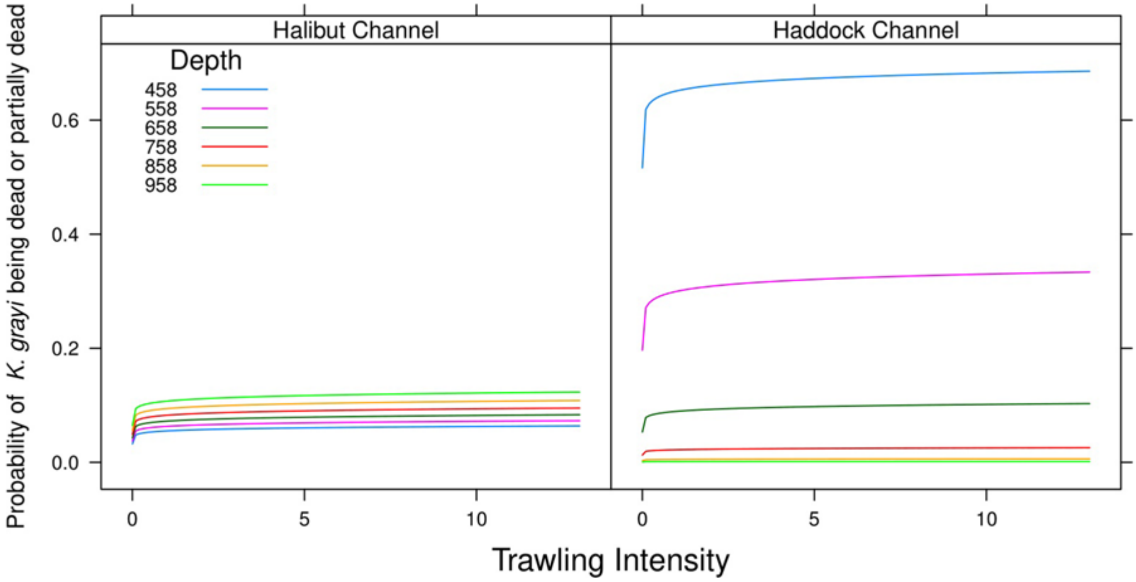

FIGURE 5 | Model predictions of the influence of trawling intensity and depth on the probability of dead/partially dead versus live *Keratoisis grayi* in Halibut Channel and Haddock Channel.

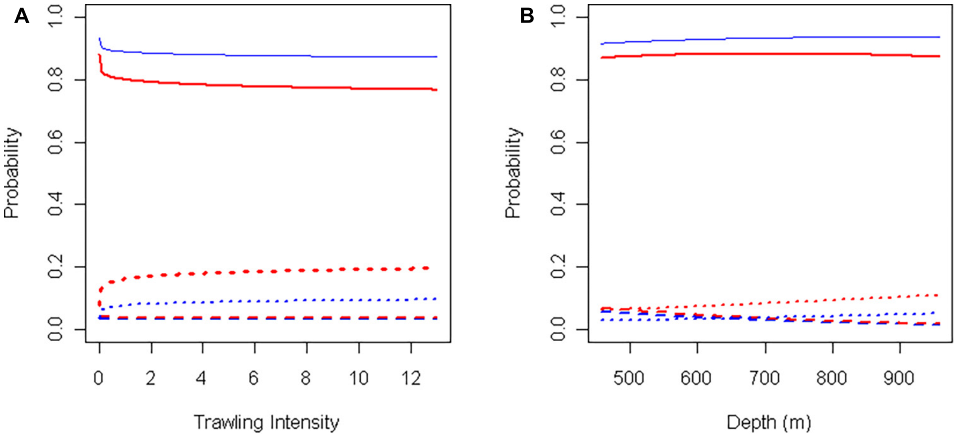

FIGURE 6 | Model predictions of the probability of intact (solid), tipped (dashed), or broken (dotted) *Keratoisis grayi* in Halibut Channel (blue) and Haddock Channel (red) in relation to **(A)** trawl intensity (depth = 650 m), and **(B)** depth (trawl intensity = 0).

Height

Colony height increased significantly with bottom depth, a pattern previously reported for bubble gum coral, *Paragorgia arborea,* in the Northeast Channel off Nova Scotia (Watanabe et al., 2009). Thresher (2009) found slower radial growth rates in bamboo corals collected in deeper waters and at lower temperatures, suggesting much longer growth periods without disturbance for deeper, taller corals than shallower, faster growing colonies.

Our models predicted that the largest bamboo coral colonies occur on boulders in Halibut Channel and boulders and cobble in Haddock Channel (acknowledging a significant positive interaction between canyon and bottom type). We suspect that the larger surface area of boulders offers a more stable surface as colonies grow in size, thus allowing a colony to grow larger before tipping and overturning the stone (Tunnicliffe and Syvitski, 1983).

As with coral abundance patterns, size, and growth rates may link to a variety of environmental factors that likely vary with depth and differ between canyons. These factors include, but are not limited to, currents, strontium/calcium ratios, surface productivity, calcium carbonate, and organic content (Weinbauer et al., 2000; Thresher, 2009).

Condition

The majority of *K. grayi* observed in both Halibut and Haddock Channels were healthy (80%) and fully living (78%). Dead/partially dead colonies of *K. grayi* were more prevalent at shallower depths in Haddock Channel than Halibut Channel, and colonies in Haddock Channel were broken more often and generally less intact compared to those in Halibut Channel. Trawling could explain this difference. Although we attempted to account for trawl intensity in our models, we may have underestimated areas of past trawling if our survey path did not intersect the trawl-door furrow. We observed a total of 80 trawls marks in Haddock Channel, compared to only 12 in Halibut Channel, and the Haddock Channel survey site is relatively close to locations where >100% of the area was trawled at least 1 year between 1980 and 2000 (Kulka and Pitcher, 2001). Therefore, in our survey areas, trawling pressure in Haddock Channel likely exceeded that in Halibut Channel and the poorer health of *K. grayi* in Haddock Channel may reflect fishing damage not captured with our methodologies. This interpretation would also explain the absence of significant differences in probability of tipped colonies between canyons. The physical force of a trawl would likely break or tip and break a colony, rather than tip a colony without breakage (Sainsbury et al., 1992; Krieger, 2001). Alternatively, many of the variables that likely differ between canyons and affect size and abundance (e.g., current velocity, sedimentation rates, and temperature), may also impact overall *K. grayi* condition and contribute to the canyon-related patterns.

Numerous mechanisms can tip and break colonies, sometimes overturning the attachment substrate (Tunnicliffe and Syvitski, 1983). For example, longlines or gillnets may hook corals (Krieger, 2001). Therefore, we cannot identify the direct mechanism responsible for the colonies that were tipped and/or broken in our video.

Trawling Impacts

Our results clearly illustrate the negative influence of trawling on the size, condition, and number of *K. grayi* off Newfoundland. However, *K. grayi* were also more likely to occur in trawled areas, perhaps because fishers target areas with high densities of fish, which could coincide with coral presence (Husebo et al., 2002; Costello et al., 2005; Stone, 2006). But corals that persist in trawled areas are more likely to exhibit damage, breakage, smaller size, and reduced abundance. These findings confirm other studies on trawling effects on vulnerable epifauna. For example, Yoklavich et al. (2018) considered only half of the bamboo corals healthy in a heavily trawled area, and observed bamboo corals sheared off at the base, and linear swaths of broken and/or dead colonies. Freese (2001) found an immediate 16% reduction in sponge density post trawling, a 21% reduction 11 months post trawling, and damaged to almost half of the sponges (46.8%) that remained in three trawl paths. Trawled seamounts exhibited significantly reduced cover of *Solenosmilia* thickets compared to seamounts that were never trawled, with significantly higher density of large gorgonians and black corals with broken stems on seamounts with active trawling (Althaus et al., 2009). One study in the Gulf of Alaska estimated that 27% of corals in a trawl net path were detached and 50–90% of these corals were missing polyps (Krieger, 2001). Damaged corals may be more susceptible to predation (Malecha and Stone, 2009), infection and disease and, ultimately, mortality (Krieger, 2001), with reduced reproductive (Henry et al., 2003; Malecha and Stone, 2009), and feeding abilities (Krieger, 2001), and slower growth rates (Meesters et al., 1994). For example, *Tritonia diomedea* actively fed on sea whips lying on the seafloor after simulated trawl disturbance (Malecha and Stone, 2009).

Our predictive models clearly corroborate previous research illustrating the significant damage caused by the first pass of a trawl. In each model, we found the largest incremental effect of trawling with the smallest number of trawls (illustrated by initial slopes in **Figures 3–6**). On the continental shelf of Australia, a single pass of a trawl removed 90% of the large epibenthic organisms in the trawl path (Sainsbury et al., 1992). A single trawl pass in the Gulf of Alaska significantly removed or damaged emergent epifauna (Freese et al., 1999). Van Dolah et al. (1987) found significantly reduced barrel sponge abundances and octocorals and stony corals broken at the base after only a single trawl pass.

Our findings use observations collected with an ROV and quantitative methods to add to the growing research demonstrating clear impacts of trawling on deep-sea ecosystems (e.g., Watling and Norse, 1998; Freese, 2001; Althaus et al., 2009; Norse et al., 2012; Clark et al., 2016; Yoklavich et al., 2018). Slow-growing and long-lived octocorals, such as *K. grayi* will require considerable time to recover from disturbances (Roberts et al., 2009), if even possible, and other taxa in the deep sea may depend on octocorals (Buhl-Mortensen et al., 2010). Collectively, these findings raise significant concerns regarding trawling impacts and sustainability of deep-sea ecosystems. Therefore, we believe protection of corals, associated taxa, and their ecosystems requires closing large areas of the seafloor to destructive fishing gear. In areas that remain open to trawling (and other fishing practices), ensuring appropriate fisheries management in an ecosystem context requires accountability and transparency (Weaver et al., 2011).

In conclusion, we used quantitative methods to clearly illustrate the negative influence of trawling on *K. grayi* counts, size, and status. Our findings also suggest fishers may preferentially, though unintentionally, target areas with *K. grayi*, underscoring the urgency of this conservation threat. Therefore, our research adds to growing evidence for the need to protect large seabed areas from bottom trawling. Such protected areas will help to reduce the overall footprint of fishing and initiate recovery efforts for deep-sea corals and associated marine fauna.

DATA AVAILABILITY

The datasets generated for this study can be found in the author's GitLab site: https://gitlab.com/krista.baker/keratoisis.

AUTHOR CONTRIBUTIONS

KB, PS, RH, EE, VW, and KG contributed to the concept and initial study design. KB and VW performed the video analysis. KB and DF performed the statistical analyses and interpretation. KB wrote the first draft of the manuscript. All authors contributed to the manuscript revisions. KB, PS, EE, VW, and KG have read and approved the submitted version of the manuscript. RH approved a previous, but very similar, version of the manuscript.

FUNDING

This research was supported by the Natural Sciences and Engineering Research Council of Canada (NSERC) Postgraduate Scholarship to KB, NSERC Ship Time Grant to A. Mercier et al., NSERC Discovery Grants to PS and EE, and Fisheries and Oceans Canada International Governance Strategy grant to KG.

ACKNOWLEDGMENTS

We sincerely thank the crews of CCGS *Hudson* and ROPOS. We also thank Brenda Oake and Calan Fisher for their help with the video analysis, and Robert Benjamin for his explanations of ClassAct Mapper. We also thank Monty Priede, Suzanne Dufour, and Annie Mercier for their comments on an earlier draft of the manuscript.

REFERENCES

Althaus, F., Williams, A., Schlacher, T. A., Kloser, R. J., Green, M. A., Barker, B. A., et al. (2009). Impacts of bottom trawling on deep-coral ecosystems of seamounts are long-lasting. *Mar. Ecol. Prog. Ser.* 397, 279–294. doi: 10.3354/meps08248

Appeltans, W., Bouchet, P., Boxshell, G. A., De Broyer, C., de Voodg, N. J., Gordon, D. P., et al. (2012). *World Register of Marine Species*. Available at: http://www.marinespecies.org. (accessed October 6, 2012)

Baillon, S., Hamel, J.-F., Wareham, V. E., and Mercier, A. (2012). Deep cold-water corals as nurseries for fish larvae. *Front. Ecol. Environ.* 10, 351–356. doi: 10.1890/120022

Baker, K. D., Wareham, V., Snelgrove, P. V. R., Haedrich, R. L., Fifield, D. A., Edinger, E. N., et al. (2012a). Distributional patterns of deep-sea coral assemblages in three submarine canyons off Newfoundland, Canada. *Mar. Ecol. Prog. Ser.* 445, 235–249. doi: 10.3354/meps09448

Baker, K. D., Haedrich, R. L., Snelgrove, P., Wareham, V., Edinger, E. N., and Gilkinson, K. (2012b). Small-scale patterns of deep-sea fish distributions and assemblages of the Grand Banks, Newfoundland continental slope. *Deep Sea Res. A Oceanogr. Res. Papers* 65, 171–188. doi: 10.1016/j.dsr.2012.03.012

Benjamin, R. (2007). *ClassAct Mapper*. Dartmouth, NS: Fisheries and Oceans Canada.

Bryan, T. L., and Metaxas, A. (2006). Distribution of deep-water corals along the North American continental margins: relationships with environmental factors. *Deep Sea Res. I Oceanogr. Res. Papers* 53, 1865–1879. doi: 10.1016/j.dsr.2006.09.006

Buhl-Mortensen, L., Vanreusel, A., Gooday, A. J., Levin, L. A., Priede, I. G., Buhl-Mortensen, P., et al. (2010). Biological structures as a source of habitat heterogeneity and biodiversity on the deep ocean margins. *Mar. Ecol.* 31, 21–50. doi: 10.1111/j.1439-0485.2010.00359.x

Clark, M. R., Althaus, F., Schlacher, T. A., Williams, A., Bowden, D. A., and Rowden, A. A. (2016). The impacts of deep-sea fisheries on benthic communities: a review. *ICES J. Mar. Sci.* 73(Suppl. 1), i51–i69. doi: 10.1371/journal.pone.0022588

Costello, M. J., McCrea, M., Freiwald, A., Lundalv, T., Jonsson, L., Bett, B. J., et al. (2005). "Role of cold-water *Lophelia pertusa* coral reefs as fish habitat in the NE Atlantic," in *Cold-Water Corals and Ecosystems*, eds A. Freiwald and J. M. Roberts (Berlin: Springer-Verlag), 771–805. doi: 10.1007/3-540-27673-4_41

CSSF (2010). *Canadian Scientific Submersible Facility*. British Columbia, BC: CSSF.

Dayton, P. K., Thrush, S. F., Agardy, M. T., and Hofman, R. J. (1995). Environmental effects of marine fishing. *Aquat. Conserv. Mar. Freshwater Ecosyst.* 5, 205–232. doi: 10.1002/aqc.3270050305

Deichmann, E. (1936). *The Alcyonaria of the western part of the Atlantic Ocean. Memoires of the Museum of Comparative Zoology*, Vol. 53. Cambridge, MA: Harvard College, 1–317.

Edinger, E. N., Baker, K. D., Devillers, R., and Wareham, V. (2007). *Coldwater Corals Off Newfoundland and Labrador: Distribution and Fisheries Impacts*. Toronto,ON: World Wildlife Fund, 41.

ESRI (2008). *ArcGIS 9.3*. Redlands, CA: Environmental Systems Research Institute.

Fossa, J. H., Mortensen, P. B., and Furevik, D. M. (2002). The deep-water coral *Lophelia pertusa* in Norwegian waters: distribution and fishery impacts. *Hydrobiologia* 471, 1–12.

Freese, J. L. (2001). Trawl-induced damage to sponges observed from a research submersible. *Mar. Fish. Rev.* 63, 7–13.

Freese, L., Auster, P. J., Heifetz, J., and Wing, B. L. (1999). Effects of trawling on seafloor habitat and associated invertebrate taxa in the Gulf of Alaska. *Mar. Ecol. Prog. Ser.* 182, 119–126. doi: 10.3354/meps182119

Gass, S. (2003). *Conservation of Deep-Sea Corals in Atlantic Canada*. Toronto, ON: World Wildlife Fun – Canada, 54.

Henry, L. A., Kenchington, E. L. R., and Silvaggio, A. (2003). Effects of mechanical experimental disturbance on aspects of colony responses, reproduction, and regeneration in the cold-water octocoral *Gersemia rubiformis*. *Can. J. Zool. Rev. Canadienne De Zool.* 81, 1691–1701. doi: 10.1139/z03-161

Husebo, A., Nottestad, L., Fossa, J. H., Furevik, D. M., and Jorgensen, S. B. (2002). Distribution and abundance of fish in deep-sea coral habitats. *Hydrobiologia* 471, 91–99.

Jackman, S., Tahk, A., Zeileis, A., Maimone, C., and Fearon, J. (2011). *Package 'pscl'*. Stanford CA: Standford University.

Koen-Alonso, M., Favaro, C., Ollerhead, N., Benoit, H., Bourdages, H., Sainte-Marie, B., et al. (2018). Analysis of the overlap between fishing effort and Significant Benthic Areas in Canada's Atlantic and Eastern Arctic marine waters. *DFO Can. Sci. Advis. Sec. Res. Doc.* 2018/015 xvii + 270.

Koenig, C. C., Shepard, A. N., Reed, J. K., Coleman, F. C., Brooke, S. D., Brusher, J., et al. (2005). Habitat and fish populations in the deep-sea Oculina coral ecosystem of the western Atlantic. *Am. Fish. Soc. Symposium* 41, 795–805.

Krieger, K. J. (2001). "Coral (*Primnoa*). impacted by fishing gear in the Gulf of Alaska," in *Proceedings of the First International Symposium on Deep Sea Corals*, eds J. H. M. Willison, J. Hall, and S. E. Gass (Halifax, NS: Ecology Action Centre), 156–165.

Kulka, D. W., and Pitcher, D. A. (2001). Spatial and temporal patterns in trawling activity in the Canadian and Pacific. *ICES CM R* 02, 1–55.

Malecha, P. W., and Stone, R. P. (2009). Response of the sea whip *Halipteris willemoesi* to simulated trawl disturbance and its vulnerability to subsequent predation. *Mar. Ecol. Prog. Ser.* 388, 197–206. doi: 10.3354/meps08145

Meesters, E. H., Noordeloos, M., and Bak, R. P. M. (1994). Damage and regeneration - links to growth in the reef-building coral *Montastrea annularis*. *Mar. Ecol. Prog. Ser.* 112, 119–128. doi: 10.3354/meps112119

Mortensen, P. B., and Buhl-Mortensen, L. (2005). "Deep-water corals and their habitats in The Gully, a submarine canyon off Atlantic Canada," in *Cold-Water Corals and Ecosystems*, eds A. Freiwald and J. M. Roberts (Berlin: Springer-Verlag), 247–277. doi: 10.1007/3-540-27673-4_12

Mortensen, P. B., Buhl-Mortensen, L., and Gordon, D. C. (2006). "Distribution of deep-water corals in Atlantic Canada," in *Proceedings of the 10th International Coral Reef Symposium*, (Okinawa), 1832–1848.

Murillo, F. J., Durán Munoz, P., Altuna, A., and Serrano, A. (2010). Distribution of deep-water corals of the Flemish Cap, Flemish Pass, and the Grand Banks of Newfoundland (Northwest Atlantic Ocean): interaction with fishing activities. *ICES J. Mar. Science* 68, 319–332. doi: 10.1093/icesjms/fsq071

Norse, E. A., Brooke, S., Cheung, W. W. L., Clark, M. R., Ekeland, L., Froese, R., et al. (2012). Sustainability of deep-sea fisheries. *Mar. Policy* 36, 307–320.

RDevCoreTeam. (2012). *R: A Language and Environment for Statistical Computing*. Vienna: R Foundation for Statistical Computing.

Roberts, J. M., Wheeler, A. J., Freiwald, A., and Cairns, S. (2009). *Cold-water Corals: The Biology and Geology of Deep-sea Coral Habitats*. New York, NY: Cambridge University Press, 334.

Roberts, S., and Hirshfield, M. (2004). Deep-sea corals: out of sight, but no longer out of mind. *Front. Ecol. Environ.* 2, 123–130. doi: 10.1890/1540-9295(2004)002%5B0123:dcoosb%5D2.0.co;2

Sainsbury, K. J., Campbell, D. E., and Whitelaw, A. W. (1992). "Effects of trawling on the marine habitat on the North West shelf of Australia and implications for sustainable fisheries management," in *Sustainable Fisheries through Sustaining Fish Habitat. Australian Society for Fish Biology Workshop*, ed. D. A. Hancock (Canberra: Australian Government Publishing Service), 137–145.

Sherwood, O. A., and Edinger, E. N. (2009). Ages and growth rates of some deep-sea gorgonian and antipatharian corals of Newfoundland and Labrador. *Can. J. Fish. Aquat. Sci.* 66, 142–152. doi: 10.1139/f08-195

Stone, R. (2006). Coral habitat in the Aleutian Islands of Alaska: depth distribution, fine-scale species associations, and fisheries interactions. *Coral Reefs* 25, 229–238. doi: 10.1007/s00338-006-0091-z

Thresher, R. E. (2009). Environmental and compositional correlates of growth rate in deep-water bamboo corals (Gorgonacea; Isididae). *Mar. Ecol. Prog. Ser.* 397, 187–196. doi: 10.3354/meps08245

Thrush, S. F., Hewitt, J. E., Funnell, G. A., Cummings, V. J., Ellis, J., Schultz, D., et al. (2001). Fishing disturbance and marine biodiversity: the role of habitat structure in simple soft-sediment systems. *Mar. Ecol. Prog. Ser.* 223, 277–286. doi: 10.3354/meps223277

Tunnicliffe, V., and Syvitski, J. P. M. (1983). Corals move boulders - an unusual mechanism of sediment transport. *Limnol. Oceanogr.* 28, 564–568. doi: 10.4319/lo.1983.28.3.0564

van der Land, J. (1994). *UNESCO-IOC Register of Marine Organisms, a common base for biodiversity inventories*. Leiden: NNM.

Van Dolah, R. F., Wendt, P. H., and Nicholson, N. (1987). Effects of a research trawl on a hard-bottom assemblage of sponges and corals. *Fish. Res.* 5, 39–54. doi: 10.1016/0165-7836(87)90014-2

Wareham, V. E., and Edinger, E. N. (2007). Distribution of deep-sea corals in the Newfoundland and Labrador region, Northwest Atlantic Ocean. *Bull. Mar. Sci.* 81, 289–313. doi: 10.1371/journal.pone.0111519

Watanabe, S., Metaxas, A., Sameoto, J., and Lawton, P. (2009). Patterns in abundance and size of two deep-water gorgonian octocorals, in relation to depth and substrate features off Nova Scotia. *Deep Sea Res. I Oceanogr. Res. Papers* 56, 2235–2248. doi: 10.1016/j.dsr.2009.09.003

Watling, L., and Norse, E. A. (1998). Disturbance of the seabed by mobile fishing gear: A comparison to forest clearcutting. *Conserv. Biol.* 12, 1180–1197. doi: 10.1046/j.1523-1739.1998.0120061180.x

Weaver, P. P. E., Benn, A., Arana, P., Ardron, J., Bailey, D. M., Baker, K. D., et al. (2011). *The impact of deep-sea fisheries and implementation of the UNGA Resolutions 61/105 and 64/72*. Report of an international scientific workshop. Southampton: National Oceanography Centre, 45.

Weinbauer, M. G., Brandstatter, F., and Velimirov, B. (2000). On the potential use of magnesium and strontium concentrations as ecological indicators in the calcite skeleton of the red coral (*Corallium rubrum*). *Mar. Biol.* 137, 801–809. doi: 10.1007/s002270000432

Yesson, C., Taylor, M. L., Tittensor, D. P., Davies, A. J., Guinotte, J., Baco, A., et al. (2012). Global habitat suitability of cold-water octocorals. *J. Biogeogr.* 39, 1278–1292. doi: 10.1111/j.1365-2699.2011.02681.x

Yoklavich, M. M., Laidig, T. E., Graiff, K., Clarke, M. E., and Whitmire, C. E. (2018). Incidence of disturbance and damage to deep-sea corals and sponges in areas of high trawl bycatch near the California and Oregon border. *Deep sea Res. II* 150, 156–163. doi: 10.1016/j.dsr2.2017.08.005

Zuur, A. F., Ieno, E. N., Walker, N. J., Saveliev, A. A., and Smith, G. M. (2009). *Mixed Effects Models and Extensions in Ecology with R*. New York, NY: Springer, 574.

Conflict of Interest Statement: The authors declare that the research was conducted in the absence of any commercial or financial relationships that could be construed as a potential conflict of interest.

frontiers in Marine Science

ORIGINAL RESEARCH
published: 11 October 2019
doi: 10.3389/fmars.2019.00596

Demersal Fishing in Areas Beyond National Jurisdiction: A Comparative Analysis of Regional Fisheries Management Organisations

James B. Bell[1]*, **Elena Guijarro-Garcia**[2] **and Andrew Kenny**[1]

[1] Centre for Environment, Fisheries and Aquaculture Science, Lowestoft, United Kingdom, [2] Instituto Español de Oceanografía, CO de Murcia, Murcia, España

In areas beyond national jurisdiction, there are ten regional fisheries bodies (RFBs) responsible for the management of bottom fisheries (ABNJ). Eight of these organizations are further termed "Regional Fisheries Management Organisations" (RFMOs) and have a legal mandate to regulate the sustainable use of marine living resources on the high seas. The remaining two, both in the equatorial Atlantic, are limited to advisory roles. Here we present comparisons between these organizations' management of deep-water demersal fisheries, with particular respect to how they have respectively, adopted the suite of available measures for the mitigation of significant adverse impacts (SAIs) upon vulnerable marine ecosystems (VMEs). Each organization was scored against 99 performance criteria that either related to their capacity to implement management measures ("Capacity"); the number and effectiveness of measures they have implemented ("Action"); and the intensity and spatial extent of the activities they regulate ("Need"). For most organizations, action and need scores were proportional, as the more actions an organization takes to reduce risk to VMEs, the more it reduces the scope for improvement. However, comparisons between capacity and action scores indicate that, in some organizations, there remain several aspects of VME impact mitigation that could be improved. In the case of RFBs, or recently established RFMOs, capacity gaps are still considerable, suggesting that these organizations receive additional scientific, technical, legal, and financial support, to ensure that they are able to meet current and future objectives. Further, there is little evidence of significant cooperation between adjacent or overlapping organizations in the development and application of conservation measures, highlighting the need for an agreement on the management of biodiversity, rather than sectors, in ABNJ.

Keywords: deep-sea, areas beyond national jurisdiction, impacts, fisheries, VME

Edited by:
Christopher Kim Pham,
University of the Azores, Portugal

Reviewed by:
Michael Vecchione,
National Oceanic and Atmospheric Administration (NOAA), United States
Jeff A. Ardron,
The University of Southampton, United Kingdom

****Correspondence:***
James B. Bell
james.bell@cefas.co.uk

Specialty section:
This article was submitted to Deep-Sea Environments and Ecology, a section of the journal Frontiers in Marine Science

Received: *07 May 2019*
Accepted: *05 September 2019*
Published: *11 October 2019*

Citation:
Bell JB, Guijarro-Garcia E and Kenny A (2019) Demersal Fishing in Areas Beyond National Jurisdiction: A Comparative Analysis of Regional Fisheries Management Organisations. Front. Mar. Sci. 6:596. doi: 10.3389/fmars.2019.00596

Abbreviations: ABNJ, areas beyond national jurisdiction; BBNJ, biodiversity beyond national jurisdiction; CAN, capacity – action – need (scoring method in comparative analysis); CCAMLR, Convention For The Conservation Of Antarctic Marine Living Resources; CECAF, Fisheries Committee For The Eastern Central Atlantic; FAO, food and agriculture organization, un; GFCM, General Fisheries Commission for the Mediterranean; GFW, Global Fishing Watch; NAFO, North West Atlantic Fisheries Organisation; NEAFC, Northeast Atlantic Fisheries Commission; NPFC, North Pacific Fisheries Commission; RFB, regional fishery body; RFMO, Regional Fisheries Management Organisation; SAI, significant adverse impact; SDM, species distribution model; SEAFO, South East Atlantic Fisheries Organisation; SIOFA, South Indian Ocean Fisheries Agreement; SPRFMO, South Pacific Regional Fisheries Management Organisation; UNGA, United Nations General Assembly; VME, Vulnerable Marine Ecosystem (variously defined); VMS, vessel monitoring system; WECAFC, Western Central Atlantic Fishery Commission; WG, working group.

INTRODUCTION

Fishing activities in the majority of the world's oceans are subject to oversight by relatively few organizations. In ABNJ, the organization responsible for management of living resources harvested by fishing is determined by whether or not the species are considered highly migratory, under Annex II of the UN Convention on the Law of the Sea. Highly migratory species are managed by organizations so-called "Tuna-RFMOs," but for demersal species or those with more restricted ranges, there are ten organizations worldwide whose areas of competence cover some 55.6% of the global ocean, including ABNJ and territorial waters (**Table 1** and **Figure 1**). Of these ten, seven have a legal mandate to enact binding measures in ABNJ and cover around 76.0% of the high seas.

The deep-sea plays host to a wide range of habitat types that are commonly, but not exclusively, characterized by low productivity. Many of the species, both those of commercial value or otherwise, that inhabit the deep-sea, display life history traits adapted to slow-growth and high longevity/late maturation (Cailliet et al., 2001), which markedly increases their vulnerability to direct exploitation or other disturbances. Owing to these vulnerabilities, deep-sea fisheries have often been characterized by short periods of high-intensity fishing that can quickly reduce fish stocks below economic levels. Deep-sea fisheries use a range of fixed and mobile gear types and are focused in depths of between 200 and 2000 m, targeting areas of continental slope, seamounts and mid-ocean ridges, both within exclusive economic zones and ABNJ. Since 1950, the mean depth of fishing activity has increased by 350 m (Mengerink et al., 2014). In this review, we consider how each organization has managed impacts that can arise from deep-water fisheries (deeper than 400 m; Mangi et al., 2016).

The FAO International guidelines for the management of deep-sea fisheries in the High Seas (FAO, 2009) are intended for use by states and RFMOs in formulating and implementing appropriate measures. However, these guidelines have been adopted only by a few coastal and flag states (Rogers and Gianni, 2010). International concern over the impacts of deep-sea fishing has been the subject of extensive debate by the UNGA, leading to the adoption of several resolutions to protect deep-sea ecosystems (UNGA resolutions 59/25; 61/105; 64/72), which have been variously adopted by each of the RFMOs (UN Secretary General, 2006; Rogers and Gianni, 2010). RFMOs are mandated to conduct assessments, as to whether significant adverse impacts (SAIs) have occurred upon VME and if stocks are exploited sustainably, and implement measures, according to the precautionary approach as necessary, to mitigate these risks (Rogers and Gianni, 2010; Gianni et al., 2016).

Both fixed and mobile fishing gears can come into contact with the sea floor during fishing operations, and consequently pose a risk of SAIs to benthic fauna, particularly those associated with vulnerable marine ecosystems (VME), which are the focus of this review. VMEs are those which host assemblages with one or more of the following attributes: relatively high proportions of rare species; important contribution to key ecosystem functions; structural fragility; and life history traits such as slow growth rates, late maturity or low/unpredictable recruitment (Kenchington et al., 2014). Such ecosystems, whilst not usually the target of commercial activity themselves, are considered to be an important source of habitat for commercial species and thus contribute toward the long-term viability of a stock (Pham et al., 2015). The scale and significance of an impact determines whether it can be considered a SAI (Martin-Smith, 2009; Kenchington et al., 2014). SAIs are negative, long-term consequences for ecosystem function and natural productivity, and the relatively low resilience of deep-sea ecosystems highlights the importance of protecting seabed habitats as an integral part of deep-sea fisheries management (Mangi et al., 2016; Kenny et al., 2018; Koen-Alonso et al., 2019). Assessments of SAIs however, do not always meet FAO criteria and fishing activities that create SAIs are still permitted over large areas of sensitive habitats (Gianni et al., 2016).

Conceptually, the application of fisheries management may be thought of as a trade-off between the "cost" of management activities (data acquisition and stock assessments, closure of fishing grounds etc.) versus the amount of expected "reward" (i.e., fisheries product) (**Figure 2**). This schema allows for the contextualization of the precautionary principle within fisheries economics, to aid in the prioritization of particular areas where increased management focus is most needed. For example, in low-effort fisheries with relatively few ecosystem impacts (e.g., the deep-sea red crab pot fishery in SEAFO Division B1), the need for explicit oversight is less warranted, and indeed less economic, than for more intensive fisheries with greater potential for impacts (e.g., demersal trawling in the NAFO regulatory area).

Some RFMOs have been proactive in formulating rules related to deep-sea fisheries exploitation but ambition and resultant implementation of these measures is uneven. While RFMOs are given a central place in the management of these fisheries, they can vary widely in scope, authority, participation by fishing nations, and the robustness of the scientific advice provided (Cullis-Suzuki and Pauly, 2010; Clark et al., 2015; Wright et al., 2015; Gianni et al., 2016). Consequently, the different scientific approaches in RFMOs for deep-sea fisheries can be quite broad when addressing issues such as: SAI thresholds, fishing footprint and fishing intensity calculation, application of models of VME indicator species occurrence, method for defining risk of impacts, scale and significance of the impact of fishing on VMEs, and encounter protocols. The most common avoidance or mitigation measures are area closures, gear limitations, encounter rules, and stricter controls upon exploratory fishing (Penney et al., 2009; Aguilar et al., 2017). There remain concerns that low observer coverage levels, inadequate measures, and poor compliance limits the effectiveness of management in these areas, particularly for the application of encounter rules (Rogers and Gianni, 2010; Auster et al., 2011; Gianni et al., 2016).

We reviewed ten organizations (**Table 1**) with the remit to advise upon and/or regulate deep-sea fishing against a set of criteria to evaluate their relative performance, with particular focus on the ways in which they mitigate impacts upon VMEs.

TABLE 1 | Organizations reviewed in this article. RFMO waters, except GFCM, are only in ABNJ. RFB waters include territorial seas (**Figure 1**).

Name	Legal status	General area of jurisdiction	Key fish stocks
Convention for the Conservation of Antarctic Marine Living Resources (CCAMLR)	RFMO*	Southern Ocean, south of sub-polar Front.	Patagonian and Antarctic Toothfish, Krill, and Mackerel Icefish.
Fisheries Committee for the Eastern Central Atlantic (CECAF)	RFB	Sub-tropical and tropical Atlantic, east of 40°W.	Multiple pelagic and demersal finfish and crustacean stocks.
General Fisheries Commission for the Mediterranean (GFCM)	RFMO	Mediterranean and Black Seas.	Multiple pelagic and demersal finfish and crustacean stocks.
Northwest Atlantic Fisheries Organization (NAFO)	RFMO	Northwest Atlantic, west of 42°W.	Temperate groundfishes (e.g. cod, redfish) and cephalopods.
North-east Atlantic Fisheries Commission (NEAFC)	RFMO	Northeast Atlantic and Arctic Oceans, 42°W – 50°E.	Temperate groundfishes (e.g. redfish, whiting) and sharks.
North Pacific Fisheries Commission (NPFC)	RFMO	North Pacific, north of 10°N.	Demersal fishes (e.g. alfonsino), and pelagic finfish and cephalopods.
South East Atlantic Fisheries Organisation (SEAFO)	RFMO	South-east Atlantic, east of 20°W.	Geryonid crabs Patagonian Toothfish Orange Roughy
South Indian Ocean Fisheries Agreement (SIOFA)	RFMO	South Indian Ocean, south of 10°S	Alfonsino, Pelagic armourhead, geryonid crabs, Patagonian Toothfish.
South Pacific Regional Fisheries Management Organisation (SPRFMO)	RFMO	South Pacific, south of 0°N	Multiple pelagic and demersal finfish and cephalopod stocks.
Western Central Atlantic Fishery Commission (WECAFC)	RFB**	Western sub-tropical and tropical Atlantic and Caribbean, west of 40°W	Spiny Lobster, small pelagic finfishes and miscellaneous demersal fishes¤

**The Convention for the Conservation of Antarctic Marine Living Resources (CCAMLR) is not officially a RFMO, but for the purposes of this review, only its roles relevant to the management of demersal fisheries are considered. **Legal status under review, with aspiration to become a RFMO. ¤As defined by FAO.*

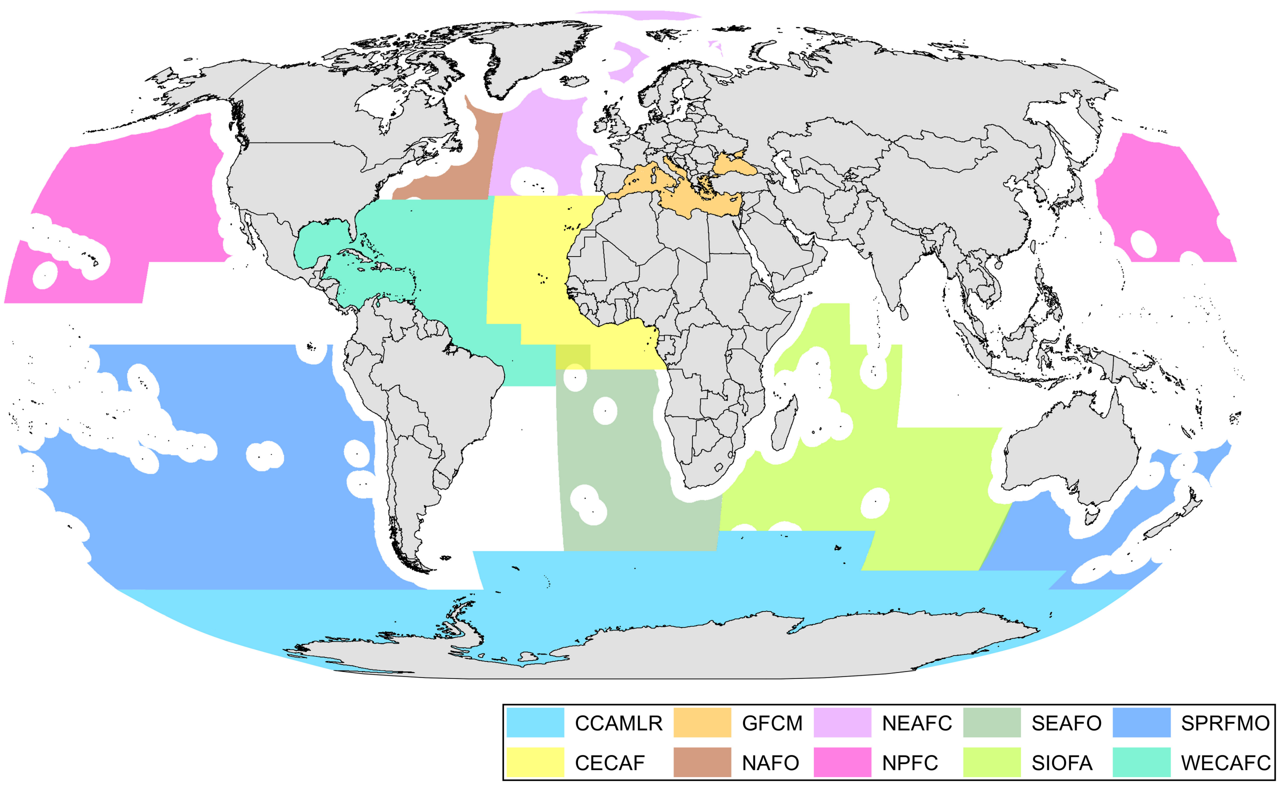

FIGURE 1 | Area of competence for each RFMO/RFB considered in the present review. GFCM is the only RFMO that includes areas within national jurisdiction. N.B. The SEAFO convention area overlaps with the CECAF area in the region to the north of Ascension Island (central Atlantic). CCAMLR – Convention for the Conservation of Antarctic Marine Living Resources; CECAF – Fisheries Committee for the Eastern Central Atlantic; GFCM – General Fisheries Commission for the Mediterranean; NAFO – Northwest Atlantic Fisheries Organization; NEAFC – North-east Atlantic Fisheries Commission; NPFC – North Pacific Fisheries Commission; SEAFO – South-east Atlantic Fisheries Organisation; SIOFA – South Indian Ocean Fisheries Agreement; SPRFMO – South Pacific Regional Fisheries Management Organisation; WECAFC – Western Central Atlantic Fishery Commission.

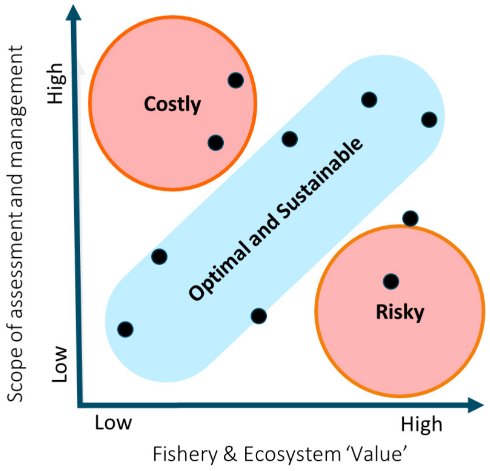

FIGURE 2 | Conceptual risk-reward framework for fisheries management.

MATERIALS AND METHODS

Each organization was scored against 99 specific criteria in May-June 2018, using information that was publicly available through their respective websites and published reports and relevant to some aspect of their organizational structure, the activities they manage, or ecological characteristics of their areas of competence. The criteria were developed with the authors of the original report (Bell et al., 2019) and staff at the European Maritime and Fisheries Fund (EMFF) with the aim of covering as many characteristics of each organization as possible (**Supplementary Appendix S1, S4**). Secretariats were not contacted to request information as part of the effort to minimize bias.

The criteria were scored using a mix of quantitative (e.g., area size of the organization's regulatory area/area of competence, or the proportion of fishing trips that are subject to independent observation) and qualitative (e.g., whether the organization has agreed a definition of VME) sources of information. Qualitative information was scored against pre-agreed criteria and all scores for a given organization were reviewed by an author not involved in the primary data collection. The criteria covered a broad range of topics, including organizational structure (e.g., annual budget of the organization); collection and use of fisheries-dependent and research data; potential sources of SAIs; and management measures adopted by the organization.

Scores from 46 of the 99 criteria were disregarded from subsequent analyses for one or more of the following reasons:

(1) A direct comparison was not considered meaningful. For instance, typical stock assessment interval varied between and within organizations, tending to be more regular in organizations with a longer history, and a higher proportion of developed Contracting Parties (, e.g., NEAFC or NAFO). However, this difference does not effectively comment on whether the stock assessment interval is adequate, so it would not be valid to assume that a shorter interval constituted "better" management;
(2) There were insufficient organizations for which data could be gathered (seven or fewer), or all organizations were scored at zero;
(3) Concerns about bias or incomparability in scores could not be resolved, particularly where concerns over differences in the quality of information reported by the organizations were raised (e.g., fishing effort was not equivalently reported by each organization).

Each of the remaining 53 criteria were classified according to whether they best represented either: organizational capacity (i.e., what the organization has the authority and resources to deliver); management actions (i.e., measures that the organization has previously implemented); or management need (i.e., the level of management measures that are still required) (**Supplementary Appendix S1**). These scores are collectively referred to as CAN scores and are analogous to the P and Q (theoretical performance, i.e., capacity, and actual performance, i.e., action, respectively) scoring method used by Cullis-Suzuki and Pauly (2010) but take an additional step of contextualizing capacity and action scores within potential threat levels (i.e., need), such as fishing intensity. Need scores also included an element of penalization (e.g., organizations scored higher in need if certain actions, such as mandated observer coverage levels, had not, or could not have been implemented; **Supplementary Appendix S1**).

Scores were also classified as relating to "fishery-ecosystem value" (**Figure 2**), a subset of scores categorized as need that excluded criteria such as whether the organization permitted the use of towed bottom-contacting gears (a management decision not related to the inherent biodiversity "value" of the area). First sale value of the fisheries could not be determined and so these scores are derived from the inference that a larger fleet, and/or higher fishing effort begets a higher "value." The ecosystem value of non-target species was indicated by scores in criteria such as the extent and diversity of the VME species and habitats present.

All scores were normalized to the maximum value within each criterion, to avoid bias/incomparability arising from the differing scales between criteria. Untransformed CAN scores were used to calculate a Euclidean dissimilarity matrix and visualized with non-metric multidimensional scaling and average linkage hierarchical clustering using the "Vegan" package in R (Oksanen et al., 2019). The mean and standard deviation within each classification was also calculated to compare each organizations' overall position and Spearman's rank correlation test applied. Relationship between scores was visualized using generalized linear models with 95% confidence intervals.

Limitations and Caveats

Since each criterion's scores were normalized (so that the highest value = 1), the results presented here should be considered relative measures only; high or low scores should not necessarily be interpreted as an organization having adopted best practice or failing to meet its objectives. The study combined criteria with categorical and quantitative scores and as such, individual criteria often had non-normal error distributions (especially for binary scores; **Supplementary Appendix S1**). Mean scores (and standard deviation) were sensitive to binary scores, but the majority of scores were objective, comparable measures (e.g., fishing effort) that largely limited the potential for this error in interpretation. Scoring methods were quantitative in as many cases as possible but some were necessarily qualitative, in which case scoring methods were standardized (**Supplementary Appendix S1**). Despite this, and the wide range of criteria used, differences in information accessibility between organizations, or between individual author's perceptions, likely still contributed some residual source of error.

Organizations were not scored for measures that were still under consideration at the time of data collection, though we note that some improvements were being considered at the time of writing (e.g., proposal of new fishery closed areas in SIOFA and GFCM). In some cases, comparable data were very difficult to acquire via publicly accessible sources of information and so, where possible, supplementary spatial data were also acquired, such as daily fishing effort data from the GFW portal (Kroodsma et al., 2018), and global bathymetric data (Ryan et al., 2009). GFW data were gridded at 0.01° resolution, and the mean number of fishing hours per cell between 2012 and 2016 was taken as an estimate of fishing intensity within each of the organizations' areas of competence. The use of GFW data means that such results are biased toward vessels that are large enough to be expected to use a position beacon, and compliant enough to ensure that the beacon is operational, but comparable estimates of fishing effort within each RFMO were otherwise impossible to constrain.

RESULTS

Typical Management Measures

All the organizations (that have had opportunity to do so), have implemented some combination of the following precautionary or reactive measures to limit or avoid the risk of SAI upon VMEs:

1. Fishery closed areas;
2. Fishing areas closed to specific gears;
3. Exploratory fishing rules, whereby fishing in new areas is subject to increased scrutiny; and
4. Encounter rules, through which vessels are expected to report instances of VME species bycatch exceeding a given threshold and cease fishing within a stated distance of the last fishing event.

However, the extent to which each of these measures has been adopted, varied widely between organizations. For example, the proportion of area closed to some or all kinds of fishing gears ranged between 0% in SIOFA and SPRFMO, to 77.4% in GFCM (though the vast majority of this area is deeper than 1000 m and closed to bottom trawling only). Where implemented, the proportion of fishing closed areas ranged between 3 and 11% of the total regulatory area, compared with a fishing footprint extent of between <1 and 37%.

Organization Scores

The capacity and action scores for each organization were broadly proportional to their need (p = 0.11 and 0.04 respectively, **Figures 3A,B**). Some organizations however, fell substantially above or below the trend, indicating where there are improvements to be made, or where management has been more precautionary. CECAF scored highest in need, and lowest in capacity and action, although capacity and action scores were comparable to WECAFC. NEAFC, NAFO, and CCAMLR were consistently the highest scoring organizations for capacity and action, with commensurately low scores in need (**Figures 3A,B**).

Comparisons between capacity and action (i.e., what an organization could have done, versus what it actually has done) highlight some interesting cases where an organization appears to be performing above or below the "expected relationship." SEAFO and GFCM were the most markedly different from the overall trend (**Figure 3C**), with SEAFO having a relatively high "action" score given its capacity, whereas for GFCM the opposite appears to be the case.

Multivariate Analyses

The strongest organizational associations were between CECAF and WECAFC, and NAFO and NEAFC. The dissimilarity between CECAF and WECAFC, and the other organizations was mainly driven by their legal status, and other differences that arise from this (e.g., they could not implement closed areas). Organizations whose convention areas are geographically close also appeared to have some degree of association (e.g., NPFC and SPRFMO, or SEAFO and CCAMLR), especially between NEAFC and NAFO. GFCM was the most distinct, with no clear association with any other organization (**Figure 5**).

There were a number of categories that were strongly covariate (**Figure 5**). For instance, if an organization had defined a fishing footprint, it would also have been more likely to have adopted exploratory fishing rules and to require vessels to report position data. Similarly, observer data collection tended to be implemented across the full suite of information sources, and there were no organizations which only mandated collection of target species data.

DISCUSSION

CAN Scores

Most organizations had proportionate scores in terms of their actions and fishery-ecosystem value and NEAFC, NAFO and CCAMLR were consistently evident as having done the most to address their management needs, expanding upon previous findings regarding CCAMLR (Gianni et al., 2016). For CECAF and WECAFC, differences largely relate to their legal status but for GFCM, which also scored poorly in terms of its relationship between capacity and action, this likely owing to its area of competence being largely contained within waters under the control of coastal states and thus heavily limiting its ability to make unilateral decisions. Most of the organizations reviewed had need and action scores that were proportional (**Figures 3**, **4**). One of the major drivers of an organization's need score related to the amount of fishing effort. CECAF had the highest need score, driven principally by the relatively high fishing effort in its area of competence (which includes territorial seas), particularly along the west African margin and was amongst the least able to address

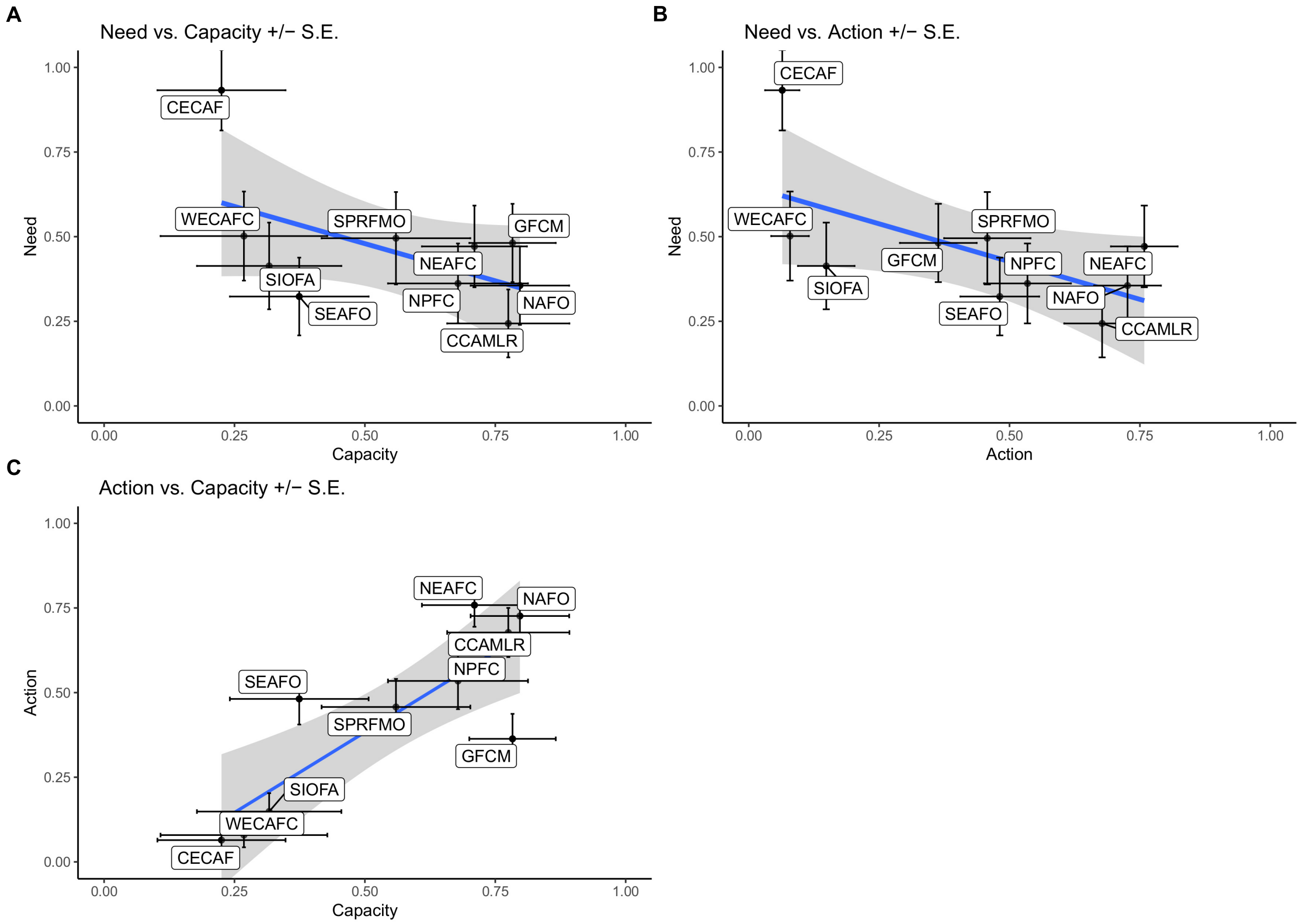

FIGURE 3 | Comparisons of the "capacity," "need" and "action" scores. Gray area = S.E. of generalized linear model (blue line). See **Supplementary Appendix S2** for 3-D CAN scores graphic. CCAMLR – Convention for the Conservation of Antarctic Marine Living Resources; CECAF – Fisheries Committee for the Eastern Central Atlantic; GFCM – General Fisheries Commission for the Mediterranean; NAFO – Northwest Atlantic Fisheries Organization; NEAFC – North-east Atlantic Fisheries Commission; NPFC – North Pacific Fisheries Commission; SEAFO – South-east Atlantic Fisheries Organisation; SIOFA – South Indian Ocean Fisheries Agreement; SPRFMO – South Pacific Regional Fisheries Management Organisation; WECAFC – Western Central Atlantic Fishery Commission.

this need, being comprised principally of lesser developed CPs and lacking a convention text. Furthermore, the coastal states bordering the CECAF region are among the least developed and there remain a considerable number of small-scale, artisanal fisheries, whose effort was not captured here but nonetheless contribute much of the fishing effort. WECAFC, although having a similar situation to CECAF in terms of capacity, had far fewer vessels and a much smaller "fishable" area for deep-water fishing (depths between 400 and 2000 m).

One of the most useful comparisons, in terms of assessing RFMO performance, was between capacity and action. Of particular interest were SEAFO and GFCM, the organizations that differed most strongly from the mean relationship (**Figure 3C**). SEAFO's scores indicate that it was relatively cautious in developing mitigation measures, given its capacity, and thus outperforming other organizations in its application of the precautionary approach. However, it has been contended by some that SEAFO's conservation measures (particularly with reference to closed and exploratory areas) are overly detrimental to the opportunities for responsible, low impact fisheries (SEAFO, personal communication). For comparison, the amount of fishing effort expended in SEAFO (mean fishing hours per $0.01^{\circ 2}$ between 2012 and 2016) is around a third of that in SIOFA or SPRFMO, and considerably less than a tenth of that of NAFO or NEAFC.

Effectiveness of Management Measures

There are several factors affecting the success of measures for the avoidance of SAIs, of which compliance is arguably the most consistent and thus, measures that are easier to enforce tend to have a higher chance of success. Encounter rules are particularly problematic, the main issues being that; (a) encounter rules are reactive and so cannot wholly exclude the risk of SAIs and (b) they rely on vessels reporting instances of VME bycatch, which is often unreliable even in the presence of independent observers (Auster et al., 2011).

In terms of mitigating potential impacts to VME, closed areas are the most effective method but come with the cost of reducing

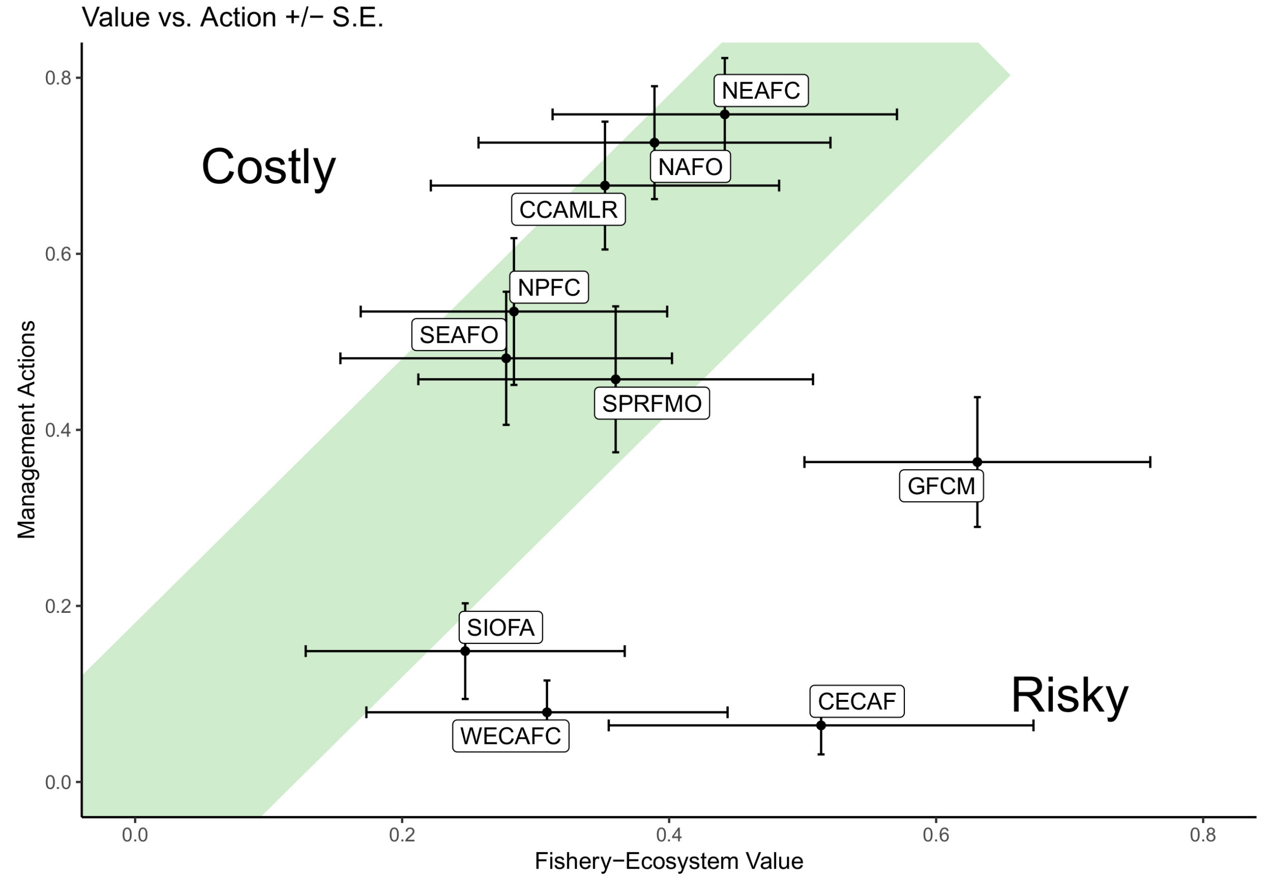

FIGURE 4 | Comparisons between the "fishery-ecosystem value" of each organization's area of competence and its historic activity. Green area represents an idealized, though arbitrary, optimal relationship between action and value (**Figure 2**). CCAMLR – Convention for the Conservation of Antarctic Marine Living Resources; CECAF – Fisheries Committee for the Eastern Central Atlantic; GFCM – General Fisheries Commission for the Mediterranean; NAFO – Northwest Atlantic Fisheries Organization; NEAFC – North-east Atlantic Fisheries Commission; NPFC – North Pacific Fisheries Commission; SEAFO – South East Atlantic Fisheries Organisation; SIOFA – South Indian Ocean Fisheries Agreement; SPRFMO – South Pacific Regional Fisheries Management Organisation; WECAFC – Western Central Atlantic Fishery Commission.

the size of the fishable area. For isolated stocks, this effectively "costs" fishery production and increases the risk of localized serial depletion elsewhere. In such cases, it may be more effective, at least in terms of balancing risk to the stock status of commercial species, to close fishing areas to specific gear types only, since the risk of SAIs is very strongly related to gear type.

There were clear differences between some groups of organizations (**Figure 5**) that tended to arise from implementation, or lack thereof, of particular measures (**Table 2**). For instance, organizations that had defined a fishing footprint, usually had also usually taken further actions, such as developing habitat suitability models for VME and establishing closures. This results in a list of relatively few criteria that may be considered to constitute a kind of a "success profile" for demersal fisheries management (**Table 2**).

Extrinsic Factors

Among the factors that were not formally captured in the analyses, one that apparently had considerable influence were the number of developed nations, as a proportion of the total membership. This theme was not captured during the review of each organization because it is largely outside of their control (e.g., NAFO, by dint of its coastal and fishing states, intrinsically has a higher proportion of developed member states than SIOFA). The history of the organization also plays an important role in some of the scores expressed here. For instance, although SIOFA has a convention text and so the means to enact measures such closed areas or mandated observer coverage levels, the scientific committee convened for the first time in 2016. This places a serious limit on the amount of progress that it could have made and, whilst a list of candidate VME closures existed in 2018 (SIOFA Scientific Committee, 2018), the Commission had not had the chance to decide whether or not to implement them. These considerations underline the amount of potential increased activity for older, better provisioned organizations, like CCAMLR or NEAFC, versus those such as CECAF or SIOFA.

We also note that WECAFC is considering its position, with a view toward establishing itself as a RFMO. It is therefore worth considering that the analyses presented here are a snapshot of each organization's policies and plans in

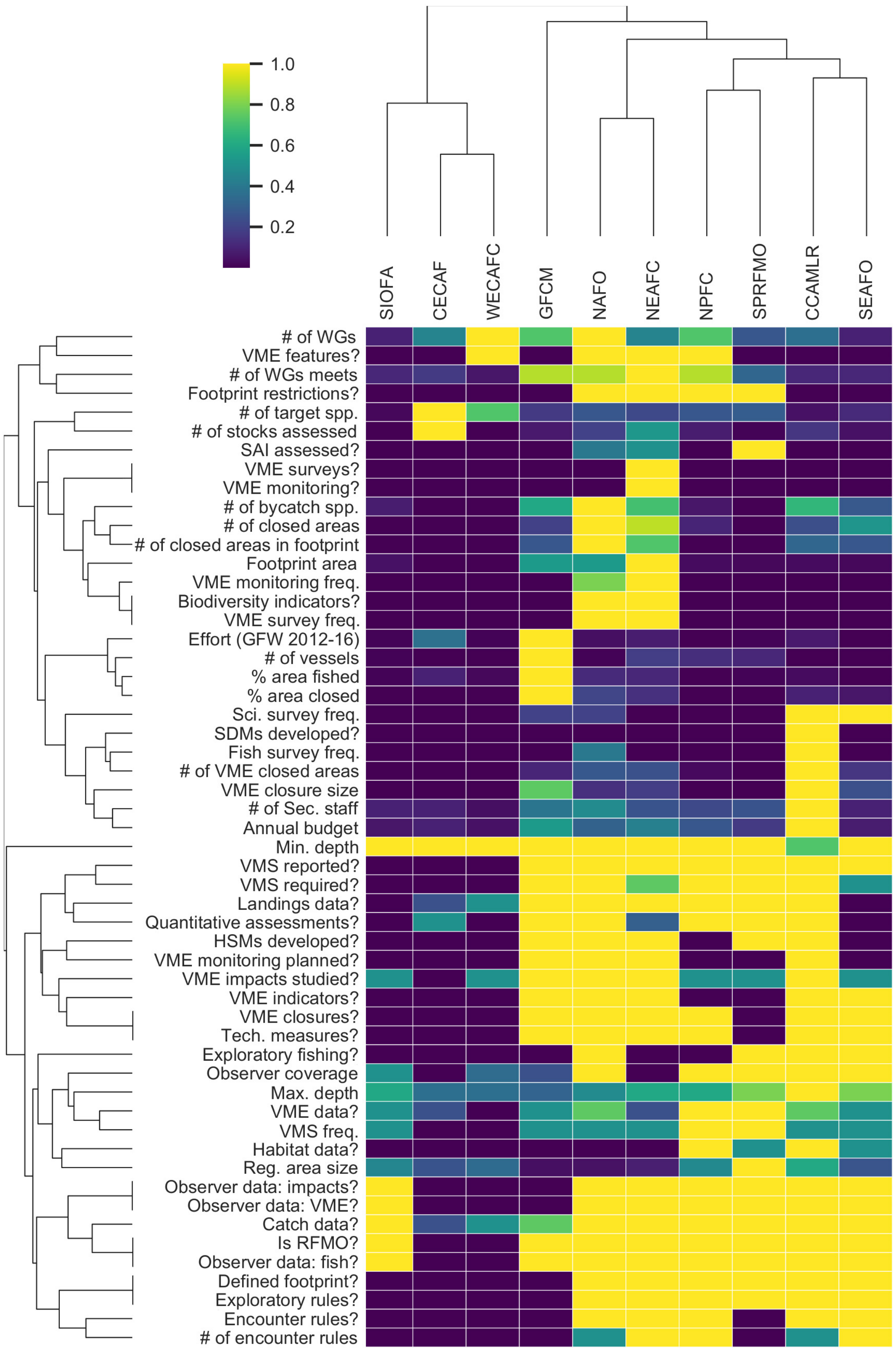

FIGURE 5 | Interactions between RFMOs and different category scores. Average linkage cluster dendrograms (based on Euclidean distance dissimilarity matrix) used to order the plot axes, with color indicating the score value. spp., species; HSM, habitat suitability model; SDM, species distribution model; VMS, vessel monitoring system. N.B. Criteria with too few scores, or where all organizations scored zero, are not included. See **Supplementary Appendix S3** for PCA ordination. CCAMLR – Convention for the Conservation of Antarctic Marine Living Resources; CECAF – Fisheries Committee for the Eastern Central Atlantic;

(Continued)

FIGURE 5 | Continued
GFCM – General Fisheries Commission for the Mediterranean; NAFO – North-west Atlantic Fisheries Organization; NEAFC – North-east Atlantic Fisheries Commission; NPFC – North Pacific Fisheries Commission; SEAFO – South-east Atlantic Fisheries Organisation; SIOFA – South Indian Ocean Fisheries Agreement; SPRFMO – South Pacific Regional Fisheries Management Organisation; WECAFC – Western Central Atlantic Fishery Commission.

mid-2018, and that if this analysis were to be repeated, some change would certainly be observable, particularly for those organizations with a relatively short history. Organizations like NAFO or NEAFC are, by comparison, much more well established and, whilst their measures continue to be reviewed, are unlikely to exhibit as much change. This consideration also underlines the need for stakeholders to focus their support upon those organizations that have the least technical, legal or financial capacity.

Particularly in the case of RFBs, the proportion of contracting parties that are developed nations is considerable relevance to an organization's performance. This stems from the legal mechanism whereby vessels flagged to a particular state are bound to its laws, as well as those of the organization in whose area it will fish. In the case of CECAF, the only mandated observer coverage is that of EU-flagged vessels, highlighting the potential for other national or multilateral agreements to assist in improving global fisheries management. In organizations like NAFO or NEAFC, this flag state influence is more prominent in terms of the amount of resource available to conduct scientific research and, for the purposes of this review, particularly that which relates to VMEs and the avoidance/mitigation of SAIs (e.g., habitat suitability modeling).

A complicating factor that emerged during this analysis was the extent to which the history and geopolitical context of each organization affects its current state. Particular organizations of note here were CCAMLR and GFCM. CCAMLR, except in the case of remote, uninhabited island territories such as South Georgia and the South Sandwich Islands or Heard and McDonald Islands, has no coastal states and all of its fisheries are comprized of industrial scale, distant water fleets. This creates a platform for an expected standard of compliance that other organizations have seemingly found difficult to replicate. GFCM by comparison, is responsible for a wide range of fishing activities, much of which occurs within the 12 nm territorial seas of its member states. Consequently, although GFCM has the same mandate, to ensure the sustainable management of marine living resources, most measures require the agreement of coastal states. This is considered to be a primary reason for the apparently low activity, relative to capacity, in GFCM.

TABLE 2 | Common characteristics of high and low-moderate scored organizations.

Relatively high scoring organizations **NEAFC, NAFO, CCAMLR, SEAFO**	**Relatively low-moderate scoring organizations*** **CECAF, SIOFA, WECAFC**
High standards of data collection for target fish stocks.	The organization has only recently been established or does not have RFMO status.
Vessel position data used.	Low numbers of permanent staff in the secretariat.
VME species/habitats identified, and habitat suitability models developed.	The secretariat has few working groups.
Fishing footprint defined and fishery closed areas implemented, both within and outside of fishing footprint.	Observer coverage is low or not mandated.
Studies of SAIs have been conducted and monitoring plans are implemented.	Lack of fishery independent surveys.

**In addition to scoring low in criteria symptomatic of higher scoring organizations.*
CCAMLR – Convention for the Conservation of Antarctic Marine Living Resources; CECAF – Fisheries Committee for the Eastern Central Atlantic; GFCM – General Fisheries Commission for the Mediterranean; NAFO – North-west Atlantic Fisheries Organization; NEAFC – North-east Atlantic Fisheries Commission; NPFC – North Pacific Fisheries Commission; SEAFO – South-east Atlantic Fisheries Organisation; SIOFA – South Indian Ocean Fisheries Agreement; SPRFMO – South Pacific Regional Fisheries Management Organisation; WECAFC – Western Central Atlantic Fishery Commission.

Regional Conservation Goals

In terms of the success or failure of wider management objectives, there is concern about the lack of a formalized process for agreeing conservation measures between overlapping or adjacent competent organizations. For example, threshold values for encounter rules are more often than not, just inherited from other, more established RFMOs, rather than being bespoke to their particular area of competence. Inter-RFMO cooperation (e.g., through ensuring that closed area networks are complementary between adjacent organizations) is apparently relatively limited, and likely worse between RFMOs and other competent authorities, such as the International Seabed Authority (Gjerde et al., 2018). Currently, there is no clear resolution in terms of which organization would take primacy in events such as the ISA wishing to license mining activities in areas of the Mid-Atlantic Ridge already designated as fisheries closed areas by NEAFC, and further covered by the mandate of the Oslo-Paris Convention. The lack of a competent organization that is able to mediate or rule upon such conflicts highlights the need for management of ("the BBNJ agreement" – Ardron et al., 2014; Gjerde et al., 2018; Wright et al., 2019), currently under consideration by the UN General Assembly, pursuant to UNGA resolutions 59/25; 66/288; 72/249. Recognizing that "the problems of ocean space are closely interrelated and need to be considered as a whole" (UNCLOS, 1982), and the need for ecosystem approaches to management, places further demand upon fisheries management organizations but, particularly in the cases of CECAF and WECAFC, these demands are often in excess of what a given organization is functionally able to deliver.

Whilst RFMOs have generally been cognizant of each other's activities, there has historically been relatively little imperative to formally cooperate with each other and with other competent authorities, despite the obvious relevance to broader biodiversity agreements (Rice et al., 2014). With regards the ecosystem-based management of VMEs, which RFMOs are already mandated to address (e.g., through UNGA 61/105), the main benefits from a BBNJ agreement would be through the development of regional plans and standardized assessment approaches, and for the harmonization of the wide range of third party agreements (van der Burght et al., 2017). Whilst we have reviewed the performance of each organization individually, the lack of regional management plans means that we cannot comment on how the links between adjacent/overlapping organizations are performing in terms of meeting broader conservation goals.

Some RFMOs have formally adopted agreements or memoranda with international organizations whose remit is focused upon specific taxa, rather than a geographic area (e.g., the North Atlantic Salmon Conservation Organization or the Agreement on the Conservation of Albatrosses and Petrels). In certain cases, these agreements oblige the organization to further develop certain conservation measures, over and above the requirements made by the various UNGA fish stock agreements. However, such arrangements are largely piecemeal, at the discretion of individual commissions, and generally lack the kinds of binding measures that could be championed by the proposed BBNJ authority.

CONCLUSION

The trends and results presented here, whilst limited to relative differences, provide useful comparisons between different regional fishery management organizations, with particular respect to how they have adopted measures to mitigate adverse impacts upon vulnerable ecosystems. Actions between organizations varied widely but so also did their needs. In considering RFMO performance within the context of indicators of management need, we have demonstrated that, most organizations are achieving a similar balance of permitting fishing activities and promoting ecosystem approach considerations.

Younger RFMOs, and RFBs, are naturally those in most need of targeted support, but there is also much room for improvement in cooperation between competent organizations and the development of standardized approaches for assessing and mitigating adverse impacts upon vulnerable marine ecosystems.

Few organizations have assessed levels of fishing intensity that result in SAIs meaning that in most cases, precautionary management still forms the basis of any conservation measures implemented. Precautionary measures however, are not made equal and have varying challenges in their application. Encounter rules for instance are only effective when observer coverage and competence is adequate and when organizations are diligent in reviewing and acting upon encounter reports. In the absence of suitable levels of scrutiny, such management may actually not be considered precautionary and underlines the need for bespoke assessment of adverse impacts in each organization.

DATA AVAILABILITY STATEMENT

All datasets generated for this study are included in the manuscript/**Supplementary Files**.

AUTHOR CONTRIBUTIONS

All authors participated in writing and commenting on all aspects of the manuscript. JB prepared the figures.

FUNDING

This work was supported by EASME, under the European Commission (EC) European Marine and Fisheries Fund (Bell et al., 2019; Framework Contract EASME/EMFF/2016/008), and we gratefully acknowledge the contributions of those involved in the preparation of the original document, upon which the present manuscript is based.

ACKNOWLEDGMENTS

We thank the associate editor and the two reviewers for their valuable contributions. The funding agency gave formal permission for these results to be published but was not involved in the preparation of the present manuscript. The results of this study are the property of the EC, but any opinions expressed in this manuscript are those of the authors, and do not necessarily represent those of the EC.

SUPPLEMENTARY MATERIAL

The Supplementary Material for this article can be found online at: https://www.frontiersin.org/articles/10.3389/fmars.2019.00596/full#supplementary-material

APPENDIX S1 | List of criteria and their scoring methods and classifications.

APPENDIX S2 | 3-D dimension relationship between organizations' CAN scores.

APPENDIX S3 | 3-D relationship between organizations along three most important principal components axes.

APPENDIX S4 | Category scores collated for each organisation.

REFERENCES

Aguilar, R., Perry, A. L., and López, J. (2017). "Conservation and management of vulnerable marine benthic ecosystems," in *Marine Animal Forests*, eds S. Rossi, B. Bramanti, A. Gofi, and C. Orejas (Berlin: Springer).

Ardron, J. A., Clark, M. R., Penney, A. J., Hourigan, T. F., Rowden, A. A., Dunstan, P. K., et al. (2014). A systematic approach towards the identification and protection of vulnerable marine ecosystems. *Mar. Policy* 49, 146–154. doi: 10.1016/j.marpol.2013.11.017

Auster, P. J., Gjerde, K., Heupel, E., Watling, L., Grehan, A., and Rogers, A. D. (2011). Definition and detection of vulnerable marine ecosystems on the high seas: problems with the "move-on" rule. *ICES J. Mar. Sci.* 68, 254–264. doi: 10.1093/icesjms/fsq074

Bell, J. B., Guijarro-García, E., Abellán, L., Carbonell-Quetglas, A., Clark, J., Durán-Muñoz, P., et al. (2019). *Scientific Approaches for the Assessment and Management of Deep-Sea Fisheries and Ecosystems in RFMOs and RFBs. EASME/EMFF/2016/008*. Lowestoft: CEFAS, 171.

Cailliet, G. M., Andrews, A. H., Burton, E. J., Watters, D. L., Kline, D. E., and Ferry-Graham, L. A. (2001). Age determination and validation studies of marine fishes: do deep-dwellers live longer? *Exp. Gerontol.* 36, 739–764. doi: 10.1016/s0531-5565(00)00239-4

Clark, N. A., Ardron, J. A., and Pendleton, L. H. (2015). Evaluatng the basic elements of transparency of regional fisheries management organizations. *Mar. Policy* 57, 158–166. doi: 10.1016/j.marpol.2015.03.003

Cullis-Suzuki, S., and Pauly, D. (2010). Failing the high seas: a global evaluation of regional fisheries management organizations. *Mar. Policy* 34, 1036–1042. doi: 10.1016/j.marpol.2010.03.002

FAO (2009). *International Guidelines for the Management of Deep-sea Fisheries in the High Seas*. Rome: FAO, 73.

Gianni, M., Fuller, S., Currie, D. E. J., Schleit, K., Pike, B., Goldsworthy, L., et al. (2016). *How Much Longer Will it Take? A ten Year Review of the Implementation of United Nations General Assembly Resolition 61/105, 64/72 and66/68 on the Management of bottom fisheries in Areas Beyondnational Jurisdiction*, Vol. 4. Amsterdam: Deep Sea Conservation Coalition.

Gjerde, K., Boteler, B., Durussel, C., Rochette, J., Unger, S., and Wright, G. (2018). *Conservation and Sustainable Use of Marine Biodiversity in Areas Beyond National Jurisdiction: Options for Underpinning a Strong Global BBNJ Agreement through Regional and Sectoral Governance*. Potsdam: IASS Policy Brief.

Kenchington, E., Murillo, F. J., Lirette, C., Sacau, M., Koen-Alonso, M., Kenny, A. J., et al. (2014). Kernel density surface modelling as a means to identify significant concentrations of vulnerable marine ecosystem indicators. *PLoS One* 9:e109365. doi: 10.1371/journal.pone.0109365

Kenny, A. J., Cambell, N., Koen-Alonso, M., Pepin, P., and Diz, D. (2018). Delivering sustainable fisheries through adoption of a risk-based framework as part of an ecosystem approach to fisheries management. *Mar. Policy* 93, 232–240. doi: 10.1016/j.marpol.2017.05.018

Koen-Alonso, M., Pepin, P., Fogarty, M. J., Kenny, A. J., and Kenchington, E. L. R. (2019). The Northwest Atlantic fisheries organisation roadmap for the development and implementation of an ecosystem approach to fisheries: structure, state of development, and challenges. *Mar. Policy* 100, 342–352. doi: 10.1016/j.marpol.2018.11.025

Kroodsma, D. A., Mayorga, J., Hochberg, T., Miller, N. A., Boerder, K., Ferretti, F., et al. (2018). Tracking the global footprint of fisheries. *Science* 359, 904–908. doi: 10.1126/science.aao5646

Mangi, S. C., Kenny, A., Readdy, L., Posen, P., Ribeiro-Santos, A., Neat, F. C., et al. (2016). The economic implications of changing regulations for deep sea fishing under the European common fisheries policy: UK case study. *Sci. Total Environ.* 562, 260–269. doi: 10.1016/j.scitotenv.2016.03.218

Martin-Smith, K. (2009). A risk-management framework for avoiding significant adverse impacts of bottom fishing gear on vulnerable marine ecosystems. *CCAMLR Sci.* 16, 177–193.

Mengerink, K. J., Van Dover, C. L., Ardron, J., Baker, M., Escobar-Briones, E., Gjerde, K., et al. (2014). A call for deep-ocean stewardship. *Science* 344, 696–698. doi: 10.1126/science.1251458

Oksanen, J., Blanchet, F. G., Friendly, M., Kindt, R., Legendre, P., McGlinn, D., et al. (2019). *Package Vegan 2.5-4*, https://cran.r-project.org/web/packages/vegan/vegan.pdf (accessed June 1, 2018).

Penney, A. J., Parker, S. J., and Brown, J. H. (2009). Protection measures implemented by New Zealand for vulnerable marine ecosystems in the South Pacific Ocean. *Mar. Ecol. Prog. Ser.* 397, 341–354. doi: 10.3354/meps08300

Pham, C. K., Vandeperre, F., Menezes, G., Porterio, F., Isidro, E., and Morato, T. (2015). The importance of deep-sea vulnerable marine ecosystems for demersal fish in the Azores. *Deep Sea Res. Part I Oceanogr. Res. Papers* 96, 80–88. doi: 10.1016/j.dsr.2014.11.004

Rice, J., Lee, J., and Tandstad, M. (2014). "Parallel initiatives: CBD's ecologically of biologically significant areas (EBSAs) and FAI's vulnerable marine ecosystems (VMEs) criteria and processes," In *Governance of Marine Fisheries and Biodiversity. Interaction and Coevolution*, S. M. Garcia., J. Rice, and A. Charlies (Hoboken: Wiley).

Rogers, A. D., and Gianni, M. (2010). *The Implementation of UNGA Resolutions 61/105 and 64/72 in the Management of Deep-Sea Fisheries on the High Seas*. Amsterdam: Deep Sea Conservation Coalition.

Ryan, W. B. F., Carbotte, S. M., Coplan, J. O., O'Hara, S., Melkonian, A., Arko, R., et al. (2009). Global multi-resolution topography synthesis. *Geochem. Geophys. Geosyst.* 10, Q03014.

SIOFA Scientific Committee (2018). *Report of the Third Meeting of the Scientific Committee of the Southern Indian Ocean Fisheries Agreement (SIOFA)*. La Réunion: SIOFA

UN General Assembly (2005). *Resolution 59/25: Sustainable Fisheries, Including Through the 1995 Agreement for the Implementation of the Provisions of the United Nationals Convention on the Law of the Sea of 10 December 1982 Relating to the Conservation and Management of Straddling Fish Stocks and Highly Migratory Fish stocks, and Related Instruments*. New York, NY: UN General Assembly.

UN General Assembly (2007). *Resolution 61/105: Sustainable Fisheries, Including Through the 1995 Agreement for the Implementation of the Provisions of the United Nationals Convention on the Law of the Sea of 10 December 1982 relating to the Conservation and Management of Straddling Fish Stocks and Highly Migratory Fish stocks, and Related Instruments*. New York, NY: UN General Assembly.

UN General Assembly (2010). *Resolution 64/72: Sustainable Fisheries, Including Through the 1995 Agreement for the Implementation of the Provisions of the United Nationals Convention on the Law of the Sea of 10 December 1982 relating to the Conservation and Management of Straddling Fish Stocks and Highly Migratory Fish stocks, and Related Instruments*. New York, NY: UN General Assembly.

UN General Assembly (2012). *Resolution 66/288: The future we want*. New York, NY: UN General Assembly.

UN General Assembly (2017). *Resolution 72/249: Intergovernmental Conference on an international legally binding instrument under the United Nations Convention on the Law of the Sea on the conservation and sustainable use of marine biological diversity of areas Beyond National Jurisdiction*. New York, NY: UN General Assembly.

UN Secretary General (2006). *Impacts of fishing on Vulnerable Marine Ecosystems: Actions Taken by States and Regional fisheries Management Organizations and Arrangements to Give Effect to Paragraphs 66 to 69 of General Assembly Resolution 59/25 on Sustainable Fisheries, Regarding the Impacts of Fishing on Vulnerable Marine Ecosystems*. Manhattan, NY: UN Secretary General.

UNCLOS (1982). *United Nations Convention on the Law of the Sea*. Montego Bay: UNCLOS.

van der Burght, N., Dupont, C., Mastor, R., Potestio, S., Smith, N., and Vancauwenbergh, S. (2017). *Research for PECH Committee – Regional Ocean Governance in Europe: The Role of Fisheries*. Brussels: European Parliament, Policy Department for Structural and Cohesion Policies, 1–122.

Wright, G., Ardron, J., Gjerde, K., Currie, D., and Rochette, J. (2015). Advancing marine biodiversity protection through regional fisheries management: a review of bottom fisheries closures in areas beyond national jurisdiction. *Mar. Policy* 61, 134–148. doi: 10.1016/j.marpol.2015.06.030

Wright, G., Gjerde, K., Johnson, D. E., Finkelstein, A., Ferreira, M. A., Dunn, D. C., et al. (2019). Marine spatial planning in areas beyond national jurisdiction. *Mar. Policy.* 832–839. doi: 10.1016/j.marpol.2018.12.003

Conflict of Interest: The authors declare that the research was conducted in the absence of any commercial or financial relationships that could be construed as a potential conflict of interest.

frontiers
in Marine Science

ORIGINAL RESEARCH
published: 14 January 2020
doi: 10.3389/fmars.2019.00791

Population Structure and Genetic Connectivity of Squat Lobsters (*Munida* Leach, 1820) Associated With Vulnerable Marine Ecosystems in the Southwest Pacific Ocean

Ruo-Jin Yan[1]*, Kareen E. Schnabel[2], Ashley A. Rowden[1,2], Xiang-Zhao Guo[1] and Jonathan P. A. Gardner[1]

[1] School of Biological Sciences, Victoria University of Wellington, Wellington, New Zealand, [2] National Institute of Water and Atmospheric Research, Wellington, New Zealand

Edited by:
Les Watling,
University of Hawai'i at Mānoa,
United States

Reviewed by:
Enrique Macpherson,
Spanish National Research Council
(CSIC), Spain
Cheryl L. Morrison,
United States Geological Survey
(USGS), United States

***Correspondence:**
Ruo-Jin Yan
rjyan@suda.edu.cn

Specialty section:
This article was submitted to
Deep-Sea Environments and Ecology,
a section of the journal
Frontiers in Marine Science

Received: *31 May 2019*
Accepted: *09 December 2019*
Published: *14 January 2020*

Citation:
Yan R-J, Schnabel KE, Rowden AA, Guo X-Z and Gardner JPA (2020) Population Structure and Genetic Connectivity of Squat Lobsters (Munida Leach, 1820) Associated With Vulnerable Marine Ecosystems in the Southwest Pacific Ocean. Front. Mar. Sci. 6:791. doi: 10.3389/fmars.2019.00791

Studies of genetic diversity and population genetic structure in deep-sea fauna mainly focus on vulnerable marine ecosystem (VME) indicator taxa, whilst relatively few studies have focussed on VME-associated taxa whose distributions are not exclusively limited to VMEs. Knowledge of genetic connectivity (gene flow) amongst populations of VME-associated taxa, such as squat lobsters, will contribute to ongoing management decision-making related to the protection of VMEs. To better understand the genetic diversity and genetic structure of squat lobster populations (*Munida isos*, *Munida endeavourae* and *Munida gracilis*) at different spatial scales (biogeographic provinces, regions and geomorphic features) in the southwest Pacific Ocean, mitochondrial cytochrome *c* oxidase subunit I (COI) region and nuclear microsatellite markers were employed. Overall, the levels of genetic diversity were high for the COI region and moderate for the microsatellite loci across the three *Munida* species. Analysis of molecular variance (AMOVA) of COI variation revealed no significant genetic differentiation, whereas AMOVA of microsatellite variation revealed significant genetic differentiation amongst the three species, but at different spatial scales. Based on microsatellite variation, a range of analyses [Structure, principal coordinate analysis (PCoA), discriminant analysis of principal components (DAPC)] provided some evidence of limited genetic differentiation at different spatial scales across the three species. Low to moderate levels of assignment success (~40–60%) based on microsatellite variation were achieved for the three *Munida* species, suggesting high levels of gene flow and possible panmixia. Nonetheless, for *M. isos*, populations from the Tasmanian slope were genetically differentiated from all other populations and may act as source populations, whereas populations from the Kermadec Ridge region may be sink populations for all three *Munida* species. Our results highlight the need to consider gene flow at trans-national scales when managing anthropogenic impacts on VMEs. The results are discussed in the context of existing marine protected areas (MPAs), which can contribute new information useful to the management of VMEs within the southwest Pacific Ocean.

Keywords: genetic diversity, genetic connectivity, management, conservation, southwest Pacific Ocean, vulnerable marine ecosystems

INTRODUCTION

The deep sea is the largest ecosystem on earth, encompassing more than 90% of the global ocean area (Ramirez-Llodra et al., 2010; Taylor and Roterman, 2017). It harbours a wide range of marine ecosystem services with unique abiotic and biological characteristics that support a rich diversity of life (Ramirez-Llodra et al., 2010). For several decades, considerable attention has been paid to the ongoing declines in marine biodiversity caused by pressures including environmental change, pollution and human exploitation (Pandolfi et al., 2003; Ramirez-Llodra et al., 2011; Cordes et al., 2016). Consequently, international agreement on the need for marine protected areas (MPAs) has been reached (Food and Agricultural Organisation of the United Nations, 2009) that is widely acknowledged to be an important step to help reduce anthropogenic impacts on biodiversity (Leathwick et al., 2008; Gjerde et al., 2016).

Vulnerable marine ecosystems (VMEs), including seamounts, canyons, hydrothermal vent and cold seep habitats, as well as cold-water coral reefs and sponge beds, are vulnerable to the impact of intense or long-term anthropogenic activities, in particular to bottom trawling (Food and Agricultural Organisation of the United Nations, 2009). There is now increasing awareness that VMEs need protection from anthropogenic activities such as trawling that have been carried out for decades, but also from future activities such as mining which may commence in the near future (e.g. Beger et al., 2014; Boschen et al., 2016; van Dover et al., 2018). MPAs provide a means to restrict damaging human activities and thereby allow for the conservation of critical natural habitats such as VMEs, which can help facilitate the maintenance and restoration of biodiversity and ecosystem structure and function (Agardy, 1994; Clark et al., 2011). Given that population declines can lead to reduced individual fitness, reduced population resilience and possible eventual extinction, an understanding of the population connectivity of VME indicator taxa is useful for informing the design and implementation of MPAs, for assessing the effectiveness of existing MPAs and for improving the management and mitigation of impacts on VMEs (Palumbi, 2003; Miller and Gunasekera, 2017).

The presence of a VME can be indicated by taxa that form a VME, e.g. coral species that form complex reef habitats (refer to Parker et al., 2009 for the South Pacific Ocean and Parker and Bowden, 2010 for the Southern Ocean and Antarctica). Whilst there are numerous studies examining the population structure of VME indicator taxa (e.g. in the southwest Pacific Ocean—Miller et al., 2010, 2011; Herrera et al., 2012; Miller and Gunasekera, 2017; Zeng et al., 2017; Holland et al., 2019; Zeng et al., 2019), relatively few studies have focussed on VME-associated taxa whose distributions are not exclusively limited to VMEs but are often found together with VMEs (e.g. crinoids, brisingid seastars *sensu*; Parker et al., 2009). Squat lobsters are highly diverse anomuran crustaceans that are sometimes, but not always, closely associated with VMEs (e.g. coral thickets and sponge gardens) (Lumsden et al., 2007; Baba et al., 2008; Baeza, 2011). As such, squat lobsters are an abundant and ecologically important group that may provide new insights into the patterns of genetic connectivity amongst VMEs.

Using a range of different genetic markers, previous studies of population genetic structure for deep-sea squat lobsters across all or parts of their ranges have, perhaps not surprisingly, failed to reveal a consistent pattern of results. Whilst several different studies have reported no genetic population differentiation (e.g. Samadi et al., 2006; Haye et al., 2010; Bors et al., 2012; Cabezas et al., 2012; Roterman et al., 2016; Wang et al., 2016), others have reported evidence of limited to moderate genetic differences amongst populations (e.g. Pérez-Barros et al., 2014; Yang et al., 2016) and still others have reported no population genetic differentiation based on one marker type but population genetic differentiation based on a different marker type (e.g. Thaler et al., 2014). As VME-associated taxa, knowledge of connectivity amongst deep-sea squat lobster populations can be used to contribute to ongoing management decision-making about protection by assessing the effectiveness of existing MPAs and informing the placement of new MPAs. However, in the absence of consistent patterns of population genetic differentiation amongst squat lobster species reported in the literature, it is clear that new and region-specific assessments of genetic connectivity need to be carried out.

In the present study, the population genetic variation of three locally abundant *Munida* species [*Munida isos* (Ahyong and Poore, 2004), *Munida endeavourae* (Ahyong and Poore, 2004) and *Munida gracilis* (Henderson, 1885)] from the southwest Pacific Ocean region are investigated to better understand genetic diversity and genetic connectivity amongst VMEs. *M. isos* and *M. endeavourae* are widespread around New Zealand and south-eastern Australia where they occur from the edge of the continental shelves (∼400 m) to bathyal depths of 1800–2700 m, respectively. *M. gracilis* is a widespread New Zealand endemic species with a slightly shallower depth distribution of about 100–1200 m (Baba et al., 2008; Schnabel, unpublished). *Munida* species have free-swimming planktonic larval phases that may drift with ocean currents, but the larval dispersal strategies of these species are unknown in detail. However, it is presumed that they have similar development to other munidids which include between four and six planktotrophic zoeal larval stages and 15–83 days of larval development (Baba et al., 2011), which in turn suggests that larval dispersal over distances of 10s, if not 100s of km is likely. *Munida* species are associated with VMEs rather than being a functional component of VMEs as are many habitat-forming corals and sponges (Zeng et al., 2017, 2019). Squat lobsters therefore are a good choice of group to help investigate patterns of gene flow and population genetic differentiation amongst VMEs, and provide a valuable contrast to the more widely studied VME-forming groups. In conjunction, information about genetic connectivity and barriers to gene flow that may result in geographic genetic differentiation and/or genetic hotspots can be used in the planning of the placement and size of new MPAs (e.g. Miller et al., 2010, 2011; Bors et al., 2012; Miller and Gunasekera, 2017; Zeng et al., 2017, 2019; Holland et al., 2019). Based on the presumptive dispersal strategies and the known habitat preferences of these species, it is hypothesised that *M. isos* and *M. endeavourae*, which are typically found on physically isolated seamounts, will exhibit population genetic heterogeneity within the study area. In contrast, it is hypothesised that *M. gracilis*, which is also found on soft sediments that are generally contiguous over large areas of the deep sea, allowing greater physical movement of adults and larvae, will exhibit higher levels of population genetic homogeneity. If the connectivity of species inhabiting only seamounts differs from the connectivity of species inhabiting seamounts and non-seamount habitats, then this has implications for spatial management measures of these species across their respective ranges. We used a spatially explicit hierarchical framework to test these hypotheses, and to explore the drivers of the observed genetic connectivity patterns, to provide information that will contribute to the management of VMEs within the southwest Pacific Ocean.

MATERIALS AND METHODS

Sample Collection and DNA Extraction

Specimens were obtained from the National Institute of Water and Atmospheric (NIWA) Research Invertebrate Collection (Wellington, New Zealand) and Museum Victoria (Melbourne, Australia). These were archived individuals collected mainly by scientific expeditions in the southwest Pacific Ocean since the 2000s. Most specimens were collected within the New Zealand's Exclusive Economic Zone (EEZ), with additional samples from the south Tasman Sea within the Australian EEZ, and from the Louisville Seamount Chain, an Area Beyond National Jurisdiction, to the northeast of New Zealand's EEZ (**Figure 1**). All specimens were preserved in > 80% ethanol after collection. The majority of specimens of *M. isos* and *M. endeavourae* were from seamount habitats, whilst the majority of specimens of *M. gracilis* were from soft sediment habitats at relatively shallower depths. Sample availability depends on collection activity at any given site with the result that our site-specific sample sizes are highly variable, but not low given these constraints. Sample details are summarised in **Table 1**; full details are presented in **Supplementary Tables S1–S3**.

Abdominal muscle or pereopod tissue samples were collected and stored individually in 95% ethanol before being transferred to the laboratory, for further analysis. Whole genomic DNA was extracted using the DNeasy Blood and Tissue kit (Qiagen, Hilden, Germany) following the manufacturer's instructions. DNA integrity and molecular weight were assessed using electrophoresis in 3% agarose gels and with a NanoPhotometer (Implen, Munich, Germany). Samples exhibiting poor quality DNA were discarded.

Squat lobster samples had previously been identified using the methods and keys described in Ahyong and Poore (2004) and Baba (2005). Species identification was further confirmed by genetic screening with GenBank accession numbers MF457406 (*M. isos*) and KJ544249 (*M. gracilis*) using the mitochondrial universal DNA barcoding primers LCO1490/HCO2198 (Folmer et al., 1994).

Data Testing Framework

For *M. isos*, for which there were large samples sizes and good spatial coverage, a spatially explicit hierarchical testing framework was employed to evaluate genetic differentiation amongst populations. This approach follows Zeng et al. (2017, 2019) and Holland et al. (2019).

First, samples of *M. isos* were assigned to the two deep, bathyal (800–3500 m), ocean floor biogeographic provinces of Watling et al. (2013); BY6, referred to here as the Northern province, and BY10 or the Southern province, with a boundary between them at approximately 45°S (**Figure 1**). The differential water mass characteristics (e.g. salinity, temperature and particulate organic carbon flux) of the two provinces may affect the Northern–Southern population distribution, resulting in a province-scale pattern of genetic differentiation across the study area.

Second, samples were assigned to three regions; North (north of Chatham Rise), Central (Chatham Rise) and South (south of Chatham Rise) regions (**Figure 1**). Subtropical Water (STW) that reaches New Zealand region via the East Australian Current and the South Pacific subtropical gyre, and Subantarctic Water (SAW) that is driven north by Ekman transport and westerly winds, meet along the Chatham Rise forming the Subtropical Front (Chiswell et al., 2015). This front may act as a barrier to pelagic larval dispersal, leading to a North–Central–South region scale pattern of genetic subdivision of populations, and a high level of genetic diversity may be expected in the Central region on the Chatham Rise where North–South population mixing may occur.

Third, samples were assigned to populations according to major geomorphic features of the seafloor in the study area: Kermadec Ridge, Louisville Seamount Chain, Hikurangi Margin, Chatham Rise, Macquarie Ridge and Tasmanian slope (**Figure 1**). Given the species-specific distribution and habitat requirement, the distinctive topographic and local hydrodynamic characteristics may act as barriers to gene flow (Rowden et al., 2010a,b; Zeng et al., 2017). Samples from Bollons Seamount were included in the province and region spatial scale analyses, but not in geomorphic feature scale analyses, due to the limited sample size.

For *M. endeavourae* and *M. gracilis*, due to patchy sampling site coverage, samples were only assigned to populations according to major geomorphic features for the assessment of genetic connectivity. For *M. endeavourae*, populations were included from the Kermadec Ridge, Louisville Seamount Chain and the Tasmanian slope. For *M. gracilis*, populations included those from the Kermadec Ridge, Chatham Rise and Challenger Plateau (**Figure 1**).

COI Sequencing and Data Analyses

The mitochondrial DNA protein encoding cytochrome *c* oxidase subunit I (COI) region was amplified for the three *Munida* species using universal invertebrate primers LCO1490 and HCO2198 (Folmer et al., 1994), yielding fragments of 649 bp in length. Reactions were performed in a 20 μL total volume containing approximately 1 μL of genomic DNA (∼30 ng/μL), 10 μL MyTaq Red Mix (Total Lab Systems Ltd., Auckland, New Zealand), 1 μL of both primers (forward and reverse) at a concentration

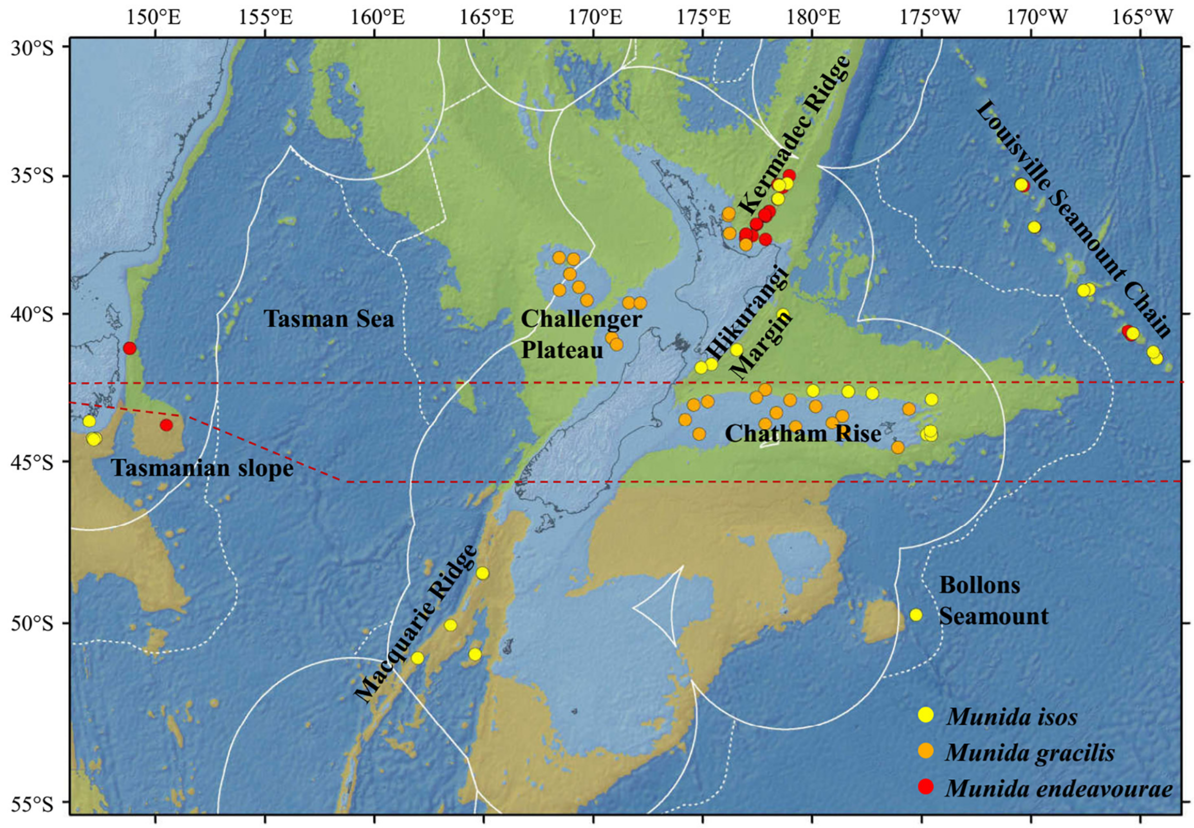

FIGURE 1 | Map showing the locations of the samples for the study species. For *Munida isos*, hierarchical testing framework was employed: (1) green (northern) and khaki (southern) backgrounds indicate the two biogeographic lower bathyal provinces (BY6 and BY10) of Watling et al. (2013) in the New Zealand region; (2) red dashed lines at 42°S and approximately 45°S represent the boundaries between the North (< 42°S), Central (42°S to 45°S) and South (>45°S) regions; (3) major geomorphic features are named on the map.

of 10 μM and with the addition of 7 μL ddH_2O. PCR amplifications for COI sequencing were carried out in a 96-well PCR Thermal Cycler (Applied Biosystems) programmed as follows: denaturation at 95°C for 5 min, followed by 40 cycles of denaturation at 95°C for 30 s, 48°C for 30 s, extension at 72°C for 45 s and a final extension at 72°C for 10 min. PCR products were visualised on a 1.5% agarose gel and then sequenced on an ABI 3730xl DNA analyser. Despite multiple attempts, some COI fragments could not be amplified for several samples. Sequences have been deposited in GenBank (MK155662–MK156049).

Cytochrome *c* oxidase subunit I sequences (forward strand only) were aligned in MEGA v7 (Kumar et al., 2016) following manual checking and editing using DNAStar software (Burland, 2000). Species-specific genetic diversity statistics including number of haplotypes (h), average number of nucleotide differences (K), number of segregating sites (S), haplotype diversity (H_d) and nucleotide diversity (π) were calculated using DNASP v6.11.01 (Rozas et al., 2017) and Arlequin v.3.5 (Excoffier and Lischer, 2010).

To assess hierarchical population genetic differentiation amongst squat lobster populations, the uncorrected p distances within/between regions were calculated in MEGA v7 (Kumar et al., 2016). Arlequin v.3.5 (Excoffier and Lischer, 2010) was used to perform a spatially explicit analysis of molecular variance (AMOVA) and to compute pairwise Φ_{ST} values. All groupings were evaluated with 10,000 permutations. Haplotype networks were constructed using a median-joining method in Popart (Leigh and Bryant, 2015). For each species, a maximum likelihood (ML) tree was drawn under the best-fit evolutionary model with the lowest Bayesian information criterion (BIC) score and 500 bootstraps in MEGA v7 (Kumar et al., 2016). Two species, *Munida thoe* (AY351013) and a yeti crab, *Kiwa tyleri* (KP763652), were designated as outgroups, the former being congeneric and the latter a more distantly related squat lobster. Nodes with bootstrap values > 90% were included on the final ML trees.

All analyses described above were carried out at three spatial scales (Northern–Southern provinces, North–Central–South regions and geomorphic features) for *M. isos*, and at the geomorphic level only for *M. endeavourae* and *M. gracilis*.

Microsatellite Genotyping and Data Analyses

From the 20 microsatellite markers described in Yan et al. (2019), 17, 11 and 9 microsatellite primer pairs were assayed for variation

TABLE 1 | Summary of sample sizes (*N*, number of specimens) for *Munida isos* at three spatial scales, and for *M. endeavourae* and *M. gracilis* at the geomorphic feature scale.

	Spatial class	Code	COI	Microsatellite
Munida isos	Northern province	Northern	214	219
	Southern province	Southern	134	136
	Total (provinces)		**348**	**355**
	North region	North	106	109
	Central region	Central	108	110
	South region	South	134	136
	Total (regions)		**348**	**355**
	Kermadec Ridge	KR	13	13
	Louisville Seamount Chain	LS	82	85
	Hikurangi Margin	HM	11	11
	Chatham Rise	CR	108	110
	Macquarie Ridge	MR	59	60
	Tasmanian slope	TA	72	73
	Total (geomorphic features)		**345**	**352**
M. endeavourae	Kermadec Ridge	KR	38	42
	Louisville Seamount Chain	LS	28	28
	Tasmanian slope	TS	23	26
	Total (geomorphic features)		**89**	**96**
M. gracilis	Kermadec Ridge	KR	19	20
	Chatham Rise	CR	154	155
	Challenger Plateau	CP	159	164
	Total (geomorphic features)		**332**	**339**

for *M. isos*, *M. endeavourae* and *M. gracilis*, respectively, based on their scoring reliability (**Supplementary Table S4**). Locus-specific PCR amplification conditions followed Yan et al. (2019). PCR products were run alongside a LIZ500 internal size standard on an ABI 3730xl DNA analyser (Sangon Inc., Shanghai, China). Alleles were scored automatically and reviewed manually using PeakScanner v2.0 (Applied Biosystems).

The genotype data were initially assessed in Lositan (Antao et al., 2008) for the neutrality test in an island model under the infinite alleles model (IAM) with 50,000 simulations. Microchecker v2.2.3 (van Oosterhout et al., 2004) was subsequently employed to detect the presence of null alleles, large allele dropout and scoring errors caused by stuttering, as well as to calculate null allele frequency (*r*) using the Brookfield (1996) method for each locus.

To quantify population genetic diversity, summary statistics including the actual number of alleles (N_A), effective number of alleles (N_E), observed (H_O) and expected (H_E) heterozygosity, polymorphism information content (*PIC*) values, allelic richness (A_R), number of private alleles (N_{AP}) and inbreeding coefficient (F_{IS}) were calculated for each locus using GenAlEx v6.5 (Peakall and Smouse, 2012), Cervus v3.03 (Kalinowski et al., 2007) and Fstat v2.9.3.2 (Goudet, 2002). Exact tests of deviation from Hardy–Weinberg equilibrium (HWE) (Guo and Thompson, 1992) for each locus × population combination and tests for genotypic linkage disequilibrium (LD) between pairs of loci were performed in Arlequin v3.5 (Excoffier and Lischer, 2010) and Genepop v4.2 (Raymond and Rousset, 1995; Rousset, 2008). Significance levels ($p < 0.05$) for multiple pair-wise tests were adjusted using the false discovery rate (FDR) correction (Benjamini and Hochberg, 1995).

To quantify population genetic differentiation, Nei's genetic distance (D_A) (Nei et al., 1983) and pairwise F_{ST} values were computed using Populations v1.2.31[1] and Arlequin v.3.5 (Excoffier and Lischer, 2010). The latter was used to perform spatially explicit AMOVA, with all groupings tested with 10,000 permutations, for the different spatial scales.

General relationships amongst individuals were depicted through a principal coordinate analysis (PCoA) on the basis of a covariance pairwise genetic distance matrix in GenAlEx v6.5 (Peakall and Smouse, 2012). Discriminant analysis of principal components (DAPC) (Jombart et al., 2010) was applied to test for genetic structure amongst populations with the 'adegenet' package v2.0.1 (Jombart and Ahmed, 2011) in the program R v3.4.1 (R Development Core Team, 2017). For *M. isos*, DAPC was conducted at region and population scales but not at the province level due to the limited number of groups. To determine the best *K*, denoting the most likely number of putative genetic clusters, a Bayesian clustering approach was implemented in Structure v2.3.4 (Pritchard et al., 2000) using an admixture ancestry model with corrected initial ALPHA values (~1/*K*), uncorrelated allele frequencies and prior location information (Hubisz et al., 2009; Wang, 2017). Preliminary testing revealed that choice of model made no substantive difference to analysis outcomes. Each Markov chain Monte Carlo (MCMC) simulation was run for 500,000 iterations, with an initial burn-in period of

---

[1] http://bioinformatics.org/~tryphon/populations/

50,000 iterations. Fifty independent runs were performed for each cluster set. The ΔK metric (Evanno et al., 2005) was employed to calculate the best K (average number of nucleotide differences) in Structure Harvester[2]. Post-processing of Structure results was carried out using CLUMPAK (Kopelman et al., 2015). A second clustering approach was carried out in BAPS v6 (Corander et al., 2008) as a complement to the Structure analyses. Calculations were performed under the mixture model, with the maximum number of populations set as the number of regions, i.e. six, three and three for *M. isos*, *M. endeavourae* and *M. gracilis*, respectively.

Individual assignment tests and first generation migrant detection with 'L_home' likelihood computation were implemented in GeneClass v2 (Piry et al., 2004). The contemporary migration rates amongst populations were calculated in BayesAss v3 (Wilson and Rannala, 2003), which can produce accurate estimates of migration and self-replenishment when F_{ST} is ≥ 0.05 (Faubet et al., 2007). Calculation parameters were set as follows: 10,000,000 iterations, of which 3,000,000 were burn-in; sampling frequency 1000; migration rates, allele frequencies and inbreeding coefficients set at 1, 1 and 1, respectively, to make the acceptance rates between 20 and 60%.

All analyses described above were carried out at three spatial scales (Northern–Southern provinces, North–Central–South regions and geomorphic features) for *M. isos*, and at geomorphic feature level for *M. endeavourae* and *M. gracilis*.

RESULTS

Population Genetic Structure Based on COI Region

Genetic Diversity

Haplotypic diversity was very high across populations for all provinces, regions and geomorphic features of the three *Munida* species. For *M. isos*, 111 haplotypes, based on a 649-bp fragment of the gene, were obtained from 348 individuals at both the province and region spatial scales. The haplotype diversity and nucleotide diversity values of populations were slightly greater in populations of the Northern province than in the Southern province, and both estimates in the North region were greater than the other two regions (detailed results are reported in **Supplementary Table S5**). At the geomorphic feature scale, a total of 110, 67 and 200 COI haplotypes were obtained from 345, 89 and 332 individuals of *M. isos*, *M. endeavourae* and *M. gracilis*, respectively. Notably, the mean population haplotype diversity and nucleotide diversity values for *M. isos* (0.764; 0.26%) were lower than for *M. endeavourae* (0.980; 0.59%) and *M. gracilis* (0.973; 0.56%), respectively.

Genetic Differentiation

As revealed by uncorrected p distances and Φ_{ST} values, genetic differentiation amongst populations of provinces, regions and geomorphic features was low in the three *Munida* species (uncorrected p distances in the range of 0.002–0.006; Φ_{ST} values in the range of 0.000–0.035). Specifically, all of the uncorrected p distances were relatively low, but within the Decapoda intraspecific barcode threshold (0.285–1.375%) (da Silva et al., 2011). Significance ($p < 0.05$) was detected for three Φ_{ST} values, all from population pairs at geographical feature scale of *M. isos*, yet none was observed amongst regions or province population pairs of *M. isos*, nor population pairs of geomorphic features for *M. endeavourae* or *M. gracilis* (**Supplementary Table S6**). This lack of differentiation was supported AMOVA results, with no significant genetic differentiation observed for all Φ-statistic values and over 99% of the variance being attributed to differences within populations (**Supplementary Table S7**).

The median-joining networks, representing the most parsimonious relationship amongst haplotypes, were plotted for the three *Munida* species. For *M. isos*, a starburst-like pattern was observed from the 111 haplotypes, but no pattern of genetic structure was detected in populations at either the province (**Supplementary Figure S1**) or region scales (**Supplementary Figure S2**). At the geomorphic feature scale, haplotypes from both *M. isos* and *M. endeavourae* populations exhibited a starburst-like pattern, consistent with the mutational evolution of new haplotypes over time (**Figure 2**). However, the number of equally parsimonious haplotype connections was too great in *M. gracilis* for the most likely network to be determined. Similarly, there was no evidence of a pattern of genetic structure amongst populations of the three *Munida* species across their distributional ranges (**Supplementary Figure S3**). The ML phylogenetic trees were similar for the three *Munida* species, with all haplotypes occurring in a major non-differentiated cluster with strong support, and clearly differentiated from the two outgroup taxa (**Supplementary Figure S4**). These analyses indicate that there is no clear evidence of genetic subdivision amongst populations at the geomorphic feature, region or province scale for the three *Munida* species.

Population Genetic Structure Based on Microsatellite Variation

Genetic Diversity

For all three species Lositan analyses indicated that no microsatellite locus was likely to be experiencing selection. Null alleles ($r > 0.2$) were detected at loci MI_06 (*M. isos*) and MI_02 (*M. gracilis*), but not observed at these loci in the two other species. Evidence of homozygote excess and stuttering was observed, but these were randomly distributed across loci in the three *Munida* species. No large allele dropout was indicated at any locus.

In total, 167, 63 and 74 alleles with size ranges of 78–134, 83–172and 82–200 bp were amplified at 17, 11 and nine microsatellite loci in *M. isos*, *M. endeavourae* and *M. gracilis*, respectively. In general, allelic variation (e.g. H_E and *PIC*) was only moderately high. Four loci (MI_21, MI_29, MI_39 and MI_40) in *M. isos*, three (MI_06, MI_10 and MI_39) in *M. endeavourae* and one (MI_14) in *M. gracilis* exhibited a relatively low level of polymorphism compared to other loci (details are summarised in **Supplementary Table S8**). The *M. isos* of the Northern province exhibited a higher level of genetic diversity than those of the Southern province. The average number of effective alleles

---

[2] http://taylor0.biology.ucla.edu/structureHarvester/

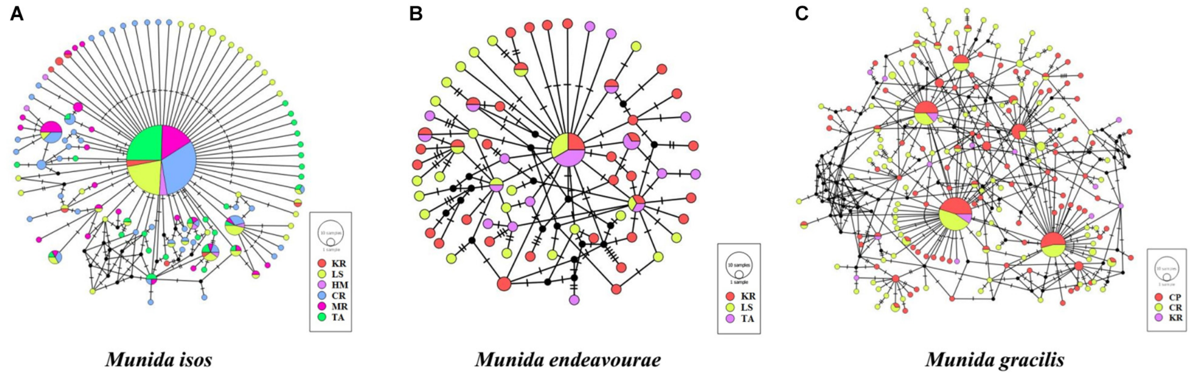

FIGURE 2 | Median-joining network of COI haplotypes of **(A)** *Munida isos*, **(B)** *M. endeavourae* and **(C)** *M. gracilis* for geomorphic features. Coloured circles represent haplotypes and circle sizes are proportional to the number of individuals. Black circles represent hypothesised (not observed) haplotypes that are intermediate between observed haplotypes. Lines denote base pair changes.

and expected heterozygosity were greatest in populations of the Central region, but the largest number of private alleles was found in the South region. At the geomorphic feature level, the observed and expected heterozygosities in the populations were reasonably consistent in all features for the three species (detailed results are reported in **Supplementary Table S5**). At the geomorphic feature scale, populations of *M. isos* and *M. gracilis* exhibited moderate levels of genetic diversity whilst *M. endeavourae* showed slightly lower genetic diversity. Private alleles were identified in nearly all populations of geomorphic features across the three *Munida* species, with the highest numbers being observed for the Chatham Rise (*M. isos* and *M. gracilis*) and Kermadec Ridge (*M. endeavourae*) populations, whilst none were detected for the Kermadec Ridge population of *M. gracilis*. Average F_{IS} values were positive across populations of geomorphic features, with the only exception being the population of *M. endeavourae* from the Tasmanian slope, which exhibited a deficit of heterozygotes.

For *M. isos*, after FDR correction for multiple comparisons, 28 (82.35%) and 37 (72.55%) tests were significantly different from HWE ($p < 0.05$) at pairwise combinations of loci × populations at the province and region spatial scales, respectively. For geomorphic features, 38 (37.25%), 5 (15.15%) and 14 (51.85%) tests were significantly different from HWE ($p < 0.05$) in *M. isos*, *M. endeavourae* and *M. gracilis*, respectively, with the majority exhibiting heterozygote deficiencies. In particular, loci MI_25 and MI_02 demonstrated significant departures from HWE within all populations at the geomorphic feature scale of *M. isos* and *M. gracilis*, respectively.

For *M. isos*, only four of 136 locus-pairs showed significant LD after FDR correction ($p < 0.05$). No evidence of LD was found in *M. endeavourae* and *M. gracilis*.

Genetic Differentiation

Genetic population differentiation was low for the three species, as revealed by Nei's genetic distance (D_A) and F_{ST} values (D_A in the range of 0.015–0.107; F_{ST} in the range of 0.001–0.051). For *M. isos*, F_{ST} values amongst populations of the two provinces and three regions remained low but significant ($p < 0.05$). For *M. isos* at the geomorphic feature scale, only the pairwise comparison between populations of the Hikurangi Margin and Tasmanian slope (F_{ST} = 0.051) exhibited a moderate level of differentiation (**Supplementary Table S6**). For population pairs of the other two species, significant difference from zero ($p < 0.05$) was detected for thirteen F_{ST} values after correction, of which 11 and two were from *M. isos* and *M. endeavourae*, respectively.

Analysis of molecular variance revealed significant genetic differentiation at different spatial levels: within all samples of *M. isos* and *M. gracilis*; amongst the populations of the two provinces, three regions, and six geomorphic features for *M. isos* and amongst populations of the three geomorphic features for *M. endeavourae* and *M. gracilis* (**Supplementary Table S7**). Nonetheless, AMOVA partitioned more than 96% of the genetic variation within samples for the three *Munida* species, leaving less than 4% variance attributable to the differences amongst populations and amongst populations within groups.

Genetic Structure

Principal coordinate analysis, with relatively low cumulative variation represented by the first two factors, revealed no evidence of genetic differentiation across populations of provinces or regions for *M. isos*, and amongst populations of geomorphic features for the three *Munida* species (**Supplementary Figures S5**, **S6**), whilst Structure showed the highest support for two clusters ($\Delta K = 2$) for all datasets. However, given that the ΔK approach is unable to detect the best K when $K = 1$, post-processing of Structure bar plots was conducted in CLUMPAK. As a result, $K = 1$ and $K = 2$ could not be successfully differentiated between for *M. isos* (10/10; 10/10) at three spatial scales (provinces, regions and geomorphic features) and *M. gracilis* (10/10; 10/10) at geomorphic feature level, whereas $K = 2$ (5/10) was rejected in favour of $K = 1$ for *M. endeavourae* (**Figures 3**, **4**). For *M. isos*, when $K = 2$, individuals from the Southern province and the South region were mostly assigned to the blue cluster based on provinces and region scales. At the geomorphic feature scale, the majority of individuals from the Hikurangi Margin, Macquarie Ridge and Tasmanian slope populations were assigned to the blue cluster, whilst populations from other features showed a more complex genetic structure

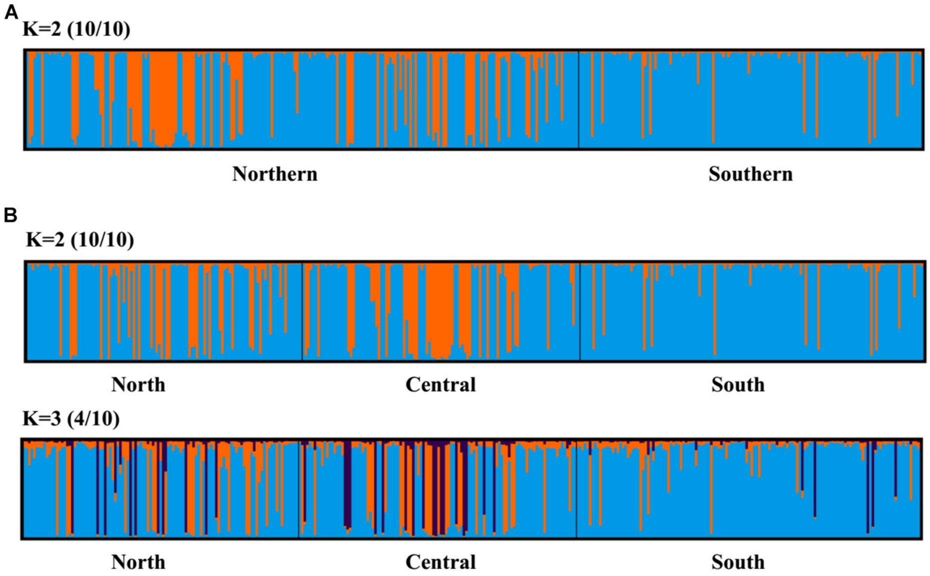

FIGURE 3 | Structure cluster analyses of *Munida isos* based on spatial differentiation of **(A)** two provinces and **(B)** three regions as revealed by microsatellite variation.

with a shared membership of both the blue and orange clusters. This finding was supported by the fact that 10 out of 11 significant pairwise F_{ST} values were detected in populations from these three geomorphic features (Hikurangi Margin, Macquarie Ridge and Tasmanian slope). For *M. endeavourae*, no pattern was revealed, with all individuals assigned equally to both clusters, indicating no structure. For *M. gracilis*, individuals from populations of all three geomorphic features were randomly assigned to two clusters, echoing the AMOVA results as major variance was attributed to the differences within geomorphic features. In the BAPS analyses, the inferred number of populations was one ($K = 1$) for all datasets of three *Munida* species, indicating no genetic structure.

Results from DAPC, an analysis that can maximise genetic variation amongst groups whilst minimising separation within groups, indicated three genetic clusters corresponding to the three regions as defined by the first two principal components (PCs) for *M. isos* (**Figure 5**). At the geomorphic feature level, two, three and three major genetic clusters were calculated for *M. isos*, *M. endeavourae* and *M. gracilis*, respectively (**Figure 6**). For *M. isos*, PC1 separated the Tasmanian slope population from the populations of all other geomorphic features. The major cluster was further divided by PC2 into individuals from populations of the Kermadec Ridge and Louisville Seamount Chain, Chatham Rise and Macquarie Ridge and the Hikurangi Margin, which was congruent with the F_{ST} and Structure results. For *M. endeavourae* and *M. gracilis*, three distinct clusters corresponding to the populations from the three geomorphic features were revealed, with clusters overlapping to different degrees for the two species.

Gene Flow and Connectivity

Assignment-based tests performed in GeneClass had a low to moderate level of classification success. For *M. isos*, 231 (65.1%) and 179 (50.4%) individuals were correctly assigned to their province and region populations, respectively. At the geomorphic feature level, a total of 143 (40.6%), 53 (55.2%) and 156 (40.0%) individuals were correctly assigned to their own geomorphic feature populations for *M. isos*, *M. endeavourae* and *M. gracilis*, respectively. The 'L_home' statistics demonstrated some evidence of first-generation migrants amongst sampled province/region/geomorphic feature populations. In total, 19, two and eight individuals were below the threshold of the assignment tests (α = 0.01) for *M. isos*, *M. endeavourae* and *M. gracilis*, respectively, increasing the possibility that these individuals may be first generation immigrants that have been introduced from an unknown source.

For *M. isos*, BayesAss analyses were unable to reach the standard of 20–60% in the province and region spatial scale datasets: only results for geomorphic features are presented. At the geomorphic feature level, estimates of contemporary migrants between populations were low, and the proportions of self-recruitment were high to very high (**Table 2**). For *M. isos*, the Macquarie Ridge (81.22%) and Tasmanian slope (96.43%) populations exhibited evidence of genetic isolation with high proportions of contribution from within each population (self-recruitment). Similar patterns were observed for individuals from the Louisville Seamount Chain for *M. endeavourae* (95.47%) and from the Challenger Plateau for *M. gracilis* (88.26%). Notably, the Kermadec Ridge region was identified as a sink population (only receiving migrants from other populations) for all *Munida* species. For *M. isos*, the Tasmanian slope population was identified as a source population (providing migrants to other populations while receiving no or few migrants). This was incongruent with findings from *M. endeavourae*, for which the Tasmanian slope population (68.01%) acted as a sink population, receiving migrants (30.27%) from the Louisville Seamount

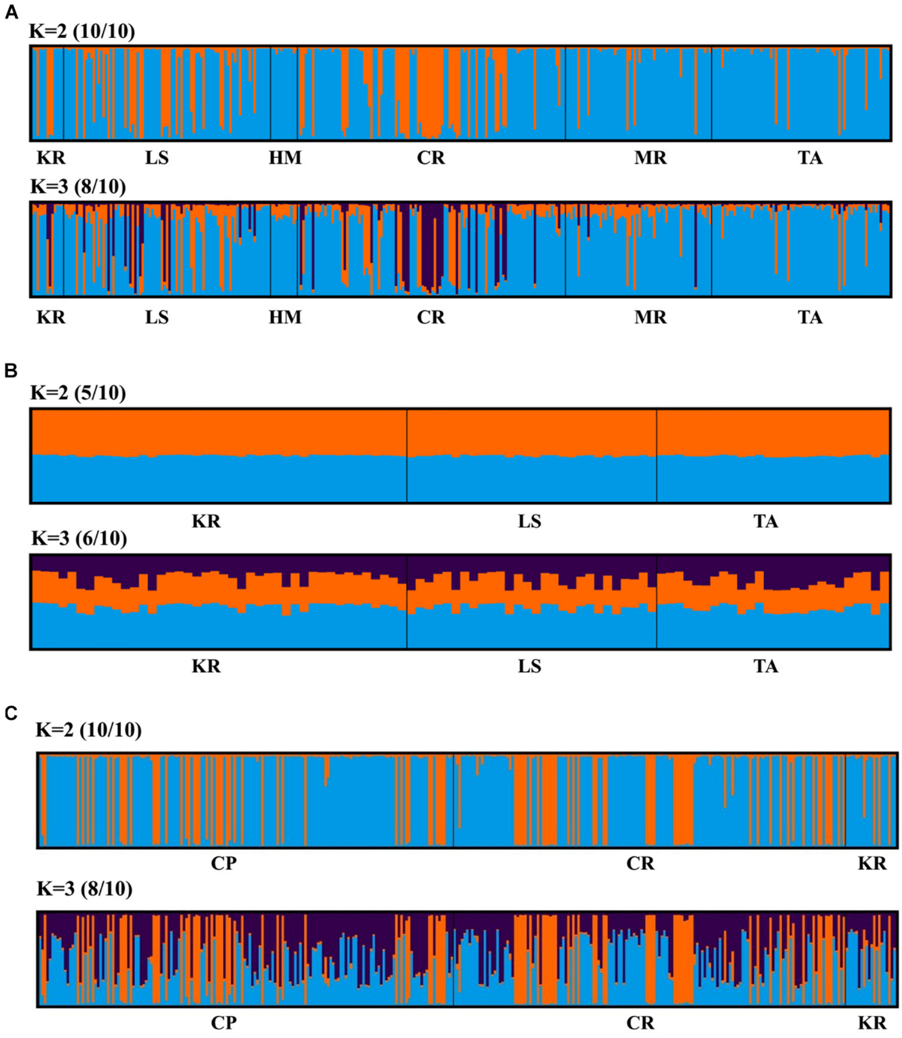

FIGURE 4 | Structure cluster analyses of **(A)** *Munida isos*, **(B)** *M. endeavourae* and **(C)** *M. gracilis* based on microsatellite variation among populations on geomorphic features.

Chain population. For *M. gracilis*, populations from both the Chatham Rise and Challenger Plateau were both source and sink populations.

DISCUSSION

Three munidid squat lobsters, *M. isos*, *M. endeavourae* and *M. gracilis*, have been tested for levels of genetic diversity and patterns of genetic connectivity in the southwest Pacific Ocean based on mitochondrial COI region and nuclear microsatellite variation. Overall, the level of genetic diversity was high as revealed by the COI region, and moderate as revealed by microsatellite markers, across all three *Munida* species. There was no evidence of genetic subdivision amongst populations of the three *Munida* species based on the COI sequence data, and only limited genetic differentiation was observed in *M. isos* and *M. gracilis* based on microsatellite variation (none was detected for *M. endeavourae* using microsatellites). These results provide new insights into the genetic connectivity of VME-associated taxa in the southwest Pacific Ocean.

Genetic Diversity

Genetic diversity of the three *Munida* species was randomly distributed across the study area, as indicated by both the COI region and microsatellite markers. The mitochondrial COI region, in particular, exhibited a high level of genetic diversity for haplotypes across the three *Munida* species. Notably, within the genus *Munida*, high levels of polymorphisms in COI can be indicative of a relatively fast mutation rate, or because population sizes are large, or because the taxa have an ancient origin, allowing for mutations to accumulate over time (Coykendall et al., 2017). The observation of high haplotype diversity was consistent with findings from other deep-sea squat lobsters, such as the chirostyloid *K. tyleri* (Roterman et al., 2016) and the munidid *Pleuroncodes monodon* (Haye et al., 2010). Nonetheless, *M. isos*

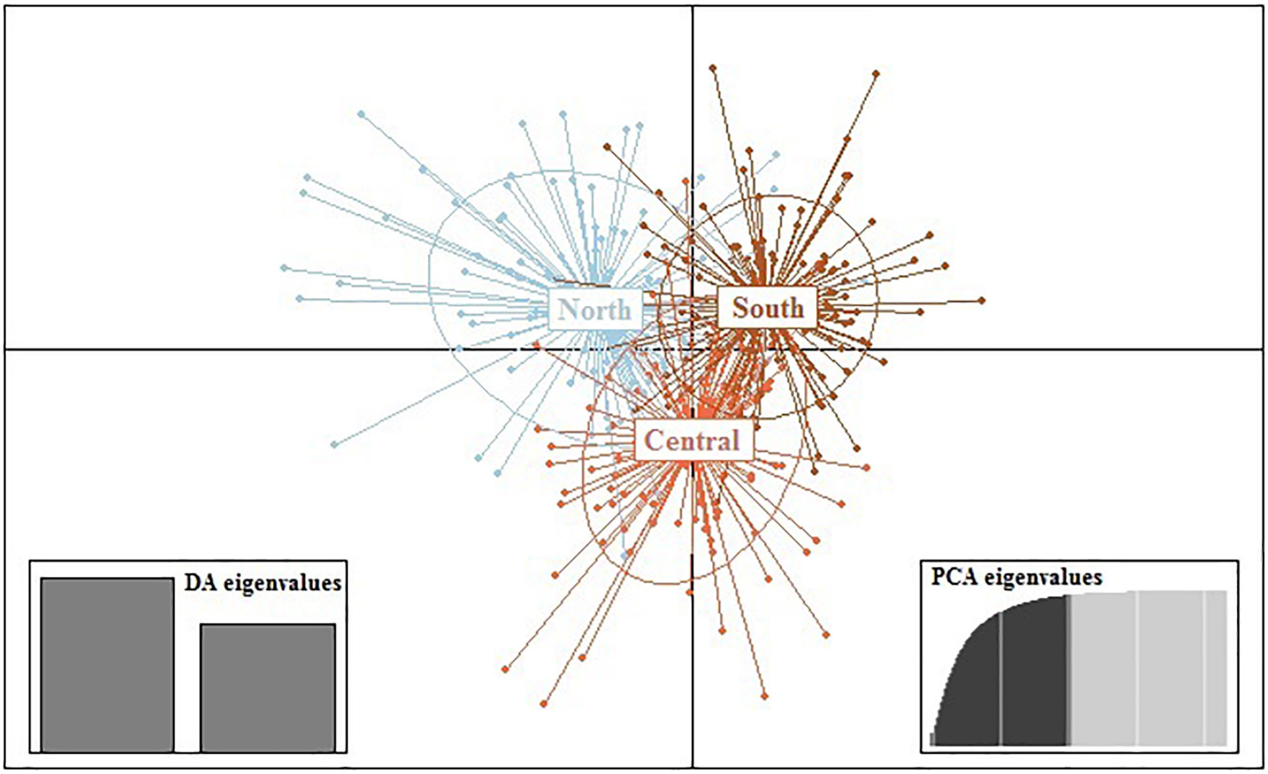

FIGURE 5 | Scatterplot generated by the discriminant analysis of principal components (DAPC) of *Munida isos* based on three regions as revealed by microsatellite variation.

exhibited lower genetic diversity compared to *M. endeavourae* and *M. gracilis*, as revealed by other genetic diversity estimates based on COI region, whilst *M. endeavourae* showed the lowest genetic diversity on the basis of microsatellite markers with respect to expected heterozygosity and effective number of alleles that could reflect genetic drift (Hedrick, 1999). Given that sample size is uneven when comparing populations of *M. isos* and *M. gracilis*, allelic richness, which is independent on sample size, is included as an index to evaluate the level of genetic diversity for the newly developed microsatellite markers. Consequently, these microsatellite markers performed reasonably well, exhibited a moderate level of genetic diversity and provided valuable genetic information for the three *Munida* species.

Significant deviations from HWE were observed in the three *Munida* species, which is common in squat lobster species (Molecular Ecology Resources Primer Development Consortium et al., 2010; Boyle et al., 2013; Nakajima et al., 2018). Deviations from HWE may be attributed to causes such as null alleles and the Wahlund effect (Johnson and Black, 1984). The presence of null alleles may result in mistyping of homozygotes and heterozygotes, leading to an over-estimation of genetic differentiation (DeWoody et al., 2006). However, null alleles are commonly observed in a variety of marine invertebrate species (e.g. Dailianis et al., 2011; Thaler et al., 2014; Roterman et al., 2016) and in population genetic studies null allele frequencies below 0.2 are commonly accepted when using microsatellite markers (Dakin and Avise, 2004). In this study, although low-to-moderate frequencies of null alleles were detected at a number of loci across the three *Munida* species, only two loci exhibited null allele frequencies above 0.2. Given that little genetic differentiation was observed amongst populations of *M. isos* and *M. gracilis*, the null alleles at these two loci were not expected to influence the overall interpretation of the results. The Wahlund effect is caused by individuals from different localities that are characterised by different genotype proportions, being mixed during sampling or during data analysis, resulting in excess homozygosity and significant F_{IS} estimates (Freeland, 2005; Waples, 2014). The highly significant deficit of heterozygote genotypes, as revealed by positive inbreeding coefficients, was obtained across all populations in the three *Munida* species with only one exception (i.e. the Tasmanian slope population of *M. endeavourae*), indicating the presence of inbreeding. Moreover, HWE deviations occurred in the form of homozygote excesses, which might also result from small sample size (e.g. populations from Kermadec Ridge and Hikurangi Margin in *M. isos*), given the potential for extensive gene flow amongst populations and population demographic history (e.g. expansions or selective sweeps). However, small sample size and limited spatial scale sampling are unavoidable constraints in population genetic studies of deep-sea organisms (Baco et al., 2016). For microsatellite-based population genetic

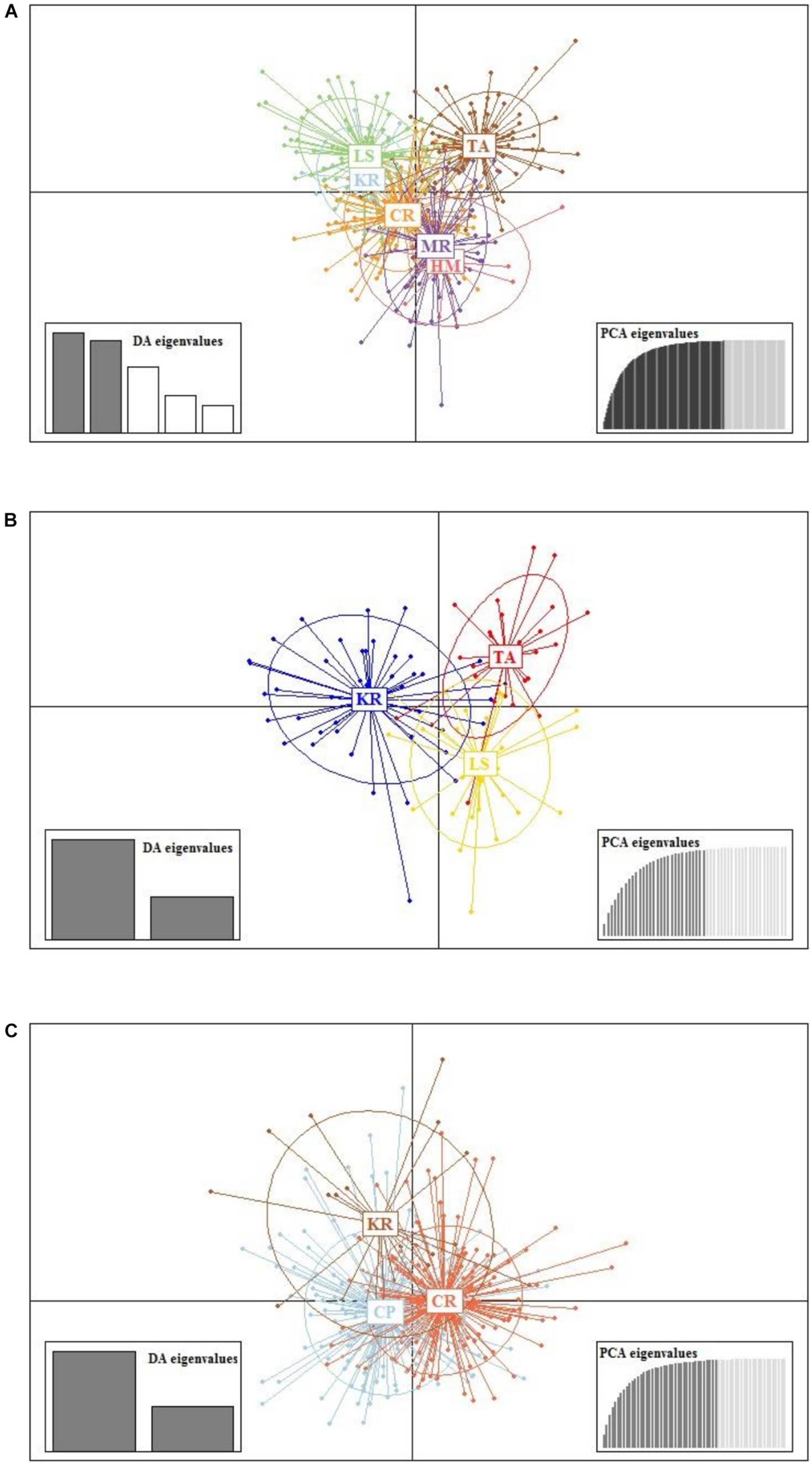

FIGURE 6 | Scatterplot generated by the discriminant analysis of principal components (DAPC) of **(A)** *Munida isos*, **(B)** *M. endeavourae* and **(C)** *M. gracilis* based on microsatellite variation among populations of geomorphic features.

TABLE 2 | Estimated migration rates from source populations (top) to recipient populations (side) for three *Munida* species based on microsatellite variation.

	Code	Source					
Munida isos		KR	LS	HM	CR	MR	TA
	KR	**68.41%**	6.59%				16.35%
	LS		**72.23%**				20.31%
	HM			**68.59%**		19.99%	5.02%
	CR				**78.74%**	6.22%	14.02%
	MR					**81.22%**	14.87%
	TA						**96.43%**
M. endeavourae		KR	LS	TA			
	KR	**79.65%**	19.45%				
	LS		**95.47%**				
	TA		30.27%	**68.01%**			
M. gracilis		KR	CR	CP			
	KR	**68.13%**	17.86%	14.00%			
	CR		**76.81%**	22.98%			
	CP		11.54%	**88.26%**			

Empty cells denote migration rates <0.05, estimates of self-recruitment in bold (on the diagonal).

studies, 25–30 individuals per population is considered sufficient to provide accurate estimations of genetic diversity and gene flow (Hale et al., 2012), and the majority of the populations tested in the three *Munida* species meet this criterion.

Genetic Differentiation and Connectivity

Genetic differentiation at different spatial scales was evaluated based on mitochondrial COI region and nuclear microsatellite marker variation in the three *Munida* species. Levels of site-specific genetic diversity are a function, at least in part, of sample size and we recognise that our sample sizes are very variable amongst our sites. This variability reflects the differential availability of archived material in the museum collections, which is itself a function of the very different sampling efforts that our sites have been subject to over the last several decades and is a known and appreciated constraint for deep-sea population genetics research (e.g. Boschen et al., 2015; Baco et al., 2016; Zeng et al., 2017, 2019). For the COI region, according to the Decapoda intraspecific barcode threshold (0.285–1.375%) (da Silva et al., 2011), the maximum pairwise uncorrected *p* distances amongst the three *Munida* populations did not suggest the presence of cryptic species. These results support previous findings for *M. gracilis* in the New Zealand region (0–1.9%) (Bors et al., 2012) and align with observations in other squat lobsters, including *Fennerogalathea chacei* (0.13–0.61%) (Rodríguez-Flores et al., 2017). Despite the large geographic coverage of sampling sites, low and statistically non-significant global Φ_{ST} values were observed for the three *Munida* species, suggesting genetic similarity in the squat lobster populations across the southwest Pacific Ocean. In contrast, microsatellite markers revealed some limited evidence of genetic differentiation amongst populations of *M. isos* and *M. gracilis*, but not *M. endeavourae*. Although nuclear microsatellite markers showed signs of low levels of genetic differentiation for the three *Munida* species, more than 96% of the variance was attributed to differences within populations, again suggesting high levels of gene flow amongst populations leading to panmixia. Collectively, little genetic differentiation was observed amongst populations of three *Munida* species in the southwest Pacific Ocean, either from seamounts or soft sediments. Therefore, the hypothesis that *M. isos* and *M. endeavourae* (typically found on isolated seamounts) exhibit population genetic differentiation was rejected, whilst the hypothesis that gene flow amongst populations of *M. gracilis,* (typically found on soft sediments) results in high levels of population genetic homogeneity was accepted. The absence of genetic structure is usually interpreted as being consistent with either panmixia or recent demographic expansion following a genetic bottleneck event can leave little or no signature in the genome. Additionally, a recent colonisation from another area of the species' distribution is possible, although we see no evidence of this. This lack of population genetic differentiation has been observed in a number of squat lobster species (e.g. Samadi et al., 2006; Haye et al., 2010; Bors et al., 2012; Cabezas et al., 2012; Wang et al., 2016), including for *M. gracilis* in the New Zealand region (Bors et al., 2012). Similarly, no significant population genetic structure was observed across the same province, region and geomorphic feature scales for a deep-sea sponge species in the study area (Zeng et al., 2019). However, this pattern of genetic similarity is not consistent across all deep-sea marine species, including corals and sponges (e.g. Miller et al., 2011; Herrera et al., 2012; Miller and Gunasekera, 2017). For example, within the Southwest Pacific region, a North–Central–South region pattern of structure has been detected in a cup coral based on ITS sequence variation (Miller et al., 2010), province-scale differentiation has been reported in branching stony corals using a combination of D-loop, ITS and microsatellite markers (Zeng et al., 2017), and genetic differentiation has been detected in a deep-sea sponge species based on province, region and geomorphic feature spatial scales as revealed by COI, Cytb and microsatellite variation (Zeng et al., 2019).

Based on mitochondrial COI sequence data, an overall lack of population genetic structure was detected for the three *Munida* species accordingly to ML tree and median-joining network. Similar haplotype networks have been reported for other squat lobster taxa, such as *K. tyleri* (Roterman et al., 2016), *Munida intermedia* (García-Merchán et al., 2012), *M. gracilis* (Bors et al., 2012), *Munida gregaria* (Pérez-Barros et al., 2014) and *P. monodon* (Haye et al., 2010). For nuclear microsatellite data, given that the differentiation amongst populations was weak for the three *Munida* species, it was difficult to infer population genetic structure. The Bayesian clustering software programmes Structure and BAPS can both perform reasonably well at low levels of genetic differentiation and are able to correctly identify the maximum (upper limit) number of genetically distinct groups (Latch et al., 2006). In this study, considering the low F_{ST} values for all three *Munida* species, Structure and BAPS were employed to calculate the best *K* (average number of nucleotide differences). Little or no structure was found for the three *Munida* species when using both approaches. Nonetheless, populations from the Tasmanian slope are potentially genetically differentiated, but not isolated, from the other *M. isos* populations as revealed by results from the F_{ST}, Structure and DAPC analyses. Considering the difficulty in detecting any structure, we refrain from speculating why *M. isos* populations are potentially more structured compared to those of the other two *Munida* species.

The three *Munida* species exhibited low to moderate levels of assignment success, indicative of panmixia across the study area, and which is most probably driven by high levels of gene flow in the region. Interestingly, estimations of migration rate were not always consistent for populations from the Tasmanian slope, which acted as a source population for *M. isos* and as a sink population for *M. endeavourae*. Moreover, populations from the Kermadec Ridge acted as sink populations in the three *Munida* species, which was inconsistent with a previous study of two stony corals where the Kermadec Ridge is a migrant source (Zeng et al., 2017). Given the fact that BayesAss can only produce accurate estimates of migration and self-replenishment when F_{ST} is ≥ 0.05 (Faubet et al., 2007), all estimates of migration rates as revealed by BayesAss should be cautiously interpreted and are best viewed in combination with other analyses.

Overall, we have evidence of moderate to high levels of gene flow, of low levels of genetic differentiation and of low levels of assignment success, all of which point to population genetic homogeneity or perhaps even panmixia at large spatial scales. But we also have evidence of limited differentiation of the Tasmanian slope populations from all other populations to the east, in the New Zealand EEZ and beyond (i.e. the Louisville Seamount Chain) based on F_{ST} values and the DAPC plots. We interpret these results as indicating that the Tasmanian slope populations are differentiated to a small extent, perhaps at the limits of detection by some of the analyses, from all other populations. Our data suggest that there is likely to be asymmetrical gene flow from the Tasmanian slope populations to the east (i.e. the Tasmanian slope populations are source populations), and this is supported by, and consistent with, the regional physical oceanography. For example, the major surface current circulation, the STW and SAW, both flow eastwards (from Australia towards New Zealand) before meeting and mixing along the Chatham Rise to the east of New Zealand (Chiswell et al., 2015). Our data point to gene flow from the Australian EEZ to the New Zealand EEZ, but not vice versa, a finding that is consistent with results for other species such as shallow water rock lobsters and the intertidal black nerite that have a long pelagic larval duration (e.g. Chiswell et al., 2003; Bruce et al., 2007; Morgan et al., 2013; Gardner et al., submitted).

Larval dispersal is crucial for connectivity and colonisation through migration in deep-sea environments. Specific larval development characteristics are unknown for *M. isos*, *M. endeavourae* and *M. gracilis* but based on egg size, a 'regular' (not abbreviated) planktotrophic larva is inferred as in other *Munida* species (Baba et al., 2011), The only complete larval development study was conducted for a congeneric species, *M. gregaria*, with a PLD that may reach 83 days at a rearing temperature of 8°C in the laboratory (Pérez-Barros et al., 2007). The potentially long PLD of the three *Munida* species that lasts for perhaps several months is but one of various possible explanations for the panmixia observed in the study region. The larval lifespans may be extended by low temperature-induced metabolic rate reduction in a low-temperature environment, lessening the impact of dispersal strategy on patterns of genetic differentiation (Roterman et al., 2016). In addition, the density of seamounts, as potential stepping stones, may be higher than is presently thought, facilitating dispersal, and deep water currents may act as a driving force for the enhancement of connectivity as well (Handayani et al., 2014). Interestingly, the estimates of genetic homogeneity in marine organisms are often found to be inconsistent with expectations from inferred PLD, which may be due to oversimplification of PLD estimation (Weersing and Toonen, 2009; Selkoe and Toonen, 2011; Faurby and Barber, 2012). Developmental biology studies of the three *Munida* species in the future should test the potential relationship between PLD and connectivity in squat lobster populations across their distributional range. Understanding this relationship will help inform the construction of biophysical models that are also used to inform the design of MPA networks (Hilário et al., 2015).

Implications for Conservation and Management

In recent years, VMEs have suffered severe damage from anthropogenic activities at a regional or local scale, as well as from physical environmental changes such as increasing ocean temperature and acidification (Thresher et al., 2015; Gollner et al., 2017). To date, some efforts have been made to lessen human impacts on the VMEs by establishing MPAs that provide a means to restrict human activity for a conservation purpose to protect critical natural habitats, which can help facilitate the protection and restoration of biodiversity and ecosystem function of VMEs (Agardy, 1994; Clark et al., 2011). An understanding of spatially explicit genetic diversity as well as patterns of connectivity within and amongst populations of deep-sea organisms that characterise or are associated with VMEs, is fundamental to inform the management of impacts on VMEs, through assessing the effectiveness of current MPAs and informing the design of the spatial arrangement of new MPAs (Palumbi, 2003; Coleman et al., 2011; Pujolar et al., 2013; Santini et al., 2016).

In 2001, New Zealand implemented a seamount management strategy, with 17 areas (containing 19 seamounts) within New Zealand's EEZ closed to all bottom trawling in order to protect the benthic habitat and communities on seamounts, including VMEs (Brodie and Clark, 2003). Following these seamount closures, in 2007 the New Zealand Government closed 17 benthic protected areas (BPAs) within the EEZ to dredging and bottom trawling (and prohibiting mid-water trawling within 50 m of the seafloor) to protect benthic biodiversity, including VMEs (Helson et al., 2010). As a consequence, 32% of New Zealand's seafloor is now protected from dredging and bottom trawling (but no other form of anthropogenic disturbance), a total area which comprises roughly four times the landmass of New Zealand (**Figure 7**). In 2007, the United Nations General Assembly Resolution 61/105 on sustainable fisheries (United Nations General Assembly, 2007) appealed to States and regional fisheries management organisations to protect VMEs from significant adverse impacts caused by destructive fishing activities in international waters. Consequently, in the South Pacific Ocean, interim measures to protect VMEs have been adopted by the South Pacific Regional Fisheries Management Organization (SPRFMO). These measures include 20 min longitude × 20 min latitude areas closed to bottom trawling, as well as areas open to trawling, some of which include the provision of a 'move-on rule' to avoid damage to VMEs (Penney et al., 2009). To date, the suitability and effectiveness of the BPAs and seamount closures within New Zealand's EEZ, and the SPRFMO interim measures, have been assessed using cost-benefit analyses (Leathwick et al., 2008; Penney and Guinotte, 2013), as well as some limited evaluation using genetic tools and connectivity patterns (e.g. Boschen et al., 2016; Holland et al., 2019).

A key finding of this study is that the relatively high levels of genetic connectivity and the low levels of genetic differentiation reported amongst geographically isolated populations of *Munida* spp. suggests that any damage to a localised site squat lobster population (e.g. natural disturbance such as slumps or man-made disturbance such as fishing or mining) may be counteracted by the high levels of larval connectivity from other sites. Whilst this appears to be true for *Munida* spp. that are associated with the VMEs, the same cannot be said of VME habitat-forming taxa such as corals and sponges (Zeng et al., 2017, 2019).

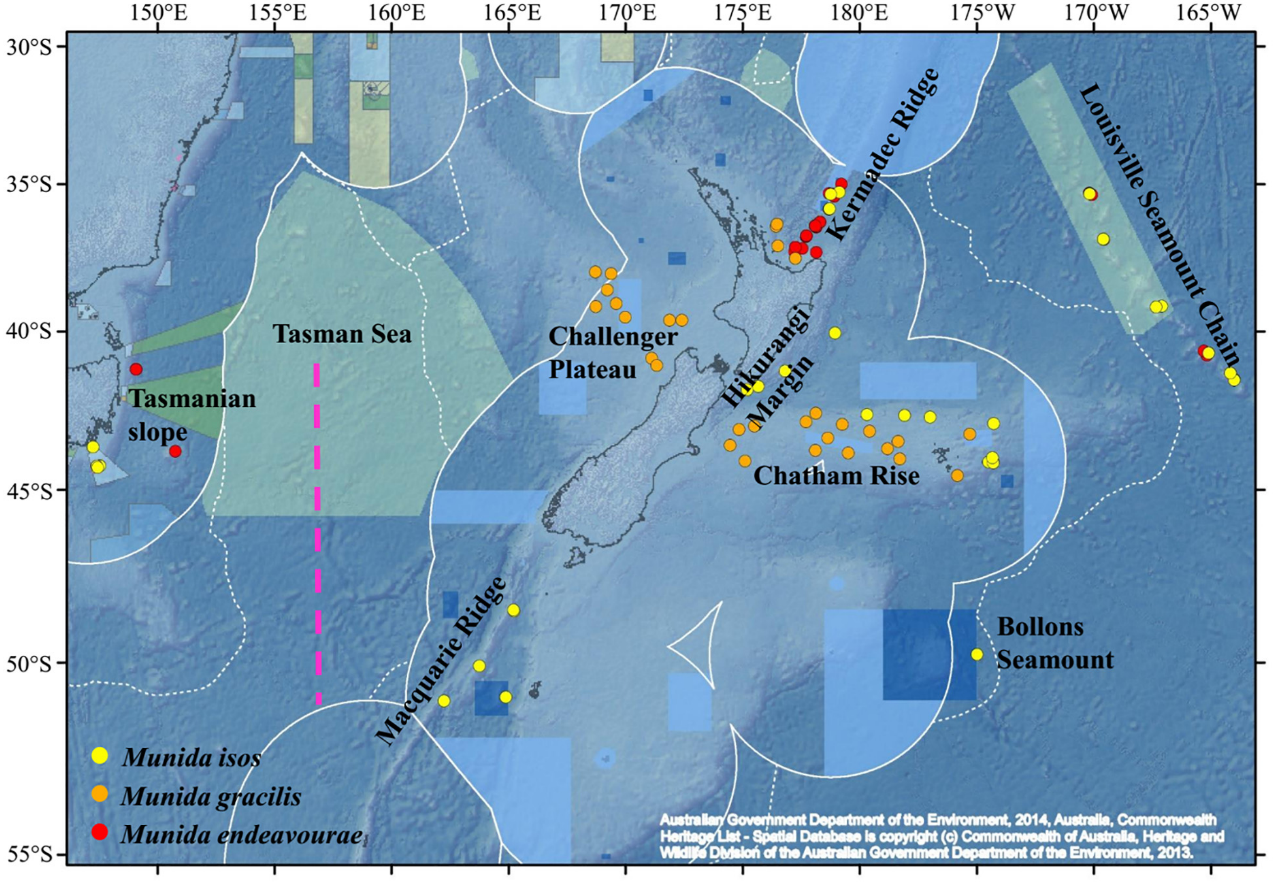

FIGURE 7 | Map showing the distribution of marine protected areas (shaded), major geomorphic features and locations of the samples in the southwest Pacific Ocean region. White solid lines indicate the boundary of economic exclusive zone. White dashed lines represent the boundary of Extended Continental Shelf. Pink dashed line is marked as the potential genetic barrier.

Squat lobster populations on the Tasmanian slope are located in the 9991 km^2 Huon Commonwealth Marine Reserve (part of the Southeast Commonwealth Marine Reserve Network) within the Australian EEZ. Three of the sample sites are within the Habitat Protection Zone (IUCN IV), with mining prohibition and commercial fishing needing to be authorised, whilst the fourth site for this population is situated in the Huon-Multiple Use Zone (IUCN VI), where activities such as mining and fishing can occur if authorised (Iftekhar et al., 2014). Thus, the conservation of populations of a VME-associated taxon on the Tasmanian slope is managed. Moreover, the population of *M. isos* in the Huon Marine Park is a potential source population for populations within New Zealand's EEZ, and therefore its protection is helpful for the conservation of the genetic diversity of this species in the New Zealand region.

Squat lobsters from within New Zealand's EEZ and beyond (i.e. at the Louisville Seamount Chain) exhibited high levels of gene flow across New Zealand's EEZ and beyond. Thus, it is essential to have MPAs distributed throughout these regions to reflect and to protect this wide-ranging genetic connectivity. Significantly, it is necessary to separately protect VMEs on the Louisville Seamount Chain, because the impacts of bottom trawling on VMEs in the SPRFMO Convention Area are managed separately from the management of similar impacts in New Zealand's EEZ. Furthermore, the currently closed areas on the Louisville Seamount Chain are part of a broader protection measure that not only distributes VME protection elsewhere in the SPRFMO Convention Area, but also includes limits on VME indicator taxa bycatch (including VME habitat associated taxa).

Ongoing monitoring of genetic diversity and patterns of connectivity within and amongst populations of deep-sea fauna before and after bottom trawling will allow researchers to evaluate the impact of anthropogenic activity on population differentiation and connectivity, and will provide valuable information to inform best practices in management and conservation. Collectively, the results of this study illustrate the importance of considering the international cross-boundary implications of conservation measures when trying to design effective MPA networks (e.g. Miller et al., 2018; van Dover et al., 2018).

DATA AVAILABILITY STATEMENT

The datasets for this study can be found in the NCBI GenBank (https://www.ncbi.nlm.nih.gov/nucleotide/).

AUTHOR CONTRIBUTIONS

AR and JG designed the research project. KS and AR contributed to the collection of the analysed samples. KS and R-JY provided the identifications of the squat lobster species. R-JY and X-ZG conducted the laboratory and statistical analyses. The first draft of the manuscript was written by R-JY. R-JY, KS, AR, and JG contributed to the reworking and editing of the draft manuscript towards the submitted version.

FUNDING

This work was supported by funding from Victoria University of Wellington to JG (SB80802), National Institute of Water and Atmospheric to Richard Wysoczanski [Crustacea as indicators of marine environmental change (CAIME)] and Sadie Mills (New Zealand Ministry for Business, Innovation and Employment core funding to NIWA under Coasts and Oceans Research Programme). Sample collections were supported by funding from the former New Zealand Foundation for Research, Science and Technology, former New Zealand Ministry of Fisheries, Land Information New Zealand, Department of Conservation (New Zealand), GNS Science (New Zealand), Auckland University and Woods Hole Oceanographic Institute (United States).

ACKNOWLEDGMENTS

Squat lobster specimens were supplied for genetic work by the National Institute of Water and Atmospheric (NIWA) Invertebrate Collection, Wellington, New Zealand, and Museum Victoria, Melbourne, Australia. Particular special thanks to Ms. Sadie Mills and Ms. Diana Macpherson of the NIWA Invertebrate Collection and Dr. Anna McCallum of the Museum Victoria, for their diligent assistance with loans.

SUPPLEMENTARY MATERIAL

The Supplementary Material for this article can be found online at: https://www.frontiersin.org/articles/10.3389/fmars.2019.00791/full#supplementary-material

REFERENCES

Agardy, M. T. (1994). Advances in marine conservation: the role of marine protected areas. *Trends Ecol. Evol.* 9, 267–270. doi: 10.1016/0169-5347(94)90297-6

Ahyong, S. T., and Poore, G. C. (2004). Deep-water Galatheidae (Crustacea: Decapoda: Anomura) from southern and eastern Australia. *Zootaxa* 472, 3–76. doi: 10.11646/zootaxa.472.1.1

Antao, T., Lopes, A., Lopes, R. J., Beja-Pereira, A., and Luikart, G. (2008). LOSITAN: a workbench to detect molecular adaptation based on a F_{ST}-outlier method. *BMC Bioinformatics* 9:323. doi: 10.1186/1471-2105-9-323

Baba, K. (2005). Deep-sea chirostylid and galatheid crustaceans (Decapoda: Anomura) from the Indo-Pacific, with a list of species. *Galathea Rep.* 20, 1–317.

Baba, K., Fujita, Y., Wehrtmann, I. S., and Scholtz, G. (2011). "Developmental biology of squat lobsters," in *The Biology of Squat Lobsters*, eds G. C. B. Poore, S. T. Ahyong, and J. Taylor, (Melbourne: CSIRO Publishing), 105–148.

Baba, K., Macpherson, E., Poore, G. C., Ahyong, S. T., Bermudez, A., Cabezas, P., et al. (2008). *Catalogue of Squat Lobsters of the World (Crustacea: Decapoda: Anomura—Families Chirostylidae, Galatheidae and Kiwaidae)*. Auckland: Magnolia Press.

Baco, A. R., Etter, R. J., Ribeiro, P. A., von der Heyden, S., Beerli, P., and Kinlan, B. P. (2016). A synthesis of genetic connectivity in deep-sea fauna and implications for marine reserve design. *Mol. Ecol.* 25, 3276–3298. doi: 10.1111/mec.13689

Baeza, J. A. (2011). "Squat lobsters as symbionts and in chemo-autotrophic environments," in *The Biology of Squat Lobsters*, eds G. C. B. Poore, S. T. Ahyong, and J. Taylor, (Melbourne: CSIRO Publishing), 249–270.

Beger, M., Selkoe, K. A., Treml, E., Barber, P. H., Von Der Heyden, S., Crandall, E. D., et al. (2014). Evolving coral reef conservation with genetic information. *Bull. Mar. Sci.* 90, 159–185. doi: 10.5343/bms.2012.1106

Benjamini, Y., and Hochberg, Y. (1995). Controlling the false discovery rate: a practical and powerful approach to multiple testing. *J. R. Stat. Soc. Ser. B Methodol.* 57, 289–300. doi: 10.1111/j.2517-6161.1995.tb02031.x

Bors, E. K., Rowden, A. A., Maas, E. W., Clark, M. R., and Shank, T. M. (2012). Patterns of deep-sea genetic connectivity in the New Zealand region: implications for management of benthic ecosystems. *PLoS One* 7:e49474. doi: 10.1371/journal.pone.0049474

Boschen, R. E., Collins, P. C., Tunnicliffe, V., Carlsson, J., Gardner, J. P. A., Lowe, J., et al. (2016). A primer for use of genetic tools in selecting and testing the suitability of set-aside sites protected from deep-sea seafloor massive sulfide mining activities. *Ocean Coast. Manag.* 122, 37–48. doi: 10.1016/j.ocecoaman.2016.01.007

Boschen, R. E., Rowden, A. A., Clark, M. R., and Gardner, J. P. A. (2015). Limitations in the use of archived vent mussel samples to assess genetic connectivity among seafloor massive sulfide deposits: a case study with implications for environmental management. *Front. Mar. Sci.* 2:105. doi: 10.3389/fmars.2015.00105

Boyle, E. A., Thaler, A. D., Jacobson, A., Plouviez, S., and Van Dover, C. L. (2013). Characterization of 10 polymorphic microsatellite loci in *Munidopsis lauensis*, a squat-lobster from the southwestern Pacific. *Conserv. Genet. Resour.* 5, 647–649. doi: 10.1007/s12686-013-9872-1

Brodie, S., and Clark, M. R. (2003). "The New Zealand seamount management strategy–steps towards conserving offshore marine habitat," in *Aquatic Protected Areas: what Works Best and How Do We Know? Proceedings of the World Congress on Aquatic Protected Areas, Cairns, Australia, August 2002*, eds J. P. Beumer, A. Grant, and D. C. Smith, (Cairns: Australian Society of Fish Biology), 664–673.

Brookfield, J. F. Y. (1996). A simple new method for estimating null allele frequency from heterozygote deficiency. *Mol. Ecol.* 5, 453–455. doi: 10.1046/j.1365-294X.1996.00098.x

Bruce, B. D., Griffin, D. A., and Bradford, R. W. (2007). *Larval Transport and Recruitment Processes of Southern Rock Lobster*. Hobart: CSIRO Marine and Atmospheric Research.

Burland, T. G. (2000). "DNASTAR's Lasergene sequence analysis software," in *Bioinformatics Methods and Protocols*, eds S. Misener, and S. A. Krawetz, (Totowa, NJ: Humana Press), 71–91. doi: 10.1385/1-59259-192-2:71

Cabezas, P., Alda, F., Macpherson, E., and Machordom, A. (2012). Genetic characterization of the endangered and endemic anchialine squat lobster *Munidopsis polymorpha* from Lanzarote (Canary Islands): management implications. *ICES J. Mar. Sci.* 69, 1030–1037. doi: 10.1093/icesjms/fss062

Chiswell, S. M., Bostock, H. C., Sutton, P. J. H., and Williams, M. J. M. (2015). Physical oceanography of the deep seas around New Zealand: a review. *N. Z. J. Mar. Freshwater Res.* 49, 286–317. doi: 10.1080/00288330.2014.992918

Chiswell, S. M., Wilkin, J., Booth, J. D., and Stanton, B. (2003). Trans-Tasman Sea larval transport: is Australia a source for New Zealand rock lobsters? *Mar. Ecol. Prog. Ser.* 247, 173–182. doi: 10.3354/meps247173

Clark, M. R., Watling, L., Rowden, A. A., Guinotte, J. M., and Smith, C. R. (2011). A global seamount classification to aid the scientific design of marine protected area networks. *Ocean Coast. Manag.* 54, 19–36. doi: 10.1016/j.ocecoaman.2010.10.006

Coleman, M. A., Chambers, J., Knott, N. A., Malcolm, H. A., Harasti, D., Jordan, A., et al. (2011). Connectivity within and among a network of temperate marine reserves. *PLoS One* 6:e20168. doi: 10.1371/journal.pone.0020168

Corander, J., Marttinen, P., Sirén, J., and Tang, J. (2008). Enhanced bayesian modelling in BAPS software for learning genetic structures of populations. *BMC Bioinformatics* 9:539. doi: 10.1186/1471-2105-9-539

Cordes, E. E., Jones, D. O., Schlacher, T. A., Amon, D. J., Bernardino, A. F., Brooke, S., et al. (2016). Environmental impacts of the deep-water oil and gas industry: a review to guide management strategies. *Front. Environ. Sci.* 4:58. doi: 10.3389/fenvs.2016.00058

Coykendall, D. K., Nizinski, M. S., and Morrison, C. L. (2017). A phylogenetic perspective on diversity of Galatheoidea (*Munida*, *Munidopsis*) from cold-water coral and cold seep communities in the western North Atlantic Ocean. *Deep Sea Res. Part II Top. Stud. Oceanogr.* 137, 258–272. doi: 10.1016/j.dsr2.2016.08.014

da Silva, J. M., Creer, S., dos Santos, A., Costa, A. C., Cunha, M. R., Costa, F. O., et al. (2011). Systematic and evolutionary insights derived from mtDNA COI barcode diversity in the Decapoda (Crustacea: Malacostraca). *PLoS One* 6:e19449. doi: 10.1371/journal.pone.0019449

Dailianis, T., Tsigenopoulos, C. S., Dounas, C., and Voultsiadou, E. (2011). Genetic diversity of the imperilled bath sponge *Spongia officinalis* Linnaeus, 1759 across the Mediterranean Sea: patterns of population differentiation and implications for taxonomy and conservation. *Mol. Ecol.* 20, 3757–3772. doi: 10.1111/j.1365-294X.2011.05222.x

Dakin, E. E., and Avise, J. C. (2004). Microsatellite null alleles in parentage analysis. *Heredity* 93, 504–509. doi: 10.1038/sj.hdy.6800545

DeWoody, J., Nason, J. D., and Hipkins, V. D. (2006). Mitigating scoring errors in microsatellite data from wild populations. *Mol. Ecol. Notes* 6, 951–957. doi: 10.1111/j.1471-8286.2006.01449.x

Evanno, G., Regnaut, S., and Goudet, J. (2005). Detecting the number of clusters of individuals using the software STRUCTURE: a simulation study. *Mol. Ecol.* 14, 2611–2620. doi: 10.1111/j.1365-294X.2005.02553.x

Excoffier, L., and Lischer, H. E. L. (2010). Arlequin suite ver 3.5: a new series of programs to perform population genetics analyses under Linux and Windows. *Mol. Ecol. Resour.* 10, 564–567. doi: 10.1111/j.1755-0998.2010.02847.x

Faubet, P., Waples, R. S., and Gaggiotti, O. E. (2007). Evaluating the performance of a multilocus Bayesian method for the estimation of migration rates. *Mol. Ecol.* 16, 1149–1166. doi: 10.1111/j.1365-294X.2007.03218.x

Faurby, S., and Barber, P. H. (2012). Theoretical limits to the correlation between pelagic larval duration and population genetic structure. *Mol. Ecol.* 21, 3419–3432. doi: 10.1111/j.1365-294X.2012.05609.x

Folmer, O., Black, M., Hoeh, W., Lutz, R., and Vrijenhoes, R. (1994). DNA primers for amplification of mitochondrial cytochrome *c* oxidase subunit I from diverse metazoan invertebrates. *Mol. Mar. Biol. Biotechnol.* 3, 294–299.

Food and Agricultural Organisation of the United Nations (2009). *International Guidelines for the Management of Deep-Sea Fisheries in the High Seas*. Rome: FAO.

Freeland, J. R. (2005). "Molecular markers in ecology," in *Molecular Ecology*, ed. H. Kirk, (Chichester: John Wiley and Sons), 31–62.

García-Merchán, V. H., Robainas-Barcia, A., Abelló, P., Macpherson, E., Palero, F., García-Rodríguez, M., et al. (2012). Phylogeographic patterns of decapod crustaceans at the Atlantic–Mediterranean transition. *Mol. Phylogenet. Evol.* 62, 664–672. doi: 10.1016/j.ympev.2011.11.009

Gjerde, K. M., Reeve, L. L. N., Harden-Davies, H., Ardron, J., Dolan, R., Durussel, C., et al. (2016). Protecting Earth's last conservation frontier: scientific, management and legal priorities for MPAs beyond national boundaries. *Aquat. Conserv.* 26, 45–60. doi: 10.1002/aqc.2646

Gollner, S., Kaiser, S., Menzel, L., Jones, D. O., Brown, A., Mestre, N. C., et al. (2017). Resilience of benthic deep-sea fauna to mining activities. *Mar. Environ. Res.* 129, 76–101. doi: 10.1016/j.marenvres.2017.04.010

Goudet, J. (2002). *FSTAT, a Program to Estimate and Test Gene Diversities and Fixation Indices, version 2.9.3*. Available at: https://www2.unil.ch/popgen/softwares/fstat.htm [accessed December 4, 2018].

Guo, S. W., and Thompson, E. A. (1992). Performing the exact test of Hardy-Weinberg proportion for multiple alleles. *Biometrics* 48, 361–372. doi: 10.2307/2532296

Hale, M. L., Burg, T. M., and Steeves, T. E. (2012). Sampling for microsatellite-based population genetic studies: 25 to 30 individuals per population is enough to accurately estimate allele frequencies. *PLoS One* 7:e45170. doi: 10.1371/journal.pone.0045170

Handayani, M., Anggoro, S., Widowati, I., and Hideyuki, I. (2014). Molecular ecology comparison of blue leg hermit crab (*Calcinus elegans*) based on spatial factor in south coast of Java Island. *Int. J. Mar. Aquat. Resour. Conserv. Coexistence* 1, 12–18. doi: 10.14710/ijmarcc.1.1.p

Haye, P. A., Salinas, P., Acuna, E., and Poulin, E. (2010). Heterochronic phenotypic plasticity with lack of genetic differentiation in the southeastern Pacific squat lobster *Pleuroncodes monodon*. *Evol. Dev.* 12, 628–634. doi: 10.1111/j.1525-142X.2010.00447.x

Hedrick, P. W. (1999). Perspective: highly variable loci and their interpretation in evolution and conservation. *Evolution* 53, 313–318. doi: 10.1111/j.1558-5646.1999.tb03767.x

Helson, J., Leslie, S., Clement, G., Wells, R., and Wood, R. (2010). Private rights, public benefits: industry-driven seabed protection. *Mar. Policy* 34, 557–566. doi: 10.1016/j.marpol.2009.11.002

Henderson, J. R. (1885). Diagnoses of new species of Galatheidae collected during the "Challenger" expedition. *Annals and Magazine of Natural History (ser. 5)* 16, 407–421. doi: 10.1080/00222938509459908

Herrera, S., Shank, T. M., and Sánchez, J. A. (2012). Spatial and temporal patterns of genetic variation in the widespread antitropical deep-sea coral *Paragorgia arborea*. *Mol. Ecol.* 21, 6053–6067. doi: 10.1111/mec.12074

Hilário, A., Metaxas, A., Gaudron, S. M., Howell, K. L., Mercier, A., Mestre, N. C., et al. (2015). Estimating dispersal distance in the deep sea: challenges and applications to marine reserves. *Front. Mar. Sci.* 2:6. doi: 10.3389/fmars.2015.00006

Holland, L. P., Rowden, A. A., Hamilton, J. Z., Clark, M. R., Chiswell, S. M., and Gardner, J. P. A. (2019). *Genetic Connectivity of Deep-Sea Corals in the New Zealand Region*. Wellington: Ministry for Primary Industries.

Hubisz, M. J., Falush, D., Stephens, M., and Pritchard, J. K. (2009). Inferring weak population structure with the assistance of sample group information. *Mol. Ecol. Resour.* 9, 1322–1332. doi: 10.1111/j.1755-0998.2009.02591.x

Iftekhar, M., Tisdell, J., and Gilfedder, L. (2014). Private lands for biodiversity conservation: review of conservation covenanting programs in Tasmania, Australia. *Biol. Conserv.* 169, 176–184. doi: 10.1016/j.biocon.2013.10.013

Johnson, M. S., and Black, R. (1984). The Wahlund effect and the geographical scale of variation in the intertidal limpet *Siphonaria* sp. *Mar. Biol.* 79, 295–302. doi: 10.1007/BF00393261

Jombart, T., and Ahmed, I. (2011). *adegenet 1.3-1*: new tools for the analysis of genome-wide SNP data. *Bioinformatics* 27, 3070–3071. doi: 10.1093/bioinformatics/btr521

Jombart, T., Devillard, S., and Balloux, F. (2010). Discriminant analysis of principal components: a new method for the analysis of genetically structured populations. *BMC Genet.* 11:94. doi: 10.1186/1471-2156-11-94

Kalinowski, S. T., Taper, M. L., and Marshall, T. C. (2007). Revising how the computer program CERVUS accommodates genotyping error increases success in paternity assignment. *Mol. Ecol.* 16, 1099–1106. doi: 10.1111/j.1365-294X.2007.03089.x

Kopelman, N. M., Mayzel, J., Jakobsson, M., Rosenberg, N. A., and Mayrose, I. (2015). CLUMPAK: a program for identifying clustering modes and packaging population structure inferences across *K*. *Mol. Ecol. Resour.* 15, 1179–1191. doi: 10.1111/1755-0998.12387

Kumar, S., Stecher, G., and Tamura, K. (2016). MEGA7: molecular evolutionary genetics analysis version 7.0 for bigger datasets. *Mol. Biol. Evol.* 33, 1870–1874. doi: 10.1093/molbev/msw054

Latch, E. K., Dharmarajan, G., Glaubitz, J. C., and Rhodes, O. E. (2006). Relative performance of Bayesian clustering software for inferring population substructure and individual assignment at low levels of population differentiation. *Conserv. Genet.* 7, 295–302. doi: 10.1007/s10592-005-9098-1

Leathwick, J., Moilanen, A., Francis, M., Elith, J., Taylor, P., Julian, K., et al. (2008). Novel methods for the design and evaluation of marine protected areas in offshore waters. *Conserv. Lett.* 1, 91–102. doi: 10.1111/j.1755-263X.2008.00012.x

Leigh, J. W., and Bryant, D. (2015). POPART: full-feature software for haplotype network construction. *Methods Ecol. Evol.* 6, 1110–1116. doi: 10.1111/2041-210X.12410

Lumsden, S. E., Hourigan, T. F., Bruckner, A. W., and Dorr, G. (2007). *The State of Deep Coral Ecosystems of the United States*. Silver Spring, MD: NOA Technical Memorandum CRCP-3.

Miller, K. A., Thompson, K. F., Johnston, P., and Santillo, D. (2018). An overview of seabed mining including the current state of development, environmental impacts and knowledge gaps. *Front. Mar. Sci.* 4:418. doi: 10.3389/fmars.2017.00418

Miller, K. J., and Gunasekera, R. M. (2017). A comparison of genetic connectivity in two deep sea corals to examine whether seamounts are isolated islands or stepping stones for dispersal. *Sci. Rep.* 7:46103. doi: 10.1038/srep46103

Miller, K. J., Rowden, A. A., Williams, A., and Häussermann, V. (2011). Out of their depth? Isolated deep populations of the cosmopolitan coral *Desmophyllum dianthus* may be highly vulnerable to environmental change. *PLoS One* 6:e19004. doi: 10.1371/journal.pone.0019004

Miller, K. J., Williams, A., Rowden, A. A., Knowles, C., and Dunshea, G. (2010). Conflicting estimates of connectivity among deep-sea coral populations. *Mar. Ecol.* 31, 144–157. doi: 10.1111/j.1439-0485.2010.00380.x

Molecular Ecology Resources Primer Development Consortium, Andris, M., Aradottir, G. I., Arnau, G., Audzijonyte, A., Bess, E. C., et al. (2010). Permanent genetic resources added to molecular ecology resources database 1 June 2010–31 July 2010. *Mol. Ecol. Resour.* 10, 1106–1108. doi: 10.1111/j.1755-0998.2010.02916.x

Morgan, E. M., Green, B. S., Murphy, N. P., and Strugnell, J. M. (2013). Investigation of genetic structure between deep and shallow populations of the southern rock lobster, *Jasus edwardsii* in Tasmania, Australia. *PLoS One* 8:e77978. doi: 10.1371/journal.pone.0077978

Nakajima, Y., Shinzato, C., Khalturina, M., Nakamura, M., Watanabe, H. K., Nakagawa, S., et al. (2018). Isolation and characterization of novel polymorphic microsatellite loci for the deep-sea hydrothermal vent limpet, *Lepetodrilus nux*, and the vent-associated squat lobster, *Shinkaia crosnieri*. *Mar. Biodivers.* 48, 677–684. doi: 10.1007/s12526-017-0704-5

Nei, M., Tajima, F., and Tateno, Y. (1983). Accuracy of estimated phylogenetic trees from molecular data. *J. Mol. Evol.* 19, 153–170. doi: 10.1007/bf02300753

Palumbi, S. R. (2003). Population genetics, demographic connectivity, and the design of marine reserves. *Ecol. Appl.* 13, 146–158. doi: 10.1890/1051-0761(2003)013%5B0146:pgdcat%5D2.0.co;2

Pandolfi, J. M., Bradbury, R. H., Sala, E., Hughes, T. P., Bjorndal, K. A., Cooke, R. G., et al. (2003). Global trajectories of the long-term decline of coral reef ecosystems. *Science* 301, 955–958. doi: 10.1126/science.1085706

Parker, S. J., and Bowden, D. A. (2010). Identifying taxonomic groups vulnerable to bottom longline fishing gear in the Ross Sea region. *CCAMLR Sci.* 17, 105–127.

Parker, S. J., Penney, A. J., and Clark, M. R. (2009). Detection criteria for managing trawl impacts on vulnerable marine ecosystems in high seas fisheries of the South Pacific Ocean. *Mar. Ecol. Prog. Ser.* 397, 309–317. doi: 10.3354/meps08115

Peakall, R., and Smouse, P. E. (2012). GenAlEx 6.5: genetic analysis in Excel. Population genetic software for teaching and research—an update. *Bioinformatics* 28, 2537–2539. doi: 10.1093/bioinformatics/bts460

Penney, A. J., and Guinotte, J. M. (2013). Evaluation of New Zealand's high-seas bottom trawl closures using predictive habitat models and quantitative risk assessment. *PLoS One* 8:e82273. doi: 10.1371/journal.pone.0082273

Penney, A. J., Parker, S. J., and Brown, J. H. (2009). Protection measures implemented by New Zealand for vulnerable marine ecosystems in the South Pacific Ocean. *Mar. Ecol. Prog. Ser.* 397, 341–354. doi: 10.3354/meps08300

Pérez-Barros, P., Lovrich, G. A., Calcagno, J. A., and Confalonieri, V. A. (2014). Is *Munida gregaria* (Crustacea: Decapoda: Munididae) a truly transpacific species? *Polar Biol.* 37, 1413–1420. doi: 10.1007/s00300-014-1531-9

Pérez-Barros, P., Thatje, S., Calcagno, J. A., and Lovrich, G. A. (2007). Larval development of the subantarctic squat lobster *Munida subrugosa* (White, 1847) (Anomura: Galatheidae), reared in the laboratory. *J. Exp. Mar. Biol. Ecol.* 352, 35–41. doi: 10.1016/j.jembe.2007.06.035

Piry, S., Alapetite, A., Cornuet, J.-M., Paetkau, D., Baudouin, L., and Estoup, A. (2004). GENECLASS2: a software for genetic assignment and first-generation migrant detection. *J. Hered.* 95, 536–539. doi: 10.1093/jhered/esh074

Pritchard, J. K., Stephens, M., and Donnelly, P. (2000). Inference of population structure using multilocus genotype data. *Genetics* 155, 945–959.

Pujolar, J. M., Schiavina, M., Di Franco, A., Melià, P., Guidetti, P., Gatto, M., et al. (2013). Understanding the effectiveness of marine protected areas using genetic connectivity patterns and Lagrangian simulations. *Divers. Distrib.* 19, 1531–1542. doi: 10.1111/ddi.12114

Ramirez-Llodra, E., Tyler, P. A., Baker, M. C., Bergstad, O. A., Clark, M. R., Escobar, E., et al. (2011). Man and the last great wilderness: human impact on the deep sea. *PLoS One* 6:e22588. doi: 10.1371/journal.pone.0022588

Ramirez-Llodra, E. Z., Brandt, A., Danovaro, R., De Mol, B., Escobar, E., German, C. R., et al. (2010). "Deep, diverse and definitely different: unique attributes of the world's largest ecosystem," in *Biogeosciences*, eds J. P. Gattuso, and J.

Kesselmeier, (Göttingen: Copernicus Publications), 2851–2899. doi: 10.5194/bg-7-2851-2010

Raymond, M., and Rousset, F. (1995). An exact test for population differentiation. *Evolution* 49, 1280–1283. doi: 10.1111/j.1558-5646.1995.tb04456.x

R Development Core Team (2017) *R: A Language and Environment for Statistical Computing*. Available at: https://www.R-project.org/

Rodríguez-Flores, P. C., Machordom, A., and Macpherson, E. (2017). Three new species of squat lobsters of the genus *Fennerogalathea* Baba, 1988 (Decapoda: Galatheidae) from the Pacific Ocean. *Zootaxa* 4276, 46–60. doi: 10.11646/zootaxa.4276.1.2

Roterman, C. N., Copley, J. T., Linse, K. T., Tyler, P. A., and Rogers, A. D. (2016). Connectivity in the cold: the comparative population genetics of vent-endemic fauna in the Scotia Sea, Southern Ocean. *Mol. Ecol.* 25, 1073–1088. doi: 10.1111/mec.13541

Rousset, F. (2008). GENEPOP'007: a complete re-implementation of the GENEPOP software for Windows and Linux. *Mol. Ecol. Resour.* 8, 103–106. doi: 10.1111/j.1471-8286.2007.01931.x

Rowden, A. A., Schlacher, T. A., Williams, A., Clark, M. R., Stewart, R., Althaus, F., et al. (2010a). A test of the seamount oasis hypothesis: seamounts support higher epibenthic megafaunal biomass than adjacent slopes. *Mar. Ecol.* 31, 95–106. doi: 10.1111/j.1439-0485.2010.00369.x

Rowden, A. A., Schnabel, K. E., Schlacher, T. A., Macpherson, E., Ahyong, S. T., and de Forges, B. R. (2010b). Squat lobster assemblages on seamounts differ from some, but not all, deep-sea habitats of comparable depth. *Mar. Ecol.* 31, 63–83. doi: 10.1111/j.1439-0485.2010.00374.x

Rozas, J., Ferrer-Mata, A., Sánchez-DelBarrio, J. C., Guirao-Rico, S., Librado, P., Ramos-Onsins, S. E., et al. (2017). DnaSP 6: DNA sequence polymorphism analysis of large data sets. *Mol. Biol. Evol.* 34, 3299–3302. doi: 10.1093/molbev/msx248

Samadi, S., Bottan, L., Macpherson, E., De Forges, B. R., and Boisselier, M.-C. (2006). Seamount endemism questioned by the geographic distribution and population genetic structure of marine invertebrates. *Mar. Biol.* 149, 1463–1475. doi: 10.1007/s00227-006-0306-4

Santini, L., Saura, S., and Rondinini, C. (2016). Connectivity of the global network of protected areas. *Divers. Distrib.* 22, 199–211. doi: 10.1111/ddi.12390

Selkoe, K. A., and Toonen, R. J. (2011). Marine connectivity: a new look at pelagic larval duration and genetic metrics of dispersal. *Mar. Ecol. Prog. Ser.* 436, 291–305. doi: 10.3354/meps09238

Taylor, M. L., and Roterman, C. N. (2017). Invertebrate population genetics across Earth's largest habitat: the deep-sea floor. *Mol. Ecol.* 26, 4872–4896. doi: 10.1111/mec.14237

Thaler, A. D., Plouviez, S., Saleu, W., Alei, F., Jacobson, A., Boyle, E. A., et al. (2014). Comparative population structure of two deep-sea Hydrothermal-Vent-Associated decapods (*Chorocaris* sp. 2 and *Munidopsis lauensis*) from southwestern Pacific back-arc basins. *PLoS One* 9:e101345. doi: 10.1371/journal.pone.0101345

Thresher, R. E., Guinotte, J. M., Matear, R. J., and Hobday, A. J. (2015). Options for managing impacts of climate change on a deep-sea community. *Nat. Clim. Chang.* 5, 635–639. doi: 10.1038/nclimate2611

United Nations General Assembly (2007). *Resolution 61/105. Sustainable Fisheries, Including through the 1995 Agreement for the Implementation of the Provisions of the United Nations Convention on the Law of the Sea of 10 December 1982 Relating to the Conservation and Management of Straddling Fish Stocks and Highly Migratory Fish Stocks, and Related Instruments. UNGA A/RES/61/105*. Available at: www.un.org/Depts/los/general_assembly/general_assembly_resolutions.htm (accessed December 4, 2018).

van Dover, C. L., Arnaud-Haond, S., Gianni, M., Helmreich, S., Huber, J. A., Jaeckel, A. L., et al. (2018). Scientific rationale and international obligations for protection of active hydrothermal vent ecosystems from deep-sea mining. *Mar. Policy* 90, 20–28. doi: 10.1016/j.marpol.2018.01.020

van Oosterhout, C., Hutchinson, W. F., Wills, D. P. M., and Shipley, P. (2004). MICRO-CHECKER: software for identifying and correcting genotyping errors in microsatellite data. *Mol. Ecol. Resour.* 4, 535–538. doi: 10.1111/j.1471-8286.2004.00684.x

Wang, C., Agrawal, S., Laudien, J., Häussermann, V., and Held, C. (2016). Discrete phenotypes are not underpinned by genome-wide genetic differentiation in the squat lobster *Munida gregaria* (Crustacea: Decapoda: Munididae): a multi-marker study covering the Patagonian shelf. *BMC Evol. Biol.* 16:258. doi: 10.1186/s12862-016-0836-4

Wang, J. (2017). The computer program STRUCTURE for assigning individuals to populations: easy to use but easier to misuse. *Mol. Ecol. Resour.* 17, 981–990. doi: 10.1111/1755-0998.12650

Waples, R. S. (2014). Testing for Hardy–Weinberg proportions: have we lost the plot? *J. Hered.* 106, 1–19. doi: 10.1093/jhered/esu062

Watling, L., Guinotte, J., Clark, M. R., and Smith, C. R. (2013). A proposed biogeography of the deep ocean floor. *Prog. Oceanogr.* 111, 91–112. doi: 10.1016/j.pocean.2012.11.003

Weersing, K., and Toonen, R. J. (2009). Population genetics, larval dispersal, and connectivity in marine systems. *Mar. Ecol. Prog. Ser.* 393, 1–12. doi: 10.3354/meps08287

Wilson, G. A., and Rannala, B. (2003). Bayesian inference of recent migration rates using multilocus genotypes. *Genetics* 163, 1177–1191.

Yan, R. J., Schnabel, K. E., Guo, X. Z., and Gardner, J. P. A. (2019). Development and characterization of 20 polymorphic microsatellite loci in the deep sea squat lobster, *Munida isos* Ahyong and Poore, 2004 and cross-amplification in two congeneric species. *J. Genet.* 98:11. doi: 10.1007/s12041-019-1062-9

Yang, C.-H., Tsuchida, S., Fujikura, K., Fujiwara, Y., Kawato, M., and Chan, T.-Y. (2016). Connectivity of the squat lobsters *Shinkaia crosnieri* (Crustacea: Decapoda: Galatheidae) between cold seep and hydrothermal vent habitats. *Bull. Mar. Sci.* 92, 17–31. doi: 10.5343/bms.2015.1031

Zeng, C., Clark, M. R., Rowden, A. A., Kelly, M., and Gardner, J. P. A. (2019). The use of spatially explicit genetic variation data from four deep-sea sponges to inform the protection of Vulnerable Marine Ecosystems. *Sci. Rep.* 9:5482. doi: 10.1038/s41598-019-41877-9

Zeng, C., Rowden, A. A., Clark, M. R., and Gardner, J. P. A. (2017). Population genetic structure and connectivity of deep-sea stony corals (Order Scleractinia) in the New Zealand region: implications for the conservation and management of vulnerable marine ecosystems. *Evol. Appl.* 10, 1040–1054. doi: 10.1111/eva.12509

Conflict of Interest: The authors declare that the research was conducted in the absence of any commercial or financial relationships that could be construed as a potential conflict of interest.

frontiers
in Marine Science

ORIGINAL RESEARCH
published: 05 February 2020
doi: 10.3389/fmars.2020.00017

Cold-Water Corals and Other Vulnerable Biological Structures on a North Pacific Seamount After Half a Century of Fishing

Cherisse Du Preez[1]*, *Kelly D. Swan*[1] *and Janelle M. R. Curtis*[2]

[1] *Institute of Ocean Sciences, Fisheries and Oceans Canada, Sidney, BC, Canada,* [2] *Pacific Biological Station, Fisheries and Oceans Canada, Nanaimo, BC, Canada*

OPEN ACCESS

Edited by:
Christopher Kim Pham,
University of the Azores, Portugal

Reviewed by:
Chris Yesson,
Zoological Society of London,
United Kingdom
Lucia Bongiorni,
Istituto di Scienze Marine (ISMAR),
Italy
Jerry R. Hoff,
National Oceanic and Atmospheric
Administration (NOAA), United States

***Correspondence:**
Cherisse Du Preez
cherisse.dupreez@dfo-mpo.gc.ca

Specialty section:
This article was submitted to
Deep-Sea Environments and Ecology,
a section of the journal
Frontiers in Marine Science

Received: *02 October 2019*
Accepted: *10 January 2020*
Published: *05 February 2020*

Citation:
Du Preez C, Swan KD and Curtis JMR (2020) Cold-Water Corals and Other Vulnerable Biological Structures on a North Pacific Seamount After Half a Century of Fishing. Front. Mar. Sci. 7:17. doi: 10.3389/fmars.2020.00017

Addressing growing threats of overexploitation to the world's oceans is especially challenging in the High Seas, where limited data and international jurisdiction make it difficult to determine where and when conservation measures are necessary. Of particular concern are vulnerable marine ecosystems (VMEs)—special habitats on the seafloor that are highly sensitive to disturbance and slow to recover. To ensure the long-term conservation and sustainable use of marine resources, regional fisheries management organizations are committed to identifying the locations of VMEs and responding to prevent significant adverse impacts (SAIs). For over 50 years, Cobb Seamount—a shallow underwater volcanic mountain in the Northeast Pacific Ocean—has been commercially fished by multiple nations using various types of gear. Here we have assimilated data from fisheries records and a recent visual survey on the seamount. Our findings show a variety of habitat-forming emergent biological structures widely distributed on Cobb Seamount and generally depth-stratified into high-density assemblages ($\geq$1 m^{-2}). Our spatial analyses show that fishing has also been widely distributed, overlapping the habitat of the biological structures. We found fewer cold-water corals, sponges, and other biological structures in areas with higher recent fishing effort and documented evidence of fishing impacts, such as extensive mats of coral rubble and a high abundance of derelict fishing gear entangled with dead or damaged organisms. Based on the average density of "lost" gear (2,785 ± 1,003 km^{-2}), we can confidently estimate that hundreds of thousands of items of derelict fishing gear are currently entangled with the seafloor of Cobb Seamount and that these pose an ongoing threat to biological structures, the biogenic habitats they create, and the species they support. Such impacts can persist for decades or centuries to come. This study contributes and discusses new information on the condition and distribution of biological structures, VME indicator taxa, physically complex biogenic ecosystems, and human impacts on Cobb Seamount. These data will be necessary to identify the location(s) of potential VMEs and SAIs on this heavily fished seamount in the High Seas.

Keywords: vulnerable marine ecosystem, bottom-contact fishing, derelict fishing gear, deep sea, biological structures, biogenic habitats, cold-water corals, indicator taxa

INTRODUCTION

Impacts of human-induced stressors are often readily visible in terrestrial and coastal ecosystems, but the same cannot be said for species and ecosystems in the deep sea. The majority of the deep sea remains unexplored (Ramirez-Llodra et al., 2010), and though much of these vast areas were once thought safe from human exploitation, technological advancements have made it steadily easier for fishing fleets to catch species far offshore and safely store them for the journey back to land (Cullis-Suzuki and Pauly, 2010). Bottom trawling and other deep-sea fishing methods have effects on the seafloor that resemble forest clearcutting and are widely regarded as a significant threat to biological diversity and economic sustainability (Watling and Norse, 1998). The threat of increased fishing pressure is compounded by climate change (Hoegh-Guldberg and Bruno, 2010), growing deep-sea mining interests (Merrie et al., 2014), and the accumulation of anthropogenic debris (Woodall et al., 2014; Gall and Thompson, 2015), such as abandoned, lost or otherwise discarded fishing gear (Macfadyen et al., 2009); hereafter, "derelict fishing gear" or DFG.

Increasing attention is being paid to these anthropogenic threats in Areas Beyond National Jurisdiction (ABNJs), which include the "High Seas" and "the Area" (i.e., the water column outside of State-managed Exclusive Economic Zones or the Territorial Sea where no EEZ has been declared, and the seabed beyond the limits of the continental shelf, respectively; Popova et al., 2019). The High Seas cover nearly 60% of the world's oceans (Cullis-Suzuki and Pauly, 2010), comprise the largest habitat for life on the planet (Verity et al., 2002; Blasiak et al., 2016), and are overseen by intergovernmental regional fisheries management organizations (RFMOs) which provide a mechanism for managing shared resources and meeting international obligations (Cullis-Suzuki and Pauly, 2010; Gilman et al., 2014). Although they are critical to the protection of marine ecosystems, many RFMOs are relatively young and still in the process of implementing the United Nations General Assembly (UNGA) Resolutions on the management of bottom fisheries in ABNJs (Gianni et al., 2016; Bell et al., 2019). Of particular concern is Resolution 61/105, which calls on individual States and RFMOs to sustainably manage fish stocks and protect vulnerable marine ecosystems (VMEs), including seamounts, hydrothermal vents, and cold-water corals and sponges, from destructive fishing practices (UNGA, 2006). Recognizing the immense value of deep-sea ecosystems and the biodiversity they contain, Resolution 61/105 further requires that RFMOs adopt conservation and management measures to prevent significant adverse impacts (SAIs) to VMEs. The Food and Agriculture Organization (FAO) has published International Guidelines for the Management of Deepsea Fisheries in the High Seas (FAO, 2009) which define a VME as an ecosystem that is easily disturbed and slow to recover (if at all), and SAIs as those that compromise ecosystem integrity in a manner that: (i) impairs the ability of affected populations to replace themselves, (ii) degrades the long-term natural productivity of habitats, or (iii) causes, on more than a temporary basis, significant loss of species richness, habitat or community type.

Vulnerable marine ecosystem identification has nonetheless proven challenging because of limited data on the response of ecosystems to fishing and their trajectory of recovery. Many RFMOs have therefore identified a suite of taxa as indicators of VMEs. For example, in its implementation of Resolution 61/105, the long-running Northwest Atlantic Fisheries Organization developed a set of physiographic and biological indicators as a proxy for VME identification (NAFO, 2018). Physiographic indicators included seamounts, canyons, knolls, shoals and steep flanks, while indicator taxa were identified on the basis of biological traits analysis (Bremner et al., 2006) and include a comprehensive list of structure-forming sponges, corals, sea pens, anemones, bryozoans, crinoids and sea squirts (NAFO, 2018). These taxa meet the FAO (2009) criteria regarding uniqueness or rarity, the functional significance of the habitat, life-history traits that make recovery difficult, and structural complexity.

The identification of potential VMEs in the North Pacific Ocean is the responsibility of a relatively newly formed RFMO: the North Pacific Fisheries Commission (founded in July 2015). To that end, the NPFC has adopted four groups of structure-forming cold-water corals as interim VME indicators: sea fans and true soft corals (both order Alcyonacea; sea fans prior epithet Gorgonacea), black corals (order Antipatharia), and stony corals (order Scleractinia) (North Pacific Fisheries Commission [NPFC], 2017, 2018).

Cobb Seamount is a shallow submarine volcanic mountain in the NPFC convention area (**Figure 1**) that was discovered in the 1950s by the commercial fisheries research vessel John N. Cobb (National Technical Information Service, 1971). Starting in the mid-1960s, Cobb Seamount was intermittently fished by Japan, United States, the Soviet Union, Canada, (Sasaki, 1985; Pearson et al., 1993; Clark et al., 2007; Douglas, 2011; Curtis et al., 2015), and likely other nations by way of unreported, unregulated, or illegal fishing (UN, 2019). Unlike the majority of North Pacific seamount fisheries, which expanded to catch North Pacific armorhead and splendid alfonsino (*Pentaceros wheeleri* and *Beryx splendens*), fisheries on Cobb Seamount have targeted sablefish (*Anoplopoma fimbria*), rockfish (*Sebastes* spp.), flatfish (Pleuronectiformes), thornyheads (*Sebastolobus* spp.), and other groundfish (Uchida and Tagami, 1984; Clark et al., 2007; Curtis et al., 2015). Over the decades, fishers have removed thousands of metric tons of fish from Cobb Seamount, at times in short bursts of heavy exploitation (Sasaki, 1985; Pearson et al., 1993; Clark et al., 2007) from which there is evidence of overfishing of at least one rockfish species (Douglas, 2011). Fishing on Cobb Seamount was ceased by the Soviet Union in the late 1960s, by Japan in the early 1990s, and by the United States in the early 2000s (Clark et al., 2007; Curtis et al., 2015). Canada is the only nation to report fishing on Cobb Seamount at present (North Pacific Fisheries Commission [NPFC], 2017); sporadic trips by Canadian vessels began in 1983 and continue to date (Curtis et al., 2015; North Pacific Fisheries Commission [NPFC], 2017) as part of the country's southern seamount fishery for sablefish (North Pacific Fisheries Commission [NPFC], 2017). The current fishing effort on Cobb Seamount is limited to one vessel per month for a 6 months season with the use of longline trap or longline hook gear (Fisheries and Oceans Canada [DFO], 2013).

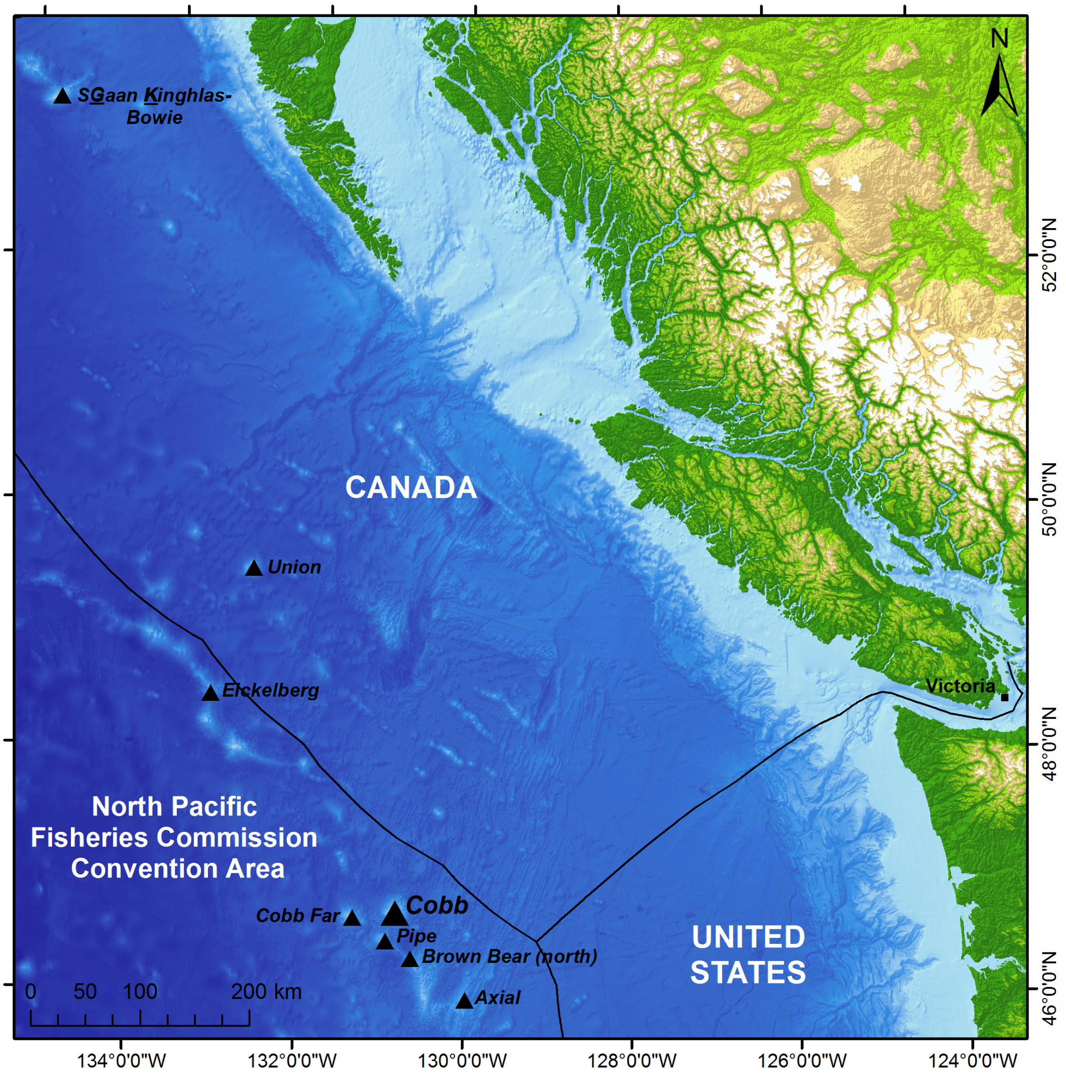

FIGURE 1 | The location of Cobb Seamount (46° 44′ 24′′ N, 130° 48′ 0′′ W), approximately 450 km off the west coast of Canada and the United States, within the North Pacific Fisheries Commission (NPFC) Convention Area of the High Seas. Also shown, seven notable seamounts, including SGaan Kinghlas-Bowie, the only other shallow-water seamount in the region (within the photic zone). The Exclusive Economic Zones are outlined.

Although the present fishing effort on Cobb Seamount is relatively modest, it has been fished for over half a century via bottom longline trap and hook gear, stern and heavy-duty tire bottom trawl nets, gill nets, and mid-water trawls (reviewed in Curtis et al., 2015). Physical contact by such fishing gear can damage, remove, and/or kill structure-forming organisms, including VME indicator taxa (Watling and Norse, 1998; Krieger, 2001; Fosså et al., 2002; Waller et al., 2007; Salgado et al., 2018). Not all fishing gear is equally destructive, but all of the gear types used on Cobb Seamount are capable of impacting VMEs. Current fishing activity on the seamount is limited to bottom longline sets; while these are intended to be stationary, with a relatively small footprint, they nonetheless move across the seafloor during deployment and retrieval, in the event of equipment failure, bad weather, strong tides and currents, operator error, entanglement with DFG, or when fishers grapple to retrieve lost gear (see NOAA Marine Debris Program, 2015 for review). Gauthier (2017) observed 81% of bottom longline sets on SGaan-Kinghlas Bowie Seamount (**Figure 1**) dragged, rolled, or bounced on the seafloor when in normal use. Historical fishing on Cobb Seamount will also have impacted the seafloor. Bottom trawling is hundreds to thousands of times more destructive than longline gear (Pham et al., 2014) and its impacts can last years to centuries (Watling, 2005). Even gear types that are not intended to make contact with the seafloor, such as gill nets and mid-water trawls, can and often do (e.g., Tingley, 2014; Salgado et al., 2018). Additionally, any gear that has been abandoned, lost, or otherwise discarded on Cobb Seamount over its long fishing history could be inflicting ongoing damage to the seafloor and its inhabitants. This includes trapping, entangling, or killing target and non-target organisms, such as VME indicator taxa (NOAA Marine Debris Program, 2015).

Our understanding of the ecological, cultural, and economic value of seamounts is growing, but so too are the threats they currently face (Pitcher et al., 2007). To adequately mitigate those threats, we must first document the diversity, distribution, and abundance of species on seamounts and assess the historical and potential footprint of anthropogenic impacts. To that end, in July 2012, Fisheries and Oceans Canada [DFO] and the National Oceanic and Atmospheric Administration (NOAA) embarked on a joint expedition to visually survey the communities, as well as fishing impacts, on Cobb Seamount at greater depths and in greater detail than ever before (Curtis et al., 2015; Du Preez et al., 2015, 2016). Here, we utilize the 2012 survey data to examine the spatial distribution of biological structures (i.e., habitat-forming organisms, such as cold-water corals, sponges, and other invertebrates; Buhl-Mortensen et al., 2010) adopted by the NPFC and other RFMOs as VME indicator taxa. We then investigate the recent footprint and effort of bottom longline fishing on Cobb Seamount and report on the prevalence of DFG and its associated impacts. Ultimately, we aim to support international commitments to Resolution 61/105 to identify VMEs and prevent SAIs by bringing together the best available data from a heavily fished seamount in the High Seas of the North Pacific Ocean.

MATERIALS AND METHODS

Study Area

Cobb Seamount is located in international waters, approximately 450 km southwest of Victoria, Vancouver Island, British Columbia (**Figure 1**). As one of many seamounts in the Cobb-Eickelberg chain (Chaytor et al., 2007), Cobb Seamount is far offshore, but not isolated. Its nearest neighbor is Pipe Seamount (also known as Cobb South), just 30 km southwest. Cobb Seamount, an ancient volcano, was formed by a hot spot that is currently active at Axial Seamount (Chaytor et al., 2007), 150 km southeast. It stands out among the Northeast Pacific Ocean's many seamounts because it is a shallow guyot. There is evidence that its last eruption was aerial and that 300 m of the summit plateau was once above sea level (Budinger, 1967; Farrow and Durant, 1985; Chaytor et al., 2007). Today, its flat-topped pinnacle rises to within 34 m of the surface, reaching well within the photic zone, while its base extends to ∼2750 m depth (**Figure 2**) (Birkeland, 1971; Parker and Tunnicliffe, 1994; Chaytor et al., 2007). The seamount has a two-dimensional (2D) area of approximately 824 km^2, and its terraced flanks average 12 degrees in slope (Budinger, 1967).

Biological surveys indicate that Cobb Seamount supports abundant, diverse, and unusual communities of organisms (Birkeland, 1971; Dower et al., 1992; Parker and Tunnicliffe, 1994; Du Preez et al., 2016). This hotspot of marine life is fueled by upwelling of nutrient-rich deep water and a Taylor cone (Dower et al., 1992), enhanced phytoplankton production (Comeau et al., 1995), trapping of diurnally migrating deep scattering layers (Curtis et al., 2015), and *in situ* primary productivity (kelp forests on the pinnacle and encrusting algae to ∼200 m depth; Parker and Tunnicliffe, 1994; Du Preez et al., 2015). The 267 taxa identified to date (historical and recent records reviewed in Du Preez et al., 2015) cluster into at least ten distinct depth-stratified benthic communities: one on the narrow pinnacle (<90 m), six on the broad summit plateau (90–350 m), and three on the steep upper flanks (350 to at least 1200 m) (Du Preez et al., 2016). The biological communities of the deeper flanks and base of Cobb Seamount have not yet been studied.

Visual Survey

Video and still imagery of the seafloor was collected along seventeen line transect surveys of Cobb Seamount from 21–26 July 2012 (**Figure 2**). Transects ranging from 350 to 1800 m in length were randomly assigned using ArcMap Generate Random Point tool (start location) and the Excel RANDBETWEEN function (bearing) to strata of varying depths, aspects, and recent fishing effort (avoiding potential hazards, e.g., slope > 30°; Curtis et al., 2015). The survey was conducted with a customized Deep Ocean Engineering Phantom HD2 + 2 remotely operated vehicle (ROV) and a SeaBED-class autonomous underwater vehicle (AUV).

The ROV was equipped with one 8 megapixel Cyclops digital still camera (C-Map Systems, Inc.), one high definition (HD) Mini Zeus video camera (1080i, Insite Pacific Inc.), and 10 cm parallel lasers to allow calculation of the field of view (and therefore densities from counts). It was piloted 0.5–1.5 m above the seafloor at a speed of approximately 0.1–0.25 m/s (0.2–0.5 knots) and completed 12 transects on the summit plateau at depths of 34–225 m (**Figure 2**). The AUV (Clarke et al., 2010) was equipped with three Prosilica GigE 14 cameras which collected digital still photographs every 10 s from a height of approximately 3 m above the seafloor. It possessed an altimeter to allow calculation of the field of view and completed four transects on the flanks of the seamount at depths of 465–1154 m (**Figure 2**).

Although the intention was to survey the entire depth range above 1200 m using the shallow-water ROV and deep-water AUV, dives between 225 and 465 m were aborted because of technical issues. One short pseudo-transect (**Figure 2**: SFU 2) was completed within the depth gap before the dive ended (Curtis et al., 2015), but data from this transect was only useful for the DFG analyses because the imagery was too poor to resolve the benthos. A total of 13.5 km or 29,364 m^2 was surveyed, including 8.3 km or 12,262 m^2 covered by the ROV and 5.2 km or 17,102 m^2 covered by the AUV (Curtis et al., 2015). Additional details on the survey design and configuration of the submersibles are provided by Clarke et al. (2010) and Curtis et al. (2015).

Imagery Annotation

During post-expedition video and photograph annotation in Video Miner (versions 2.1.3 and 2.1.4; a custom DFO image annotation software), we counted organisms using the methodologies outlined in Du Preez et al. (2016). The ROV-collected videos were annotated in 10-s intervals (approximately 5 m^2; supplemented with stills) and the non-overlapping AUV-collected still photographs were annotated in their entirety (approximately 5 m^2). We calculated the average densities per 10-s ROV video interval or high-altitude AUV photograph (where each interval or photo is one record and density is reported as per square meter) for a comprehensive list of

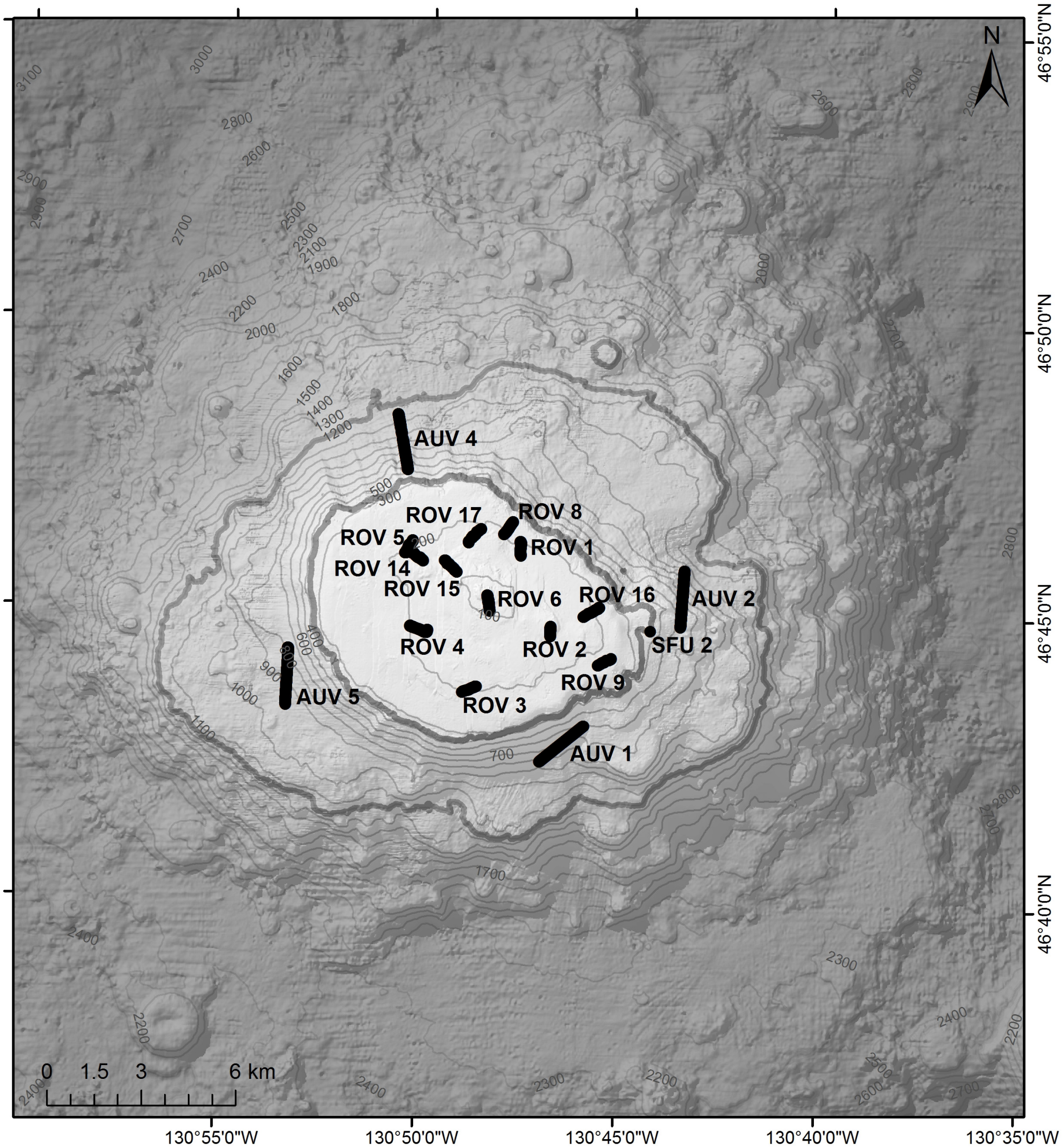

FIGURE 2 | The study area, topography, and transects. Black lines show the locations of the 17 visual survey dives in 2012 on Cobb Seamount, an unusually shallow guyot rising from ∼2750 m depth (∼map boundary) to within 24 m of the surface. The imagery of the pinnacle and shallow seamount summit plateau was collected using a remotely operated vehicle (ROV), imagery at the summit ridge was collected using a ROV during a single short, aborted dive (SFU), and the imagery of the upper flanks was collected using an autonomous underwater vehicle (AUV). The maximum depth for the ROV dives was ∼225 m, the SFU dive was at ∼350 m (bold contour), and the maximum depth for the AUV dives was ∼1200 m (bold contour). Contour lines = 100 m depth intervals.

organisms that meet the FAO criteria outlined for VME indicator taxa (FAO, 2009) and have been adopted by one or more RFMOs (**Table 1**). The taxonomic groups were soft corals (order Alcyonacea), black corals (order Antipatharia), stony corals (order Scleractinia), hydrocorals (family Stylasteridae), sea pens (order Pennatulacea), the crinoid *Florometra serratissima*, the giant scallop *Crassadoma gigantea* (presence only; individuals could not be confidently resolved from the continuous and encrusted mats of this taxon), and glass sponges (class Hexactinellida) (example images in **Figure 3**). The VME indicator taxa were grouped at the lowest level of taxonomic resolution possible based on morphotype (Du Preez et al., 2015). VME indicator taxa that were too rare for inclusion in our analyses and were grouped at higher levels include Isididae (*Keratoisis* sp. A and B, and *Isidella tentaculum*), Primnoidae (*Plumarella superba* and *Primnoa pacifica*), and Rossellidae (cf *Acanthascus* spp., *Rhabdocalyptus* spp., *Staurocalyptus* spp., and Bathydorous sp.).

We also recorded all DFG and noted instances where this gear was entangled in damaged, broken, toppled, or dead biological structures. Gear type identification was made by comparing close-up imagery to published descriptions and photographs

TABLE 1 | The occurrences of 19 groupings of habitat-forming biological structures on Cobb Seamount, observed during a 2012 visual survey.

Taxonomic group (common name)	VME indicator taxa	RFMOs	General location	No. of transects	No. of individuals/colonies	When present, av. density ± SE (1 m^{-2})	Maximum density (1 m^{-2})
Alcyonacea, non-gorgonians (true soft corals)	***Gersemia* sp.**	All[1−6]	Flank	2	47	0.67 ± 0.16	2.12
	Heteropolypus ritteri [2]		Flank	4	259	0.27 ± 0.01	2.04
Alcyonacea, gorgonians (sea fans)	**Isididae**	All	Flank	3	625	0.53 ± 0.03	3.76
	Primnoidae		Summit	2	2	na	na
			Flank	3	180	0.28 ± 0.02	1.39
	Swiftia simplex [2,3]		Flank	4	30	0.22 ± 0.00	0.27
Antipatharia (black corals)	***Chrysopathes speciosa***	All	Flank	3	84	0.27 ± 0.02	1.19
	***Bathypathes* sp.**		Flank	4	397	0.28 ± 0.01	1.36
	Lillipathes lillei		Flank	4	310	0.29 ± 0.01	1.81
	Antipatharia sp.		Flank	4	30	0.3 ± 0.06	1.58
	***Stichopathes* sp.** [4]		Flank	4	76	0.33 ± 0.03	0.87
Scleractinia (stony corals)	***Desmophyllum dianthus***	All	Summit	8	968	0.74 ± 0.09	11.44
			Flank	1	9	na	na
	Desmophyllum pertusum		Summit	3	16 bioherms	na (continuous)	na
Stylasteridae (hyrocorals)	***Stylaster* spp.**	Half, not NPFC [2,5,6]	Summit	9	215,555	39.98 ± 3.11	193.75
			Flank	2	57	0.47 ± 0.09	1.60
Pennatulacea (sea pens)	***Anthoptilum* spp.**	All except NPFC [2−6]	Flank	4	106	0.24 ± 0.01	0.81
	Halipteris willemoesi		Summit	9	87	0.15 ± 0.01	0.33
			Flank	2	14	0.22 ± 0.00	0.23
Crinoidea (crinoids)	***Florometra serratissima*** [2]	Most, not NPFC [2,3,5,6]	Summit	9	82,844	35.5 ± 2.91	>>100 (continuous)
			Flank	2	26	0.29 ± 0.04	0.89
Bivalvia (e.g., scallops)	***Crassadoma gigantea*** [2]	One, not NPFC [2]	Pinnacle	1	na	na	na (continuous)
Hexactinellida (glass sponges)	***Farrea omniclavata*** [4]	All except NPFC	Flank	3	46 large colonies	na (colonies > 1 m^2)	na
	Rossellidae		Flank	4	105	0.42 ± 0.02	1.15
	Sub-total for NPFC VME indicator taxa only				**3,034**		
	Total				**301,874**		

The listed taxa are vulnerable marine ecosystem (VME) indicators according to one or more regional fisheries management organizations (n = six RFMOs; listed in footnotes). A strikethrough superscript in the VME indicator column means that while the Taxonomic Group is listed as a VME indicator by the RMFO, the specific taxa we observed is not. See ***Figure 3*** *for representative photographs. [1]North Pacific Fisheries Commission (North Pacific Fisheries Commission [NPFC], 2017, 2018); [2]Commission for the Conservation of Antarctic Marine Living Resources (Commission for the Conservation of Antarctic Marine Living Resources [CCAMLR], 2009, 2013) (included because of its role in the management of bottom-contact fisheries even though it is not officially an RMFO; Bell et al., 2019); [3]Northwest Atlantic Fisheries Organization (North Atlantic Fisheries Organization [NAFO], 2009, 2010; Murillo et al., 2011); [4]North East Atlantic Fisheries Commission (NEAFC, 2015); [5]South East Atlantic Fisheries Organisation (South East Atlantic Fisheries Organisation [SEAFO], 2016); [6]South Pacific Regional Fisheries Management Organisation (South Pacific Regional Fisheries Management Organisation [SPRFMO], 2019); according to the Food and Agriculture Organization (FOA), the General Fisheries Commission for the Mediterranean (GFCM) and South Indian Ocean Fisheries Agreement (SIOFA) has not yet adopted VME indicator taxa (FAO, 2019).*

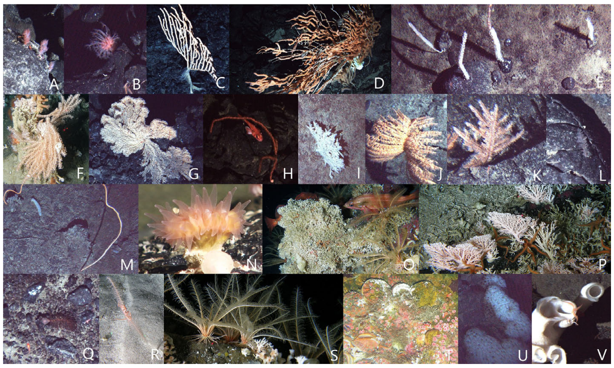

FIGURE 3 | Representative photographs of the 19 groupings of habitat-forming biological structures on Cobb Seamount, observed during the 2012 visual survey. The listed taxa are vulnerable marine ecosystem (VME) indicators according to one or more regional fisheries management organizations (RFMOs; see **Table 1**). The Alcyonacea soft corals **(A)** *Gersemia* sp., **(B)** *Heteropolypus ritteri*, **(C)** *Isidella tentaculum*, **(D)** *Keratoisis* sp. A, **(E)** *Keratoisis* sp. B, **(F)** *Primnoa pacifica*, **(G)** *Plumarella superba*, and **(H)** *Swiftia simplex*. The Antipatharia black corals **(I)** *Chrysopathes speciosa*, **(J)** *Bathypathes* sp., **(K)** *Lillipathes lillei*, **(L)** Antipatharia sp., and **(M)** *Stichopathes* sp. The Scleractinia stony corals **(N)** *Desmophyllum dianthus* and **(O)** *D. pertusum* (prior epithet *Lophelia pertusa*). The hydrocorals, *Stylaster* spp. **(P)**, the two Pennatulacea sea pens, **(Q)** *Anthoptilum* spp. and **(R)** *Halipteris willemoesi*, **(S)** the crinoid *Florometra serratissima*, **(T)** the giant scallop, *Crassadoma gigantean*, and the two Hexactinellida glass sponges, **(U)** *Farrea omniclavata* and **(V)** Rossellidae.

of DFG (e.g., Donaldson et al., 2010; Ragnarsson et al., 2017; Salgado et al., 2018; Baco et al., 2019). We distinguished between longline groundlines stretched across the seafloor (continuing beyond the field of view in both directions), clumps of rope in large piles, and pieces of rope which could have originated from longline groundlines but were short (i.e., ends were visible in the field of view). Putative drag marks were also noted; an incident equated to any observations of one or more drag marks across the substrate but not associated with the presence of DFG. The observed DFG was standardized to both km^{-1} and 2D km^{-2} for each transect (for ease of reference and comparability with our studies). We also annotated any other observable evidence of damage to VME indicators caused by physical contact.

Geospatial and Statistical Analyses

All annotated data was georeferenced (with latitude, longitude, and depth) using the navigational data of the ROVs and AUV. Mapping and geospatial analyses were executed in ArcMap 10.4. We used locations of seamounts in Canada, the United States, and adjacent ABNJ (e.g., DFO, 2019a) to measure the distance between seamounts and the continental slope and thus quantify the isolation of habitats on Cobb Seamount. For depth data (and as the base layer for our maps), we used the published 20 m × 20 m bathymetric raster data obtained by NOAA in 2000 using a SeaBeam2112 onboard the NOAA Ship RV *Ronald Brown* (survey RB0002). Statistical analyses were run in RStudio 1.1.442 starting with Shapiro Normality Tests and reporting averages ± standard error and a significant $p\text{-value} \leq 0.05$.

Recent Fishing Footprint and Effort Analysis

The recent Canadian longline fishing effort does not represent the full fishing footprint, given the extended duration and nature of historical fishing on Cobb Seamount. We nonetheless included it in our study to examine the most recent impacts of fishing. We obtained DFO fisheries records for commercial sablefish bottom longline fishing on Cobb Seamount over 22 years, from 1996 to 2017, inclusive. There is no comparable data for earlier trips (i.e., 1983–1995). The fisheries records included the start and end set locations, gear used (trap or hooks), and trap size from each fishing event ($n = 466$) over 87 trips.

We used the Wilcoxon Test to test for a change in fishing depth over time by calculating the average deepest and shallowest point of each longline set and comparing the averages for two equal time periods (1996–2005 and 2006–2017). For our spatial analyses, we used a conservative assumption that longlines were set straight across from the start to the end of set locations. We generated grid cells of 500 m by 500 m to cover the seamount and mapped fishing effort as the number of sets transecting each cell. We do not display cells fished by two or fewer vessels (applies to 40% of cells) to comply with DFO's "three-party rule" to respect the privacy of commercial fishers. This results in an underrepresentation of the depth limits and spatial coverage of fishing in our maps. We executed a spatial (Spearman) correlation of VME indicator densities and fishing effort by averaging the density of VME indicators within each cell.

Area Affected by the Recent Fishing

During bottom longline fishing, at a minimum, the anchors, longline, branch lines, and ±60 traps make contact with the seafloor, impacting biological structures within the footprint through entanglement, crushing, and by shearing (Doherty and Cox, 2017). For a range of conservative estimates of the area affected by the bottom longlines and traps, we calculated different scenarios: one assuming little to no gear movement and one incorporating a modest amount of movement (as documented in Gauthier, 2017). For each scenario, 2D area affected was calculated using ArcMap tools Buffer (with dissolve) and Clip to generate a footprint for each 50 m depth bin. We measured the longline string length for each set and used the average trap width of 137 cm (DFO fisheries records).

The two scenarios calculated:

> Scenario 1: area affected = longline string length × trap width
>
> Scenario 2: area affected = longline string length × 100 m moderate swept area of gear-drag during the deployment and retrieval (calculation from DFO, 2018; aligns with the nature of the trap movement documented by Gauthier, 2017).

For example, using scenario 1 and an average longline string length of 2,915 ± 25 m (DFO fisheries records), we estimate the average set's bottom footprint was 3,994 ± 34 m^2. This footprint is comparable to the estimate of 3,200 m^2, made using *in situ* video, accelerometer, and depth sensor data from sablefish bottom longline trap gear on SG̲aan-K̲inghlas Bowie Seamount (Doherty and Cox, 2017) but is very conservative in comparison to scenario 2, which is over 72 times larger, assuming a 100 m lateral movement (sweep) of the gear, based on expert opinion (DFO, 2018) (i.e., almost 300,000 m^2 for an average longline set). While the range of these scenarios may seem large, they do not account for the broader area affected by secondary impacts (e.g., the sediment resuspension from gear movement; DFO, 2018).

Derelict Fishing Gear

To estimate the amount of DFG within the fishable depths of Cobb Seamount, we extrapolated the average density of DFG (km^{-2}) we observed to the 2D surface area above 1200 m (220 km^2) (n = 16 transects; data from Curtis et al., 2015). Although SFU 2 appeared to have one of the highest densities of DFG, it was excluded from the estimate because we could not confidently calculate area (i.e., poor visual quality).

RESULTS

Biological Structures and Their Biogenic Habitats

We generated 5,143 spatial records (each ~5 m^2) which contain the identification, abundance, and location of 301,874 individual biological structures belonging to one of 19 groupings of VME indicator taxa (26 individual resolvable taxa) (**Table 1** and **Figure 3**). Of the 19 taxonomic groupings, 12 are recognized as VME indicators by all RFMOs (those with published lists of VME indicator taxa; **Table 1**) and are relatively well studied. However, these soft, black, and stony corals comprised just ~1% of colonies/individuals recorded during the survey (**Table 1**). The remaining 99% of individuals recorded during the survey were comprised of seven taxa which are presently adopted as VME indicators by one or more RFMOs, but not by the NPFC. These include the hydrocorals (*Stylaster* spp.), crinoids (*F. serratissima*), sea pens (order Pennatulacea), scallops (*C. gigantea*), and glass sponges (**Table 1**). Overall, hydrocorals and crinoids were the most numerically abundant VME taxa we observed, comprising 71% and 27% of all individuals, respectively. These taxa both formed the densest aggregations, with maximum counts of over one hundred individuals/colonies·m^{-2} attained before individuals blended into broad continuous fields (**Table 1**).

While in relatively low abundances, there was diversity in the cold-water coral biological structures. Of the soft coral taxa, the majority were large, erect, branching corals. The most abundant soft corals, the Isididae species, included individuals up to ~2 m tall. Two large *Paragorgia* sp. colonies were also observed, but the species was too rare to include in this study. We observed two taxa of low-relief true soft corals: *Gersemia* sp. and *Heteropolypus ritteri*. The black coral taxa recorded included one whip-like coral (*Stichopathes* sp.) and four branching, bush-like corals (e.g., *Bathypathes* sp.). Soft and black corals aggregated in high-density forest-like patches, whereas the stony corals aggregated in low-relief clusters, with the exception of the stony coral *Desmophyllum pertusum* (prior epithet *Lophelia pertusa*; Addamo et al., 2016) which formed large erect, complex bioherms.

Hydrocorals

Hard hydrocoral colonies ~20 cm tall covered the boulders and bedrock along entire transects and did not generally co-occur in high abundances with other biological structures (i.e., soft corals, black corals, sponges, or scallops). However, they were often associated with dense and diverse assemblages of other mobile, sedentary and/or sessile animals. The most conspicuous associates were small rockfish species (e.g., rosethorn rockfish, *Sebastes helvomaculatus*; **Figure 4A**), white-spined sea cucumbers (*Apostichopus leukothele*), nudibranchs (order Nudibranchia), and hermit crabs (*Elassochirus cavimanus*). While these large mobile animals were tucked between and against hydrocoral colonies, small sedentary and sessile animals were observed attached to the live coral branches, such as brittle stars (class Ophiuroidea; **Figure 4B**), zoanthids (order Zoantharia), pale urchins (*Strongylocentrotus pallidus*), California lamp shells (*Laqueus californianus*), hydroids (class Hydrozoa), caprellids (family Caprellidae), sea stars (class Asteroidea), and tubeworms (order Sabellida). Transects typified by fields of hydrocorals also supported abundant large rockfish, including large blackspotted and rougheye rockfish (*Sebastes melanostictus* and *S. aleutianus*).

Many of the attached hydrocorals we observed on the summit of Cobb Seamount were dead (i.e., skeleton exposed with no living tissue). For over half of the colonies we observed, only the base stump remained (with or without some severely reduced branches). All colonies entangled in, or directly adjacent to, DFG were reduced to dead stumps (**Figure 4C**). Hydrocorals on flat surfaces, such as low-lying boulders and smooth bedrock, were also dead and stripped of branches (**Figure 4D**). These dead corals hosted caprellids, hydroids, and other fouling epifauna. Detached coral rubble carpeted the sediment between boulders or in pockets on bedrock, forming nearly continuous mats of dead corals and branch fragments (**Figure 4F**). Live colonies were patchy and most often associated with substrate of higher physical complexity. Some large stumps showed signs of new growth, such as small, live branches (**Figure 4E**).

Crinoids

Crinoids attached to bedrock created dense, continuous fields along current-swept transects (10–100 s of individuals·m^{-2}; **Table 1**). Similar to hydrocoral fields, crinoids were usually the dominant or the only distinguishable biological structures when present. While many epifauna co-occurred with crinoids (e.g., tubeworms, demosponges, hydroids, anemones), they were attached to the rocks and not on the crinoids themselves. During close visual investigations, we observed small rockfish (including juveniles; species list in Du Preez et al., 2015) tucked under the arms of the crinoids and remaining stationary despite strong currents.

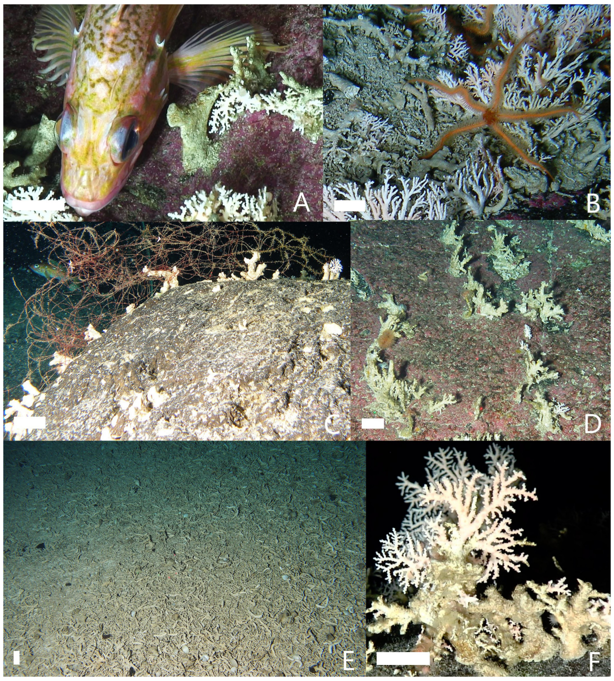

FIGURE 4 | Examples of associations and conditions of hydrocorals (*Stylaster* spp.). Common associates with hydrocorals were **(A)** small rockfish species (e.g., rosethorn rockfish, *Sebastes helvomaculatus*) tucked against colonies and **(B)** ophiuroids (class Ophiuroidea) perched on colonies. Colonies of hydrocorals **(C)** entangled in derelict fishing gear (DFG) and **(D)** on flat surfaces were most often reduced to dead branchless stumps. **(E)** Detached corals covered the sediment in continuous mats of rubble. **(F)** There were signs of new growth, some large stumps supported small live branches. White scale bars = 2 cm.

Giant Scallops

Giant scallops may have been present in even higher densities than the hydrocorals and crinoids, but we could not confidently resolve individuals within their almost completely encrusted, continuous mats. These bivalves were the foundation of complex living carpets of various encrusting sponges, strawberry anemones (*Corynactis californica*), coralline algae (*Lithothamnoin* spp. and *Lithophyllum* spp.), bushes of unidentified tube worms, and encrusting bryozoans (*Reginella hippocrepis*). During the shallowest transect of the survey, we observed schools of widow and rosy rockfish (*S. entomelas* and *S. rosaceus*) above the scallop biogenic habitat.

Other Biological Structures

Not all biological structures occurred in high abundances or were photographed equally well. Close-up imagery from the AUV was rare, so we were not able to resolve the taxa for all biological structures —specifically those present on deeper transects. Of the sea pens, *Halipteris willemoesi* was present in low densities over the shallow sandy bottom and was usually home to a single *Asteronyx loveni* brittle star (as reported in Du Preez et al., 2016). In comparison, *Anthoptilum* spp. rock pens were twice as abundant but inhabited deep, hard substratum. When present, the glass sponges were often the largest biological structures, especially in the case of the reef-forming species *Farrea omniclavata*, which formed complex, emergent mounds. Rare or small VME indicator taxa that could not be confidently resolved or counted—and therefore were not included in the analyses of this study—include anemones, tubeworms, and demosponges (order Actiniaria, family Sabellidae, class Demospongiae).

Distribution of Biogenic Habitats

Nearly 80% of the spatial records contain one or more VME indicators (79.5 ± 5.8% of records per transect; **Figure 5**), and almost half contain dense ($\geq$1 individual/colony·m^{-2}) assemblages of VME indicators (45.6 ± 9.6%; **Figure 5**). VME indicators were present at all depths, but density decreased as depth increased. Only one section of a single transect at depths below 465 m supported dense assemblages of VME indicators-the deepest end of AUV 4 (just 2.0 ± 2.0% of records per transect on the seamount flanks; **Figure 5**). Along the summit plateau, 60% (±9.5) of records per transect supported dense assemblages. The two shallowest transects, on or adjacent to the pinnacle (ROV 2 and 6; between 35 and 138 m depth), supported dense assemblages over their entire lengths (671 and 352 m). Records containing no VME indicators (0 individuals/colonies·m^{-2}) occurred most often on transects over sand.

Only three biological structures listed as NPFC VME indicator taxa (Primnoidae, *D. dianthus*, *D. pertususum*) were present on the summit plateau (**Figure 5A**); the rest of the NPFC VME indicators were concentrated below 225 m depth (**Figure 6**). Between ~160 and 200 m depth, low-density patches or built-up bioherms of *D. pertusum* were observed (**Figure 6**) but were rare (only 16 locations; **Table 1**). This stony coral occasionally co-occurred with hydrocorals and crinoids (e.g., **Figure 7A**). The small solitary stony cup coral (*D. dianthus*) had a similar depth distribution (**Figure 6**) but occurred more frequently (**Table 1**). From the small amount of imagery at 370 m (SFU 2, aborted dive), it is evident that we likely failed to detect dense aggregations of *Primnoa pacifica* that exist within the narrow sampling depth gap (**Figure 6**). These large Primnoidae corals co-occurred with sparsely distributed hydrocorals (**Figure 7B**). Within the deeper range of the survey, we observed forests of live soft corals and black corals (**Figures 7C,D**) concentrated on the flanks (**Figure 6**).

In comparison, the other VME indicator taxa (adopted by one or more RMFOs but not by the NPFC) were observed across the seamount (**Figure 5B**) and over the entire depth range surveyed in 2012 (**Figure 6**). The majority of these taxa were strongly depth-stratified (**Figure 6**), with the continuous living carpets of epifaunal-encrusted giant scallops (**Figure 7E**) found only on the vertical wall of the pinnacle, vast fields of hydrocorals (**Figure 7F**) and dense aggregations of crinoids (**Figure 7G**) mainly on the summit plateau, scattered sea pens on both the summit and flanks, and glass sponges on the flanks. It is likely that soft corals can inhabit shallower depths than we observed (i.e., above 225 m), given that we came across many dead Primnoidae remains on the summit plateau in the form of large stumps attached to the tops of boulders (**Figure 8**).

Geospatial analyses of Cobb Seamount in the context of the Northeast Pacific Ocean revealed that the 64 km^2 summit

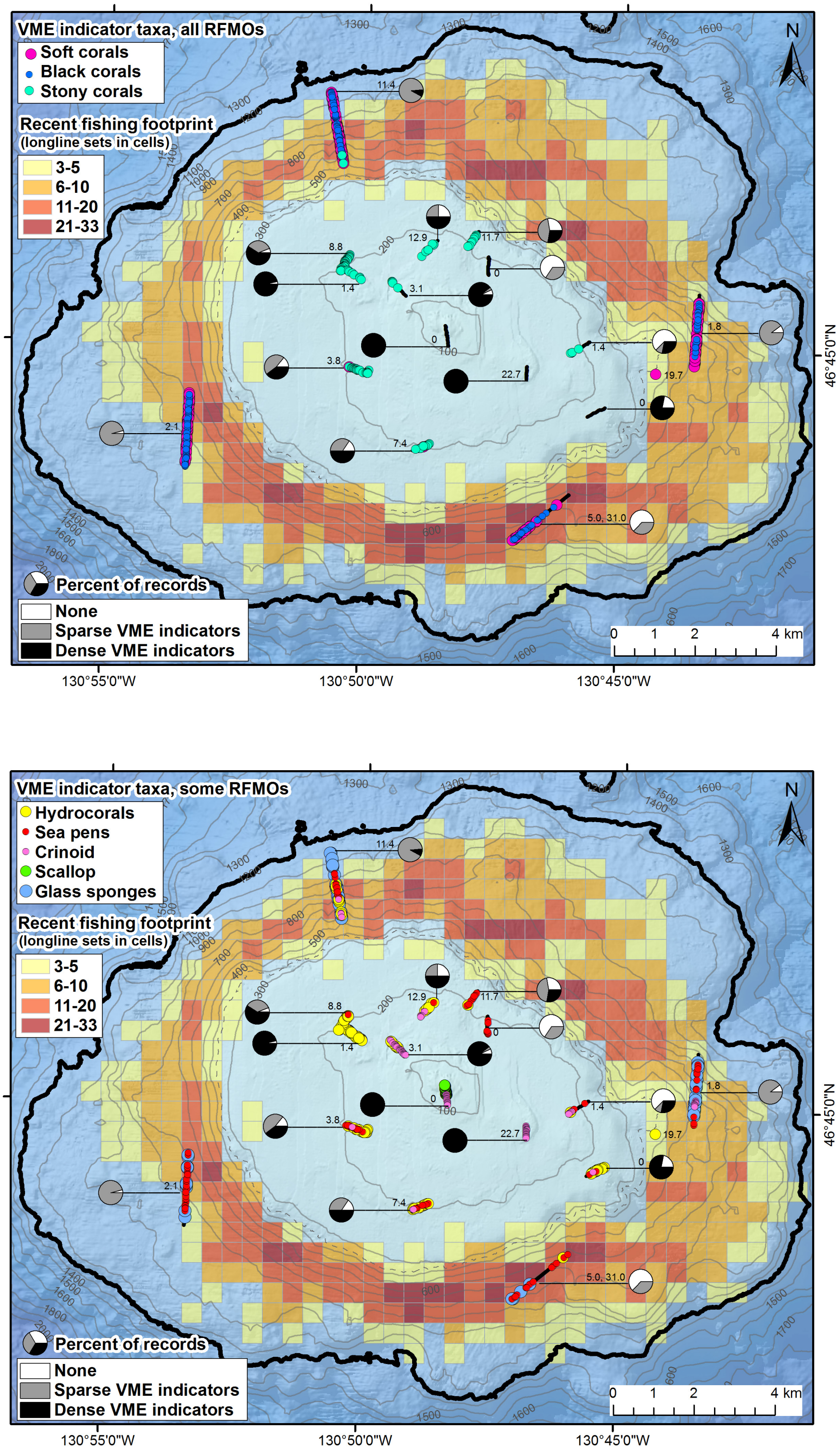

FIGURE 5 | Maps showing the densities and distributions of vulnerable marine ecosystem (VME) indicators, the recent longline fishing footprint and effort (1996–2017), and density of derelict fishing gear on Cobb Seamount. Pie charts show the percent of records per transect with no VME indicators (0 m^{-2}), sparse VME indicators (>0 and <1 m^{-2}), and dense VME indicators ($\geq$1 m^{-2}). The distributions of VME indicators are shown for taxa recognized by **(A)** all regional fisheries management organizations (RFMOs) and **(B)** those only recognized by some (not the North Pacific Fisheries Commission). The colored grid cells (500 m by 500 m) indicate the number of longline sets transecting each cell (cells with < 3 vessel removed to comply with "three-party rule"). The number adjacent to the transect is the density (km^{-1}) of derelict fishing gear observed (DFG; AUV 5 includes a second number, the density of drag mark incidents). Contour lines, 100 m depth intervals (350 and 1200 m in gray dashed and black bold, respectively).

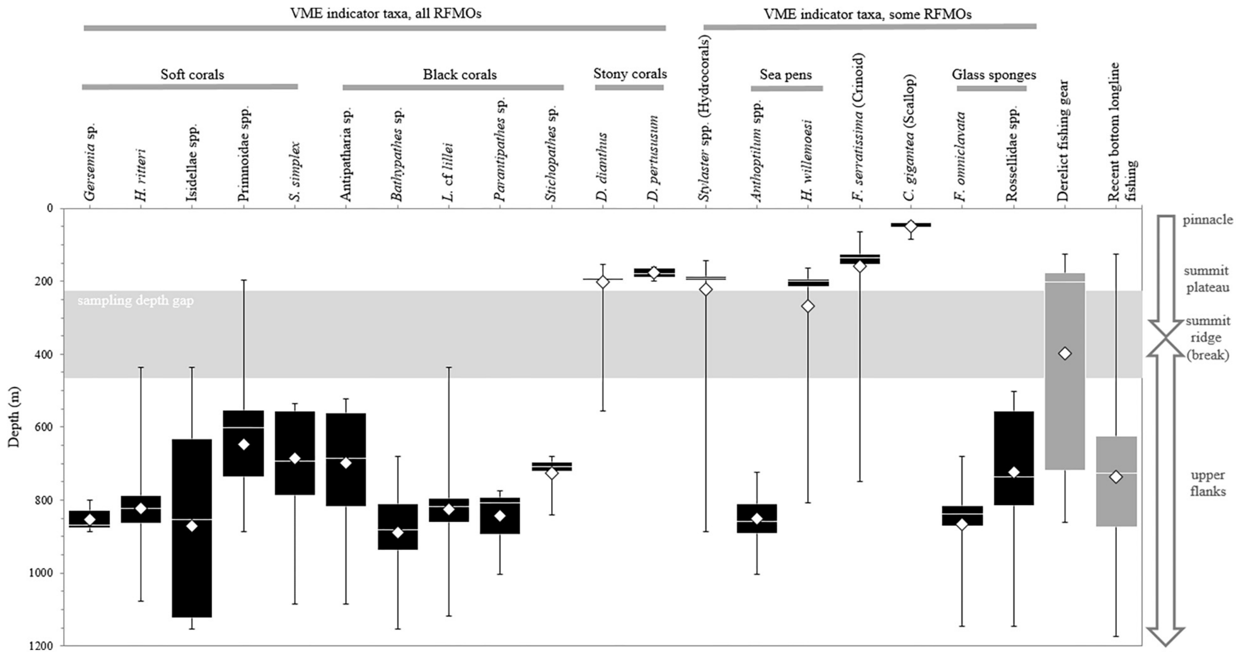

FIGURE 6 | Depth ranges of 19 groupings of habitat-forming biological structures and derelict fishing gear (DFG) on Cobb Seamount, observed during the 2012 visual survey, as well as the recent longline fishing effort. The listed taxa are vulnerable marine ecosystem (VME) indicators according to one or more regional fisheries management organizations (RFMOs; see **Table 1**). Boxes represent the 1st and 3rd quartile intervals, the white band represents the median (2nd quartile), the whiskers represent the minimum and maximum, and the diamonds represent the mean. There was a survey sampling depth gap between 225 and 465 m (shaded area).

plateau (2D area; **Figure 9A**) is regionally unique habitat. The nearest seafloor to Cobb Seamount above 350 m depth is 340–400 km away, either on the small summit of Union Seamount or the top of the Canadian continental shelf (**Figure 1**). In comparison, approximately 70 km^2 of the seamount is between 350 and 900 m depth (2D area; **Figure 9A**)—the seafloor within this depth range occurs on three seamounts within 100 km of Cobb Seamount (Pipe, Cobb Far, Brown Bear; **Figure 1**).

Distribution of Recent Fishing

We obtained information on the fishing activity of 12 Canadian-registered vessels operating on Cobb Seamount between January 1996 and December 2017. Over this period, Canadian vessels deployed 466 bottom longline sets on the seamount: 95% longline traps and 5% fixed hook. Sablefish were landed during nearly every set (99%), while rockfish, other groundfish, and crabs were also landed with some frequency (e.g., 22% of fishing events landed rougheye rockfish).

Over the 22 years, Canadian fishing efforts spanned depths from 96 to 1253 m on Cobb Seamount, with an average fishing depth of 736 ± 1.39 m (**Figure 6**). The majority of fishing occurred between 625 and 875 m depth (1st and 3rd quantiles; **Figure 6**) with only two sets extending below 1200 m. These intensively fished depths overlap with the observed depth distribution of multiple VME indicator taxa, including all of the soft and black corals, as well as the rock pen and glass sponges (1st and 3rd quantiles; **Figure 6**).

From the survey transects that occurred within the fishing footprint (**Figure 5**), we recorded a significant, negative correlation between the number of longline sets and the average density of VME indicators (Spearman test r −0.650, n 20, p 0.002; **Figure 10**). We observed an average of approximately one individual/colony·m^{-2} in a cell (500 m by 500 m) fished once, and almost no VME indicators in cells fished 20 or more times. Our dataset included up to 25 longline sets in a single cell (**Figure 10**). Contrary to the trend of lower VME indicator density at greater depths, the only dense assemblages of VME indicators ($\geq$1 individual/colony·m^{-2}) were observed at some of the deepest depths surveyed (960–1154 m depth), on the northern AUV 4 transect below the fishing footprint (**Figure 5B**).

The recent bottom longline fishing footprint provides a conservative estimate of the VME indicator habitat impacted by fishing. In total, we estimate the area affected by direct physical contact with recent bottom longline gear (above 1200 m depth) is 1.8 km^2 (0.8%) assuming little to no gear movement (scenario 1) or 74.4 km^2 (33.8%) assuming moderate gear movement (scenario 2; **Figure 9B**). This fishing intensity (and therefore potential for impact) was not evenly distributed, with some areas fished multiple times (i.e., several overlapping sets; **Figure 5**). The intensity of fishing impact was also interpreted in light of the bathymetry. Each depth interval has a different total area (**Figure 9A**). Thus, while 800–850 m is the most fished depth-interval, if we account for the area of each depth band, the relatively thin 650–700 m depth interval had the highest relative impact from fishing under scenario 2 (7.4 km^2, or 84.9% of the

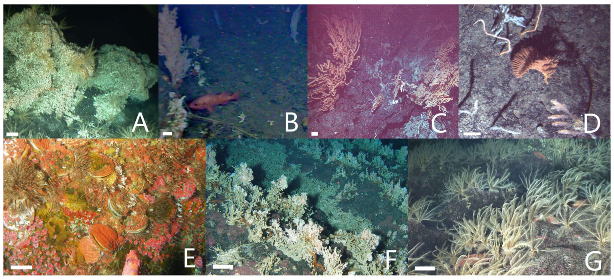

FIGURE 7 | Examples of potential vulnerable marine ecosystems (VMEs): biogenic habitats typified by a variety of biological structures, all of which are VME indicator taxa adopted by one or more regional fisheries management organizations (RMFOs; see **Table 1**) and within the fishing footprint. **(A)** Mixed gardens including stony coral bioherms (*Desmophyllum pertusum*). **(B)** Diverse forests including soft corals and others (*Primnoa pacifica*, *Desmophyllum dianthus*, *Stylaster* spp.). **(C)** Aggregations of soft corals (*Keratoisis* spp. A). **(D)** Diverse clusters of soft and black corals (*Heteropolypus* ritteri, *Keratoisis* sp. B, *Bathypathes* sp., *Lillipathes lillei*, *Chrysopathes speciosa*). **(E)** Epifauna-encrusted mats of giant scallops (*Crassadoma gigantean*). **(F)** Vast fields of hydrocorals (*Stylaster* spp.). **(G)** Dense aggregations of crinoids (*Florometra serratissima*) hiding barely visible small rockfish (*Sebastes* spp.). Most images are side-view (from the ROV on the pinnacle or summit plateau) with the exceptions of **(C,D)**, which are downward-facing (from the AUV on the flanks). **(B)** Is a lower quality side-view (from the aborted dive SFU 2 at the summit ridge). White scale bars =10 cm.

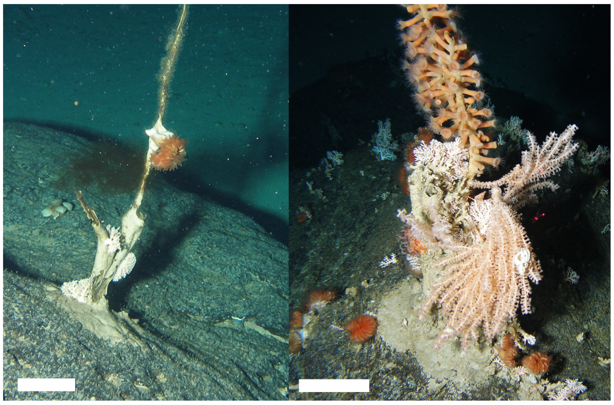

FIGURE 8 | Large stumps attached to the tops of boulders constituted the majority of "soft coral" observations on the summit plateau (cf Primnoidae). Scale bars, 10 cm.

depth band; **Figures 9B,C**). Based on only this one fishing dataset, we estimate ≥75% of the seafloor between 550 and 850 m depth has been impacted (under scenario 2; **Figure 9C**).

While the intensity of fishing was not even among all depths, the general distribution of fishing shows only slight spatial patterns related to aspect: there were 20% fewer sets on the western flank compared to the eastern flank, but no notable difference in fishing effort on the northern and southern flanks (**Figure 5**). There was also no difference in the distribution of fishing effort in relation to traps or hooks.

While this recent fishery has mainly focused on the upper flanks of Cobb Seamount, Canada's sablefish fishing has shoaled slightly over time: the average shallowest and deepest points of longline sets changed from 689 ± 14 to 599 ± 16 m depth and 866 ± 13 to 826 ± 14 m depth (Wilcox Test p 0.002 and $<<$ 0.001) between 1996 to 2005 (n = 246) and 2006 to 2017 (n = 220). The reason for the shift by tens of meters is unknown, but could be the result of a change in the orientation of the sets. Earlier sets were mostly orientated with-slope (crossing a large depth range), whereas latter sets were orientated more across-slope just below the summit ridge (crossing a narrower depth range). This spatial data is not shown to respect privacy considerations for commercial fishers.

Distribution and Impacts of DFG

As is typical of deep-sea benthic visual surveys, the 13.5 km of annotated transects cover just 0.0001% of the seafloor above 1200 m depth on Cobb Seamount (i.e., 0.029364 km^2 of the 220 km^2 fishable 2D area). Yet, within that small area, we observed 102 incidents of DFG (n = 72) or putative drag marks (n = 30) (**Table 2**). We distinguished eight categories of gear (**Table 2**): longline groundlines (36% of gear incidents; **Figure 11A**), pieces of rope (26%), monofilament gill netting (21%; **Figures 11B,C**), rope netting (7%; **Figure 11D**), clumps of rope or netting (4%), anchors (2%), anchored float lines (1%), and trawl netting (1%). We observed some DFG outside of the recent fishing footprint (**Figure 5**) and depth distribution (**Figure 6**), suggesting that it was lost many years to decades ago by historical fishing. We also noted some gear was lost so long ago that there was coral growth on it (e.g., on lines extending into the water column; **Figure 11E**). Other types of anthropogenic litter were also observed, such as fabrics, plastics, and aluminum cans.

Derelict fishing gear was identified on 82% of transects, for an average frequency of 7 incidents·km^{-1} (**Figure 5**). The highest density of gear on a single transect was 22.7 incidents·km^{-1} (ROV 5; **Figure 5**). The majority of gear was observed between 176 and 718 m depth (1st and 3rd quantiles; **Figure 6**). While a mix of gear was observed on the summit plateau and ridge (≤350 m depth), the gear most frequently observed on the flanks was longline groundlines (**Table 2**). Over half of these observations were from a single transect on the northern flank, AUV 4 (**Figure 5**). Drag marks in the absence of DFG were only observed on one deep transect (AUV 1, between 620 and 820 m depth), on the southeast flank, at a frequency of 31 incidents·km^{-1} (**Figure 5**). It is impossible to say for certain whether each photo of drag marks represents its own fishing event (**Figure 11F**) or whether some of the spatially distinct photos documented drag marks created by the same fishing event, but it is likely most were separate events since the drag marks did not run parallel to the transect line (we assumed straight line sets), and the drag marks were within one of the heaviest recently fished areas (**Figure 5**).

For 58% of DFG we detected, there was an associated observable ongoing impact, such as habitat alteration and ghost fishing (**Table 2**). Gear entangled in corals was the most frequently observed form of habitat alteration (49%). Entangled corals, such as tall stands of branching soft corals (**Figure 11A**) or large clusters of short hydrocorals (**Figure 11B**), were either dead, damaged, or toppled. Within the limited field of view (∼2 m

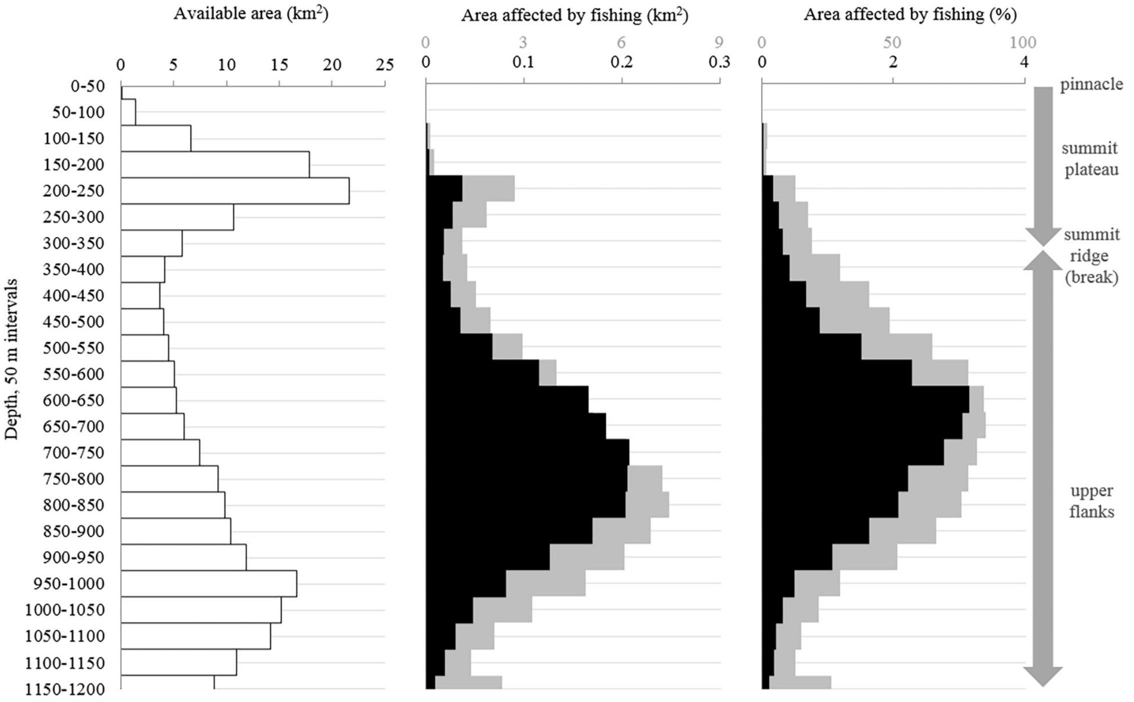

FIGURE 9 | The distribution of **(A)** the available area of each 50 m depth-interval, **(B)** the area affected by the 1996–2017 bottom longline fishing using two scenarios, and **(C)** the percentage of the available area affected by the fishing. Scenario 1 assumes there is little to no movement of traps on the seafloor (black). Scenario 2 assumes there is moderate movement (100 m lateral sweep; gray).

across on average), we observed almost 60% of derelict longline ground lines entangled in dead or damaged corals. Almost all nets were entangled in corals, dead fish, or both (**Figures 11B–D**). Although it was not possible to resolve all dead fauna, the fresh carcasses of widow rockfish were readily visible (**Figure 11C**).

DFG was observed at an average density of 2,785 ± 1,003 observations·km^{-2}. At this rate, we estimate a comprehensive survey of the seamount would encounter DFG 612,651 ± 220,565 times. If we err on the conservative side by omitting DFG that would likely be encountered numerous times on such a survey (i.e., the expansive longline ground lines, which accounted for 26 or ~1/3 of our DFG observations; e.g., **Figure 11E**), an estimated 408,434 ± 147,043 separate observations of DFG might still be recorded on Cobb Seamount, based solely on the frequency of relatively confined clumps of net or lines we identified. Given that the 2012 survey overlapped a small fraction of the recently fished areas, excluding the areas of highest intensities (**Figures 5**: dark red cells), we should consider this extrapolation to be a conservative one.

DISCUSSION

VME Indicator Taxa

Like some other RMFOs, the NPFC has a descriptive definition of VMEs but is still in the process of identifying the minimum density, abundance, and/or spatial footprint at which certain biological structures would constitute a VME. Thus we cannot identify locations of VMEs from our data at this point, but we can describe the distribution and nature of habitat-forming organisms regarded as indicators of VMEs.

We found VME indicator taxa widely distributed on Cobb Seamount and forming biogenic habitats that meet the descriptive VME criteria defined by FAO (e.g., summits and flanks of seamounts with cold-water corals and sponges and communities of dense emergent fauna that form an important structural component of the habitat; FAO, 2009). The majority of the seafloor surveyed supported at least sparsely distributed VME indicators, and nearly half of the surveyed area supported dense assemblages with at least one VME indicator per square meter. In a first pass consensus of experts from around the world, 0.1 colonies per square meter for soft or black corals was commonly considered to constitute a VME (data from three oceans, including the Pacific Ocean; Baco-Taylor et al., 2019). The most densely aggregated VME indicators occurred on the shallow summit plateau and pinnacle, while a small patch occurred much deeper, below the recent fishing footprint.

Our observations of close associations between VME indicators and a variety of other taxa align with the documented role of these biological structures as substrates for attachment, nursery grounds, feeding grounds, and refugia that generally support higher levels of biodiversity and productivity than surrounding habitats (cf Hart and Chute, 2004; Buhl-Mortensen et al., 2010). Hydrocorals and crinoids,

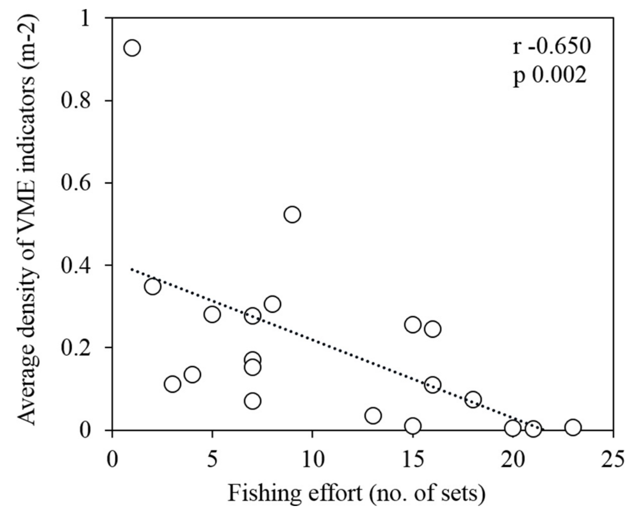

FIGURE 10 | A significant negative correlation between the average density of vulnerable marine ecosystem (VME) indicators (m^{-2}) and the fishing effort (number of transecting longline sets) within grid cells of 500 m by 500 m (Spearman test r –0.650, n 20, p 0.002).

in particular, were observed in association with commercially important fish (also documented on the adjacent continental slope; Stone, 2006; Tissot et al., 2006). Areas with the highest densities of biological structures (hydrocorals and crinoids) also supported the highest density and richness of rockfish (cf Du Preez et al., 2016). Similar usage of coral structures by rockfish to seemingly station-hold has also been documented on the adjacent coast (Du Preez and Tunnicliffe, 2011).

The composition and density of biological structures were strongly depth-stratified (cf Du Preez et al., 2016). Two major bathymetric boundaries between the biogenic habitats were evident, with continuous mats of giant scallops on the pinnacle above 90 m depth, fields of hydrocorals and fields of crinoids on the summit plateau between 90 and 350 m, and sparser forests of soft and black corals on the upper flanks below 350 m. Above the summit plateau ridge, on the shallower section of the seamount, biological structures tended to occur as single-taxon dominated assemblages in high densities over large areas. Below the ridge, biological structures were distributed in patches of mixed assemblages. There are likely other biogenic habitat types that merit conservation and management considerations in deeper waters of Cobb Seamount; our observations are limited to the biological structures above 1200 m depth. Ideally, future surveys of Cobb Seamount would include the deeper regions of the flanks, as well as the depth range "missed" by the 2012 expedition.

Fishing

Cobb Seamount has been impacted by historical fishing, which included heavy-duty bottom tire trawls, a recent bottom longline fishery for sablefish, which focuses predominantly on the upper flanks of the seamount but is showing evidence of moving shallower and close to the summit ridge, and widely distributed DFG resulting from these activities. These past and present fisheries represent over 50 years of (known) fishing on the summit plateau and upper flanks above 1200 m depth of the seamount, a relatively small area of less than ∼20 km by 15 km or ∼220 km^2.

Our impacted area estimates highlight the critical value of spatial fishing data and the importance of comprehensive fishing records when mapping fishing effort. Our impacted area estimates of 1.8–74.4 km^2 (0.8–33.8% of the seamount surface; scenario 1 and 2) include just 87 trips by Canadian vessels over 22 years. While we don't have data on the historical fishing effort of other nations bordering the North Pacific Ocean, US fishing vessels made twice as many trips to Cobb Seamount in almost half the time with mid-water trawl and bottom longline gear (1991–2003; Douglas, 2011). Presumably, the collective footprint of Japanese, Russian, American, and Canadian fisheries (using a variety of gear types) is an order of magnitude larger than we have documented for the Canadian Sablefish fishery alone. The longline fishery is considered to have a lower impact on VMEs than bottom trawls (Pham et al., 2014). While traps have a small footprint and are intended to be stationary, bottom trawls can be 75–150 times as wide (100–200 m; Clark and Koslow, 2007) and are specifically engineered to drag across the seafloor (∼footprint = tow distance × door or beam spread; DFO, 2018). In addition, undocumented (illegal, unreported, and unregulated) fishing is a major issue to ocean sustainable development, recently identified as such by the United Nations goal to conserve and sustainably use the oceans, sea and marine resources (no. 14; UN, 2019). The combined historical and undocumented fishing footprints would undoubtedly show that the proportion of each impacted habitat type (i.e., depth band) is more substantial than our estimates.

Based on the consolidation of the best available information and the recent Canadian fishing effort, it is reasonable to infer the bottom-contact fishing footprint on Cobb Seamount extends from its pinnacle to at least 1200 m depth, inclusive of the summit plateau, summit ridge, and the upper flanks. Since fisheries target the summits of seamounts and bottom trawl gear is at least landed on the summit to stabilize before towing down the flank (Clark and Dunn, 2012), it is highly likely the summit plateau and ridge were at least fished by bottom trawling. Use of this gear on the summit plateau could explain the large scale hydrocoral rubble fields. The depth distributions of the dominant rockfish species caught by the bottom-contact and mid-water fisheries (summarized in Curtis et al., 2015) further support the inference that the summit plateau was historically fished: rougheye and widow rockfish were observed on Cobb Seamount confined between 107 and 373 and 37 and 198 m depth, respectively (Du Preez et al., 2015). Moving deeper, the main commercial depth range for sablefish in the region covers the upper flanks of Cobb Seamount, from 500 to 1000 m depth (Clark et al., 2015). That said, the recent Canadian sablefish fishing effort extends from approximately 100 to beyond 1200 m depth (Fisheries and Oceans Canada [DFO], 2013).

TABLE 2 | Documentation of derelict fishing gear (DFG) abandoned, lost, or otherwise discarded, and observable impacts during 2012 visual survey.

Derelict gear	Incidents, *n*	Depth, av. (m)	Percent with observable impact(s)	Primary observable impact(s)
Longline ground line	26	528	58%	Entangled in dead/damaged coral
Pieces of line	19	596	16%	Entangled in dead/damaged coral
Monofilament net	15	171	93%	Entangled in dead/damaged coral; caught, dead fish
Rope net	5	176	100%	Entangled in dead/damaged coral; caught, dead fish
Mass of rope/net	4	191	100%	Entangled in habitat/smothering
Anchor	2	153	50%	Entangled in habitat/smothering
Anchor and float line	1	176	0%	Entangled in habitat
Total				
Putative drag mark(s)	30	718	0%	na

*See **Figure 11** for representative photographs.*

Spatial Overlap of Fishing and VME Indicators

All the VME indicators we observed on the 2012 survey (living or dead) overlap with the known fishing footprint on Cobb Seamount. We also documented a negative correlation between the density of VME indicators and the intensity of the known fishing effort. Ideally, we would have compared Cobb Seamount as a whole to a similar but unfished neighboring seamount, but Cobb Seamount is unique and no such site exists. Further research is necessary to determine if and how fishing influences VME indicator densities; however, we noted that every hydrocoral field we surveyed (n = 9 transects) showed signs of physical damage. While colonies of *Stylaster* spp. are relatively short (<20 cm) in comparison to some of the soft corals and glass sponges (meters tall), they are the densest and most abundant coral observed on Cobb Seamount. Kaiser et al. (2006) recognized that even a low-level impact that occurs on a relatively large spatial or temporal scale can result in serious ecological consequences. Du Preez et al. (2015) estimated that over half the substrate in the hydrocoral communities on Cobb Seamount was comprised of mixed mats of dead hydrocoral rubble. We observed live corals in areas that could be regarded as natural refuges from gear (i.e., areas of higher physical complexity). The hydrocoral fields were observed in a small, rare depth-interval (between ∼150 and 250 m depth, an area of only 40 km^2); beyond Cobb Seamount, the nearest seafloor at this depth interval is 340–400 km away.

We recognize that our visual observations represent the minimal damage experienced as some evidence of impacts would have been removed as bycatch (entire organisms or colonies), washed away by currents (fragments), decomposed, degraded, or consumed. This is especially true for fishing events that occurred in previous years and decades. On Cobb Seamount, we did not observe enduring evidence of physical damage to many of the VME indicator taxa. For instance, even though *F. serratissima* is semi-mobile and able to swim short distances when disturbed (Lambert and Austin, 2007), such crinoids are known to be easily destroyed by physical contact with mobile fishing gear (Smith et al., 2000). Similarly, the brittle tissue of glass sponges cannot withstand the mechanical impact of fishing gear and readily crumbles into fragments (Krautter et al., 2001). The persistent signs of physical damage to VME indicator taxa on Cobb Seamount were largely limited to the robust calcium carbonate skeletons of corals that remain on the seafloor and also the punitive drag marks, which can persist for years to decades on deep soft-sediment (Clark et al., 2015; De Leo et al., 2017).

DFG, Impacts and Potential Consequences for VME Taxa

It is expected the full impact of DFG is more extensive than what we observed in our snapshot of Cobb Seamount. The longline groundlines extended beyond our visual field of view. If entire longline sets were lost or abandoned, these incidents could represent, on average, almost 3 km of longline groundline, plus the associated traps or hooks, and the anchors, float lines, etc. While the majority of DFG was anchored or entangled and had spatial footprints on the order of meters-squared or less, this does not necessarily equate to a small impact. For instance, we observed "fresh" fish carcasses entangled in small clumps of gill nets. The last reported use of gill nets on Cobb Seamount is in 1989 (Douglas, 2011), meaning that it is possible this DFG has continued to ghost fish and self-bait for at least 30 years. In addition to the impact of DFG potentially having a large temporal scale, the spatial scale is magnified when the entangled biogenic structures (e.g., coral skeletons) eventually breakdown, freeing the gear to be mobile once again.

The spatial frequency of the DFG observations was, in general, a magnitude greater than reports from similar ROV surveys on offshore fishing grounds. We observed an average of 7 items·km^{-1} and up to 29 items·km^{-1} of DFG. In comparison, the litter density on Condor Seamount (Azores) was estimated as 3 items·km^{-1} (DFG and other types of litter; Pham et al., 2013) while the maximum observed on the seamounts of Gorringe Bank (Southwest of Portugal, in ABNJ) was up to 4 items·km^{-1} (Vieira et al., 2015). Our densities are more comparable to observations of litter or derelict commercial gear in nearshore deep-water systems (e.g., litter in Saint Vicente canyon: av. 16.7 ± 14.4 items·km^{-1}; litter in Lisbon canyon: 13.2 items·km^{-1}; commercial fishing gear off central California: 5-7 ± 1-2 items·km^{-1}; Watters et al., 2010; Mordecai et al., 2011; Oliveira et al., 2015). Considering the seamount's remote location, and given findings from other fishing grounds, the density of DFG observed on Cobb Seamount in 2012 is unexpectedly high.

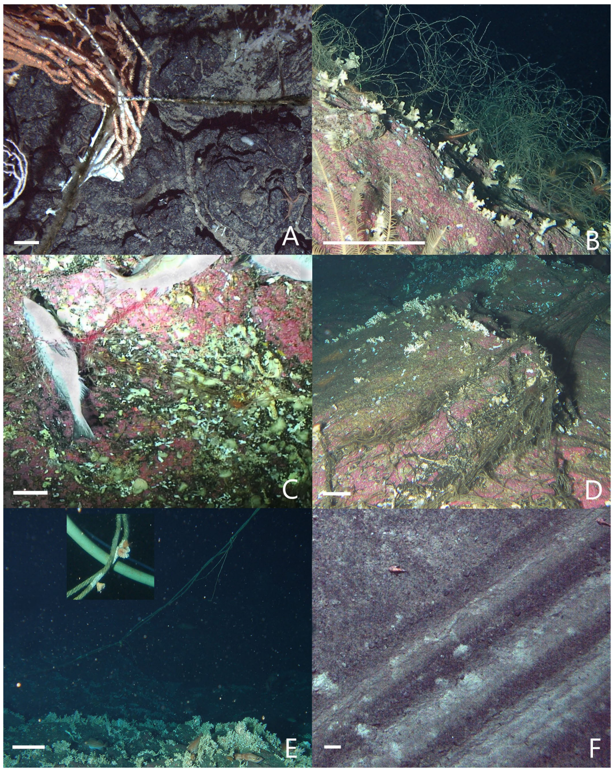

FIGURE 11 | Examples of observable impacts caused by derelict fishing gear (DFG) abandoned, lost, or otherwise discarded on Cobb Seamount, from the 2012 visual survey. **(A)** A fouled longline passing through a toppled and damaged large sea fan (*Keratoisis* sp. A), surrounded by fragments of broken corals. **(B)** Monofilament net entangled in the stumps of dead and broken hydrocorals (*Stylaster* spp.) and **(C)** the carcasses of dead rockfish (*Sebastes* spp.). **(D)** A rope net spread across coral habitat, overlaying stumps of dead and broken corals. **(E)** An anchored longline groundline with dangling branch lines, attatched to floating gear, ascending into the water column. Cup coral growth on the gear is evidence it was lost years to decades ago (shown in inset image). **(F)** Putative drag marks in soft sediment with no associated DFG. Most images are side-on view, but the first and last images are downward-facing (from AUV). White scale bars =10 cm.

We propose the high density of DFG on Cobb Seamount is the result of a combination of factors and also not the result of the recent fishing alone. For instance, the majority of DFG observations did not overlap with the recent fishing footprint and over 27% of DFG were nets (not bottom longlines). The seamount is an attractive fishing ground due to its unusually shallow, flat top and *in situ* primary production by kelp and other algae, but fishers report very rugged terrain and gear hazards (Pearson et al., 1993; Douglas, 2011), which may convey a greater risk of entanglement and gear loss. Cobb Seamount was also heavily fished by multiple nations using multiple gear types for over half a century before the cooperative management and oversight of the NPFC came into force in July 2015 (North Pacific Fisheries Commission [NPFC], 2017, 2018). Not all of the DFG on Cobb Seamount would include items that could harm vulnerable species, and not all types of lost gear are equally damaging, but we can confidently estimate that tens to hundreds of thousands of items of DFG currently exist on Cobb Seamount. This DFG poses an ongoing threat to biological structures, the biogenic habitats they create, and the species they support.

Conservation and Management Applicability

Identification of VMEs

The NPFC is authorized to adopt conservation and management measures to prevent SAIs to VMEs in its convention area (North Pacific Fisheries Commission [NPFC], 2017, 2018). The presence of an indicator alone is not sufficient to identify a VME (FAO, 2009); however, the distribution, density, and nature of structure-forming species is highly relevant to the definition and identification of VMEs. Thus our survey data, along with surveys of other North Pacific seamounts (e.g., Miyamoto et al., 2017; Baco et al., 2019), can provide scientific guidance. Once the crucial VME definitions are established for application in the North Pacific Ocean, these data may be useful to identify VMEs in the NPFC convention area (North Pacific Fisheries Commission [NPFC], 2017, 2018). Presently, there are two potential VMEs identified in the NPFC convention area on C-H and Koko seamounts. Both are part of the Hawaiian-Emperor seamount chain in the Northwest Pacific Ocean (North Pacific Fisheries Commission [NPFC], 2018); but there are none yet identified in the Northeast Pacific Ocean (North Pacific Fisheries Commission [NPFC], 2017).

Like most RFMOs, the NPFC presently employs a move-on rule to limit damage to potential VMEs (North Pacific Fisheries Commission [NPFC], 2017, 2018); this rule establishes a 50 kg bycatch limit/threshold for soft, black, and stony coral taxa. When this threshold is reached, a >2 nautical mile fishing buffer is required to prevent SAIs, and the encounter would then be reported to the NPFC Secretariat so appropriate measures can be adopted in respect of the potential VME (North Pacific Fisheries Commission [NPFC], 2017, 2018). While this move-on rule is an important measure, it is subject to the catchability bias of different types of gear and organisms (Auster et al., 2010). For instance, while trawl nets are more likely to retain large durable intact organisms as bycatch, light, brittle, and flexible organisms, such as abundant hydrocorals on Cobb Seamount, readily pass through the mesh (Auster et al., 2010). Other types of gear with the potential to shear and entangle organisms (e.g., the longlines, traps, and hooks currently used on Cobb Seamount) do a poor job at retaining most types of VME indicator taxa (Auster et al., 2010). Using the combination of data from the 2012 visual survey and previous collections, we can estimate that a relatively small ~30 m^2 patch of a hydrocoral field supports the equivalent of the bycatch limit, ~50 kg of hydrocorals. This relationship between the bycatch limit and *in situ* images is based on the average height and density of colonies from the visual survey (conservatively 10 cm and 40.0 colonies·m^2) and unpublished wet weight data for 53 specimens from the Royal BC Museum collection (average height-weight ratio 44.8 g for 10 cm tall hydrocoral colonies/fragments; Merlin Best, personal communication). In comparison, the footprint of a single bottom-contact fishing event is several orders of magnitude larger than the area estimated to support 50 kg of this VME indicator taxa.

Non-invasive identification of VMEs, such as visual surveys and predictive models, and spatial management, such as fishing closures, are likely to be more effective at protecting potential or established VMEs than bycatch move-on rules (Clark and Dunn, 2012). Efforts to standardize methods for VME identification from image-based data are ongoing (Morato et al., 2018; Baco-Taylor et al., 2019; Deep-Ocean Stewardship Initiative [DOSI], 2019) and will be necessary to reduce the overlap between fishing effort and VMEs.

While image-based surveys for VME-indicators are promising, the data are not without limitations. The VME indicator taxa found on Cobb Seamount may tolerate wider depth ranges than those we documented, but we did not survey the distribution, density, or composition of benthic ecosystems pre-disturbance or post-recovery. Our observations are a snapshot of only those taxa that have persisted at detectable levels after over half a century of bottom-contact fishing activity. Because non-detection alone is not evidence of species absence, the results we present are a conservative estimate of where VME indicator taxa may be found. For future work, it would be highly valuable to obtain estimates of detection probability for VME indicator taxa when using ROVs and AUVs.

Identification of SAIs

Once VMEs are defined and identified, determining whether the impacts of fishing gear to biological structures and the biogenic habitats they create qualify as an SAI—therefore requiring actions be taken to prevent these impacts—requires consideration of six factors identified by FAO (2009) and the North Pacific Fisheries Commission [NPFC] (2017, 2018). Our findings provide new scientific information for many of these factors, such as the intensity of the impact at the specific site and the impact relative to the availability of the habitat type affected. While many questions remain concerning the severity of the ecosystem-level impacts of bottom-contact fishing, it is prudent to respond quickly to the best available scientific information to establish appropriate and effective conservation measures that protect vulnerable biological structures persisting on Cobb Seamount, such as on its unique summit plateau, and elsewhere in ABNJ. Once the long-term consequences to benthic communities are readily apparent and repeatedly documented, the opportunity to conserve these unique offshore oases may no longer exist, especially if fishing activity shifts in location (e.g., shoaling on Cobb Seamount) or intensity increases over time.

Potential for Recovery

While our study did not attempt to quantify ecosystem-level consequences or SAIs of bottom-contact fishing on Cobb Seamount, we anticipate that the degradation or complete removal of the vulnerable biological structures has and will continue to negatively impact the functional significance of these ecosystems. These impacts may be exacerbated by larger-scale threats to deep-sea environments, such as the ongoing expansion of the Northeast Pacific Ocean oxygen minimum zone attributed to global climate change (Whitney et al., 2007; Cummins and Ross, in review). Further, the ability of the unique ecosystems on Cobb Seamount to recover from historical and ongoing harm may be hampered by a low probability of rescue from adjacent (but distant) populations by immigration or dispersal of new recruits. However, to determine if rescue events are possible, further research is required to examine the endemism and connectivity of populations on submarine features in the Northeast Pacific Ocean (Shank, 2010), potentially building on dispersal strategy research by Parker and Tunnicliffe (1994).

Even after recolonization, the rate of ecosystem recovery is likely to be on the order of decades to centuries for many of the slow-growing biological structures we observed on Cobb Seamount (Roberts and Hirshfield, 2004; Murillo et al., 2011; Clark et al., 2019). Some scallops and crinoids are estimated to live decades (MacDonald et al., 1991; Murillo et al., 2011), glass sponges can live hundreds of years (Samadi et al., 2007), and sea fans can grow as little as a centimeter or two per year (Andrews et al., 2002, 2009) and live thousands of years (Roark et al., 2006; Rogers et al., 2007). That said, in 2012, we observed signs that damaged hydrocoral fields on Cobb Seamount might be starting to recover from large-scale physical impacts, 30 years after the last documented trawling events occurred in the area. These observations were limited to some branch regrowth on dead hydrocoral stumps and small live colonies amid the rubble of dead colonies and are similar to findings on previously heavily fished seamounts within the Northwest Pacific Ocean (Baco et al., 2019).

NPFC VME Indicator Taxa List

Most of the dense aggregations of biological structures we documented on Cobb Seamount are considered to be VME indicators by other RFMOs and commissions (Commission for the Conservation of Antarctic Marine Living Resources, Northwest Atlantic Fisheries Organization, North East Atlantic Fisheries Commission, South East Atlantic Fisheries Organisation, South Pacific Regional Fisheries Management Organisation), but are not currently listed as such by the NPFC (**Table 1**). These include hydrocorals, sea pens, crinoids, giant scallops, and sponges. These taxa are equally fragile and vulnerable to SAIs from bottom-contact fishing damage as those on the interim list of NPFC VME indicators (already assessed by other RFMOs; **Table 1**). They are also a hundred times more abundant on Cobb Seamount and typify the largest biogenic habitats. We documented further evidence of their functional significance and regional uniqueness, and have reviewed obstacles to their recovery (criteria of VMEs; North Pacific Fisheries Commission [NPFC], 2017, 2018).

The current interim NPFC VME indicator taxa were based on the analysis of bottom-trawling bycatch that landed on deck (Miyamoto and Kiyota, 2017). Ideally, VME indicator taxa would be identified by fishery-independent means, given that trawl nets, longlines, and other bottom-fishing gear have low catchability for most sessile benthic organisms (Ardron et al., 2014) and are therefore heavily biased against sponges, fragments of hydrocorals, and other fragile animals. If Cobb

Seamount is an indicator of the North Pacific Ocean in general, the exclusion of hydrocorals, crinoids, and sponges from the NPFC's interim VME indicator list creates a depth- and spatial-related bias in potential VME protection, given that these species form extensive biogenic habitats on the historically heavily fished summit plateau of Cobb Seamount, rather than in the deeper waters inhabited by the NPFC's interim VME indicator taxa.

One systematic approach considers a high ranking in just one VME criterion to be sufficient for a taxon to be considered a potential VME indicator (Ardron et al., 2014). Given that hydrocorals and sponges meet multiple FAO VME criteria and occur throughout the North Pacific Ocean (e.g., Miyamoto and Kiyota, 2017), a resolution to include them among the NPFC VME-indicator taxa was recently proposed at the 2018 NPFC/FAO Workshop on the Protection of VMEs in Yokohama, Japan (Rooper and Kiyota, 2018). This resolution has not yet passed, but capacity and precedence to do so exists—the NPFC ranks relatively high among RFMOs for its management resources (Bell et al., 2019) and other RFMOs have adopted additional VME indicators in light of new information (e.g., North Atlantic Fisheries Organization [NAFO], 2009; Murillo et al., 2011). Not all of the VME indicator taxa included in this study are adopted by every RFMO, but the survey of biogenic habitats on Cobb Seamount supports the inclusion of these taxa as VME indicators within the North Pacific Ocean.

Protection of Northeast Pacific Seamounts

If partial protection for Cobb Seamount was to be considered (similar to the two existing Northwest Pacific Ocean closures; North Pacific Fisheries Commission [NPFC], 2018), our data could be useful to managers seeking to maximize ecological benefits and minimize economic impacts. That said, partial protection of marine features can be problematic, given the minimal operational area requirements for fishing activities, the tendency for the most productive and most fished areas to overlap, and because the spatial scales functionally meaningful to organisms may be large or difficult to determine (Clark and Dunn, 2012). While the current fishing effort on Cobb Seamount is relatively modest, it has fluctuated over time and could increase again, should existing or future Members of the NPFC request to fish the same footprint or new areas of the seamount (North Pacific Fisheries Commission [NPFC], 2017, 2018).

Any historical or future bottom-contact fishing impacts on Cobb Seamount are likely to be exacerbated due to the volcano's conical shape and steep flanks, which support a high-turnover of habitats associated with narrow depth bands (cf McClain et al., 2010; Du Preez et al., 2016; Victorero et al., 2018). In other words, each depth-stratified biogenic habitat on this seamount exists in a naturally fragmented and finite area and is relatively rare—rarer still considering the surrounding deep seafloor and open ocean. According to ecological niche and island biogeography theories, rarity and isolation increase the vulnerability of these habitats to an unnatural increase in disturbance regime (MacArthur and Wilson, 2001; Gallagher et al., 2015), such as that caused by bottom-contact fishing.

Cobb Seamount is already classified by the Convention on Biological Diversity as an Ecologically and Biologically Significant Area (EBSA) that supports ocean health and ecological services, predominantly because of its benthic ecosystems (Convention on Biological Diversity [CBD], 2016) and a high threat of human impact (considering the history of bottom trawling; Taranto et al., 2012). It is notable that the EBSA criteria encompass the FAO VME criteria (Ardron et al., 2014). Under the language within the United Nations General Assembly Resolution 61/105 (FAO, 2009), Cobb Seamount may also be considered a VME in its entirety, given that seamounts are among their physiographic indicators (FAO, 2009; Watling and Auster, 2017; NAFO, 2018).

Within the Northeast Pacific Ocean there are hundreds of known seamounts in the Exclusive Economic Zones of Canada and the United States (US)—all of which have been assessed and are now protected from bottom-contact gear. In 2006, seamounts in the Gulf of Alaska and off the US West Coast were recognized for their unique ecological characteristics and protected from all bottom-contact gear (Hourigan, 2009). In 2016, Canadian seamounts were identified as EBSAs (Ban et al., 2016), and in 2017, bottom-contact fishing was prohibited on all known seamounts within fishable depths within the Canadian Pacific Ocean (DFO, 2019a,b,c). Of the hundreds of seamounts in the region, only one falls in the same biophysical class as Cobb Seamount, but it is 800 km away (**Figure 1**) and supports different species assemblages (SG̲aan K̲inghlas-Bowie Seamount; Canessa et al., 2003; Gauthier et al., 2018a,b,c; DFO, 2019a). At present, seamounts in the Northeast Pacific ABNJ, including the regionally unique Cobb Seamount, are the only ones known to be fished with bottom-contact gear.

Summary

- Cobb Seamount is inhabited by a diverse assemblage of habitat-forming emergent biological structures adopted as VME indicator taxa. Dense aggregations of these taxa create depth-distributed biogenic habitats, such as the living carpets of epifauna-encrusted scallops on the pinnacle, extensive fields of hydrocorals and crinoids with patches of coral bioherms and forests on the summit plateau and ridge, and diverse gardens of large soft corals, black corals, and glass sponges on the upper flanks. Almost half of the seafloor surveyed in 2012 supported dense assemblages of VME indicators, at one or more individuals or colonies per square meter.
- The two most abundant biogenic habitats were formed by hydrocorals and crinoids—both of which supported dense and diverse assemblages of other animals, including commercially-important fishes. Therefore, the present NPFC VME indicator list of soft, black, and stony corals does not represent the majority of biogenic habitats observed on Cobb Seamount.
- Several of the shallow (<350 m) depth-distributed biogenic habitats are regionally unique or rare, isolated by hundreds of kilometers, potentially inhibiting recolonization and as such recovery.

- All the VME indicators we observed on the 2012 survey (living or dead) overlap with the known fishing footprint on Cobb Seamount.
- We estimate that hundreds of thousands of items of derelict fishing gear currently exist on Cobb Seamount and that these pose an ongoing threat to biological structures, the biogenic habitats they create, and the associated species they support, which could persist for decades or centuries to come.
- Historical bottom-contact fishing impacts (e.g., fields of coral rubble, ghost fishing) appear to have persisted decades after the fishing activity occurred. Therefore, to assess VMEs and SAIs, it is imperative management organizations collect the best available spatial information for historical fisheries, especially in the case of bottom trawling. Such information is also required to identify and assess signs of potential recovery (coral growth).
- While life on Cobb Seamount continues to experience impacts outside our current realm of control (e.g., DFG), relief from future direct stressors, including future bottom-contact fishing, is possible through management organizations. This study aims to contribute information to potentially help identify some of the first VMEs and SAIs in the High Seas of the North Pacific Ocean.

DATA AVAILABILITY STATEMENT

The raw data supporting the conclusions of this article will be made available by the authors without undue reservation, to any qualified researcher, except for the fisheries data. The Fisheries and Oceans Canada fisheries datasets for this manuscript are not publicly available to respect the privacy of commercial fishers. Requests to access the datasets should be directed to CD (cherisse.dupreez@dfo-mpo.gc.ca).

AUTHOR CONTRIBUTIONS

JC conceived and planned the visual survey. CD and JC performed the visual survey. CD, KS, and JC contributed to the design of the research and to the writing of the manuscript. CD performed the image annotation and analysis of the results. All authors provided critical feedback and helped shape the research, analysis and manuscript.

FUNDING

This research was supported by a grant from DFO's International Governance Strategy to JC.

ACKNOWLEDGMENTS

This research was supported by Fisheries and Oceans Canada, with field support from the United States National Oceanic and Atmospheric Administration (NOAA). This article benefited from reviews by Chris Rooper, Stephanie Archer, Candice St Germain, and Eddy Kennedy. We thank Wolfgang Carolsfeld, Sarah Davies, James Pegg, and Jonathan Martin for their assistance in collecting data from the ROV transects. Species and habitat data from the AUV transects were kindly provided by M. Elizabeth Clarke, Erica Fruh, Jeremy Taylor and Curt Whitmire. We thank Katie Gale for her assistance with extracting the sablefish bottom longline data from DFO databases. Merlin Best and Heidi Gartner kindly provided unpublished *Stylaster* spp. data from their analyses of the Royal British Colombia Museum collection. Bathymetry data were obtained from NOAA. We appreciated our discussions with Tammy Norgard and Miriam O, and gratefully acknowledge constructive comments on previous drafts of our analyses and manuscript from Jim Boutillier, Lisa Lacko, M. Elizabeth Clarke, and Verena Tunnicliffe.

REFERENCES

Addamo, A. M., Vertino, A., Stolarski, J., García-Jiménez, R., Taviani, M., and Machordom, A. (2016). Merging Scleractinian genera: the overwhelming genetic similarity between solitary *Desmophyllum* and colonial *Lophelia*. *BMC Evol. Biol.* 16:108. doi: 10.1186/s12862-016-0654-8

Andrews, A. H., Cordes, E. E., Mahoney, M. M., Munk, K., Coale, K. H., Cailliet, G. M., et al. (2002). Age, growth and radiometric age validation of a deep-sea, habitat-forming gorgonian (Primnoa resedaeformis) from the Gulf of Alaska. *Hydrobiologia* 471, 101–110.

Andrews, A. H., Stone, R. P., Lundstrom, C. C., and De Vogelaere, A. P. (2009). Growth rate and age determination of bamboo corals from the northeastern Pacific Ocean using refined 210Pb dating. *Mar. Ecol. Prog. Ser.* 397, 173–185. doi: 10.3354/meps08193

Ardron, J. A., Clark, M. R., Penney, A. J., Hourigan, T. F., Rowden, A. A., Dunstan, P. K., et al. (2014). A systematic approach towards the identification and protection of vulnerable marine ecosystems. *Mar. Policy* 49, 146–154. doi: 10.1016/j.marpol.2013.11.017

Auster, P. J., Gjerde, K., Heupel, E., Watling, L., Grehan, A., and Rogers, A. D. (2010). Definition and detection of vulnerable marine ecosystems on the high seas: problems with the "move-on" rule. *ICES J. Mar. Sci.* 68, 254–264. doi: 10.1093/icesjms/fsq074

Baco, A. R., Roark, E. B., and Morgan, N. B. (2019). Amid fields of rubble, scars, and lost gear, signs of recovery observed on seamounts on 30-to 40-year time scales. *Sci. Adv.* 5:eaaw4513. doi: 10.1126/sciadv.aaw4513

Baco-Taylor, A. R., Ross, R., Althaus, F., Bridges, A., Brix, S., Colaço, A., et al. (2019). *A Community Consensus on Designating Vulnerable Marine Ecosystems From Imagery*. San Diego, CA: Ocean Sciences Meeting.

Ban, S., Curtis, J. M. R., St. Germain, C., Perry, R. I., and Therriault, T. W. (2016). Identification of ecologically and biologically significant areas (EBSAs) in Canada's offshore pacific bioregion. *DFO Can. Sci. Advis. Sec. Res. Doc.* 2016/034. x + 152 p.

Bell, J., Guijarro, E., and Kenny, A. (2019). Demersal fishing in areas beyond national jurisdiction: a comparative analysis of regional fisheries management organisations. *Front. Mar. Sci.* 6:596. doi: 10.3389/fmars.2019.00596

Birkeland, C. (1971). Biological observations on cobb seamount. *N. W. Sci.* 45, 193–199.

Blasiak, R., Pittman, J., Yagi, N., and Sugino, H. (2016). Negotiating the use of biodiversity in marine areas beyond national jurisdiction. *Front. Mar. Sci.* 3:224. doi: 10.1016/j.marpol.2017.03.004

Bremner, J., Rogers, S., and Frid, C. (2006). Methods for describing ecological functioning of marine benthic assemblages using biological traits analysis (BTA). *Ecol. Indic.* 6, 609–622. doi: 10.1016/j.ecolind.2005.08.026

Budinger, T. F. (1967). Cobb seamount. *Deep Sea Res.* 14, 191–201. doi: 10.1016/0011-7471(67)90005-8

Buhl-Mortensen, L., Vanreusel, A., Gooday, A. J., Levin, L. A., Priede, I. G., Buhl-Mortensen, P., et al. (2010). Biological structures as a source of habitat heterogeneity and biodiversity on the deep ocean margins. *Mar. Ecol.* 31, 21–50. doi: 10.1111/j.1439-0485.2010.00359.x

Canessa, R. R., Conley, K., and Smiley, B. D. (2003). Bowie seamount pilot marine protected area: an ecosystem overview report. *Can. Tech. Rep. Fish. Aquat. Sci.* 2461: xi + 85 p.

Chaytor, J. D., Keller, R. A., Duncan, R. A., and Dziak, R. P. (2007). Seamount morphology in the bowie and cobb hot spot trails Gulf of Alaska. *Geochem. Geophy. Geosy.* 8:Q09016.

Clark, M. R., Althaus, F., Schlacher, T. A., Williams, A., Bowden, D. A., and Rowden, A. A. (2015). The impacts of deep-sea fisheries on benthic communities: a review. *ICES J. Mar. Sci.* 73(Suppl. 1), i51–i69. doi: 10.1093/icesjms/fsv123

Clark, M. R., Bowden, D. A., Rowden, A. A., and Stewart, R. (2019). Little evidence of benthic community resilience to bottom trawling on seamounts after 15 years. *Front. Mar. Sci.* 6:63. doi: 10.3389/fmars.2019.00063

Clark, M. R., and Dunn, M. R. (2012). Spatial management of deep-sea seamount fisheries: balancing sustainable exploitation and habitat conservation. *Environ. Conserv.* 39, 204–214. doi: 10.1017/s0376892912000021

Clark, M. R., and Koslow, J. A. (2007). "Impacts of fisheries on seamounts," in *Seamounts: Ecology, Fisheries, and Conservation*, eds T. J. Pitcher, P. J. B. Hart, M. R. Clark, N. Haggan, and R. S. Santos, (Wiley-Blackwell), 413–441. doi: 10.1002/9780470691953.ch19

Clark, M. R., Vinnichenko, V. I., Gordon, J. D., Beck-Bulat, G. Z., Kukharev, N. N., and Kakora, A. F. (2007). "Large-scale distant-water trawl fisheries on seamounts," in *Seamounts: Ecology, Fisheries, and Conservation*, eds T. J. Pitcher, P. J. B. Hart, M. R. Clark, N. Haggan, and R. S. Santos, (Wiley-Blackwell), 361–399. doi: 10.1002/9780470691953.ch17

Clarke, M. E., Whitmire, C., Fruh, E., Anderson, J., Taylor, J., Rooney, J., et al. (2010). "Developing the SeaBED AUV as a tool for conducting routine surveys of fish and their habitat in the Pacific," in *Proceedings of the 2010 IEEE/OES Autonomous Underwater Vehicles conference proceedings*, Monterey, CA.

Comeau, L. A., Vézina, A. F., Bourgeois, M., and Juniper, S. K. (1995). Relationship between phytoplankton production and the physical structure of the water column near Cobb Seamount, northeast Pacific. *Deep Sea Res.* 42, 993–1005. doi: 10.1016/0967-0637(95)00050-g

Commission for the Conservation of Antarctic Marine Living Resources [CCAMLR], (2009). *CCAMLR VME Taxa Classification Guide 2009*. Hobart: CCAMLR.

Commission for the Conservation of Antarctic Marine Living Resources [CCAMLR], (2013). *Interim Measure for Bottom Fishing Activities Subject to Conservation Measure 22-06 Encountering Potential Vulnerable Marine Ecosystems in the Convention Area. CM 22-07*. Hobart: CCAMLR.

Convention on Biological Diversity [CBD], (2016). *Ecologically or Biologically Significant Areas (EBSAs) North-East Pacific Ocean Seamounts. 204132-2.* New York, NY: Convention on Biological Diversity.

Cullis-Suzuki, S., and Pauly, D. (2010). Failing the high seas: a global evaluation of regional fisheries management organizations. *Mar. Policy* 34, 1036–1042.

Curtis, J. M. R., Du Preez, C., Davis, S. C., Pegg, J., Clarke, M. E., Fruh, E. L., et al. (2015). 2012 Expedition to Cobb Seamount: survey methods, data collections, and species observations. *Can. Tech. Rep. Fish. Aquat. Sci.* 3124: xii + 145.

De Leo, F. C., Gauthier, M., Nephin, J., Mihaly, S., and Juniper, S. K. (2017). Bottom trawling and oxygen minimum zone influences on continental slope benthic community structure off Vancouver Island (NE Pacific). *Deep Sea Res. Pt II* 137, 404–419. doi: 10.1016/j.dsr2.2016.11.014

Deep-Ocean Stewardship Initiative [DOSI], (2019). *New Technologies for Environmental Impact Assessments in the Deep Sea*. New York, NY: DOSI.

DFO, (2018). *Framework to Support Decisions on Authorizing Scientific Surveys with Bottom Contacting Gears in Protected Areas with Defined Benthic Conservation Objectives. Can. Sci. Adv. Sec. Sci. Res. 043*. Available at: https://waves-vagues.dfo-mpo.gc.ca/Library/40726277.pdf (accessed October 1, 2019).

DFO, (2019a). *Biophysical and ecological overview of the offshore Pacific Area of interest (AOI). Can. Sci. Adv. Sec. Sci. Res. 011*. Available at: http://publications.gc.ca/collections/collection_2019/mpo-dfo/fs70-7/Fs70-7-2019-011-eng.pdf (accessed October 1, 2019).

DFO, (2019b). *Offshore Pacific Seamounts and Vents Closure [Online]*. Available at: http://www.dfo-mpo.gc.ca/oceans/oeabcm-amcepz/refuges/offshore-hauturiere-eng.html (accessed September 9, 2019).

DFO, (2019c). *SGaan Kinghlas- Bowie Seamount 2019 Marine Protected Area Management Plan*. Minato: DFO.

Doherty, B., and Cox, S. (2017). *Data summary of trap camera video obtained during sablefish bottom longline fishing at SGaan Kinghlas-Bowie Seamount, 2014-2015. Can. Dat. Rep. Fish. Aquat. Sci. 1276*. Available at: http://publications.gc.ca/collections/collection_2017/mpo-dfo/Fs97-13-1276-eng.pdf (accessed October 1, 2019).

Donaldson, A. B., Gabriel, C., Harvey, B., and Carolsfeld, J. (2010). Impacts of fishing gears other than bottom trawls, dredges, gillnets and longlines on aquatic biodiversity and vulnerable marine ecosystems. *DFO Can. Sci. Adv. Sec. Sci. Res.* 2010/011. vi + 84 p.

Douglas, D. A. (2011). *The Oregon Shore-Based Cobb Seamount Fishery, 1991-2003: Catch Summaries and Biological Observations*. Newport, OR: Marine Resources Program.

Dower, J., Freeland, H., and Juniper, K. (1992). A strong biological response to oceanic flow past cobb seamount. *Deep Sea Res. Pt A.* 39, 1139–1145. doi: 10.1016/0198-0149(92)90061-w

Du Preez, C., Curtis, J. M. R., Davies, S. C., Clarke, M. E., and Fruh, E. L. (2015). Cobb seamount species inventory. *Can. Tech. Rep. Fish. Aquat. Sci.* 3122: viii + 108 p.

Du Preez, C., Curtis, J. M., and Clarke, M. E. (2016). The structure and distribution of benthic communities on a shallow seamount (Cobb Seamount, Northeast Pacific Ocean). *PLoS One* 11:e0165513. doi: 10.1371/journal.pone.0165513

Du Preez, C., and Tunnicliffe, V. (2011). Shortspine thornyhead and rockfish (Scorpaenidae) distribution in response to substratum, biogenic structures and trawling. *Mar. Ecol. Prog. Ser.* 425, 217–231. doi: 10.3354/meps09005

FAO, (2009). *International Guidelines for the Management of Deep-Sea Fisheries in the High Seas*. Rome: Food and Agriculture Organization.

FAO, (2019). *Vulnerable Marine Ecosystems [Online]*. Rome: FAO.

Farrow, G. E., and Durant, G. P. (1985). Carbonate-basaltic sediments from Cobb Seamount, northeast Pacific: zonation, bioerosion and petrology. *Mar. Geol.* 65, 73–102. doi: 10.1016/0025-3227(85)90047-7

Fisheries and Oceans Canada [DFO], (2013). *A Review of Sablefish Population Structure in the Northeast Pacific Ocean and Implications for Canadian Seamount Fisheries. Can. Tech. Rep. Fish. Aquat. Sci. 017*. Available at: https://waves-vagues.dfo-mpo.gc.ca/Library/349898.pdf (accessed October 1, 2019).

Fosså, J. H., Mortensen, P., and Furevik, D. M. (2002). The deep-water coral *Lophelia pertusa* in Norwegian waters: distribution and fishery impacts. *Hydrobiologia.* 471, 1–12.

Gall, S. C., and Thompson, R. C. (2015). The impact of debris on marine life. *Mar. Pollut. Bull.* 92, 170–179. doi: 10.1016/j.marpolbul.2014.12.041

Gallagher, A. J., Hammerschlag, N., Cooke, S. J., Costa, D. P., and Irschick, D. J. (2015). Evolutionary theory as a tool for predicting extinction risk. *Trends Ecol. Evol.* 30, 61–65. doi: 10.1016/j.tree.2014.12.001

Gauthier, M. (2017). *Trap Camera Videos From Sgaan Kinghlas-Bowie Seamount: Overview of Data Obtained During Sablefish Bottom Longline Trap Fishing in 2016. Can. Dat. Rep. Fish. Aquat. Sci. 1279*. Available at: http://publications.gc.ca/collections/collection_2017/mpo-dfo/Fs97-13-1279-eng.pdf (accessed October 1, 2019).

Gauthier, M., Curtis, J., Gale, K., Archer, S., and Haggarty, D. (2018c). *SGaan Kinghlas-Bowie Seamount Marine Protected Area Species Inventory: Invertebrates (Annelida, Arthropoda, Brachiopoda, Ctenophora, Echinodermata and Mollusca). Can. Tech. Rep. Fish. Aquat. Sci. 3198*. Available at: http://publications.gc.ca/collections/collection_2018/mpo-dfo/Fs97-6-3198-eng.pdf (accessed October 1, 2019).

Gauthier, M., Curtis, J. M. R., Gale, K. S. P., Archer, S. K., and Haggarty, D. R. (2018a). SGaan Kinghlas-Bowie Seamount marine protected area species inventory: Algae, Cnidaria, Bryozoa and Porifera. *Can. Tech. Rep. Fish. Aquat. Sci.* 3196: vi + 56 p.

Gauthier, M., Curtis, J. M. R., Gale, K. S. P., and Haggarty, D. (2018b). SGaan Kinghlas-Bowie Seamount marine protected area species inventory: Chordata. *Can. Tech. Rep. Fish. Aquat. Sci.* 3197: vi + 48 p.

Gianni, M., Fuller, S., Currie, D., Schleit, K., Goldsworthy, L., Pike, B., et al. (2016). *How Much Longer Will It Take? A Ten-Year Review Of The Implementation of United Nations General Assembly Resolutions 61/105, 64/72 and 66/68 On The Management of Bottom Fisheries In Areas Beyond National Jurisdiction. Deep Sea Conservation Coalition*. Available at: http://www.savethehighseas.org/wp-content/uploads/2016/07/DSCC-Review-2016_Launch-29-July.pdf (accessed October 1, 2019).

Gilman, E., Passfield, K., and Nakamura, K. (2014). Performance of regional fisheries management organizations: ecosystem-based governance of bycatch and discards. *Fish. Fish.* 15, 327–351. doi: 10.1111/faf.12021

Hart, D. R., and Chute, A. S. (2004). *Essential Fish Habitat Source Document. Sea Scallop, Placopecten Magellanicus, Life History And Habitat Characteristics*. Silver Spring, MD: NOAA.

Hoegh-Guldberg, O., and Bruno, J. F. (2010). The impact of climate change on the world's marine ecosystems. *Science* 328, 1523–1528. doi: 10.1126/science.1189930

Hourigan, T. (2009). Managing fishery impacts on deep-water coral ecosystems of the USA: emerging best practices. *Mar. Ecol. Prog. Ser.* 397, 333–340. doi: 10.3354/meps08278

Kaiser, M., Clarke, K., Hinz, H., Austen, M. C., Somerfield, P. J., and Karakassis, I. (2006). Global analysis of response and recovery of benthic biota to fishing. *Mar. Ecol. Prog. Ser.* 311, 1–14. doi: 10.3354/meps311001

Krautter, M., Conway, K. W., Barrie, J. V., and Neuweiler, M. (2001). Discovery of a "living dinosaur": globally unique modern hexactinellid sponge reefs off British Columbia, Canada. *Facies* 44, 265–282. doi: 10.1007/bf02668178

Krieger, K. J. (2001). "Coral (Primnoa) impacted by fishing gear in the gulf of alaska," in *Proceedings of the First International Symposium on Deep-Sea Corals*, Nova Scotia.

Lambert, P., and Austin, W. C. (2007). *Brittle Stars, Sea Urchins and Feather Stars Of British Columbia, Southeast Alaska and Puget Sound*. Victoria, BC: Royal British Columbia Museum.

MacArthur, R. H., and Wilson, E. O. (2001). *The Theory of Island Biogeography*. Princeton, NJ: Princeton university press.

MacDonald, B., Thompson, R., and Bourne, N. (1991). Growth and reproductive energetics of three scallop species from British Columbia (*Chlamys hastata*, *Chlamys rubida*, and *Crassadoma gigantea*). *Can. J. Fish. Aquat. Sci.* 48, 215–221. doi: 10.1139/f91-029

Macfadyen, G., Huntington, T., and Cappell, R. (2009). *Abandoned, Lost Or Otherwise Discarded Fishing Gear. UNEP Regional Seas Reports and Studies No.185, FAO Fisheries and Aquaculture Technical Paper, No. 523*. Rome: UNEP.

McClain, C. R., Lundsten, L., Barry, J., and DeVogelaere, A. (2010). Assemblage structure, but not diversity or density, change with depth on a northeast Pacific seamount. *Mar. Ecol.* 31, 14–25. doi: 10.1111/j.1439-0485.2010.00367.x

Merrie, A., Dunn, D. C., Metian, M., Boustany, A. M., Takei, Y., Elferink, A. O., et al. (2014). An ocean of surprises–trends in human use, unexpected dynamics and governance challenges in areas beyond national jurisdiction. *Global Environ. Chang.* 27, 19–31. doi: 10.1016/j.gloenvcha.2014.04.012

Miyamoto, M., and Kiyota, M. (2017). Application of association analysis for identifing indicator taxa of vulnerable marine ecosystems in the Emperor Seamounts area, North Pacific Ocean. *Ecol. Indic.* 78, 301–310. doi: 10.1016/j.ecolind.2017.03.028

Miyamoto, M., Kiyota, M., Hayashibara, T., Nonaka, M., Imahara, Y., and Tachikawa, H. (2017). Megafaunal composition of cold-water corals and other deep-sea benthos in the southern Emperor Seamounts area, North Pacific Ocean. *Galaxea. J. Coral Reef Stud.* 19, 19–30. doi: 10.3755/galaxea.19.1_19

Morato, T., Pham, C. K., Pinto, C., Golding, N., Ardron, J. A., Muñoz, P. D., et al. (2018). A multi criteria assessment method for identifying vulnerable marine ecosystems in the North-East Atlantic. *Front. Mar. Sci.* 5:460. doi: 10.3389/fmars.2018.00460

Mordecai, G., Tyler, P. A., Masson, D. G., and Huvenne, V. A. (2011). Litter in submarine canyons off the west coast of Portugal. *Deep Sea Res. Pt II* 58, 2489–2496. doi: 10.1016/j.dsr2.2011.08.009

Murillo, F. J., Kenchington, E., Sacau-Cuadrado, M. D. M., Piper, D., Wareham, V., and Muñoz, A. (2011). *New VME Indicator Species (Excluding Corals and Sponges) and Some Potential VME Elements of the NAFO (North Atlantic Fisheries Organization) SCR Doc. 11/73*. Available at: https://archive.nafo.int/open/sc/2011/scr11-073.pdf (accessed October 1, 2019).

NAFO (2010). *Sponge Identification Guide NAFO Area. Northwest Atlantic Fisheries Organization Scientific Council Studies*. Dartmouth: NAFO.

NAFO (2018). *Northwest Atlantic Fisheries Organization conservation and Enforcement Measures. NAFO/FC Doc 18-01*. Dartmouth: NAFO.

National Technical Information Service (1971). *Development of a Fixed, Permanent Mooring System on the Pinnacle of Cobb Seamount*. Springfield, VA: National Technical Information Service.

NEAFC (2015). *Recommendation on the Protection of Vulnerable Marine Ecosystems in the NEAFC Regulatory Area. North East Atlantic Fisheries Commission*. Available at: http://extwprlegs1.fao.org/docs/pdf/mul165665.pdf (accessed October 1, 2019).

NOAA Marine Debris Program (2015). *Report on the Impacts of "Ghost Fishing" Via Derelict Fishing Gear*. Silver Spring, MD: NOAA Marine Debris Program.

North Atlantic Fisheries Organization [NAFO] (2009). *Coral Identification Guide NAFO Area. Northwest Atlantic Fisheries Organization Scientific Council Studies*. Dartmouth: NAFO.

North Pacific Fisheries Commission [NPFC] (2017). *Conservation and Management Measure for Bottom Fisheries and Protection of Vulnerable Marine Ecosystems in the Northeastern Pacific Ocean. North Pacific Fisheries Commission. CMM 2017-16*. Available at: https://www.npfc.int/system/files/2017-09/CMM%202017-06%20FOR%20BOTTOM%20FISHERIES%20AND%20PROTECTION%20OF%20VULNERABLE%20MARINE%20ECOSYSTEMS%20IN%20THE%20NORTHEASTERN%20PACIFIC%20OCEAN.pdf (accessed October 1, 2019).

North Pacific Fisheries Commission [NPFC] (2018). *Conservation and Management Measure for bottom fisheries and Protection of Vulnerable Marine Ecosystems in the Northeastern Pacific Ocean. North Pacific Fisheries Commission. CMM 2018–2015*. New York, NY: NPFC.

Oliveira, F., Monteiro, P., Bentes, L., Henriques, N. S., Aguilar, R., and Gonçalves, J. M. (2015). Marine litter in the upper São Vicente submarine canyon (SW Portugal): Abundance, distribution, composition and fauna interactions. *Mar. Pollut. Bull.* 97, 401–407. doi: 10.1016/j.marpolbul.2015.05.060

Parker, T., and Tunnicliffe, V. (1994). Dispersal strategies of the biota on an oceanic seamount: implications for ecology and biogeography. *Biol. Bull.* 187, 336–345. doi: 10.2307/1542290

Pearson, D. E., Douglas, D. A., and Barss, B. (1993). Biological observations from the Cobb Seamount rockfish fishery. *Fish. Bull.* 91, 573–576.

Pham, C., Gomes-Pereira, J., Isidro, E., Santos, R., and Morato, T. (2013). Abundance of litter on condor seamount (Azores, Portugal, Northeast Atlantic). *Deep Sea Res. Pt II* 98, 204–208. doi: 10.1016/j.dsr2.2013.01.011

Pham, C. K., Diogo, H., Menezes, G., Porteiro, F., Braga-Henriques, A., Vandeperre, F., et al. (2014). Deep-water longline fishing has reduced impact on vulnerable marine ecosystems. *Sci. Rep.* 4:4837. doi: 10.1038/srep04837

Pitcher, T. J., Morato, T., Hart, P. J. B., Clark, M. R., Haggan, N., and Santos, R. S. (2007). "The depths of ignorance: an ecosystem evaluation framework for seamount ecology, fisheries and conservation," in *Seamounts: Ecology, Fisheries & Conservation*, eds T. J. Pitcher, T. Morato, P. J. B. Hart, M. R. Clark, N. Haggan, and R. S. Santos, (Hoboken, NJ: Blackwell Publishing), 476–488. doi: 10.1002/9780470691953.ch21

Popova, E., Vousden, D., Sauer, W. H., Mohammed, E. Y., Allain, V., Downey-Breedt, N., et al. (2019). Ecological connectivity between the areas beyond national jurisdiction and coastal waters: Safeguarding interests of coastal communities in developing countries. *Mar. Policy* 104, 90–102. doi: 10.1016/j.marpol.2019.02.050

Ragnarsson, S. A., Burgos, J. M., Kutti, T., van den Beld, I., Egilsdóttir, H., Arnaud-Haond, S., et al. (2017). "The impact of anthropogenic activity on cold-water corals," in *Marine Animal Forests: The Ecology of Benthic Biodiversity Hotspots*, eds S. Rossi, L. Bramanti, A. Gori, and C. Orejas, (Berlin: Springer), 1–35. doi: 10.1007/978-3-319-17001-5_27-1

Ramirez-Llodra, E., Brandt, A., Danovaro, R., De Mol, B., Escobar, E., German, C., et al. (2010). Deep, diverse and definitely different: unique attributes of the world's largest ecosystem. *Biogeosciences* 7, 2851–2899. doi: 10.5194/bg-7-2851-2010

Roark, E. B., Guilderson, T. P., Dunbar, R. B., and Ingram, B. L. (2006). Radiocarbon-based ages and growth rates of Hawaiian deep-sea corals. *Mar. Ecol. Prog. Ser.* 327, 1–14. doi: 10.3354/meps327001

Roberts, S., and Hirshfield, M. (2004). Deep-sea corals: out of sight, but no longer out of mind. *Front. Ecol. Environ.* 2, 123–130. doi: 10.2307/3868237

Rogers, A. D., Baco, A., Griffiths, H., Hart, T., and Hall-Spencer, J. M. (2007). "Corals on seamounts," in *Seamounts: Ecology, Fisheries and Conservation*, eds N. Haggan, T. Morato, R. S. Santos, P. J. B. Hart, and M. R. Clark, (Blackwell), 141–169. doi: 10.1002/9780470691953.ch8

Rooper, C., and Kiyota, M. (2018). Applying global experiences to regional assessments: A workshop on the Protection of Vulnerable Marine Ecosystems in the North Pacific Fisheries Commission Area. *PICES Press* 26, 8–12.

Salgado, E. J., Nehasil, S. E., and Etnoyer, P. J. (2018). Distribution of deep-water corals, sponges, and demersal fisheries landings in Southern California, USA: implications for conservation priorities. *PeerJ* 6:e5697. doi: 10.7717/peerj.5697

Samadi, S., Schlacher, T., Richer, and de Forges, B. (2007). "Seamount benthos," in *Seamounts: Ecology, Fisheries And Conservation*, eds N. Haggan, T. Morato, R. S. Santos, P. J. B. Hart, and M. R. Clark, (Blackwell), 119–140.

Sasaki, T. (1985). Development and present status of Japanese trawl fisheries in the vicinity of seamounts. *Bull. JPN Soc. Fish. Oceanogr.* 47, 161–166.

Shank, T. M. (2010). Seamounts: deep-ocean laboratories of faunal connectivity, evolution, and endemism. *Oceanography* 23, 108–122. doi: 10.5670/oceanog.2010.65

Smith, C., Papadopoulou, K., and Diliberto, S. (2000). Impact of otter trawling on an eastern Mediterranean commercial trawl fishing ground. *ICES J. Mar. Sci.* 57, 1340–1351. doi: 10.1006/jmsc.2000.0927

South East Atlantic Fisheries Organisation [SEAFO], (2016). *Report of the 12th SEAFO Scientific Committee*. Available at: http://www.seafo.org/media/4ca98f5f-c111-4bcf-875b-36ac3213b8b7/SEAFOweb/pdf/SC/open/eng/SC%20Report%202016_pdf (accessed October 1, 2019).

South Pacific Regional Fisheries Management Organisation [SPRFMO], (2019). *Conservation and Management Measure For The Management Of Bottom Fishing in the SPRFMO Convention Area. South Pacific Regional Fisheries Management Organisation. CMM-03-2019*. Available at: https://www.sprfmo.int/assets/Fisheries/Conservation-and-Management-Measures/2019-CMMs/CMM-03-2019-5Mar2019.pdf (accessed October 1, 2019).

Stone, R. (2006). Coral habitat in the Aleutian Islands of Alaska: depth distribution, fine-scale species associations, and fisheries interactions. *Coral Reefs* 25, 229–238. doi: 10.1007/s00338-006-0091-z

Taranto, G. H., Kvile, K. O., Pitcher, T. J., and Morato, T. (2012). An ecosystem evaluation framework for global seamount conservation and management. *PLoS One* 7:e42950. doi: 10.1371/journal.pone.0042950

Tingley, G. (2014). *An Assessment of the Potential for Near-Seabed Midwater Trawling to Contact the Seabed and to Impact Benthic Habitat and Vulnerable Marine Ecosystems (VMEs). SPRFMO Technical Paper. SC-02-10.* Available at: https://www.sprfmo.int/assets/Meetings/Meetings-2013-plus/SC-Meetings/2nd-SC-Meeting-2014/Papers/SC-02-10-Midwater-trawls-potential-for-benthic-impacts.pdf (accessed October 1, 2019).

Tissot, B. N., Yoklavich, M. M., Love, M. S., York, K., and Amend, M. (2006). Benthic invertebrates that form habitat on deep banks off southern California, with special reference to deep sea coral. *Fish. Bull.* 104, 167–181.

Uchida, R. N., and Tagami, D. T. (1984). Groundfish fisheries and research in the vicinity of seamounts in the North Pacific Ocean. *Mar. Fish. Rev.* 46, 1–17.

UN, (2019). *The Sustainable Development Goals Report*. Available at: https://unstats.un.org/sdgs/report/2019/The-Sustainable-Development-Goals-Report-2019.pdf (accessed November 14, 2019).

UNGA, (2006). *United Nations General Assembly Resolution 61/105 (UNGA 61/105). Sustainable Fisheries, Including Through The 1995 Agreement for the Implementation of the Provisions of the United Nations Convention on the Law of the Sea of 10 December 1982 relating to the Conservation and Management of Straddling Fish Stocks and Highly Migratory Fish Stocks, And Related Instruments*. Available at: https://documents-dds-ny.un.org/doc/UNDOC/GEN/N06/500/73/PDF/N0650073.pdf?OpenElement (accessed October 1, 2019).

Verity, P. G., Smetacek, V., and Smayda, T. J. (2002). Status, trends and the future of the marine pelagic ecosystem. *Environ. Conserv.* 29, 207–237. doi: 10.1111/jfb.12759

Victorero, L., Robert, K., Robinson, L. F., Taylor, M. L., and Huvenne, V. A. (2018). Species replacement dominates megabenthos beta diversity in a remote seamount setting. *Sci. Rep.* 8:4152.

Vieira, R. P., Raposo, I. P., Sobral, P., Gonçalves, J. M., Bell, K. L., and Cunha, M. R. (2015). Lost fishing gear and litter at Gorringe Bank (NE Atlantic). *J. Sea Res.* 100, 91–98. doi: 10.1016/j.seares.2014.10.005

Waller, R., Watling, L., Auster, P., and Shank, T. (2007). Anthropogenic impacts on the Corner Rise seamounts, north-west Atlantic Ocean. *J. Mar. Biol. Assoc. U.K.* 87, 1075–1076. doi: 10.1017/s0025315407057785

Watling, L. (2005). "The global destruction of bottom habitats by mobile fishing gear," in *Marine Conservation Biology: The Science Of Maintaining The Sea's Biodiversity*, eds L. B. Crowder, and E. A. Norse, (Washington, DC: Island Press), 198–210.

Watling, L., and Auster, P. J. (2017). Seamounts on the high seas should be managed as vulnerable marine ecosystems. *Front. Mar. Sci.* 4:14. doi: 10.3389/fmars.2017.00014

Watling, L., and Norse, E. A. (1998). Disturbance of the seabed by mobile fishing gear: a comparison to forest clearcutting. *Conserv. Biol.* 12, 1180–1197. doi: 10.1046/j.1523-1739.1998.0120061180.x

Watters, D. L., Yoklavich, M. M., Love, M. S., and Schroeder, D. M. (2010). Assessing marine debris in deep seafloor habitats off California. *Mar. Pollut. Bull.* 60, 131–138. doi: 10.1016/j.marpolbul.2009.08.019

Whitney, F. A., Freeland, H. J., and Robert, M. (2007). Persistently declining oxygen levels in the interior waters of the eastern subarctic Pacific. *Prog. Oceanogr.* 75, 179–199. doi: 10.1016/j.pocean.2007.08.007

Woodall, L. C., Sanchez-Vidal, A., Canals, M., Paterson, G. L., Coppock, R., Sleight, V., et al. (2014). The deep sea is a major sink for microplastic debris. *R. Soc. Open Sci.* 1:140317. doi: 10.1098/rsos.140317

Conflict of Interest: CD and JC have acted as part of the Canadian delegation at North Pacific Fishery Commission (NPFC) scientific committee meetings and workshops. JC is presently the Chair of the scientific committee.

The remaining author declares that the research was conducted in the absence of any commercial or financial relationships that could be construed as a potential conflict of interest.

frontiers
in Marine Science

ORIGINAL RESEARCH
published: 21 February 2020
doi: 10.3389/fmars.2020.00095

Determining Coral Density Thresholds for Identifying Structurally Complex Vulnerable Marine Ecosystems in the Deep Sea

Ashley A. Rowden[1,2]*, *Tabitha R. R. Pearman*[3], *David Anthony Bowden*[1], *Owen F. Anderson*[1] and *Malcolm Ross Clark*[1]

[1] National Institute of Water and Atmospheric Research, Wellington, New Zealand, [2] Victoria University of Wellington, Wellington, New Zealand, [3] Ocean and Earth Science, University of Southampton, Southampton, United Kingdom

Vulnerable marine ecosystems (VMEs) are at risk from the impacts of deep-sea trawling. Identifying the presence of VMEs in high seas fisheries management areas has to date relied mainly on presence records, or on habitat suitability models of VME indicator taxa (e.g., the stony coral species *Solenosmilia variabilis* Duncan, 1873) as proxies for the occurrence of VMEs (e.g., cold-water coral reefs). However, the presence or predicted presence of indicator taxa does not necessarily equate to the occurrence of a VME. There have been very few attempts to determine density thresholds of VME indicator taxa that relate to a "significant concentration" which supports a "high diversity" of associated taxa, as per the current criterion for identifying structurally complex VMEs (FAO, 2009). Without knowing such thresholds, identifications of VMEs will continue to be subjective, impeding efforts to design effective spatial management measures for VMEs. To address this issue, we used seafloor video and still image data from the Louisville Seamount Chain off New Zealand to model relationships between the densities of live *Solenosmilia variabilis* coral heads, as well as percent cover of live and dead coral matrix, and the number of other epifauna taxa present. Analyses were conducted at three spatial scales; 50 and 25 m^2 for video, and 2 m^2 for stills. Model curves exhibited initial steep positive responses reaching thresholds for the number of live coral heads at 0.11 m^{-2} (50 m^2), 0.14 m^{-2} (25 m^2), and 0.85 m^{-2} (2 m^2). Both live and dead coral cover were positively correlated with the number of associated taxa up to about 30% cover, for all spatial scales (24.5–28%). We discuss the results in the context of past and future efforts to develop criteria for identifying VMEs.

Keywords: ***Solenosmilia variabilis*, cold-water coral reef, density threshold, VME, deep sea**

Edited by:
Sandra Brooke,
Florida State University, United States

Reviewed by:
Tina Molodtsova,
P.P. Shirshov Institute of Oceanology (RAS), Russia
Saskia Brix,
Senckenberg Museum, Germany

Correspondence:
Ashley A. Rowden
ashley.rowden@niwa.co.nz

Specialty section:
This article was submitted to Deep-Sea Environments and Ecology, a section of the journal Frontiers in Marine Science

Received: *03 October 2019*
Accepted: *05 February 2020*
Published: *21 February 2020*

Citation:
Rowden AA, Pearman TRR, Bowden DA, Anderson OF and Clark MR (2020) Determining Coral Density Thresholds for Identifying Structurally Complex Vulnerable Marine Ecosystems in the Deep Sea. Front. Mar. Sci. 7:95. doi: 10.3389/fmars.2020.00095

INTRODUCTION

Deep-sea trawling impacts the structure and function of seafloor communities and habitats (see review by Clark et al., 2016). In 2006 and 2009, the United Nations General Assembly (UNGA) called upon regional fisheries management organizations (RFMOs) to develop and adopt binding conservation management measures requiring their members to protect vulnerable marine ecosystems (VMEs) from significant adverse impacts of bottom fishing (Resolutions 61/105 and 64/72; UNGA, 2006, 2009). The Fisheries Agricultural Organisation (FAO) International Guidelines for the Management of Deep-sea Fisheries in the High Seas provides guidance for defining and identify VMEs (FAO, 2009). Although the guidelines have served as the principal means for RFMOs to define and identify VMEs, they did not provide any clear guidance on what constitutes evidence of an encounter with a VME during bottom fishing operations or analytical approaches for identifying areas containing VMEs.

Occurences of VME indicator taxa are routinely used by RFMOs as surrogates for VME identification and delimitation. VME indicator taxa may be recorded from trawling bycatch and used for encounter protocols [e.g., Parker et al., 2009 for the South Pacific Regional Fisheries Management Organisation (SPRFMO)] or their distribution may be predicted by habitat suitability modeling (also called species distribution modeling) (e.g., Georgian et al., 2019 for SPRFMO). However, the distribution of a VME indicator taxon does not necessarily correlate with the distribution of the VME itself. For example, Howell et al. (2011) noted that the observed distribution of a coral reef in the North Atlantic is a subset of the wider predicted distribution the indicator taxon *Desmophyllum pertusum* (Linnaeus, 1758) [formerly *Lophelia pertusa*] that can form such a VME when it occurs in sufficient density. Most methods used to date to distinguish VMEs involve some subjective judgment, and therefore the veracity of these methods depends upon a number of untested assumptions. For example, Rowden et al. (2017) used abundance-based habitat suitability models of a coral species and a subjective density-based definition of a coral reef to predict VME distribution. However, the definition used was not related directly to any of the criteria that the FAO guidelines specify for what constitutes a VME (FAO, 2009).

The FAO guidelines have 5 criteria for identifying VMEs, one of which is: "*Structural complexity – an ecosystem that is characterized by complex physical structures created by significant concentrations of biotic and abiotic features. In these ecosystems, ecological processes are usually highly dependent on these structured systems. Further, such ecosystems often have high diversity, which is dependent on the structuring organisms*" (FAO, 2009). This criterion emphasizes two obvious components that can be measured, and which can therefore be used to determine objectively a threshold for identifying a VME. That is, the threshold of the "significant concentrations" of the structure forming organism that supports a "high diversity" of the organisms that are dependent on the structuring organisms. Thresholds for identifying cold-water coral reefs are beyond the remit of the FAO guidelines, and of the few thresholds that have been published independently none are based on a quantitative analysis of the direct relationship between coral density and associated biodiversity. These threshold estimates for identifying distinct coral reef habitat range widely between 15 and >60% coral cover (Vertino et al., 2010; Rowden et al., 2017), presumably at least in part because of taxa and site/regional differences in the relationship between coral cover and the formation of a recognizable reef structure, but also potentially because of the subjective nature of the threshold estimate. Ideally, if habitat suitability models or even direct observation of VMEs are going to be used to inform spatial management of bottom trawling, then studies are required that objectively derive VME thresholds where VME indicator taxa densities are sufficient to provide specific ecological functions. Such studies will need to be specific to the taxa encountered in a RFMO area.

Solenosmilia variabilis is a stony coral VME indicator species that is structurally complex, long-lived, fragile, and widespread within the SPRFMO Convention Area (Anderson et al., 2016). This coral species can form structurally complex reef that provides habitat for diverse communities in the region, which can be impacted by bottom trawling (Koslow et al., 2001; Althaus et al., 2009; Clark and Rowden, 2009; Williams et al., 2010; Clark et al., 2019). The aim of the present study was to examine the relationship between the density of *S. variabilis* and the diversity of associated organisms, and to determine if it is possible to identify a density threshold at which a demonstrable elevated biodiversity is supported by the coral habitat, and which can be used practically to identify a VME. While a density threshold identified by the study may not be transferable to other taxa/regions, the methodology can be used for similar determinations in other RFMO areas. That is, our overall purpose is to operationalize one of the FAO's criteria for identifying VMEs so that it can be used as a basis for devising spatial management measures to prevent significant adverse impacts by fishing.

MATERIALS AND METHODS

Study Area and Sampling

Data used in the analysis were collected during a survey of six seamounts on the Louisville Seamount Chain to field test habitat suitability models for VME indicator taxa (Anderson et al., 2016). The Louisville Seamount Chain lies to the east of New Zealand in the SPRFMO Convention Area, the region of the South Pacific beyond areas of national jurisdiction. Analysis was conducted on data from one of these seamounts, Forde Guyot, situated at the North-West of the part of the Louisville Seamount Chain sampled by the survey (**Figure 1**). Forde Guyot was chosen for the analysis because historically it has received the least fishing pressure (of the six seamount features surveyed) and is now closed to bottom trawling (since May 2008), and thus represents an environment in which the coral reef habitat formed by *S. variabilis* is unlikely to have been modified by bottom trawling (no indication of trawling impacts – trawl net/door marks, discarded gear etc – were observed in the camera survey of this seamount). The survey used a towed camera system (Hill, 2009) with video (HD1080, 45° forward-orientation) and stills (24 mp DSLR, vertical orientation) cameras. The tow speed, camera and light settings, and transect length were optimized for imaging and quantifying benthic epifauna communities (see Anderson et al., 2016 for deployment details). Imagery from both cameras was analyzed to obtain data on the abundance and distribution of *S. variabilis* and all visible epifauna. These data were used to

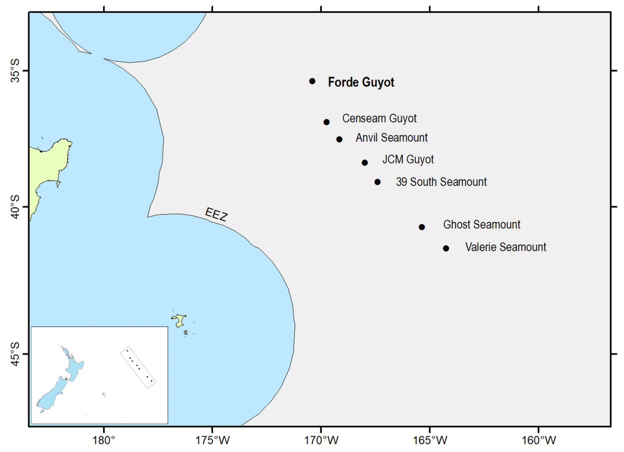

FIGURE 1 | Map showing the summit location of Forde Guyot (bolded feature name) in relation to other seamount features on part of the Louisville Seamount Chain. Inset map shows these seamounts in relation to New Zealand (modified from Rowden et al., 2017).

not only test regional habitat suitability models, but to also make abundance-based models of *S. variabilis* (Rowden et al., 2017).

Data and Data Processing

Video data from Rowden et al. (2017), detailing faunal occurrences and substrate types were reviewed, and nine transects from Forde Guyot in which *S. variabilis* was present were used in the analysis (**Figure 2** and **Table 1**). For the current study, still images from these transects were also analyzed (**Table 1**; after review to remove overlapping images, poor quality images, and images taken at >3 m altitude) with *S. variabilis* and all other visible epifauna ('morphospecies' > 10 mm) being counted (using the image annotation platform BIIGLE 2.0; Langenkämper et al., 2017). Because much of the *S. variabilis* matrix of colonies observed was evidently not alive (dark coloration with no live polyps visible in high resolution still imagery), which is apparently typical for such cold-water coral reef habitat (e.g., Clark and Rowden, 2009; Vertino et al., 2010, and see **Figure 3**), occurrence of this taxon was recorded in three ways: percent cover of the seabed for live and dead "intact coral" matrix, percent cover of dead broken-up matrix termed "coral rubble," and counts of distinct live coral colonies or "coral heads" on which live polyps were visible (**Figure 3**). A coral head was considered distinct if the separation between colonies with live polyps was visually obvious (typically > 5 cm). No minimum or maximum size criteria were used to identify a live coral head, but they were typically in the range of 15–40 cm in diameter.

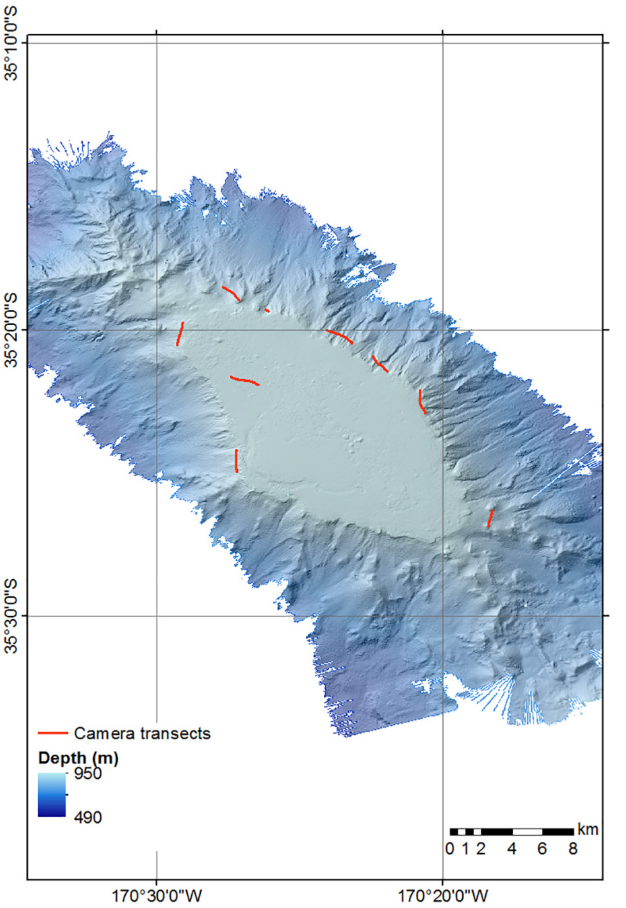

FIGURE 2 | Bathymetric map of Forde Guyot showing the location of the camera transects analyzed for this study.

Coral and other epifauna records were determined at three spatial scales: per 50 m^2 segment of video transect (~2 m transect image width × 24 m along the transect track), per 25 m^2 segment of video transect (~2 m transect image width × 12 m along the transect track) and from individual still frames per 2 m^2 (~ 2 m × 1 m still image view). Analyses at these spatial scales allow for an examination of whether any identified VME density thresholds were scale dependent, and allow for comparisons with previously published threshold estimates for coral reef habitat.

Data Analysis

Welch's ANOVA was first used to test if coral habitat (live and dead intact coral and coral rubble) is associated with higher species richness (number of other epifaunal 'morphospecies') than non-coral habitat (mainly unconsolidated substrates such as sand and mud). Welch's ANOVA was used because data had unequal variances.

Data exploration indicated a lack of homogeneity and non-linear relationships within the datasets, which together with the nested structure of the data violate statistical assumptions of methods that fit curves to raw data (**Supplementary Figure S1**). Thus, general additive models (GAMs) were applied to the datasets to model the relationship between the coral density parameters noted above (predictor variables) and the species richness of other epifauna (response variable). GAMs are generalized models with smoothers and link functions based on an exponential relationship between the response variable and the predictor variables (Zuur et al., 2014b). GAMs have previously been used to model relationships between

TABLE 1 | Length of each camera transect, video duration, total number of still images taken and retained for analysis, and % of video transect represented by the retained images.

Camera transect	Length (m)	Duration (hh:mm:ss)	Total images	Images retained	% Video sampled	Mid transect depth (m)
TAN1402/06	1268	01:02:43	251	217	34	1217
TAN1402/09	1648	01:02:50	258	234	28	1105
TAN1402/12	1734	00:28:05	258	206	24	1472
TAN1402/13	335	00:11:22	100	34	20	1375
TAN1402/18	1264	01:02:53	254	157	25	1483
TAN1402/19	1550	00:55:30	228	210	27	1227
TAN1402/20	1469	00:58:03	259	218	30	1234
TAN1402/25	1151	00:47:42	199	192	33	1430
TAN1402/27	1668	01:02:48	256	250	30	1053

environmental variables and species richness (Robert et al., 2015; Song and Cao, 2017) and to identify ecological response thresholds (Foley et al., 2015; Large et al., 2015). GAMs were chosen because they can accommodate non-linear relationships and produce ecologically intuitive outputs by identifying the shape and strength of the relationship between the response and predictor variables (Zuur et al., 2014a). Non-linear threshold responses are common in ecological systems, but some non-linear phenomena may not be of direct interest and need to be accounted for when making inferences about the variables in question. Depth and spatial proximity of data points to one another can influence biological responses and were integrated into models via the categorical variable 'transect.' To further account for inherent spatial autocorrelation in the data an additional predictor variable, the residual autocovariate (RAC) was calculated and added to the model. The RAC represents the similarity between the residuals from initial models at a location compared with those of neighboring locations. This method can account for spatial autocorrelation without compromising model performance (Crase et al., 2012).

The degree of smoothing in the fitting of the explanatory variables was based on the generalized cross validation (GCV) method and a log link function. For the 2 m^2 dataset smooth terms allowing up to 4 degrees of freedom were used, due to the low variability in the response values at this resolution. A negative binomial distribution with no transformation was chosen (in part because this provided better fits given the high proportion of zero values) after exploring several alternative distributions (Poisson, quasi-Poisson, zero inflated) and model set ups (different variable explanatory variables and optimized under parsimony). Significance of terms in the model were tested with ANOVA. Model accuracy was assessed by variance in species richness explained by each model (Adjusted R^2) and model fit by Akaike's Information Criterion score (AIC). All statistical analyses were conducted using the open source software R (R Core Team, 2014), packages "mgcv," "gbm," "raster" and "vegan."

Thresholds are characterized by a non-linear change in response to a predictor variable (Foley et al., 2015; Large et al., 2015). Based on ecological theory, we expect the relationship between coral density parameters and associated species richness to exhibit an initial relatively steep positive relationship before flattening off to a plateau or exhibiting a slight drop off as coral density increases. That is, as the amount or density of structurally complex habitat increases so does the number of species that can be supported by this habitat, up until a point where the concentration of habitat has reached a level where all physical niches are occupied by species that have become associated with the habitat (Rosenzweig, 1995, pp. 32–36, and references therein). As the density of the structural habitat increases beyond this threshold, it is possible that the number of associated species

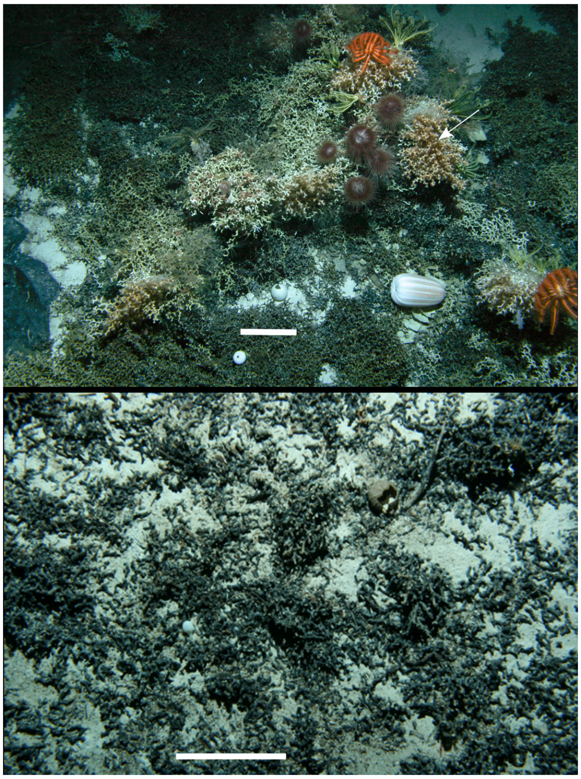

FIGURE 3 | Still images of the seafloor on Forde Guyot showing: **(top)** intact dead (brown)/live (white and pale orange) coral matrix with live coral heads (distinct pale orange colonies with live polyps; arrow indicates an example of a coral head) of *Solenosmilia variabilis*, and associated epifauna taxa; **(bottom)** broken-down dead coral matrix or coral rubble. Scale bar = 20 cm.

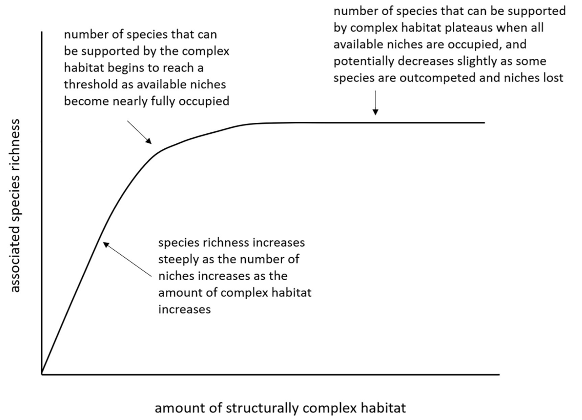

FIGURE 4 | Theoretical relationship between the amount of structurally complex habitat and associated species richness.

may decrease slightly as some species are outcompeted and the number of niches is reduced, assuming an increase in density is associated to some extent with an increase in time (Rosenzweig, 1995, pp. 186–189, and references therein) (**Figure 4**). Potential coral density thresholds for species richness were identified from the GAMs using four methods: (1) the intersections of linear regressions through the initial and final 5% of the data; (2) the intersection of a linear regression through the initial 5% of data with a horizontal line extended from the maximum cumulative value; (3) the point on a curve fit to the data that is closest to the top-left corner; and (4) the point that maximizes the distance between the curve and a line drawn between the extreme points on the curve (Youden Index) (**Supplementary Figure S2**). Where possible, all four threshold values were determined for each of the coral density parameters, and the average threshold for each spatial scale calculated.

RESULTS

See **Supplementary Material** for species richness data for each spatial scale of the analysis.

One hundred and thirty-six epifaunal morphospecies were identified from the datasets. Epifauna exhibited a patchy distribution, reflected in the species richness counts that were relatively low, and which reached maximum values of 10 at 50 m^2, 8 at 25 m^2 and 9 at 2 m^2. *Solenosmilia variabilis* also exhibited a patchy distribution occurring at low density across the study transects (**Figure 5**).

At all spatial scales, average epifaunal species richness was significantly higher for the intact live and dead coral matrix (2.35 50 m^{-2}, 3.28 25 m^{-2}, 2.6 2 m^{-2}), compared to coral rubble (0.98 50 m^{-2}, 1.56 25 m^{-2}, 1.09 2 m^{-2}) and non-coral habitat (0.81 50 m^{-2}, 1.27 25 m^{-2}, 1.15 2 m^{-2}) (Welch's ANOVA for 50 m^2 F2, 168 = 61.49, $p < 0.001$; 25 m^2 F2, 258 = 77.886, $p < 0.001$; 2 m^2 F2, 227 = 20.51, $p < 0.001$).

The number of live S. *variabilis* coral heads had the greatest influence on the models for species richness, followed by % cover of intact coral, whilst coral rubble had no significant influence, except at the 50 m^2 spatial scale. This result is consistent across spatial scales (**Table 2**).

Species richness exhibited an initial shallow positive response to % intact coral, which flattened or dropped off after reaching thresholds of 26% (50 m^2), 24.5% (25 m^2) and 28% (2 m^2) (**Figure 5** and **Table 3**). The relationships between species richness and % coral rubble were too 'flat' to determine thresholds (**Figure 6**).

Species richness exhibited an initial steep positive relationship with the number of live coral heads of *S. variabilis*, before reaching an identifiable threshold beyond which the relationship flattened off in an undulating or slightly decreasing curve (**Figure 6**). The multimodal response beyond the threshold at the 50 and 25 m^2 spatial scales appears to reflect inter-transect variability driven by the high density of S. *variabilis* recorded from one transect (station TAN1402/18) which is responsible for the second maxima. The average density threshold for the number of *S. variabilis* live heads is similar for both 50 and 25 m^2 spatial scales of the analysis, when expressed as number of coral heads m^{-2}; 0.11 and 0.14 m^{-2}, respectively. The average density threshold for number of live coral heads was 0.85 m^{-2} at the 2 m^2 spatial scale of the analysis (**Table 3**).

DISCUSSION

We determined density thresholds that can be used to objectively identify structurally complex coral reef VMEs in the SPRFMO Convention Area. We used a methodology that operationalizes one of the criteria for identifying VMEs by determining the "significant concentrations" of a structure forming organism that supports a "high diversity" of associated fauna that are dependent on this structuring organism (FAO, 2009).

Our initial analysis of image data from Forde Guyot on the Louisville Seamount Chain demonstrated that cold-water coral reef habitat formed by the stony coral *Solenosmilia variabilis* supports elevated levels of biodiversity compared to less structurally complex substrates such as nearby mud and sand. Elevated levels of biodiversity associated with habitat formed by other stony coral species, compared to other deep-sea habitats, have been demonstrated previously in other ocean regions (e.g., *Desmophyllum pertusum* in the North Atlantic - Henry and Roberts, 2007). However, we are unaware of any published study that has examined the direct relationship between density parameters of cold-water coral reefs and the richness of associated species [but see acknowledgments, and Beazley et al. (2015) and Ashford et al. (2019) for examinations of the density/biomass of other VME indicatar taxa and associated species richness]. A study by Van Den Beld et al. (2017) examined the separate relationships between stony coral cover and the abundance (but not species richness) of solitary coral taxa, and no density threshold for the abundances of these taxa was observed.

Our modeling analysis demonstrated a relationship between coral density and associated species richness at three spatial scales, and identified density thresholds at which coral reef habitat supports relatively higher levels of associated biodiversity.

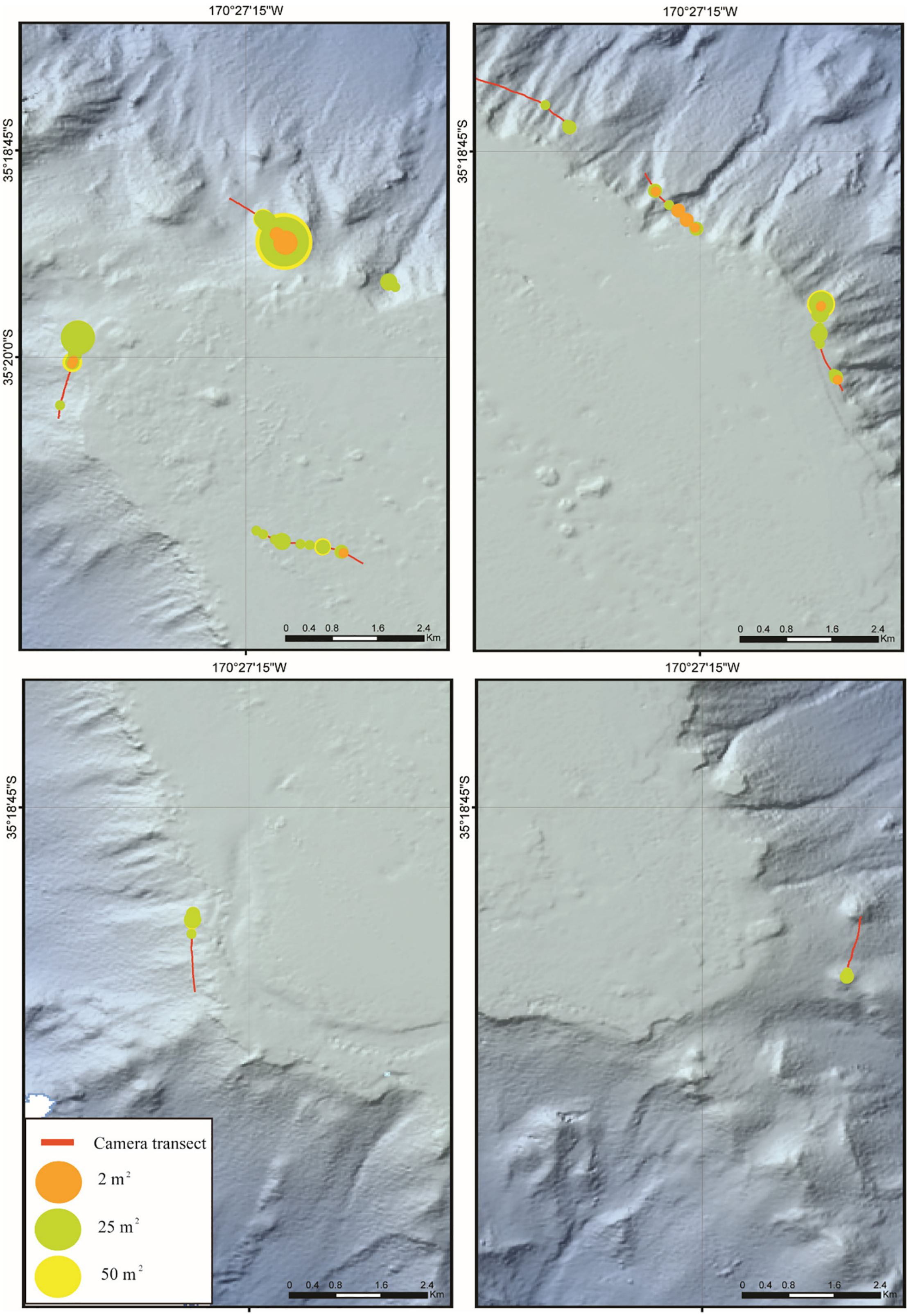

FIGURE 5 | Maps showing the distribution of the abundance of the stony coral *Solenosmilia variabilis* at three spatial scales (50, 25, and 2 m^2). Relative abundance expressed by expanding circles (see key for values). Symbols plotted at the midpoints of the 50 m^2, 25 m^2 sections of the camera transects, and at the exact image location for 2 m^2.

TABLE 2 | Results of the GAM models at three spatial scales.

	Spatial scale		
	50 m^2	25 m^2	2 m^2
Variable	**Approximate significance of smoother terms (ANOVA)**		
Number of live coral heads	3 (4), 580 = 2e-16***	4 (5), 1153 ≤ 2e-16***	2 (3), 1658 = 1.24e-08***
% intact coral	2 (9), 580 = 0.00586**	2 (9), 1153 = 0.00096***	2 (3), 1658 = 6.47–06***
% coral rubble	2 (9), 580 = 0.00461**	1 (9), 1153 = 0.0982	1 (3), 1658 = 0.273
Transect	8,580 ≤ 2e-16***	8,1153 ≤ 2e-16***	8, 1658 ≤ 2e-16***
RAC	1,580 ≤ 2e-16***	1,1153 ≤ 2e-16***	1,1658 ≤ 2e-16***
Adjusted R^2	48%	36%	26%
AIC	1723	2793	4550

Explanatory contribution of each variable indicated by approximate significance of the smoother terms. Model accuracy assessed by variance in species richness explained by each model (Adjusted R^2) and model fit by Akaike's Information Criterion score (AIC).

The non-linear relationship conformed to the theoretical expectation on which our study was based (see section Materials and Methods). We acknowledge that a possible alternative explanation, in addition to competition, for any apparent decrease in the number of species associated with coral densities above the thresholds could be related to lower detection probability as habitat-forming taxa become more abundant and increase in complexity. Somewhat surprisingly, the density thresholds for the % cover of the intact coral matrix were similar across all spatial scales (ranging from 24.5 to 28%), as were the thresholds for the number of live coral heads at the 50 m^2 and 25 m^2 spatial scales (0.11 and 0.14 m^{-2}, respectively). The higher coral head density threshold observed for the 2 m^2 spatial scale (0.85 m^{-2}) could potentially be explained by a range of factors associated with the two camera systems, including: different observation viewpoints in video and still images; image resolution and lighting differences; and differing spatial scales of observation. The angled viewpoint of the video means that it is possible some coral heads may be obscured by coral matrix in front of them, whereas the vertical viewpoint of the still images will ensure that all live coral heads are observable, thereby resulting in a higher count. The still images are of higher resolution and more evenly lit than the video imagery, which could also result in higher detection rates of the live coral heads in the still images. It is also possible that the identification of thresholds for individual live coral heads are scale-dependent. The cold-water coral reefs were patchy, and because still images sample a smaller seabed area than does video, they are less likely to encounter coral reef patches, which will influence the counts of live coral heads. A further consequence of the smaller seabed area within individual still images (which is typically smaller than the coral patches) is that counts of live coral head density may be higher in still images because larger coral reef patches are more likely to be detected multiple times by the images than smaller habitat patches (assuming larger patches are more dense than smaller patches). Observations made by video at the 50 m^2 and 25 m^2 spatial scale will more likely capture whole coral reef patches, and thereby result in more stable and reliable density estimates. Thus, it is clear that scale-related sampling effects should be considered when attempting to determine reliable density estimates of fauna that generate patchy habitats (Andrew and Mapstone, 1987). However, the results for the two larger spatial scales, both derived from the same imaging system, suggest that the relationships and thresholds observed are ecologically fundamental. This finding provides support for the practical application of such objectively identified quantitative thresholds in the identification and mapping of structurally complex VME habitats.

TABLE 3 | Results of the analysis to determine coral density thresholds for identifying structurally complex vulnerable marine ecosystems at three spatial scales (see section Materials and Methods for description of numbered threshold methods).

Threshold method	**Spatial scale**		
	50 m^2	25 m^2	2 m^2
% Intact coral cover			
1	NA	NA	NA
2	NA	NA	NA
3	22	19	25
4	32	30	31
Average	24.5	26	28
Number of coral heads m^{-2}			
1	0.11	NA	NA
2	0.10	0.13	0.80
3	0.10	0.15	0.65
4	0.11	0.15	1.10
Average	0.11	0.14	0.85

Vertino et al. (2010) subjectively identified 20–40% coverage of live and/or dead coral colonies as a threshold at a spatial scale of 2.4 m^2 in the Mediterranean Sea. Their result, even though a different species in a different ocean was broadly similar to our objectively derived thresholds of 24.5 – 28% cover. For the one quantitative examination that we know of that examined the relationship between % coral cover and community structure (Price et al., 2019), the derived density threshold is also similar to the one we identify more directly for species richness. Price et al. (2019) found through multivariate analysis that the proportion

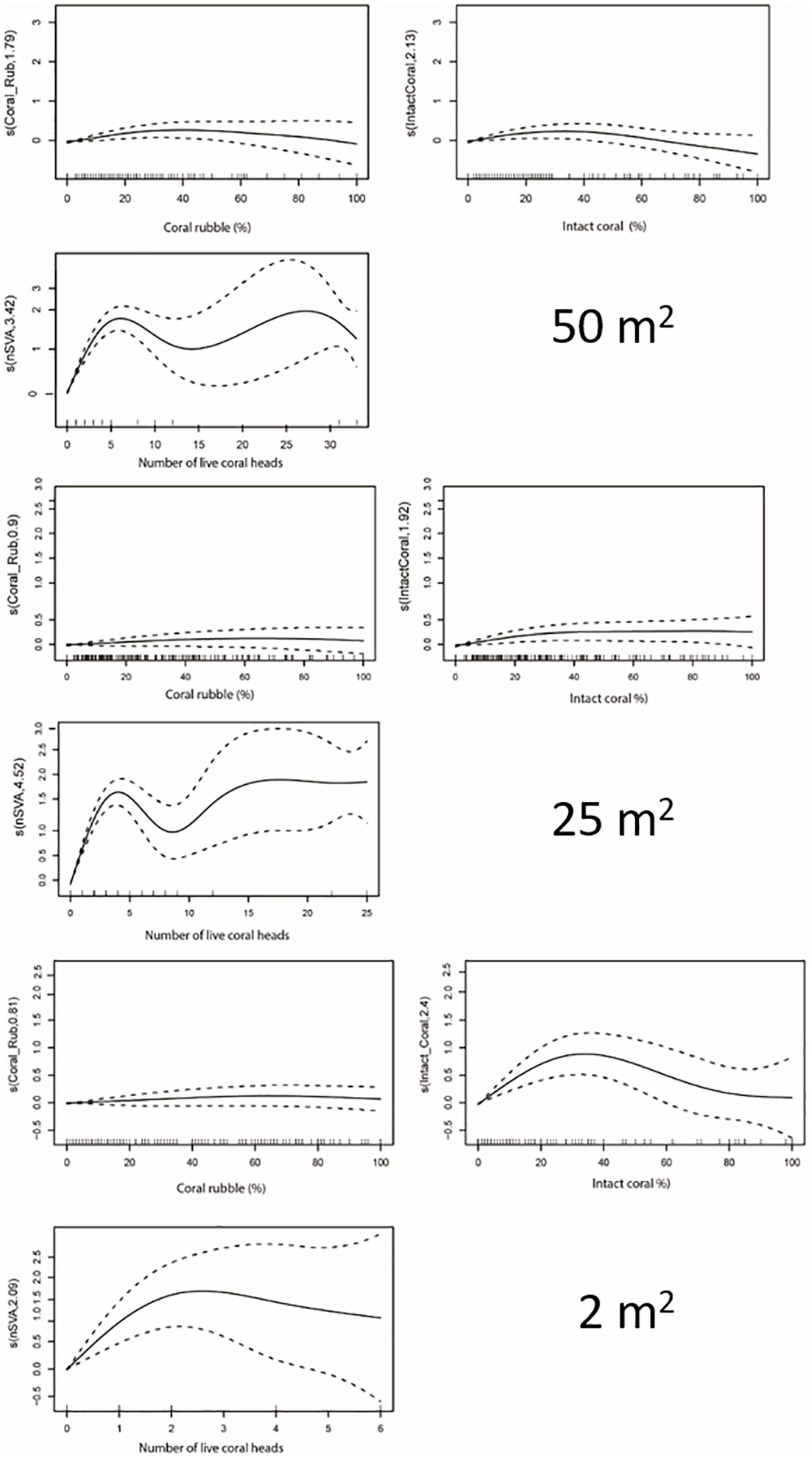

FIGURE 6 | General Additive Model smoother outputs showing the relationship between coral density (% coral rubble, % intact coral, number of live coral heads) and species richness at three spatial scales.

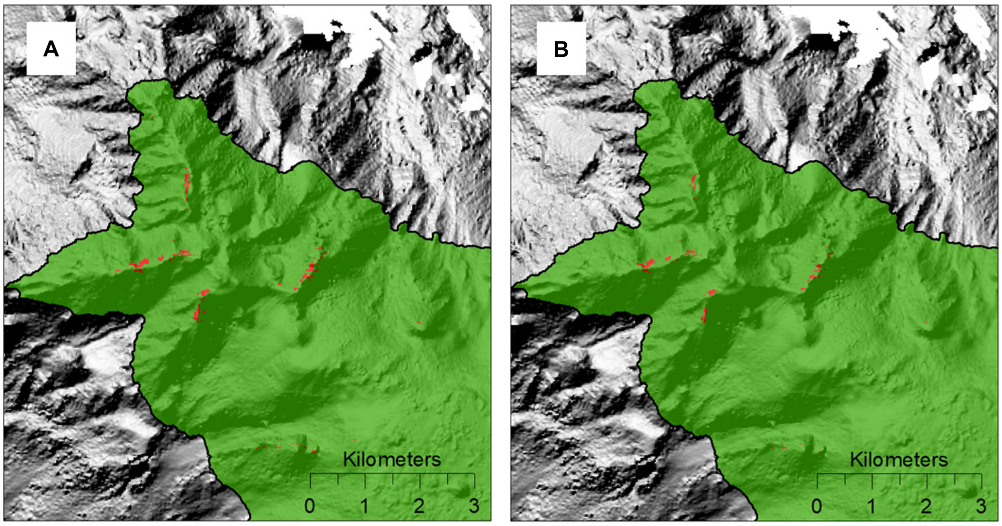

FIGURE 7 | Predicted coral reef VME habitat (red patches) on the north-west portion of Forde Guyot, identified by applying a density threshold for live coral heads to an abundance-based habitat suitability model for *Solenosmilia variabilis* (Rowden et al., 2017); **(A)** using the subjectively derived threshold of 2.78 live coral heads 25 m^{-2} from Rowden et al. (2017), and **(B)** the objectively derived threshold of 3.5 live coral heads 25 m^{-2} from the present study.

of live and dead coral cover of stony coral (predominantly *Madrepora oculata* Linnaeus, 1758 and *Desmophyllum pertusum*) in the Whittard Canyon (North East Atlantic) was apparently related to community structure, and that coral reef communities become distinct somewhere between a coral cover of 28 and 36% (they suggested 30% as an approximation) at a spatial scale of 10 s of meters. They demonstrated more directly using GAMs that species richness began to plateau at a particular level of structural complexity (0.7 vector ruggedness measure), which they reported (but did not show) as being equivalent to 30% coral cover.

The density thresholds we identified for live coral heads using video data, 0.11 m^{-2} and 0.14 m^{-2} (at 50 m^2 and 25 m^2, respectively), were the same or similar to the threshold of 0.11 m^{-2} used previously to identify coral reef VME on the Lousiville Seamount Chain (coverted from 2.78 live heads per 25 m^2, Rowden et al., 2017). The density threshold used by Rowden et al. (2017) was from the same video data but derived by a different methodology, and based on a subjective definition of what constitutes a coral reef "sensitive environment" according to regulations devised to prevent impacts to such habitats by human activities in the New Zealand EEZ[1]. The similarity between the thresholds appears to offer some support for the subjective-based threshold. However, Rowden et al. (2017) urged caution of the use of the threshold they applied, describing it as a subjective regional translation of the "you will know when you see it" descriptions of cold-water coral reefs, and argued for the implementation of quantitative studies such as the present work to objectively identify VMEs. Having now established a quantitative-based threshold to identify VMEs, it is possible to re-map the coral reef habitat on the study seamounts of the Louisville Seamounts Chain. Although the objective and subjective-based thresholds were apparently similar, application of the new density threshold for 25 m^2 indicates that there is ~60% less coral reef VME habitat on Forde Guyot than previously estimated (Rowden et al., 2017; 0.12 km^2 compared to 0.20 km^2, **Figure 7**).

In the present study, low sample size and uneven sampling posed some limitations for modeling the relationship between coral density parameters and associated species richness. However, it appears that low coral density and a patchy distribution is inherent in the nature of the cold-water coral reefs on Forde Guyot, and indeed other seamounts on the Louisville Seamount Chain (Rowden et al., 2017). Future studies should endeavor to better accommodate such heterogeneity in analyses of the relationships that we examined. Despite the potential limitations, we hope our work will encourage future efforts to look further at the taxa/regional-specific or universal nature of the density thresholds determined here for identifying structural complex coral reef VMEs. Quantitative studies establishing the association between coral density parameters and the structural or functional attributes that distinguish VMEs are few, and this lack is currently hindering efforts to devise measures to protect VMEs from the impacts of fishing.

CONCLUSION

Our data and previous findings suggest that approximately 30% intact coral cover represents a significant concentration which supports a high diversity of associated taxa. This threshold could be used broadly to distinguish deep-sea coral reef VMEs made by structurally complex stony coral species such as *Solenosmilia variabilis*, *Madrepora oculata*, and *Desmophyllum pertusum*. Furthermore, specific threshold density metrics for particular species and regions, such as we derived for number of live coral heads of *S. variabilis* for the South Pacific, can be used to threshold abundance-based habitat suitability model

---

[1] http://www.mfe.govt.nz/marine/legislation/regulations-under-eez-act

predictions to make maps that can be used by RFMOs to design spatial management measures to prevent significant adverse impacts to VMEs.

DATA AVAILABILITY STATEMENT

All datasets generated for this study are included in the article/**Supplementary Material**.

AUTHOR CONTRIBUTIONS

AR conceived of the study, led the writing, and drafted text for the manuscript. AR, MC, and DB designed the field survey. MC, DB, and OA collected the data from the field survey. TP analyzed the images, conducted the statistical analysis, and contributed draft text to the manuscript. All authors interpreted all data, revised and approved the final version of the manuscript.

FUNDING

This work was based on data obtained during the NIWA-led South Pacific Vulnerable Marine Ecosystems Project funded by the New Zealand Ministry for Business, Innovation and Employment (C01X1229). AR, DB, OA, and MC's contribution to the research reported here was funded by NIWA's Fisheries Centre. TP's contribution to the research was funded by the Southampton Partnership for Innovative Training of Future Investigators Researching the Environment, which supported her internship at NIWA while a Ph.D. student at the University of Southampton.

ACKNOWLEDGMENTS

We acknowledge that our study was partly inspired by the poster displayed by Lenaick Menot et al. at the 2018 Deep Sea-Biology Symposium in Monterey, United States (The ecological role of patchy cold-water coral habitats: Does coral density influence local biodiversity in submarine canyons in the Bay of Biscay? http://dsbsoc.org/wp-content/uploads/2014/12/15thDSBS_Abstracts.pdf). We thank Tom Ezard, from the National Oceanography Centre, for his discussions of statistical model validation plots.

SUPPLEMENTARY MATERIAL

The Supplementary Material for this article can be found online at: https://www.frontiersin.org/articles/10.3389/fmars.2020.00095/full#supplementary-material

REFERENCES

Althaus, F., Williams, A., Schlacher, T. A., Kloser, R. K., Green, M. A., Barker, B. A., et al. (2009). Impacts of bottom trawling on deep-coral ecosystems of seamounts are long-lasting. *Mar. Ecol. Progr. Ser.* 397, 279–294. doi: 10.3354/meps08248

Anderson, O. F., Guinotte, J. M., Rowden, A. A., Clark, M. R., Mormede, S., Davies, A. J., et al. (2016). Field validation of habitat suitability models for vulnerable marine ecosystems in the South Pacific Ocean: implications for the use of broad-scale models in fisheries management. *Ocean Coast. Manag.* 120, 110–126. doi: 10.1016/j.ocecoaman.2015.11.025

Andrew, N. L., and Mapstone, B. D. (1987). Sampling and the description of spatial pattern in marine ecology. *Oceanogr. Mar. Biol.* 25, 39–90.

Ashford, O. S., Kenny, A. J., Barrio Froján, C. R. S., Downie, A.-L., Horton, T., and Rogers, A. D. (2019). On the influence of Vulnerable Marine Ecosystem habitats on peracarid crustacean assemblages in the Northwest Atlantic Fisheries Organisation regulatory area. *Front. Mar. Sci.* 6:401. doi: 10.3389/fmars.2019.00401

Beazley, L., Kenchington, E., Yashayaev, I., and Murillo, F. J. (2015). Drivers of epibenthic megafaunal composition in the sponge grounds of the Sackville Spur, northwest Atlantic. *Deep Sea Res. Part I Oceanogr. Res. Pap.* 98, 102–114. doi: 10.1016/j.dsr.2014.11.016

Clark, M. R., Althaus, F., Schlacher, T. A., Williams, A., Bowden, D. A., and Rowden, A. A. (2016). The impacts of deep-sea fisheries on benthic communities: a review. *ICES J. Mar. Sci.* 73, i51–i69. doi: 10.1371/journal.pone.0022588

Clark, M. R., Bowden, D. A., Rowden, A. A., and Stewart, R. (2019). Little evidence of benthic community resilience to bottom trawling on seamounts after 15 Years. *Front. Mar. Sci.* 6:63. doi: 10.3389/fmars.2019.00063

Clark, M. R., and Rowden, A. A. (2009). Effect of deep water trawling on the macro-invertebrate assemblages of seamounts on the Chatham Rise. *New Zealand. Deep Sea Res. I* 56, 1540–1554. doi: 10.1016/j.dsr.2009.04.015

R Core Team, (2014). *R: A language and environment for statistical computing. R Foundation for Statistical Computing*. Vienna: R Core Team.

Crase, B., Liedloff, A. C., and Wintle, B. A. (2012). A new method for dealing with residual spatial autocorrelation in species distribution models. *Ecography* 35, 879–888. doi: 10.1111/j.1600-0587.2011.07138.x

Duncan, P. M. (1873). A description of the Madreporaria dredged up during the Expeditions of H.M.S. 'Porcupine' in 1869 and 1870. *Trans. Zool. Soc. London* 8, 303–344.

FAO, (2009). *Management of Deep-Sea Fisheries in the High Seas*. Rome: FAO.

Foley, M. M., Martone, R. G., Fox, M. D., Kappel, C. V., Mease, L. A., Erickson, A. L., et al. (2015). Using ecological thresholds to inform resource management: current options and future possibilities. *Front. Mar. Sci.* 2:95. doi: 10.3389/fmars.2015.00095

Georgian, S. E., Anderson, O. F., and Rowden, A. A. (2019). Ensemble habitat suitability modeling of vulnerable marine ecosystem indicator taxa to inform deep-sea fisheries management in the South Pacific Ocean. *Fish. Res.* 211, 256–274. doi: 10.1016/j.fishres.2018.11.020

Henry, L. A., and Roberts, J. M. (2007). Biodiversity and ecological composition of macrobenthos on cold-water coral mounds and adjacent off mound habitat in the bathyal Porcupine Seabight. *Ne Atlantic. Deep Sea Res I* 54, 654–672. doi: 10.1016/j.dsr.2007.01.005

Hill, P. (2009). Designing a deep-towed camera vehicle using single conductor cable. *Sea Technol.* 50, 49–51.

Howell, K. L., Holt, R., Endrino, I. P., and Stewart, H. (2011). When the species is also a habitat: comparing the predictively modelled distributions of Lophelia pertusa and the reef habitat it forms. *Biol. Conservat.* 144, 2656–2665. doi: 10.1016/j.biocon.2011.07.025

Koslow, J. A., Gowlett-Holmes, K., Lowry, J. K., O'hara, T., Poore, G. C. B., and Williams, A. (2001). Seamount benthic macrofauna off southern Tasmania: community structure and impacts of trawling. *Mar. Ecol. Progr. Ser.* 213, 111–125. doi: 10.3354/meps213111

Langenkämper, D., Zurowietz, M., Schoening, T., and Nattkemper, T. W. (2017). BIIGLE 2.0 - *Browsing and annotating large marine image collections. Front. Mar. Sci.* 4:83. doi: 10.3389/fmars.2017.00083

Large, S. I., Fay, G., Friedland, K. D., and Link, J. S. (2015). Critical points in ecosystem responses to fishing and environmental pressures. *Mar. Ecol. Progr. Ser.* 521, 1–17. doi: 10.3354/meps11165

Linnaeus, C. (1758). *Systema Naturae Per Regna Tria Naturae, Secundum Classes, Ordines, Genera, Species, Cum Characteribus, Differentiis, Synonymis, Locis*, 10th Edn, Vol. 1. Holmiae: Laurentius Salvius, 824. doi: 10.5962/bhl.title.542

Parker, S. J., Penney, A. J., and Clark, M. R. (2009). Detection criteria for managing trawl impacts to Vulnerable Marine Ecosystems in high seas fisheries of the South Pacific Ocean. *Mar. Ecol. Progr. Ser.* 397, 309–317. doi: 10.3354/meps08115

Price, D. M., Robert, K., Callaway, A., Lo Lacono, C., Hall, R. A., and Huvenne, V. A. I. (2019). Using 3D photogrammetry from ROV video to quantify cold-water coral reef structural complexity and investigate its influence on biodiversity and community assemblage. *Coral Reefs* 38, 1007–1021. doi: 10.1007/s00338-019-01827-3

Robert, K., Jones, D. O. B., Tyler, P. A., Van Rooij, D., and Huvenne, V. A. I. (2015). Finding the hotspots within a biodiversity hotspot: fine-scale biological predictions within a submarine canyon using high-resolution acoustic mapping techniques. *Mar. Ecol.* 36, 1256–1276. doi: 10.1111/maec.12228

Rosenzweig, M. L. (1995). *Species diversity in space and time*. Cambridge: Cambridge University Press.

Rowden, A. A., Anderson, O. F., Georgian, S. E., Bowden, D. A., Clark, M. R., Pallentin, A., et al. (2017). High-resolution habitat suitability models for the conservation and management of vulnerable marine ecosystems on the Louisville Seamount Chain, South Pacific Ocean. *Front. Mar. Sci.* 4:335. doi: 10.3389/fmars.2017.00335

Song, C., and Cao, M. (2017). Relationships between plant species richness and terrain in middle sub-tropical eastern China. *Forests* 8:344. doi: 10.3390/f8090344

UNGA, (2006). *United Nations General Assembly. Sustainable fisheries, including through the 1995 agreement for the implementation of the provisions of the United Nations convention on the law of the sea of 10 December 1982 relating to the conservation and management of straddling fish stocks and highly migratory fish stocks, and related instruments*. New York: UNGA.

UNGA, (2009). *United Nations General Assembly. Sustainable fisheries, including through the 1995 agreement for the implementation of the provisions of the United Nations convention on the law of the sea of 10 December 1982 relating to the conservation and management of straddling fish stocks and highly migratory fish stocks, and related instruments. General Assembly Resolution 64/72, 2009; A/RES/64/72*. New Yorl: UNGA.

Van Den Beld, I. M. J., Bourillet, J.-F., Arnaud-Haond, S., De Chambure, L., Davies, J. S., Guillaumont, B., et al. (2017). Cold-water coral habitats in submarine canyons of the Bay of Biscay. *Front. Mar. Sci.* 4, 1–30. doi: 10.3389/fmars.2017.00118

Vertino, A., Savini, A., Rosso, A., Di Geronimo, I., Mastrototaro, F., Sanfilippo, R., et al. (2010). Benthic habitat characterization and distribution from two representative sites of the deep-water SML Coral Province (Mediterranean). *Deep Sea Res. Part II Top. Stud. Oceanogr.* 57, 380–396. doi: 10.1016/j.dsr2.2009.08.023

Williams, A., Schlacher, T. A., Rowden, A. A., Althaus, F., Clark, M. R., Bowden, D. A., et al. (2010). Seamount megabenthic assemblages fail to recover from trawling impacts. *Mar. Ecol.* 31, 183–199. doi: 10.1111/j.1439-0485.2010.00385.x

Zuur, A., Ieno, E., Walker, N., Saveliev, A., and Smith, G. (2014a). *Mixed effects models and extensions in ecology with R*. Berlin: Springer.

Zuur, A., Saveliev, A., and Ien, E. (2014b). *A beginner's Guide to Generalised Additive Mixed Models with R*. United Kingdom: Kingdom.

Conflict of Interest: The authors declare that the research was conducted in the absence of any commercial or financial relationships that could be construed as a potential conflict of interest.

frontiers
in Marine Science

ORIGINAL RESEARCH
published: 18 March 2020
doi: 10.3389/fmars.2020.00155

A Data-Informed Approach for Identifying Move-on Encounter Thresholds for Vulnerable Marine Ecosystem Indicator Taxa

Shane W. Geange[1]*, Ashley A. Rowden[2,3], Simon Nicol[4], Tiffany Bock[5] and Martin Cryer[5]

[1] Department of Conservation, Wellington, New Zealand, [2] National Institute of Water and Atmospheric Research, Wellington, New Zealand, [3] School of Biological Sciences, Victoria University of Wellington, Wellington, New Zealand, [4] Institute for Applied Ecology, University of Canberra, Bruce, ACT, Australia, [5] Fisheries New Zealand, Ministry for Primary Industries, Wellington, New Zealand

OPEN ACCESS

Edited by:
Les Watling,
University of Hawai'i at Mānoa,
United States

Reviewed by:
Angelo Fraga Bernardino,
Federal University of Espirito Santo,
Brazil
Peter J. Auster,
University of Connecticut,
United States

***Correspondence:**
Shane W. Geange
sgeange@doc.govt.nz

Specialty section:
This article was submitted to
Deep-Sea Environments and Ecology,
a section of the journal
Frontiers in Marine Science

Received: 28 August 2019
Accepted: 28 February 2020
Published: 18 March 2020

Citation:
Geange SW, Rowden AA, Nicol S,
Bock T and Cryer M (2020) A
Data-Informed Approach
for Identifying Move-on Encounter
Thresholds for Vulnerable Marine
Ecosystem Indicator Taxa.
Front. Mar. Sci. 7:155.
doi: 10.3389/fmars.2020.00155

The United Nations General Assembly has called for the adoption of conservation management measures to protect vulnerable marine ecosystems (VMEs) from significant adverse impacts outside of areas of national jurisdiction. In response, many regional fisheries management organizations (RFMOs) have implemented move-on rules triggered by encounter threshold levels for the biomass of VME indicator taxa retained as bycatch. However, due to uncertainty of the relationships between catch, catch efficiency and the *in situ* biomass of VME indicator taxa, move-on rules alone may not be enough to prevent significant adverse impacts on VMEs. Although spatial management measures present one possible solution to these concerns, a lack of empirical data on the distribution of VMEs within the high seas means spatial management is often informed by model predictions of the spatial distribution of VME indicator taxa. Given the uncertainty associated with predicted distributions, move-on rules can provide immediate responses when spatial management measures may not be providing the expected conservation benefits. Using bycatch data from 9,771 New Zealand bottom trawls within the South Pacific RFMO Convention Area, we illustrate a data-informed approach for selecting high move-on encounter thresholds that may suggest the predicted distributions of VME taxa used to underpin spatial management are highly inaccurate. The reasoning that high thresholds act as a safeguard against uncertainty in the performance of spatial management measures requires untested assumptions regarding the level of permissible bycatch before further management action is required, with the acceptance of those assumptions a management decision balancing the sensitivity of the move-on rule with uncertainty regarding the effectives of the spatial management measures. Additional work is required to support these management decisions, including the determination of taxa-specific catchability estimates, and the seafloor density/biomass of VME indicator taxa that represents a VME. Obtaining this information will allow for the identification of encounter thresholds that are more ecologically meaningful. In the interim, the choice of thresholds should be re-evaluated as more experience with their application is gathered.

Keywords: VME, vulnerable marine ecosystem, indicator taxa, encounter protocol, move-on rule, bycatch thresholds, SPRFMO, high seas

INTRODUCTION

Based on growing concern about the risks to vulnerable marine ecosystems from fishing activities, the 2005 United Nations General Assembly (UNGA) has called for application of a precautionary approach and ecosystem approaches in the identification of vulnerable marine ecosystems, assessments of whether individual bottom fishing activities would cause significant adverse impacts to those ecosystems, and the closure of areas where vulnerable marine ecosystems are known or likely to occur until conservation and management measures have been established to prevent significant adverse impacts (United Nations General Assembly [UNGA], 2005, 2007). In support of the UNGA, the United Nations Food and Agriculture Organization (FAO) developed guidelines that included five criteria for defining VMEs (uniqueness or rarity; functional significance; fragility; probability of recovery; and structural complexity) and examples of VME indicator taxa (including: cold-water corals and hydroids; sponge-dominated communities; and seep and vent communities) (Food and Agriculture Organisation [FAO], 2009). The guidelines also defined significant adverse impacts as those compromising ecosystem structure or function, and identified six factors for determining the scale and significance of an impact (intensity of impact, spatial extent of impact relative to the availability of the habitat type affected, sensitivity to the impact, ability to recover, the extent to which ecosystems are altered by the impact, and the timing and duration of the impact). Although the guidelines have served as the principle means for RFMOs to define and manage significant adverse impacts on VMEs, they do not provide any clear guidance on what constitutes evidence of an encounter with a VME during bottom fishing operations or analytical approaches for identifying whether an area contains a VME or not. In addition, the guidelines provide only limited guidance on the spatial scale at which impact assessments should be conducted, referring to the terms areas, populations, habitats and ecosystems. Recognizing a lack of specificity in the guidelines, and that the actions that they had called for had not been sufficiently implemented by all RFMOs, the UNGA has become increasingly explicit regarding the need to develop science-based protocols to define evidence of encounters with VMEs, including the implementation of indicator-specific encounter thresholds, which in turn trigger a response, such as ceasing fishing operations and relocating elsewhere (i.e., the ‘move-on rule’) (United Nations General Assembly [UNGA], 2010, 2012). An ongoing challenge for RFMOs and member states is how to determine, based on best available scientific information and the precautionary principle, suitable encounter threshold levels that take into consideration other management measures (e.g., effort controls, spatial restrictions or closures, changes in gear design and/or operational measures) that are in place to prevent significant adverse impacts on VMEs.

Encounter thresholds, which are usually expressed as the quantity of a VME indicator taxon retained by the fishing gear, should ideally be specific to area, gear type and taxon, and based on historic bycatch levels and catchability estimates (Ardron et al., 2014). However, while scientifically validated thresholds are preferable (Food and Agriculture Organisation [FAO], 2016), in practice, most RFMOS have developed thresholds based on best judgment, with only a few RFMOs having developed thresholds based on historical catch records from either the fisheries for which the threshold is required, or from similar fisheries. For example, Kenchington et al. (2009) initially proposed the use of percentiles to identify thresholds from cumulative bycatch records for the North Atlantic Fisheries Organization (NAFO) region, and later used a kernel density approach to re-adjust the encounter threshold weights (Kenchington et al., 2014). New Zealand used historic bycatch records for the period 1990–2007 from within the South Pacific RFMO (SPRFMO) convention area, supplemented with data from the New Zealand exclusive economic zone, to determine encounter thresholds for 11 designated VME indicator taxa (at taxonomic levels ranging from phylum to order) (Parker et al., 2009). Using these data, the 50th percentile of the cumulative weight frequency distributions for each of the six primary indicator taxa (“the fishery norm”) was selected as a weight threshold (Parker et al., 2009). Recognizing that with increasing numbers of VME indicator taxa caught within a tow suggests an increased likelihood that the trawl had encountered a VME, the New Zealand encounter protocol for SPRFMO also included a ‘biodiversity’ threshold; the presence of three primary or secondary high-level VME indicator taxa retained within tows was selected as the biodiversity threshold (Parker et al., 2009). Therefore, within move-on areas (spatial management measures at the time also included closed areas and open areas within which the move-on rule did not apply) the encounter protocol for New Zealand-flagged fishing vessels was triggered by either the presence of three or more high-level VME indicator taxa, or by the catch of a single taxon above a taxon-specific weight threshold (Penney et al., 2009).

Once encounter thresholds have been exceeded, fishing vessels are typically required to move a minimum distance away from the location where VME indicator taxa were encountered. However, the conservation value associated with move-on rules is dependent on several assumptions that threshold values and move-on distances are adequate to prevent significant adverse impacts on VMEs. For example, although bycatch is assumed to be an indicator of *in situ* VME biomass and composition, the limited studies that have evaluated this assumption indicate that bottom-fishing gear (which is designed to catch fish) is inefficient at sampling VMEs, such that large quantities of VMEs might be destroyed on the seabed before an amount exceeding encounter thresholds is brought to the surface (Auster et al., 2010). Freese et al. (1999) found that catch efficiency for asteroids, echinoids and mollusk was <1%, and <5% for holothurians for trawls deployed in shallow water (∼200–280 m depth). With an encounter threshold set at 30 kg (the New Zealand threshold for stony corals under SPRFMO CMM-03 2017), a catch efficiency of 5% could potentially mean 600 kg of stony corals on the seafloor had been impacted. An additional concern with move-on rules is the sensitivity of the threshold; thresholds that are too sensitive result in frequent move-on events and the spreading of fishing effort away from preferred fishing grounds and, potentially, across the entire extent of a VME (Auster et al., 2010).

With concerns about the setting of encounter threshold levels and the general efficacy of move-on rules, there has been an increasing emphasis on the importance of implementing effective and representative spatial closures as a management measure to prevent significant adverse impacts on VMEs (Ardron et al., 2008, 2014; de Juan and Lleonart, 2010; Clark and Dunn, 2012; Wright et al., 2015; Thompson et al., 2016; Bell et al., 2018; Rowden et al., 2019). Bell et al. (2018) concluded that the use of closed areas is the most effective management tool for avoiding significant adverse impacts on VMEs, and encounter protocols the least effective. However, the design of spatial management is complicated by data availability. Relatively few data are available on the distribution and abundance of VME indicator taxa to use for the objective planning of spatial management measures. Consequently, spatial management is increasingly informed by combining limited biological records with environmental data in habitat suitability models to predict where VMEs are likely to occur. For example, habitat suitability models have recently been used to design spatial closures to avoid significant adverse impacts on VMEs in the SPRFMO Convention Area (Georgian et al., 2019; SPRFMO CMM 03-2019). The resulting spatial management measures close the great majority of the SPRFMO Convention Area to bottom trawling, concentrating fishing in areas that contain few cells where habitat suitability models predict high conservation value for VMEs. However, predictive habitat suitability models have associated uncertainty and may generate both false positives (VME indicator taxa are predicted to be more widespread than in actuality, potentially over-estimating the conservation value of closed areas) and false negatives (VME indicator taxa exist at high density in areas open to fishing but are not predicted by the models, potentially exposing them to fishing impacts). To address this uncertainty, SPRFMO's current approach is to use move-on rules to provide for rapid responses to unexpectedly large benthic bycatch events (relative to the predicted distributions of VME indicator taxa used to underpin spatial management) in open areas while work to reassess the effectiveness of the spatial management measures in preventing significant adverse impacts continues. Recognizing that in the SPRFMO case spatial management measures are the primary mechanism preventing significant adverse impacts on VMEs, SPRFMO's Scientific Committee agreed that any thresholds should be set relatively high so that they indicate when encounters are unexpected based on the relevant VME habitat suitability models (SPRFMO, 2017). Like SPRFMO, other RFMOs have controls on where fishing can occur combined with VME encounter protocols; however, key differences between SPRFMO's approach and other RFMOs is that the latter place emphasis on encounter protocols as a key tool (rather than spatial management as a key tool), only closing designated VMEs (rather than closing the majority of the Convention Area to bottom fishing and opening areas predicted to be of low conservation value for VMEs), and thereby appear to focus on managing significant adverse impacts on VMEs at local scales (rather than at broader spatial scales).

The aim of the present study was to reassess the SPRFMO bycatch encounter thresholds using SPRFMO-specific data, including that used by Parker et al. (2009), and a range of quantitative methods to establish encounter thresholds in accordance with direction from the SPRFMO's Scientific Committee that thresholds should be set high. Specifically, we (i) use historical bycatch data from within the SPRFMO Convention Area to construct taxon-specific cumulative distributions of VME indicator taxa bycatch and calculate a range of candidate weight and biodiversity thresholds; (ii) calculate the position of reference points on cumulative distributions to inform the systematic selection of a range of high weight and biodiversity thresholds from the suite of candidate values, from which decision-makers can choose depending on the desired sensitivity of the move-on rule. We also briefly discuss potential modifications that can be made to the approach where management objectives require more sensitive thresholds to prevent significant adverse impacts on VMEs.

MATERIALS AND METHODS

The data we used in the analysis were extracted from the Fisheries New Zealand Centralized Observer Database (*cod*) (accessed 14 May 2019). Data were collected by scientific observers (the New Zealand bottom trawl fleet has 100% observer coverage in the SPRFMO Convention Area) and included 9,771 New Zealand trawl tows (including both bottom and mid-water trawls) targeting black oreo (*Allocyttus niger*), alfonsinos (*Beryx splendens* and *B. decadacylus*), cardinal fish (*Epigonus telescopus*), orange roughy (*Hoplostethus atlanticus*), and spiky oreo (*Neocyttus rhomboidalis*). All tows were conducted within an assessed area within the western part of the SPRFMO Convention Area (west of 143°E longitude; **Figure 1**) between depths of 70 – 1,328 m (median = 955 m) over the period 2008–2018. These data consisted of tow-by-tow observer data with one record per benthic taxon encountered on each tow, and included trip number, tow number, fishing method, trawl type, benthic species code, common name, bycatch weight, method of weight analysis, information on whether the benthic material was encrusting anything or encrusted by something else, and observer comments. We partitioned the data extract to retain only those tows that included VME indicator taxa as bycatch. We designated VME indicator taxa using a modification of criteria defined by Parker et al. (2009) (**Table 1**). For tows containing VME indicator taxa as bycatch, we aggregated individual VME indicator species into higher-order VME indicator taxa using taxonomic designations from the World Register of Marine Species (Horton et al., 2019) (RRID:SCR_013312), resulting in a final dataset consisting of 3,048 bottom trawl tows and 4,502 aggregated VME indicator taxa records (see **Supplementary Material** for the allocation of New Zealand fisheries codes to VME indicator taxa).

Prior to analysis we checked the data for spurious bycatch weights. Of the 5,079 VME indicator taxa records, 80 had no or zero specified weight due to either small samples (<0.1 kg) not being accurately weighed at sea, rounding error, or presence only being recorded. Because zero weights are indicative of the presence of VME indicator taxa, we retained all zero weights in the analysis. Twenty-five records included bycatch weights

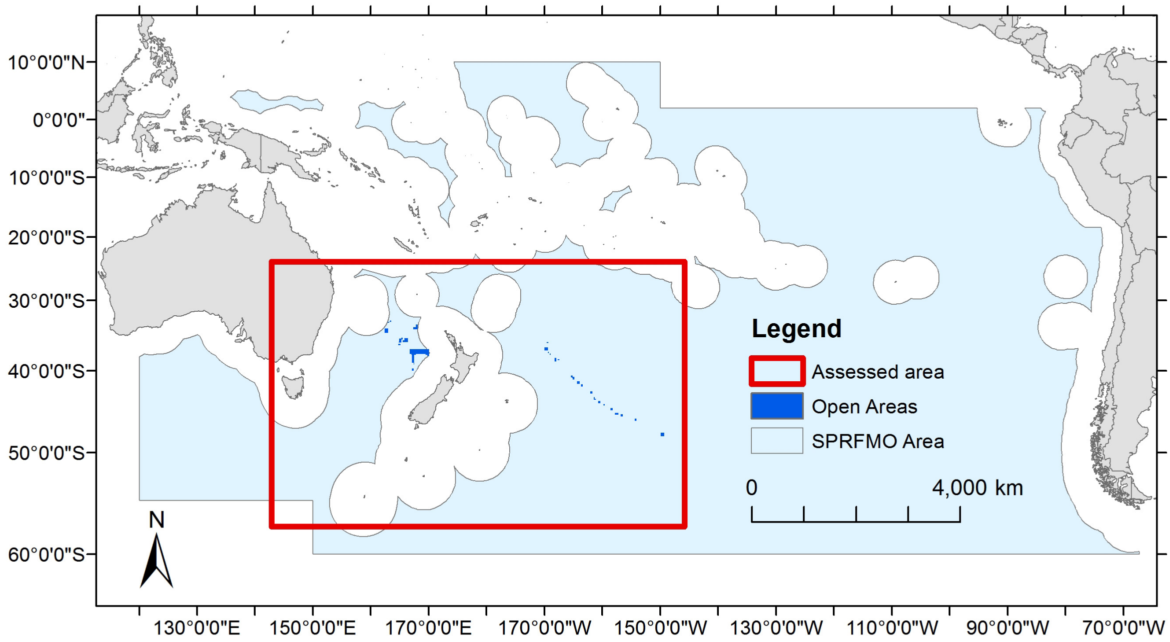

FIGURE 1 | The SPRFMO Convention Area with the location of the assessed area from within which data collected by scientific observers from 9,771 New Zealand bottom trawl tows over the period 2008–2018 was used in this analysis. Also shown as dark blue polygons are the locations of areas open to bottom trawling under SPRFMO CMM03-2019.

over 100 kg. For each of these records we reviewed observer comments, bycatch forms and any available photographs to verify that samples did include VME indicator taxa and weren't composite samples that also included non-VME indicator components. None of the records greater than 100 kg were recorded as encrusting something, and only four were recorded as being encrusted by something else. For all but three of the 25 records (Porifera 1091 kg; Scleractinia 200 and 120 kg), all weights over 100 kg were estimated by eye. Because we found no compelling evidence that the reported weights were incorrect, all records were retained in subsequent analyses. We also evaluated if bycatch weights had decreased over time (potentially as a result of historical fishing), which would suggest the calculation of thresholds should be based on bycatch weights from more recent fishing events. Finding no consistent relationship between bycatch weight and year across VME indicator taxa, we included the entire temporal dataset in subsequent analyses.

For each VME indicator taxon we calculated a range of percentiles from the ordered bycatch weights, with the percentiles serving as candidate encounter threshold values. Because the distribution of bycatch weights was not normally distributed (see section Results), we used ordered values rather than interpolation to calculate percentiles. Further, because the theoretical lower limit of the sample size required for the estimation of the 100α and 100(1-α) percentile from ordered values is equal to 1/α (e.g., the estimation of the 99.5th percentile requires 1/0.005 = 300 values) some taxa had insufficient bycatch samples to calculate the full range of percentiles using ordered data. Consequently, the number of candidate weight and biodiversity thresholds differed between VME indicator taxa.

To inform the systematic selection of weight and biodiversity thresholds for individual taxa from the candidate values, taxon-specific cumulative catch curves were examined to distinguish between the initial part of the curve associated with linear increase, and the final part of the curve associated with asymptotic decrease in slope. Assuming a strong relationship between the weight of VME indicator taxa landed on deck as bycatch and the functional role of VMEs, the transition between these two parts of the curve, especially if sharp, could potentially indicate a naturally occurring or ecologically relevant reference point (**Figure 2**); e.g., the biomass of the indicator taxon has reached a point where it is sufficient to constitute a distinct VME, such as coral reef or sponge garden (Kenchington et al., 2009). Weight thresholds indicating unexpectedly large catches that suggest the models used to predict the distribution of VME indicator taxa have a high level of inaccuracy should ideally fall to the right of such points, whereas biodiversity thresholds indicating increasing numbers of taxa in a single tow at weights below the threshold trigger should occur to the left. We used three different methods to calculate ecologically relevant reference points for taxa with sample sizes large enough to calculate the 99.5th percentile (**Figure 3**): (1) the position of the final breakpoint of a three-parameter segmented regression fitted to the data using the package 'segmented' in R (R Core Team, 2019) (RRID:SCR_001905); (2) the point on the cumulative distribution that is closest to the top-left corner (0,1), calculated as $q_1 = \min\{\sqrt{(1-y)^2 + (1-x)^2}\}$ for each point belonging to the cumulative distribution M(1-y,x) (Tilbury et al., 2000); and (3) the point on the cumulative distribution that maximizes the distance between the curve and a line drawn between the

TABLE 1 | Rationale for the designation of VME Indicator taxa (modified from Parker et al., 2009).

FAO Code	VME Indicator taxa	Comments	Relationship to FAO listings
PFR	Porifera (Phylum) *Sponges*	Includes the classes Demospongiae and Hexactinellida. These are found in the deep sea, can form complex structures and are vulnerable to disturbance by fishing gears. Longevity and resilience of cold-water sponges is unknown.	Sponge dominated communities are specifically listed by the FAO guidelines as vulnerable ecosystem components to protect. Sponge fields and large colonies form complex structures and may provide habitat for many species.
AJZ	Alcyonacea (Order) *Soft corals*	Alcyonacea other than gorgonians. Deep-sea species may be erect, large and branching, providing structural habitats and associated with other VME taxa.	Specifically listed by FAO guidelines as one of the main target taxonomic groups of the VME definition. If found in high densities, they would be vulnerable to fishing gear.
-	Gorgonian Alcyonacea *Tree-like forms, sea fans, sea whips, bottlebrush*	Includes the suborders Holaxonia, Calcaxonia, and Scleraxonia. Gorgonians (Sea fans) have been revised and subsumed into the Alcyonacea (soft corals) but are left separated here as important VME taxa that may be complex, large, fragile, and form complex biogenic structure.	Specifically listed by FAO guidelines as one of the main target taxonomic groups of the VME definition. This group includes several large structure-forming species that may provide habitat to other species.
AXT	Stylasteridae (Family) *Hydrocorals*	Covers a wide range of taxa from small (cm scale) to massive *Macropora* reef, but if big enough to be caught by fishing gear, they are indicative of VME.	Specifically listed by FAO guidelines as one of the main target taxonomic groups of the VME definition. They can form very large complex, yet brittle structures.
CSS	Scleractinia (Order) *Stony corals*	Includes six complex branching, thicket or mound forming genera matching VME criteria: *Solenosmilia; Goniocorella; Oculina; Enallopsammia; Madrepora*; and *Lophelia*.	Specifically listed by FAO guidelines as one of the main target taxonomic groups of the VME definition. They are slow growing, structure-forming species vulnerable to disturbance by fishing gear, with unknown recovery rates. Accordingly, a high importance is given.
AQZ	Antipatharia (Order) *Black corals*	All taxa are structure forming, fragile and associated with habitats that tend to be more diverse (heterogeneous seabed with accelerated current flow).	Specifically listed by FAO guidelines as one of the main target taxonomic groups of the VME definition. They are low productivity, structure-forming species vulnerable to fishing gears.
ATX	Actiniaria (Order) *Anemones*	Anemones are not listed by Food and Agriculture Organisation [FAO] (2009) but can be large and are indicators of hard substrate and habitats that support corals, so are included as an indicator of vulnerable species.	As an indicator of other VME components.
NTW	Pennatulacea (Order) *Sea pens*	They are typical of softer substrates but do provide complex structure, have been associated with fish species and are vulnerable to trawl gear because they can be tall and often live in trawlable habitat.	Specifically listed as VME examples by FAO guidelines, but do not indicate hard substrate or stony corals. They do, however, suggest a different type of VME. They are scored as an indicator of habitat containing vertical structure.
CWD	Crinoidea (Class) *Sea lilies*	All taxa are fragile and associated with habitats that tend to be more diverse (heterogeneous seabed with accelerated current flow)	Not specifically identified by FAO guidelines, but identified by Parker et al. (2009) as a habitat indicator of VME taxa. Once detected, crinoids are an indicator of suitable VME substrate.
BHZ	Brisingida (Order) *'Armless' stars*	All taxa are fragile and associated with habitats that tend to be more diverse (Heterogeneous seabed with accelerated current flow)	Not specifically identified by FAO guidelines, but identified by Parker et al. (2009) as a habitat indicator of VME taxa. Once detected, armless stars are an indicator of suitable VME substrate.

FAO does not currently have a three-letter alpha code assigned to gorgonian Alcyonacea.

extreme points on the curve (Youden Index), calculated as $q_2 = \max\{y + x - 1\}$ for each point belonging to the cumulative distribution M(1-y,x) (Ruopp et al., 2008). Segmented regressions are commonly used to identify breakpoints which differentiate data into different groups based on changes in the relationship between dependent and independent variables (e.g., Ochoa-Quintero et al., 2015; Robertson et al., 2016). Points on a curve closest to (0,1) or which maximize Youden Index are commonly used in medical research to identify thresholds and facilitate treatment decisions (e.g., Youden, 1950; Tilbury et al., 2000) and can provide identical estimates for smooth curves without large steps, which was the case in our study. We therefore omit reporting on the Youden Distance in the results.

Percentiles that exceeded the maximum ecologically relevant reference point across all taxa, calculated by either method were selected as weight thresholds (rounded to the nearest 5 kg) by policy makers. Similarly, policy makers selected biodiversity thresholds (rounded to the nearest 5 kg if greater than 1 kg) as the percentile that was lower than the minimum references point across all taxa, calculated by either method. To inform how many VME indicator taxa are required to exceed their specific biodiversity thresholds before a move-on event is triggered, we explored the number of VME indicator taxa caught per fishing event with weights above the taxon-specific biodiversity thresholds (**Table 2**). Policy makers chose three or more taxa as an appropriately sensitive trigger level given the spatial management measures in place.

To evaluate the potential future implications of the thresholds for fishers, we applied an encounter protocol consisting of the rounded weight and biodiversity thresholds directly to the 9,771

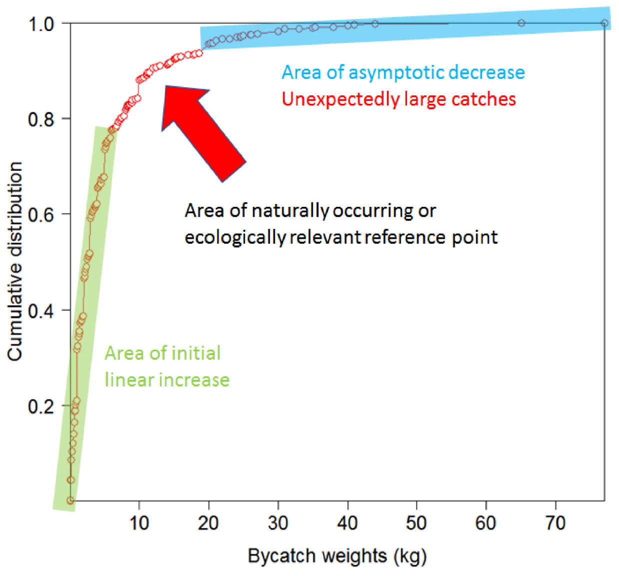

FIGURE 2 | Cumulative distribution curve for the weight of Actiniaria bycatch from the 2008–2018 New Zealand bottom trawl fishery in the SPRFMO Convention Area, where the initial part of the curve associated with linear increase is distinguished from the final part of the curve associated with asymptotic decrease. The area distinguishing between these two parts of the curve potentially indicates a naturally occurring or ecologically relevant reference point. Thresholds indicating unexpectedly large catches that indicate the models used to predict the distribution of VME indicator taxa are highly inaccurate should ideally fall to the right of such points, whereas "biodiversity weights" indicating increasing numbers of taxa in a single tow at weights below the threshold triggers indicating unexpectedly large catches should occur to the left.

historic bottom trawl tows. We considered that a move-on event would have been triggered by either a single VME indicator taxon exceeding its specific weight threshold, or three or more VME indicator taxa exceeding their biodiversity thresholds, and report how many times the move-on would have been triggered had the move-on rule been in effect. All analysis was conducted in R 3.6.1 (R Core Team, 2019) (RRID:SCR_001905).

RESULTS

The prevalence of each of the ten VME indicator taxa in the 9,771 bottom trawl tows conducted by New Zealand in the SPRFMO Convention Area between 2008 and 2018 was highly variable, ranging from two observations (<0.5% of tows) for Alcyonacea (excluding the gorgonian Alcyonacea) to 1,344 observations (approximately 15% of tows) for Scleractinia (**Table 3**). Similarly, the maximum observed bycatch weight was highly variable, ranging from 0.5 kg for Alcyonacea to 5,000 kg for Scleractinia (**Table 3** and **Figure 4**). The distributions of non-zero catch weights for all taxa show that, relative to the range of observed bycatch weights, most catches were small, with many fewer large catches (**Figure 5**).

Of the ten VME indicator taxa, five (Porifera, gorgonian Alcyonacea, Scleractinia, Antipatharia, and Actiniaria) had sample sizes large enough to calculate the 99.5th percentile from ordered values (**Table 3**). For these taxa, maximum ecologically relevant reference points ranged between 2.4 kg for Antipatharia to 60 kg for Scleractinia, with the 99th percentile exceeding the maximum reference points for all species (**Table 3**). Based on the 99th percentile, weight thresholds rounded to the nearest 5 kg ranged between 5 kg for Antipatharia and 250 kg for Scleractinia (**Table 4**).

Minimum reference points ranged between 1.3 kg for Antipatharia and 11.4 kg for Porifera, with the 80th percentile lower than the minimum ecologically relevant reference point for all species. Based on the 80th percentile, biodiversity thresholds ranged between 5 kg (for Porifera, Scleractinia, and Actiniaria) and 1 kg (for all other taxa) (**Table 4**).

Applying an encounter protocol based on the weight and biodiversity thresholds presented in **Table 4** directly to the 9,771 bottom trawl tows conducted in the SPRFMO Convention Area by New Zealand between 2008–2018 suggest that, had the protocol been in place in all areas fished, the move-on rule would have been triggered in 53 tows (<1%), almost always as a result of an individual taxon exceeding its weight threshold. The VME indicator taxa most often triggering their weight thresholds were Scleractinia and Antipatharia (**Table 4**). The biodiversity component of the encounter protocol would have been triggered only rarely (13 times), and for seven tows would have led to a move-on when no individual taxa weight threshold was triggered.

DISCUSSION

Move-on rules were not originally intended as stand-alone measures to protect VMEs from significant adverse impacts by fishing and should be complemented with spatial closures or other measures. However, there has been wide variation in the interpretation of the UNGA resolutions and FAO guidelines by RFMOs and member states, and some RFMOs or member states continue to use move-on rules within historic fishing footprints as the sole management measure preventing significant adverse impacts of bottom trawling on VMEs (e.g., member states within SIOFA). The spatial management measures currently used by SPRFMO (SPRFMO CMM 03-2019) are based on habitat suitability models (Georgian et al., 2019) and only areas containing no or few cells with high conservation value for VME indictor taxa are open to bottom trawling (Delegation of New Zealand, 2019). However, to mitigate risks caused by uncertainty in these models, we present a data-informed approach for selecting taxon-specific encounter thresholds for a move-on rule to rapidly put a stop to fishing in areas where there is an unexpectedly high catch of VME indicator taxa. This approach sets thresholds for triggering a move-on event relatively high, indicating that habitat suitability models underpinning the spatial closures might be highly inaccurate. When encounter protocols are triggered, SPRFMO CMM 03-2019 requires that: an area around the relevant trawl tow is immediately closed to fishing; the encounter must be reviewed by the Scientific Committee; and the Commission must determine if the closure should stay in effect or be lifted. The review process must

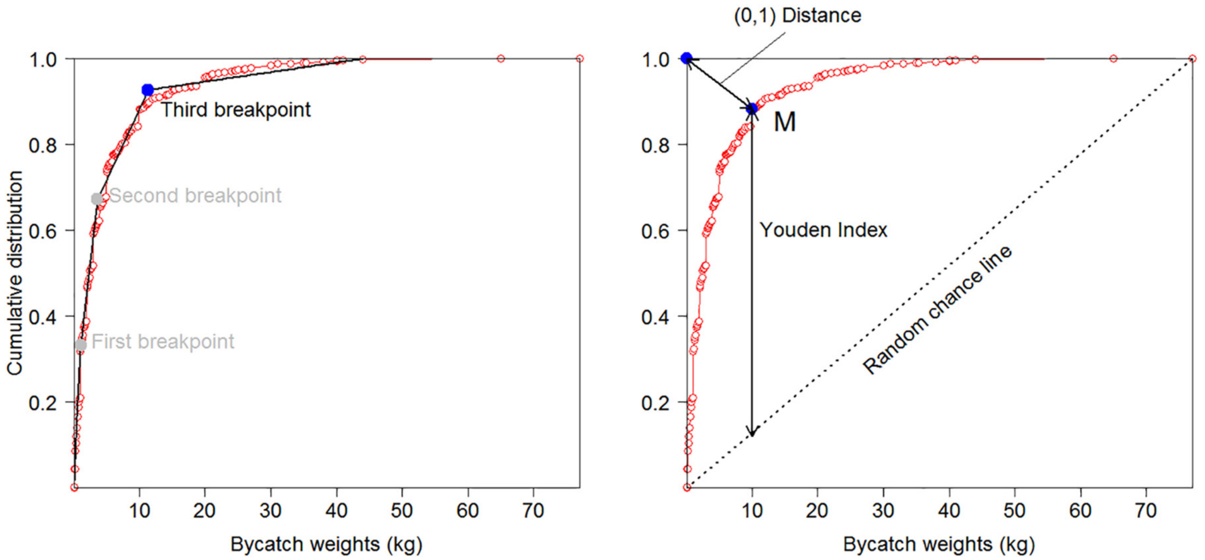

FIGURE 3 | Cumulative distribution curve for the weight of Actiniaria bycatch from the 2008–2018 New Zealand bottom trawl fishery in the SPRFMO Convention Area and three approaches used to distinguish between the initial part of the curve associated with linear increase and the final part of the curve associated with asymptotic decrease (i.e., identification of ecologically relevant reference points): (1) the third breakpoint in a 3-parameter segmented regression (left-hand panel); (2) the point on the curve that is closest to the top-left corner [(0,1) Distance, right-hand panel]; and (3) the point on the curve that maximizes the distance between the curve and a random chance line drawn between the extreme points on the curve (Youden Index, right hand panel).

consider, amongst other things, previous VME encounters within the vicinity of the new encounter (and all information on benthic bycatch), habitat suitability model predictions of VME indicator taxa, details of relevant fishing activity, and any other information the Scientific Committee considers relevant.

Because the selection of encounter thresholds by policy makers took into consideration that spatial management measures would be adopted as a key tool for preventing significant adverse impacts on VMEs in SPRFMO, the thresholds identified for some taxa in this study are higher than those used by some other RFMOs to trigger move-on events. For example, the threshold weight for Scleractinia identified in our study for the SPRFMO Convention Area is 250 kg, compared with 60 kg used by the South East Atlantic Fisheries Organization (SEAFO). However, the 50 kg encounter threshold identified for Porifera in this study is lower than the 600 kg threshold used for sponges by SEAFO. These differences in the thresholds reflect differences in the approaches taken to set thresholds, but potentially also regional differences in the relative abundance of the taxa. But, as already noted, the thresholds developed in this study must be understood as complementing spatial management (which has been evaluated as protecting approximately 85% of the predicted distribution of VME indicator taxa, Cryer et al., 2018) rather than operating in isolation. The FAO acknowledges that the role of thresholds can vary between regions and depends on the fisheries and the level of development of other elements of the VME-related management framework in place (Food and Agriculture Organisation [FAO], 2016; Thompson et al., 2016).

An encounter protocol using the thresholds presented in **Table 4** applied to all areas in which historic tows occurred would have led to 53 of the historic tows triggering move-on events. Conversely, only 16 tows within "move-on areas" where lower weight and biodiversity thresholds were applied by New Zealand under SPRFMO CMM 03-2017 would have triggered move-on events. This difference in the number of encounters is primarily driven by differences in the spatial application of a move-on rule. Under SPRFMO CMM 03-2019 higher thresholds are applied to all areas open to bottom trawling, whereas New Zealand's measures under CMM 03-2017 applied lower thresholds within "move-on areas" only, with approximately 50% of the areas open to trawling by New Zealand vessels not subjected to a move-on rule. Further, because the fishing industry actively avoided move-on areas to avoid triggering VME thresholds, tows within a historic dataset are disproportionately distributed within areas that were not subjected to a move-on rule under CMM 03-2017. These differences highlight the need to take into consideration other management measures in place when determining the sensitivity of thresholds.

TABLE 2 | The number and percent of 9,771 bottom trawl tows recording 0 to >4 VME indicator taxon groups exceeding taxon-specific biodiversity thresholds, as reported in **Table 4**.

	Number of VME indicator taxa exceeding taxon-specific biodiversity thresholds					
	0	1	2	3	4	>4
Number of fishing events	8,858	779	121	8	5	0
Percent of fishing events	90.7%	8.0%	1.2%	0.1%	0.1%	0.0%

TABLE 3 | The number of bottom trawl tows recorded as bycatch (n), range in bycatch weight (kg), percentiles in bycatch weight, and reference points per VME indicator taxon using ordered values from all New Zealand bottom trawls within the western SPRFMO Convention Area between 2008 and 2018.

FAO Code	VME Indicator taxa	n	Range in weight (kg)	Percentiles (kg) 0.8	0.9	0.95	0.97	0.98	0.99	0.995	Reference points Segmented regression	(0,1) distance
PFR	Porifera (Phylum) Sponges	845	0–1091.2	3.0	7.7	13.5	20.0	25.0	50.0	95.0	11.4	26
AJZ	Alcyonacea (Order) Soft corals	2	0.2Ű0.5	NA	NA	NA	NA	NA	NA	NA	NA	NA
–	Gorgonian Alcyonacea *Tree-like forms, sea fans, sea whips, bottlebrush corals*	630	0–200.0	1.0	2.0	5.4	15.2	24.1	32.0	60.0	2.6	6
AXT	Stylasteridae (Subclass) Hydrocorals	24	0–8.0	1.0	1.7	2.0	NA	NA	NA	NA	NA	NA
CSS	Scleractinia (Order)Stony corals	1344	0–5000.0	5.0	10.0	25.0	40.0	80.0	250.0	700.0	8.5	60.0
AQZ	Antipatharia (Order) Black corals	695	0–10.4	1.0	1.9	3.0	4.0	4.8	5.8	7.6	2.4	1.3
ATX	Actiniaria (Order) Anemones	814	0.02–77.0	7.4	12.0	20.0	24.5	30.0	35.3	40.1	11.3	10
NTW	Pennatulacea (Order) Sea pens	83	0–3.6	1.0	1.0	1.0	1.0	1.0	NA	NA	NA	NA
CWD	Crinoidea (Class) Sea lilies	37	0 -2.0	0.4	1.0	1.0	1.0	NA	NA	NA	NA	NA
BHZ	Brisingida (Order) ŚArmlessŠ stars	28	0.02–5.0	1.0	2.0	3.0	NA	NA	NA	NA	NA	NA

For taxa with sample sizes large enough to calculate the 0.995 percentile, dark blue shading indicates percentiles that are higher than both ecologically relevant reference points, and light blue shading indicates percentiles that are lower than both ecologically relevant reference points. Gray cells indicate percentiles could not be calculated from ordered values due to insufficient sample sizes. The FAO does not currently have a three-letter alpha code assigned to gorgonian Alcyonacea.

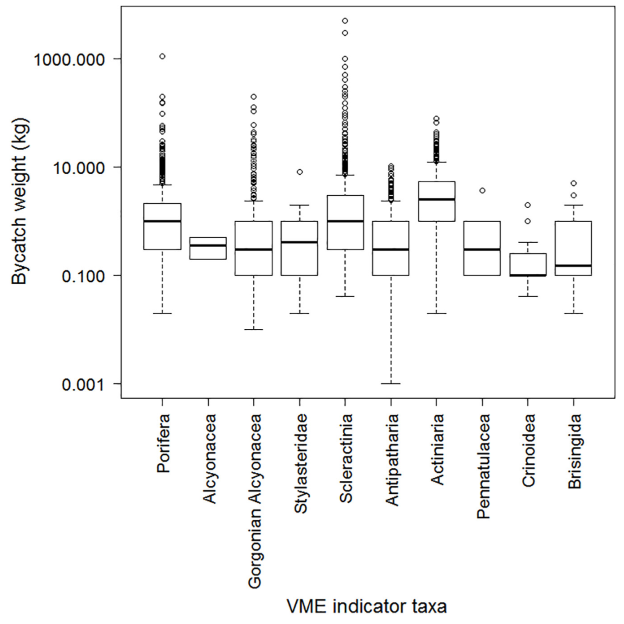

FIGURE 4 | Bycatch weight (kg) of VME indicator taxa in New Zealand bottom trawls within the SPRFMO Convention Area as reported by observers for the 2008–2018 period. Within each boxplot the line indicates the 50th percentile (median), the box encompasses 50% of the data, from the 25th to the 75th percentile and the dashed vertical lines extend to 1.5 times the interquartile range, with circles indicating "outliers." Note that the *y*-axis is plotted on a log-scale.

An important difference between the analysis presented in this paper and an earlier analysis used to inform the thresholds that were incorporated within the current encounter protocol (SPRFMO CMM 03-2019) is the differentiation of gorgonian Alcyonacea from other Alcyonacea. Although taxonomists consider Alcyonacea to include gorgonians, we have separated the suborders Holaxonia, Calcaxonia, and Scleraxonia here because of their contrast in structure-forming characteristics to other Alcyonacea. This separation differs from that used to inform the thresholds included in current encounter protocol, which distinguished VME indicator taxa explicitly coded as Gorgonacea from all other Alcyonacea, but which didn't consistently separate out the Holaxonia, Calcaxonia, and Scleraxonia suborders. Consequently, the thresholds in the current encounter protocol for both Alcyonacea and Gorgonacea differ from those calculated in this study. Further, the grouping of Holaxonia, Calcaxonia, and Scleraxonia into gorgonian Alcyonacea meant that there were only two bycatch samples coded as Alcyonacea, which raises doubt about the suitability of Alcyonacea as a VME indicator taxon if it is not being retained in bycatch samples. We therefore suggest that future reviews of the conservation and management measure include both a re-evaluation of the list of VME indicator taxa and their associated threshold weights.

There are several ongoing challenges with the approach we have taken to select encounter thresholds. First, due to a lack of data, we were unable to calculate area-specific thresholds.

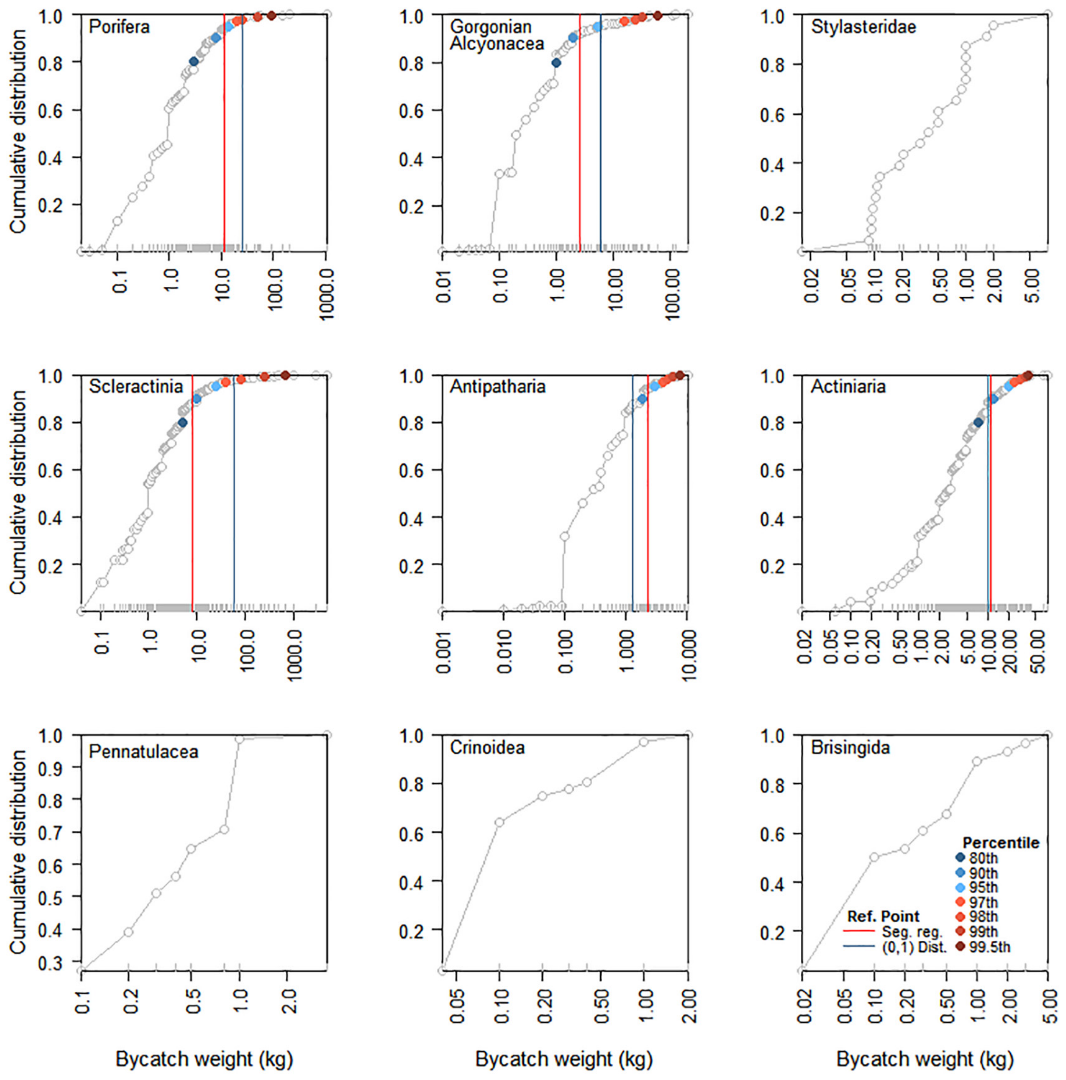

FIGURE 5 | Cumulative distributions of bycatch weight (kg) of VME indicator taxa in New Zealand bottom trawls within the SPRFMO Convention Area as reported by observers for the 2008–2018 period. Percentiles and naturally occurring or ecologically relevant reference points calculated using 3-parameter segmented regressions and the (0,1) distance are shown for the five taxa with sample sizes large enough to calculate the 99.5th percentile. Note that the *x*-axis is on the log-scale, and the limits of the x-axis differ between panels.

Although the portion of the SPRFMO Convention Area within which New Zealand bottom trawling occurs can be divided into two distinct geographical areas, the Louisville Seamount Chain to the east of New Zealand (where trawls are seamount feature-based and typically short), and the various Tasman Sea fisheries to the west of New Zealand (where trawls may also occur on the slope and are of longer duration), there were insufficient data for many taxa within each area to enable the generation of area-specific weight thresholds. Therefore, VME indicator taxa-specific weight thresholds were generated for the entire western SPRFMO area combined, and even then, there was insufficient data to calculate taxa-specific weight thresholds for all VME indicator taxa.

Second, is an implicit assumption that the threshold weights used to trigger move-on rules are related in some way to the presence of a VME. Previous studies linking the density or biomass of VME indicator taxa on the seafloor to bycatch indicate that bycatch of individual trawl events may be a poor indicator of the composition and density of VME indicator taxa on the seabed (Freese et al., 1999; Auster et al., 2010; Watling and Auster, 2017). The implication is that the methods used to select threshold values would ideally be supported by an explicit demonstration of a relationship between an ecologically significant biomass or density of VME indicator taxa on the seafloor (i.e., a VME such as coral reef or sponge garden), the catch efficiency of bottom trawl gear, and the biomass of VME indicator taxa retained as bycatch on the deck of fishing vessels. Unfortunately, we currently do not have those data available to quantify these relationships. The reasoning that the threshold weights and encounter protocol acts as a "backstop"

TABLE 4 | Single-taxon thresholds for a move-on rule, and number of times thresholds triggered by 9,771 historic trawls had the move-on rule been in place.

FAO Code	VME Indicator taxa	Weight threshold (kg)	Biodiversity threshold (kg)	No. times weight threshold triggered	No. times contributed to biodiversity rule being triggered
PFR	Porifera (Phylum) *Sponges*	50	5	10	9
AJZ	Alcyonacea (Order) *Soft corals*	–	1	10	11
–	Gorgonian Alcyonacea *Tree-like forms, sea fans, sea whips, bottlebrush corals*	30	1	–	–
AXT	Stylasteridae (Subclass) *Hydrocorals*	–	1	–	3
CSS	Scleractinia (Order)*Stony corals*	250	5	14	8
AQZ	Antipatharia (Order) *Black corals*	5	1	13	12
ATX	Actiniaria (Order) *Anemones*	35	5	10	–
NTW	Pennatulacea (Order) *Sea pens*	–	1	–	–
CWD	Crinoidea (Class) *Sea lilies*	–	1	–	–
BHZ	Brisingida (Order) *'Armless' stars*	–	1	–	1

Weight and biodiversity thresholds (kg) are equivalent, respectively, to the 99th and 80th percentiles of the distribution of positive records for each of ten VME indicator taxa recorded in the 2008–2018 New Zealand bottom trawl bycatch data for the SPRFMO Convention Area. The FAO does not currently have a three-letter alpha code assigned to gorgonian Alcyonacea.

to spatial management therefore requires untested assumptions regarding the level of permissible bycatch before further "real time" management action is required. The choice of whether to accept or reject those assumptions is a management decision that must consider uncertainty in the effectiveness of other management measures preventing significant adverse impacts on VMEs. Where managers are comfortable with the effectiveness of other management measures in preventing significant adverse impacts on VMEs, there is scope to select less-sensitive encounter thresholds. However, where managers are uncomfortable with the level of uncertainty in the information underpinning those management measures (including information related to the performance of spatial management measures or the relationship between the biomass of VME indicator taxa on the seabed and that landed on deck as bycatch), or the encounter protocol is the primary mechanism for preventing significant adverse impacts on VMEs, they might select more sensitive encounter thresholds to trigger a move-on rule. Where more sensitive thresholds are required, one approach would be to use a scalar to better link the biomass of VME indicator taxa on the seafloor to bycatch landed on the deck. For example, assuming a catch efficiency of 10%, a multiplier of 0.1 could be applied to the raw data prior to analysis, resulting in down-scaled, more precautionary thresholds. Alternatively, the approach used in this paper can be modified to select thresholds lower on the cumulative distribution curve of bycatch weight. For example, the first breakpoint in the three-parameter segmented regression could be used as the ecologically relevant reference point when selecting weight thresholds, which would provide policy makers with a broader range of increasingly sensitive thresholds from which to select. Similarly, the sensitivity of the biodiversity threshold could be increased by relaxing the number of taxa required to exceed taxon-specific biodiversity thresholds before the encounter protocol is triggered.

Additional work is required, to support the approach taken by SPRFMO in developing encounter protocols as a safeguard against the uncertainty associated with the effectiveness of spatial management measures in preventing significant adverse impacts on VMEs. We think this work should include the determination of taxa-specific catchability estimates (e.g., by comparing VME indicator taxa bycatch weights from trawls to those determined from seafloor imagery from the same area swept by the trawls), and the determination of the particular seafloor density/biomass of VME indicator taxa that represents an actual VME [e.g., by examining the relationship between the density/biomass of a VME indicator taxa and the diversity of associated species, see Rowden et al. (2020) this issue]. Obtaining this information will allow for the identification of encounter thresholds that are more ecologically meaningful and at the same time prevent trawling impacts to VMEs while assessing the accuracy of the habitat suitability models on which the spatial management measures are based. In the interim, and while additional work is underway, the choice of thresholds was reviewed by the SPRFMO Commission in February 2020, taking into consideration the precautionary approach as required by various UNGA resolutions and the SPRFMO Convention text. As a result, the threshold in the encounter protocol for stony corals was reduced from 250 to 80 kg, leaving the thresholds for other VME indicator taxa and the biodiversity component unchanged. SPRFMO's bottom fishing measures will be reviewed by the Commission again in early 2021.

DATA AVAILABILITY STATEMENT

The data analyzed in this study was obtained from the Ministry for Primary Industries and is classified as "Commercial and in Confidence." Requests to access these datasets should be directed to the Ministry for Primary Industries Data Management Team for their approval (rdm@mpi.govt.nz).

AUTHOR CONTRIBUTIONS

SG, AR, MC, and SN designed the study. SG and AR compiled the data. SG and MC checked the data for obvious errors. SG and AR analyzed the data. All authors wrote the manuscript.

FUNDING

This research was primarily funded by the Department of Conservations Marine Ecosystems Team and Fisheries New Zealand (Projects: SEA2018/14 and SPR2018/01) with additional funding to support the production of the manuscript provided by the New Zealand Sustainable Seas National Science Challenge (Project: SUSS16203) and aligned funding from the NIWA Coasts and Oceans Programme (Project: COME1803).

ACKNOWLEDGMENTS

We are grateful for comments, suggestions, and inputs from the Fisheries New Zealand's South Pacific Fishery Assessment Working Group and the South Pacific Regional Fisheries Management Organization's Scientific Committee.

SUPPLEMENTARY MATERIAL

The Supplementary Material for this article can be found online at: https://www.frontiersin.org/articles/10.3389/fmars.2020.00155/full#supplementary-material

REFERENCES

Ardron, J., Gjerde, K., Pullen, S., and Tilot, V. (2008). Marine spatial planning in the high seas. *Mar. Policy* 32, 832–839. doi: 10.1016/j.marpol.2008.03.018

Ardron, J. A., Clark, M. R., Penney, A. J., Hourigan, T. F., Rowden, A. A., Dunstan, P. K., et al. (2014). A systematic approach towards the identification and protection of vulnerable marine ecosystems. *Mar. Policy* 49, 146–154. doi: 10.1016/j.marpol.2013.11.017

Auster, P. J., Gjerde, K., Heupel, E., Watling, L., Grehan, A., and Rogers, A. D. (2010). Definition and detection of vulnerable marine ecosystems on the high seas: problems with the "move-on" rule. *ICES J. Mar. Sci.* 68, 254–264. doi: 10.1093/icesjms/fsq074

Bell, J., Guijarro-Garcia, E., and Kenny, A. (2018). *Scientific Approaches for the Assessment and Management of Deep Sea Fisheries and Ecosystems in RFMOs and RFBs*. 171. Final Report for European Commission Framework Contract EASME/EMFF/2016/008. Brussels: European Commission.

Clark, M. R., and Dunn, M. R. (2012). Spatial management of deep-sea seamount fisheries: balancing exploitation and habitat conservation. *Environ. Conserv.* 39, 204–214. doi: 10.1017/S0376892912000021

Cryer, M., Geange, S. W., and Bock, T. (2018). *Methods for Designing Spatial Management Areas Using Outputs From Zonation Software and Other Spatial Data*. SPRFMO SC6-DW11. Wellington: SPRFMO.

de Juan, S., and Lleonart, J. (2010). A conceptual framework for the protection of vulnerable habitats impacted by fishing activities in the Mediterranean high seas. *Ocean Coast. Manag.* 53, 717–723. doi: 10.1016/j.ocecoaman.2010.10.005

Delegation of New Zealand, (2019). *A Proposal for a Revised Bottom Fishing Conservation and Management Measure for SPRFMO*. SPRFMO COMM7-Prop 03.1. Wellington: SPRFMO.

Food and Agriculture Organisation [FAO] (2009). *International Guidelines for the Management of Deep-Sea Fisheries in the High Seas*. Rome: Food and Agriculture Organisation, 73.

Food and Agriculture Organisation [FAO] (2016). *Report of the FAO Workshop on Encounter Protocols and Impact Assessments, 5–8 May 2015.* FAO Fisheries and Aquaculture Report. No. 1178. Rome: FAO, 51.

Freese, L., Auster, P. J., Heifetz, J., and Wing, B. L. (1999). Effects of trawling on seafloor habitat and associated invertebrate taxa in the Gulf of Alaska. *Mar. Ecol. Prog. Ser.* 182, 119–126. doi: 10.3354/meps182119

Georgian, S. E., Anderson, O. F., and Rowden, A. A. (2019). Ensemble habitat suitability modeling of vulnerable marine ecosystem indicator taxa to inform deep-sea fisheries management in the South Pacific Ocean. *Fish. Res.* 211, 256–274. doi: 10.1016/j.fishres.2018.11.020

Horton, T., Kroh, A., Ahyong, S., et al. (2019). *World Register of Marine Species*. Available at: https://www.marinespecies.org at VLIZ (accessed August 22, 2019).

Kenchington, E., Cogswell, A., Lirette, C., and Murillo, F. J. (2009). *The Use of Density Analyses to Delineate Sponge Grounds and Other Benthic VMEs from Trawl Survey Data*. NAFO SCR Doc. 09/6. Dartmouth, NS: Northwest Atlantic Fisheries Organization.

Kenchington, E., Murillo, F. J., Lirette, C., Sacau, M., Koen-Alonso, M., Kenny, A., et al. (2014). Kernel density surface modelling as a means to identify significant concentrations of vulnerable marine ecosystem indicators. *PLoS One* 9:e109365. doi: 10.1371/journal.pone.0109365

Ochoa-Quintero, J. M., Gardner, T. A., Rosa, I., de Barros Ferraz, S. F., and Sutherland, W. J. (2015). Thresholds of species loss in Amazonian deforestation frontier landscapes. *Cons. Biol.* 29, 440–451. doi: 10.1111/cobi.12446

Parker, S. J., Penney, A. J., and Clark, M. R. (2009). Detection criteria for managing trawl impacts on vulnerable marine ecosystems in high seas fisheries of the South Pacific Ocean. *Mar. Ecol. Prog. Ser.* 397, 309–317. doi: 10.3354/meps08115

Penney, A. J., Parker, S. J., and Brown, J. H. (2009). Protection measures implemented by New Zealand for vulnerable marine ecosystems in the South Pacific Ocean. *Mar. Ecol. Prog. Ser.* 397, 341–354. doi: 10.3354/meps08300

R Core Team, (2019). *R: A Language and Environment for Statistical Computing*. Vienna: R Foundation for Statistical Computing.

Robertson, B. P., Savage, C., Gardner, J. P., Robertson, B. M., and Stevens, L. M. (2016). Optimising a widely-used coastal health index through quantitative ecological group classifications and associated thresholds. *Ecol. Indic.* 69, 595–605. doi: 10.1016/j.ecolind.2016.04.003

Rowden, A. A., Pearman, T. R. R., Bowden, D. A., Anderson, O. F., and Clark, M. R. (2020). Determining Coral Density Thresholds for Identifying Structurally Complex Vulnerable Marine Ecosystems in the Deep Sea. *Front. Mar. Sci.* 7:95. doi: 10.3389/fmars.2020.00095

Rowden, A. A., Stephenson, F., Clark, M. R., Anderson, O. F., Guinotte, J. M., Baird, S. J., et al. (2019). Examining the utility of a decision-support tool to develop spatial management options for the protection of vulnerable marine ecosystems on the high seas around New Zealand. *Ocean Coast. Manage.* 170, 1–16. doi: 10.1016/j.ocecoaman.2018.12.033

Ruopp, M. D., Perkins, N. J., Whitcomb, B. W., and Schisterman, E. F. (2008). Youden Index and optimal cut-point estimated from observations affected by a lower limit of detection. *Biometrical J.* 50, 419–430. doi: 10.1002/bimj.200710415

SPRFMO, (2017). *Report of the 5th Scientific Committee Meeting*. Shanghai: SPRFMO.

Thompson, A., Sanders, J., Tandstad, M., Carocci, F., and Fuller, J. (2016). "Vulnerable marine ecosystems: processes and practices in the high seas," *FAO Fisheries and Aquaculture Technical Paper* 595, (Rome: FAO), 185.

Tilbury, J. B., Van Eetvelt, W. J., Garibaldi, J. M., Curnsw, J. S. H., and Ifeachor, E. C. (2000). Receiver operating characteristic analysis for intelligent medical systems-a new approach for finding confidence intervals. *IEEE T. Bio-Med. Eng.* 47, 952–963. doi: 10.1109/10.846690

United Nations General Assembly [UNGA], (2005). *Resolution 59/25: Sustainable fisheries, including through the 1995 Agreement for the Implementation of the Provisions of the United Nations Convention on the Law of the Sea of 10 December 1982 relating to the Conservation and Management of Straddling Fish Stocks and Highly Migratory Fish Stocks, and related instruments, UNGA A/RES/59/25, United Nations General Assembly*. New York, NY: UNGA.

United Nations General Assembly [UNGA], (2007). *Resolution 61/105: Sustainable fisheries, including through the 1995 Agreement for the Implementation of the Provisions of the United Nations Convention on the Law of the Sea of 10 December 1982 relating to the Conservation and Management of Straddling*

Fish Stocks and Highly Migratory Fish Stocks, and related instruments, UNGA A/RES/61/105, United Nations General Assembly. New York, NY: UNGA.

United Nations General Assembly [UNGA], (2010). *Resolution 64/72: Sustainable fisheries, including through the 1995 Agreement for the Implementation of the Provisions of the United Nations Convention on the Law of the Sea of 10 December 1982 relating to the Conservation and Management of Straddling Fish Stocks and Highly Migratory Fish Stocks, and related instruments, UNGA A/RES/64/72, United Nations General Assembly*. New York, NY: UNGA.

United Nations General Assembly [UNGA], (2012). *Resolution 66/68: Sustainable fisheries, including through the 1995 Agreement for the Implementation of the Provisions of the United Nations Convention on the Law of the Sea of 10 December 1982 relating to the Conservation and Management of Straddling Fish Stocks and Highly Migratory Fish Stocks, and related instruments, UNGA A/RES/66/68, United Nations General Assembly*. New York, NY: UNGA.

Watling, L., and Auster, P. J. (2017). Seamounts on the high seas should be managed as vulnerable marine ecosystems. *Front. Mar. Sci.* 4:14. doi: 10.3389/fmars.2017.00014

Wright, G., Ardron, J., Gjerde, K., Currie, D., and Rochette, J. (2015). Advancing marine biodiversity protection through regional fisheries management: a review of bottom fisheries closures in areas beyond national jurisdiction. *Mar. Policy* 61, 134–148. doi: 10.1016/j.marpol.2015.06.030

Youden, W. J. (1950). Index for rating diagnostic tests. *Cancer* 3, 32–35. doi: 10.1002/1097-0142(1950)3:1<32::aid-cncr2820030106>3.0.co;2-3

Conflict of Interest: The authors declare that the research was conducted in the absence of any commercial or financial relationships that could be construed as a potential conflict of interest.

frontiers in Marine Science

ORIGINAL RESEARCH
published: 03 April 2020
doi: 10.3389/fmars.2020.00187

True Size Matters for Conservation: A Robust Method to Determine the Size of Deep-Sea Coral Reefs Shows They Are Typically Small on Seamounts in the Southwest Pacific Ocean

Alan Williams[1]*, Franziska Althaus[1], Mark Green[1], Kylie Maguire[1], Candice Untiedt[1], Nick Mortimer[2], Chris J. Jackett[1], Malcolm Clark[3], Nicholas Bax[1,4], Roland Pitcher[5] and Thomas Schlacher[6]

[1] CSIRO Oceans and Atmosphere, Hobart, TAS, Australia, [2] CSIRO Oceans and Atmosphere, Perth, WA, Australia, [3] National Institute of Water and Atmospheric Research, Wellington, New Zealand, [4] Institute for Marine and Antarctic Science, University of Tasmania, Hobart, TAS, Australia, [5] CSIRO Oceans and Atmosphere, Brisbane, QLD, Australia, [6] School of Science and Engineering, University of the Sunshine Coast, Maroochydore, QLD, Australia

OPEN ACCESS

Edited by:
Christopher Kim Pham,
University of the Azores, Portugal

Reviewed by:
Peter Etnoyer,
National Centers for Coastal Ocean Science (NOAA), United States
Joana R. Xavier,
University of Porto, Portugal

***Correspondence:**
Alan Williams
Alan.Williams@csiro.au

Specialty section:
This article was submitted to Deep-Sea Environments and Ecology, a section of the journal Frontiers in Marine Science

Received: *18 October 2019*
Accepted: *10 March 2020*
Published: *03 April 2020*

Citation:
Williams A, Althaus F, Green M, Maguire K, Untiedt C, Mortimer N, Jackett CJ, Clark M, Bax N, Pitcher R and Schlacher T (2020) True Size Matters for Conservation: A Robust Method to Determine the Size of Deep-Sea Coral Reefs Shows They Are Typically Small on Seamounts in the Southwest Pacific Ocean. Front. Mar. Sci. 7:187. doi: 10.3389/fmars.2020.00187

Protection of vulnerable marine ecosystems (VME) is a critical goal for marine conservation. Yet, in many deep-sea settings, where quantitative data are typically sparse, it is challenging to correctly identify the location and size of VMEs. Here we assess the sensitivity of a method to identify coral reef VMEs based on bottom cover and abundance of the stony coral *Solenosmilia variabilis* on deep seamounts, using image data from a survey off Tasmania, Australia, in 2018. Whilst there was some detectable influence from varying coral cover and the abundance of live coral heads, the distribution of coral reef VMEs was not substantially shifted by changing these criteria or altering the attributes of a moving window used to spatially aggregate coral patches. Whilst applying stricter criteria for classifying VMEs predictably produced smaller areas of coral reef VME, these differences were not sizeable and were often negligible. Coral reef VMEs formed large contiguous "blankets," mainly on the peaks and flanks of seamounts, but were absent from the continental slope where *S. variabilis* occurred at low abundance (cover) and/or had no living colonies. The true size of the Tasmanian coral reef VMEs ranged from 0.02 to 1.16 km^2; this was relatively large compared to reefs of *S. variabilis* mapped on New Zealand seamounts, but is small compared to the scales used for regional model predictions of suitable habitat (typically 1 km^2 grid cell), and much smaller than the smallest units of management interest (100s–1000s km^2). A model prediction of the area of suitable habitat for coral reef in the Tasmanian area was much greater than the area of coral reef estimated in this study. That the method to estimate VME size is not overly sensitive to the choice of criteria is highly encouraging in the context of designing spatial conservation measures that are robust, although its broader application, including to other VME indicator taxa, needs to be substantiated by scenario testing in different environments. Importantly, these results should give confidence for stakeholder uptake and form the basis for better predictive VME models at larger spatial scales and beyond single taxa.

Keywords: vulnerable marine ecosystem, VME, *Solenosmilia*, seamount, towed-camera, deep sea, coral, fisheries management

INTRODUCTION

Vulnerable marine ecosystems (VME) in the deep sea are typically defined by criteria originating from international policies and actions to manage fishing impacts and conserve biodiversity (FAO, 2009). Often these criteria are based on a suite of attributes that make particular ecosystems potentially vulnerable to threatening processes, especially bottom-contact fishing; VME species have traits such as being rare, habitat-forming, fragile, functionally significant, slow to recover, or low biological productivity (Ardron et al., 2014). The criteria have mostly been applied to "indicator" species, or higher-level taxa, resulting in methods that primarily use the presence of indicator taxa to identify VME locations. These methods have become increasingly quantitative, progressing from relatively simple threshold approaches (e.g., Auster et al., 2011) to multi-criteria mapping that combines information on the vulnerability traits and abundances of target taxa with estimates of the confidence in data quality (Morato et al., 2018). Quantitative measures of indicator taxa density and spatial extent of associated habitat are viewed as the preferred technique to identify VMEs, but in the deep sea this is rarely possible using data that are independent from fisheries bycatch information (Ardron et al., 2014).

An alternative method to identifying VME locations when reliable data are lacking is using models to predict the potential suitable habitat of VME indicator taxa based on environmental variables (Vierod et al., 2014; Anderson et al., 2016b). Models are particularly useful in deep-sea settings because the areas of interest (fishery regions or bioregions) are typically large and distribution data for species and habitats sparse – a juxtaposition that is common for most of the deep ocean (Ross and Howell, 2013). The performance of habitat suitability modeling has been improved by: (i) incorporating high-resolution terrain data at regional scales (Rengstorf et al., 2013), (ii) improving faunal metrics derived from *in situ* video data (Rengstorf et al., 2014), (iii) validating predictions using sampling and photographic images (Anderson et al., 2016a; Rooper et al., 2016), and (iv) combining models in ensemble techniques that can improve accuracy over single models (Robert et al., 2016) and provide additional estimates of model uncertainty (Georgian et al., 2019). Habitat suitability modeling lends itself well to management applications such as conservation planning to identify potentially important habitats for reserves (Ross and Howell, 2013) and areas where managing fishery impacts could be more effective (Penney and Guinotte, 2013; Georgian et al., 2019). Despite these technical advances, most models are typically based on presence-absence or presence-only data and therefore provide no information about the abundance of VME indicator taxa. Moreover, models of presence-absence data that give the most precise predictions tend to be poorly calibrated and overconfident in their estimates (Norberg et al., 2019). The best performing models may vary according to the structure of the underlying community and how the data are collected, substantiating the approach of using multiple models and assessing the consistency between them (Norberg et al., 2019). Even where multi-criteria assessments (Morato et al., 2018) take account of abundance in point collections of fauna (e.g., fishery bycatch), there is uncertainty about how well the collections represent faunal density on the seabed because of gear selectivity and differences in the catchability of taxa. *In situ* photographic image data have the potential to provide abundance data on deep-sea VME taxa when the field-of-view is quantified (Althaus et al., 2009; Clark et al., 2019), and have shown that physical (sled) collections in the deep-sea are prone to underestimate faunal density – possibly by a considerable degree (Williams et al., 2015).

Habitat suitability models based on environmental data can reveal potential distributions of VME indicator taxa over data-sparse areas (Tittensor et al., 2009). Few studies have, however, attempted to define the true spatial extents of VMEs based on detailed *in situ* data. Quantitative *in situ* observations have the advantage that thresholds for defining distributions and densities of VME taxa can be determined from direct observation of deep-sea communities. Implied community or functional "ecosystem" descriptors based on observations of individual taxa can be tested for their efficacy in defining the spatial scales of VMEs, addressing directly the question of what constitutes a functional VME ecosystem unit, and how to define it based on our ecological knowledge and *in situ* observation.

Stony corals that build thickets or reefs and are classified as "habitat-forming," a key attribute for VME taxa (Buhl-Mortensen et al., 2010). Reefs of the widely distributed stony corals *Lophelia pertusa* (Linnaeus, 1758) (currently accepted, and referred to hereafter, as *Desmophyllum pertusum*) and *Solenosmilia variabilis* Duncan, 1873 are viewed as "hot spots" of biomass and carbon-cycling on continental margins (van Oevelen et al., 2009), that harbor distinct fauna assemblages in greater abundance and diversity than those in nearby areas without corals (Henry and Roberts, 2007; Roberts et al., 2008; Althaus et al., 2009). Fine-scale mapping of coral thickets composed of *D. pertusum* and *Madrepora oculata* Linnaeus, 1758 (Vertino et al., 2010) showed the importance of distinguishing between areas where coral (live and dead) predominate from areas where corals were sparse or absent, and identifying thresholds to classify seabed cover of coral communities based on images.

In the deep sea of the southwest Pacific, *S. variabilis* is the dominant reef-building stony coral in terms of biomass and distribution. It is pivotal in forming habitat patches that support higher biomass and diversity on seamounts compared

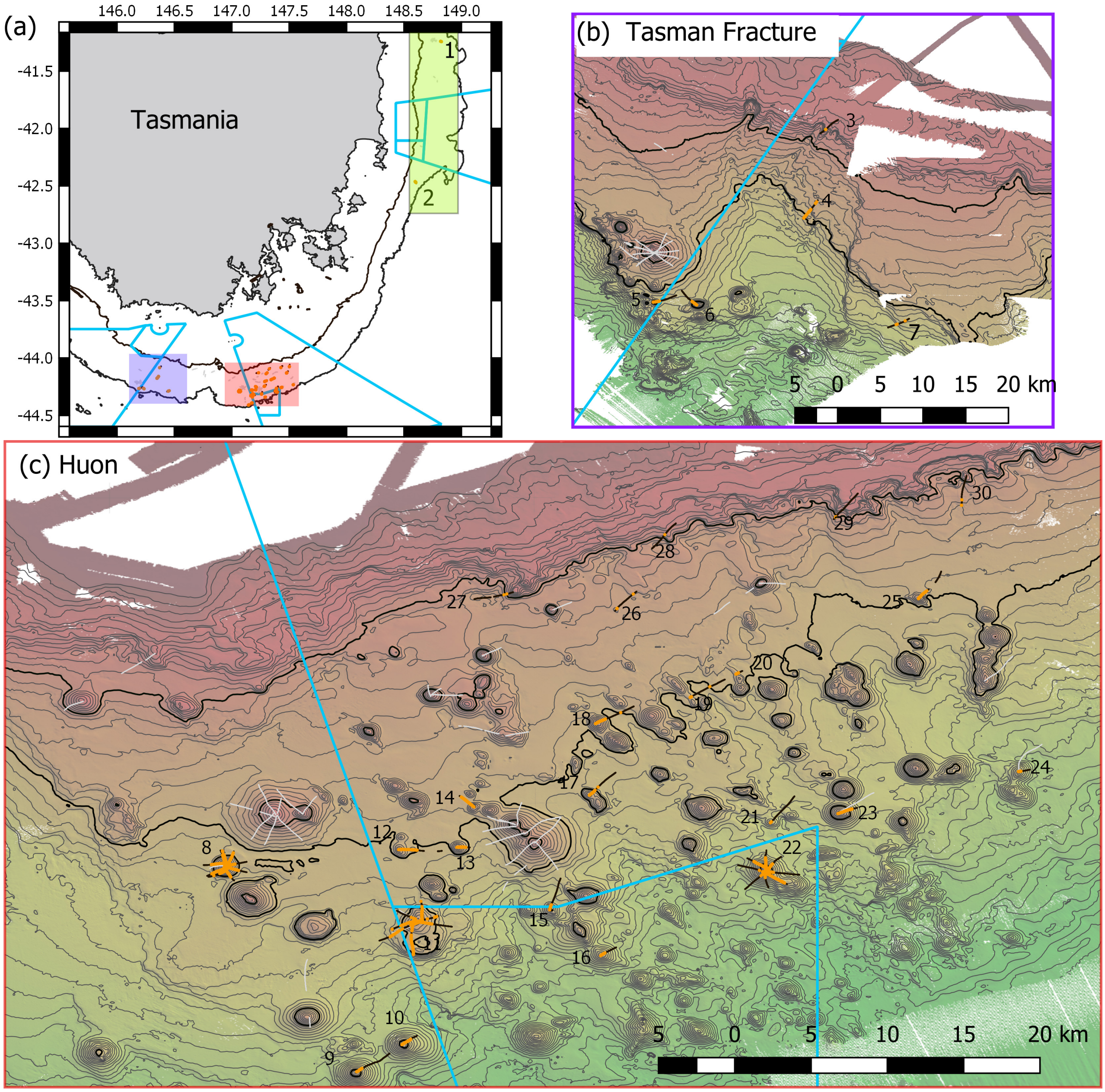

FIGURE 1 | Maps of Tasmanian Seamounts survey area showing locations of the 30 transect sites sampled: **(a)** overview map showing east coast sub-area (green shaded box; sites 1 and 2) and south coast sub-areas – orange and mauve boxes; **(b)** south coast Tasman Fracture sub-region (sites 3–7); **(c)** south coast Huon sub-region (sites 8–30). Photographic transects (black lines) with distribution of the stony coral *Solenosmilia variabilis* matrix (live and dead) overlaid (orange); transects with fishing impacts eliminated from analysis (gray lines). Boundaries of Australian Marine Parks (blue lines); Depth contours: panel **(a)** 250 and 2000 m – define the limits of the survey area; panels **(b,c)** 50 m intervals with 950 and 1350 lines bolded.

to adjacent slopes (Rowden et al., 2010), including distinct assemblages of some groups (e.g., ophiuroids, O'Hara et al., 2008). Reefs of this species have been mapped off New Zealand from *in situ* image-based data by Rowden et al. (2017) using a quantitative two stage method. First, seabed cover of coral reef and the presence of live coral, brisingids, crinoids along towed video transects was mapped to classify seabed with VME status, and then patches of reef with VME status were further assessed for the presence of live coral heads (above a pre-defined threshold) and used as input to habitat suitability models for a larger area. Despite having developed this abundance-based and high-resolution model ensemble approach Rowden et al. (2017) recognized that their method and model parameters needed to be tested in other areas.

In this paper, we apply the Rowden et al. (2017) method to an area of seamounts off southern Australia and test the consistency of results when parameters for identifying coral reef VME are changed. Our primary goal is to determine the robustness of the method to changes in these parameters and whether the method is sufficiently consistent to be recommended as a method to improve VME mapping as input to distribution models used to support conservation practice and fishery management.

MATERIALS AND METHODS

Sampling Design

We test the sensitivity of Rowden et al.'s (2017) model to changes in mapping parameters, including the mechanics of a moving window used to define coral reef VMEs. Our test is based on sampling coral matrix formed predominantly by *S. variabilis* in a similar environment using very similar methods, but on seamounts that are topographically markedly different. Our data from Tasmania, Australia, are from the same general depth range (∼500–2000 m) as the New Zealand surveys, and represent a very similar South West Pacific (SWP) deep-sea megabenthic fauna; this has many identical and similar taxa, including VME indicator taxa such as the dominant habitat-forming stony coral, *S. variabilis*. The Tasmanian seamounts are, however, smaller (∼1–25 km^2 base size) conical mounts compared with the substantially larger (253–725 km^2) guyots off New Zealand sampled by Rowden et al. (2017). Both areas have a known and continuing history of bottom trawl impacts from fisheries for orange roughy (*Hoplostethus atlanticus*, Collett, 1889; Tingley and Dunn, 2018), which makes them directly relevant to the FAO goal of managing both for sustainable fisheries and the protection of VMEs (FAO, 2009).

Data Collection

The study area in Australian waters lies off the east and south coasts of Tasmania (**Figure 1**). Data were collected during a voyage in November-December 2018 on Australia's National Marine Facility vessel, the RV *Investigator*. The "Tasmanian Seamounts" area is known from a previous study of seabed habitats and megabenthos associated with some 130 small conical volcanic seamounts; the earlier study focused on trawling impact (Althaus et al., 2009) and faunal recovery (Williams et al., 2010) following commercial bottom trawling for orange roughy.

In the present study, the extents of stony coral VMEs were estimated from image data taken by a towed camera along transects that were typically 2 km in length. Transects were located in space using a flexible spatially balanced design (Foster et al., 2020) and were of three types: (1) randomized "radial" transects on selected seamounts; (2) randomized "baseline transects" that crossed slope and seamount habitats; and (3) "ad hoc" transects that were completed during vessel transits between pre-determined sites under designs 1 and 2. The two criteria for transect selection in this analysis were: (1) that the highly dominant reef-forming stony coral *S. variabilis* (**Figure 2**) (referred to in this paper as "coral" and "coral reef") was present along a transect, and (2) that transects had not been impacted by bottom trawling. This resulted in a total of 52 transects suitable for analysis in this study. The historical distribution of trawling effort was available from logbook data recorded by the Australian Fisheries Management Authority (AFMA) at 0.01° resolution (see methods in Althaus et al., 2009), from information provided by knowledgeable commercial fishers, and from observations during the previous studies. Most of the sites selected lie within or between the Huon and Tasman Fracture Australian Marine Parks that were closed to trawling in 2007 (**Figure 1**). Details of the 30 study sites are provided in **Table 1**.

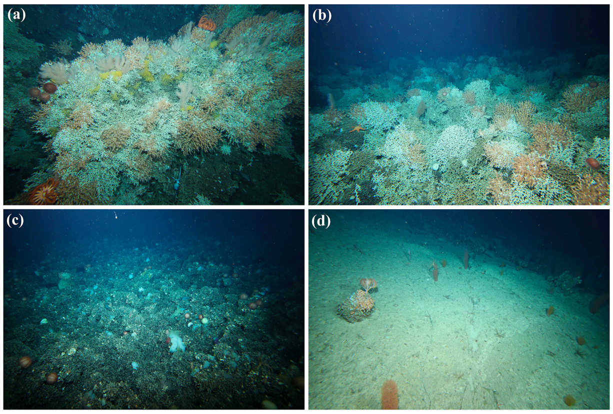

FIGURE 2 | Examples of reef formed by the stony coral *Solenosmilia variabilis* on Tasmanian seamounts showing: **(a,b)** high % cover and many live coral heads (living polyps are orange); **(c)** high % cover of dead matrix with no live coral heads; **(d)** low % cover and isolated single live head.

The towed camera system was similar to the one used in the previous study (detailed in Althaus et al., 2009), but fitted with higher resolution cameras and a USBL that recorded with higher accuracy and frequency. In brief, a Canon EOS-1DX video camera provided continuous HD video imagery and a calibrated pair of Canon EOS-1DX Mark II still cameras provided image pairs at 5-s intervals (Marouchos et al., 2017). The system was towed at a speed of 1 knot (0.5 ms^{-1}) at a height of 2 m (±+0.5 m) off bottom by a pilot using camera vision transmitted back to the vessel in real-time. Video was geolocated at 1-s intervals, and all stills individually geolocated. Video was annotated for dominant substrate type on the vessel; this enabled the presence (and absence) of intact coral reef (dead or alive), and the presence of coral rubble, to be mapped along all transects. Subsequent lab-based annotation provided more detailed mapping and recorded the number of live coral heads within the portions of transects with coral reef for analysis in slow-speed replays of the video footage. Annotation was done in the Video Annotation and Reference System (VARS) developed by the Monterey Bay Aquarium Research Institute (Schlining and Jacobsen Stout, 2006) where annotations were georeferenced through linking to the processed USBL data from the camera system.

Image Data Processing and Analysis

Image data were processed in two stages following, as closely as possible, the method described by Rowden et al. (2017). In the first stage, the coral VME status of individual 12-s video segments was assessed and segments with VME habitat status were grouped

TABLE 1 | List of sites sampled in the seamounts study area off Tasmania, Australia, detailing site reference numbers, location descriptors, and summary metrics for sample sizes and coral habitat.

Site no.	Region	Location type	Location Name	Number of transects	Total no. 1-s annotations	Total number of 25 m^2 segments	Percent matrix	Total number live heads	Estimated size of coral reef VME km^2
1	East coast Tasmania	Seamount	St Helens E	1	2103	88	37.2	851	0.21
2	East coast Tasmania	Seamount	Reidle Hill	1	4155	174	29.4	1568	0.04
3	Tasman Fracture	Slope	Slope_101	1	3388	142	0.7	0	0
4	Tasman Fracture	Seamount	Slope_100	1	2994	126	17.1	584	0.04
5	Tasman Fracture	Seamount	z110	1	3754	157	22.9	975	0.14
6	Tasman Fracture	Seamount	z99	1	3411	143	17.3	437	0.25
7	Tasman Fracture	Slope	Slope_099	1	3845	161	1	0	0
8	Huon	Seamount	z16	9	17959	755	64.1	14912	1.16
9	Huon	Seamount	z103	1	3257	136	13.6	29	0.08
10	Huon	Seamount	Hill V	1	1749	74	59.2	155	0.02
11	Huon AMP	Seamount	Hill U	8	18994	794	39.5	6952	1.16
12	Huon AMP	Seamount	z34	1	2240	96	39.2	1250	0.1
13	Huon AMP	Seamount	z20	1	1277	54	57.5	834	0.22
14	Huon AMP	Seamount	Little Sister	1	1997	84	80.1	1272	0.11
15	Huon AMP	Seamount	z53	1	3890	163	15.7	138	0.05
16	Huon AMP	Seamount	z44	1	1644	69	28.4	1	0
17	Huon AMP	Seamount	z5	1	3694	155	15.2	491	0.21
18	Huon AMP	Seamount	z8	1	3606	151	20.8	766	0.53
19	Huon AMP	Seamount	New 1	1	2907	123	4.4	35	0
20	Huon AMP	Seamount	z96	1	694	29	25.6	93	0.04
21	Huon AMP	Seamount	z77	1	3582	150	3.3	0	0
22	Huon AMP	Seamount	Hill K1	8	21875	918	28.4	1968	0.29
23	Huon AMP	Seamount	z24	1	1704	71	55.2	659	0.86
24	Huon AMP	Seamount	z91	1	1270	53	17.2	0	0
25	Huon AMP	Seamount	z12	1	2357	102	33.1	516	0.28
26	Huon AMP	Slope	Slope_154	1	2281	96	1.1	3	0
27	Huon AMP	Slope	Slope_129	1	3193	135	0.3	1	0
28	Huon AMP	Slope	Slope_133	1	3313	140	0.1	1	0
29	Huon AMP	Slope	Slope_134	1	3577	150	0.5	4	0
30	Huon AMP	Slope	Slope_136	1	3604	151	0.6	17	0

into patches along transects; in the second stage, coral VME abundance was accounted for in a spatial (predictive) expansion of the patches across broader areas of the seabed.

Transect segments were classified as having "*VME habitat status*" if they met criteria based on the bottom cover (% by area) of seabed composed of intact coral matrix (live or dead) and the presence of live coral heads. Segments meeting these criteria ("eligible" segments) were then grouped into contiguous areas along transects ("*patches*"). To identify the boundary between contiguous patches and adjacent areas, which might also include isolated coral heads, segment data were processed with a moving "window" that had the effect of smoothing the patch structure over multiple segments. The effect of altering the size of this moving window was examined. Contiguous patches were identified as "*coral reef VME*" only if they had an abundance of live coral heads exceeding a "*threshold*" – a mean abundance of live heads per segment. The effect of altering this threshold was examined. The detailed data processing and analytical steps are detailed below, and the overall method is summarized schematically in **Figure 3**.

Stage 1 Analysis

Step 1 – data on % coral cover and live coral heads were aggregated to the smallest spatial unit of analysis, being a segment of ∼25 m^2 size (∼12 m long × 2 m plan view wide). We used elapsed time to identify the 12 m long segments along the transect path (24 × 1-s frames at an average speed of 0.5 ms^{-1}) together with a diminishing perspective overlay in our oblique field-of-view annotation to achieve a 2 m wide scoring corridor.

Step 2 – a segment (as defined in step one) was classified as having VME habitat status if it satisfied two criteria: (i) coral matrix covered an area of the seafloor above a particular value of % cover; and (ii) live coral heads were present (i.e., VME status of segments depended on both the cover and the occurrence of live corals).

Step 3 – A segment with VME habitat status was incorporated into a patch with VME habitat status only when it satisfied

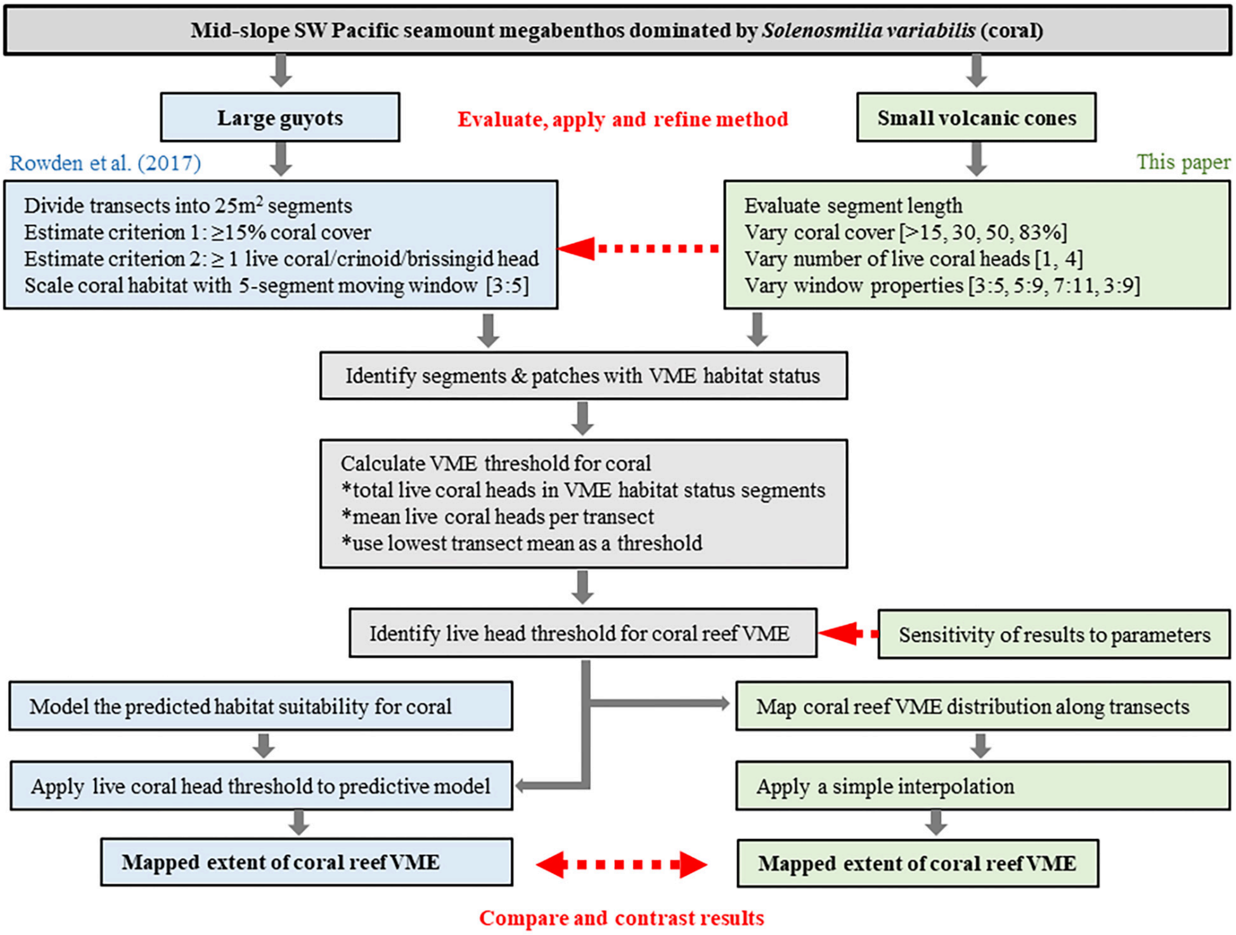

FIGURE 3 | Schematic showing overview of process to evaluate and develop the method of Rowden et al. (2017) to spatially define coral reef VME habitat using image-derived data. The red arrows identify key phases of the process: (1) evaluate, apply and refine the method; (2) identify sensitivities to changes in methodology; (3) interpret the output for Tasmanian seamounts.

the requirement of a moving window. The requirement (rule) was for a minimum "*ratio*" of segments across the window to have VME habitat status, e.g., ≥3 of 5; if satisfied, the window then attributes VME habitat status to the single segment in the center of the window; each segment is sequentially classified in this way as the window moves along the transect (**Figure 4**).

Step 4 – Coral reef VME is attributed to segments with VME habitat status by applying a live coral head threshold. This was calculated as the number of live coral heads per segment averaged over those segments that were identified in previous analytical steps as having VME habitat status on an individual transect; the smallest value was applied as the threshold to map coral reef VMEs for the entire data set.

The stage 1 analysis (steps 1–4) is illustrated for site 8 (Seamount Z16) a symmetrical cone with simple topography in **Figure 5**. This shows the progression from locating coral matrix with live heads within 12 m long segments (**Figure 5a**), to applying the criteria for cover of coral matrix and presence of live coral heads (**Figure 5b**); to mapping segments with VME habitat status into patches (**Figure 5c**), to applying a calculated minimum threshold of number of live heads per segment (**Figure 5d**).

Stage 2 Analysis

Step 5 – The distribution of coral reef VME (as defined in step 4 above) was then spatially expanded, by simple extrapolation (below). We did not proceed to the development of a predictive spatial model for the entire area (e.g., Rowden et al., 2017), principally because this demanded greater resolution of physical covariates than we had available.

Scenario Testing

The classification of coral reef VME using transect data, pioneered by Rowden et al. (2017), used a single value for percentage cover (≥15%) and live coral abundance (≥1 live head), and a 5-segment moving window requiring 3 segments with VME habitat status (a 3:5 ratio) to qualify as being part of a patch with VME habitat status. We used these parameter values as a base-case scenario and examined how varying theses

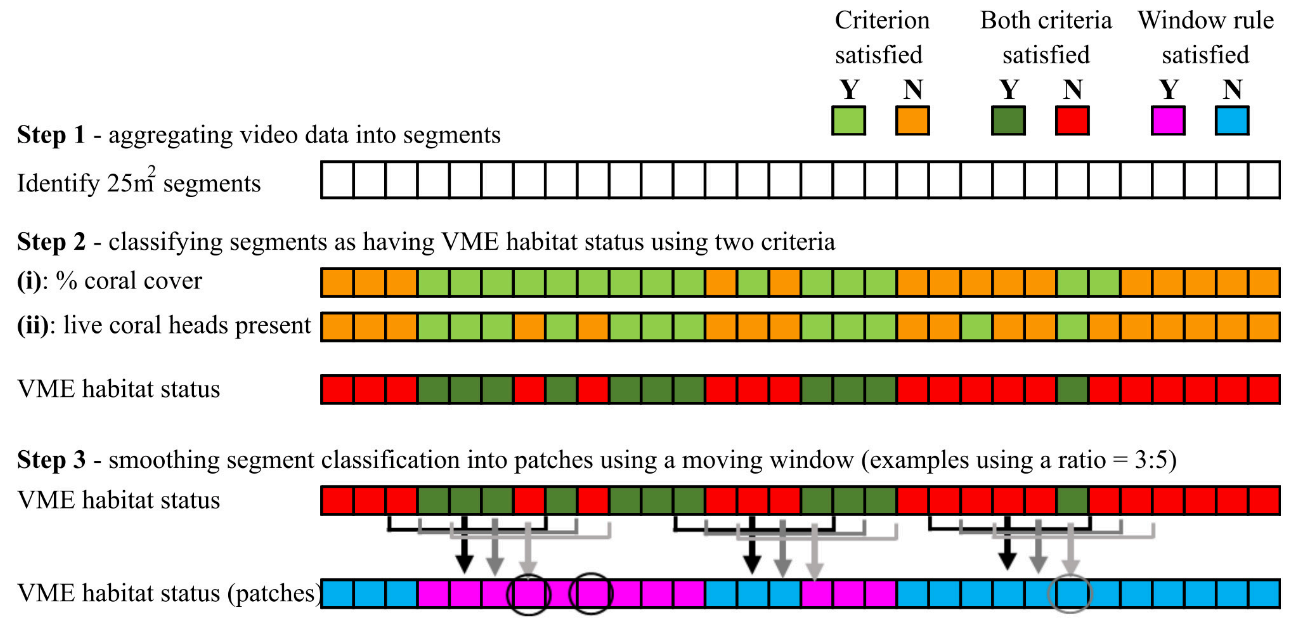

FIGURE 4 | Schematic illustration of how VME habitat status is classified at segment scale (steps 1 and 2), and the use of a moving window to aggregate segments into patches by smoothing (step 3). In the example shown here, the smoothing rule for the moving window is for a ratio of ≥3 of 5 segments inside the window to have VME habitat status. Where the rule is satisfied, the window attributes VME habitat status to the single segment in the center of the window as it moves along the transect. Circles show examples of how smoothing may result in misclassifications.

values (setting more conservative criteria and the properties of the moving window more and less strictly) influenced the distribution and area of seabed estimated to have VME habitat status. We first increased the percentage of % cover of coral matrix from 15% cover to 25% to match the base-case threshold of 15% over 100 m^2, i.e., the size of a 5-segment moving window with a 3:5 ratio rule, and then added 50 and 83% cover per segment (equivalent to 30 and 50% of a 5-segment moving window). The number of live heads was increased arbitrarily from the base-case of presence (≥1) to an abundance of ≥4 live heads. Scenarios applying different combinations of parameter values were examined for the total dataset (52 transects) and the effects measured by % change in two survey-scale metrics: (1) the number of transects in which ≥1 patch of VME habitat status was identified, and (2) the total area of seabed classified with VME habitat status combined over all transects.

We then explored how varying the length of the moving window and the number of segments required to have VME habitat status within the window (the ratio) influenced patch structure classification (length and distribution). A moving window "smooths" the patch-level classification by incorporating lone segments without VME habitat status into patches with VME habitat status and *vice versa* (**Figure 4**). Smoothing correctly classifies some lone segments but may misclassify others that occur in groups smaller than the number required by the rule for VME habitat status, e.g., groups of 2 where the rule is 3 (as for the base-case 3:5 ratio) (**Figure 4**).

We expected that the window's smoothing effects – either patch-joining (creating fewer but longer patches) or patch-splitting (more but shorter patches) – would vary with window length, the required ratio of segments with VME habitat status, *and* the interaction of these two properties. Thus, across scenarios we aimed to provide a contrast in window length while keeping the ratio similar to base-case (3:5) and, additionally, provide a contrast in the ratio. Three scenarios were tested: (1) a longer window with similar (slightly lower) ratio = 5:9; (2) a very long window with similar (slightly higher) ratio = 7:11; and (3) a longer window and small ratio = 3:9. The effects on patch structure classification from different scenarios were examined at patch scale across transects, and at segment scale within patches. Changes across transects were measured by two transect-scale metrics: (1) the mean number of patches with VME habitat status, irrespective of patch size, across all transects with patches; and (2) the mean maximum patch size per transect. Changes in the number and distribution of segments as the result of patch-forming and patch-breaking were visualized at site 11 (Hill U), a complex seamount feature comprised of a cone with an adjacent caldera and extensive areas of rough seabed.

The basis for spatial expansion from patches with VME habitat status to areas of coral reef VME was based on calculating a live coral head threshold in the same way as Rowden et al. (2017). This was achieved by calculating the mean number of live coral heads over all segments with VME habitat status in each transect separately, and then using the minimum transect mean as the threshold for the entire data set. The Rowden et al. (2017) value (2.78) was used as the base-case. Those authors applied the live coral head threshold to predictive models that had previously mapped habitat suitability (HS) for *S. variabilis* on a series of large guyots; threshold-based mapping identified where coral reef VME habitat occurred

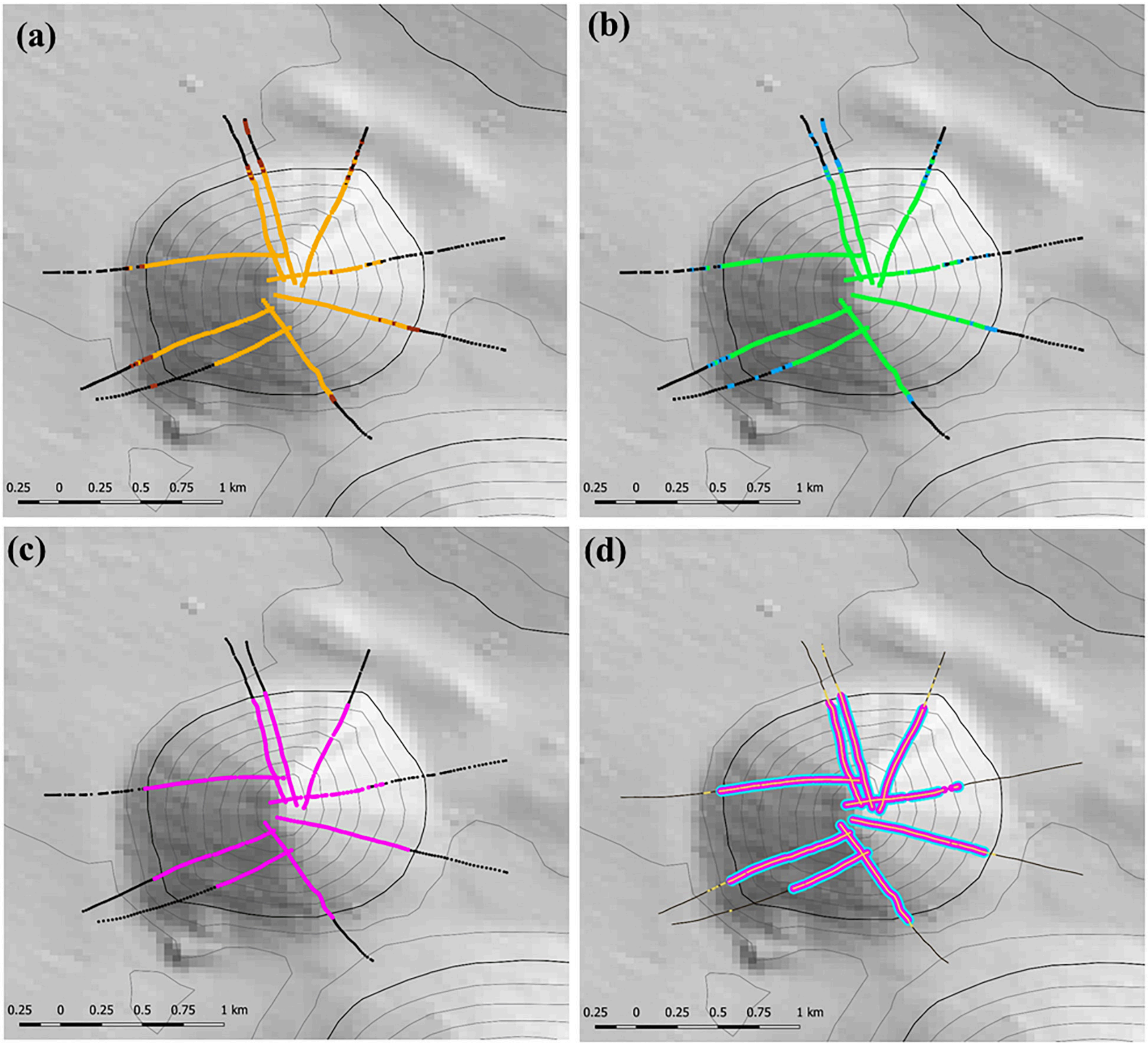

FIGURE 5 | Illustration of the initial steps used to identify the presence and location of VME habitats at study site 8 (Seamount Z16) where camera transects were conducted; heavy depth contour = 1350 m depth: **(a)** step 1 – locating the presence of the matrix-forming stony coral *Solenosmillia variabilis* in 12 m long segments – orange = live coral, brown = dead coral; **(b)** step 2 – applying criteria of percentage cover and presence of live coral heads to identify segments representing VME habitat status (base-case scenario of 15% cover of coral matrix and ≥1 live coral head) – black meets neither criteria, blue meets one criterion, green meets both criteria; **(c)** step 3 – mapping segments with VME habitat status into patches with VME habitat status (pink) using a classification that requires ≥3 segments in a five segment moving window (3:5 ratio) to have VME habitat status; and **(d)** step 4 – coral reef VME (blue) is identified and mapped along patches with VME habitat status by applying a (minimum) live coral head threshold calculated across all transects. Depth contours: 50 m intervals with 1350 line bolded.

within the broader areas previously identified as having some level of habitat suitability for *S. variabilis*. We did not have a comparable model or a suite of co-variate environmental data (notably seabed backscatter) of sufficient quality and at suitably fine spatial scales to emulate their model application. Instead, we applied a simple extrapolation of our observed VME habitat status distributions between adjacent radial transects, or around single transects. This was accomplished by extending the VME boundary, by eye, using the adjacent 50 m isobaths to generate polygons that represent the approximate estimated extent of coral reef VME. These estimates permit direct comparison of *S. variabilis* coral reef VME extents (sizes) in the 500–2000 m depth range on large guyots and small volcanic cones (**Figure 3**).

RESULTS

Vulnerable marine ecosystems habitat status was not very sensitive to changes in key parameters used for classification

TABLE 2 | Summary outputs from modeling scenarios used to classify habitats as having VME status; key parameters (column 1) are varied in order to test the sensitivity of the method.

Scenario: parameters are % cover – live heads – moving window ratio*	Nos. transect with VME habitat status	Threshold – min. no. live heads**	Max. no. live heads	Percent area: VME habitat status	Percent area: coral reef habitat calculated threshold (column 3)	Percent area: coral reef habitat base-case threshold (2.78)
15% – 1–3:5	40	5.6	50.9	25.92	20.46	22.62
15% – 1–3:9	41	3.5	49.27	30.12	22.23	23.21
15% – 1–5:9	40	5.6	50.9	25.89	20.34	22.38
15% – 1–7:11	39	5.75	51.92	24.22	19.8	21.58
25% – 1–3:5	40	5.6	50.9	25.66	20.39	22.45
25% – 1–3:9	41	3.5	49.27	29.91	22.23	23.17
25% – 1–5:9	40	5.6	50.9	25.46	20.21	22.18
25% – 1–7:11	39	5.75	51.92	23.87	19.75	21.44
50% – 1–3:5	40	5.6	51.34	24.17	19.79	21.56
50% – 1–3:9	41	3.5	49.27	28.21	21.79	22.62
50% – 1–5:9	40	5.6	51.34	24.11	19.66	21.38
50% – 1–7:11	39	5.75	52.58	22.75	19.18	20.66
83% – 1–3:5	39	5.6	52.58	21.81	18.6	19.95
83% – 1–3:9	39	3.5	49.27	25.87	21.03	21.68
83% – 1–5:9	39	5.6	52.58	22.23	18.81	20.16
83% – 1–7:11	39	5.75	54.64	20.34	17.78	18.87
15% – 4–3:5	39	5.75	53.46	22.3	19.98	21.31
15% – 4–3:9	40	4.67	51.76	26.21	21.08	22.54
15% – 4–5:9	38	7	54.38	22.18	19.31	21.01
15% – 4–7:11	37	7	55.25	20.69	18.56	19.98
25% – 4–3:5	39	5.75	53.46	22.15	19.91	21.21
25% – 4–3:9	40	4.67	51.76	26.06	21.08	22.5
25% – 4–5:9	38	7	54.38	22.06	19.26	20.94
25% – 4–7:11	37	7	55.25	20.59	18.49	19.88
50% – 4–3:5	39	5.75	53.96	21.31	19.36	20.55
50% – 4–3:9	40	4.67	51.76	25.05	20.74	22.02
50% – 4–5:9	38	7	54.91	21.35	18.81	20.37
50% – 4–7:11	37	7	55.81	20.05	18.14	19.41
83% – 4–3:5	39	5.75	53.96	19.98	18.4	19.34
83% – 4–3:9	39	4.67	51.76	23.76	20.2	21.26
83% – 4–5:9	38	7	54.91	20.04	18.07	19.33
83% – 4–7:11	37	7	55.81	18.46	16.99	18.01

**% Cover = cover of stony coral reef per segment; live heads = number of live head per segment; moving window ratio = proportion of segments with VME habitat status required in window. **Minimum excludes two transects on Hill K1 (site 22) where some fishing impact was observed.*

(**Table 2** and **Figures 6**, **7**). Our scenario testing showed nil, negligible, or small (0–4%) changes from the base-case, either in terms of the number of transects or the area of transects identified as having VME habitat status. All effects of changing key parameters were consistently nil to very low for scenarios varying the seabed cover of corals (i.e., from a 15% base-case to 25 and 50%), and the number of live coral heads (i.e., from ≥1 base-case to ≥4 live heads).

Similarly, we found no substantial effects of changing the length of the moving window or the proportion of VME habitat segments required within its length (i.e., from a 3:5 ratio in the base-case to ratios of 3:9, 5:9, and 7:11) (**Figure 6**). A few larger changes (>4%) were observed only when we combined the largest parameter changes, being a 50 and 83% seabed cover and a ratio of 7:11 in the moving window; none, however, exceed a 6% change from the base-case. The least strict condition for the window (3:9 ratio) had the effect of increasing the computed VME area (**Figure 7D**).

Our scenario testing also showed small changes in patch structure from the base-case as measured by the mean number of patches with VME habitat status per transect, and the mean maximum patch size per transect (**Figures 8A,B**, respectively); the only sizeable difference was between the single segment (no smoothing) and all moving window scenarios. The effects of varying parameters on patch structure on individual transects are illustrated for the topographically complex site 11 (seamount "Hill U") using selected scenarios (**Supplementary Figure 1**) and the four moving window ratios (3:5 base-case, 3:9, 5:9, and 7:11) (**Supplementary Figure 2**).

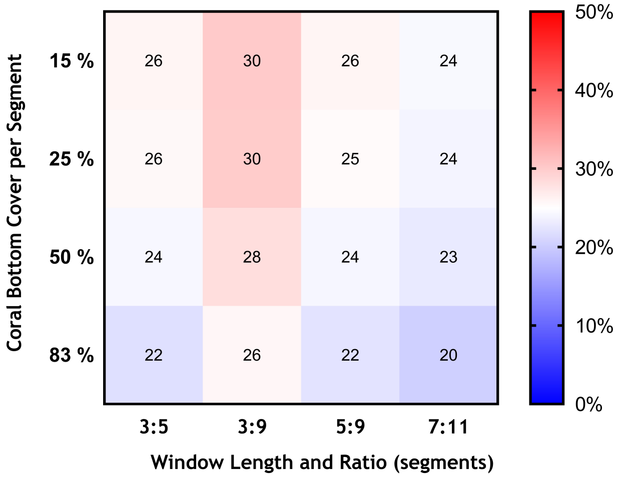

FIGURE 6 | Effects of changing the bottom cover of coral matrix (from 15 to 83%), and the length of the moving window and ratio of VME habitat segments required within its length (3:5 base-case and 3:9, 5:9, and 7:11) in terms of the area of VME habitat identified across transects expressed as percentage of total area surveyed (color scale).

Any changes to patch structure that result from adding or subtracting segments with VME habitat status under different scenarios had the potential to affect the calculation of the live head threshold applied to the final spatial expansion of coral reef VMEs. Thus, in an overall exploration of methodology it was also necessary to change the live head threshold for mapping. All combinations of criteria and window properties affected the threshold value for our data, and across our scenarios this value was in a range of ∼3.5 to 7 minimum mean live heads per transect (**Table 2**, column 3), although with consistently lower values (3.5–4.67) when applying the least strict (3:9 ratio) moving window. Applying the Rowden et al. (2017) base-case scenario to the Tasmanian data set – 15% coral cover, 1-live coral head and a 3:5 moving window – resulted in a threshold value of 5.6 (**Table 2**). The effects of this higher threshold compared to the base-case (2.78) are illustrated at transect level using site 11 (Hill U) as an example (**Figure 9**). Compared to the base-case (**Figure 9a**) our higher live head threshold eliminated one deep patch of coral reef VME on transect 2 and slightly shortened patch lengths on transects 4, 6, and 7; there was also a patch break on transect 4 (**Figure 9b**). An increase of the % cover criterion to 25% made no observable difference (**Figure 9d**).

A scenario of 25% cover of coral reef and 1 live head, a moving window with a ratio of 3:5, and a live head threshold of 5.6) was applied to all transects to map coral reef VME over the study area (**Figure 10**). The estimated size (spatial extent) of coral reef VMEs estimated from simple extrapolation showed the largest coral reef VMEs are at sites 8 (1.16 km^2), 11 (1.16 km^2), and 23 (0.86 km^2); the smallest is at site 10 (0.02 km^2) (**Table 1** and **Figure 11**). Extrapolation appeared robust for symmetrical volcanic cones, especially where there were replicate radial transects, and supported its application to cones with single transects. Mapping on volcanic cones clearly shows a depth-related transition between coral reef VME and VME habitat around 1300–1400 m depth; contiguous intact reef extends through this depth range, but the abundance of live *S. variabilis* diminishes to zero and transect segments no longer meet both the % cover and live heads criteria. Mapping also clearly demonstrated where coral reef VME is absent (sites 3, 7, 16, 19, 21, 24, 26–30), even if dead or isolated small clumps of coral reef substrate were observed in the videos. Extrapolation can be done with least confidence where replicate transects show inconsistency (site 11), and on rugged rocky bottom without clear contours or morphology (sites 2, 4, 14, 20).

DISCUSSION

Robustness of the Method

The method of Rowden et al. (2017) to identify and map coral reef VME from image data was explored and further developed to provide an objective way of defining distributions of coral reef VME habitat formed by the stony coral *S. variabilis* on Tasmanian seamounts. The result successfully represented VME distribution at the feature-scale by distinguishing living coral reef from dead reef, reflecting the abundance of live coral, mapping the spatial extents of VME patches using a simple extrapolation, and by not being sensitive to a range of practical choices of parameter values chosen for VME identification from photographic transects.

The steps for identifying coral reef VME – establishing the VME habitat status of segments and combining them into patches before defining patches as coral reef VME (steps 1–4 in our method) – were robust to modest changes in parameter values or properties of the moving window. Marked differences to using the Rowden et al. (2017) base-case outcomes for classifying VME habitat status were identified only for combinations of the strictest changes to parameter values (50 and 83% cover; 4 live coral heads and an 11-segment moving window) and least-strict ratio (3:9) for the moving window. Similarly, there were only minimal differences to base-case outcomes for patch structure. Mapped scenarios for the seven transects on the example seamount (the topographically complex Hill U) showed relatively small changes in patch distributions as parameter values and window properties varied – despite many changes to the VME habitat status of individual segments. Segment-level changes affected patches mostly by shortening them; relatively few patches were eliminated, and none were created in the scenarios tested. Changes in segment status typically occurred at the ends of patches and were concentrated toward the deep distributional limit of *S. variabilis* around 1200–1300 m depths. The requirement to calculate a locally specific live head abundance threshold to map coral reef VME (step 4) also appeared to be robust because the threshold value calculated for the Tasmanian seamounts (5.6) was nearly double the New Zealand value (2.78) but resulted in only small changes in identified areas on the example Hill U seamount.

These patterns of low sensitivity to different analytical scenarios are partly explained by the coral reefs on Tasmanian seamounts being typically large, contiguous structures with high abundances of live coral heads. We expect there will be higher

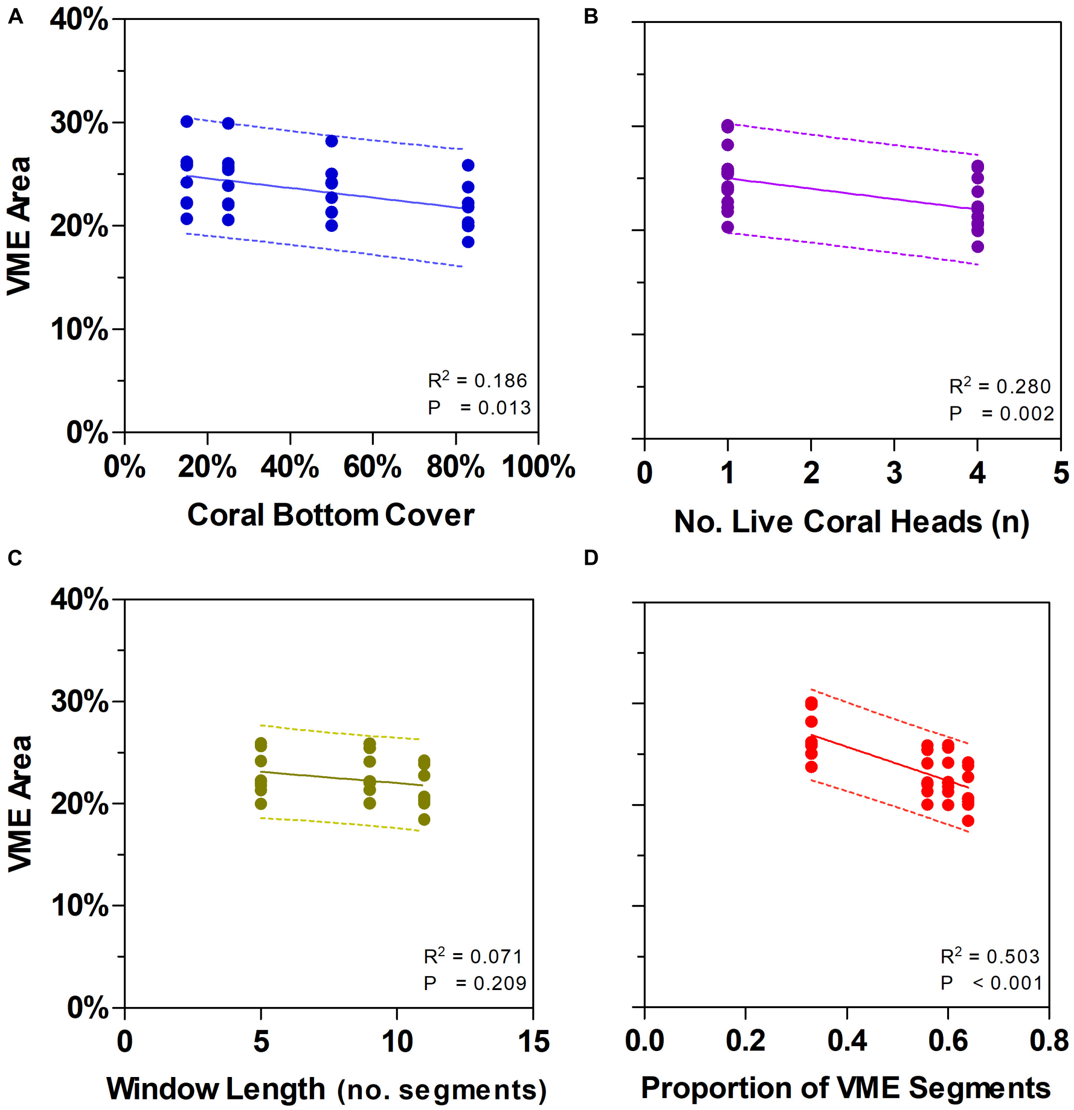

FIGURE 7 | Effects of changing some key parameters in scenario modeling to gauge the sensitivity of a method to classify areas of deep seabed as vulnerable marine ecosystems (VME). Top row shows how changes in the criteria of bottom cover by stony corals **(A)** and the number of live coral heads per segment **(B)** influence the proportion of the sampled seabed that is classed as VME based on individual segments. Bottom row shows how segments along transect lines can be aggregated into patches using a moving window that can vary in length **(C)** and in the proportion of segments having to meet the criteria under **(A)** and **(B)** above inside a window (the ratio) **(D)**. Panel **(C)** shows the effect of varying window length with similar ratio (~3:5, 5:9, 7:11); panel **(D)** includes window with a small ratio (3:9).

sensitivity to variation in parameters where *S. variabilis* reefs are more patchy. This prediction is supported by our observation that on Tasmanian seamounts, changes to VME mapping were concentrated toward the deep ends of transects where coral reefs became more fragmented. The method was applied successfully to the Louisville Seamount Chain guyots off New Zealand where coral reef VMEs are typified by smaller patches and relatively high proportions of dead coral matrix (Rowden et al., 2017). Collectively, these are positive indications for the overall robustness of the method, but its broader application needs to be substantiated by scenario testing in different environments. There are therefore no strong arguments to change the parameter values or moving window properties. We do note, however, that a 15% cover of coral reef (criterion 1) per segment needs to become 25% across the length of a 5-segment window to satisfy the minimum requirement of a 3:5 rule. Irrespective, this remains an arbitrary value that is not founded on a relationship between % cover of coral reef and its ecological significance and represents a valuable future refinement to the method.

Stage 2 of the method (step 5) requires spatial expansion of transect-based patches of coral reef VME to larger areas. Ideally this would be accomplished using a predictive modeling approach (e.g., Rowden et al., 2017), but there are demanding requirements for suitable environmental covariate data in the

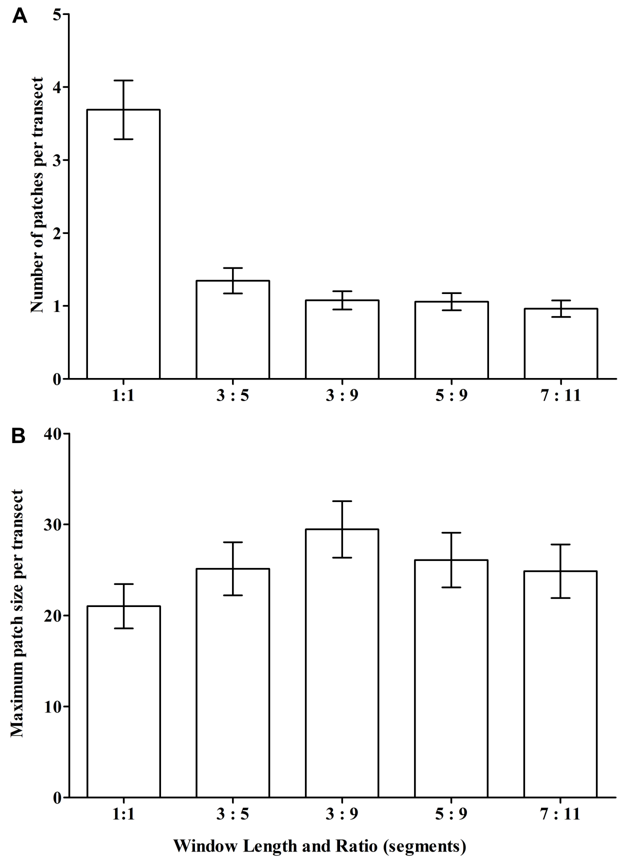

FIGURE 8 | Sensitivity of VME classification to changes in the length (number of segments) of the moving window and the ratio of VME habitat segments required within a window to identify contiguous patches with coral VME habitat status along transects. The effects of changing the moving window ratio from base-case (3:5) is compared to single segments (unsmoothed) and ratios of 3:9, 5:9 and 7:11 as measured across all transects in terms of changes to **(A)** the number of patches; and **(B)** the maximum patch length per transect.

deep-sea context. Predictor variables need to be available for large areas but have both a native resolution that matches the spatial scale of ecological analysis (10s–100s of meters) and low uncertainty. Where abundance is a desired outcome of models, predictor variables also need to be relevant to abundance and not just presence.

Options for predictor variables in the deep sea are therefore restricted to seabed depth, derivatives of seabed bathymetry, and seabed backscatter provided by multi-beam sonar (MBS). Many of the variables derived from bathymetry are highly correlated and spatially auto-correlated, but after appropriate treatment in model data they are well suited to identifying fine-scale topography that may be informative about the fine-scale distribution of faunal abundance (Anderson et al., 2016b; Georgian et al., 2019). As well, good quality bathymetry data are typically acquired during surveys over large areas. In our area, depth makes a useful contribution to defining coral reef VME for *S. variabilis* because the species has a relatively narrow depth range of occurrence here (∼950–1350 m). Backscatter data have high potential for fine-scale predictive analysis because they can provide information on seabed hardness and roughness that will have often have strong correlation with the abundances of sessile benthos including corals. However, while backscatter data are collected simultaneously with bathymetry data, their quality can be insufficient for predictive mapping. We found that even after rigorous post-processing of noisy data generated by ship turns and nadir, our data were still of insufficient quality for modeling over the scale of the study area due to variations in sea state and ship direction. Carefully controlled collection of backscatter data is required to provide data sets that are fit-for-purpose for predictive modeling. Hence, we elected to estimate spatial extents of coral reef VMEs using a simple depth-based extrapolation because our initial and primary focus was at the site and feature scale. This was robust for symmetrical volcanic cones, especially where there were replicate radial transects, and supported extrapolation on cones where we had only single transects. Extrapolation was weakest where replicate transects on individual features showed inconsistency in coral reef VME distribution with depth, and on rugged rocky bottom that lacked clearly defined feature-scale topography and depth boundaries. Identifying and quantifying VME distributions on these types of locations across a regional setting will depend on whether fine-scale bathymetry-derived covariates have predictive value.

Sizes and Structure of Coral Reef VMEs on the Tasmanian Seamounts

The seabed areas identified as coral reef VME on Tasmanian seamounts were typically characterized by long contiguous patches of reef supporting highly abundant live coral heads. Coral reef VME occurred mainly on the peaks and flanks of seamounts in a depth range of approximately 950 to 1350 m; these areas were distinguished from areas where *S. variabilis* reef grew at low abundance (cover) and/or had no living colonies; these were mostly on the continental slope, and the deeper flanks of seamounts or near the base of seamounts (>1350 m depth) (**Figure 10**).

Locations of coral reef VMEs included sites where there were replicate radial transects on individual seamounts; some showed consistent and relatively uniform VME distribution on symmetrical conical features, i.e., site 8 (Seamount Z16), and others a more heterogenous distribution, particularly in areas of complex topography (e.g., over the caldera at site 11 (Hill U) and the extension of rugged bottom southwards of site 22 (Seamount K1) (**Figure 11**). On features where only a single transect was sampled, VME distributions were consistently mapped over the peaks and flanks of individual seamounts (**Figure 11**). Importantly, coral reef VME was always absent on the continental slope below the shelf edge and typically absent on flat unstructured areas of continental slope between seamounts despite some *S. variabilis* present as dead matrix or in small isolated clumps (**Figures 2d**, **10**). These observations indicated that any subsequent prediction of coral reef VMEs over a broad area around Tasmania could be completed with a higher overall confidence in a predictive model. However,

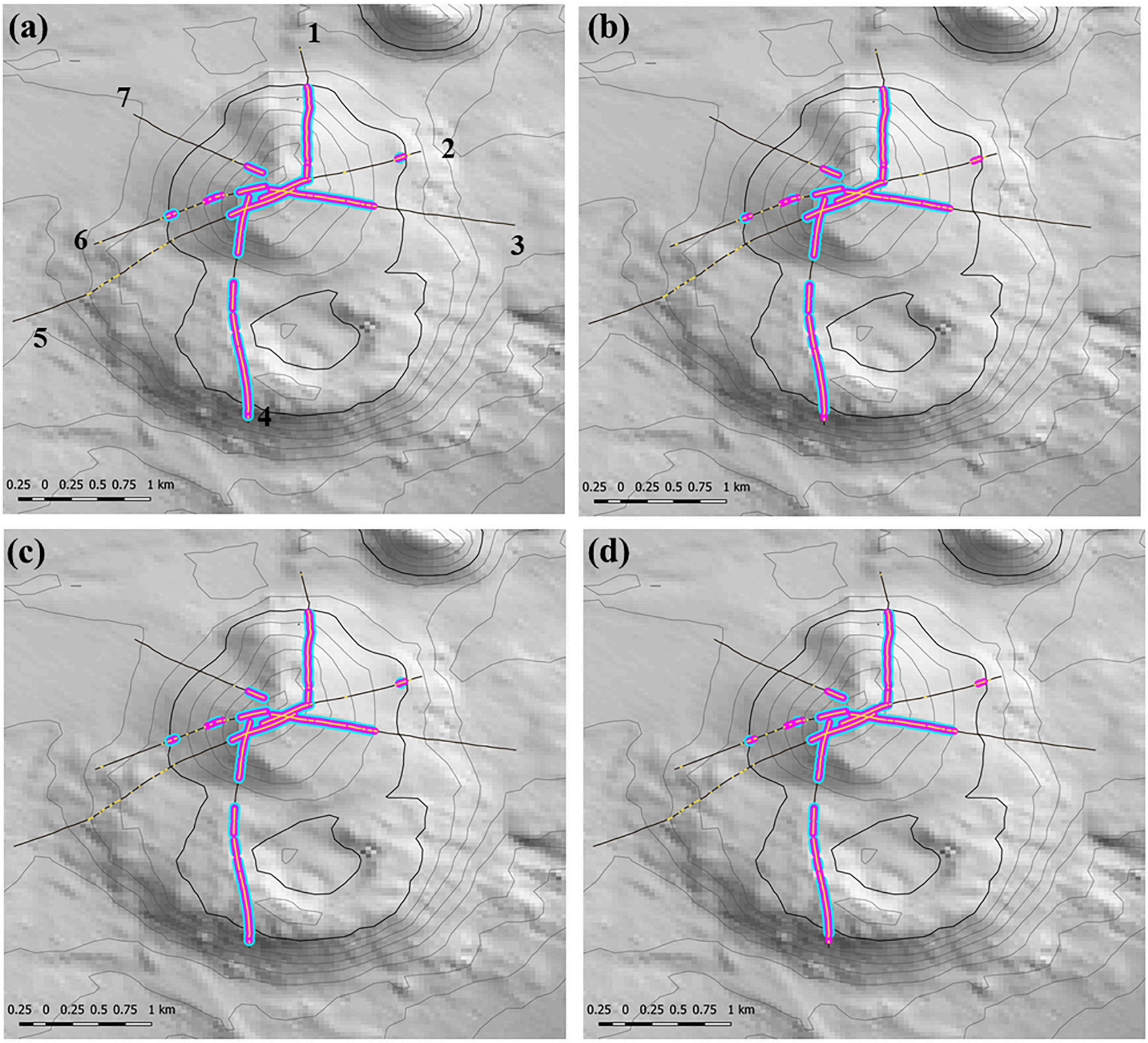

FIGURE 9 | Transect-scale effects of changing parameters used to map coral reef VME habitat: example from site 11 (Hill U). Maps show transects (heavy black lines), the raw distribution of the matrix-forming stony coral *Solenosmillia variabilis* (yellow); segments defined as having VME habitat status (pink), and coral reef VME habitat (blue). Panel **(a)** shows transect numbers. Scenarios: **(a)** base-case with 2.78 live head threshold; **(b)** base-case with 5.6 live head threshold; **(c)** 25% cover and 2.78 live head threshold; **(d)** 25% cover and 5.6 live head threshold. Depth contours: 50 m intervals with 1350 line bolded.

observations of coral reef VME away from seamounts, one associated with an extensive area of flat but rugged bottom that extended between small seamount cones at site 14 (Little Sister Seamount), another with an unusually pronounced area of raised topography on the continental margin at site 2 (Riedle Hill), and a third on the rugged bottom of the continental margin (site 4) (**Figure 11**), suggest the need for including fine-scale (25 m^2) bathymetry-derived covariates in any model that aims to predict the distribution of coral reef VME over a broad area, and especially away from areas of high and contiguous abundance.

Coral reef VMEs on the Tasmanian seamounts are large in spatial extent (0.02–1.16 km^2) when compared to those mapped on the Louisville Seamount Chain (LSC) off New Zealand (0.0006–0.0425 km^2) by Rowden et al. (2017). There are also large relative differences in terms of the proportions of total areas of coral reef VME on individual seamounts. Thus, the largest and smallest estimated proportions of coral reef VME on Tasmanian seamounts are, respectively, 65% on Seamount Z16 (site 11) and 0.3% on Seamount Hill V (site 10), and correspondingly on the LSC are 0.085% on the Valerie Seamount and 0.001% on the Ghost Seamount. Thus, compared to the largest proportion of VME on an LSC seamount, the smallest and largest Tasmanian VME proportions are 3.5 and some 750 times greater. These differences in size are accompanied by differences in reef form

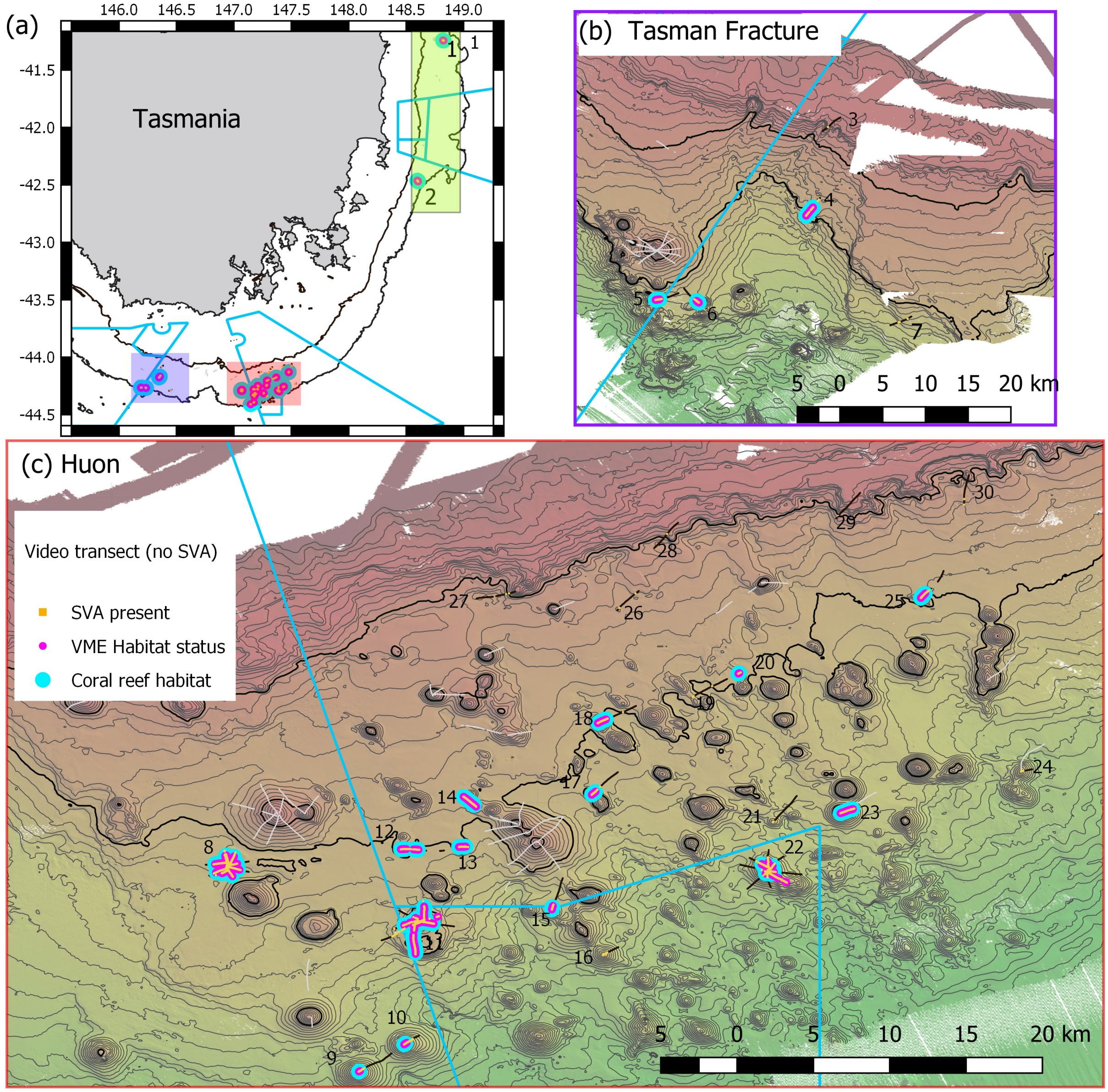

FIGURE 10 | Distribution of *Solenosmilia variabilis* coral reef VME habitat (blue) across all sites. Scenario uses criteria of 25% cover of coral reef and 1 live head, a moving window with a ratio of 3:5, and a live head threshold of 5.6). Depth contours: panel **(a)** 250 and 2000 m – define the limits of the survey area; panels **(b,c)** 50 m intervals with 950 and 1350 lines bolded.

(**Figure 11** and Rowden et al., 2017, **Figure 8**), with coral reef VMEs on the smaller Tasmanian seamount cones composed of large contiguous "blankets" and those on the LSC guyots being more numerous, smaller and distributed patches.

How Big Is Big Enough for VME Classification?

Using the Rowden et al. (2017) method, the spatial extent of *S. variabilis* coral reef VME on seamounts in the Southwest Pacific Ocean was found to vary widely, from small isolated patches of 625 m^2 (the minimum scale of modeling) to extensive "blankets" covering 1.16 km^2 or more. This considerable size range raises the question of whether there are thresholds in terms of coral densities and/or reef sizes that can be considered as ecologically functional units? An answer will depend largely on the type of function considered (e.g., productivity, habitat provision, bio-geochemical processing, nursery area, refuge etc.) and the body size and mobility of associated fauna. Thus, even small reefs can be "functionally important" for small individual and/or species, particularly in a seascape setting where such feature are rare and scattered. The dominant northern hemisphere reef-builder, *D. pertusum*, typically creates reefs composed of live and dead coral which are numerous (e.g., ∼6000

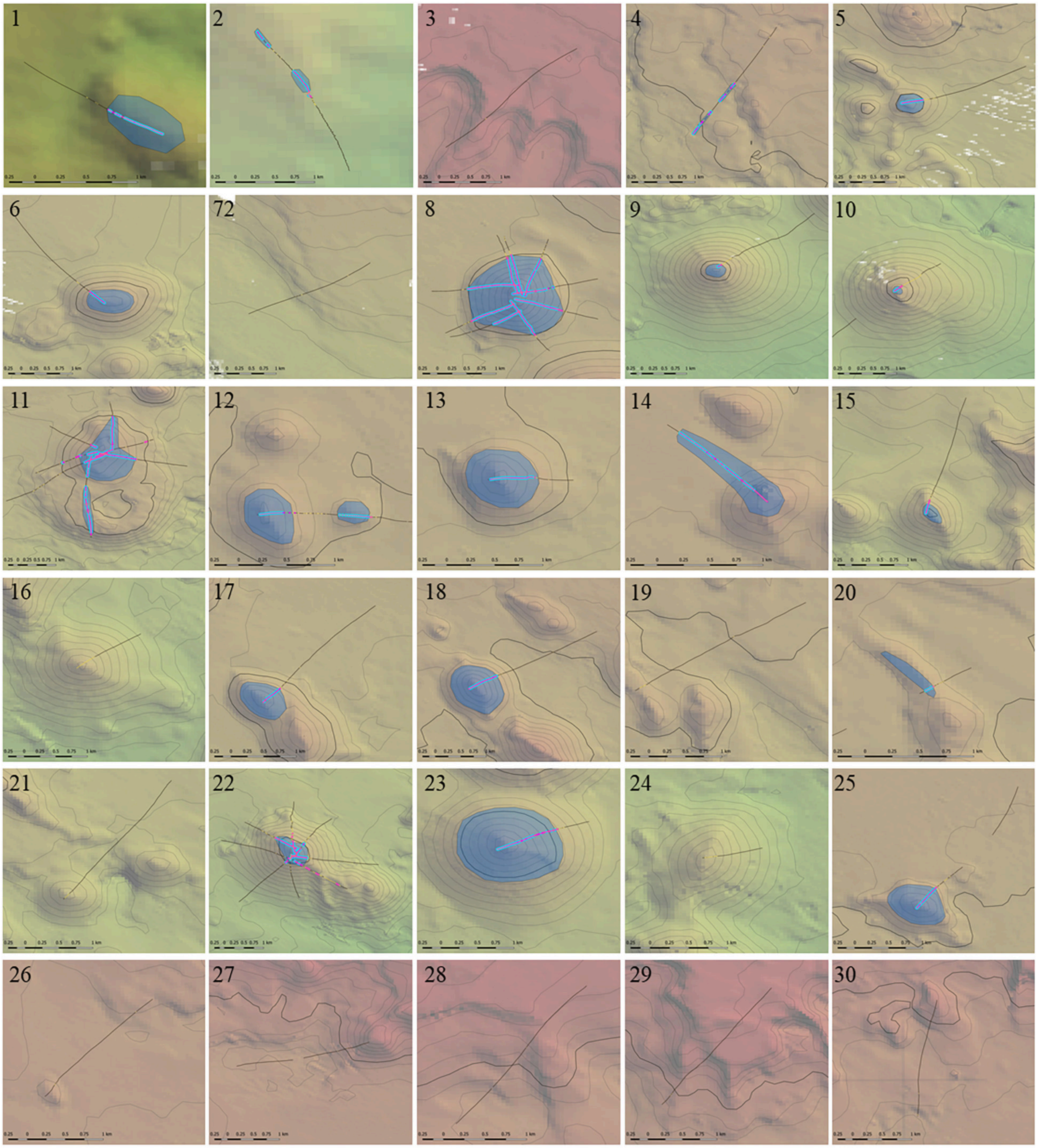

FIGURE 11 | The estimated extent (size) of *Solenosmilia variabilis* coral reef VME at individual study sites extrapolated from coral reef VME mapped along transects. Mapping method as per **Figure 9**, with coral reef VME extent underlaid as gray polygons. Scenario uses criteria of 25% cover of coral reef and 1 live head, a moving window with a ratio of 3:5, and a live head threshold of 5.6). Depth contours: 50 m intervals with 950 and 1350 lines bolded.

reefs off Norway alone), round or narrow in shape and up to several 100 m in length (Buhl-Mortensen et al., 2010). A high level of biogeochemical recycling was demonstrated by Cathalot et al. (2015) at a reef of 1,767 m^2 in size, indicating that relatively small areas within individual reefs can make significant contributions to ecosystem processes. The localized high abundance of *S. variabilis* on Tasmanian seamounts was suggested by Miller and Gunasekera (2017) to be partly attributable to heavy reliance on asexual clonal reproduction for localized recruitment, with negligible dispersal of sexually produced larvae. These life history characteristics result in smaller, isolated genetic populations and a susceptibility to the effects of genetic drift, loss of genetic diversity and adaptive capacity which make the species more vulnerable to anthropogenic impacts than other reef-building coral species with relatively higher rates of sexual reproduction and more widespread dispersal – including *D. pertusum*. On the other hand, the minimum size for a self-sustaining population of a clonal reproducing species would be expected to be smaller than that for a population reproducing via dispersed larvae. *D. pertusum* also recruits through a combination of sexual and asexual reproduction but, whilst these proportions vary geographically, it has a lower proportion of clonal reproduction and therefore may be less vulnerable to impacts (Miller and Gunasekera, 2017). These observations indicate there is no single answer to the question of a minimum size for a coral reef VME, but suggest that size-based criteria need to be at least species and region specific.

For this method to be applied to other VME indicator taxa, the majority of which do not form reef-like structures, would require development of density thresholds for each taxon or group of taxa of interest. The live vs. dead criterion may be important if indicator taxa are associated with biogenic habitat, but it will be more important to assess taxa density or cover within transect segments and relate these numbers to the area over which the taxa is distributed. Applications to taxa that, compared to stony corals, have greater ranges of abundance at the spatial scales of analysis (segments and patches) and occur over much greater areas, may also benefit from exploring alternative properties for the moving window in conjunction with the density threshold.

Management Applications of Data

We anticipate that these results will assist the development of models that predict VME distributions. The use of such models has been recommended as part of the process for designing management plans to protect VMEs from fishing impacts (Ardron et al., 2014; Vierod et al., 2014), but it is acknowledged that models generally overpredict the occurrence of VMEs (Rengstorf et al., 2013; Buhl-Mortensen et al., 2019) due to not having predictors relevant to the ecological responses of VME taxa and at the relevant spatial scales. For reef-building corals there may be considerable differences between the predicted distribution of reef habitats and the broader species distribution (Howell et al., 2011). This is well demonstrated for reef-forming corals in the South Pacific Ocean by Anderson et al. (2016a) who tested model predictions with photographic field validation sampling and found that the observed frequency of corals was much lower than predicted, and correlation between observed and predicted coral distribution was moderately poor.

Recent ensemble habitat suitability modeling for a suite of VME indicator taxa in the Southwest Pacific Ocean (Georgian et al., 2019) indicated there was extensive suitable habitat (at 1 km^2 grid scale) for *S. variabilis* across much of the modeled domain. This included the Tasmanian seamount areas mapped herein, where model diagnostics indicated good performance and low uncertainty in predictions. In the Huon sub-region (**Figure 10c**) their model predicted at least 770 km^2 of suitable habitat for *S. variabilis*. In contrast, our analysis identified about 5 km^2 of coral reef VME (**Figure 11** and **Table 2**), and, based on the restriction of coral reef VME largely to seamount peaks in 950–1350 m depths, suggests there is 106 km^2 of coral reef VME at most, of which some 58 km^2 (55%) is on seamounts where bottom trawling has occurred. Hence, our results provide evidence that the true scales of *S. variabilis* coral reef VMEs are relatively small when compared to regional model predictions of suitable habitat (typically smaller than a 1 km^2 model prediction grid cell), and much smaller than the smallest units of management interest (100s–1000s km^2). While it is sometimes considered precautionary to provide maximum estimates of the spatial extent of vulnerable populations, this is only true at the initial stages of developing management measures. Once the broad area of concern has been identified, more accurate predictions are required to ensure the most important areas are protected (avoiding erroneous assumptions that vulnerable populations occur throughout the range of predicted suitable habitat), and to minimize the economic consequences of management measures. Our observations point to the need for more caution to be used in designating spatially managed areas and management tools using predictions from models, which often appear to be too optimistic. However, our evaluation of the Rowden et al. (2017) method also shows that there is a solid basis for producing accurate and reliable maps of the coral reef VMEs at the scale of individual seabed features and hence an effective and simple means to strengthen both feature-based conservation and model predictions of VME distributions at broader spatial scales.

DATA AVAILABILITY STATEMENT

The data generated for this study is available on the CSIRO Data Access Portal at https://doi.org/10.25919/5e7951b49d279.

AUTHOR CONTRIBUTIONS

AW, MC, NB, and TS designed the study. AW, MG, KM, CU, NM, MC, NB, and TS acquired the data at sea. AW, FA, MG, KM, CU, NM, and CJ acquired and processed the image-derived data. FA and AW performed the analyses. AW led the writing. All authors made substantial contributions to discussing the methods and results and revising the manuscript.

FUNDING

This work originates from a project that is funded, collectively, by the CSIRO Oceans and Atmosphere, Parks Australia and the Australian Government National Environmental Science Program (NESP), Marine Biodiversity Hub. Project data were collected during a voyage on Australia's Marine National Facility Vessel, RV Investigator, funded through the Australian Government.

ACKNOWLEDGMENTS

We acknowledge the committees and staff of Australia's Marine National Facility (MNF) for access to the research vessel RV

Investigator, and the captain and the crew of the vessel for their hard work in making the survey successful. We also thank the sea-going staff from the MNF whose support was vital to the field collection of data. We especially thank our many colleagues from CSIRO Oceans and Atmosphere and Parks Australia, and Dr. Tiffany Sih, who helped process photographic imagery whilst at sea, and gratefully acknowledge the many other engineering, technical and administrative staff at CSIRO who contributed in various ways to supporting the project that provided the data for this manuscript. In particular, for the design and fabrication of the camera platform, and for maintaining and piloting the system at sea, we thank Matt Sherlock, Jeff Cordell, Karl Forcey, and Aaron Tyndall, and for advice and assistance with various aspects data preparation and survey design we are indebted to Scott Foster, Amy Nau and Jasmine Bursic (CSIRO), and Jan Jansen and Vanessa Lucieer (University of Tasmania). Finally, we thank staff from the IT and Data Centre at CSIRO, notably Pamela Brodie and Peter Shanks, made invaluable contributions to handling and processing the image data sets.

SUPPLEMENTARY MATERIAL

The Supplementary Material for this article can be found online at: https://www.frontiersin.org/articles/10.3389/fmars.2020.00187/full#supplementary-material

REFERENCES

Althaus, F., Williams, A., Schlacher, T. A., Kloser, R. J., Green, M. A., Barker, B. A., et al. (2009). Impacts of bottom trawling on deep-coral ecosystems of seamounts are long-lasting. *Mar. Ecol. Prog. Ser.* 397, 279–294. doi: 10.3354/meps08248

Anderson, O. F., Guinotte, J. M., Rowden, A. A., Clark, M. R., Mormede, S., Davies, A. J., et al. (2016a). Field validation of habitat suitability models for vulnerable marine ecosystems in the South Pacific Ocean: implications for the use of broad-scale models in fisheries management. *Ocean Coast. Manag.* 120, 110–126. doi: 10.1016/j.ocecoaman.2015.11.025

Anderson, O. F., Guinotte, J. M., Rowden, A. A., Tracey, D. M., Mackey, K. A., and Clark, M. R. (2016b). Habitat suitability models for predicting the occurrence of vulnerable marine ecosystems in the seas around New Zealand Deep sea research part I. *Oceanogr. Res. Pap.* 115, 265–292. doi: 10.1016/j.dsr.2016.07.006

Ardron, J. A., Clark, M. R., Penney, A. J., Hourigan, T. F., Rowden, A. A., Dunstan, P. K., et al. (2014). A systematic approach towards the identification and protection of vulnerable marine ecosystems. *Mar. Policy* 49, 146–154. doi: 10.1016/j.marpol.2013.11.017

Auster, P. J., Gjerde, K., Heupel, E., Watling, L., Grehan, A., and Rogers, A. D. (2011). Definition and detection of vulnerable marine ecosystems on the high seas: problems with the "move-on" rule Ices. *J. Mar. Sci.* 68, 254–264. doi: 10.1093/icesjms/fsq074

Buhl-Mortensen, L., Burgos, J. M., Steingrund, P., Buhl-Mortensen, P., Ólafsdóttir, S. H., and Ragnarsson, S. (2019). *Vulnerable Marine Ecosystems (VME): Coral and Sponge VMEs in Arctic and Sub-arctic Waters - Distribution and Threats.* Rosendahls: Nordic Council of Ministers, 155.

Buhl-Mortensen, L., Vanreusel, A., Gooday, A. J., Levin, L. A., Priede, I. G., Buhl-Mortensen, P., et al. (2010). Biological structures as a source of habitat heterogeneity and biodiversity on the deep ocean margins. *Mar. Ecol.* 31, 21–50. doi: 10.1111/j.1439-0485.2010.00359.x

Cathalot, C., Van Oevelen, D., Cox, T. J. S., Kutti, T., Lavaleye, M., Duineveld, G., et al. (2015). Cold-water coral reefs and adjacent sponge grounds: hotspots of benthic respiration and organic carbon cycling in the deep sea. *Front. Mar. Sci.* 2:37. doi: 10.3389/fmars.2015.00037

Clark, M. R., Bowden, D. A., Rowden, A. A., and Stewart, R. (2019). little evidence of benthic community resilience to bottom trawling on seamounts after 15 years. *Front. Mar. Sci.* 6:63. doi: 10.3389/fmars.2019.00063

FAO (2009). "International guidelines for the management of deep-sea fisheries in the high Seas," in *Food and Agricultural Organisation of the United Nations*, Rome: FAO, 73.

Foster, S. D., Hosack, G., Monk, J., Lawrence, E., Barrett, N., Williams, A., et al. (2020). Spatially-balanced designs for transect-based surveys. *Methods Ecol. Evol.* 11, 95–105. doi: 10.1111/2041-210X.13321

Georgian, S. E., Anderson, O. F., and Rowden, A. A. (2019). Ensemble habitat suitability modeling of vulnerable marine ecosystem indicator taxa to inform deep-sea fisheries management in the South Pacific Ocean. *Fish. Res.* 211, 256–274. doi: 10.1016/j.fishres.2018.11.020

Henry, L. A., and Roberts, J. M. (2007). Biodiversity and ecological composition of macrobenthos on cold-water coral mounds and adjacent off-mound habitat in the bathyal Porcupine Seabight. NE Atlantic. *Deep Sea Re.s I* 54, 654–672. doi: 10.1016/j.dsr.2007.01.005

Howell, K. L., Holt, R., Endrino, I. P., and Stewart, H. (2011). When the species is also a habitat: comparing the predictively modelled distributions of Lophelia pertusa and the reef habitat it forms. *Biol. Conserv.* 144, 2656–2665. doi: 10.1016/j.biocon.2011.07.025

Marouchos, A., Sherlock, M., Filisetti, A., and Williams, A. (2017). "Underwater imaging on self-contained tethered systems," in *IEEE Oceans Anchorage*, Anchorage, 18–21.

Miller, K. J., and Gunasekera, R. M. (2017). A comparison of genetic connectivity in two deep sea corals to examine whether seamounts are isolated islands or stepping stones for dispersal. *Nat. Sci. Rep.* 7:46103.

Morato, T., Pham, C. K., Pinto, C., Golding, N., Ardron, J. A., Muñoz, D. P., et al. (2018). A multi criteria assessment method for identifying vulnerable marine ecosystems in the north-east Atlantic. *Front. Ma. Sci.* 5:460. doi: 10.3389/fmars.2018.00460

Norberg, A., Abrego, N., Blanchet, F. G., Adler, F. R., Anderson, B. J., Anttila, J., et al. (2019). A comprehensive evaluation of predictive performance of 33 species distribution models at species and community levels. *Ecol. Monogr.* 89:e01370.

O'Hara, T. D., Rowden, A. A., and Williams, A. (2008). Cold-water coral habitats on seamounts: do they have a specialist fauna? *Divers. Distrib.* 14, 925–934. doi: 10.1111/j.1472-4642.2008.00495.x

Penney, A. J., and Guinotte, J. M. (2013). Evaluation of New Zealand's high-seas bottom trawl closures using predictive habitat models and quantitative risk assessment. *PLoS One* 8:e82273. doi: 10.1371/journal.pone.0082273

Rengstorf, A. M., Mohn, C., Brown, C., Wisz, M. S., and Grehan, A. J. (2014). Predicting the distribution of deep-sea vulnerable marine ecosystems using high-resolution data: considerations and novel approaches Deep Sea Research Part I. *Oceanogr. Res. Pap.* 93, 72–82. doi: 10.1016/j.dsr.2014.07.007

Rengstorf, A. M., Yesson, C., Brown, C., and Grehan, A. J. (2013). High-resolution habitat suitability modelling can improve conservation of vulnerable marine ecosystems in the deep sea. *J. Biogeogr.* 40, 1702–1714. doi: 10.1111/jbi.12123

Robert, K., Jones, D. O. B., Roberts, J. M., and Huvenne, V. A. I. (2016). Improving predictive mapping of deep-water habitats: considering multiple model outputs and ensemble techniques Deep Sea Research Part I. *Oceanogr. Res. Pap.* 113, 80–89. doi: 10.1016/j.dsr.2016.04.008

Roberts, J. M., Henry, L. A., Long, D., and Hartley, J. P. (2008). Cold-water coral reef frameworks, megafauna communities and evidence for coral carbonate mounds on the Hatton Bank, north east Atlantic. *Facies* 54, 297–316. doi: 10.1007/s10347-008-0140-x

Rooper, C. N., Sigler, M. F., Goddard, P., Malecha, P., Towler, R., Williams, K., et al. (2016). Validation and improvement of species distribution models for structure-forming invertebrates in the eastern Bering Sea with an independent survey. *Mar. Ecol. Prog. Ser.* 551, 117–130. doi: 10.3354/meps11703

Ross, R. E., and Howell, K. L. (2013). Use of predictive habitat modelling to assess the distribution and extent of the current protection of 'listed' deep-sea habitats. *Divers. Distrib.* 19, 433–445. doi: 10.1111/ddi.12010

Rowden, A. A., Anderson, O. F., Georgian, S. E., Bowden, D. A., Clark, M. R., Pallentin, A., et al. (2017). High-resolution habitat suitability models for the conservation and management of vulnerable marine ecosystems on the Louisville Seamount Chain, South Pacific Ocean. *Front. Mar. Sci.* 4:335. doi: 10.3389/fmars.2017.00335

Rowden, A. A., Schlacher, T. A., Williams, A., Clark, M. R., Stewart, R., Althaus, F., et al. (2010). A test of the seamount oasis hypothesis: seamounts support higher epibenthic megafaunal biomass than adjacent slopes. *Mar. Ecol.* 31, 95–106. doi: 10.1111/j.1439-0485.2010.00369.x

Schlining, B., and Jacobsen Stout, N. (2006). "MBARI's video annotation and reference system," in *In: Proceedings of the Marine Technology Society/Institute of Electrical and Electronics Engineers Oceans Conference*, Boston, MA, 1–5.

Tingley, G., and Dunn, M. (eds) (2018). "Global review of orange roughy (Hoplostethus atlanticus), their fisheries, biology and management," in *FAO Fisheries and Aquaculture Technical Paper No.* 622, Rome, 128.

Tittensor, D. P., Baco, A. R., Brewin, P. E., Clark, M. R., Consalvey, M., Hall-Spencer, J., et al. (2009). Predicting global habitat suitability for stony corals on seamounts. *J. Biogeogr.* 36, 1111–1128. doi: 10.1111/j.1365-2699.2008.02062.x

van Oevelen, D., Duineveld, G., Lavaleye, M., Mienis, F., Soetaert, K., and Heip, C. H. R. (2009). The cold-water coral community as a hot spot for carbon cycling on continental margins: a food-web analysis from Rockall Bank (northeast Atlantic). *Limnol. Oceanogr.* 54, 1829–1844. doi: 10.4319/lo.2009.54.6.1829

Vertino, A., Savini, A., Rosso, A., Di Geronimo, I., Mastrototaro, F., Sanfilippo, R., et al. (2010). Benthic habitat characterization and distribution from two representative sites of the deep-water sml coral province (Mediterranean) Deep Sea Research Part II. *Top. Stud. Oceanogr.* 57, 380–396. doi: 10.1016/j.dsr2.2009.08.023

Vierod, A. D. T., Guinotte, J. M., and Davies, A. J. (2014). Predicting the distribution of vulnerable marine ecosystems in the deep sea using presence-background models. *Deep Sea Res. II* 99, 6–18. doi: 10.1016/j.dsr2.2013.06.010

Williams, A., Althaus, F., and Schlacher, T. A. (2015). Towed camera imagery and benthic sled catches provide different views of seamount benthic diversity. *Limnol. Oceanogr. Methods* 13, 62–73.

Williams, A., Schlacher, T. A., Rowden, A. A., Althaus, F., Clark, M. R., Bowden, D. A., et al. (2010). Seamount megabenthic assemblages fail to recover from trawling impacts. *Mar. Ecol.* 31, 183–199. doi: 10.1111/j.1439-0485.2010.00385.x

Conflict of Interest: The authors declare that the research was conducted in the absence of any commercial or financial relationships that could be construed as a potential conflict of interest.

frontiers
in Marine Science

ORIGINAL RESEARCH
published: 23 June 2020
doi: 10.3389/fmars.2020.00457

Ecosystem Functioning Under the Influence of Bottom-Trawling Disturbance: An Experimental Approach and Field Observations From a Continental Slope Area in the West Iberian Margin

***Sofia P. Ramalho*[1,2]*, *Lidia Lins*[2], *Karline Soetaert*[3], *Nikolaos Lampadariou*[4], *Marina R. Cunha*[1], *Ann Vanreusel*[2] and *Ellen Pape*[2]**

[1] Centre for Environmental and Marine Studies, Department of Biology, Universidade de Aveiro, Aveiro, Portugal, [2] Marine Biology Research Group, Department of Biology, Ghent University, Ghent, Belgium, [3] NIOZ Royal Netherlands Institute for Sea Research, Department of Estuarine and Delta Systems, Utrecht University, Utrecht, Netherlands, [4] Hellenic Centre for Marine Research, Institute of Oceanography, Heraklion, Greece

Edited by:
Les Watling,
University of Hawai'i at Mānoa,
United States

Reviewed by:
Ian David Tuck,
National Institute of Water and Atmospheric Research,
New Zealand
Jacobo Martin,
Consejo Nacional de Investigaciones Científicas y Técnicas, Argentina

***Correspondence:**
Sofia P. Ramalho
sramalho@ua.pt

Specialty section:
This article was submitted to Deep-Sea Environments and Ecology, a section of the journal Frontiers in Marine Science

Received: 17 September 2019
Accepted: 22 May 2020
Published: 23 June 2020

Citation:
Ramalho SP, Lins L, Soetaert K, Lampadariou N, Cunha MR, Vanreusel A and Pape E (2020) Ecosystem Functioning Under the Influence of Bottom-Trawling Disturbance: An Experimental Approach and Field Observations From a Continental Slope Area in the West Iberian Margin. Front. Mar. Sci. 7:457. doi: 10.3389/fmars.2020.00457

Understanding the effects of bottom-trawling induced changes in benthic community structure, diversity and ecosystem functioning across different benthic-size components is imperative to determine the future sustainability of bottom-trawling fisheries in deep-sea regions. In this study, we combined field sampling observations with a pulse-chase experiment on sediments obtained from two stations of interest along the West Iberian Margin (WIM) distinguished by different trawling pressures. We compared these two stations in terms of meio- and macrofauna (infauna) standing stocks, biodiversity and several ecosystem function proxies. These proxies included: (i) ^{13}C uptake by bacterial communities, (ii) infauna respiration rates, (iii) penetration of ^{13}C in the sediment, and (iv) sediment pore-water nutrient concentrations. The pulse-chase experimental results were complemented with a larger biological dataset partially compiled from previous studies in the area, to investigate structural and functional diversity ecosystem functioning (respiration) patterns across the WIM. Our observations indicated that different regimes of trawling pressure influenced both macrofaunal respiration rates with disturbed sediments predominantly composed of deposit-/detritus-feeding smaller-sized macrofauna species. Moreover, sediment biogeochemical functioning (ammonium profiles) and ^{13}C bacterial uptake showed differences among the two disturbance regimes. On the contrary, the biomass of small-sized biota, including bacteria and meiofauna, did not show marked differences between stations. The general depletion in macrofauna species richness across impacted areas of the study region was also correlated with a reduction in total biomass and respiration, suggesting that the long history of trawling disturbance at the WIM may affect regulatory ecosystem functions. These preliminary findings alert for the impacts of trawling on crucial functions of benthic ecosystems that may be imperceptible to the current tools used in monitoring programs.

Keywords: bacteria, meiofauna, macrofauna, pulse-chase experiment, bottom-trawling disturbance, deep sea

INTRODUCTION

There is cumulative evidence on the influence of anthropogenic activities on marine biodiversity (Ramirez-Llodra et al., 2011). This includes the deep sea, where exploitation of marine resources has been frequently associated with changes in benthic structure and biodiversity loss (Ramirez-Llodra et al., 2011 and references therein; Vanreusel et al., 2016; Stratmann et al., 2018).

Since biodiversity is potentially linked to ecosystem functions and services (Strong et al., 2015), the increasing pressure of human-induced disturbance raises serious concerns about the deterioration of ecosystem functioning and its integrity (Worm et al., 2006; Danovaro et al., 2008). In marine sediments, benthic organisms are responsible for supporting various ecosystem functions in the sediment, which varies according to their traits (e.g., size, mobility capacity, and feeding strategies). These functions can be either represented by sediment reworking, feeding and respiration activities, that directly/indirectly affect organic material mineralization and by other biogeochemical processes (Aller, 1982; Lohrer et al., 2004; Braeckman et al., 2010). The macrofauna size fraction in particular (animals generally $\geq$ 250 μm to few centimeters) plays a fundamental role in sustaining sediment biogeochemistry fluxes, as well as diversity and efficiency of microbial communities, either through bioturbation (particle mixing), bio-irrigation (solute transfer and sediment permeability; Aller, 1982; Lohrer et al., 2004; Braeckman et al., 2010), and/or through biological interactions (e.g., carbon transfer by predation). Similarly, certain meiofaunal taxa (i.e., Foraminifera, nematodes) also contribute to sediment processes via micro-bioturbation, particularly in the absence of diverse macrofaunal assemblages (Rysgaard et al., 2000; Bonaglia et al., 2014). As such, even small alterations in infauna standing stocks, community structure, diversity and functional traits, may result in changes in oxygen and nutrient penetration depth in the sediment, and affect microbial-mediated processes such as carbon remineralization and nutrient cycling (Aller, 1982; Lohrer et al., 2004; Braeckman et al., 2010).

Among the most destructive anthropogenic activities in the deep sea, bottom-trawling fisheries severely affect benthic organisms and may consequently have an impact on ecosystem functioning (Martín et al., 2014a; Clark et al., 2016; Sciberras et al., 2018). High faunal damage and mortality rates and marked alterations of seabed habitats have been reported in both shelf and deep-sea studies (National Research Council [NRC], 2002; Hiddink et al., 2006; Clark et al., 2016 and references therein). In soft sediments, trawl nets typically homogenize the sediment surface and, depending on trawling frequency and intensity, these may also modify sediment biogeochemistry (Sañé et al., 2013; Oberle et al., 2016). Sediment removal and remixing by trawl gears causes thick nepheloid layers, reduces sediment surface organic matter concentrations and increases sediment sorting and porosity, which inevitably weakens water-sediment nutrient fluxes (Sañé et al., 2013; Martín et al., 2014a,b,c; Oberle et al., 2016). In extreme cases, repeated bottom-trawl fisheries have physically modified entire benthic basins in terms of its composition, texture and morphology (Martín et al., 2014a). Moreover, the induced faunal mortality and alteration of habitat can modify faunal interactions and benthic community structure, and induce biodiversity loss of functionally important benthic components (National Research Council [NRC], 2002; Clark et al., 2016; Ramalho et al., 2018). Noteworthy is that effects of trawling on the benthos appear to vary depending on their size and position in relation to the seabed (infauna/epifauna), with larger-sized fauna, such as mega-epifauna and macro-infauna typically more susceptible to removal or damage by trawl gears (Jennings et al., 2001a,b; Queirós et al., 2006; Clark et al., 2016) by comparison to small-sized biota (e.g., bacteria and meiofauna; Jennings et al., 2001b; Schratzberger et al., 2002; Queirós et al., 2006).

So far, few studies have addressed the structure and diversity of infauna communities in parallel with ecosystem functions in areas affected by bottom trawling (Duplisea et al., 2001; Hiddink et al., 2006; Sciberras et al., 2016, 2017; Hale et al., 2017) and even less so in the deep sea (Pusceddu et al., 2014; Leduc et al., 2016). The study of Ramalho et al. (2017) have examined, the changes in mega-epibenthic assemblages associated with trawling, while the study of Ramalho et al. (2018), investigated changes in diversity in the infaunal component of the sediment, the macrobenthos. Both studies were carried in a continental slope area in the Western Iberian Margin (WIM) that has been subjected to intensive bottom-trawling fisheries for several decades (Leocádio et al., 2012). These studies showed that the main fishing ground area was subject to a decrease of species richness and presented important taxonomic and trophic changes in comparison to undisturbed areas, with a higher prevalence of opportunistic taxa. Moreover, macrofaunal communities in the fishing grounds showed lower trophic redundancy, which likely makes these assemblages functionally vulnerable to further increases in disturbance, as functional (trophic) complexity was sustained by fewer species when compared to undisturbed locations (Ramalho et al., 2018).

Following these studies, the present work aimed to further explore the disturbance influence on the two major components of infauna (macro- and meiofaunal) standing stocks and diversity patterns in concert with several ecosystem functions. Specifically, the first part of the study we aim to determine the existence of a biodiversity-ecosystem functioning relationships [BEF; in the sense of Solan et al. (2004)] across different locations in the SW Iberian margin. The assessment of how biodiversity relates with ecosystem functioning can assist predicting the efficiency and stability of an ecosystem under (anthropogenic) disturbance (Strong et al., 2015). In the second part of the study, we investigated in detail, using an experimental approach, several faunal parameters in relation to bioturbation activity and ecosystem function proxies (i.e., bacterial production and biogeochemical functioning) in two locations fishing ground (FG) and an adjacent area under low trawl pressure (AA).

Overall, we hypothesized that changes in infaunal standing stocks, functional traits (e.g., feeding strategies and mean size) and diversity associated with different trawling disturbance regimes, observed in previous studies, will (i) reduce bioturbation and organic matter processing in the sediment; (ii) lead to a reduction of nutrient fluxes in the sediment, and (iii) these responses will be primarily linked with changes in macrobenthic assemblages rather by meiofauna. Finally, we hypothesize that the decrease of biological diversity across the region will negatively affect secondary productivity in the fishing ground.

MATERIALS AND METHODS

Study Area

The West Iberian continental margin (WIM) presents complex and diverse geomorphological features (Relvas et al., 2007; Maestro et al., 2013), such as submarine canyons and rocky outcrops. These features interact with several water masses and fronts, determining its spatial and temporal variability in salinity, temperature and oxygen content (Relvas et al., 2007).

Under the influence of the Iberian upwelling system, the high seasonal primary production along the WIM (associated with upwelling) determines productive fisheries' conditions (Santos, 2001; Picado et al., 2014; Kämpf and Chapman, 2016). Specifically, the south and southwest regions off Portugal are among the most disturbed in Europe by bottom-contact trawling fisheries (Eigaard et al., 2016), where the majority (93.6%) of the seabed between 200 and 1000 m water depth being disturbed at least once a year. Furthermore, these fisheries are also associated with an enormous footprint per unit of landings (ca. 17 km^{-2} t^{-1}; Eigaard et al., 2016), and high by-catch and discard rates (ca. 40 − 70%; Borges et al., 2001; Monteiro et al., 2001).

Sampling Strategy and Onboard Sample Processing

During the RV Belgica cruises B2013/17 (10/06/2013–18/06/2013) and B2014/15 (02/06/2014–10/06/2014), a total of seven stations were sampled along the upper continental slope off Sines and near the Setúbal Canyon (ca. 250 − 550 m depth) for the analysis of sediment environmental parameters, and meiofauna and macrofauna assemblages, in areas subjected to varying trawling pressure (**Figure 1** and **Supplementary Tables 1, 2**). Sampling stations were initially selected based on trawling pressure information obtained from Vessel monitoring systems (VMS) data compiled by the Direção Geral de Recursos Marinhos − DGRM (MAMAOT, 2012) and as in Bueno-Pardo et al. (2017). Estimation of the pressure induced by trawling fisheries to the seabed surface is here expressed as surface swept area ratio (grid cell 0.05 × 0.05 degrees). Swept area ratio values were obtained from the OSPAR Data & Information Management system database for both 2013 and 2014 (**Figure 1**; OSPAR Data & Information Management System database, 2020). This, together with the visual assessment of the seabed conditions (i.e., presence and condition of the trawl scars; Ramalho et al., 2017) allowed us to confidently allocate each station to one of the following categories: not trawled (NT), an adjacent area to the main fishing ground (AA) and the fishing ground (FG). The NT label was only assigned to the stations safeguarded by current legal restrictions and where trawling has not occurred for the past decades (st. 9 and st. 10 in the vicinity of the Setúbal canyon head; null swept area ratio). The adjacent area (AA) stations correspond to those that have been either undisturbed or subjected to very few trawl passages in time and space (st. 2 and st. 6; swept area ratio ranging between 0.32 and 0.93), but are adjacent to the main fishing ground (**Figures 1B,C**). This AA area presented overall very few and mostly eroded trawl scars during ROV video surveys (Ramalho et al., 2017). Fishing ground (FG) stations were located in the area where crustacean otter trawlers are typically fishing (st. 1, st. 4, and st. 7; swept area ratio ≥ 1.5) and video surveys detected a high number of apparently recent trawl scars on the seabed (**Figures 1B,C**; Ramalho et al., 2017).

In each station three replicate samples were collected for environmental and meiofauna analysis with a multicorer (MUC, Ø 10 cm), whereas those for macrofauna analysis were collected with a NIOZ box corer (Ø 32 cm; **Supplementary Tables 1, 2**). Meiofauna and environmental samples were sliced every centimeter down to 10 cm depth and preserved in borax-buffered 4% formalin and frozen at −20°C, respectively. Macrofauna samples were initially processed by collecting the small fraction of water on the surface of each core and sieve it through a 250 μm mesh. Then the sediment was subsampled at three depth layers (0−1, 1−5, and 5−15 cm). To facilitate sediment washing and sorting procedure, each layer was washed onboard through a set of 1 mm, 500 μm and 250 μm sieves and fixed with 96% ethanol. Amongst the seven stations surveyed, two (st. 6 and st. 7) were selected for the collection of additional MUC cores in order to perform an onboard pulse-chase experiment to explore ecosystem function aspects in comparable sites at different levels of trawling pressure (see section "Time-Series Isotope Enrichment Experiment"). This selection was determined by the fact that these were the only two stations with a similar environmental setting [depth and sediment composition, being muddy-sand sediments (Instituto Hidrográfico, 2005a,b)], but different trawling pressure regimes (with swept area ratio of 0.9 and 1.5 for the st. 6 and st. 7, respectively, for the year of 2014). Even though we recognize the importance of including a true control (NT) in our experimental set up, due to differences in depth and grain-size differences with the main fishing ground/adjacent areas, this undisturbed location could not be included.

Field Sample Analyses

Environmental Variables

Sediment environmental characterization analyses included sediment grain size, total organic carbon and total nitrogen content, obtained from Lins et al. (2017); Ramalho et al. (2018) for all sampled stations (**Supplementary Tables 1, 2**). Grain-size distribution was determined using a particle size analyzer Malvern Mastersizer 2000, with a particle size range of 0.02–2000 μm and then classified into five categories following the Wenthworth (1922) scale: silt + clay (<63 μm), very fine sand (63 – 125 μm), fine sand (125 − 250 μm), medium sand (250 – 500 μm), and coarse sand (500 μm − 2 mm). Total organic carbon (TOC) and total nitrogen (TN), expressed as percentage of sediment dry weight, were measured using a Carlo Erba25 elemental analyzer, after acidification with 1% HCl to eliminate carbonates.

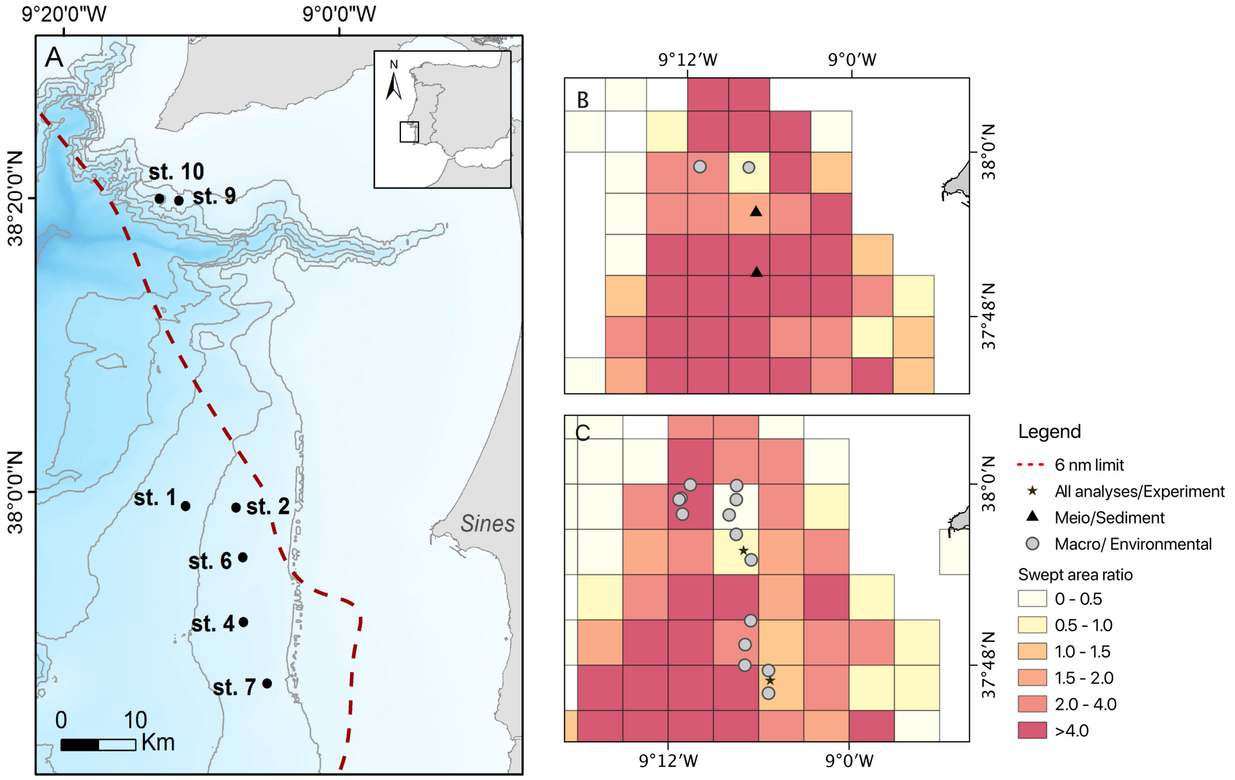

FIGURE 1 | (A) Study area with an indication of all sampled stations and their position in relation to bottom trawling surface swept area ratio for panels **(B)** 2013 and **(C)** 2014, with the corresponding analysis: meiofauna, macrofauna and environmental parameters (sediment) or pulse-chase experiment. The Setúbal canyon area (st. 9 and st. 10) was only sampled for macrofauna and environmental parameters; bottom trawling surface swept area ratio for these stations are not shown here due to null trawling pressure values (NT). Surface swept area data was compiled from the OSPAR Data & Information Management system database (grid cell 0.05 × 0.05 degrees). Bathymetry data obtained from EMODNet Bathymetry database (2017). The red dashed line denotes the six nautical miles limit from the coastline, where trawling activities are legally prohibited.

Macro- and Meiofaunal Community Analyses

Both meiofauna and macrofauna composition data were collected from the Lins et al. (2017), Ramalho et al. (2018), respectively.

In summary, sediments retained in between 32 and 1000-µm sieves, were centrifuged using colloidal silica polymer LUDOX HS-40 (specific gravity 1.19) for extraction of meiofauna organisms. This dataset, included total abundances of exclusively metazoan meiobenthic organisms classified following Higgins and Thiel (1988), Giere (2009). In addition, a list of the nematode genera abundance was also provided from the sediment surface slice (0−1 cm), estimated from a randomly picked subset of 100 to 120 nematodes mounted on permanent slides (or all nematodes when abundances were lower than 120 per sample). Deeper sediment layer were not analyzed in terms of nematode genera identification due to laboratory time restrictions. The nematodes were identified to genus level using the pictorial keys provided by Platt and Warwick (1983, 1988), online identification keys and other relevant literature available in the Nemys Database (Guilini et al., 2016[1]). Each nematode genus was allocated to a matching trophic group, following the Wieser (1953) classification: selective deposit feeders (1A), non-selective deposit feeders (1B), epistratum feeders (2A), and predators/scavengers (2B).

Macrofauna (≥250 µm; Gage et al., 2002) individuals were sorted and identified to the lowest taxonomical level possible, and in the cases where a match with a species name was not possible; each taxon was ascribed with a consistent code across all sampled stations. To avoid overlap in the faunal size-groups investigated, "typical" meiofauna taxa, i.e., Nematoda, Copepoda and Ostracoda, were excluded from this dataset. Each taxon was assigned to a matching trophic guild according to its food source (or foraging behavior), feeding mode and food type/size, following the classification proposed by Macdonald et al. (2010) and other relevant literature available (e.g., Fauchald and Jumars, 1979; Jumars et al., 2015). The following categories were considered for: (a) food source: epibenthic (EP), sediment surface (SR), and sediment subsurface (SS); (b) feeding mode: omnivorous (Om), deposit feeders (De), detritus feeders (Dt), grazers (Gr), scavengers (Sc), predators (Pr), suspension/filter feeders (Su), mixotrophs (Mx) and suctorial parasites (Sp); and (c) food type/size: sediment (sed), particulate organic matter (poc) microfauna (mic), meiofauna (mei), macrofauna (mac), zooplankton (zoo), and fish (fis).

---

[1] http://nemys.ugent.be

Biomass

Nematode biomass measured in this study was determined for a subsample of 100−120 individuals per sediment layer. Individual nematode length [excluding filiform tail tips; L (μm)] and maximum body width [W (μm)] was measured under the compound microscope (Olympus BX-50) with Olympus Cellˆ D software, and body volume estimated by applying Andrassy's formula (wet weight; Andrassy, 1956; Wieser, 1960). A ratio of a 0.124 was assumed to convert nematode wet weight into carbon weight (μgC; Baguley et al., 2004).

Macrofauna biomass data obtained from Ramalho et al. (2018), as wet weight (mg) grouped by specimens of the same family for sample and each sediment layer (0−1; 1−5; and 5−15 cm), was converted into carbon weight (mgC) following the taxa-specific conversion factors of Rowe (1983). Due to their small values, macrofaunal wet weights were measured by transferring all individuals belonging to the same family in each sub-sample to previously weighed microtubes containing 96% ethanol that were then weighed again to obtain the wet weight of the lot.

Individual mean biomass was calculated as the weight of the taxon group divided by the number of individuals counted, while total biomass was calculated as the sum of the products of individual biomass and abundance of each taxon. Total biomass for meio- and macrofauna were expressed as mg $C.m^{-2}$.

Allometric Respiration Rates

Allometric respiration estimates were calculated for both nematode (meiofauna) and macrofauna assemblages following Mahaut's formula (Mahaut et al., 1995). The mass dependent respiration rate (R, d^{-1}) was calculated as:

$$R=a \times W^b,$$

where W is the mean individual biomass (in mg C), and the constant $\alpha=7.4 \times 10^{-3}$ and $b=-0.24$. Total community respiration of both meiofaunal and macrofaunal assemblages was calculated as the product of the mass-dependent respiration rate (R) and total biomass (in $mgC.m^{-2}$), expressed as $mgC.m^{-2}.d^{-1}$.

Time-Series Isotope Enrichment Experiment

Experimental Set-Up

In addition to field sampling, a pulse-chase experiment was performed during the B2014/15 cruise, aiming to measure bioturbation and different proxies of ecosystem functioning at three distinct time points: at the start of the experiment (T0), after 3 (T3), and 5 (T5) days. The end of the experiment (T5) was determined by the ship time available, and T3 was considered as a mid-point observation. Sediments were collected from two 300-m deep stations that exhibited distinct trawling disturbance regimes, i.e., st. 6 (AA) and st. 7 (FG; **Figure 1**), but similar environmental setting (muddy-sand sediments), initially established from detailed sediment charts from Instituto Hidrográfico (2005a,b). By choosing two areas with similar environmental characteristics we attempted to attenuate the influence of important environmental conditions on our observations (e.g., grain size, permeability and food availability), known to strongly shape deep-sea infauna assemblages, as well as oxygen and nutrient fluxes in the sediment (Levin et al., 2001; Glud, 2008). Furthermore, even though we recognize the importance of including an area close to pristine conditions and legally protected (NT) in the experimental set up, due to differences in depth and grain-size differences with the main fishing ground, this could not be included in the experimental set-up.

In total, 18 MUC cores were collected: nine at each station (AA and FG) with three replicates at each time point (**Supplementary Table 2**). The cores were maintained in a cold room in the dark for 24h at *in situ* water temperature, i.e., 12°C, and constant oxygen flow provided by aquarium pumps. After acclimatization, each core was randomly assigned to a distinct sampling time step (n = 3 for T0, T3, and T5) and, except for the cores assigned to T0 that were used as controls, a suspension of ^{13}C labeled algae (*Skeletonema costatum*) was added homogeneously to the sediment surface of each core with a long pipette (ca. 2.6 mg C per core; 26% of ^{13}C enrichment). *S. costatum* was chosen because it is a common diatom species in phytoplankton assemblages throughout the year along the Iberian Margin (Silva et al., 2009). At each time step, the selected cores from each trawl pressure group were sliced per centimeter down to 10 cm, and subsampled for the analysis of: ^{13}C uptake by sedimentary total organic carbon (ca. 2 ml), ^{13}C uptake by bacteria-specific phospholipid-derived fatty acids (PLFAs) (ca. 10 ml), and pore-water nutrients concentrations (remaining sediment for both ammonium and nitrate concentrations). Sub-samples for pore-water nutrient concentrations were stored at −20°C, while the remaining sub-samples were stored at −80°C for further laboratory analysis. Bacterial biomass from the T0 samples was used in conjunction with meio- and macrofaunal biomass to compare infaunal standing stocks between AA and FG (only possible for the surface layer 0−1 cm).

Assessment of Biogeochemical Functioning, Bioturbation and Bacterial Biomass and Production

The pore-water dissolved inorganic nitrogen concentrations, specifically ammonium and nitrate concentrations (expressed as $\mu mol.l^{-1}$), were investigated along the vertical sediment profile (down to 10 cm), as a proxy for biogeochemical functioning. Changes in these nutrients concentrations within the sediment column can indirectly indicate changes in bioirrigation and bioturbation, as well as carbon remineralization processes (Lohrer et al., 2004; Volkenborn et al., 2007). The pore-water was extracted from each sub-sample through Whatman GF/C filters and analyzed using a continuous flow analyzer the SKALAR SAN.

Bioturbation was inferred from ^{13}C incorporation in the sediment. Each sediment sub-sample was first freeze-dried and grinded. Quantification of organic carbon content and isotopic ratios were then carried out using a Thermo Flash EA 1112 element analyzer, coupled with a Thermo Delta V Advantage Isotopic mass spectrometer (Thermo Fisher scientific). Due to laboratory and analysis constraints, ^{13}C labeled algae content in the sediment and corresponding total organic carbon and total nitrogen values in the experimental cores were only measured down to 5 cm depth.

Bacteria ^{13}C algae uptake (production) and biomass were derived from the concentrations of bacteria-specific phospholipid-derived fatty acids PLFA's, for the layers 0−1 cm and 4−5 cm as described by van Oevelen et al. (2006). The polar lipid fraction was extracted from the freeze-dried and grinded sediments and derivatized using the mild alkaline methanolysis to yield fatty acid methyl esters (FAMEs), following the Bligh and Dyer method (Bligh and Dyer, 1959; Boschker, 2004). ^{13}C concentrations of this component were analyzed with a gas chromatography combustion interface isotope-ratio mass spectrometer (GC-C-IRMS). Due to laboratory and analysis constraints we analyzed only 0−1 and 4−5 cm for comparison. The bacteria-specific PLFAs used included the i14:0 and ai15:0, present in all of our samples, and accounted roughly for 8% of all bacterial PLFAs (Middelburg et al., 2000) and 5.6% of the total carbon content in bacterial cells (Brinch-Iversen and King, 1990), allowing for the estimation of total bacterial biomass.

Data Analyses

BEF Relationships Under Different Trawling Regimes at the WIM

Correlations between structural diversity and ecosystem functions (i.e., respiration rate and total respiration) for the whole meio- and macrofauna field dataset (both B2013/17 and B2014/15 campaigns), was explored by means of non-parametric Spearman rank correlations using the software GraphPad PRISM v6. Similar procedure was applied for analyzing the relationship between ecosystem functions (i.e., respiration rate and total respiration) and trawling pressure (swept area ratio). Significant *p*-Values were adjusted for multiple testing using the Bonferroni correction (Shaffer, 1995), by dividing the significance value of each test by the number of hypotheses tested. Biodiversity indices for all seven stations were calculated using the software PRIMER v6 (Clarke and Gorley, 2006).

Comparison Between the Highly Disturbed and Low Disturbed Stations (FG and AA)

The biological and environmental data from the field samples collected at the same time and location as the samples for the pulse-chase experiment (B2014/15; st. 6 and st. 7, from here on designated as the AA and FG stations, respectively), were tested for differences by means of non-parametric Mann-Whitney *U*-tests, after rejection of normality and homogeneity of dispersion (Quinn and Keough, 2002), using the software GraphPad PRISM v6. The environmental parameters tested for the surface (0−1 cm) and sub-surface (4−5 cm) by means of non-parametric Mann-Whitney *U*-tests included: grain-size, porosity, total organic carbon (TOC) and total nitrogen (TN). Biological parameters were only compared from the surface layer (0−1 cm), and included total bacterial biomass, meio- and macrofaunal abundance, meio- and macrofaunal mean individual biomass/total biomass and meio- and macrofaunal respiration rate/total respiration. Note that comparisons for the deeper layers (>1 cm) were not done here due to the absence of consistent data for all benthic size-groups for the different sediment depth layers. Nematodes were the dominant meiofaunal taxon (68−90%), and thus with "meiofauna" diversity and biomass, we are only referring to the nematodes. Taxonomic and functional (trophic) biodiversity patterns were also analyzed for meio- and macrofauna for both stations (AA and FG) using several diversity indices, namely: species or genus richness/trophic guilds richness (S/TG), Shannon-Wiener diversity (H'), evenness (J') (Pielou, 1966) and Hurlbert's expected number of taxa or trophic guilds ($ES_{(n)}/ETG_{(n)}$) for 20 individuals (Hurlbert, 1971). These biodiversity indices were calculated using the software PRIMER v6 (Clarke and Gorley, 2006), and were also tested for differences between stations by means of non-parametric Mann-Whitney *U*-tests, using GraphPad PRISM v6.

Ecosystem functions investigated during the enrichment experiment included: biogeochemical functioning (by assessing vertical profiles of pore-water ammonium and nitrate), bioturbation (^{13}C sediment uptake) and bacterial production (^{13}C bacterial uptake). These variables were tested separately for differences between stations subjected to distinct trawling pressures ["Station(TP)"] over time ("Time") and accounting for sediment depth dependency ("Sediment depth"), by means of a permutational multivariance analysis of variance (PERMANOVA) using PRIMER v6 and the PERMANOVA + add-on (Clarke and Gorley, 2006; Anderson et al., 2008). These tests were applied on a Euclidean distance matrix after normalization of the dataset. The PERMANOVA design followed a 4-factor layout, with "Station (TP)" as a fixed factor (levels: AA and FG); "Time" as a fixed factor [levels: T0 (only for ammonium/nitrate concentrations), T3, T5]; "Sediment depth" as a fixed factor (levels: every cm down to 10 cm for biogeochemical functioning, and 0−1 and 4−5 cm for the other variables), and "replicate core" as a random factor nested in "Station (TP) × Time." This design allowed to account for the dependency of the depth layers within each replicate. When a statistically significant effect ($p \leq 0.05$) was found for any of the factors investigated in the PERMANOVA main test, pair-wise pseudo-*t*-tests were subsequently performed. Homogeneity of multivariate dispersions was also tested using the PERMDISP routine, but none of the factors identified by the PERMANOVA tests showed a significant dispersion effect. Corresponding total organic carbon and nitrogen content in the experimental cores down to 5 cm were also investigated using similar statistical analyses.

RESULTS

BEF Relationships Under Different Trawling Regimes at the WIM

We identified significant negative correlations, after Bonferroni correction, between trawling pressure and macrofauna total respiration ($R = -0.512$; $p \leq 0.01$; **Figure 2F**), and total macrofauna biomass ($R = -0.514$; $p \leq 0.01$; **Figure 2B**), while respiration rates were positively correlated with trawling pressure ($R = 0.363$; $p \leq 0.01$; **Figure 2D**). Note that between trawling pressure and different measures of meiofauna/nematode

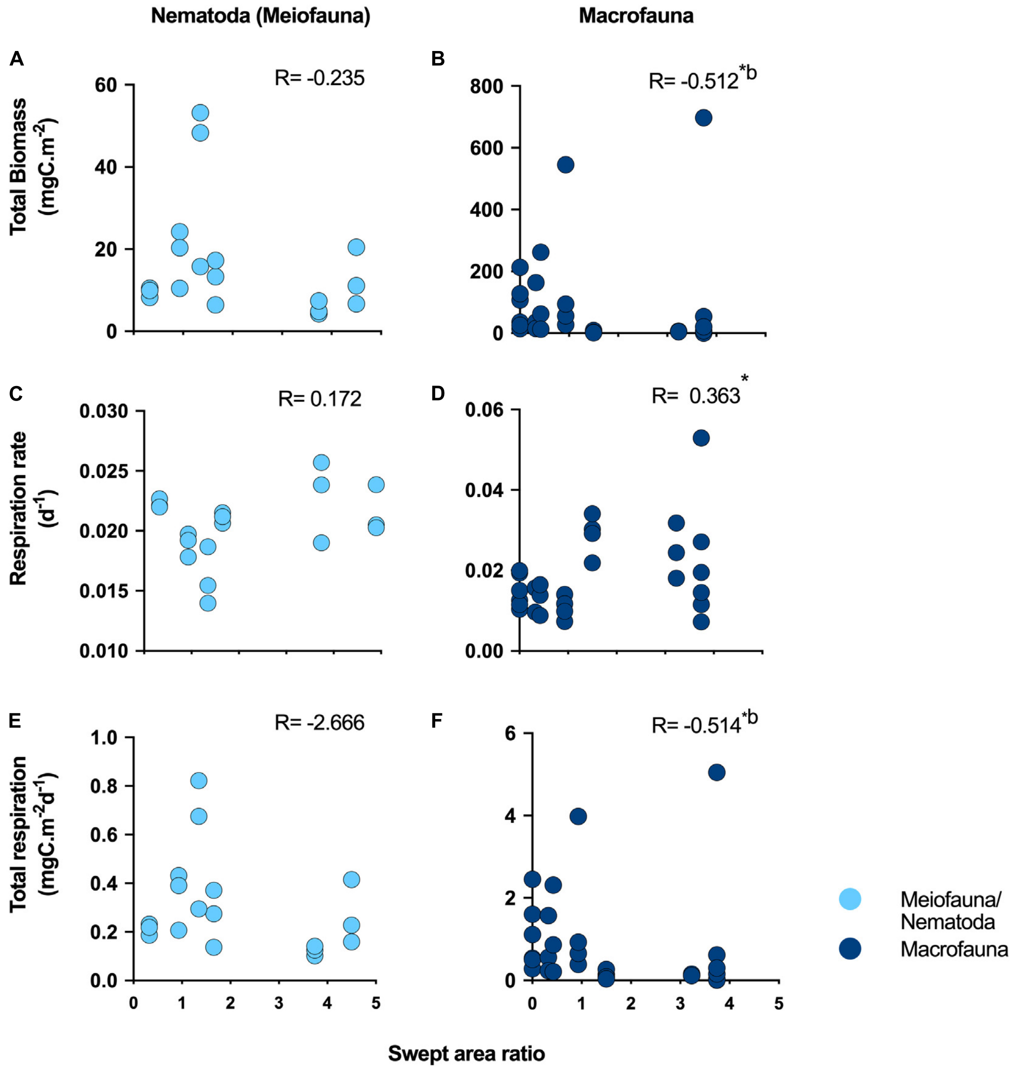

FIGURE 2 | Ecosystem functioning relationship with bottom trawling surface swept area ratio. Ecosystem functions investigated included **(A,B)** total biomass; **(C,D)** respiration rate and **(E,F)** total respiration on the sediment surface (0–1 cm) for Nematoda (meiofauna) and macrofauna, respectively. *Indicates statistically significant correlations; ^{b}indicates statistical significance after Bonferroni correction.

abundance and diversity no significant correlations were detected (**Supplementary Figure 1**), nor between trawling pressure and nematode respiration rates and total respiration (**Figures 2A,C,E**).

Macrofauna BEF relationships investigated through correlations between species richness and ecosystem metabolism proxies (respiration rates and total respiration) were only significant (positive) for total respiration ($R = 0.433$; $p \leq 0.05$) (**Table 1**). Significant positive correlations were also identified between macrofauna species richness and biomass ($R = 0.030$; $p \leq 0.05$; **Table 1**). (Negative) BEF correlations for meiofauna were identified between nematode genus richness and respiration rates ($R = -0.683$, $p \leq 0.01$), however, only within FG stations (**Supplementary Table 3**).

Significant positive relationships after Bonferroni corrections were identified between macrofauna species richness and trophic (functional) diversity ($R = 0.754$; $p \leq 0.01$; **Table 1**). Specifically, predator-feeding guilds were positively linked with species richness ($R = 0.732$; $p \leq 0.01$; **Table 1**), despite the comparable relative contribution of these feeding guilds to the macrofauna trophic structure among all stations (**Table 1**).

Comparison Between the Highly Disturbed and Low Disturbed Stations (FG and AA)

Environmental Parameters

Generally, similar environmental conditions were observed at the two stations sampled for the pulse-chase experiment (AA and FG) in both the surface (0−1 cm) and sub- surface layers (4−5 cm; **Table 2**). Overall, sediments were characterized as muddy-sand (silt + clay content > 10%) composed of high

TABLE 1 | Overview of the non-parametric Spearman-rank correlations results for macrofauna species richness and macrofauna biomass, macrofauna associated ecosystem function (respiration), and functional (trophic) diversity.

		Macrofauna species richness	
		Spearman R	***P*-value**
Macrofauna Respiration rate	NT	0.086	0.919
	AA	−0.104	0.750
	FG	−0.002	0.991
	ALL	−0.171	0.366
Macrofauna Total respiration	NT	0.543	0.297
	AA	0.214	0.550
	FG	0.442	0.114
	ALL	0.433	**0.017**
Macrofauna Total biomass	NT	0.543	0.297
	AA	0.214	0.550
	FG	0.372	0.190
	ALL	0.030	**0.030**
Macrofauna Trophic diversity	NT	−0.577	0.190
	AA	0.680	**0.036**
	FG	0.764	**0.002**
	ALL	0.754	**<0.0001**[b]
Macrofauna Predator diversity	NT	0.820	0.067
	AA	0.545	0.105
	FG	0.612	**0.022**
	ALL	0.732	**<0.0001**[b]

Trawling pressure categories include: NT, not trawled; AA, adjacent area to the fishing ground; FG, fishing ground. Bold values denote significant results. [b]*indicates significance after Bonferroni correction.*

TABLE 2 | Overview of the sediment environmental characteristics (average ± standard error) at the fishing ground (FG) and its adjacent area (AA) stations in the sediment surface (0−1) and subsurface layers (4−5) cm.

Environmental Variables	**AA (st. 6)**		**FG (st. 7)**	
	0−1 cm	**4−5 cm**	**0−1 cm**	**4−5 cm**
Silt + Clay (%)	10.2 ± 2.02	12.9 ± 2.88	15.7 ± 1.24	17.4 ± 2.17
Very Fine Sand (%)	16.5 ± 2.49	17.2 ± 0.93	13.6 ± 1.62	14.1 ± 1.32
Fine Sand (%)	38.2 ± 0.56	35.8 ± 0.46	25.2 ± 0.60	25.3 ± 0.93
Medium Sand (%)	29.2 ± 2.64	27.3 ± 1.47	30.3 ± 2.41	29.1 ± 3.11
Coase sand (%)	5.9 ± 2.43	6.8 ± 1.88	15.2 ± 1.04	14.0 ± 0.55
Porosity	0.53 ± 0.002	0.49 ± 0.002	0.54 ± 0.070	0.48 ± 0.006
TOC (%)	0.42 ± 0.011	0.50 ± 0.039	0.38 ± 0.081	0.40 ± 0.027
TN (%)	0.05 ± 0.026	0.06 ± 0.017	0.04 ± 0.010	0.05 ± 0.007

proportions of both very fine and fine sand content (ca. 40−55%), with no significant differences in terms of sediment porosity for either the surface layer ($U = 3$; $p > 0.99$) and sub-surface ($U = 2$; $p > 0.80$). TOC and TN concentrations were also similar in both stations, both at surface ($U = 2$; $p > 0.80$ and $U = 2$; $p > 0.80$) and sub-surface layers ($U = 0$; $p > 0.20$ and $U = 1$; $p > 0.40$).

Infaunal Standing Stock, Diversity, and Trophic Composition

The infauna (meio- and macrofauna combined) showed consistently higher abundances in the 0−1 cm layer at FG (st. 7) than at AA (st. 6; **Figure 3A**). Total macrofauna abundances were 672 ± 194.7 and 1035 ± 145.9 ind.m^{-2} at the AA and FG station, respectively, and differed significantly ($U = 0$; $p \leq 0.05$). Meiofauna was typified by the dominance of nematodes (68−90%) and total abundances found in the AA and FG station, respectively, were 39367 ± 5948.8 and 49070 ± 7656.6 ind.m^{-2}. No significant differences among stations were found for meiofauna total abundances ($U = 1$; $p > 0.05$).

Unlike abundance, benthic biomass showed contrasting trends between stations, dependent of the size group. Overall, bacteria were the main contributor to total biomass at both stations (**Figure 3B**), with a higher average contribution at FG (91%) than at AA (67%), although not significantly different ($U = 1$; $p > 0.05$). Nematoda (meiofauna) was identified as the second most important contributor to total benthic biomass at FG with larger nematode genera, while macrofauna relative contribution prevailed over meiofauna at AA (macrofauna ca. 30% at AA vs. 1% at FG). Macrofauna biomass was significantly different between these stations ($U = 0$; $p \leq 0.05$; **Figure 3B**), associated with a much higher mean individual weight at the sediment surface (0−1 cm) of AA (st. 6; 0.34 ± 0.227 mgC; **Figure 3C**).

Macrofauna and nematode biodiversity indices did not differ significantly between the AA and FG stations ($p > 0.05$), with the exception of macrofauna ETG$_{(20)}$ ($U = 0$; $p \leq 0.05$), which indicated a higher trophic (functional) diversity at AA when compared to FG (**Table 1**). Macrofauna trophic structure was more complex (**Supplementary Figure 2B**) in the AA sediments. This resulted from relatively even contributions of the various trophic groups that comprised the macrofaunal assemblages at AA station. At the AA station, the relative contribution of deposit and detritus feeders (37%) was highest, followed of predators (23%), suspension feeders (16%), omnivores (8%), and gazers (5%; **Supplementary Figure 2B**). The FG station was characterized by a larger contribution of both surface and subsurface deposit and detritus feeders (56%). Nematode trophic composition at AA was also composed by lower contributions of Wieser (1953) equivalent to deposit/detritus feeding guilds (1A + 1B; 41%) when compared to FG (53%; **Supplementary Figure 2A**).

Ecosystem Functions

Total nematode respiration estimates varied between 0.34 ± 0.069 and 0.59 ± 0.111 mgC.10 m^{-2}d^{-1} in AA and FG sediments, respectively, not differing significantly ($U = 2$; $p > 0.05$; **Figure 3D**). Total respiration estimates for the macrofauna assemblages showed significantly higher values ($U = 0$; $p \leq 0.05$) in AA (1.49 ± 1.676 mgC.m^{-2}d^{-1}) than in FG sediments (0.13 ± 0.098 mgC.m^{-2}d^{-1}) (**Figure 3D**).

Biogeochemical functioning, investigated through pore-water nutrient concentrations, showed marginally significant higher concentration of ammonium in FG ($F = 5.3926$; $p = 0.0485$). Ammonium concentrations increased with depth

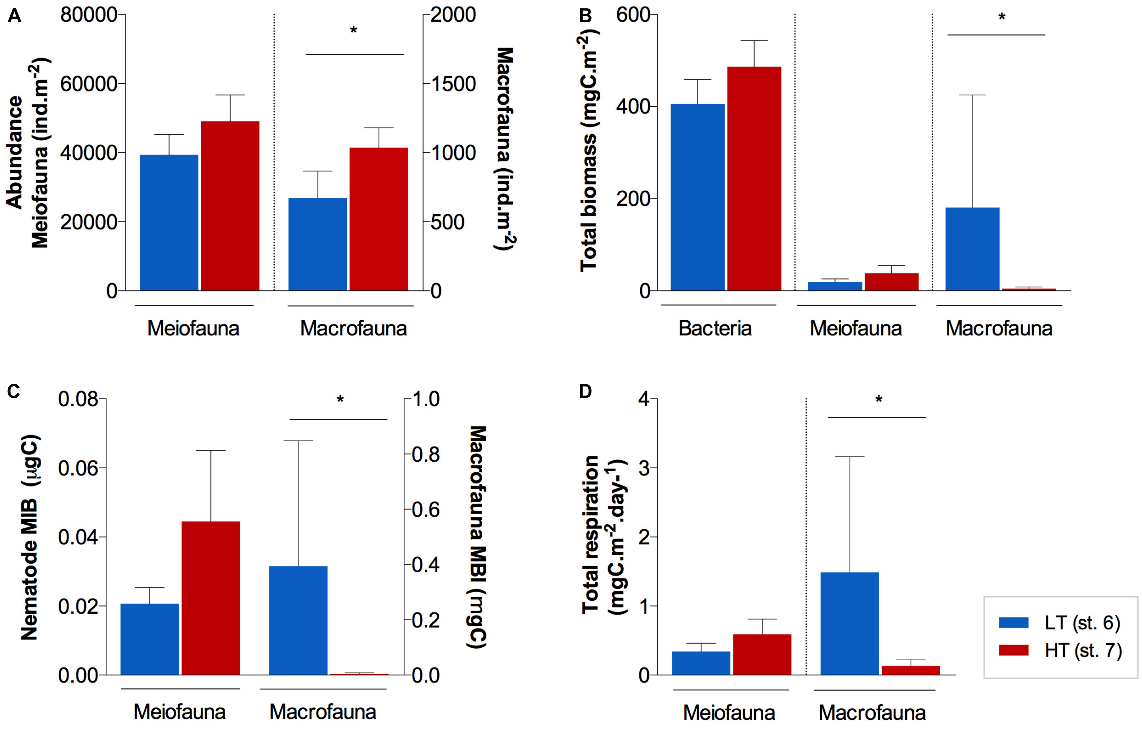

FIGURE 3 | Average (±standard error) benthic **(A)** abundances, **(B)** biomass, **(C)** mean individual biomass (MIB), and **(D)** total respiration for all size groups (bacteria, meiofauna and macrofauna) at the surface of the sediments (0–1 cm) of station AA and FG. Note that for bacteria, only biomass measurements were available. *Indicates significant differences between stations ($p \leq 0.05$).

($F = 27.609$; $p \leq 0.01$); with the increase in ammonium concentrations in sediment layers deeper than 5 cm relative to the surface and subsurface layers (0 – 4 cm; **Supplementary Tables 4, 5**), within the first 3 days of experiment (**Figures 4A,B**). Ammonium profiles were similar after 5 days in both AA and FG stations (**Figure 4C**). Pore-water nitrate concentrations significantly decreased below 3 cm depth, but no significant differences were detected between the profiles of the two studied stations for the whole experiment duration (**Figures 4D–F** and **Supplementary Tables 6, 7**).

The ^{13}C labeled algae added were detected within the first 3 days of the experiment down to 3—4 cm sediment depth. After 5 days, the ^{13}C labeled algae signal was detected in both AA and FG down to the deepest sediment layer investigated (4—5 cm), yet no significant differences were detected between the two stations ($F = 0.505$; $p > 0.05$). Significant differences were found between the sediment depth layers ($F = 68.702$; $p \leq 0.01$) over time ($F = 5.549$; $p \leq 0.05$) associated with evident transport of the ^{13}C labeled algae to the deeper layer over the course of the experiment (**Figures 5A,B** and **Supplementary Tables 8, 9**). FG sediments showed overall significantly higher concentrations of organic carbon (%) in the sediment surface layers over the course of the experiment (**Supplementary Figure 3** and **Supplementary Tables 10, 11**), while nitrogen concentrations were more variable among replicates (**Supplementary Tables 12, 13**).

The average uptake of the ^{13}C labeled algae by bacteria (bacterial production) showed significant differences between stations with different trawling pressure and sediment depths (interaction of both factors; $F = 9.777$; $p \leq 0.05$; **Supplementary Table 14**), mostly due to higher uptake in the surface layer (0—1 cm; pair-wise test $t = 2.957$; $p \leq 0.05$; **Supplementary Table 15**). The higher bacterial uptake was consistently observed at the AA station after both 3 and 5 days (**Figures 5C,D**).

DISCUSSION

Bottom trawling activities are effectively associated with the deterioration of the seabed integrity, not only by altering topography, substrate structure, but also by causing both direct and indirect changes on the benthic assemblages (Martín et al., 2014a; Clark et al., 2016). As a consequence of this activity, changes in taxonomic and functional diversity (e.g., Duplisea et al., 2001; National Research Council [NRC], 2002; Lohrer et al., 2004) may occur, leading to altered ecosystem functions in the sediment. Our primary goal in this study was to investigate how changes in both meio- and macrofauna standing stocks diversity and traits (feeding preferences, size-spectra) are related to sediment ecosystem functions in areas subjected to different trawling pressure regimes. To our knowledge, trawling pressure on benthic processes has received little attention in

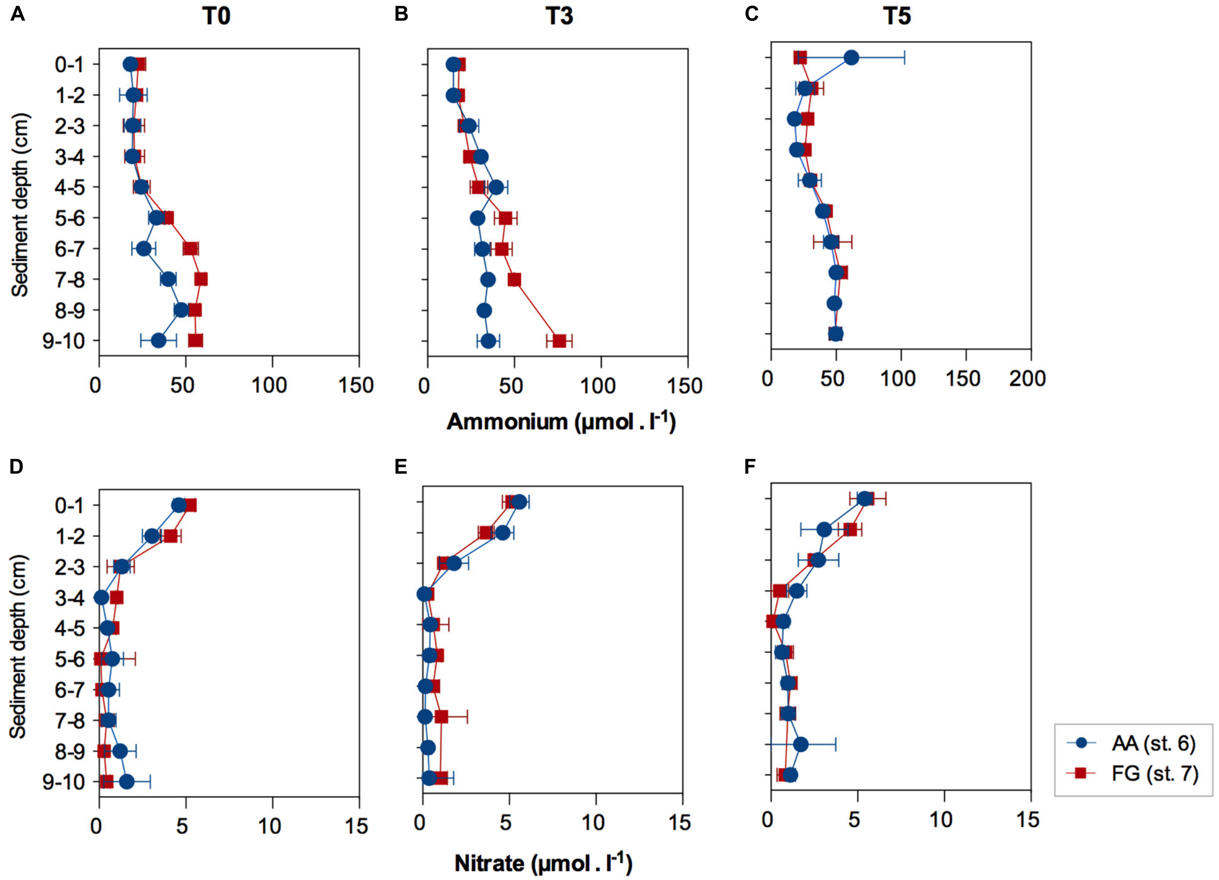

FIGURE 4 | Pore-water ammonium and nitrate concentrations (average ± standard error) in function of sediment depth at the AA and FG stations, after **(A,D)** acclimatization (T0), **(B,E)** three (T3) and **(C,F)** five (T5) days. Values expressed as average ± standard error.

the deep sea, such as the Western Iberian margin (WIM), where trawling is known to impose an enormous pressure on benthic habitats (Eigaard et al., 2016). In the context of the European Union's Marine Strategy Framework Directive 2008/56/EC (MSFD, European Commission, 2008) the existing assessment of Good Environmental Status (GES) have a low degree of confidence, and is hindered by the limited availability of data (MAMAOT, 2012), including for key descriptors, such as descriptor 1 (biodiversity is maintained) and descriptor 6 (seafloor integrity insures functioning of the ecosystems) (European Commission, 2008).

Diversity and Ecosystem Function Trends Across the WIM

General diversity trends investigated in field samples (Lins et al., 2017; Ramalho et al., 2018) allowed us to account for the spatial heterogeneity beyond the two stations investigated during the pulse-chase experiment. Overall there was a general decrease in species richness with increasing trawling pressure for macrofaunal assemblages (Ramalho et al., 2018), but not for meiofaunal genus richness. This cannot be interpreted as a non-detrimental influence of trawling pressure on nematode diversity, since unlike the macrofauna, nematodes were not identified down to species level, and also because the metrics investigated may not be sensitive enough to detect effects on nematode assemblages. However, as nematode biodiversity showed no correlation with increasing trawling pressure, further interpretation of the BEF relationship (even if absent) cannot assist predicting nematode-related ecosystem functioning alterations under trawling disturbance conditions in the present study.

Regarding macrofauna assemblages, the highly disturbed locations showed overall a decrease in biomass with increasing trawling pressure, which suggests that the shift in the benthos size structure under conditions of high disturbance may be consistent across the study region. Furthermore, we identified significant positive correlations between macrofauna species richness and total biomass and respiration, and with trophic (functional) diversity, where both NT and AA displayed consistently the highest functional diversity, including predator richness. Baldrighi and Manini (2015), Baldrighi et al. (2017), found similar positive correlations (both linear and exponential) between biodiversity and functions related to macrofaunal assemblages (i.e., biomass, trophic diversity, predator richness), despite larger sample size, differences in geographical areas, depth

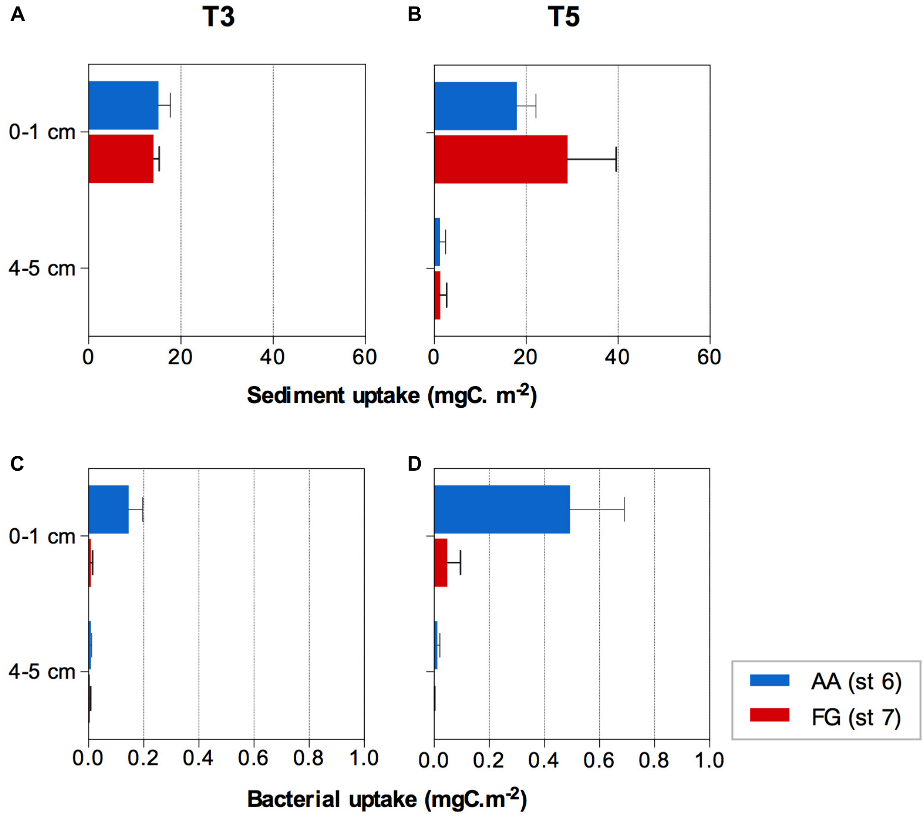

FIGURE 5 | ^{13}C algae uptake by the **(A,B)** sediment and **(C,D)** bacterial communities at the AA and FG station after three (T3) and five (T5) days, respectively. Values expressed as average ± standard error.

ranges and biodiversity (species richness) ranges investigated in their studies. The observed alterations of the trophic structure, respiration rates and benthic secondary production (indirectly assessed by biomass), in relation to trawling disturbance, is an indication of its negative influence on nutrient and energy fluxes across the food web. As energy transfer in marine systems (across the food web) is predominantly determined by biotic interactions among organisms (e.g., predation, but also competition, facilitation; Strong et al., 2015; Spiers et al., 2016), the capture and conversion of primary production into secondary production by consumers is a key function of the benthos (Strong et al., 2015). Moreover, there is increased evidence that loss of species at higher trophic levels would have more severe effects on the stability of food webs through top-down control, and thus groups such as predators can have a crucial role in carbon and energy cycling (Atwood et al., 2015; Spiers et al., 2016).

Despite the indication of detrimental effects suggested by our results, they need to be interpreted with caution owing to the poor replication in relation to spatial environmental heterogeneity and trawling disturbance intensity. Additional observations are needed to determine if the observed significant BEF relations can be extrapolated across depth-ranges and along the WIM. This will be key to predict, with high confidence, how disturbance patterns (e.g., exploitation of new fishing grounds) may affect ecosystem functions that are facilitated by the infaunal communities in the region.

Changes in Benthic Infauna and Associated Ecosystem Functions

Different benthic faunal compartments (e.g., macrofauna and meiofauna) have different capacities to sustain, recolonize and re-establish after one or several disturbance events. Their distinct responses will depend on both the assemblage traits, turnover rates and faunal interactions (e.g., prey-predator relations, facilitation processes; Sciberras et al., 2017), as well as on the post-disturbance habitat conditions (Clark et al., 2016 and references therein; Yesson et al., 2016). Post-disturbance environmental conditions in soft sediments habitats will be determined by direct changes in sediment structure (e.g., porosity and permeability), but also by alterations of the biotic and abiotic processes that follow.

Our results suggest that some of ecosystem functions investigated may be impaired, under conditions of varying disturbance history. These differences were primarily perceived by an increase of total macrofaunal abundances in the FG station, which was in fact mostly due to an increase of the smaller sized taxa (lower MIB) inhabiting disturbed sediments. This was also associated with differences in trophic structure in the two investigated stations (larger proportion of surface and subsurface deposit and detritus feeders in the fishing ground; Ramalho et al., 2018). The influence of trawling disturbance on macrofauna was also evident in the lower total respiration for macrofauna in FG (st. 7), but not in nematode (meiofauna) assemblages.

The shift in species size and traits toward smaller opportunistic taxa under conditions of disturbance also observed in mega-epibenthic taxa by Ramalho et al. (2017) has been associated with a lower recovery capacity of sediment biogeochemical conditions, as mediation of macronutrients and carbon cycling was decoupled (Hale et al., 2017). In the present study, in addition to the differences in terms of traits of macrobenthos (both trophic, mean size, and respiration rates) between the two FG and AA stations, we have also observed significant differences in bacterial uptake rates and biogeochemical functions based on ammonium concentrations in sediments collected in these stations. Specifically, bacterial uptake rates associated with the carbon transformation processes were lower in FG sediments, while an increase in ammonium concentrations was observed in FG sediments in deeper and typically anoxic layers during the first 3 days of the experiment. Increases in ammonium concentration in anoxic layers can occur under alterations of the denitrifying bacterial communities and/or depleted oxygen concentrations required to convert ammonium into N_2 via anaerobic ammonium oxidation (anammox) (Laverock et al., 2011). Similar rises in ammonium concentrations were found by Hale et al. (2017), while also similarly to this study, nitrate profiles showed no differences between sediments of low to high fishing disturbance. The high ammonium concentrations found here, together with the presence of smaller-sized macrofaunal individuals (lower MIB) in the FG sediments compared to the AA sediments could point to inefficient bioturbation activity in the disturbed area that could indirectly affect biogeochemical functions and bacterial productivity. Smaller macrofauna individuals (lower MIB), but conversely larger nematode genera in FG sediments when compared to AA sediments, are congruent with a deprived oxygen provision in the deeper layers of the sediments in highly disturbed seafloor areas. A decrease in macrofauna standing stock (Levin, 2002) and the prevalence of larger-sized nematodes (larger MIB observed in FG than in AA sediments) has been observed in oxygen-deprived deep-sea areas. The latter has been considered an adaption to maximize oxygen absorption under oxygen-deprived conditions (Jensen, 1986). Although the present results give some indication of changes in ecosystem function depending on trawling disturbance, a direct link between changes in macrofauna size-spectra and a depletion of biogeochemical functions and bacterial productivity cannot be effectively established. The investigated faunal variables (e.g., trophic preferences, biomass, and diversity) were not assessed on the same sediment cores as the biogeochemical function proxies and therefore spatial variability cannot be excluded as a factor in the observed differences. Furthermore, the hypothesis that changes in faunal assemblages will cause altered bioturbation potential of the sediments remains unanswered (no significant differences observed among treatments) probably owing to the low number of replicates used. Finally, even though we recognize the importance of including an area close to pristine conditions and legally protected (NT) in the experimental set up, due to differences in depth and grain-size differences between the only close NT area and the main fishing ground/adjacent areas, this undisturbed location could not be included, and thus biogeochemical functions and ^{13}C bacterial uptake in undisturbed conditions at the WIM remain untested.

Noteworthy is that, in opposition to what was observed for macrofauna, the absence of a significant effect of trawling pressure on meiofaunal standing stocks (both abundance and biomass), community composition (Lins et al., 2017) and respiration, advocates for an overall absence of a detrimental effect on the measured meiofauna/nematode variables. These results contradict the results obtained by Pusceddu et al., 2014. The contrasting results may be related with the differences in organic matter concentrations under different conditions of trawling pressure. Here at the start of the experiment, the first 5 cm of sediment showed similar environmental conditions in both AA and FG, including in terms of organic carbon and nitrogen, while Pusceddu et al., 2014 showed decreased organic carbon concentrations with increased trawling pressure. Generally, meiofaunal standing stocks are positively related with food availability and quality in deep-sea sediments (e.g., Ingels et al., 2009; Pape et al., 2013; Lins et al., 2017), so this may partially explain the decreased in meiobenthos with increasing trawling pressure in the study of Pusceddu et al. (2014). Other differences identified between these two studies were varying habitat conditions (e.g., depths, canyon vs. slope) and/or differences in sample size (c.a. 50% more samples analyzed by Pusceddu et al., 2014). Nevertheless, while meiofauna can contribute to ecosystem processes via micro-bioturbation (Rysgaard et al., 2000; Bonaglia et al., 2014), in high diversity systems such as the study area (Ramalho et al., 2018), the influence of strong interactions with the macrofauna (competition and predation), may mask or decrease the relevance of the meiofauna to sediment biogeochemical functioning comparatively to macrofauna (Rysgaard et al., 2000; Bonaglia et al., 2014).

CONCLUSION

The present study suggested a negative influence of trawling disturbance on the benthos and related ecosystem functions. The most evident effects were detected for the macrofauna assemblages, with a prevalence of small-sized opportunistic species under high physical disturbance conditions (fishing grounds). Moreover, the general decline in macrofauna species richness, functional (trophic) diversity and total respiration, suggests that the long history of trawling disturbance along the WIM may be affecting the integrity of the seafloor and the capacity of the benthos to ensure fundamental ecosystem functions and services. In contrast, the biomass of the small-sized biota (meiofauna and bacteria) showed no marked differences associated with trawling regimes, although bacterial production (^{13}C uptake) was reduced in the FG sediments investigated during the pulse-chase experiment. Trawling-induced changes in macrofauna traits and size structure may result in an inefficient bioturbation and low bioirrigation potential affecting both biogeochemical functioning and productivity in marine sediments. Further investigation is required to substantiate the observed function impairment across the study area, including larger sampling effort within AA and FG areas and a comparison with pristine locations.

DATA AVAILABILITY STATEMENT

The datasets generated for this study are available on request to the corresponding author.

AUTHOR CONTRIBUTIONS

MC, AV, EP, and NL generated the study idea and funding. MC, AV, SR, EP, and LL were responsible for sample collection and experimental set-up, further analyzed by SR, EP and LL. KS was the main responsible for ^{13}C and PLFA sample processing analyses. SR and EP wrote the manuscript with significant contribution from all authors. All authors contributed to the article and approved the submitted version.

FUNDING

This work was supported by the CESAM (UIDP/50017/2020 + UIDB/50017/2020) funds, granted by FCT/MCTES through national funds. SR work was funded through a MARES Grant (FPA 2011-0016) and is currently supported by national funds (OE), through the FCT – Fundação para a Ciência e a Tecnologia, I.P., in the scope of the “CEEC Individual 2017” contract (CEECIND/00758/2017). LL work as funded by the BOF (12/DOS/006) and CAPES (BEX 11595/13-2) grants. EP was financed by the FWO project “Unraveling the enigma of nematode success in the deep sea” (G083512N).

ACKNOWLEDGMENTS

We thank all scientific parties, the captain, and the crew, for their excellent logistical support during the RV Belgica 2013/2017 and RV Belgica 2014/2015 cruises. We are thankful to Pieter Van Rijswijck (NIOZ Yerseke) for his work with the ^{13}C and PLFA sample processing.

SUPPLEMENTARY MATERIAL

The Supplementary Material for this article can be found online at: https://www.frontiersin.org/articles/10.3389/fmars.2020.00457/full#supplementary-material

REFERENCES

Aller, R. C. (1982). “The effects of macrobenthos on chemical properties of marine sediment and overlying water,” in *Animal-Sediment Relations. Topics in Geobiology*, Vol. 100, eds P. L. McCall and M. J. S. Tevesz (Boston, MA: Springer), 53–102. doi: 10.1007/978-1-4757-1317-6_2

Anderson, M. J., Gorley, R. N., and Clarke, R. K. (2008). *Permanova+ for Primer: Guide to Software and Statistical Methods*. Plymouth: PRIMER-E Ltd.

Andrassy, I. (1956). Die rauminhalts- und gewichtsbestimmung der fadenwurmer (Nematoden). *Acta Zool.* 2, 1–15.

Atwood, T. B., Connolly, R. M., Ritchie, E. G., Lovelock, C. E., Heithaus, M. R., Hays, G. C., et al. (2015). Predators help protect carbon stocks in blue carbon ecosystems. *Nat. Clim. Chang* 5, 1038–1045. doi: 10.1038/nclimate2763

Baguley, J. G., Hyde, L. J., and Montagna, P. A. (2004). A semi-automated digital microphotographic approach to measure meiofaunal biomass. *Limnol. Oceangr.* 2, 181–190. doi: 10.4319/lom.2004.2.181

Baldrighi, E., Giovannelli, D., D’Errico, G., Lavaleye, M., and Manini, E. (2017). Exploring the relationship between macrofaunal biodiversity and ecosystem functioning in the deep sea. *Front. Mar. Sci.* 4:198. doi: 10.3389/fmars.2017.00198

Baldrighi, E., and Manini, E. (2015). Deep-sea meiofauna and macrofauna diversity and functional diversity: are they related? *Mar. Biodivers* 45, 469–488. doi: 10.1007/s12526-015-0333-9

Bligh, E. G., and Dyer, W. J. (1959). A rapid method of total lipid extraction and purification. *Can. J. Biochem. Physiol.* 37, 911–917. doi: 10.1139/o59-099

Bonaglia, S., Nascimento, F. J. A., Bartoli, M., Klawonn, I., and Br¨chert, V. (2014). Meiofauna increases bacterial denitrification in marine sediments. *Nat. Commun.* 5:5133. doi: 10.1038/ncomms6133

Borges, T. C., Erzini, K., Bentes, L., Costa, M. E., Goncalves, J., Lino, P. G., et al. (2001). By-catch and discarding practices in five Algarve (southern Portugal) metiers. *J. Appl. Ichthyol.* 17, 104–114. doi: 10.1111/j.1439-0426.2001.00283.x

Boschker, H. T. S. (2004). “Linking microbial community structure and functioning: stable istope (13C) labeling in combination with PLFA analysis,” in *Molecular Microbial Ecology Manual*, 2nd Edn, ed. G. A. Kolwalchuk (Dordrecht: Kluwer Academic Publishers), 1673–1688.

Braeckman, U., Provoost, P., Gribsholt, B., Van Gansbeke, D., Middelburg, J. J., Soetaert, K., et al. (2010). Role of macrofauna functional traits and density in biogeochemical fluxes and bioturbation. *Mar. Ecol. Prog. Ser.* 399, 173–186. doi: 10.3354/meps08336

Brinch-Iversen, J., and King, G. M. (1990). Effects of substrate concentration, growth-state, and oxygen availability on relationships among bacterial carbon, nitrogen and phospholipid phosphorus-content. *FEMS Microbiol. Ecol.* 74, 345–355. doi: 10.1016/0378-1097(90)90687-L

Bueno-Pardo, J., Ramalho, S. P., García-Alegre, A., Morgado, M., Vieira, R. P., Cunha, M. R., et al. (2017). Deep-sea crustacean trawling fisheries in portugal: quantification of effort and assessment of landings per unit effort using a vessel monitoring system (VMS). *Sci. Rep.* 7:40795. doi: 10.1038/srep40795

Clark, M. R., Althaus, F., Schlacher, T. A., Williams, A., Bowden, D. A., and Rowden, A. A. (2016). The impacts of deep-sea fisheries on benthic communities: a review. *ICES J. Mar. Sci.* 73:fsv123. doi: 10.1093/icesjms/fsv123

Clarke, K. R., and Gorley, R. N. (2006). *PRIMER Version 6: User Manual/Tutorial*. Plymouth: PRIMER-E Ltd.

Danovaro, R. C., Gambi, M. C., Dell’Anno, A., Corinaldesi, C., Fraschetti, S., Vanreusel, A., et al. (2008). Exponential decline of deep-sea ecosystem functioning linked to benthic biodiversity loss. *Curr. Biol.* 18, 1–8. doi: 10.1016/j.cub.2007.11.056

Duplisea, D. E., Jennings, S., Malcolm, S. J., Parker, R., and Sivyer, D. B. (2001). Modelling potential impacts of bottom trawl fisheries on soft sediment biogeochemistry in the North Sea. *Geochem. Trans.* 2:112. doi: 10.1039/b108342b

Eigaard, O. R., Bastardie, F., Hintzen, N. T., Buhl-Mortensen, L., Buhl-Mortensen, P., Catarino, R., et al. (2016). The footprint of bottom trawling in European waters: distribution, intensity, and seabed integrity. *ICES J. Mar. Sci.* 74, 847–865. doi: 10.1093/icesjms/fsw194

European Commission. (2008). *Directive 2008/56/EC of the European Parliament and of the Council of 17 June 2008*. Brussels: Official Journal of the European Union.

Fauchald, K., and Jumars, P. A. (1979). The diet of worms: a study of polychaete feeding guilds. *Oceanogr. Mar. Biol. Annu. Rev.* 17, 193–284.

Gage, J. D., Hughes, D. J., and Vecino, J. L. G. (2002). Sieve size influence in estimating biomass, abundance and diversity in samples of deep-sea macrobenthos. *Mar. Ecol. Prog. Ser.* 225, 97–107. doi: 10.3354/meps225097

Giere, O. (2009). *Meiobenthology: The Microscopic Motile Fauna of Aquatic Sediments*. Berlin: Springer-Verlag.

Glud, R. N. (2008). Oxygen dynamics of marine sediments. *Mar. Biol. Res.* 4, 243–289. doi: 10.1080/17451000801888726

Guilini, K., Bezerra, T. N., Deprez, T., and Fonseca, G. F. C. (2016). *NeMys: World Database of Free-Living Marine Nematodes*. Avaliable at: https://nemys.ugent.be/. (accessed December 3, 2015)

Hale, R., Godbold, J. A., Sciberras, M., Dwight, J., Wood, C., Hiddink, J. G., et al. (2017). Mediation of macronutrients and carbon by post-disturbance shelf sea sediment communities. *Biogeochemistry* 135, 121–133. doi: 10.1007/s10533-017-0350-9

Hiddink, J. G., Jennings, S., Kaiser, M. J., Queirós, A. M., Duplisea, D. E., and Piet, G. J. (2006). Cumulative impacts of seabed trawl disturbance on benthic biomass, production, and species richness in different habitats. *Can. J. Fish. Aquat. Sci.* 63, 721–736. doi: 10.1139/f05-266

Higgins, R. P., and Thiel, H. (1988). *Introduction to the Study of Meiofauna*. Washington D.C: Smithsonian Institution Press.

Hurlbert, S. H. (1971). The nonconcept of species diversity: a critique and alternative parameters. *Ecology* 52, 577–586. doi: 10.2307/1934145

Ingels, J., Kiriakoulakis, K., Wolff, G. A., and Vanreusel, A. (2009). Nematode diversity and its relation to the quantity and quality of sedimentary organic matter in the deep Nazaré Canyon. Western Iberian Margin. *Deep-Sea Res. Part I* 56, 1521–1539. doi: 10.1016/j.dsr.2009.04.010

Instituto Hidrográfico (2005a). *Carta dos Sedimentos Superficiais da Plataforma Continental Portuguesa - Folha 5 - Escala 1, 150 000*. Portugal: Instituto Hidrográfico.

Instituto Hidrográfico (2005b). *Carta dos Sedimentos Superficiais da Plataforma Continental Portuguesa - Folha 6A - Escala 1, 150 000*. Portugal: Instituto Hidrográfico.

Jennings, S., Dinmore, T. A., Duplisea, D. E., Warr, K. J., and Lancaster, J. E. (2001a). Trawling disturbance can modify benthic production processes. *J. Anim. Ecol.* 70, 459–475. doi: 10.1046/j.1365-2656.2001.00504.x

Jennings, S., Pinnegar, J. K., Polunin, N. V., and Warr, K. J. (2001b). Impacts of trawling disturbance on the trophic structure of benthic invertebrate communities. *Mar. Ecol. Prog. Ser.* 213, 127–142. doi: 10.3354/meps213127

Jensen, P. (1986). Nematode fauna in the sulphide-rich brine seep and adjacent bottoms of the East Flower Garden. NW Gulf of Mexico. *Mar. Biol.* 92, 489–503. doi: 10.1007/BF00392509

Jumars, P. A., Dorgan, K. M., and Lindsay, S. M. (2015). Diet of worms emended: an update of polychaete feeding guilds. *Ann. Rev. Mar. Sci.* 7, 497–520. doi: 10.1146/annurev-marine-010814-020007

Kämpf, J., and Chapman, P. (2016). *Upwelling Systems of the World*. Switzerland: Springer International Publishing.

Laverock, B., Gilbert, J. A., Tait, K., Osborn, A. M., and Widdicombe, S. (2011). Bioturbation: impact on the marine nitrogen cycle. *Biochem. Soc. Trans.* 39, 315–320. doi: 10.1042/BST0390315

Leduc, D., Pilditch, C. A., and Nodder, S. D. (2016). Partitioning the contributions of mega-, macro- and meiofauna to benthic metabolism on the upper continental slope of New Zealand: potential links with environmental factors and trawling intensity. *Deep-Sea Res. Part I* 108, 1–12. doi: 10.1016/j.dsr.2015.12.003

Leocádio, A. M., Whitmarsh, D., and Castro, M. (2012). Comparing trawl and creel fishing for norway lobster (*Nephrops norvegicus*): biological and economic considerations. *PLoS One* 7:e39567. doi: 10.1371/journal.pone.0039567.t006

Levin, L. A. (2002). Deep-ocean life where oxygen is scarce. *Am. Sci.* 90, 436–444. doi: 10.1511/2002.5.436

Levin, L. A., Etter, R. J., Rex, M. A., Gooday, A. J., Smith, C. R., Pineda, J., et al. (2001). Environmental Influences on regional deep-sea species diversity. *Annu. Rev. Ecol. Syst.* 32, 51–93. doi: 10.1146/annurev.ecolsys.32.081501.114002

Lins, L., Leliaert, F., Riehl, T., Ramalho, S. P., Cordova, E. A., Esteves, A. M., et al. (2017). Evaluating environmental drivers of spatial variability in free-living nematode assemblages along the Portuguese margin. *Biogeosciences* 14, 651–669. doi: 10.5194/bg-14-651-2017

Lohrer, A. M., Thrush, S. F., and Gibbs, M. M. (2004). Bioturbators enhance ecosystem function through complex biogeochemical interactions. *Nature* 431, 1092–1095. doi: 10.1038/nature03042

Macdonald, T. A., Burd, B. J., Macdonald, V. I., and van Roodselaar, A. (2010). *Taxonomic and Feeding Guild Classification for the Marine Benthic Macroinvertebrates of the Strait of Georgia, British Columbia*. Sidney, BC: Fisheries and Oceans Canada.

Maestro, A., López-Martínez, J., Llave, E., Bohoyo, F., Acosta, J., Hernández-Molina, F. J., et al. (2013). Geomorphology of the Iberian Continental Margin. *Geomorphol.* 196, 13–35. doi: 10.1016/j.geomorph.2012.08.022

Mahaut, M. L., Sibuet, M., and Shirayama, Y. (1995). Weight-dependent respiration rates in deep-sea organisms. *Deep Sea Res. Part I* 42, 1575–1582. doi: 10.1016/0967-0637(95)00070-M

MAMAOT (2012). *Estratégia Marinha Para a subdivisão do Continente. Diretiva Quadro Estratégia Marinha*. Lisbon: Ministério da Agricultura, do Mar.

Martín, J., Puig, P., Palanques, A., and Giamportone, A. (2014a). Commercial bottom trawling as a driver of sediment dynamics and deep seascape evolution in the. *Anthropocene* 7, 1–15. doi: 10.1016/j.ancene.2015.01.002

Martín, J., Puig, P., Palanques, A., and Ribó, M. (2014b). Trawling-induced daily sediment resuspension in the flank of a mediterranean submarine canyon. *Deep Sea Res. Part II* 104, 174–183. doi: 10.1016/j.dsr2.2013.05.036

Martín, J., Puig, P., Masqué, P., Palanques, A., and Sánchez-Gómez, A. (2014c). Impact of bottom trawling on deep-sea sediment properties along the flanks of a submarine canyon. *PLoS One* 9:e104536. doi: 10.1371/journal.pone.0104536

Middelburg, J. J., Barranguet, C., Boschker, H. T. S., Herman, P. M., Moens, T., and Heip, C. H. (2000). The fate of intertidal microphytobenthos carbon: an in situ 13C-labeling study. *Limnol. Oceangr.* 45, 1224–1234. doi: 10.4319/lo.2000.45.6.1224

Monteiro, P., Araújo, A., Erzini, K., and Castro, M. (2001). Discards of the Algarve (southern Portugal) crustacean trawl fishery. *Hydrobiologia* 449, 267–277. doi: 10.1023/A:1017575429808

National Research Council [NRC] (2002). *Effects of Trawling and Dredging on Seafloor Habitat*. Washington, DC: The National Academies Press.

Oberle, F. K. J., Storlazzi, C. D., and Hanebuth, T. J. J. (2016). What a drag: quantifying the global impact of chronic bottom trawling on continental shelf sediment. *J. Mar. Syst.* 159, 109–119. doi: 10.1016/j.jmarsys.2015.12.007

Pape, E., Jones, D. O., Manini, E., Bezerra, T. N., and Vanreusel, A. (2013). Benthic-pelagic coupling: effects on nematode communities along southern European continental margins. *PLoS One* 8:e59954. doi: 10.1371/journal.pone.0059954

Picado, A., Alvarez, I., Vaz, N., Varela, R., Gomez-Gesteira, M., and Dias, J. M. (2014). Assessment of chlorophyll variability along the northwestern coast of Iberian Peninsula. *J. Sea Res.* 93, 2–11. doi: 10.1016/j.seares.2014.01.008

Pielou, E. C. (1966). The measurement of diversity in different types of biological collections. *J. Theor. Biol.* 13, 131–144. doi: 10.1016/0022-5193(66)90013-0

Platt, H. M., and Warwick, R. M. (1983). *Free Living Marine Nematodes. Part 1: British Enoplids. Pictorial key to World Genera and Notes for the Identification of British Species*. Cambridge: Cambridge University Press.

Platt, H. M., and Warwick, R. M. (1988). *Free-Living Marine Nematodes. Part II: British Chromadorids*. Cambridge: Cambridge University Press.

Pusceddu, A., Bianchelli, S., Martín, J., Puig, P., Palanques, A., Masqué, P., et al. (2014). Chronic and intensive bottom trawling impairs deep-sea biodiversity and ecosystem functioning. *Proc. Nat. Acad. Sci. U.S.A.* 111, 8861–8866. doi: 10.1073/pnas.1405454111

Queirós, A. M., Hiddink, J. G., Kaiser, M. J., and Hinz, H. (2006). Effects of chronic bottom trawling disturbance on benthic biomass, production and size spectra in different habitats. *J. Exp. Mar. Bio. Ecol.* 335, 91–103. doi: 10.1016/j.jembe.2006.03.001

Quinn, G. P., and Keough, M. J. (2002). *Experimental Design and Data Analysis for Biologists*. Cambridge: Cambridge University Press.

Ramalho, S. P., Almeida, M. D., Esquete, P., Génio, L., Ravara, A., Rodrigues, C. F., et al. (2018). Bottom trawling fisheries influence on macrofauna standing stocks, community composition and diversity from the West Iberian Margin. *Deep Sea Res. Part I* 138, 131–145. doi: 10.1016/j.dsr.2018.06.004

Ramalho, S. P., Lins, L., Bueno-Pardo, J., Cordova, E. A., Amisi, J. M., Lampadariou, N., et al. (2017). Deep-sea mega-epibenthic assemblages from the SW Portuguese margin (NE Atlantic) subjected to bottom trawling fisheries. *Front. Mar. Sci.* 4:350. doi: 10.3389/fmars.2017.00350

Ramirez-Llodra, E., Tyler, P. A., Baker, M. C., Bergstad, O. A., Clark, M. R., Escobar, E., et al. (2011). Man and the last great wilderness: human impact on the deep sea. *PLoS One* 6:e22588. doi: 10.1371/journal.pone.0022588

Relvas, P., Barton, E. D., Dubert, J., Oliveira, P. B., Peliz, Á, da Silva, J. C. B., et al. (2007). Physical oceanography of the western Iberia ecosystem: latest views and challenges. *Prog. Oceanogr* 74, 149–173. doi: 10.1016/j.pocean.2007.04.021

Rowe, G. T. (1983). "Biomass and production of the deep-sea macrobenthos," in *Deep-Sea Biology - The Sea*, ed. G. T. Rowe (New York, NY: John Wiley and Sons), 97–121.

Rysgaard, S., Christensen, P. B., Sorensen, M. V., Funch, P., and Berg, P. (2000). Marine meiofauna, carbon and nitrogen mineralization in sandy and soft sediments of Disko Bay. West Greenland. *Aquat. Microb. Ecol.* 21, 59–71. doi: 10.3354/ame021059

Sañé, E., Martín, J., Puig, P., and Palanques, A. (2013). Organic biomarkers in deep-sea regions affected by bottom trawling: pigments, fatty acids, amino acids and carbohydrates in surface sediments from the La Fonera (Palamós) Canyon. NW Mediterranean Sea. *Biogeosciences* 10:8093. doi: 10.5194/bg-10-8093-2013

Santos, A. (2001). Sardine and horse mackerel recruitment and upwelling off Portugal. *ICES J. Mar. Sci.* 58, 589–596. doi: 10.1006/jmsc.2001.1060

Schratzberger, M., Dinmore, T. A., and Jennings, S. (2002). Impacts of trawling on the diversity, biomass and structure of meiofauna assemblages. *Mar. Biol.* 140, 83–93. doi: 10.1007/s002270100688

Sciberras, M., Hiddink, J. G., Jennings, S., Szostek, C. L., Hughes, K. M., Kneafsey, B., et al. (2018). Response of benthic fauna to experimental bottom fishing: a global meta-analysis. *Fish. Fish.* 19, 698–715. doi: 10.1111/faf.12283

Sciberras, M., Parker, R., Powell, C., Robertson, C., Kröger, S., Bolam, S. G., et al. (2016). Impacts of bottom fishing on the sediment infaunal community and biogeochemistry of cohesive and non-cohesive sediments. *Limnol. Oceangr.* 61, 2076–2089. doi: 10.1002/lno.10354

Sciberras, M., Tait, K., Brochain, G., Hiddink, J. G., Hale, R., Godbold, J. A., et al. (2017). Mediation of nitrogen by post-disturbance shelf communities experiencing organic matter enrichment. *Biogeochemistry* 135, 135–153. doi: 10.1007/s10533-017-0370-5

Shaffer, J. P. (1995). Multiple hypothesis-testing. *Ann. Rev. Psychol.* 46, 561–584. doi: 10.1146/annurev.ps.46.020195.003021

Silva, A., Palma, S., Oliveira, P. B., and Moita, M. T. (2009). Composition and interannual variability of phytoplankton in a coastal upwelling region (Lisbon Bay. Portugal). *J. Sea Res.* 62, 238–249. doi: 10.1016/j.seares.2009.05.001

Solan, M., Cardinale, B. J., Downing, A. L., Engelhardt, K. A. M., Ruesink, J. L., and Srivastava, D. S. (2004). Extinction and ecosystem function in the marine benthos. *Science* 306, 1177–1180. doi: 10.1126/science.1103960

Spiers, E. K. A., Stafford, R., Ramirez, M., Izurieta, D. F. V., Cornejo, M., and Chavarria, J. (2016). Potential role of predators on carbon dynamics of marine ecosystems as assessed by a Bayesian belief network. *Ecol. Inform.* 36, 77–83. doi: 10.1016/j.ecoinf.2016.10.003

Stratmann, T., Lins, L., Purser, A., Marcon, Y., Rodrigues, C. F., Ravara, A., et al. (2018). Abyssal plain faunal carbon flows remain depressed 26 years after a simulated deep-sea mining disturbance. *Biogeosciences* 15, 4131–4145. doi: 10.5194/bg-15-4131-2018

Strong, J. A., Andonegi, E., Bizsel, K. C., Danovaro, R. C., Elliott, M., Franco, A., et al. (2015). Marine biodiversity and ecosystem function relationships: the potential for practical monitoring applications. *Estuar. Coast. Shelf Sci.* 161, 46–64. doi: 10.1016/j.ecss.2015.04.008

van Oevelen, D., Moodley, L., Soetaert, K., and Middelburg, J. J. (2006). The trophic significance of bacterial carbon in a marine intertidal sediment: results of an in situ stable isotope labeling study. *Limnol. Oceangr.* 51, 2349–2359. doi: 10.4319/lo.2006.51.5.2349

Vanreusel, A., Hilario, A., Ribeiro, P. A., Menot, L., and Arbizu, P. M. (2016). Threatened by mining, polymetallic nodules are required to preserve abyssal epifauna. *Sci. Rep.* 6:26808. doi: 10.1038/srep26808

Volkenborn, N., Hedtkamp, S. I. C., van Beusekom, J. E. E., and Reise, K. (2007). Effects of bioturbation and bioirrigation by lugworms (*Arenicola marina*) on physical and chemical sediment properties and implications for intertidal habitat succession. *Estuar. Coast. Shelf Sci.* 74, 331–343. doi: 10.1016/j.ecss.2007.05.001

Wenthworth, C. K. (1922). The Wenthworth scale of grain size for sediments. *J. Geol.* 30, 377–392. doi: 10.1086/622910

Wieser, W. (1953). Die beziehung zwischen mundhöhlengestalt, ernährungsweise und vorkommen bei freilebenden marinen nematoden. *Ark. Zool.* 4, 439–484.

Wieser, W. (1960). Benthic studies in buzzards bay II: the meiofauna. *Limnol. Oceangr.* 5, 121–137. doi: 10.4319/lo.1960.5.2.0121

Worm, B., Barbier, E. B., Beaumont, N., Duffy, J. E., Folke, C., Halpern, B. S., et al. (2006). Impacts of biodiversity loss on ocean ecosystem services. *Science* 314, 787–790. doi: 10.1126/science.1132294

Yesson, C., Fisher, J., Gorham, T., Turner, C. J., Hammeken Arboe, N., Blicher, M. E., et al. (2016). The impact of trawling on the epibenthic megafauna of the west Greenland shelf. *ICES J. Mar. Sci.* 74, 866–876. doi: 10.1093/icesjms/fsw206

Conflict of Interest: The authors declare that the research was conducted in the absence of any commercial or financial relationships that could be construed as a potential conflict of interest.

frontiers in Marine Science

ORIGINAL RESEARCH
published: 29 June 2020
doi: 10.3389/fmars.2020.00460

Identification of a Soft Coral Garden Candidate Vulnerable Marine Ecosystem (VME) Using Video Imagery, Davis Strait, West Greenland

Stephen Long[1,2]*, Bridget Sparrow-Scinocca[3], Martin E. Blicher[4], Nanette Hammeken Arboe[4], Mona Fuhrmann[2], Kirsty M. Kemp[2], Rasmus Nygaard[4], Karl Zinglersen[4] and Chris Yesson[2]

[1] *Department of Geography, University College London, London, United Kingdom,* [2] *Institute of Zoology, Zoological Society of London, London, United Kingdom,* [3] *Department of Life Sciences, Imperial College London, London, United Kingdom,* [4] *Greenland Institute of Natural Resources, Nuuk, Greenland*

OPEN ACCESS

Edited by:
Christopher Kim Pham,
University of the Azores, Portugal

Reviewed by:
Travis William Washburn,
University of Hawai'i at Mānoa,
United States
Tina Molodtsova,
P. P. Shirshov Institute of Oceanology
(RAS), Russia

****Correspondence:***
Stephen Long
Stephen.long.16@ucl.ac.uk

Specialty section:
This article was submitted to
Deep-Sea Environments and Ecology,
a section of the journal
Frontiers in Marine Science

Received: *31 October 2019*
Accepted: *22 May 2020*
Published: *29 June 2020*

Citation:
Long S, Sparrow-Scinocca B, Blicher ME, Hammeken Arboe N, Fuhrmann M, Kemp KM, Nygaard R, Zinglersen K and Yesson C (2020) Identification of a Soft Coral Garden Candidate Vulnerable Marine Ecosystem (VME) Using Video Imagery, Davis Strait, West Greenland. Front. Mar. Sci. 7:460. doi: 10.3389/fmars.2020.00460

The term vulnerable marine ecosystem (VME) was introduced to facilitate the spatial management of deep-seas, identifying those habitats vulnerable to anthropogenic disturbance, such as trawling. Consistent interpretation of the VME definition has been hampered by an underlying paucity of knowledge about the nature and distribution of deep-sea habitats. Photographic and video platforms yield data rich, quantifiable imagery to address these knowledge gaps. A low-cost towed benthic video sled has been used to investigate deep-sea habitats and trawling impacts in west Greenland. A review of imagery from multiple cruises highlighted an area where benthic megafauna contributes to notable structural complexity on the continental slope of the Toqqusaq Bank. Quantitative analysis of imagery from this area provides the first description of a soft coral garden habitat and other communities. The coral garden and observed densities are considered in relation to the VME guidelines (FAO, 2009) and wider literature. The study proposes a 486 km^2 area spanning ~60 km of continental slope as a VME. This has direct implications for the management of economically important deep-sea trawl fisheries, which are immediately adjacent. This furthers our knowledge and understanding of VMEs in North Atlantic, in a previously understudied region and demonstrates the utility of a low-cost video sled for identifying and describing VMEs.

Keywords: deep-sea, coral garden, spatial management, fishery management, towed video sled, cauliflower corals, benthic habitats

INTRODUCTION

The deep-sea (> 200 m) is the world's largest habitat covering ~65% of the earth's surface (Danovaro et al., 2017) and is increasingly subject to anthropogenic disturbance from fishing (Morato et al., 2006). Typically, deep-sea species are characterized by traits, including slow growth, late-maturity, and longevity, which can render populations, communities and habitats vulnerable to exploitation and disturbance (Ramirez-Llodra et al., 2010). Recognizing this, the

United Nations General Assembly (UNGA) Resolution 61/105 called upon States to take action to protect vulnerable marine ecosystems (VMEs) (UNGA, 2006). Following a period of consultation, the Food and Agriculture Organization (FAO) defined VMEs as exhibiting one or more of the following criteria: (i) unique or rare; (ii) functionally significant, (iii) fragile, (iv) containing component species whose life-history traits make recovery difficult; or (v) structurally complex (Gjerde et al., 2008; FAO, 2009).

The term VME has subsequently been applied to a wide variety of deep-sea habitats in both areas beyond national jurisdiction (ABNJ) and within exclusive economic zones (EEZs) around the world. States and regional fisheries management organizations (RFMOs) have adopted differing approaches for both identifying VMEs (Ardron et al., 2014) and implementing measures to protect them (Rogers and Gianni, 2011), which includes bycatch thresholds and move-on rules (Auster et al., 2010). Frequently, identification of VMEs has been based on the occurrence of VME indicator species, such as cold-water coral or sponges, at significant concentrations, which is a matter of expert judgment in the absence of explicit thresholds in the FAO guidance (Auster et al., 2010). This has led efforts to establish more consistent, quantitative and systematic approaches for identifying VMEs (Ardron et al., 2014; Morato et al., 2018). Fundamentally, adoption of a consistent systematic approach requires a sound understanding of the underlying nature and distribution of VMEs and indicator species globally. Currently, biases in survey effort mean that regions such as the Northeast Atlantic have received considerable attention (e.g., Muñoz and Sayago-Gil, 2011; Buhl-Mortensen et al., 2015; Huvenne et al., 2016), whilst others remain comparatively poorly known.

Survey approaches which yield quantifiable seafloor imagery by employing remote operated vehicles (ROVs), manned submersibles or towed cameras are among the preferred approaches for identifying VMEs. Morato et al. (2018) observe that the cost of obtaining and deploying equipment capable of imaging deep-sea environments has limited the identification of VMEs, with only a minute fraction of the deep-sea floor having been surveyed to date. Nevertheless, they predict that the rapid advance in technologies will reduce costs and increase coverage.

Despite having an EEZ of over 2.2 million km^2, Greenland has few Marine Protected Areas (MPAs). These are exclusively in inshore waters totalling ~4.5% of the EEZ (UNEP-WCMC, 2019), with none designated to protect known VMEs. A number of "Technical Conservation Measures" introduced by Executive Orders have been used to limit the use of bottom-contact fishing gears in some areas, of these only two are associated with the presence of VME indicator species. Specifically, there is a ~6.5 km^2 area in southwest Greenland bounding a single observation of *Desmophyllum pertusum* (Government of Greenland, 2017; Kenchington et al., 2017) and 11 discrete areas within the offshore region of Melville Bay closed to bottom trawling "*based on significant observations of sea pens*" (*Umbellula* sp.). (Cappell et al., 2018; Government of Greenland, 2018). This paucity of spatial management measures to protect VMEs is principally due to a lack of knowledge about the nature and distribution of VMEs within the Greenlandic EEZ, representing a knowledge gap in the North Atlantic.

Greenland is economically dependent on fisheries which account for 80–95% of the country's export income (Mortensen, 2014; The Economic Council, 2017; Jacobsen, 2018). The majority of this income is from deep-sea fisheries for prawns (*Pandalus borealis*) and Greenland halibut (*Reinhardtius hippoglossoides*) in west Greenland, though there is a growing contribution from pelagic fisheries in east Greenland. Since 2011, a program of benthic surveys using a drop camera (Yesson et al., 2015, 2017; Gougeon et al., 2017) and more recently a benthic video sled, has been working to quantify the impacts of trawling on benthic habitats by sampling across a spectrum of fishing effort. A series of stations from the western slope of the Toqqusaq Bank between 274 and 585 m, appear to show varied communities, with notable concentrations of cauliflower corals (Nephtheidae) and other VME indicator species, on rocky and mixed substrates.

Coral gardens are characterized by aggregations of one or more species (typically of non-reef forming coral), on a wide range of hard and soft substrates, supporting diverse benthic and epi-benthic fauna (ICES, 2007; OSPAR Commission, 2010). There is considerable diversity among coral garden communities, which may be dominated by soft corals (Alcyonacea), sea pens (Pennatulacea), black corals (Antipatharia), and stony corals (Scleractinia), often with sponges (Porifera) abundant but not dominant. Coral gardens dominated by cauliflower corals from four genera (*Gersemia, Duva*, *Drifa,* and *Pseudodrifa*), found on hard and mixed substrates are sometimes referred to as "cauliflower coral gardens" (Davies et al., 2017; Buhl-Mortensen et al., 2019). These have previously been observed in northwest and southeast Iceland (J. Burgos, pers. comm.; Buhl-Mortensen et al., 2019), Norway (Guillaumont et al., 2016) and eastern Canada (B. de Moura Neves, pers. comm.). Recognizing the vulnerability of cauliflower corals to physical disturbance, especially trawling (Devine et al., 2019), these cauliflower coral gardens have been considered VMEs by some including the North East Atlantic Fisheries Commission (NEAFC) (NEAFC, 2014; Buhl-Mortensen et al., 2019).

This study presents imagery collected using a custom built, low-cost benthic sled (total cost ~5,000 USD), which utilizes a commercially available action camera (GoPro). Imagery is used to produce a quantitative description of soft coral garden habitat in west Greenland, in the Northwest Atlantic. The findings are used to propose an area of continental slope as a soft coral garden VME, with reference to the FAO guidance and the wider literature.

MATERIALS AND METHODS

Study Site

The study site lies on the west Greenland continental slope, where the shallower Davis Strait separates the deeper northern Labrador Sea and Baffin Bay basins. The continental shelf in west Greenland can extend > 100 km offshore with numerous deep troughs and shallow banks (Jørgensen et al., 2018). Historically, the banks in west Greenland have been important fishing grounds for cod and more presently for prawns. Monitoring studies suggest that hydrographic conditions can stimulate high pelagic primary production across the edge of these banks (Poulsen and Reuss, 2002; Juul-Pedersen et al., 2015). Water mass characteristics are determined by the strength and mixing of two currents, the warm saline Irminger Current and colder, fresher East Greenland current (Myers et al., 2007). Icebergs scour the seabed to maximum depth of 600 m and deposit terrigenous sediments and dropstones (Gutt, 2002; Streuff et al., 2017). The diversity of topographic features and oceanographic influences results in diversity and heterogeneity of benthic communities (Gougeon et al., 2017).

Since 2011, benthic camera surveys (∼30–1,500 m) have been used to map habitats and quantify trawling impacts in west Greenland, employing a drop camera (Yesson et al., 2015, 2017; Gougeon et al., 2017) and benthic video sled from 2017. The benthic video sled was deployed during two *RV Sanna* research cruises in October 2018 and May 2019, dedicated to the Toqqusaq Bank area. Video imagery from these cruises and a smaller number of video stations obtained opportunistically on other cruises were reviewed. This highlighted that a subset of stations appeared to show structurally complex habitats with higher densities of cauliflower corals, VME indicator taxa and other structure forming taxa than had been observed elsewhere. Constraints prevent a comprehensive characterization of all the habitats in this area using all available imagery. Instead the focus is on producing a quantitative description of the habitats in a subset of stations where the review highlighted notable structural complexity created by benthic macrofauna. This subset of stations selected during the review ($n = 18$), are at depths from 274 to 585 m, on the continental slope on the western edge of the Toqqusaq Bank, in Greenlandic waters (NAFO Areas 1C + D) (**Figure 1**).

The study area sits directly between two Marine Stewardship Council (MSC) certified deep-sea trawl fisheries. Namely, the West Greenland Offshore Greenland Halibut Fishery (800–1,500 m) (Cappell et al., 2017) and the West Greenland Coldwater Prawn Fishery, which targets areas on the continental shelf and slope (200–500 m) (Cappell et al., 2018; **Figure 1**). In the southern part of the study area there has been additional fishing pressure from an emerging cod (*Gadus morhua*) fishery. Following collapse of the west Greenland offshore cod fishery in the early 1990s, a management plan introduced a closure in 2014 to allow recovery. This was overturned and a Total Allowable Catch (TAC) of 5,000 tonnes was set for 2015–2018, inclusive (ICES, 2019b). In 2018, 4,187 t was landed by trawlers (61%) and longliners (39%), half of which (2,666 t) was from NAFO 1C/D (ICES, 2019a), with the main fishing grounds being the Toqqusaq Bank, at the top of the slope (∼200–300 m) centered on the NAFO 1C/D boundary (**Figure 1**; ICES, 2019b).

Benthic Video Sled

Imagery from 14 stations sampled with *RV Sanna* (SA, 2018–2019) was supplemented with a single station from *RV Paamiut* (PA, 2017) and three stations from *MT Helga Maria* (HM, 2019). All stations were sampled between May and October. Imagery was collected using a towed benthic video sled with an oblique angled centrally mounted video camera, lights, scaling lasers and an echo sounder unit. Illumination was provided by two Group-Binc Nautilux 1,750 m LED torches arranged either side of the camera and angled inwards to achieve as close to even illumination as possible. A pair of green Z-Bolt lasers (wavelength = 515 nm) in custom-made housings, were positioned 20 cm apart directly below the camera to provide an indication of scale. The position of the sled relative to the seafloor was monitored from the bridge using a Marport Trawl Eye Explorer (echo sounder unit) fixed to the top of the sled, which reported the depth (± 0.1 m), pitch and roll of the sled. Once the sled had made bottom contact it was towed at a target speed of 0.8–1 knots for a minimum of 15 min and up to 45 min. Longer tow times were used where time allowed, or to ensure adequate footage was obtained when there were potential issues (e.g. rough sea) during deployment.

Video was collected using a GoPro action camera in Group-Binc housings, which have a flat acrylic port. A GoPro4 recording 1,920 × 1,080 pixels at 48 frames per second (fps) was used in 2017, in a Group-Binc Scout housing. Subsequently, a GoPro5 was used, recording at the same aspect ratio (16 × 9) but higher resolution of 2,704 × 1,520 pixels at 60 fps, in a Group-Binc Benthic 3 housing.

The "Medium FOV" setting was used on both cameras. Per the manufacturer's specifications this provides the same field of view (FOV), with vertical (α_{air}) and horizontal (β_{air}) aperture angles in air of 55 and 94.4°, respectively. Guided by the discussion in Treibitz et al. (2011), these were corrected for refraction according to Snell's Law of refraction, which means it is necessary to correct for refraction by the bulk medium (seawater) but not the acrylic lens of the housing. This allows the vertical (α) and horizontal (β) aperture angles in seawater to be determined (Eqs. 1 and 2).

$$\alpha = 2.\sin^{-1}\left(\frac{\sin(0.5 \times \alpha_{air})}{r}\right) \tag{1}$$

$$\beta = 2.\sin^{-1}\left(\frac{\sin(0.5 \times \beta_{air})}{r}\right) \tag{2}$$

Where, r is the refractive index of seawater, for which a value of 1.34 was used based on the likely range of depth, temperature and salinity encountered in this study (Millard and Seaver, 1990). The calculated values were $\alpha = 40.3°$, $\beta = 66.4°$.

Due to the oblique angle the very uppermost part of the image is difficult to interpret due to a lack of reflected light and taxa appearing smaller furthest from the camera. The distribution of all annotations made was reviewed, there were none in the top hundredth of the image. Excluding this unannotated area reduces the likelihood of artificially underestimating faunal density. Thus the area of seafloor in the annotated FOV is calculated for *JBDK*, a subset of *ABDE,* where length JB is 0.99 of the length AB (**Figure 2**).

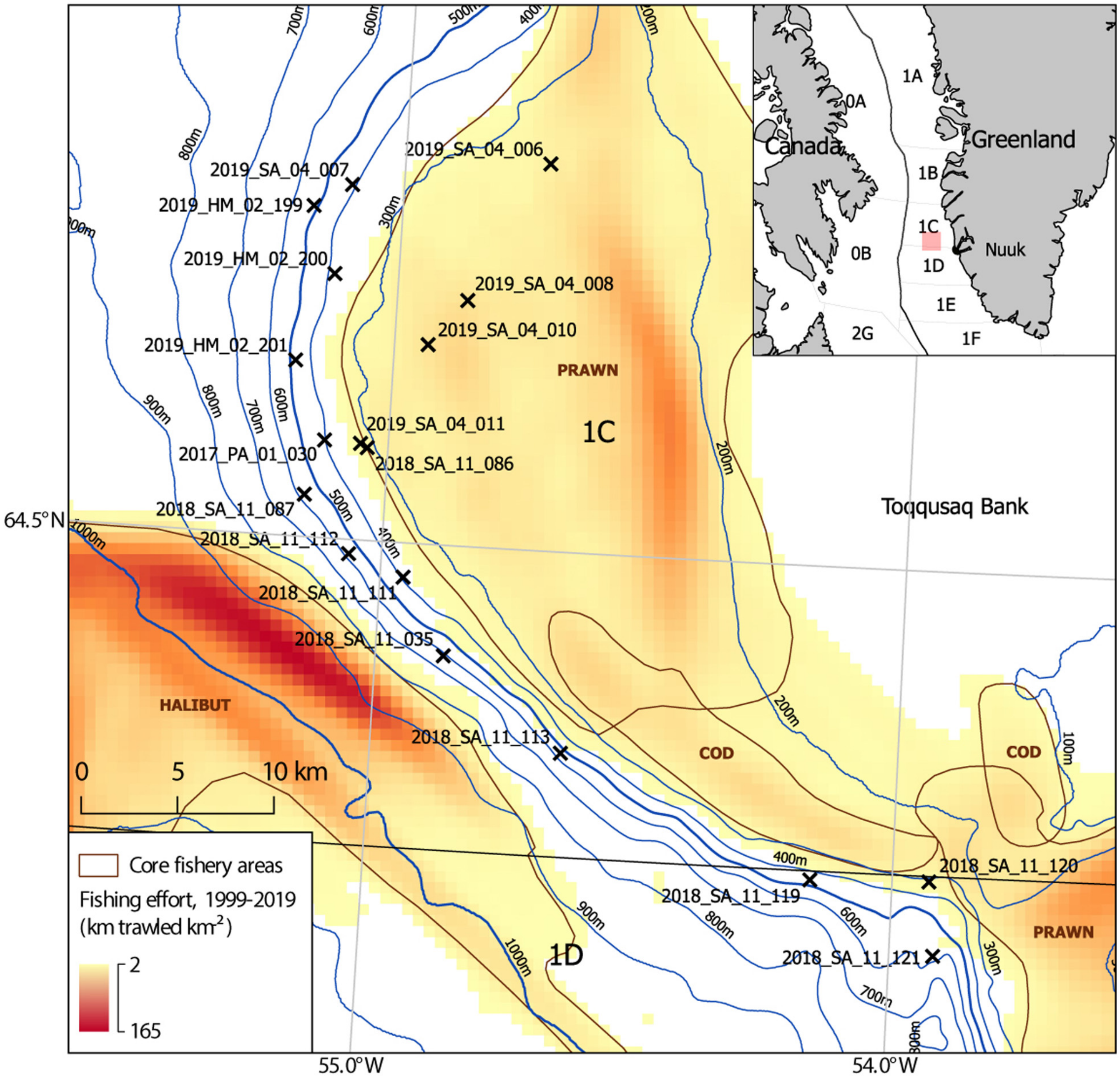

FIGURE 1 | Map of study site showing the location of benthic video sled survey stations (*n* = 18), on the continental slope of the Toqqusaq Bank, west Greenland. NAFO Divisions are indicated. Video sled stations (X) are drawn at the ship's position at the middle of each tow. The video sled station name indicates the year, vessel, cruise number, and station number (Year_Ship_Leg_Station number). The two letter ship codes indicate the *RV Paamiut* (PA), *RV Sanna* (SA), or *MT Helga Maria* (HM). Fishing effort is based on haul by haul logbook data from 1999 to 2019, used to determine the distance trawled per unit area (km trawled km^{-2}). The core target areas of halibut, prawn and cod trawling effort are annotated (brown), based on visual review of the effort dataset. This is intended to be indicative.

The method described by Nakajima et al. (2014) is modified to allow the estimation of the area *JBDK* (Eqs. 3–8).

$$\delta = \pi - \left(\frac{\pi}{2} + \theta + \alpha\right) \tag{3}$$

$$\gamma = 0.99\alpha \tag{4}$$

$$JK = 2\tan\left(\frac{\beta}{2}\right) \times \frac{OH}{\cos(\delta+\gamma)} \tag{5}$$

$$BD = 2\tan\left(\frac{\beta}{2}\right) \times \frac{OH}{\cos(\delta)} \tag{6}$$

$$GF = OH(\tan(\delta+\gamma) - \tan(\delta)) \tag{7}$$

$$JBDK = \frac{(JK+BD)}{2} \times GF \tag{8}$$

Where, *OH* the height of the camera was 0.55 m, θ the angle of incidence with the seafloor was 28.8° and the aperture angles (α and β) are determined as above (Eqs. 1 and 2). The area of seafloor analyzed in each image (*JBDK*) was estimated to be 8.23 m^2. This value is used throughout for estimating densities of taxa.

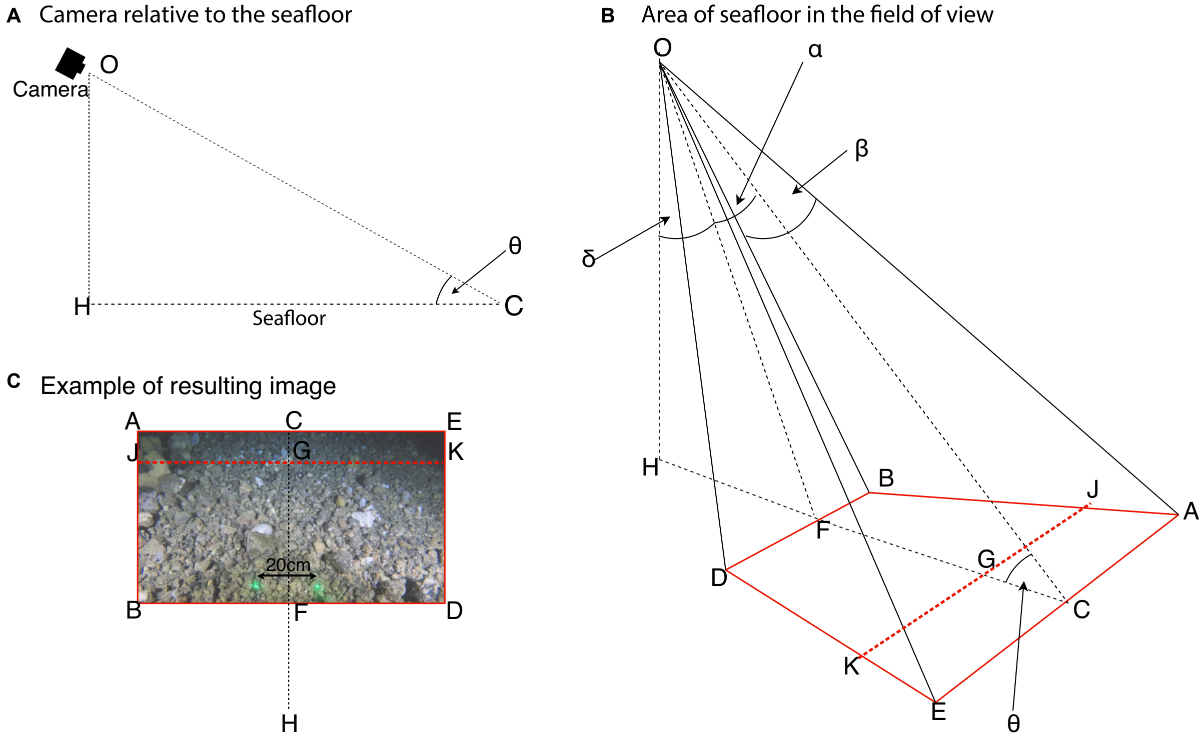

FIGURE 2 | Diagrammatic representation of the benthic video sled camera for determining the area of the field of view. **(A)** Shows the camera orientation relative to the seafloor. **(B)** Shows the camera position, aperture angles and area of seafloor (*ABDE*) in the camera's FOV (red line); with a cut-off line JK to exclude the portion of the image unsuitable for analysis (red dashed line). **(C)** Shows an example image of the seafloor, in relation to **(A,B)**, for which the area *JBDK* is calculated and used in the estimation of fauna density. Adapted from: Nakajima et al. (2014).

Image Processing

Extraction of Images

Quantitative analysis was conducted on still images extracted from videos. All footage was reviewed and useable video segments identified, excluding segments where: (i) suspended sediment or other material obscured > 5% of the screen; (ii) illumination was inadequate due to one or more torches being partially or wholly obscured; (iii) the sled was not level and on the seabed; (iv) the sled was stationary; or (iv) the sled was moving too fast, which occurs at the end of tow when the winch is being used to retrieve the sled. Stills were extracted at 15 s intervals, from the useable segments. At each 15 s interval the frame with the sharpest focus within that second of video was selected, where 1 s of video was represented by 48 frames (GoPro4) or 60 frames (GoPro5).

The frame with sharpest focus was that with the highest value of standard deviation based on the Laplacian Convolution Kernal of a grayscaled version of each frame, determined using the "convolve" function of the R package "imager" (R Core Team, 2013; Barthelmé, 2017). Convolution kernels are an established way of measuring the focus of an image within a range of similar images (Riaz et al., 2008). The resulting stills were reviewed to ensure they met the criteria above, any exceptions were removed.

Processing of Images

The images were then uploaded to a browser based annotation platform, BioImage Indexing, Graphical Labeling and Exploration 2.0 (BIIGLE 2.0) (Ontrup et al., 2009; Langenkämper et al., 2017). The platform allows the creation of custom hierarchical label trees, which can be used to annotate features within images and/or be applied at the level of the image. A representative subset of the images was reviewed by the team to agree on a consistent approach to annotation. This was informed by previous experience of image and physical sampling surveys in the region. To ensure consistency a single member of the team made all primary annotations, for both fauna and substrate.

Fauna annotation

The nature of the imagery means not all fauna can be consistently seen and reliably identified. For example, small fauna closest to the camera (bottom of the image) may not necessarily be visible or identifiable at the back of the field of view (top of the image). Therefore, only taxa that could be consistently identified within and between images were selected for annotation and analysis. Additionally, annotation was restricted to those taxa that form structurally significant/complex components of the habitats and thus are of relevance to criteria (iv) of the FAO's VME definition (FAO, 2009). To allow density estimation only taxa where discrete individuals or colonies could be identified were annotated. The taxa which met these conditions, are shown with reference to whether they are considered VME indicator taxa by Northwest Atlantic Fisheries Organization (NAFO) and NEAFC (**Table 1**).

When annotating each image the section of video that it was obtained from was reviewed alongside the image. A moving perspective was found to be useful in aiding identification of taxa and distinguishing individuals or differentiating between separate colonies.

Genera of Nephtheidae (*sensu lato*) found in west Greenland are *Gersemia, Duva*, *Drifa*, and *Pseudodrifa* (Jørgensen et al., 2013). The current taxonomy in the World Register of Marine Species (WoRMS) lists all these as belonging to the family Nephtheidae. Although the genus *Gersemia* is currently still formally placed in Nephtheidae, it is widely regarded as Alcyoniidae (McFadden et al., 2006; Williams, 2013). These genera are hard to distinguish from imagery (Buhl-Mortensen et al., 2019) and so throughout this study have been treated as Nephtheidae (*sensu lato*) and collectively referred to a cauliflower corals.

Substrate annotation

Substrates were determined by annotation at the level of the image. The revised EUNIS Habitat Classification (Davies et al., 2004), which includes deep-sea specific categories, was previously adapted by Gougeon et al. (2017) for classifying substrates in imagery from west Greenland. For the purpose of this study this is further modified with clarified descriptions (A6.1.4 and A6.2.1) and two new subclasses (A6.1.5 and A6.2.2). Only those sub-classes used in this study are described here (**Table 2** and **Figure 3**).

TABLE 1 | Taxa selected for annotation in images. For each taxon NAFO (NAFO, 2012) and NEAFC (2014) guidance was consulted to determine if the taxa is considered a VME indicator.

Common name(s)	Phylum	Taxon/ annotation label	VME indicator?	
			NAFO	NEAFC
Bryozoans	Bryozoa	Alcyonidiidae* (*Alcyonidium gelatinosum*)	No	No
Anemones	Cnidaria	Actiniaria	No	No
Gorgonians	Cnidaria	Acanthogorgiidae	Yes	Yes
		Paragorgiidae	Yes	Yes
		Plexauridae	Yes	Yes
		Primnoidae	Yes	Yes
Soft corals	Cnidaria			
Mushroom soft corals		Alcyoniidae	No	No
Cauliflower corals		Nephtheidae	No	Yes
Feather stars	Echinodermata	Antedonidae	Yes†	Yes
Sponges	Porifera	Axinellidae	Yes	Yes
		Geodiidae	Yes	Yes
		Polymastiidae	Yes	Yes
		Rossellidae	Yes	Yes
		Porifera massive		
		Porifera branching		
		Porifera encrusting		

**It is thought that all annotations made using this label were of Alcyonidium gelatinosum. †Only Trichometra cubensis from the Antedonidae family.*

Modeling

Data processing and analysis was performed in R (R Core Team, 2013). A probabilistic approach was used to determine whether the taxa selected for annotation were positively, negatively, or randomly associated with one another. The observed co-occurrence was compared to the expected co-occurrence where the latter is the product of the two species' probability of occurrence multiplied by the number images (n = 1,239) (Veech, 2013). Associations were considered significant where the probability of the observed frequency of concurrence is < 0.05, were the taxa distributed independently of one another. This was performed using the "co-occur" package in R (Griffith et al., 2016).

Mapping

The BedMachine version 3, 150 m resolution bathymetry grid (Morlighem et al., 2017) was used to produce bathymetric contours in figures and for describing the boundary of the proposed VME.

Representation of fishing effort is based on haul-by-haul logbook data from the Greenland Fishery Licence Control (GFLK) from fisheries employing demersal trawl gear from 1999 to 2019, all species and vessels inclusive. Raw data from GFLK was processed and recalculated in SAS statistical software (SAS Institute, 2019) to establish an annual data set with information on the target species, gear type, position, haul distance, and speed. No information on gear width is available, so the transversal coverage of each haul is unknown. The data set was further processed using Safe FME Workbench software (Safe Software, 2019) to establish line vectors from start and end haul positions, removing displaced positions and unrealistic long and fast hauls. The line vectors representing the hauls were interpolated with Python using the ESRI Spatial Analyst Line Density function (ESRI, 2013) with a 5 km search radius to a 1 km grid, and the result hereof further calculated against a mask of the proportion of sea and land. The resulting raster represents the distance trawled per unit area (km trawled km^{-2}).

RESULTS

Station Data

A total of 18 video sled stations were selected from which 1,239 images were extracted for annotation (**Table 3**). This represents a total area analyzed of ~10,000 m^2.

Fauna Observations

A total of 44,035 annotations of the selected fauna were made. The most numerous annotations were anemones (15,531) and cauliflower corals (11,633). The anemones appeared to be predominantly Hormathiidae. The least frequent were gorgonians, with just 250 annotations of Acanthogorgiidae,

TABLE 2 | Substrate classes used to label images sampled from videos. Substrate classes are based on the revised EUNIS Habitat Classification (Davies et al., 2004), as adapted by Gougeon et al. (2017) and further modified here.

EUNIS	Sub-class	Description
A Marine habitats		
A6 Deep-sea bed		
A6.1 Deep sea bedrock and artificial hard substrate		
	A6.1.4 Coarse rocky ground (R)	Predominantly rocky material of varying sizes including gravel (< 4 cm) and cobbles (4–20 cm).
	A6.1.5 Coarse rocky ground with boulders (Rb)	Rocky material of varying sizes including gravel (< 4 cm) and cobbles (4–20 cm), with boulders (> 20 cm) present.
A6.2 Deep-sea mixed substrata		
	A6.2.1 Gravelly mud (M)	Mud with gravel (< 4 cm).
	A6.2.2 Gravelly mud with boulders (Mb)	Mud with gravel (< 4 cm), with boulders (> 20 cm) present.

Only those sub-classes used in this study are described.

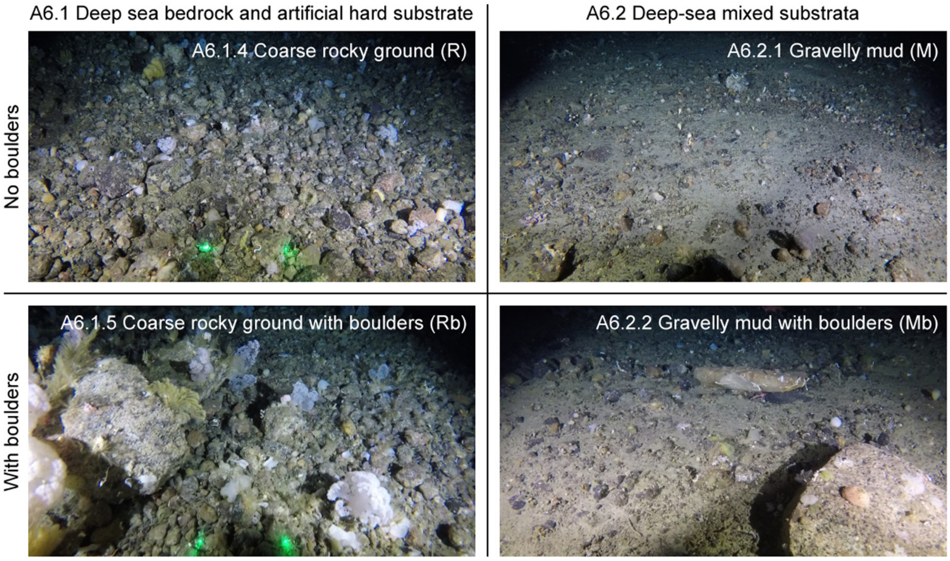

FIGURE 3 | Example image of each type of substrate class used to label images sampled from videos. Substrate classes are based on the revised EUNIS Habitat Classification (Davies et al., 2004), as adapted by Gougeon et al. (2017) and further modified here. Examples are taken from images used in the analysis. Where present laser dots (green) are 20 cm apart.

Paragorgiidae, Plexauridae, and Primnoidae combined. The mean (**Table 4**), minimum and maximum (**Table 5**) densities of annotated taxa are shown for each station, aggregated to a parent label where appropriate. Cauliflower corals were the only coral present at all stations, with a maximum density of 9.36 m^{-2}. The maximum density of any coral taxa was mushroom soft corals 13.37 m^{-2}. The maximum density of any taxa was anemones 18.23 m^{-2}.

There were a number of different distinct assemblages, often characterized by a high density of one particular taxon. Examples of the differing assemblages showing high densities of particular taxa are shown (**Figure 4**). Assemblages dominated by cauliflower corals on rocky substrates, with and without boulders, up to a maximum density of 9.36 m^{-2} (**Figure 4A**), were seen at multiple stations, with varying densities of feather stars, anemones and sponges also present. In some cases a similar assemblage was seen, in terms of species composition but instead dominated by high densities of anemones (**Figure 4B**), feather stars (**Figure 4C**), and sponges (**Figure 4D**). Patches dominated by mushroom soft corals, with other megafauna absent or occasional, were observed on rocky ground, where the substrate was largely homogenous gravel (< 4 cm) (**Figure 4E**). This assemblage was common in images from stations 2018_SA_11_087 and 2018_SA_11_112, with a maximum observed mushroom soft coral density of 13.37 m^{-2} (**Table 5**). Assemblages dominated by the bryozoan *Alcyonidium gelatinosum,* sometimes with sponges present were seen on both rocky and muddy substrates to a maximum density of 7.90 *A. gelatinosum* m^{-2} (**Figure 4F**).

There was considerable heterogeneity in the abundance and composition both within and between stations (**Tables 4**, **5** and **Figure 5**). Cauliflower corals, anemones, and sponges were present at all stations, whilst the bryozoan *A. gelatinosum*, gorgonians, feather stars and mushroom soft corals were not observed at all stations. Comparing those stations where taxa were present, the mean density varied by at least an order of magnitude in each taxon, with the exception of sponges whose

TABLE 3 | List of stations where the benthic video sled was deployed on the continental slope of the Toqqusaq Bank, west Greenland.

Station	Position	Mean depth (m)	Duration (mins)	Tow length (m)	Images	Area in images (m^2)
2017_PA_01_030	64.580°N, 55.122°W	401	15	402	23	189
2018_SA_11_035	64.409°N, 54.871°W	446	15	415	44	362
2018_SA_11_086	64.576°N, 55.040°W	321	46	1,500	131	1,078
2018_SA_11_087	64.535°N, 55.154°W	585	48	1,835	133	1,095
2018_SA_11_111	64.472°N, 54.956°W	391	30	1,129	77	634
2018_SA_11_112	64.488°N, 55.062°W	579	30	978	81	667
2018_SA_11_113	64.335°N, 54.638°W	561	30	982	84	691
2018_SA_11_119	64.243°N, 54.155°W	415	30	975	110	905
2018_SA_11_120	64.246°N, 53.930°W	314	30	915	107	881
2018_SA_11_121	64.185°N, 53.917°W	557	15	481	37	305
2019_HM_02_199	64.771°N, 55.171°W	537	19	634	59	486
2019_HM_02_200	64.717°N, 55.123°W	368	15	416	39	321
2019_HM_02_201	64.644°N, 55.187°W	482	17	490	22	181
2019_SA_04_006	64.817°N, 54.721°W	274	17	561	60	494
2019_SA_04_007	64.790°N, 55.100°W	390	15	485	60	494
2019_SA_04_008	64.702°N, 54.865°W	287	15	539	63	518
2019_SA_04_010	64.663°N, 54.936°W	293	15	696	53	436
2019_SA_04_011	64.579°N, 55.053°W	315	15	488	56	461
Totals			**417**	**13,921**	**1,239**	**10,198**

The following are provided for each station: the position (ship's location at the midpoint of tow), mean depth (m), duration of tow (minutes), length of tow (m), number of images extracted from the video and total area of the extracted images (m^2). The duration of the tow (minutes) is provided along with the number of images extracted for analysis from the video. The Station name indicates the year, vessel, cruise number and station number (Year_Ship_Leg_Station number). The two letter ship codes indicate the RV Paamiut (PA), RV Sanna (SA), or MT Helga Maria (HM).

TABLE 4 | Observed mean (standard deviation) densities (individuals or colonies m^{-2}) of taxa at each station, based on the number of annotations from all images for each station, adjusted for the area of the field of view in the images (8.23 m^2).

Station	Mean (standard deviation) density, individuals or colonies m^{-2}						
	Bryozoan *(A. gelatinosum)*	Anemones	Gorgonians	Mushroom soft corals	Cauliflower corals	Feather stars	Sponges
2017_PA_01_030	0.11 (0.17)	0.64 (0.51)	0.01 (0.03)	–	2.92 (1.25)	0.08 (0.17)	1.91 (0.70)
2018_SA_11_035	0.06 (0.10)	0.03 (0.07)	0.25 (0.23)	0.00 (0.02)	1.74 (0.91)	0.01 (0.03)	0.72 (0.50)
2018_SA_11_086	0.14 (0.18)	8.92 (3.75)	0.00 (0.03)	–	0.65 (0.71)	0.00 (0.01)	0.42 (0.37)
2018_SA_11_087	0.04 (0.08)	0.18 (0.29)	0.03 (0.14)	0.89 (2.14)	2.41 (1.65)	1.69 (2.08)	0.70 (0.63)
2018_SA_11_111	0.06 (0.13)	0.21 (0.18)	0.05 (0.13)	–	2.30 (1.17)	0.02 (0.09)	1.06 (0.63)
2018_SA_11_112	–	0.07 (0.12)	0.05 (0.17)	0.88 (1.57)	0.67 (0.85)	1.42 (2.50)	0.41 (0.34)
2018_SA_11_113	0.01 (0.06)	0.05 (0.08)	0.04 (0.13)	0.03 (0.13)	0.20 (0.28)	0.09 (0.22)	0.78 (0.53)
2018_SA_11_119	0.00 (0.02)	0.01 (0.03)	0.00 (0.03)	0.01 (0.04)	0.28 (0.66)	0.05 (0.13)	1.60 (0.68)
2018_SA_11_120	2.26 (1.68)	0.01 (0.04)	0.00 (0.05)	–	2.18 (1.98)	0.00 (0.02)	0.77 (0.60)
2018_SA_11_121	–	0.00 (0.02)	0.03 (0.08)	0.02 (0.10)	0.06 (0.12)	0.54 (0.63)	0.88 (0.52)
2019_HM_02_199	0.01 (0.04)	0.14 (0.25)	–	0.01 (0.06)	0.04 (0.10)	0.35 (0.79)	0.48 (0.43)
2019_HM_02_200	0.01 (0.03)	0.39 (0.29)	0.02 (0.05)	–	2.30 (1.69)	0.01 (0.03)	1.10 (0.91)
2019_HM_02_201	–	0.03 (0.09)	0.01 (0.04)	–	0.96 (0.86)	0.53 (0.79)	0.75 (0.60)
2019_SA_04_006	–	0.01 (0.04)	–	–	0.10 (0.12)	–	1.45 (0.77)
2019_SA_04_007	0.02 (0.06)	0.23 (0.26)	–	–	2.31 (1.91)	0.02 (0.05)	0.98 (0.65)
2019_SA_04_008	1.50 (1.01)	0.01 (0.03)	–	–	0.03 (0.08)	–	0.86 (0.47)
2019_SA_04_010	0.00 (0.02)	0.00 (0.02)	–	–	0.24 (0.27)	–	0.70 (0.45)
2019_SA_04_011	–	10.94 (2.85)	–	–	1.37 (0.61)	0.00 (0.02)	0.37 (0.31)

A dash (–) indicates the taxon was not observed in the images extracted from the video obtained at that station. Gorgonians includes the annotation labels Acanthogorgiidae, Paragorgiidae, Plexauridae, and Primnoidae. Sponges includes the annotation labels Axinellidae, Geodiidae, Polymastiidae, Rossellidae, Porifera massive, Porifera branching, and Porifera encrusting.

density was more evenly distributed (**Table 4**). There was also considerable variation in densities within stations demonstrated by the range in minimum and maximum values (**Table 5**). This indicates an inherent patchiness, which is illustrated by visualizing data from 2018_SA_11_087 (**Figure 5**). Areas where the assemblage is dominated by cauliflower corals, feather stars

TABLE 5 | The minimum and maximum (min-max) densities (individuals or colonies m^{-2}) of taxa observed within a single image for each station, based on the number of annotations adjusted for the area of the field of view in the image (8.23 m^2).

Station	Minimum and maximum (min-max) density within a single image, individuals or colonies m^{-2}						
	Bryozoan *(A. gelatinosum)*	Anemones	Gorgonians	Mushroom soft corals	Cauliflower corals	Feather stars	Sponges
2017_PA_01_030	0.00–0.49	0.12–1.94	0.00–0.12	–	0.97–6.32	0.00–0.73	0.49–3.40
2018_SA_11_035	0.00–0.36	0.00–0.24	0.00–0.85	0.00–0.12	0.12–3.89	0.00–0.12	0.00–2.79
2018_SA_11_086	0.00–0.85	0.85–18.23	0.00–0.24	–	0.00–5.47	0.00–0.12	0.00–2.19
2018_SA_11_087	0.00–0.36	0.00–2.43	0.00–1.22	0.00–13.37	0.00–8.63	0.00–8.38	0.00–4.01
2018_SA_11_111	0.00–0.61	0.00–0.85	0.00–0.73	–	0.12–4.62	0.00–0.73	0.12–2.55
2018_SA_11_112	–	0.00–0.49	0.00–1.09	0.00–6.80	0.00–3.52	0.00–11.66	0.00–1.22
2018_SA_11_113	0.00–0.49	0.00–0.36	0.00–0.97	0.00–0.97	0.00–1.34	0.00–1.09	0.00–2.92
2018_SA_11_119	0.00–0.12	0.00–0.12	0.00–0.24	0.00–0.24	0.00–6.56	0.00–0.85	0.24–3.40
2018_SA_11_120	0.00–7.90	0.00–0.24	0.00–0.49	–	0.00–8.38	0.00–0.12	0.00–3.40
2018_SA_11_121	–	0.00–0.12	0.00–0.36	0.00–0.49	0.00–0.49	0.00–2.07	0.12–1.94
2019_HM_02_199	0.00–0.24	0.00–1.46	–	0.00–0.36	0.00–0.49	0.00–4.13	0.00–1.82
2019_HM_02_200	0.00–0.12	0.00–1.22	0.00–0.24	–	0.00–5.83	0.00–0.12	0.00–5.59
2019_HM_02_201	–	0.00–0.36	0.00–0.12	–	0.00–2.67	0.00–2.19	0.00–1.70
2019_SA_04_006	–	0.00–0.12	–	–	0.00–0.36	–	0.24–3.28
2019_SA_04_007	0.00–0.36	0.00–1.34	–	–	0.00–9.36	0.00–0.24	0.24–3.65
2019_SA_04_008	0.00–5.22	0.00–0.12	–	–	0.00–0.36	–	0.12–2.31
2019_SA_04_010	0.00–0.12	0.00–0.12	–	–	0.00–1.34	–	0.00–1.82
2019_SA_04_011	–	6.56–16.28	–	–	0.24–3.40	0.00–0.12	0.00–1.22

A dash (–) indicates the taxon was not observed in the images extracted from the video obtained at that station. Gorgonians includes the annotation labels Acanthogorgiidae, Paragorgiidae, Plexauridae, and Primnoidae. Sponges includes the annotation labels Axinellidae, Geodiidae, Polymastiidae, Rossellidae, Porifera massive, Porifera branching, and Porifera encrusting.

and sponges (**Figures 5A,C**) are interspersed by patches of mushroom soft corals (**Figure 5B**) where other taxa are absent.

Significant positive and negative associations between pairs of taxa were observed (**Figure 6**). Cauliflower corals were positively associated with feather stars, gorgonians and anemones, which was more positive associations than any other taxa. Co-occurrence of cauliflower corals with feather stars and anemones was readily apparent in the imagery (**Figures 4A–D**).

There were other taxa, which could not be consistently identified and/or annotated in the imagery, but contributed to the structural diversity of the habitats. They can be observed in some sections of video and where abundant clearly form a significant component of this habitat. Specifically this includes, calcified bryozoans, from the families Celleporidae, Flustridae, Horneridae, Myriaporidae, and Phidoloporidae, as well as hydrozoans from the families Aglaopheniidae and Sertulariidae.

Substrates

The dominant substrates were coarse rocky ground (R and Rb), with these being the only substrates identified in 11 of the stations ($n = 18$) (**Figure 7**). Conversely, gravelly mud substrates (gM and GMb) were the only substrates in just two of the stations. Boulders were present at all the stations (**Figure 7**), and were typically observed intermittently during the course of a tow (**Figure 5**).

The number of annotations of some taxa varied with substrate. Anemones, mushroom soft corals, feather stars and cauliflower corals were more prevalent on hard substrates (R and Rb) (**Figure 8**). Habitats dominated by cauliflower corals and or feather stars were typically found where there was a heterogeneity in size of the rocky material, with a combination of gravel, cobbles, and boulders (**Figures 4A,C,D**). Conversely, patches of mushroom soft corals appeared to only be found on more uniform gravel substrates (**Figure 4E**). These differences in the size of rocky material were not quantified, with the exception of differentiating between the presence and absence of boulders.

DISCUSSION

Analysis of the imagery from 18 stations showed heterogeneity in the substrates and communities on the slope of the Toqqusaq Bank. This patchiness was observed within stations, with notable variation across single video sled tows as well as between stations. Several distinct assemblages were observed, in some cases the assemblage was dominated by a single taxa forming a patch of habitat, with anemone fields, mushroom soft coral beds and areas dominated by the bryozoan *A. gelatinosum*. The assemblages which appeared to be most structurally complex and diverse, were those characterized by high densities of cauliflower corals, feather stars and sponges. In such assemblages the combined effect of observed densities is a habitat with considerable structural heterogeneity, found on coarse rocky substrates. Intuitively, substrate likely plays an important part in determining the assemblage present. Previously, Baker et al. (2012) found that substrate type had a clear influence on the occurrence and abundance of deep-sea corals in the Labrador Sea, they reported that the greatest diversity was seen in video

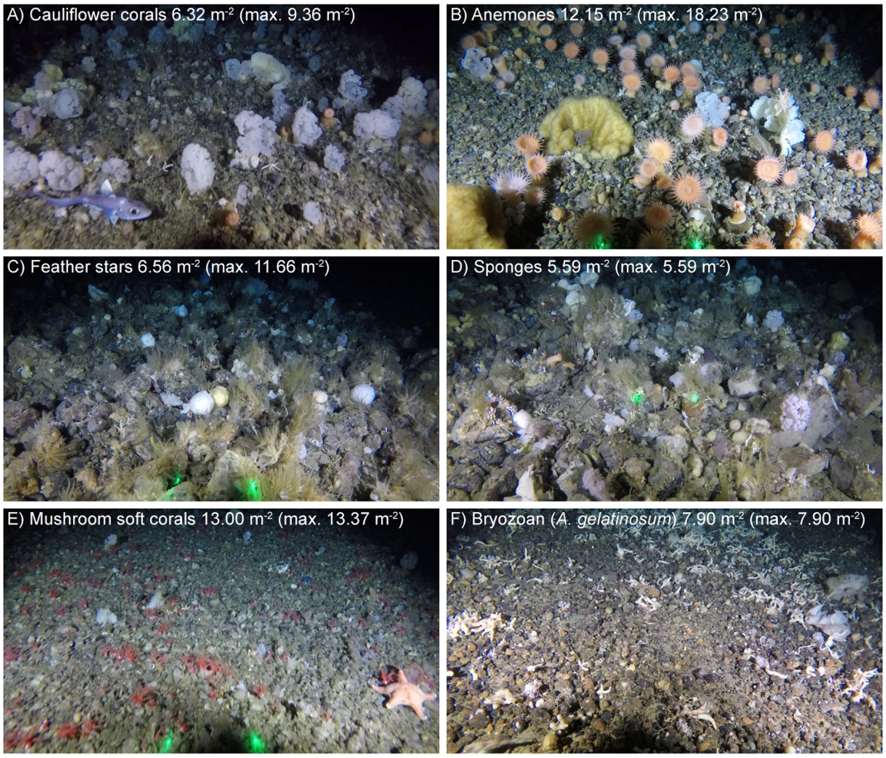

FIGURE 4 | Examples of different assemblages with high density of: **(A)** Cauliflower corals; **(B)** Anemones; **(C)** Feather stars; **(D)** Sponges; **(E)** Mushroom soft corals; and **(F)** Bryozoan (*A. gelatinosum*). Images were selected for illustrative clarity. The density of the highlighted taxa within each image is reported (along with the maximum observed density in all images for reference). Where present, laser dots (green) are 20 cm apart.

transects with a mosaic of substrate types. Many of the taxa selected for annotation in this study are sessile and require a hard substrate for attachment, for example it is known that most soft corals and gorgonians require hard substrates for larval settlement and growth (Pérez et al., 2016). Some taxa (anemones, mushroom soft corals, feather stars and cauliflower corals) showed a clear preference for the coarse rocky substrates, whilst annotations of other taxa were more evenly distributed across the substrate classes.

Defining Soft Coral Gardens

Habitat classification systems support conservation goals by providing universally understood definitions that can be used to describe and map the distribution of habitats, a necessary pre-requisite for spatial management (Howell et al., 2010). The term "coral garden" was first applied to dense aggregations of non-reef forming corals, dominated by gorgonians (Bullimore et al., 2013). A formal definition offered by the Oslo and Paris Conventions (OSPAR) applies to a much wider range of cold-water corals on both hard and soft substrates (ICES, 2007; OSPAR Commission, 2010). This definition captures a range of different habitats and does not therefore represent a single ecological unit (Bullimore et al., 2013).

In their cold-water coral classification scheme, Davies et al. (2017) proposes a biotope consisting of cold-water Alcyoniina on hard/mixed substrate, specifically, Nephtheidae (cauliflower corals) and *Anthomastus* sp. (mushroom soft coral, family: Alcyoniidae). Whilst the proposed biotope refers to *Anthomastus* sp., we suggest that this could be interpreted more broadly as mushroom soft corals, given: (i) the known diversity of mushroom soft coral species in the North Atlantic (Molodtsova, 2013); (ii) the taxonomic revision of genera in Alcyoniidae; and (iii) the fact that close relatives have similar gross morphologies and likely occupy similar niches. In the present study, the imagery does not allow greater taxonomic resolution with regards mushroom soft corals. The supplementary material in the Davies et al. (2017) classification scheme, describes the cold-water Alcyoniina on hard/mixed substrate biotope as being known from depths of 600 m in Iceland and Norway (Guillaumont et al., 2016) and provides an example image. The example image is comparable to the coral garden habitat described here. The NEAFC consider cauliflower corals to be a VME indicator taxa for a VME habitat type described as "cauliflower coral fields," which is listed as a soft-bottom habitat (NEAFC, 2014).

There is no accepted quantitative definition of soft coral gardens or coral gardens more broadly. Rogers et al. (2015) propose that to qualify the density of coral garden species must exceed 10 times the background level. Practically this relies on a good understanding of the background level which is rarely the case, including in this context. Further, since coral gardens by their nature are comprised of multiple species, it is not clear whether densities should be considered

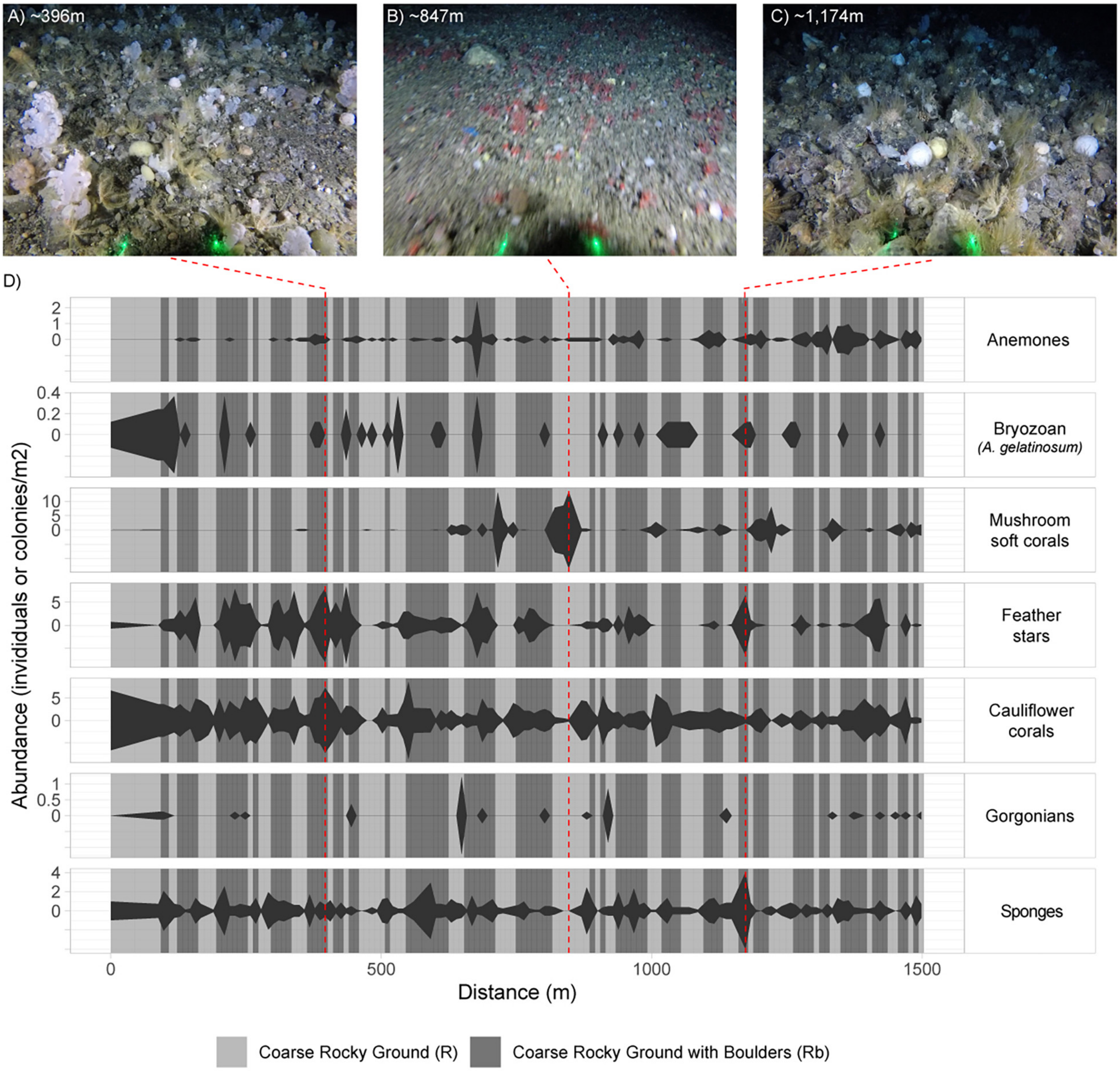

FIGURE 5 | Kite diagram showing variation in faunal abundance and substrate across an example station (2018_SA_11_087), based on fauna and substrate annotations of images sampled from the video. The width of kite is determined by the observed abundance in the image sampled at that distance along the tow. Distance is based on the speed of the vessel and the time elapsed from touchdown. The background is shaded according to substrate observed in each image. Substrate type and faunal abundance is interpolated between images to produce an illustrative representation. The example images **(A–C)** are included to illustrate the variation across the station as described by **(D)**. The left and right extremities of example images have been cropped and thus do not display the full field of view (FOV). Laser dots (green) are 20 cm apart.

individually or the combined density of the species present compared with combined background level. Thus, this study must rely on the application of "expert" judgment to make a determination and in doing so provide a quantitative description that can be used to inform the development of revised definitions in the future. This judgment is guided by the indicative densities in the description of the broader coral garden habitat type (ICES, 2007; OSPAR Commission, 2010). Specifically, these suggest colony densities of 1–7 m^{-2} generally, 0.5–2 m^{-2} for small gorgonians (Acanthogorgiidae and Primnoidae) and 0.01–0.02 m^{-2} for larger gorgonians (Paragorgiidae). It has been suggested that these ranges can be used to differentiate between comparatively sparse and dense coral gardens (ICES, 2007). These indicative density thresholds are not accompanied by a requirement for the density to be present over a minimum area, which would be

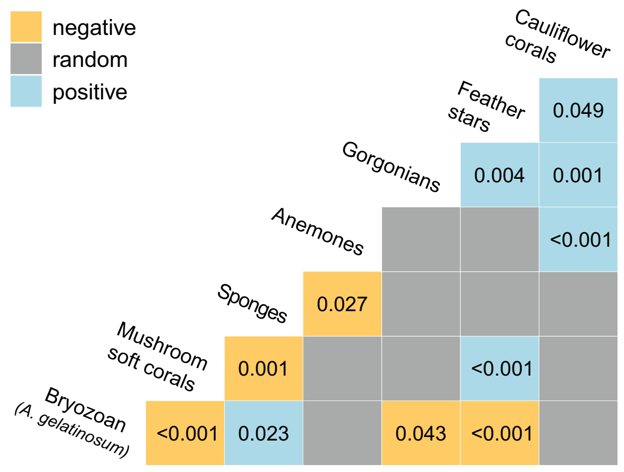

FIGURE 6 | Heat map showing the positive and negative associations between taxa as determined by a probabilistic co-occurrence model (Veech, 2013). For each pair the observed frequency of co-occurrence within images ($n = 1,239$) is either, significantly large and greater than expected (positive association), significantly small and less than expected (negative association), or not significantly different and approximately equal to expected (random association). Associations are considered significant where the probability of the observed frequency of concurrence is < 0.05 were the taxa distributed independently of one another. *P*-values are provided for significant associations.

a useful additional guidance, pending consensus among the scientific community.

Cauliflower corals are the most abundant corals in the study area. They make a significant contribution to structural complexity and exhibited more positive associations than any other taxa. They are therefore an obvious candidate to serve as an indicator species for this soft coral garden habitat. A mean density threshold of 1 colony m^{-2} is applied to determine those stations where the soft coral garden habitat is present. The lower bound of the generic indicative density suggested by OSPAR is used, as it is recognized that the study area is inherently patchy. To use a higher threshold would potentially exclude stations with patches of cauliflower corals at significant densities, indicating areas of coral garden. Excluding these would not recognize their presence in an ecosystem displaying a mosaic nature, with patches of soft coral garden present among differing substrates and assemblages. Those 8 out of 18 stations which meet this threshold are highlighted (**Figure 9**).

Does This Soft Coral Garden Constitute a Vulnerable Marine Ecosystem (VME)?

Soft coral gardens and cauliflower corals more generally, are both recognized as VMEs and VME indicators, respectively, by NEAFC, the RFMO for the Northeast Atlantic (NEAFC, 2014). Conversely, neither are considered a VME or indicator by NAFO, the RFMO for the Northwest Atlantic (NAFO, 2012). This apparent inconsistency could in theory reflect a fundamental difference in the nature of deep-sea benthic ecosystems in the Northwest Atlantic compared to those in the Northeast Atlantic, though no such rational is provided by either RFMO. More likely this is the product of differing interpretations of the VME definition by experts in separate RFMOs. This lack of coordination and harmonization between adjacent RFMOs has been noted by others (Bell et al., 2019). Therefore here, direct reference is made to the underlying VME definition, with each criteria addressed in turn (FAO, 2009).

Uniqueness or Rarity

There is no evidence to support recognition as a VME by virtue of the unique or rare criteria. The taxa observed have a wide distribution and are not known to be threatened globally. The rarity of the habitat is not known but similar assemblages have been reported elsewhere in the North Atlantic. The true spatial extent within Greenlandic waters is not known but it may well extend beyond the present study area along the continental slope.

Functional Significance of the Habitat

The soft coral garden habitat likely plays a functionally significant role, though this is not directly assessed here and only limited inferences can be made from the imagery. In general more is known about gorgonians than cauliflower corals. Buhl-Mortensen and Mortensen (2005) reported finding 114 associated species and nearly 4,000 individuals on the 25 *Paragorgia arborea* and *Primnoa resedaeformis* colonies they sampled. Krieger and Wing (2002) observed 10 mega faunal groups (rockfish, sea stars, nudibranchs, feather stars, basket stars, crabs, shrimps, snails, anemones, and sponges) associated with *Primnoa* spp., which was used to either prey on, suspension feed from, or provide protection. Cauliflower corals are known to host a variety of species. *Gersemia* spp. can be considered habitat-forming species, as the embryonic development of the basket stars (*Gorgonocephalus* spp.) may occur within the coral's tissues, with juveniles attached to the outside whilst feeding (Patent, 1970). As many as 118 small basket stars have been found on a single cauliflower colony (B. de Moura Neves, pers. comm.). Whilst not quantified, *Gorgonocephalus* spp. were observed on cauliflower corals in video and images in this study. The presence of cephalopods, decapods, Rajiformes and various fish was noted in images from this habitat. Grenadier fish (Macrouridae) and redfish (*Sebastes* spp.) were commonly encountered in videos and sampled images. Unpublished data from prawn stock assessment trawl and beam trawl surveys provides further insights into a rich community of benthic invertebrates associated with the observed soft coral garden habitat (**Supplementary Table 1**).

Fragility

The habitat should be considered fragile, as it is vulnerable to degradation by physical disturbance, especially trawling. The vulnerability of deep-sea gorgonians to trawling is well established (e.g., Freese et al., 1999; Witherell and Coon, 2000). The largest and perhaps most vulnerable species present was *Paragorgia arborea*. The ability to retract and recover from acute local injury may render cauliflower corals less vulnerable to mechanical disturbance than other corals with rigid skeletons and unretractable colonies (Henry et al., 2003). Nevertheless, these responses do not provide protection against removal. It

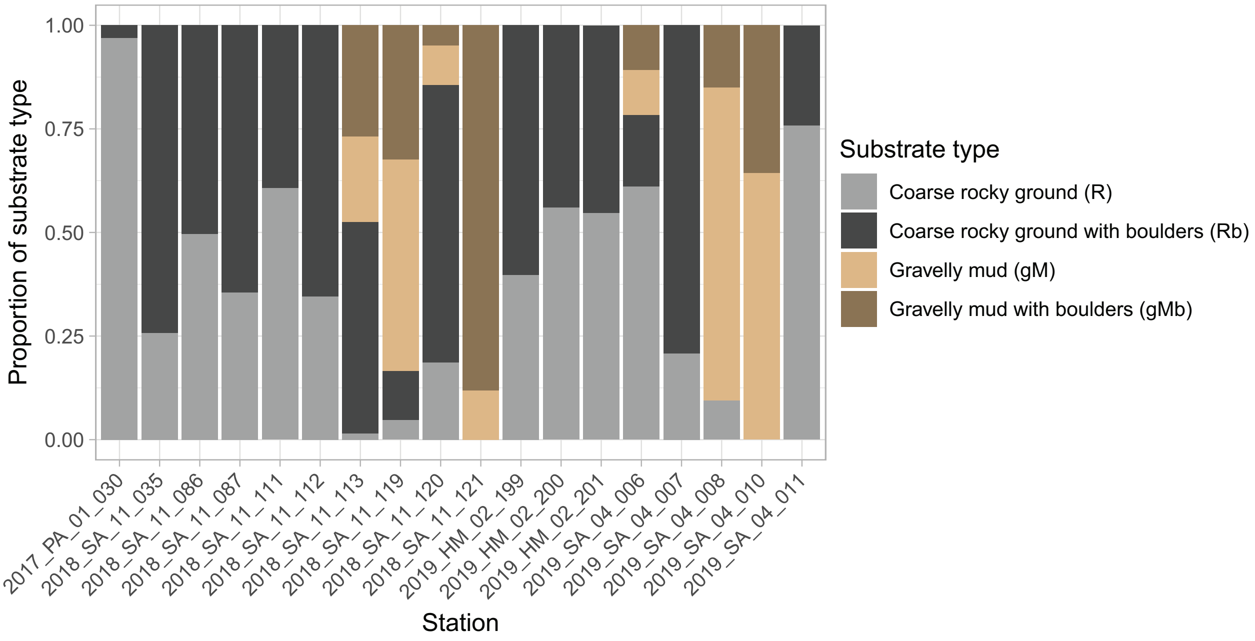

FIGURE 7 | Stacked bar chart showing proportion of each substrate type in images from each station. Substrate classes are based on the revised EUNIS Habitat Classification (Davies et al., 2004), as adapted by Gougeon et al. (2017) and further modified for the purposes of this study.

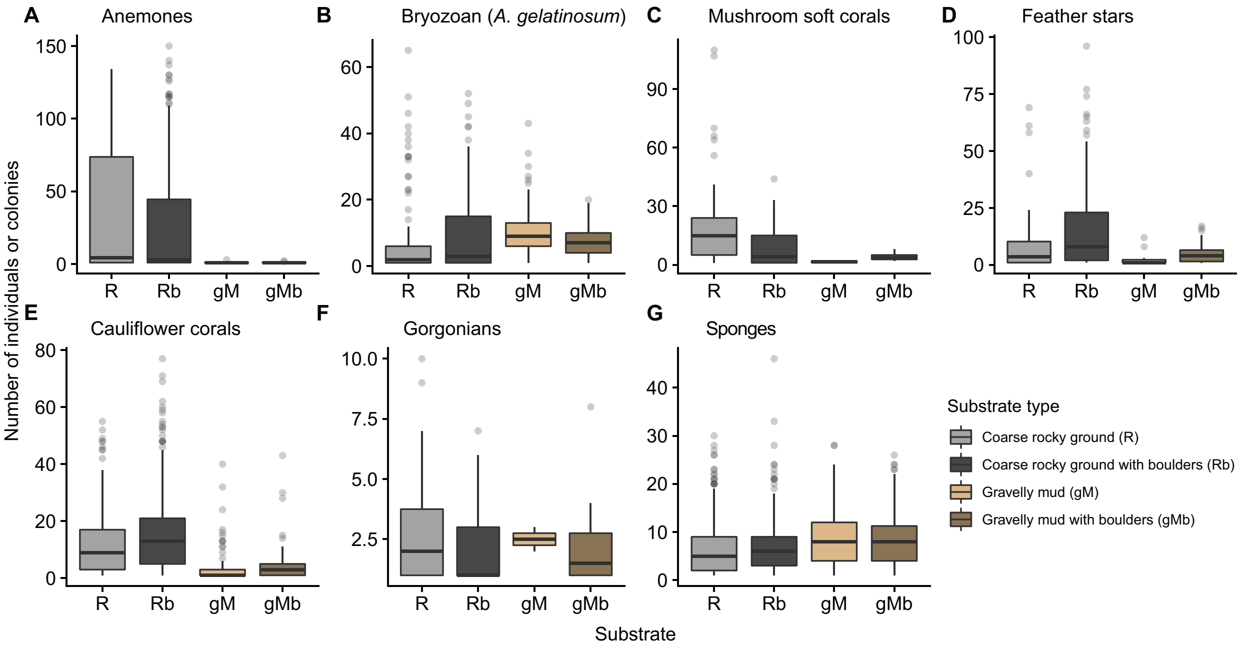

FIGURE 8 | Box-whisker plot showing the number of annotations of seven taxa **(A–G)** in images, which were annotated with one of four classes of substrate type. Substrate classes are based on the revised EUNIS Habitat Classification (Davies et al., 2004), as adapted by Gougeon et al. (2017) and further modified for the purposes of this study.

has been noted that cauliflower corals are prone to incidental bycatch in emerging deep-sea fisheries (Devine et al., 2019). Groundfish survey trawl data from the Grand Banks and Flemish Cap, confirm that soft coral biomass was the largest component of bycatch and that abundance was significantly lower in previously trawled areas (Murillo et al., 2010). In the Bering Sea, the biomass of *Gersemia* spp. has been found to be highest in untrawled areas (McConnaughey et al., 2000).

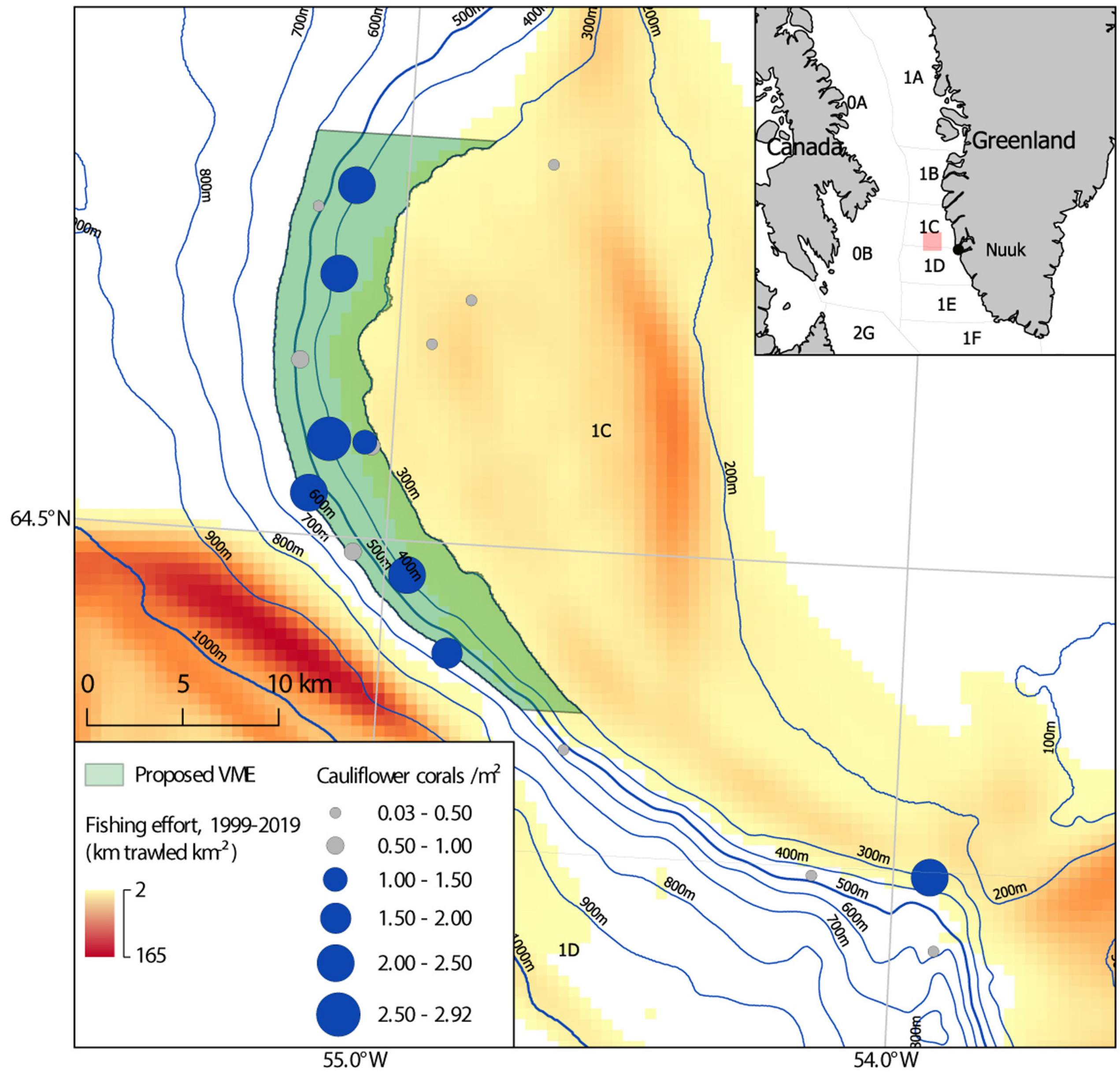

FIGURE 9 | Map of the 486 km^2 proposed soft coral garden vulnerable marine ecosystem (VME) (light green), on the continental slope of the Toqqusaq Bank, west Greenland. NAFO Divisions are indicated. The mean density of cauliflower coral colonies is shown (circles), with those stations exhibiting a density $\geq$ 1 m^2 highlighted in blue (< 1 m^2 gray). Fishing effort is based on haul by haul logbook data from 1999 to 2019, used to determine km trawled km^{-2}.

Similarly, Jørgensen et al. (2013) consider *Gersemia fruticosa, G. rubiformis, Drifa glomerata,* and *Duva florida* to be at "high risk" from trawling and found the highest biomass outside trawled areas in the Barents Sea. In the present study the lowest densities of cauliflower corals were seen in those stations (2019_SA_006, 2019_SA_008 and 2019_SA_010) within the trawling footprint, with gorgonians and mushroom soft corals also being absent there. This supports the idea that the component taxa of this soft coral garden are vulnerable to trawling. It may be the case that this coral garden assemblage is only observed in the relatively narrow section of the continental slope that has not been subject to fishing pressure to date.

Life-History Traits of Component Species That Make Recovery Difficult

Slow growth and long-life are exhibited by component taxa of this habitat, rendering recovery slow. To date studies on growth rates and longevity in deep-sea octocorals have focused on gorgonians (Pérez et al., 2016), whereas cauliflower corals have received less attention, not least because of the challenges associated with measuring soft coral colonies. Sherwood and Edinger (2009) report gorgonian axial growth rates as little as 0.56 cm year^{-1} for *Paramuricea* spp., 1.62 cm year^{-1} for *Paragorgia arborea*, and 1.00 cm year^{-1} for *Primnoa resedaeformis*, with ages exceeding 100 years. Laboratory study of larval and early growth of *G. fructicosa* and *D. florida*, found post-settlement growth to be very slow, suggesting a "sluggish recovery" following anthropogenic disturbance (Sun et al., 2011). Although, the authors note that this may be partially offset by the small size at sexual maturity and the potential for disturbance to release planulae from fertile colonies that grow into viable offspring. A similar study with *Drifa* sp. and *D. glomerata*, also suggested that early growth rates of primary polys was extremely slow with no budding of the primary polys of *Drifa* sp. in 21 months (Sun et al., 2010). Cordes et al. (2001) monitored *Heteropolypus ritteri* (mushroom soft coral; in the family Alcyoniidae; formerly in the genus *Anthomastus*) in the laboratory, finding slow initial growth became more rapid at intermediate size, before approaching an asymptote at 26–30 years. They observed that the slow growth and relative longevity was typical of other deep-sea organisms. Watling and Auster (2005) conclude that growth rates and patchy recruitment mean that recovery of alcyonacean communities following removal is likely to take a very long time.

Structural Complexity

Perhaps the most compelling justification for consideration as a VME, provided by the imagery collected, is the structural complexity created by the biotic components of this habitat. The combined effect of all the taxa annotated but especially cauliflower corals, feather stars, sponges and gorgonians, adds considerable structure at varying scales to the otherwise limited complexity of the coarse rocky substrates (**Figure 10**). Further structural complexity is added by the abundant bryozoans and hydrozoans that are present but were not quantified (**Figure 10**). As discussed above, these structures play a functional role in the ecosystems, for example by providing refugia and supporting filter feeding organisms, resulting in high diversity and abundance. These habitats are patchy in nature; denser areas of cauliflower corals are interspersed with other assemblages, for example, areas dominated by anemones (**Figure 4B**) and mushroom soft corals (**Figure 4E**). Similarly, substrates varied within and between stations from coarse rocky ground to gravelly mud substrates. This mosaic nature and resulting variation in structural complexity on a larger spatial scale, is likely to support greater diversity of species and functions.

Those highlighted stations (**Figure 9**) exhibiting the soft coral garden habitat, would appear to meet multiple criteria for a VME (FAO, 2009). Therefore it is proposed that this area be recognized as a VME.

Implications for Management

It is widely recognized that spatial closures are the most effective method of avoiding serious adverse impacts on VMEs (Bell et al., 2019). Executive Order No.4, 30 March 2017, Section 13, introduced by the Government of Greenland makes provision for the closure of areas to bottom gears where VMEs are identified in Greenlandic waters (Government of Greenland, 2017). The soft coral garden habitat identified is immediately adjacent to the MSC certified cold-water prawn (Cappell et al., 2018) and Greenland halibut fisheries (Cappell et al., 2017). This certification requires that measures are in place to ensure that fisheries do not cause serious or irreversible harm to VMEs (MSC, 2014). It should be acknowledged that the coarse rocky ground in the proposed VME area is not necessarily optimal for the prawn fishery and too shallow for the halibut fishery. Therefore, the most immediate threat maybe from the emerging cod fishery (ICES, 2019b), as the slope of the Toqqusaq Bank may be suitable ground for targeting cod. The soft coral garden habitat identified is also partially overlapped by a hydrocarbon exploration and exploitation license, which is currently pending (License: No. 2019/02) (Government of Greenland, 2020).

A bounding polygon for this candidate VME is proposed encompassing seven of the eight stations where the soft coral garden habitat was identified (**Figure 9**). These seven stations were spatially contiguous in the northern portion of the study area, within a 60 km span of continental slope. In the southern portion of the study area only one station (2018_SA_11_120) out of four exceeded the mean cauliflower corals density threshold (> 1 m^2) used to determine the presence of the soft coral garden habitat. This suggests the soft coral garden habitat was not a dominant habitat there. On that basis the southern portion of the study area was not included in the proposed VME area.

The depth range (314–585 m) of those eight stations where the soft coral garden habitat was found is used as the upper and lower boundary on the continental slope of the Toqqusaq Bank. For both pragmatic and precautionary reasons this is rounded down to 300 m and up to 600 m. Bathymetric contours are used to form the eastern (300 m contour) and western (600 m contour) edges of the polygon. The latitudinal extent is determined by the latitude of the most northerly (2019_SA_04_007) and southerly (2018_SA_11_035) of these seven stations. A 5 km latitudinal buffer is added, rounded to the nearest minute (one nautical mile). The proposed VME area can be described as the area with depths of 300–600 m between 64°50′N and 64°22′N on the western edge of the Toqqusaq Bank. This 486 km^2 area, spans ~60 km of the continental slope and is intended to be pragmatic from a spatial management perspective, whilst affording protection to known areas of this soft coral garden habitat.

The VME area proposed here is based on multiple, adjacent observations, which are sufficient to justify the introduction of spatial management measures. It is acknowledged that the data show this soft coral garden habitat is present toward the southern extremity of the study area at a single station. Thus patches of this habitat are present along at least 100 km^2 of continental slope. The true spatial range may well be greater, possibly extending a considerable distance along the continental slope of west Greenland. Management and future research should draw on other data, including unpublished GINR surveys (stock assessment trawl bycatch and beam trawls). Further research should address whether the VME area proposed in this study should be extended, especially in terms of its latitudinal extent.

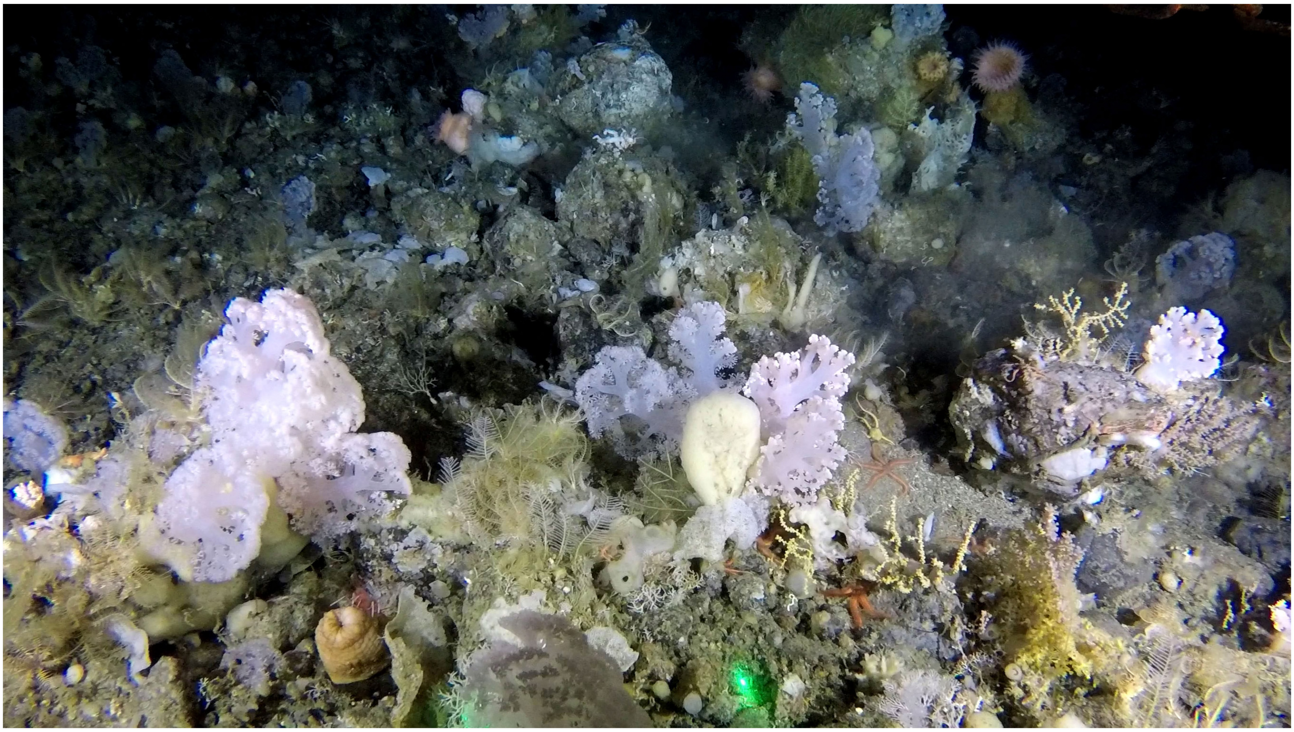

FIGURE 10 | Example still showing the structural complexity of the soft coral garden habitat, from Station 2018_SA_11_087, at a depth of 585 m, on the continental slope of Toqqusaq Bank, west Greenland. Cauliflower corals, feather stars, gorgonians, sponges, anemones, brittle stars, hydrozoans, and calcified bryozoans, are present. Laser dots (green) are 20 cm apart; the left hand dot is partially obscured.

The role of fishing effort, substrate and other environmental variables should be subject to investigation, as one or more of these may explain the distribution of this habitat and abundance of its component species.

Limitations

A fundamental methodological decision was to annotate images sampled from stills rather than directly analyze videos. This was in part due to pragmatic constraints (time) but also provides greater scope for revision and further work on the images and annotations. However, it should be acknowledged that a considerable amount of data contained in the videos are therefore excluded. This impacts our understanding of the abundance of sparser (e.g., *Paragorgia arborea*) and mobile fauna, particularly fish, which are less likely to be sampled in images.

The nature of imagery means only certain taxa can be identified and limits the taxonomic resolution that can be obtained during annotation. A more complete taxa inventory based on unpublished beam trawl and stock assessment trawls from the proposed VME area is included for reference (**Supplementary Table 1**). Efforts were made to annotate different sponge taxa and morphologies but these were ultimately aggregated to achieve consistency. Aggregation of multiple taxa to a parent label, for example into "sponges," results in a more general picture and does not allow more specific taxa associations with other taxa and substrates to be determined. The approach of annotating individuals or colonies means some taxa (e.g., hydrozoans) that formed significant components of the habitats were not quantified in this study. To do so would require a different annotation strategy and likely require considerably more time investment, the latter being a familiar problem in the benthic imaging field.

The resolution within the substrate classes themselves limited their explanatory power. In the images gorgonians were only ever seen attached to hard substrates. It was anticipated that inclusion of a sub-class "with boulders" into gravel mud, would add explanatory power accounting for the presence of gorgonians in gravelly mud substrates. Clearly this was not adequate, with some gorgonians annotated on gravelly mud substrates (gM) (**Figure 8**). In such cases the gorgonians were attached to rocky material that did not exceed the 20 cm boulder threshold, thus the substrate in the image was classed as gravelly mud (gM) and not gravelly mud with boulders (gMb). The proportion and size of hard substrates for attachment varies considerably within classes and some images exhibit a range of substrates. A higher resolution approach to substrate annotation would enable further conclusions to be drawn regarding the relationship between substrates and the observed assemblage and abundance of taxa. This could be achieved by the introduction of additional substrate classes or sub-classes, or alternatively by applying substrate labels to discrete areas within the images. The optimum approach would depend on the question(s) being addressed.

CONCLUSION

Despite the limitations identified, the benthic video sled employed proved to be a low-cost effective tool to collect imagery suitable for identifying and providing a quantitative description of a proposed VME. This allowed the first description of this soft coral garden habitat, characterized by a high density of cauliflower corals, on the continental slope of the Toqqusaq Bank. This structurally complex habitat appears to meet the definition of a VME as provided by the FAO. The vulnerability and potential ecological value mean there is a need for effective spatial management measures, given the proximity of economically important halibut and prawn fisheries along with the emerging cod fishery. A candidate VME area of 486 km^2 is therefore proposed, from which activities liable to cause serious or irreversible harm, such as benthic trawling, should be excluded.

DATA AVAILABILITY STATEMENT

All datasets generated for this study are included in the article/**Supplementary Material**.

AUTHOR CONTRIBUTIONS

SL, MB, NH, KK, and CY contributed to the conception and design of the study. SL, MB, NH, MF, and CY collected the video imagery. BS-S performed the image extraction and annotation. RN and KZ prepared fishing effort data. SL and CY conducted the analyses and produced the figures. SL drafted the manuscript. All authors contributed to manuscript revision, read and approved the submitted version.

FUNDING

This research was an outcome of the project “Fish, plankton and seabed – ecological dynamics on Toqqusaq and Fyllas Bank.” The majority of data were collected during two ship surveys planned and funded by the Greenland Institute of Natural Resources (GINR) (Project Nos. 3205 and 2458). This research was partially conducted under an IUCN BEST 2.0 funded project (Reference No. 1586), led by Zoological Society of London (ZSL), with Sustainable Fisheries Greenland (SFG) as a project partner. This research was also associated with a wider ongoing Benthos Monitoring Programme of the Greenland Institute of Natural Resources (GINR). The GINR was financially supported by the North Atlantic Cooperation (nora.fo; J. No. 510-151), the Ministry for Research in Greenland (IKIIN), the Environmental Protection Agency (Dancea) of the Ministry of Environment and Food of Denmark (J. No. mst-112-00272), and the Nordic Council of Ministers (Project No. 15002). SL was funded by a Ph.D. studentship from the Natural Environment Research Council (NERC) (Grant No. NE/L002485/1). Open access publishing fees were paid by University College London (UCL).

ACKNOWLEDGMENTS

We wish to acknowledge the following contributions to this study. The crews of the R. V. Paamiut, R. V. Sanna, and M. T. Helga Maria, helped deploy the video sled. Aaamal Hussain provided input into trigonometric approaches to determining the area of the field of view. The Institute of Making at UCL and the Department of Mechanical Engineering at UCL assisted with the design and manufacture of the laser housings. Tim Nattkemper and Daniel Langenkämper facilitated the authors' use of the BIIGLE platform. Michael Darling assisted with video sled deployment and video data management during the cruise aboard *MT Helga Maria*. The manuscript was improved by the comments of two reviewers.

SUPPLEMENTARY MATERIAL

The Supplementary Material for this article can be found online at: https://www.frontiersin.org/articles/10.3389/fmars.2020.00460/full#supplementary-material

REFERENCES

Ardron, J. A., Clark, M. R., Penney, A. J., Hourigan, T. F., Rowden, A. A., Dunstan, P. K., et al. (2014). A systematic approach towards the identification and protection of vulnerable marine ecosystems. *Mar. Policy* 49, 146–154. doi: 10.1016/j.marpol.2013.11.017

Auster, P. J., Gjerde, K., Heupel, E., Watling, L., Grehan, A., and Rogers, A. D. (2010). Definition and detection of vulnerable marine ecosystems on the high seas: problems with the “move-on” rule. *ICES J. Mar. Sci.* 68, 254–264. doi: 10.1093/icesjms/fsq074

Baker, K. D., Wareham, V. E., Snelgrove, P. V., Haedrich, R. L., Fifield, D. A., Edinger, E. N., et al. (2012). Distributional patterns of deep-sea coral assemblages in three submarine canyons off Newfoundland, Canada. *Mar. Ecol. Prog. Ser.* 445, 235–249. doi: 10.3354/meps09448

Barthelmé, S. (2017). *imager: Image Processing Library Based on 'CImg'. R package Version 0.40.2*. Available online at: https://CRAN.R-project.org/package=imager (accessed April 12, 2018).

Bell, J., Guijarro, E., and Kenny, A. (2019). Demersal fishing in areas beyond national jurisdiction: a comparative analysis of Regional Fisheries Management Organisations. *Front. Mar. Sci.* 6:596. doi: 10.3389/fmars.2019.00596

Buhl-Mortensen, L., Buhl-Mortensen, P., Dolan, M. F., and Holte, B. (2015). The MAREANO programme–A full coverage mapping of the Norwegian offshore benthic environment and fauna. *Mar. Biol. Res.* 11, 4–17. doi: 10.1080/17451000.2014.952312

Buhl-Mortensen, L., Burgos, J. M., Steingrund, P., Buhl-Mortensen, P., Ólafsdóttir, S. H., and Ragnarsson, S. Á. (2019). *Vulnerable Marine Ecosystems (VMEs): Coral and Sponge VMEs in Arctic and Sub-Arctic Waters–Distribution and Threats*. Copenhagen: Nordic Council of Ministers.

Buhl-Mortensen, L., and Mortensen, P. B. (2005). “Distribution and diversity of species associated with deep-sea gorgonian corals off Atlantic Canada,” in *Cold-Water Corals and Ecosystems*, eds A. Freiwald, and J. M. Roberts (Berlin: Springer), 849–879. doi: 10.1007/3-540-27673-4_44

Bullimore, R. D., Foster, N. L., and Howell, K. L. (2013). Coral-characterized benthic assemblages of the deep Northeast Atlantic: defining “Coral Gardens” to support future habitat mapping efforts. *ICES J. Mar. Sci.* 70, 511–522. doi: 10.1093/icesjms/fss195

Cappell, R., Lassen, H., Holt, T., and Bekkevold, S. (2017). *Public Certification Report for the Initial Assessment of the West Greenland Offshore Greenland halibut fishery*. Høvik: DNV GL Business Assurance.

Cappell, R., Mouat, B., and Hambrey, J. (2018). *West Greenland Coldwater Prawn Fishery: Public Certification Report*. Edinburgh: Acoura Marine Ltd.

Cordes, E., Nybakken, J., and VanDykhuizen, G. (2001). Reproduction and growth of *Anthomastus ritteri* (Octocorallia: Alcyonacea) from Monterey Bay, California, USA. *Mar. Biol.* 138, 491–501. doi: 10.1007/s002270000470

Danovaro, R., Aguzzi, J., Fanelli, E., Billett, D., Gjerde, K., Jamieson, A., et al. (2017). An ecosystem-based deep-ocean strategy. *Science* 355, 452–454. doi: 10.1126/science.aah7178

Davies, C. E., Moss, D., and Hill, M. O. (2004). *EUNIS Habitat Classification Revised 2004*. Paris: European Topic Centre on Nature Protection and Biodiversity, 127–143.

Davies, J., Guillaumont, B., Tempera, F., Vertino, A., Beuck, L., Ólafsdóttir, S., et al. (2017). A new classification scheme of European cold-water coral habitats: implications for ecosystem-based management of the deep sea. *Deep Sea Res. Part II Top. Stud. Oceanogr.* 145, 102–109. doi: 10.1016/j.dsr2.2017.04.014

Devine, B. M., Wheeland, L. J., de Moura Neves, B., and Fisher, J. A. D. (2019). Baited remote underwater video estimates of benthic fish and invertebrate diversity within the eastern Canadian Arctic. *Polar Biol.* 42, 1323–1341. doi: 10.1007/s00300-019-02520-5

ESRI (2013). *ArcGIS, Version 10.1*. Relands, CA: Environmental Systems Research Unit.

FAO (2009). *Report of the Technical Consultation on International Guidelines for the Management of Deep-sea Fisheries in the High Seas*. Rome: Food and Agriculture Organisation.

Freese, L., Auster, P. J., Heifetz, J., and Wing, B. L. (1999). Effects of trawling on seafloor habitat and associated invertebrate taxa in the Gulf of Alaska. *Mar. Ecol. Prog. Ser.* 182, 119–126. doi: 10.3354/meps182119

Gjerde, K., Clark, M. R., Rogers, A., and Hall-Spencer, J. (2008). *The Science Behind the Guidelines: A Scientific Guide to the FAO Draft International Guidelines (December 2007) for the Management of Deep-Sea Fisheries in the High Seas and Examples of How the Guidelines may be Practically Implemented*. Plymouth: University of Plymouth.

Gougeon, S., Kemp, K., Blicher, M., and Yesson, C. (2017). Mapping and classifying the seabed of the West Greenland continental shelf. *Estuar. Coast. Shelf Sci.* 187, 231–240. doi: 10.1016/j.ecss.2017.01.009

Government of Greenland (2017). *Selvstyrets Bekendtgørelse nr. 4 af 30. Marts 2017 om Tekniske Bevaringsforanstaltninger i Fiskeriet. Government of Greenland Executive Order no. 4 of 30 March 2017 on Technical Conservation Measures in Fishing*. Nuuk: Departementet for Finanser og Skatter.

Government of Greenland (2018). *Beskyttelse af de Sårbare og Tidligere Uberørte Havmiljøområder i Melvillebugten*. Available: https://naalakkersuisut.gl//da/Naalakkersuisut/Nyheder/2018/01/2301_melvillebugten (accessed August 22, 2019).

Government of Greenland (2020). *Minerals and Petroleum Licence Map. Mineral Resources Authority*. Available online at: https://asiaq.maps.arcgis.com/apps/webappviewer/index.html?id=819ff201b76f44f99b31da7ef630c18e&locale=en (accessed April 04, 2020).

Griffith, D. M., Veech, J. A., and Marsh, C. J. (2016). Cooccur: probabilistic species co-occurrence analysis in R. *J. Stat. Softw.* 69, 1–17.

Guillaumont, B., Tempera, F., Vertino, J., Beuck, L., Ólafsdóttir, S., Smith, C., et al. (2016). *CoralFISH Northeast Atlantic and Mediterranean Cold-Water Coral Habiats Catalogue (version 2)*. Anavyssos: Hellenic Centre for Marine Research.

Gutt, J. (2002). "On the direct impact of ice on marine benthic communities, a review," in *Ecological Studies in the Antarctic Sea Ice Zone*, eds W. E. Arntz et al. (Berlin: Springer), 157–168. doi: 10.1007/978-3-642-59419-9_21

Henry, L., Kenchington, E. L., and Silvaggio, A. (2003). Effects of mechanical experimental disturbance on aspects of colony responses, reproduction, and regeneration in the cold-water octocoral *Gersemia rubiformis*. *Can. J. Zool.* 81, 1691–1701. doi: 10.1139/z03-161

Howell, K., Davies, J., and Narayanaswamy, B. (2010). Identifying deep-sea megafaunal epibenthic assemblages for use in habitat mapping and marine protected area network design. *J. Mar. Biol. Assoc. U.K.* 90, 33–68. doi: 10.1017/s0025315409991299

Huvenne, V., Bett, B., Masson, D., Le Bas, T., and Wheeler, A. (2016). Effectiveness of a deep-sea cold-water coral Marine Protected Area, following eight years of fisheries closure. *Biol. Conserv.* 200, 60–69. doi: 10.1016/j.biocon.2016.05.030

ICES (2007). *Report of the Working Group on Deep-water Ecology (WGDEC)*. Copenhagen: International Council for the Exploration of the Seas.

ICES (2019a). "Cod (*Gadus morhua*) in NAFO divisions 1A–1E, offshore (West Greenland)," in *ICES Advice on Fishing Opportunities, Catch, and Effort, Arctic Ocean and Greenland Sea Ecoregions*, (Copenhagen: International Council for the Exploration of the Seas).

ICES (2019b). "Cod (*Gadus morhua*) in NAFO Subdivisions 1A–1E (Offshore West Greenland)," in *North Western Working Group (NWWG) Scientific Reports*, ed. K. Kristinsson (Copenhagen: International Council for the Exploration of the Seas).

Jacobsen, R. B. (2018). "The sustainability of what? Stocks, communities, the public purse?" in *The Politics of Sustainability in the Arctic*, eds U. P. Gad and J. Strandsbjerg (Abingdon: Routledge), 33–47.

Jørgensen, L. L., Blicher, M., Bluhm, B., Christiansen, J. S., Fredriksen, R., Hammeken, N., et al. (2018). *Detecting Changes in the Arctic Ecosystem–Long-Term Benthos Monitoring Network for Detecting Changes in the Arctic Benthic Ecosystem (LTM-Benthos) 2017–2020*. Bergen: Norwegian Institute of Marine Research.

Jørgensen, O. A., Tendal, O. S., and Arboe, N. H. (2013). "Preliminary mapping of the distribution of corals observed off West Greenland as inferred from bottom trawl surveys 2010-2012," in *Proceedings of the 35th Scientific Council Research Meeting NAFO*, Halifax, NS.

Juul-Pedersen, T., Arendt, K. E., Mortensen, J., Krawczyk, D., Retzel, A., Nygaard, R., et al. (2015). "The MarineBasis programme 2015," in *Nuuk Ecological Research Operations 9th Annual Report, 2015*, eds E. Topp-Jørgensen, J. Hansen, and T. R. Christensen (Aarhus: Aarhus University).

Kenchington, E., Yashayaev, I., Tendal, O. S., and Jørgensbye, H. (2017). Water mass characteristics and associated fauna of a recently discovered *Lophelia pertusa* (Scleractinia: Anthozoa) reef in Greenlandic waters. *Polar Biol.* 40, 321–337. doi: 10.1007/s00300-016-1957-3

Krieger, K. J., and Wing, B. L. (2002). Megafauna associations with deepwater corals (*Primnoa* spp.) in the Gulf of Alaska. *Hydrobiologia* 471, 83–90.

Langenkämper, D., Zurowietz, M., Schoening, T., and Nattkemper, T. W. (2017). BIIGLE 2.0 - browsing and annotating large marine image collections. *Front. Mar. Sci.* 4:83. doi: 10.3389/fmars.2017.00083

McConnaughey, R., Mier, K., and Dew, C. (2000). An examination of chronic trawling effects on soft-bottom benthos of the eastern Bering Sea. *ICES J. Mar. Sci.* 57, 1377–1388. doi: 10.1006/jmsc.2000.0906

McFadden, C. S., France, S. C., Sánchez, J. A., and Alderslade, P. (2006). A molecular phylogenetic analysis of the Octocorallia (Cnidaria: Anthozoa) based on mitochondrial protein-coding sequences. *Mol. Phylogenet. Evol.* 41, 513–527. doi: 10.1016/j.ympev.2006.06.010

Millard, R., and Seaver, G. (1990). An index of refraction algorithm for seawater over temperature, pressure, salinity, density, and wavelength. *Deep Sea Res. Part A Oceanogr. Res. Pap.* 37, 1909–1926. doi: 10.1016/0198-0149(90)90086-b

Molodtsova, T. N. (2013). Deep-sea mushroom soft corals (Octocorallia: Alcyonacea: Alcyoniidae) of the northern mid-Atlantic ridge. *Mar. Biol. Res.* 9, 488–515. doi: 10.1080/17451000.2012.750427

Morato, T., Pham, C. K., Pinto, C., Golding, N., Ardron, J. A., Muñoz, P. D., et al. (2018). A multi criteria assessment method for identifying Vulnerable Marine Ecosystems in the North-East Atlantic. *Front. Mar. Sci.* 5:460. doi: 10.3389/fmars.2018.00460

Morato, T., Watson, R., Pitcher, T. J., and Pauly, D. (2006). Fishing down the deep. *Fish Fish.* 7, 24–34. doi: 10.1111/j.1467-2979.2006.00205.x

Morlighem, M., Williams, C. N., Rignot, E., An, L., Arndt, J. E., Bamber, J. L., et al. (2017). BedMachine v3: Complete bed topography and ocean bathymetry mapping of Greenland from multibeam echo sounding combined with mass conservation. *Geophys. Res. Lett.* 44, 11051–11061.

Mortensen, B. O. G. (2014). The quest for resources – the case of Greenland. *J. Military Strateg. Stud.* 15, 93–128.

MSC (2014). *MSC Fisheries Certification Requirements and Guidance, Version 2.0*. London: Marine Stewardship Council.

Muñoz, P. D., and Sayago-Gil, M. (2011). An overview of cold-water coral protection on the high seas: the Hatton bank (NE Atlantic)—a case study. *Mar. Policy* 35, 615–622. doi: 10.1016/j.marpol.2011.01.023

Murillo, F. J., Durán Muñoz, P., Altuna, A., and Serrano, A. (2010). Distribution of deep-water corals of the Flemish Cap, Flemish Pass, and the Grand Banks of Newfoundland (Northwest Atlantic Ocean): interaction with fishing activities. *ICES J. Mar. Sci.* 68, 319–332. doi: 10.1093/icesjms/fsq071

Myers, P. G., Kulan, N., and Ribergaard, M. H. (2007). Irminger water variability in the West Greenland Current. *Geophys. Res. Lett.* 34:L17601.

NAFO (2012). *Report of the Scientific Council Meeting. NAFO SCS Doc 12/19*. Dartmouth, NS: NAFO.

Nakajima, R., Komuku, T., Yamakita, T., Lindsay, D. J., Jintsu-Uchifune, Y., Watanabe, H., et al. (2014). A new method for estimating the area of the seafloor from oblique images taken by deep-sea submersible survey platforms. *JAMSTEC Rep. Res. Dev.* 19, 59–66. doi: 10.5918/jamstecr.19.59

NEAFC (2014). *Recommendation on the Protection of Vulnerable Marine Ecosystems in the NEAFC Regulatory Area*. London: North East Atlantic Fisheries Commission.

Ontrup, J., Ehnert, N., Bergmann, M., and Nattkemper, T. W. (2009). "BIIGLE-Web 2.0 enabled labelling and exploring of images from the Arctic deep-sea observatory HAUSGARTEN," in *Proceedings of the International Oceans '09 Conference and Exhibition OCEANS 2009-EUROPE* (Piscataway, NJ: IEEE).

OSPAR Commission (2010). *Biodiversity Series Background Document for Coral Gardens*. Paris: OSPAR.

Patent, D. H. (1970). Life history of the basket star, *Gorgonocephalus eucnemis* (Müller & Troschel)(Echinodermata; Ophiuroidea). *Ophelia* 8, 145–159. doi: 10.1080/00785326.1970.10429556

Pérez, C. D., de Moura Neves, B., Cordeiro, R. T., Williams, G. C., and Cairns, S. D. (2016). "Diversity and distribution of Octocorallia," in *The Cnidaria, Past, Present and Future*, eds S. Goffredo and Z. Dubinsky (Berlin: Springer), 109–123. doi: 10.1007/978-3-319-31305-4_8

Poulsen, L. K., and Reuss, N. (2002). The plankton community on Sukkertop and Fylla Banks off West Greenland during a spring bloom and post-bloom period: hydrography, phytoplankton and protozooplankton. *Ophelia* 56, 69–85. doi: 10.1080/00785236.2002.10409491

R Core Team (2013). *R: A Language and Environment for Statistical Computing*. Vienna: R Foundation for Statistical Computing.

Ramirez-Llodra, E., Brandt, A., Danovaro, R., De Mol, B., Escobar, E., German, C., et al. (2010). Deep, diverse and definitely different: unique attributes of the world's largest ecosystem. *Biogeosciences* 7, 2851–2899. doi: 10.5194/bg-7-2851-2010

Riaz, M., Park, S., Ahmad, M. B., Rasheed, W., and Park, J. (2008). "Generalized laplacian as focus measure," in *International Conference on Computational Science*, eds M. Bubak, G. D. van Albada, J. Dongarra, and P. M. A. Sloot (Berlin: Springer).

Rogers, A. D., and Gianni, M. (2011). *Implementation of UNGA Resolutions 61/105 and 64/72 in the Management of Deep-Sea Fisheries on the High Seas*. Darby, PA: DIANE Publishing.

Rogers, A. D., Kemp, K. M., Davies, A. J., and Lisa Taylor, M. (2015). The diseases of deep-water corals. *Dis. Coral* 416–441. doi: 10.1002/9781118828502.ch32

Safe Software (2019). *Safe FME*. Vancouver: Safe Software.

SAS Institute (2019). *SAS*. Cary, NC: SAS Institute Inc.

Sherwood, O. A., and Edinger, E. N. (2009). Ages and growth rates of some deep-sea gorgonian and antipatharian corals of Newfoundland and Labrador. *Can. J. Fish. Aquat. Sci.* 66, 142–152. doi: 10.1139/f08-195

Streuff, K., Cofaigh, C. Ó., Hogan, K., Jennings, A., Lloyd, J. M., Noormets, R., et al. (2017). Seafloor geomorphology and glacimarine sedimentation associated with fast-flowing ice sheet outlet glaciers in Disko Bay, West Greenland. *Quat. Sci. Rev.* 169, 206–230. doi: 10.1016/j.quascirev.2017.05.021

Sun, Z., Hamel, J.-F., and Mercier, A. (2010). Planulation periodicity, settlement preferences and growth of two deep-sea octocorals from the northwest Atlantic. *Mar. Ecol. Prog. Ser.* 410, 71–87. doi: 10.3354/meps08637

Sun, Z., Hamel, J. F., and Mercier, A. (2011). Planulation, larval biology, and early growth of the deep-sea soft corals *Gersemia fruticosa* and *Duva florida* (Octocorallia: Alcyonacea). *Invertebr. Biol.* 130, 91–99. doi: 10.1111/j.1744-7410.2011.00229.x

The Economic Council (2017). *Nunatta Aningaasaqarnera: Greenland's Economy*. Nuuk: The Economic Council.

Treibitz, T., Schechner, Y., Kunz, C., and Singh, H. (2011). Flat refractive geometry. *IEEE Trans. Patt. Anal. Mach. Intell.* 34, 51–65. doi: 10.1109/tpami.2011.105

UNEP-WCMC (2019). *Protected Area Profile for Greenland from the World Database of Protected Areas, October 2019*. Available online at: https://www.protectedplanet.net/country/GL (accessed October 25, 2019).

UNGA (2006). *Resolution 61/105. Sustainable Fisheries, Including Through the 1995 Agreement for the Implementation of the Provisions of the United Nations Convention on the Law of the Sea of 10 December 1982 Relating to the Conservation and Management of straddling Fish Stocks and Highly Migratory Fish Stocks, and Related Instruments*. New York, NY: United Nations General Assembly.

Veech, J. A. (2013). A probabilistic model for analysing species co-occurrence. *Glob. Ecol. Biogeogr.* 22, 252–260. doi: 10.1111/j.1466-8238.2012.00789.x

Watling, L., and Auster, P. J. (2005). "Distribution of deep-water Alcyonacea off the Northeast Coast of the United States," in *Cold-Water Corals and Ecosystems*, eds A. Freiwald, and J. M. Roberts (Berlin: Springer), 279–296. doi: 10.1007/3-540-27673-4_13

Williams, G. C. (2013). New taxa and revisionary systematics of alcyonacean octocorals from the Pacific coast of North America (Cnidaria, Anthozoa). *ZooKeys* 283, 15–42.

Witherell, D., and Coon, C. (2000). "Protecting gorgonian corals off Alaska from fishing impacts," in *Proceedings of the Nova Scotian Institute of Science*, Halifax, NS, 117–115.

Yesson, C., Fisher, J., Gorham, T., Turner, C. J., Arboe, N. H., Blicher, M. E., et al. (2017). The impact of trawling on the epibenthic megafauna of the west Greenland shelf. *ICES J. Mar. Sci.* 866–876. doi: 10.1093/icesjms/fsw206

Yesson, C., Simon, P., Chemshirova, I., Gorham, T., Turner, C., Arboe, N. H., et al. (2015). Community composition of epibenthic megafauna on the West Greenland Shelf. *Polar Biol.* 38, 2085–2096. doi: 10.1007/s00300-015-1768-y

Conflict of Interest: The Zoological Society of London (ZSL) has previously received funding from Sustainable Fisheries Greenland (SFG), who were a partner in the IUCN BEST 2.0 project detailed in the Funding Statement. The nature of this partnership is that ZSL maintains complete academic independence. SFG play no role in the design, execution, or interpretation of research conducted by authors at ZSL, including this study.

frontiers in Marine Science

PERSPECTIVE
published: 25 May 2021
doi: 10.3389/fmars.2021.622586

Vulnerable Marine Ecosystems, Communities, and Indicator Species: Confusing Concepts for Conservation of Seamounts

Les Watling[1] and Peter J. Auster[2,3]*

[1] *School of Life Sciences, University of Hawai'i at Mānoa, Honolulu, HI, United States,* [2] *Mystic Aquarium—Sea Research Foundation, Mystic, CT, United States,* [3] *Department of Marine Sciences, University of Connecticut, Groton, CT, United States*

OPEN ACCESS

Edited by:
Anthony Grehan,
National University of Ireland Galway,
Ireland

Reviewed by:
Chris Yesson,
Zoological Society of London,
United Kingdom
Nadia Papadopoulou,
Hellenic Centre for Marine Research
(HCMR), Greece

***Correspondence:**
Les Watling
watling@hawaii.edu

Specialty section:
This article was submitted to
Deep-Sea Environments and Ecology,
a section of the journal
Frontiers in Marine Science

Received: *28 October 2020*
Accepted: *26 April 2021*
Published: *25 May 2021*

Citation:
Watling L and Auster PJ (2021)
Vulnerable Marine Ecosystems,
Communities, and Indicator Species:
Confusing Concepts for Conservation
of Seamounts.
Front. Mar. Sci. 8:622586.
doi: 10.3389/fmars.2021.622586

The concept of "vulnerable marine ecosystem" (VME) was included in United Nations (UN) General Assembly Resolution 61/105 as part of an international effort to minimize the effects of seafloor fisheries on the high seas. However, defining a VME was left to be developed by technical guidance to the UN Food and Agricultural Organization. In that venue certain categories of organisms were deemed to be indicator species, suggesting that areas with those species would be considered VMEs with subsequent management measures implemented to conserve those ecosystem attributes. We note that on seamounts VME indicator species can be distributed widely, in dense clusters or sparsely. A dense cluster, for example, of scleractinian corals or sponges, is most often referred to as a VME, but we argue that any such dense cluster is not an ecosystem, rather it is a community, likely one of many that make up the ecosystem. Other communities on the seamount that are not part of that dense cluster could include many small species (some yet to be discovered) who are also part of the ecosystem because they are part of the web of interactions and flow of materials/energy on the seamount. We also suggest that a seamount ecosystem might extend over several or many seamounts in a biogeographic area. We conclude that the term "ecosystem" in the VME concept outlined by the United Nations needs to be re-evaluated from a classical ecological perspective leading to spatial management approaches that better address ecologically relevant space and time scales.

Keywords: vulnerable marine ecosystem, seamount, marine communities, *Solenosmilia*, fisheries

INTRODUCTION

Seamount habitats harbor diverse assemblages of suspension-feeding organisms, usually attached to the hard substrate, and often extending a meter or more into the overlying water. Many, if not most, of these organisms have life history characteristics that identify them as indicators of vulnerable marine ecosystems (VMEs, but we will use VMEcosystems, to distinguish between the ecosystem and the indicator species usage of the acronym VME). In general, the VME indicator species are long-lived, with ages extending from many decades to several centuries and longer; they are fragile, having become adapted to places where water flow, even when enhanced, generally does not exceed a few centimeters per second; their reproductive habits, when known, suggest infrequent or aperiodic spawning, often on scales of years between spawning events, the exception perhaps being in areas with seasonal and dense phytoplankton blooms with subsequent transport to the seafloor; and their larvae are mostly unknown, as is the distance over which they are capable of dispersing [Food and Agriculture Organization of the United Nations (FAO), 2009].

The problem with the identification of VMEcosystems and deciding how to manage them is that there is no agreement on delimitation of the ecosystem. Noteworthy is that the original UNGA resolution 61/105 included the phrase "vulnerable marine ecosystem" as critical terminology (paragraphs 76–95) so the Expert Consultation tasked to develop the initial draft of the guidelines needed to start with this as the foundation [Food and Agriculture Organization of the United Nations (FAO), 2009]. The panel considered how to address the ecosystem-scale scope of the term but reduced the level of complexity for implementation to the scales of populations, communities, and habitats (paragraphs 14–16 in the guidelines) which are the units that would experience any alterations. Indeed, the guidelines that describe and define VMEcosystems acknowledge that Regional Fisheries Management Organizations (RFMOs) and their member states would want some flexibility in implementation.

Determining whether a vulnerable marine ecosystem is present is predicated on finding pre-determined indicator species (UNGA Resolution 64/72). The characteristics of indicator species were determined to have a particular set of attributes that make them especially vulnerable to the impacts of bottom contact fishing gear [Food and Agriculture Organization of the United Nations (FAO), 2009]: (1) uniqueness or rarity of the species; (2) functionally significant to the habitat; (3) body fragility; (4) life-history characteristics that make probability of recolonization after impact low or unpredictable; and (5) species that serve as habitat for other species through their structural complexity. On seamounts much attention has been given to species of corals and sponges since they generally fit at least one, and often several, of the criteria to be considered as VME indicator species (Ardron et al., 2014).

The concept of vulnerability is a critical element for implementing the guidelines. Paragraph 14 of UNGA Resolution 62/72 states (italics ours for emphasis): "[v]ulnerability is related to the likelihood that a population, community, or habitat will experience substantial alteration from short-term or chronic disturbance, and the likelihood that it would recover and in what time frame. *These are, in turn, related to the characteristics of the ecosystems themselves, especially biological and structural aspects.* VME features may be physically or functionally fragile. The most vulnerable ecosystems are those that are both easily disturbed and very slow to recover, or may never recover." Therefore, the concept of a VME is linked to the **ecosystem** in which populations, communities and habitats are nested and interact at a functional level.

In much of the subsequent literature and discussion on the issue, as well as the application of the guidelines, the concept of indicator species has been conflated with the ecosystem itself so that when some authors speak of VMEs they are simultaneously speaking of the presence of indicator species but also, by inference, evaluating the presence of a vulnerable ecosystem. The problem, of course, is that we see many examples where the occasional presence (i.e., sparse distribution) of indicator species is interpreted to mean that we are not in a VMEcosystem. However, it is important to remember that these are *indicator species* and are meant to represent all the other species not considered or sampled in the ecosystem.

DISTRIBUTION OF INDICATOR SPECIES, COMMUNITIES, AND ECOSYSTEMS ON SEAMOUNTS

Some seamounts, especially at high latitudes (but see Baco et al., 2017 for an example of a low latitude example) harbor extensive thickets or reefs created by colonies of hard corals. In the Southwest Pacific, the coral *Solenosmilia variabilis*, is the primary species of the coral thickets (Thresher et al., 2011). Elsewhere, *Madrepora* or *Desmophyllum* can fill the same role. The importance of these thickets is that they form habitat for an unknown number of other species, most of which have not been documented outside of the NE Atlantic. Images from the Tasmanian seamounts show most octocorals growing on the dead skeletons of the *Solenosmilia* colonies. In addition, large sea urchins and other invertebrates, including bryozoans and hydroids were utilizing this habitat (Thresher et al., 2011). When most people think of VMEcosystems, reef and thicket habitats are what come to mind. But seamounts, especially along ridges created by the erosion and slumping of the seamount flanks, can have high densities of bush-like octocorals with an understory of smaller species, including sponges, most if not all fragile and functionally significant as habitat (e.g., for commensal species). Diversity in these "coral gardens" or "forests" is probably quite high, but they have not yet been adequately sampled to better quantify this relationship.

In our opinion and extensive observation, most people, when referring to VMEcosystems are in fact really talking about VMCommunities (VMCs). Indeed it has been fundamental in ecological science that ecosystems are composed of many habitat types that support communities of several kinds (see Allee et al., 1949, for example). In the South Pacific, Rowden et al. (2017) mapped in detail the distribution of the hard coral, *S. variabilis*, over several seamounts. They found the distributions of brisingid starfish and crinoids to closely parallel that of the hard coral. They refer to this as the *Solenosmilia* VME, but in fact, it is the *Solenosmilia* **community**, one of many communities on those seamounts, the others generally not discussed in detail (but see Clark et al., 2015), that are made up of gorgonians, black corals, sponges, and small organisms living in the sand. With the possible exception of the sand, one could think of the coral groups and sponges as characterizing a suspension-feeder community, partly separate from, but perhaps also overlapping with the *Solenosmilia* community. The sand community comprises worms, nematodes, harpacticoid copepods, and others., but are poorly studied. The sand communities are connected through water flow, larval distribution, and the flux of materials from proximate coral and suspension-feeding communities (e.g., Bourque and Demopoulos, 2018; Pierrejean et al., 2020), thus justifying the concept of the seamount as a series of functionally interrelated and spatially overlapping communities making up part of an ecosystem which potentially comprises multiple seamounts.

Many studies, from Remotely Operated Vehicle (ROV) dives to towed camera transects, have demonstrated that VME indicator species are not homogeneously distributed across seamount substrates (e.g., Victorero et al., 2018). Seamounts are complex geomorphological structures composed largely of basalt rock in the form of ridges and flat plains, but also as vertical cliffs with all angles of slopes in between. Depending on the geological history of the seamount, there may also be areas of compressed ash, or breccias consisting of stones and boulders of various sizes, and biogenic sand. All these factors contribute to seamounts possessing a range of potential habitats (**Figure 1**) in which vulnerable species can live (Auster et al., 2005). In addition, seamount sandy habitats harbor unique small species, some of which have so far been found nowhere else. A good example are the 54 new species of the sediment-dwelling harpacticoid copepods found on the flat summit of Great Meteor Seamount in the Northeast Atlantic (George and Schminke, 2002). Dredge samples from the summits of the Meteor and Lusitanian seamount groups, which are separated by about 1,000 km, also produced 30 new species of small gastropods in the family Rissoidae (Gofas, 2007).

The ICES Working Group on Deep-Sea Ecology (WGDEC) has been asked, over multiple years, to refine the operational definition of VMEcosystems and the associated use of indicator species in the decision process for spatial management. This effort has led to a series of reports and articles that address indicator species distribution, abundance, vulnerability, and uncertainties regarding indication of a VMEcosystem, in an effort to clarify recommended areas for protection in the North Atlantic where bottom trawl fishing is occurring (Morato et al., 2018, 2021). But, while numerical approaches are being used to identify vulnerable components of VMEcosystems, they do not provide insights into the functioning of vulnerable marine ecosystems. That is, the understanding and delimitation of the ecosystem also requires a "process-functional" approach which accounts for energy flow. Thus, ". . . we see the ecosystem as a dual entity. In one dimension it is structured according to constraints involving organism interaction and natural selection. In another dimension it is structured according to constraints that involve mass balance and thermodynamics" (O'Neill et al., 1986: 209). In the sea, which is a relatively open system, ecosystems are typically large, boundaries are created by water masses and fronts, thus encompassing several hundred thousand square kilometers measured at the ocean surface (Sherman and Duda, 1999). At depth, we do not yet know the extent of the ecosystem, although there are proposals for province boundaries (Watling et al., 2013).

Does the VMEcosystem cover only a single seamount or are there multiple seamounts in a VMEcosystem? The communities that make up an ecosystem can range over very large distances. Common examples are the communities of sandy beaches or rocky shores along continental coastlines, both of which are commonly thought of as ecosystems. Each contains their own common set of species, and each might not be contiguous throughout the range, but each also might have in common the dispersal of individuals from one part of the ecosystem to another, through the movements of either the larval or adult stages of the populations. The same can be said for seamounts within a biological province. A community dominated by several species of bamboo corals or the scleractinian *Solenosmilia* might extend along the whole or part of a seamount chain, or range over seamounts located in large sections of the ocean basin. Those distributions and estimates of the genetic connectivity or how much genetic variation exists over the whole of the range of a species is just becoming known (e.g., Thoma et al., 2009; Radice et al., 2016). Some information is available for species, such as brittle stars and chirostylid galatheid crabs associated with the corals, rather than the corals themselves (Samadi et al., 2006; Cho and Shank, 2010).

Determining the extent of VMEcosystems begins with mapping the distribution of biogeographic provinces in the ocean, which in turn uses the distributions of species that make up the communities that have so far been investigated. While deep-sea biogeography has been an area of study since the time of Ekman (Watling et al., 2013), it was only the recent funding for deep-diving ROVs and funding for ecological exploration of continental margins and deep sea regions that has allowed scientists to begin to map the bathyal benthos of the ocean away from the continental shelves (e.g., Kennedy et al., 2019; Lapointe et al., 2020). Much of the data thus procured has been archived in Ocean Biogeographic Information System (OBIS) and is available to anyone who wants to use it (e.g., Costello et al., 2017). One method of differentiating seamounts or seamount groups as VMEcosystems, is to determine which of the many seamounts in the ocean are similar to each other in some characteristic way. Clark et al. (2011) developed a classification system using several physical and biological features including summit depth, organic matter flux, distance to nearest seamount, and dissolved oxygen in the surrounding water. This method divided the estimated global 10,604 large seamounts (estimate from Kitchingman and Lai, 2004) with summit depths in the bathyal (<3,500 m) into 194 groups distributed over the 14 bathyal provinces of Watling et al. (2013). In the biogeographic province in which the Louisville seamounts are located (BY6), for example, there were 517 seamounts divided into 17 groups, of which four occurred at various points along the Louisville chain.

It is very rare that more than two or three ROV dives are conducted on any one seamount, so variation in community composition based on depth (water mass characteristics), orientation to principle current regime, and effects of species interactions are generally not well-known. Seamounts with multiple dives on the summit and flanks include Kelvin (Lapointe et al., 2020) and Anton Dohrn (Davies et al., 2015) in the North Atlantic, Davidson (McClain et al., 2010) and Cobb (Du Preez et al., 2016) in the Northeast Pacific, Necker Ridge (Morgan et al., 2015) in the Central Pacific, and the Graveyard seamounts NE of New Zealand (Clark and O'Driscoll, 2003). Other ROV programs, such as those of the *Okeanos Explorer* and *Nautilus*, are exploratory and rarely do more than two dives on any seamount

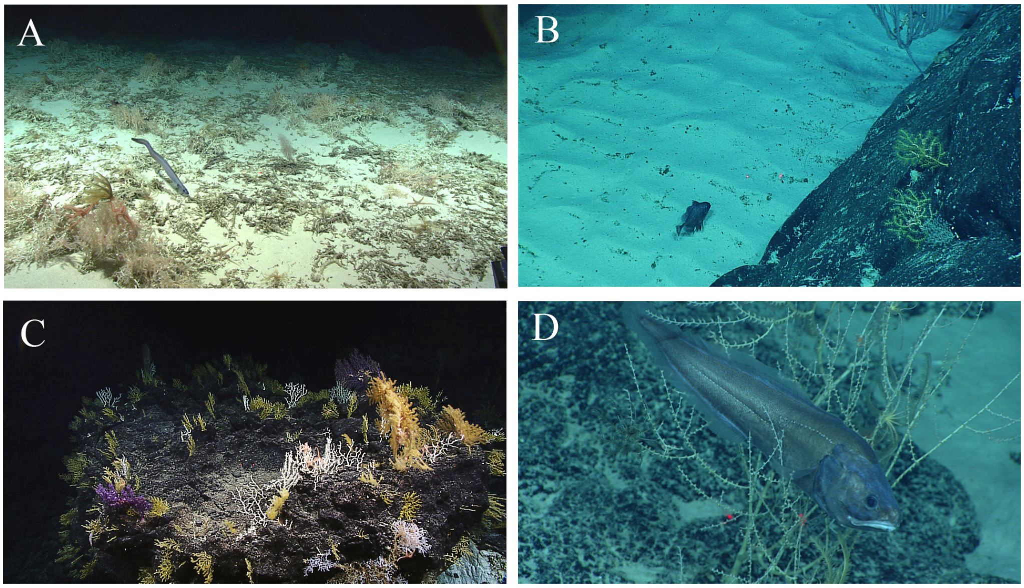

FIGURE 1 | Typical communities commonly seen on Pacific seamounts that exhibit a diversity of species in different settings with no single indicator species that would characterize these places. **(A)** A mixed coral, coral rubble, and sand habitat at 803 m off Jarvis Island with roaming *Bathycongrus*. **(B)** Sparse corals and *Neocyttus* cf. *acanthorhynchus* along the margin of basaltic ridge and sand habitats, 1,140 m, Titov Seamount. **(C)** A mixed coral community on the flank of Swordfish Seamount, 970 m. **(D)** *Diplacanthopoma* sp. among octocoral branches in a mixed basalt and sand habitat. All images courtesy of NOAA Okeanos Program and CAPSTONE Science Team, fish identifications from annotations during the dives by B. Mundy, NOAA Fisheries.

(Kennedy et al., 2019). As a result we have a more or less detailed look at the distribution of organisms on only a few seamounts and so cannot say much about the distribution of communities on any one seamount. In the SW Pacific, a TowCam system was used to cover at least the summit area of a number of seamounts. In most cases those seamounts had relatively small summit areas so the TowCam transects were arranged to produce coverage of a significant proportion of the summit and approaching flanks. In other cases, such as the Louisville Seamounts, most of the transect coverage was on the summits (Clark et al., 2015).

In order to determine the boundary of an ecosystem it is important to know the limits of the component communities, both horizontally and vertically. Efforts to plot or model the distribution of the most abundant indicator species may not account for the whole ecosystem or spatially distinct but nonetheless vulnerable communities within the seamount landscape (e.g., Rowden et al., 2017). As well, we know that fishing at a selective depth can have impacts far deeper than the target fishing depth due to the vertical movements and other density dependent responses of fish species (Bailey et al., 2009; Priede et al., 2011). For several seamounts in the Louisville Seamount chain, various models were applied to towed camera image data to determine that three VME indicator species, *S. variabilis* coral heads and matrix, brisingid starfish, and crinoids, were located near the summit edges, and that other parts therefore could be trawled due to the absence or low abundance of those species. Rowden et al. (2017) refer to the *S. variabilis* matrix as if it is a VMEcosystem on its own, and so, by presumption, the remainder of the summit of the seamount does not belong to that ecosystem and is therefore not vulnerable. We have already suggested that Rowden et al. (2017) were actually determining the extent of the *Solenosmilia* community, which is only a part of the larger ecosystem. Whole seamounts need to be treated as VMEcosystems (Watling and Auster, 2017), or more likely, as part of a larger ecosystem.

CONCLUSION AND RECOMMENDATIONS

We find the term "ecosystem" as currently applied to VMEs to be confused in use and application since its roots in the ecosystem concept are broader and more holistic. This confusion has led to use of VME indicator species being conflated to indicate whether a VMEcosystem is present or not, often ignoring the connections of such species to the communities of organisms in which they reside. Most importantly, this interpretation leads to gaps in meeting overall conservation goals. Seamount communities are not well known due to minimal or a wholesale lack of survey effort on individual seamounts. Focusing on single easily detected species (i.e., captured in fishing gear as bycatch or in image surveys) does not equate to the extent of the interactions defining the ecosystem or the connectivity of the vulnerable seafloor community. Protecting only part of a seamount does not necessarily protect the integrity of the seamount communities, making the whole community vulnerable. Furthermore, the seamount ecosystem most likely will extend over multiple seamounts, the extent to be determined by geography and hydrography. "An "ecosystem plan" that fails to protect all of the species associated with a particular natural community can only be characterized as deficient" (Wilcove, 1994: 327). This statement was written as part of the legal argument for saving the whole of the old growth forest of the northwestern United States as habitat for the northern spotted owl. Wilcove showed that a management plan targeted at a single species was unlikely to protect the full diversity of interacting and vulnerable species in the ecosystem and thus the spotted owl, itself.

Identifying the presence, distribution, and abundance of an indicator species defines the state of that species at a moment (or period) in time. It does not define the composition of an associated community, the suite of species interactions that define and sustain the community, or the flows of materials and energy that define the bounds of the ecosystem. Most important, it is those details about species interactions (including population connectivity, energy flow that mediates growth and reproduction, and interactions mediated by the local oceanographic regime) that will be needed to understand and predict the extent to which fishing and other human activities produce significant adverse impacts. Significant adverse impacts to indicator species alone simply defines a set of minimum bounds on the effects of human actions on VMEcosystems.

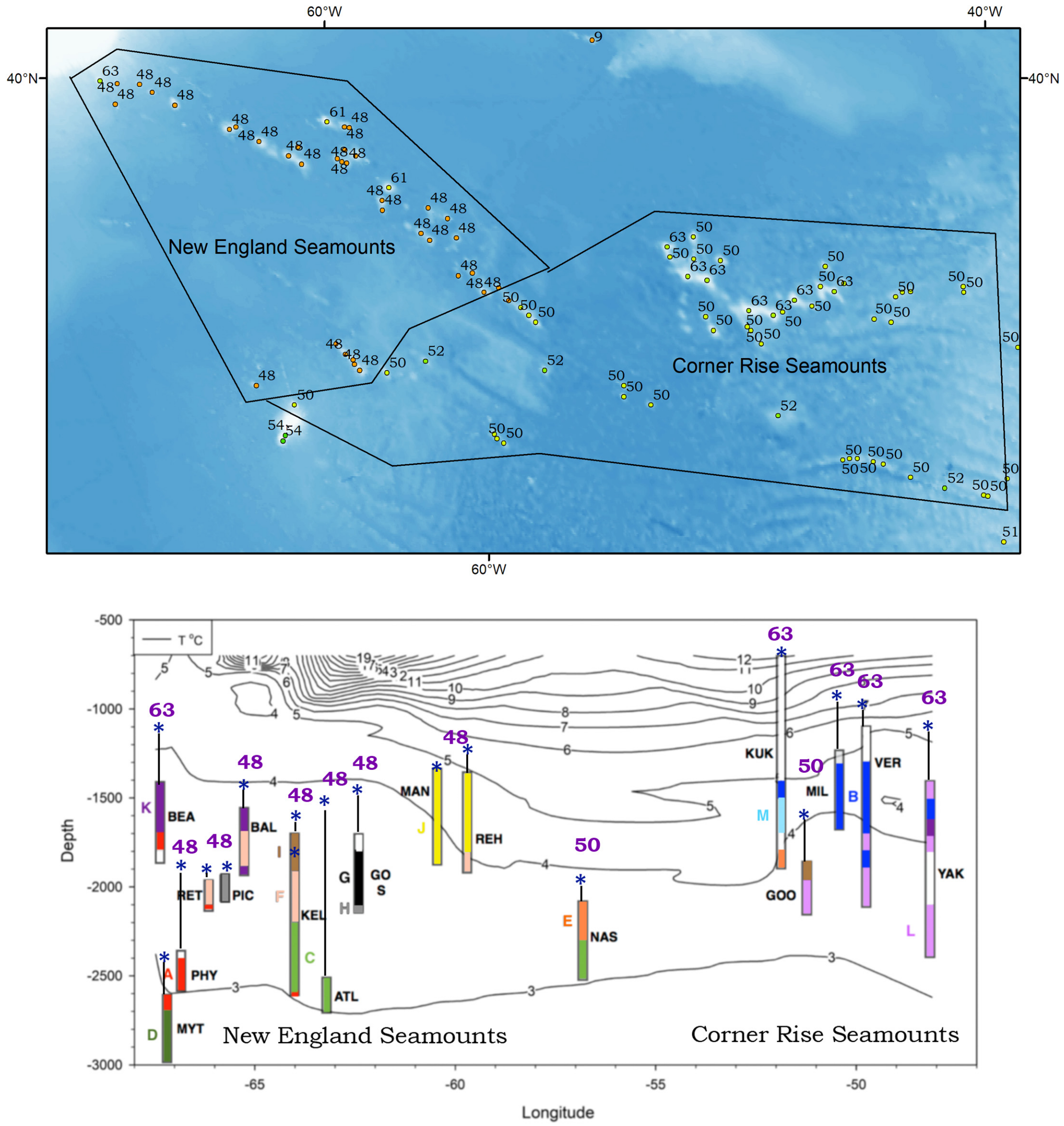

FIGURE 2 | Application of the Clark et al. (2011) seamount classification system to the seamounts of the New England and Corner Rise seamount groups, NW Atlantic whose summits were shallower than 3,500 m. Top panel: Numbers indicate in which group the seamount was included. Seamount groups were distinguished globally using factors such as summit depth, organic matter flux to the seamount summit, temperature at the summit, etc. Lower panel: A chart showing the arrangement of megafaunal assembles on the flanks of the seamounts from the upper panel that were surveyed by submersible or ROV (modified from Lapointe et al., 2020). Colors represent distinct megafaunal assemblages (white indicates areas not surveyed), asterisks indicate summit depths, numbers above the asterisks are the classification group from Clark et al. (2011), and the three letter acronyms represent seamount names (see Lapointe et al., 2020 for details).

From these considerations we make the following recommendations: (1) use indicator species to identify individual seamount VMCommunities recognizing that protecting part of a seamount identified only by the presence and distribution of an indicator species is not enough (Watling and Auster, 2017); (2) use the seamount classification system of Clark et al. (2011) or it's equivalent to delimit groups of similar seamounts to focus conservation management efforts and to distinguish between rare and abundant seamount types; (3) examine the similarities among adjacent groups of seamounts to see whether they should be considered to be part of a larger ecosystem group; and (4) evaluate the spatial extent of these larger units so that "significant adverse impacts" measures can be used to determine whether to allow some bottom fishing within a seamount ecosystem group (e.g., allowing one or two seamounts in each ecosystem group to be fished). We show in **Figure 2** the classification system as applied to the New England and Corner Rise Seamounts in the NW Atlantic along with the distribution of megafaunal assemblages on some of those seamounts as determined by Lapointe et al. (2020) to illustrate the complexity of the ecosystem problem. Only by defining the boundaries in which fishing impacts occur can we evaluate the impacts to VMEcosystems and those interacting communities within.

DATA AVAILABILITY STATEMENT

The original contributions presented in the study are included in the article/supplementary material, further inquiries can be directed to the corresponding author/s.

AUTHOR CONTRIBUTIONS

LW and PA drafted and reviewed the manuscript, and prepared it for publication. Both authors contributed to the article and approved the submitted version

ACKNOWLEDGMENTS

This perspective is modified from a position manuscript by the authors submitted as background for the 8th Scientific Committee of the South Pacific Regional Fisheries Management Organization. The comments of D. Currie, A. Grehan, and the reviewers are much appreciated. The views expressed herein are those of the authors and do not necessarily reflect the views of the authors institutions, collaborators, or funding agencies. This is publication number 108 from the School of Life Sciences, University of Hawai'i at Mānoa.

REFERENCES

Allee, W. C., Emerson, A. E., Park, O., Park, T., and Schmidt, K. P. (1949). *Principles Of Animal Ecology*. Philadelphia: W.B. Saunders Co.

Ardron, J. A., Clark, M. R., Penney, A. J., Hourigan, T. F., Rowden, A. A., Dunstan, P. K., et al. (2014). A systematic approach towards the identi fi cation and protection of vulnerable marine ecosystems. *Mar. Policy* 49, 146–154. doi: 10.1016/j.marpol.2013.11.017

Auster, P. J., Moore, J., Heinonen, K. B., and Watling, L. (2005). "A habitat classification scheme for seamount landscapes: assessing the functional role of deep-water corals as fish habitat," in *Cold-water Corals and Ecosystems*, eds A. Freiwald and J. M. Robeerts (Berlin: Springer-Verlag), 761–769. doi: 10.1007/3-540-27673-4_40

Baco, A. R., Morgan, N., Roark, E. B., Silva, M., Shamberger, K. E. F., and Miller, K. (2017). Defying dissolution: discovery of deep-sea scleractinian coral reefs in the North Pacific. *Sci. Rep.* 7, 1–11. doi: 10.1038/s41598-017-05492-w

Bailey, D. M., Collins, M. A., Gordon, J. D. M., Zuur, A., and Priede, I. G. (2009). Long-term changes in deep-water fish populations in the northeast Atlantic: a deeper reaching effect of fisheries?. *Proc. R. Soc. B Biol. Sci.* 276, 1965–1969. doi: 10.1098/rspb.2009.0098

Bourque, J. R., and Demopoulos, A. W. J. (2018). The influence of different deep-sea coral habitats on sediment macrofaunal community structure and function. *PeerJ* 6:e5276. doi: 10.7717/peerj.5276

Cho, W., and Shank, T. M. (2010). Incongruent patterns of genetic connectivity among four ophiuroid species with differing coral host specificity on North Atlantic seamounts. *Mar. Ecol.* 31, 121–143. doi: 10.1111/j.1439-0485.2010.00395.x

Clark, M., and O'Driscoll, R. (2003). Deepwater fisheries and aspects of their impact on seamount habitat in New Zealand. *J. Northw. Atl. Fish. Sci.* 31, 441–458. doi: 10.2960/j.v31.a34

Clark, M. R., Anderson, O. F., Bowden, D. A., Chin, C., George, S. G., Glasgow, D. A., et al. (2015). *Vulnerable marine ecosystems of the Louisville Seamount chain: voyage report of a survey to evaluate the efficacy of preliminary habitat suitability models. New Zealand Aquatic Environment and Biodiversity Report (Wellington)*. Wellington: New Zealand Aquatic Environment, 1–87.

Clark, M. R., Watling, L., Rowden, A. A., Guinotte, J. M., and Smith, C. R. (2011). A global seamount classification to aid the scientific design of marine protected area networks. *Ocean Coast. Manag.* 54, 19–36. doi: 10.1016/j.ocecoaman.2010.10.006

Costello, M. J., Tsai, P., Wong, P. S., Cheung, A. K. L., Basher, Z., and Chaudhary, C. (2017). Marine biogeographic realms and species endemicity. *Nat. Commun.* 8, 1–9. doi: 10.1038/s41467-017-01121-2

Davies, J. S., Stewart, H. A., Narayanaswamy, B. E., and Jacobs, C. (2015). Benthic Assemblages of the Anton Dohrn Seamount (NE Atlantic): Defining Deep-Sea Biotopes to Support Habitat Mapping and Management Efforts with a Focus on Vulnerable Marine Ecosystems. *PLoS One* 10:e0124815. doi: 10.1371/journal.pone.0124815

Food and Agriculture Organization of the United Nations [FAO] (2009). *International Guidelines for the Management of Deep-sea Fisheries in the High Seas*. Rome: Food and Agriculture Organization of the United Nations.

George, K. H., and Schminke, H. K. (2002). Harpacticoida (Crustacea, Copepoda) of the Great Meteor Seamount, with first conclusions as to the origin of the plateau fauna. *Mar. Biol.* 141, 887–895. doi: 10.1007/s00227-002-0878-6

Gofas, S. (2007). Rissoidae (Mollusca: Gastropoda) from northeast Atlantic seamounts. *J. Nat. Hist.* 41, 779–885. doi: 10.1080/00222930701298085

Kennedy, B. R., Cantwell, K., Malik, M., Kelley, C., Potter, J., Elliott, K., et al. (2019). The unknown and the unexplored: insights into the Pacific deep-sea following NOAA CAPSTONE expeditions. *Front. Mar. Sci.* 6, 1–21. doi: 10.3389/fmars.2019.00480

Kitchingman, A., and Lai, S. (2004). Inferences on potential seamount locations from mid-resolution bathymetric data. *Univ. Br. Columbia Fish. Cent. Res. Rep.* 12, 7–12.

Lapointe, A. E., Watling, L., France, S. C., and Auster, P. J. (2020). Megabenthic assemblages in the lower bathyal (700–3000 m) on the New England and Corner Rise Seamounts, Northwest Atlantic. *Deep. Res. Part I Oceanogr. Res. Pap.* 165:103366. doi: 10.1016/j.dsr.2020.103366

McClain, C. R., Lundsten, L., Barry, J., and DeVogelaere, A. (2010). Assemblage structure, but not diversity or density, change with depth on a northeast Pacific seamount. *Mar. Ecol.* 31, 14–25. doi: 10.1111/j.1439-0485.2010.00367.x

Morato, T., Pham, C. K., Fauconnet, L., Taranto, G. H., Chimienti, G., Cordes, E. E., et al. (2021). North Atlantic basin-scale multi-criteria assessment database to inform effective management and protection of Vulnerable Marine Ecosystems. *Front. Mar. Sci.* 8, 1–7. doi: 10.3389/fmars.2021.637078

Morato, T., Pham, C. K., Pinto, C., Golding, N., Ardron, J. A., Muñoz, P. D., et al. (2018). A multi criteria assessment method for identifying vulnerable marine ecosystems in the North-East Atlantic. *Front. Mar. Sci.* 5:460. doi: 10.3389/fmars.2018.00460

Morgan, N. B., Cairns, S., Reiswig, H., and Baco, A. R. (2015). Deep-Sea Research I Benthic megafaunal community structure of cobalt-rich manganese crusts on Necker Ridge. *Deep. Res. 1 Oceanogr. Res. Pap.* 104, 92–105. doi: 10.1016/j.dsr.2015.07.003

O'Neill, R. V., DeAngelis, D. L., Waide, J. B., and Allen, T. F. H. (1986). *A hierarchical concept of ecosystems*. Princeton: Princeton University Press.

Pierrejean, M., Grant, C., de Moura Neves, B., Chaillou, G., Edinger, E., Blanchet, F. G., et al. (2020). Influence of Deep-Water Corals and Sponge Gardens on Infaunal Community Composition and Ecosystem Functioning in the Eastern Canadian Arctic. *Front. Mar. Sci.* 7:495. doi: 10.3389/fmars.2020.00495

Du Preez, C., Curtis, J. M. R., and Clarke, M. E. (2016). The structure and distribution of benthic communities on a shallow seamount (Cobb Seamount, Northeast Pacific Ocean). *PLoS One* 11:e0165513. doi: 10.1371/journal.pone.0165513

Priede, I. G., Godbold, J. A., Niedzielski, T., Collins, M. A., Bailey, D. M., Gordon, J. D. M., et al. (2011). A review of the spatial extent of fishery effects and species vulnerability of the deep-sea demersal fish assemblage of the Porcupine Seabight, Northeast Atlantic Ocean (ICES Subarea VII). *ICES J. Mar. Sci.* 68, 281–289. doi: 10.1093/icesjms/fsq045

Radice, V. Z., Quattrini, A. M., Wareham, V. E., Edinger, E. N., and Cordes, E. E. (2016). Vertical water mass structure in the North Atlantic influences the bathymetric distribution of species in the deep-sea coral genus Paramuricea. *Deep. Res. 1 Oceanogr. Res. Pap.* 116, 253–263. doi: 10.1016/j.dsr.2016.08.014

Rowden, A. A., Anderson, O. F., Georgian, S. E., Bowden, D. A., Clark, M. R., Pallentin, A., et al. (2017). High-resolution habitat suitability models for the conservation and management of vulnerable marine ecosystems on the Louisville Seamount Chain, South Pacific Ocean. *Front. Mar. Sci.* 4:335. doi: 10.3389/fmars.2017.00335

Samadi, S., Bottan, L., Macpherson, E., De Forges, B. R., and Boisselier, M. C. (2006). Seamount endemism questioned by the geographic distribution and population genetic structure of marine invertebrates. *Mar. Biol.* 149, 1463–1475. doi: 10.1007/s00227-006-0306-4

Sherman, K., and Duda, A. M. (1999). An ecosystem approach to global assessment and management of coastal waters. *Mar. Ecol. Prog. Ser.* 190, 271–287. doi: 10.3354/meps190271

Thoma, J. N., Pante, E., Brugler, M. R., and France, S. C. (2009). Deep-sea octocorals and antipatharians show no evidence of seamount-scale endemism in the NW Atlantic. *Mar. Ecol. Prog. Ser.* 397, 25–35. doi: 10.3354/meps08318

Thresher, R. E., Adkins, J., Fallon, S. J., Gowlett-Holmes, K., Althaus, F., and Williams, A. (2011). Extraordinarily high biomass benthic community on Southern Ocean seamounts. *Sci. Rep.* 1:119. doi: 10.1038/srep00119

Victorero, L., Robert, K., Robinson, L. F., Taylor, M. L., and Huvenne, V. A. I. (2018). Species replacement dominates megabenthos beta diversity in a remote seamount setting. *Sci. Rep.* 8:4152. doi: 10.1038/s41598-018-22296-8

Watling, L., and Auster, P. J. (2017). Seamounts on the high seas should be managed as vulnerable marine ecosystems. *Front. Mar. Sci.* 4:14. doi: 10.3389/fmars.2017.00014

Watling, L., Guinotte, J., Clark, M. R., and Smith, C. R. (2013). A proposed biogeography of the deep ocean floor. *Prog. Oceanogr.* 111, 91-112. doi: 10.1016/j.pocean.2012.11.003

Wilcove, D. S. (1994). "Turning conservation goals into tangible results: the case of the spotted owl and old-growth forests," in *Large-Scale Ecology and Conservation Biology*, eds P. J. Edwards, R. M. May, and N. R. Webb (Oxford: Blackwell Science, Ltd), 313–329

Conflict of Interest: The authors declare that the research was conducted in the absence of any commercial or financial relationships that could be construed as a potential conflict of interest.

frontiers
in Marine Science

ORIGINAL RESEARCH
published: 05 October 2021
doi: 10.3389/fmars.2021.520713

The Discovery and Preliminary Geological and Faunal Descriptions of Three New Steinahóll Vent Sites, Reykjanes Ridge, Iceland

James Taylor[1]*, Colin Devey[2], Morgane Le Saout[2], Sven Petersen[2], Tom Kwasnitschka[2], Inmaculada Frutos[3], Katrin Linse[4], Anne-Nina Lörz[5], Dominik Pałgan[6], Anne H. Tandberg[7], Jörundur Svavarsson[8], Daniel Thorhallsson[8], Adrianna Tomkowicz[6], Hrönn Egilsdóttir[9], Stefán Á. Ragnarsson[9], Jasmin Renz[1], Elena L. Markhaseva[10], Sabine Gollner[11], Eva Paulus[11], Jon Kongsrud[7], Jan Beermann[12,13], Kevin M. Kocot[14,15], Karin Meißner[1], Alexander Bartholomä[16], Leon Hoffman[16], Pauline Vannier[17,18], Viggó Þ. Marteinsson[17,18], Hans T. Rapp[19]†, Guillermo Díaz-Agras[20], Ramiro Tato[20] and Saskia Brix[1]

[1] Senckenberg am Meer, German Centre for Marine Biodiversity Research (DZMB) c/o Biocenter Grindel, Center of Natural History, Universität Hamburg, Hamburg, Germany, [2] GEOMAR Helmholtz Centre for Ocean Research Kiel, Kiel, Germany, [3] Department of Invertebrate Zoology and Hydrobiology, University of Lodz, Łódź, Poland, [4] British Antarctic Survey, Cambridge, United Kingdom, [5] Institute for Marine Ecosystems and Fisheries Science, Center for Earth System Research and Sustainability (CEN), University of Hamburg, Hamburg, Germany, [6] Institute of Oceanography, University of Gdańsk, Gdynia, Poland, [7] University of Bergen, University Museum of Bergen, Bergen, Norway, [8] Institute of Biology, University of Iceland, Reykjavík, Iceland, [9] Marine and Freshwater Research Institute, Hafnarfjörður, Iceland, [10] Zoological Institute, Russian Academy of Sciences, Saint Petersburg, Russia, [11] Department of Ocean Systems, Royal Netherlands Institute for Sea Research and Utrecht University, Texel, Netherlands, [12] Alfred Wegener Institute, Helmholtz Centre for Polar and Marine Research, Bremerhaven, Germany, [13] Helmholtz Institute for Functional Marine Biodiversity, Oldenburg, Germany, [14] Department of Biological Sciences, The University of Alabama, Tuscaloosa, AL, United States, [15] Alabama Museum of Natural History, The University of Alabama, Tuscaloosa, AL, United States, [16] Department of Marine Geology, Senckenberg am Meer, Wilhelmshaven, Germany, [17] Department of Research and Innovation, MATIS, Reykjavík, Iceland, [18] Faculty of Food Science and Nutrition, University of Iceland, Reykjavík, Iceland, [19] Department of Biological Sciences and K.G. Jebsen Centre for Deep-Sea Research, University of Bergen, Bergen, Norway, [20] Estación de Biología Marina de La Graña, Universidade de Santiago de Compostela, A Coruña, Spain

OPEN ACCESS

Edited by:
Christopher Kim Pham,
University of the Azores, Portugal

Reviewed by:
Mustafa Yucel,
Middle East Technical University, Turkey
Daphne Cuvelier,
Marine and Environmental Sciences Centre (MARE), Portugal

****Correspondence:***
James Taylor
james.taylor@senckenberg.de

†Died: 7th March 2020

Specialty section:
This article was submitted to Deep-Sea Environments and Ecology, a section of the journal Frontiers in Marine Science

Received: *16 December 2019*
Accepted: *31 August 2021*
Published: *05 October 2021*

Citation:
Taylor J, Devey C, Le Saout M, Petersen S, Kwasnitschka T, Frutos I, Linse K, Lörz A-N, Pałgan D, Tandberg AH, Svavarsson J, Thorhallsson D, Tomkowicz A, Egilsdóttir H, Ragnarsson SÁ, Renz J, Markhaseva EL, Gollner S, Paulus E, Kongsrud J, Beermann J, Kocot KM, Meißner K, Bartholomä A, Hoffman L, Vannier P, Marteinsson VÞ, Rapp HT, Díaz-Agras G, Tato R and Brix S (2021) The Discovery and Preliminary Geological and Faunal Descriptions of Three New Steinahóll Vent Sites, Reykjanes Ridge, Iceland. Front. Mar. Sci. 8:520713. doi: 10.3389/fmars.2021.520713

During RV *MS Merian* expedition MSM75, an international, multidisciplinary team explored the Reykjanes Ridge from June to August 2018. The first area of study, Steinahóll (150–350 m depth), was chosen based on previous seismic data indicating hydrothermal activity. The sampling strategy included ship- and AUV-mounted multibeam surveys, Remotely Operated Vehicle (ROV), Epibenthic Sledge (EBS), and van Veen grab (vV) deployments. Upon returning to Steinahóll during the final days of MSM75, hydrothermal vent sites were discovered using the ROV Phoca (Kiel, GEOMAR). Here we describe and name three new, distinct hydrothermal vent site vulnerable marine ecosystems (VMEs); Hafgufa, Stökkull, Lyngbakr. The hydrothermal vent sites consisted of multiple anhydrite chimneys with large quantities of bacterial mats visible. The largest of the three sites (Hafgufa) was mapped, and reconstructed in 3D. In total 23,310 individual biological specimens were sampled comprising 41 higher taxa. Unique fauna located in the hydrothermally venting areas included two putative new species of harpacticoid copepod (*Tisbe* sp. nov. and *Amphiascus* sp. nov.), as well as the sponge *Lycopodina cupressiformis* (Carter, 1874). Capitellidae Grube, 1862 and Dorvilleidae Chamberlin, 1919 families dominated hydrothermally influenced samples for polychaetes. Around the hydrothermally influenced sites we observed a notable lack of megafauna, with only a few species being present. While we observed hydrothermal associations, the overall species composition is very similar to that seen at other shallow water vent sites in the north of Iceland, such as the Mohns Ridge vent fields, particularly with peracarid crustaceans. We therefore conclude the community overall reflects the usual "background" fauna of Iceland rather than consisting of "vent endemic" communities as is observed in deeper vent systems, with a few opportunistic species capable of utilizing this specialist environment.

Keywords: hydrothermal vent, VME, conservation, benthic fauna, infauna, bacteria, habitat, vent-associated

INTRODUCTION

Iceland is one of only two areas on Earth where a mid-ocean ridge has been elevated above the sea level, making it a remarkable laboratory for studying spreading-associated geological, biological, chemical, and physical processes (Sæmundsson, 1979). The island relief is a surface reflection of an underlying hotspot, which by interfacing with a mid-ocean ridge (i.e., Mid-Atlantic Ridge) makes it an ideal location to investigate the plume-ridge interaction and the effects it has on the evolution of Iceland and surrounding seafloor. The ∼26 Ma yearlong geological history of Iceland's development is directly correlated with the repeated eastward rift jumps that allowed the spreading center to remain fixed over the Icelandic hotspot (Sæmundsson, 1979; Foulger and Anderson, 2005; Martin et al., 2011).

The Geological Background

The Reykjanes Ridge (**Figure 1A**) is the longest oblique, hotspot-influenced section of the global mid-ocean ridge system (Talwani et al., 1971; Searle et al., 1998; Sandwell et al., 2014). This ∼950 km segment of the northern Mid-Atlantic Ridge is spreading at 1 cm y^{-1} half rate (Talwani et al., 1971; DeMets et al., 1990) and is located between Iceland (64°N) and the Bight Fracture Zone near 57°N. In general, the depth of the Reykjanes Ridge gradually shallows from south to north from ∼2500 m depth near Bight Fracture Zone (Keeton et al., 1997) to ∼300 m depth near 63°N (Pałgan et al., 2017). The ridge axis is divided into two morphological types: the area south of 59°N is defined by a prominent median valley (2.5 km deep and 15 km wide), while north of 59°N has a dome-shaped axial high; resembling mid-ocean ridges of higher spreading rate, e.g., East Pacific Rise (Talwani et al., 1971). The Reykjanes Ridge lacks first-order transform offsets (Keeton et al., 1997), but instead shows a short-wavelength segmentation composed of individual Axial Volcanic Ridges (AVRs) (Murton and Parson, 1993; Keeton et al., 1997; Searle et al., 1998). These ridges have a right-stepping echelon arrangement, are separated from one-another by 3–10 km of flatter seafloor, and usually overlap with each other in a spreading-parallel direction over a distance of one third of their length (Murton and Parson, 1993; Keeton et al., 1997; Searle et al., 1998; Höskuldsson et al., 2007; Pałgan et al., 2017). The surfaces of AVRs are characterized by either rough, untectonized, or clearly dissected tectonic deformation volcanic terrain. Volcanic features building AVRs include individual hummocks, hummocky ridges, fissure-, conical-, cratered- and flat-topped volcanoes up to several kilometers in diameter (Searle et al., 1998; Höskuldsson et al., 2007; Pałgan et al., 2017). It has been confirmed that the volcanic activity along the northern Reykjanes Ridge has been extensive throughout recorded times, with at least 14 documented eruptions between 63°10′N and Iceland (Thorarinsson, 1969; Jakobsson et al., 1978; Johnsson and Jakobsson, 1985; Höskuldsson et al., 2007). However, further south along the ridge, historic activity has not been documented and is unknown.

Hydrothermal activity has been poorly pinpointed along the Reykjanes Ridge. An extensive survey along the ridge was performed in 1990 (German et al., 1994). This led to the discovery of a hydrothermal plume near 63°06′N, which was called the namesake Steinahóll vent field. High concentrations of dissolved methane (18 nmol/1), hydrogen (30 nmol/1), silica (∼2 μmol/l), and total dissolvable manganese (∼60 nmol/l) characterize the vent plume. Moreover, the same plume was recorded by a high frequency (38 kHz) echosounder which mapped streams of bubbles rising from the seafloor. Due to technological limitations (lack of high-resolution bathymetric data) the data from German et al. (1994) could not precisely locate the source of the mapped plume. They indicated, however, that the field is located in the northern part of a prominent axial volcanic ridge (AVR). A cruise carried out in 2010 by the Marine and Freshwater Research Institute (Iceland) also observed areas of vent effluent indicated through the presence of bacterial mats (unpubl. obs.). More recent geological interpretations of that area by Pałgan et al. (2017), together with results from numerical modeling of fluid flow at mid-ocean ridges (Bani-Hassan et al., 2012), indicate that hydrothermal flow tends to focus toward topographic highs, suggesting that the Steinahóll Vent Field is located along a shallow (∼250 m depth) and 500 m long eruptive fissure situated between two east-facing faults. Hence, it has been suggested that the dikes intruding into the northern part of the AVR provide the heat necessary to drive hydrothermal flow while constant slip of the faults provides high crustal permeability (Pałgan et al., 2017).

Marine Vent Fields and Their Biology

The northern Reykjanes Ridge is a direct underwater continuation of the on-land fissures and volcanic systems of the southern Icelandic Reykjanes Peninsula (Jakobsson et al., 1978; Murton and Parson, 1993; Pedersen and Grosse, 2014; Pałgan et al., 2017), but relatively little is known about the volcanic and geothermal activity offshore (Hannington et al., 2001) and even less on the biological diversity of these active

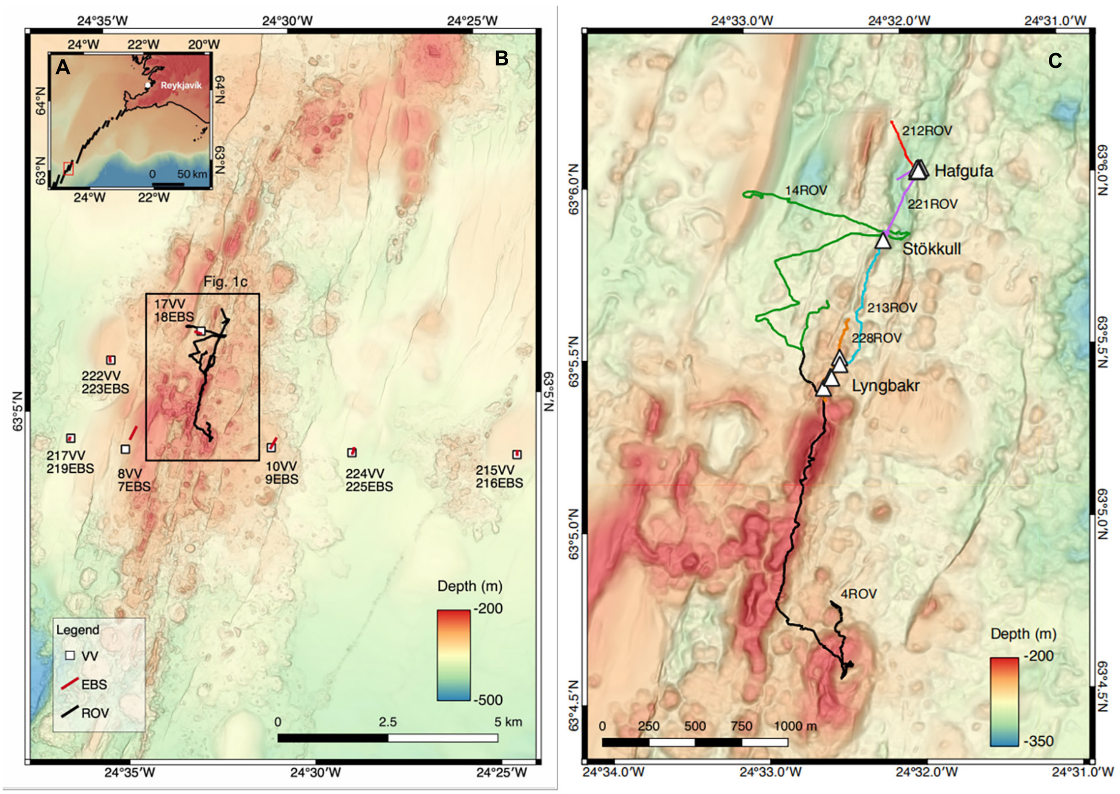

FIGURE 1 | **(A)** Regional map showing the northern section of the Reykjanes Ridge, indicated by a black line. The red box show the extent of the study area **(B)**. **(B)** Map of Steinahóll axial volcanic ridge at 5 m resolution with ROV tracks shown in black. The different sampling stations are located and named. Epibenthic sled (EBS) track are shown by a red line, ROV dive track by a black line, and Van Veen grab (vV) position is indicated by white squares. The black box shows the extent of **(C)**. **(C)** Map of the Steinahóll vent sites. Hydrothermal vents (white triangles) are grouped in three hydrothermal field named Hafgufa, Stökull, and Lyngbakr. Venting is indicated by white triangles. ROV dives are individualized by different color lines.

sites (Fricke et al., 1989; Eythorsdottir et al., 2016). Over the last decades, information has been published on the biodiversity of the known hydrothermal vent fields on the Mid-Atlantic Ridge (MAR) and the Arctic Mid Ocean Ridge (AMOR). To date in the North Atlantic, the biology of 12 vent fields along the MAR has been described for the area between 12° and 45°N, at depths ranging from 850 to 4200 m (Desbruyères et al., 2000; 2006; Wheeler et al., 2013). At the same time, biology has been studied on only few shallow water vent fields ($\leq$500 m deep), e.g., Kolbeinsey at AMOR (located at depth of ~100 m, Fricke et al., 1989). Moreover, only bacterial studies have been carried out along the AMOR (Wheeler et al., 2013). The macrofauna of the deep MAR vent fields is characterized by the presence of vent-endemic and chemosynthetic taxa, dominated by such as the alvinocarid shrimps *Mirocaris* Vereshchaka, 1997 and *Rimicaris* Williams and Rona, 1986, the bivalve *Bathymodiolus* Kenk and B.R. Wilson, 1985 or the gastropod *Peltospira* McLean, 1989 (e.g., Desbruyères et al., 2000, 2006; Tarasov et al., 2005; Wheeler et al., 2013).

Van Dover et al. (2018) describe hydrothermal vent ecosystems as "natural wonders of the ocean" that help us to understand the intersection of life and Earth processes, and are acting as storehouses of endemic marine genetic diversity. Under the United Nations General Assembly (UNGA) resolution 61/105, management of fisheries in areas beyond national jurisdiction requires identification of vulnerable marine ecosystems (VMEs). Criteria to designate a VME include uniqueness, functional significance, fragility, structural complexity, and certain life history traits. Hydrothermal vent fields can be viewed as small islands within the different habitats of the ocean floor, being colonized by endemic and mostly rare species (Van Dover et al., 2018). They show such a high natural variability that it is difficult to designate a "representative" ecosystem in the northern MAR according to the work of Desbruyères et al. (2000), wherein species composition and abundances at eight known active vents along the MAR in the North Atlantic are compared. Their results exemplify the ecological rarity and vulnerable status of active hydrothermal vents. Statutes for full protection of ecosystems at active hydrothermal vents have been enacted by several coastal States (e.g., Canada, Mexico, New Caledonia, Portugal, United States) through establishment and management of area-based protection (LeBris et al., 2016). Furthermore, the Oslo and Paris Commission for the Convention for the Protection of the Marine Environment of the North-East Atlantic (OSPAR) recommends protection and conservation of hydrothermal vent fields as "priority habitats" (OSPAR, 2008, 2014) in the OSPAR maritime area (NE Atlantic). Similar reasoning, with the aid of advice from organizations such as The International Council for the Exploration of the Sea (ICES), has lead the North-East Atlantic Fisheries Commission (NEAFC) to restrict and close certain areas of the NE Atlantic for certain fishing practices. Thus, active vents are recognized as vulnerable through multiple international instruments that call for their protection.

Tarasov et al. (2005) state that hydrothermal vent communities split into a "shallow-water" (<200 m) and a "deep-sea" (>200 m) group, with the former having none or few vent-obligate taxa, while the latter is characterized by chemosynthetic vent-endemic taxa. They postulate that the proportion of organic matter derived from photosynthesis and chemosynthesis might play a crucial role in the evolutionary history of the faunal communities. Over the recent decades, the benthic fauna around Iceland has been subject to comprehensive biodiversity surveys under the umbrellas of the international projects BIOICE (Benthic Invertebrates of Icelandic waters; 1992–2004) and IceAGE (Icelandic marine Animals: Genetics and Ecology; 2011—ongoing), encompassing 23 research cruises and samples from more than 1700 locations (Brix et al., 2014a,b; Meißner et al., 2014). While the benthic megafauna of the Reykjanes Ridge from the shelf to the lower bathyal zones has been studied thoroughly in the past (Copley et al., 1996), during IceAGE samples were taken to compare stations on the East and West side of the Reykjanes Ridge (Brix et al., 2018a,b). However, no focused biological sampling has been done in close proximity to hydrothermally active sites of Steinahóll before this study. Previous cruises conducted in the area by the Icelandic Marine and Freshwater Research Institute (MFRI) (2004 and 2010) and Ifremer/MFRI (2012), with the goal of researching coral reefs and fishing impacts, have yielded large quantities of video/image material, of which contains indications of hydrothermal activity (unpubl. obs.), aiding in location selection for the dives accomplished during MSM75 cruise.

Hunting the Steinahóll Vent Sites, Discovery, and Preliminary Descriptions of the Geological and Biological Composition

Steinahóll was detected in 1990 during a response cruise following a seismic event south of Iceland (Palmer et al., 1995). Water column studies, echosounding and towed video indicated the presence of a hydrothermal plume that was later confirmed and more precisely located in 1993 near 63°06′N, 24°32′W (German et al., 1994). Based on the coordinates given in German et al. (1994) and previous cruise reports by French and Icelandic projects, our aim was first to detect and bathymetrically map the exact location of the Steinhóll vent field and the surrounding area. More importantly, the mapping is accompanied by the first biological description of faunal communities proximal and distal to the venting sites. We hypothesized from our knowledge of two shallow-water venting sites North of Iceland, that the Steinahóll fauna resembles the adjacent fauna as already described from the Mohns (Schander et al., 2010) and Kolbeinsey Ridges (Fricke et al., 1989). However, the fauna at Steinahóll should vary from those found at the vent sites in the North. This is based on our knowledge about the different biogeographic regions and faunal composition in the Arctic water mass influenced north and the Atlantic water mass influenced south of Iceland (Brix and Svavarsson, 2010; Dauvin et al., 2012; Jochumsen et al., 2016; Brix et al., 2018a,b).

During the final days of the expedition MSM75 we discovered what could be interpreted as the previously detected vent fields, after a previous search in the area which had proven unfruitful. Upon locating the vent fields, our geological aim was to map and document the discovery. The aim of the biological part of this study was to give an introductory description of potential vent-influenced fauna compared to non-vent-influenced fauna at the Steinahóll area of the Reykjanes Ridge. We also compare this to other shallow reduced habitats examined in the North Atlantic. This is part of ongoing assessment in the area with further expeditions planned.

MATERIALS AND METHODS

Deployment of Sampling Gear

During the research cruise MSM75 onboard the R/V *Maria S. Merian* between June and August 2018, we mapped the Steinahóll area using the ship's hull-mounted Kongsberg EM712 75 kHz echo-sounder at a speed of 5 knots. The shallow depth along the ridge (less than 500 m) allowed a 5 m resolution to be achieved (**Figure 1B**). In addition to the bathymetric maps, Steinahóll was also surveyed by the Autonomous Underwater Vehicle (AUV) Abyss from GEOMAR equipped with an Edgetech sidescan sonar 2200-S 120/410 kHz and with turbidity, CTD, and redox potential sensors. The combined data were used to target potential hydrothermally active sites and to plan further dives with the Remotely Operated Vehicle (ROV) Phoca from GEOMAR.

During ROV deployments, samples were collected using the operational arm, net, and scoop. Overall 19 samples yielding biological results were taken (10 via arm, 8 via net, and 1 via scoop). A complete station list of the IceAGE project is available via OBIS (Brix and Devey, 2019). Further biological samples (**Tables 1**, **2**) were taken with an epibenthic sled (EBS; Brenke, 2005) and van Veen grab (vV; van Veen, 1933). Locations for EBS and vV sampling were chosen with a minimum distance of 1 km from discovered vent activity, and using bathymetric maps from the AUV and backscatter data to ensure the presence of "soft bottom" areas. Prior to each EBS deployment, a vV was deployed adjacent to the planned EBS track to recover sediment samples and to verify the composition of the bottom substrate, ensuring to the best of our abilities that venting areas were protected. EBS and vV samples were taken at different distances from the Steinahóll vent site. All EBS trawls, after the third deployment (station 24EBS), were equipped with a Sonardyne system ultra-short baseline (USBL) pinger (ranger 2712) to provide maximum precision in EBS positioning. The trawl distance for EBS deployments was 300 m. In total, we deployed six vV grabs

TABLE 1 | Station list of biological sampling locations; *: hydrothermally influenced sample.

Station	**Dive/Deployment No.**	**Gear**	**Cast**	**Date**	**Start°N and°W -**	**Depth**
		(Sampling equipment)			**End°N and° W**	**(m)**
MSM75-4	**ROV 4**	**ROV**		01.07.18	63°05.496′/24°32.569′ -63°04.744′/24°32.485′	200–245
		(Arm)	*1*		*63°04.404′/24°32.634′*	*233*
		(Arm)	*2**		*63°05.376′/24°32.587′*	*225*
		(Net)	*4*		*63°04.707′/24°32.771′*	*242*
		(Arm)	*5*		*63°04.645′/24°32.632′*	*205*
		(Net)	*6**		*63°04.597′/24°32.521′*	*242*
MSM75-13	**ROV 13**	**ROV**	*Video only*	03.07.18	63°05.521′/24°32.525′–63°05.523′/24°32.775′	230–261
MSM75-14	**ROV 14**	**ROV**		03.07.18	63°05.588ß/24°32.552′ –63°06.039′/24°33.177′	253–300
		(Arm)	*3*		*63°05.901′/24°32.833′*	*295*
MSM75-212	**ROV 212**	**ROV**		03.08.18	63°06.100′/24°32.007′–63°05.965′/24°31.905′	289–315
		(Arm)	*1**		*63°06.028′/24°31.918′*	*310*
		(Net)	*2**		*63°06.024′/24°31.918′*	*310*
		(Net)	*3**		*63°06.026′/24°31.916′*	*311*
		(Arm)	*4**		*63°06.012′/24°31.918′*	*308*
		(Arm)	*5**		*63°06.014′/24°32.129′*	*306*
MSM75-213	**ROV 213**	**ROV**		03.08.18	63°05.829′/24°32.139′–63°05.443′/24°32.517′	157–260
		(Net)	*1**		*63°05.830′/24°32.147′*	*259*
		(Net)	*3*		*63°05.482′/24°32.472′*	*235*
MSM75-228	**ROV 228**	**ROV**		05.08.18	63°05.623′/24°32.449′–63°05.407′/24°32.544′	250–274
		(Net)	*1**		*63°05.484′/24°32.461′*	*236*
		(Scoop)	*2*		*63°05.488′/24°32.477′*	*234*
		(Arm)	*3*		*63°05.488′/24°32.478′*	*234*
		(Arm)	*5**		*63°05.430′/24°32.522′*	*235*
		(Arm)	*6*		*63°05.430′/24°32.516′*	*239*
		(Net)	*7*		*63°05.361′/24°32.564′*	*211*
MSM75-7	**EBS 7**	**EBS**		02.07.18	63°04.687′/24°34.581′ –63°04.619′/24°34.665′	250–277
MSM75-9	**EBS 9**	**EBS**		02.07.18	63°04.469′/24°30.849′ –63°04.433′/24°30.897′	293–286
MSM75-18	**EBS 18**	**EBS**		04.07.18	63°05.889′/24°32.741′ –63°05.898′/24°32.794′	294–293
MSM75-216	**EBS 216**	**EBS**		03.08.18	63°04.348′/24°24.238′ –63°04.348′/24°24.239′	314–315
MSM75-219	**EBS 219**	**EBS**		03.08.18	63°04.563′/24°36.326′ –63°04.564′/24°36.324′	356–355
MSM75-223	**EBS 223**	**EBS**		04.08.18	63°05.708′/24°35.154′ -63°05.708′/24°35.155′	281-281
MSM75-225	**EBS 225**	**EBS**		04.08.18	63°04.470′/24°28.623′ -63°04.470′/24°28.623′	360-359
MSM75-8	**vV 8**	**vV**		02.06.18	63°04.520′/24°34.784′	286
MSM75-10-1	**vV 10-1**	**vV**		02.07.18	63°04.443′/24°30.876′	286
MSM75-10-2	**vV 10-2**	**vV**		02.07.18	63°04.441′/24°30.875′	286
MSM75-17	**vV 17**	**vV**		04.07.18	63°05.903′/24°32.648′	302
MSM75-215	**vV 215**	**vV**		03.08.18	63°04.239′/24°24.260′	323
MSM75-217	**vV 217**	**vV**		03.08.18	63°04.652′/24°36.270′	360
MSM75-222	**vV 222**	**vV**		04.08.18	63°05.582′/24°35.155′	291
MSM75-224	**vV 224**	**vV**		04.08.18	63°04.343′/24°28.707′	363

and seven EBS. Overall, there were six deployments (dives) of the ROV Phoca. ROV biological sampling took place at 19 discrete locations, sampling hydrothermally active localities with bacterial mats and inactive localities for comparison. Specifically, the Steinahóll vent field explored during the ROV dives was sampled in regard to bacterial mats and vent-associated macrofauna using nets with a mesh size of 1 mm, and scoops of sediment were taken and transferred to closable bioboxes.

Samples were washed in chilled, filtered seawater directly on board, with EBS and vV samples being sieved through four size classifications (1 cm, 1 mm, 500 μm, and 300 μm). All samples were live-sorted for large specimens over the period of 1 h after sampling and treated "on ice" (Riehl et al., 2014). After the live sorting, all specimens were immediately fixed either in −20°C precooled 96% undenatured ethanol, RNAlater, 4% buffered formaldehyde solution, or frozen at −80°C. RNAlater and frozen samples were photographed and stored along with a representative sample specimen fixed in 96% undenatured ethanol. Sorting of the Steinahóll samples was finalized in the laboratory of the DZMB Hamburg, Germany using Leica MZ 12.5 binocular microscopes.

TABLE 2 | Faunal composition showing total individuals of each taxa sampled at the Steinahóll vent fields.

	Gear	**ROV**					**EBS**							**vV**						
Taxa	**Station**	**4**	**14**	**212**	**213**	**228**	**7**	**9**	**18**	**216**	**219**	**223**	**225**	**8**	**17**	**215**	**217**	**222**	**224**	**Total**
Porifera																				
Porifera		19	2	2	–	26	47	1	4	2	–	2	80	–	11	–	5	18	20	**239**
Cnidaria																				
Anthozoa		–	–	–	–	1	5	1	–	–	–	–	2	–	–	–	1	–	1	**11**
Hydrozoa		10	1	–	14	–	33	–	–	–	–	1	–	–	–	10	1	36	–	**106**
Ctenophora																				
Ctenophora		–	–	–	–	–	–	–	–	–	1	–	–	–	–	–	–	–	–	**1**
Annelida																				
Polychaeta		280	2	255	146	755	1766	20	1	102	4	7	399	2	59	81	132	126	194	**4331**
Oligochaeta		13	–	19	4	7	53	–	–	–	–	–	–	–	5	–	1	1	–	**103**
Sipuncula																				
Sipuncula		2	–	2	–	3	6	–	–	2	–	–	5	–	1	4	3	4	3	**35**
Platyhelminthes																				
Platyhelminthes		–	–	–	–	–	4	–	–	–	–	–	–	–	–	–	–	–	–	**4**
Cephalorhyncha																				
Priapulida		–	–	–	1	1	–	–	–	–	–	–	–	–	1	–	–	–	–	**3**
Mollusca																				
Aplacophora		–	–	4	–	–	49	–	–	4	–	–	7	–	–	2	4	2	2	**74**
Bivalvia		14	–	–	–	2	141	2	1	139	3	–	109	–	9	46	16	12	34	**528**
Cephalopoda		–	–	–	–	–	–	–	–	–	–	–	1	–	–	–	–	–	–	**1**
Gastropoda		18	–	3	–	7	271	4	–	16	2	–	–	1	3	1	1	1	–	**328**
Polyplacophora		–	–	–	–	1	17	–	–	–	–	–	–	–	2	–	–	–	–	**20**
Scaphopoda		–	–	–	–	–	98	–	–	–	30	–	19	–	1	12	1	19	6	**186**
Arthropoda																				
Pycnogonida		1	–	–	–	–	40	2	–	4	1	–	3	–	–	1	–	–	–	**52**
Acarina		2	–	4	–	6	–	–	–	–	–	–	–	–	–	–	–	–	–	**12**
Crustacea																				
Ostracoda		50	–	–	1	13	372	9	–	16	1	1	43	–	12	1	6	6	74	**605**
Copepoda Calanoida		43	–	8	8	14	795	501	1335	920	79	524	2079	–	14	8	35	26	201	**6590**
Copepoda Harpacticoida		33	–	173	14	1109	54	–	–	–	–	–	1	–	–	–	1	1	1	**1387**
Cirripedia		–	–	–	1	–	1	–	–	–	–	–	–	–	–	–	–	–	–	**2**
Leptostaca		–	–	–	–	2	5	–	–	–	–	–	–	–	–	–	–	–	–	**7**
Amphipoda		258	–	60	66	356	1299	8	2	29	2	3	101	2	33	15	23	16	5	**2278**

(Continued)

TABLE 2 | (Continued)

	Gear	ROV					EBS							vV						
Taxa	**Station**	**4**	**14**	**212**	**213**	**228**	**7**	**9**	**18**	**216**	**219**	**223**	**225**	**8**	**17**	**215**	**217**	**222**	**224**	**Total**
Cumacea		–	–	1	–	1	474	1	–	32	2	1	55	–	–	–	–	–	2	**569**
Isopoda		52	–	24	1	35	463	13	1	6	1	2	87	–	21	5	6	9	5	**731**
Mysida		–	–	–	1	2	51	1	1	10	1	–	69	–	–	–	–	–	–	**136**
Tanaidacea		2	–	5	–	2	54	1	–	–	–	3	2	–	3	–	5	7	4	**88**
Euphausiacea		–	–	1	1	–	–	–	5	2	–	–	–	–	–	–	–	1	–	**10**
Decapoda		–	–	–	–	–	5	1	–	–	–	–	–	–	–	–	–	–	–	**6**
Echinodermata																				
Asteroidea		–	–	–	–	–	7	–	–	–	–	–	–	–	–	–	–	–	–	**7**
Ophiuroidea		21	1	1	4	7	2323	7	2	59	1	2	62	–	–	–	–	–	–	**2490**
Crinoidea		–	–	–	–	–	5	–	–	–	–	–	4	–	–	–	–	–	–	**9**
Echinoidea		2	–	–	–	–	–	–	–	–	–	–	–	1	1	–	–	–	–	**4**
Holothuroidea		1	–	–	–	–	91	–	–	11	1	–	43	–	2	3	2	6	20	**180**
Brachiopoda																				
Brachiopoda		20	–	–	–	–	12	–	–	1	–	–	–	1	1	–	1	5	–	**41**
Bryozoa																				
Bryozoa		11	–	–	6	10	41	–	7	4	1	5	28	–	–	3	2	24	5	**147**
Chaetognatha																				
Chaetognatha		–	–	–	–	4	17	1	–	–	–	3	9	–	–	–	–	–	–	**34**
Nematoda																				
Nematoda		687	–	65	1	176	472	7	1	3	–	1	19	–	20	9	194	111	23	**1789**
Nemertea																				
Nemertea		29	–	14	24	11	22	–	–	2	–	–	–	1	–	–	1	1	6	**111**
Hemichordata																				
Enteropneusta		–	–	–	–	–	32	–	–	–	–	–	–	–	1	–	–	–	–	**33**
Chordata																				
Tunicata		–	–	–	–	–	17	–	–	–	–	3	–	–	1	–	–	–	1	**22**
	Total	1568	6	641	293	2551	9142	580	1360	1364	130	558	3227	8	201	201	441	432	607	**23310**

For the photogrammetric surveys a CANON Eos 6D SLR of 20 MP resolution with a 15 mm fisheye lens (CANON 8–15 mm f4.5 zoom) was employed as part of the DeepSurveyCam package described in Kwasnitschka et al. (2016). This system was developed for the GEOMAR AUV Abyss and uses a high power LED strobe. Of the three strobe arrays normally employed only two were carried on either manipulator of the ROV. The mounting of the strobe arrays onto the manipulator arms meant it was possible to precisely adapt the illumination pattern to the requirements of the terrain. The camera was mounted on the starboard front porch on a hydraulic tilt unit, oriented in landscape mode relative to the direction of travel. Visibility varied between sites due to varying particulate matter in the water column, so an optimum altitude of four meters was aimed for. Useful results were gathered at up to 6 m altitude while the continuity of the reconstruction could still be maintained at 8 m altitude. At an across track field of view of 160°, we obtained a track width of approximately 15 m, limited by scattering and absorption. Minimum altitude was around 2 m dictated by the amount of overlap between each image.

As an important note, we point out that, as typical for an exploratory scientific cruise, samples were not taken quantitatively and without direct replicates for each station.

Data Analysis

The ship-based bathymetry was post-processed on board using QPS Qimera software and its 3D Swath Editor to flag false data. The processed data was then exported and integrated in the open source software QGIS and used as based map for preliminary geological interpretations and the plan of ROV dive tracks and sampling stations.

Chimney samples and crusts were described macroscopically on board for their major mineralogical components. Further investigation of trace minerals and geochemical composition are pending. The van Veen sediment samples have been dialyzed to remove the salt. The separation of the sand fraction (>63 μm) and the mud fraction (<63 μm) has been realized by wet sieving with a mesh size of 63 pm. The grain-size analyses of the dispersed sediments were performed by a Sedigraph5100 (Micromeritics^{TM}) particle analyzer (see e.g., Bianchi et al., 1999). The system determines the size distribution of particles dispersed in a liquid assuming Stokes' Law of settling. It measures the attenuation of a finely collimated X-ray beam as a function of time and height in a settling suspension. By means of the standard Micro-meritics software (version 3·07) for the Sedigraph the changes of attenuation over time were transformed into grain size fraction ranging from coarse of silt to clay.

Photogrammetric 3D reconstructions were done using the Agisoft Photoscan Pro software as detailed in Kwasnitschka et al. (2016). Processing involved the correlation and cross-referencing of USBL and DVL navigation records, which then served as a first order pose estimation to initialize the photogrammetric reconstruction and, together with multibeam maps, form the basis for georeferencing of the reconstructions. Camera orientation was logged inside the camera housing and was fused with other navigation information.

Upon review of the ROV and EBS samples it was evident that Porifera were underrepresented compared with what was observed during the ROV dives. This is predominantly due to the Porifera inhabiting hard bottom substrata, including large pillow larva. As we did not use the EBS in these areas for protection and the ROV being used for mainly exploratory purposes, it was decided to use the HD front-view video for qualitative (presence/absence) registration of Porifera, as well as noting their proximity to venting areas.

The preliminary results of the microbial diversity were obtained by 16S rRNA gen sequencing, Samples were collected and conserved for molecular analysis and for cultivation of microbes.

RESULTS

Hydrothermal Vent Field Discovery and Naming the Single Venting Spots

In order to help identify areas of hydrothermal activity, the ship-based multibeam echosounding system was used in the water-column mode in order to detect bubble streams. The newly discovered vent fields were given names of traditional maritime mythological folk creatures (Illhveli; "evil-whales") thought to reside in the treacherous waters surrounding Iceland so to represent and reflect the local culture and traditions.

We named the largest vent field (**Figure 1**) "Hafgufa," known in multiple folklores as the Kraken. The first known record of Hafgufa (haf = ocean; gufa = steam) is in the 12th century Norwegian saga Konungsskuggsjá (Kings mirror). In Örvar-Odds saga, an Icelandic saga from the 13th century, the creature is described as an enormous and evil beast, able to devour whole ships along with its men. At low tide, her nose would rise out of the water to be mistaken for two massive rocks rising from the sea.

The Southernmost vent field is named "Lyngbakr" (Lyng = heather; bakr = back) from Örvar-Odds saga. Lyngbakr is an enormous whale-like beast with a back that resembles a heather strewn island. Unlike Hafgufa is thought to be benign, but if unsuspecting seafarers take land on its back, often mistaking the creature's eyes as pools of freshwater, they may drown if Lyngbakr decides to dive.

The Illhveli "Stökkull" (stökk = jump) was used to name the middle vent field and is described in Íslenzkar þjóðsögur og aevintýri, 1862, edited by Jón Árnason. Stökkull would jump out of the sea and onto ships, leaving them in danger of sinking to the bottom of the sea. To prevent this, Saint Brendan requested divine intervention, receiving it in large flaps that covered the creature's eyes, rendering it blind. However, this did not prevent the creature from maintaining its destructive strategy and nature, remaining a threat to those ships unfortunate to encounter one.

Hafgufa

Indications for gas venting were observed 1.4 km north of the shallowest point of the Steinahóll area. These indications were later confirmed to originate from a dense area of venting with dimensions of 60 m in N/S direction and a width of 35 m (Hafgufa; **Figure 1C**). Hafgufa is located at a water depth of ca. 300 m, close to the first fault on the eastern ridge flank in this area. The vent site was associated with pillow lava and located in the hanging-wall of the fault, with its location appearing to follow a ridge-parallel fault trace in the sub-sea floor. Hydrothermal activity was shown by small anhydrite chimneys, commonly < 1 m in height, and abundant bacterial mats. Some of the chimneys sat on small mounds (only a few meters in diameter; **Figures 2A,B**) consisting of sand-sized talus material, as well as siliceous and barite-bearing slabs (**Figure 2C**). The largest of the mounds, also hosting the largest chimney ("Central Chimney" 2.5 m in height) had a diameter of approximately 7 m. The chimneys were located at the periphery of small depressions, the largest of these being 15 m in diameter. Additional small depressions were located just south of the largest chimney and were aligned parallel to the fault scarp in the east. The elevated rim around the depressions consisted of clay-rich hydrothermal precipitates and talus material, including crusts. This indicates that hydrothermal activity has been present in the area for some time. The formation of the depressions is likely the result of the collapse of anhydrite-bearing material during waning stages of hydrothermal activity, as anhydrite has a retrograde solubility and dissolves in cold seawater. This process has been

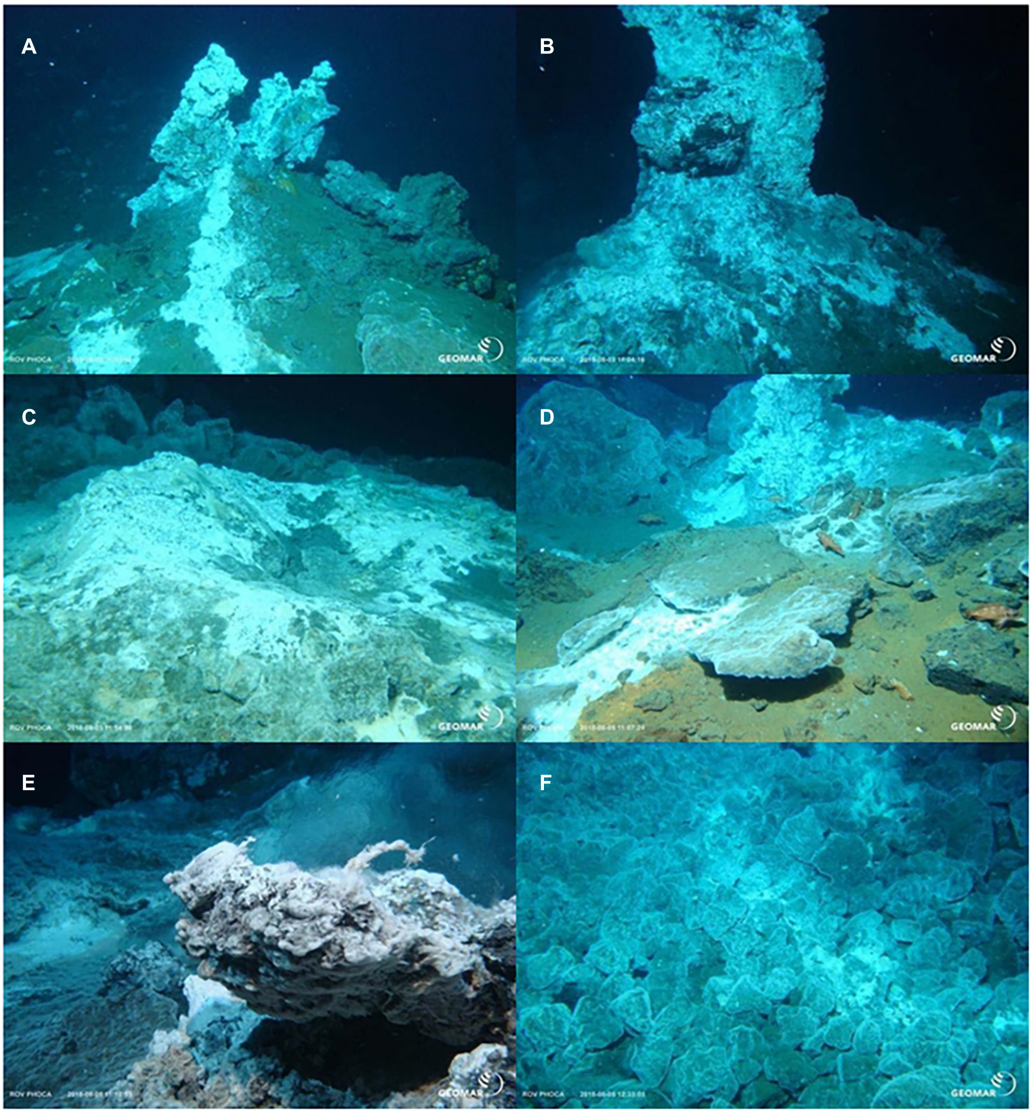

FIGURE 2 | (A) Small anhydrite chimney with associated bacterial mats located on top of a small mound at Hafgufa (212ROV-T11:33). **(B)** Base of largest chimney (2.5 m height) observed in the Steinahóll area. The chimney at Hafgufa is largely composed of anhydrite with minor pyrite/marcasite (212ROV-T11:04). **(C)** Small circular depression at Hafgufa with raised clay- rich rim covered in microbial mats. The elevated nature of the rim indicates a hydrothermal formation while anhydrite dissolution might be responsible for the formation of the depression (212ROV-T11:54). **(D)** Vent site at Lyngbakr with large anhydrite blocks, bacterial mats, and siliceous crusts in the foreground. Iron-staining is visible in the sediments (228ROV- T11:07). **(E)** Diffuse venting of clear fluids from a small chimney at Lyngbakr. All rock surfaces are covered by bacterial mats (228ROV-T11:12). **(F)** Bacterial mats coating basaltic talus indicating more widespread diffuse venting (228ROV-T12:33).

invoked for the formation of breccias at the active TAG mound (Humphris et al., 1995) and for similar depressions in the serpentinite-hosted Logatchev hydrothermal field (Petersen et al., 2009). Fluid flow was subdued and consisted of transparent fluids containing gas bubbles. Filamentous bacterial mats were present in areas of diffuse fluid venting, as well as covering larger areas of the seafloor. Bacterial mats were also widespread in talus piles indicating diffuse venting from below through the highly permeable pillow talus material. Together with anhydrite from chimneys (**Figure 3A**) a few massive to semi-massive pyrite-marcasite-bearing sulfides (**Figure 3B**) have been collected from underneath siliceous barite-rich slabs (**Figures 3C,D**) while Fe-oxyhydroxides were rare. Photometric surveys during ROV 221 allowed the mapping and 3D reconstruction of Hafgufa (**Supplementary Figure 1**).

Stökkull

Subsequent ROV dives located small patches of venting along the central volcanic chain itself. These sites, each only a few meters in diameter, were not connected to ridge-parallel faults and the heat distribution was along pillow margins, talus pieces, and cracks in the youngest volcanic rocks. Gas bubbles were observed at all chimneys. The second vent site was located 400 m south of Hafgufa and consisted of isolated patches of hydrothermal venting with bacterial mats, hydrothermal crusts, and small (<1 m in height) anhydrite chimneys (259 m water depth; **Figure 1C**).

Lyngbakr

Additional, more isolated, anhydrite chimneys and associated hydrothermal crusts were found in a water depth of around 235 m, closer to the local axial high. The sites are distributed over a strike length of 300 m with all chimneys occurring in a water depth of around 235 m. The northernmost site of Lyngbakr is located 700 m south of Stökkull (Lyngbakr; **Figure 1C**). Again, anhydrite-chimneys and siliceous crusts dominated the hydrothermal precipitates. As with the Stökkull site, individual vent sites at Lyngbakr are only a few meters in diameter. These vent sites were characterized by diffuse fluid venting and bacterial mats on the surrounding talus material (**Figures 2D–F**).

Biological Description of Steinahóll

Higher Taxon/Family Level

In total 23,310 individual specimens were collected and identified (to varying taxonomic levels, dependant on group) over the span of six ROV (5,059 ind.), seven EBS (16,361 ind.), and six vV (1,890

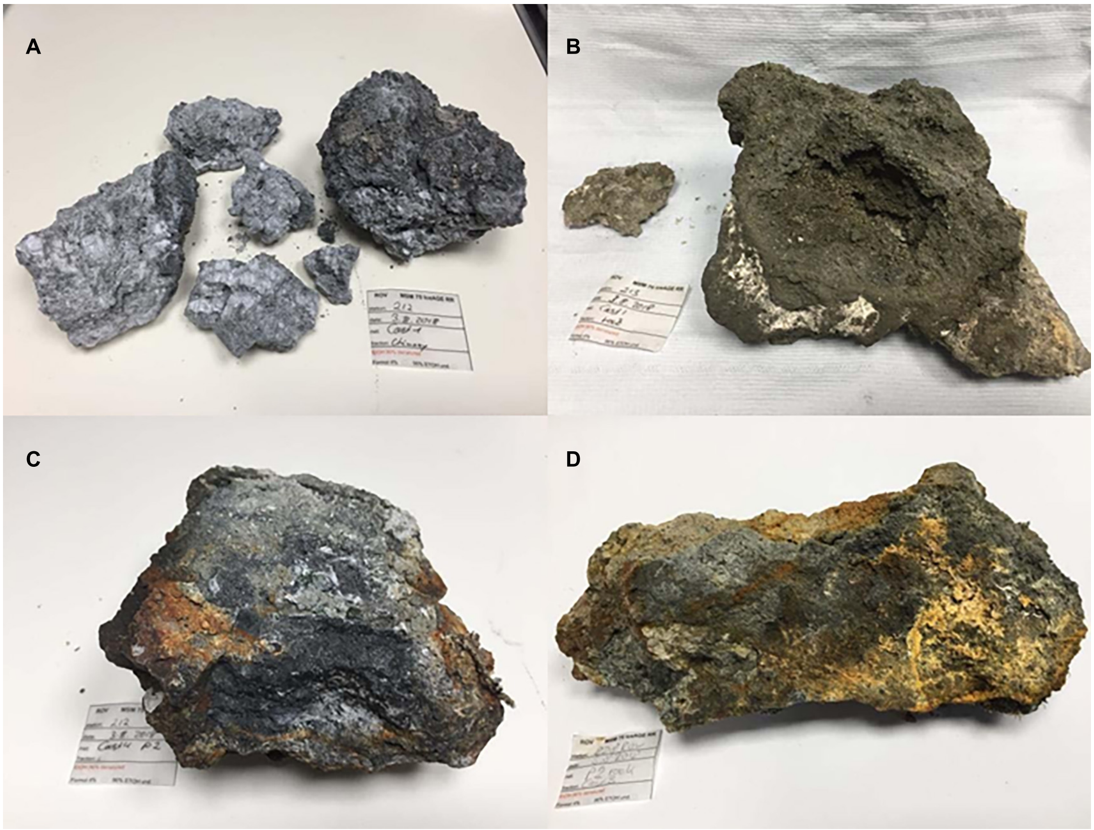

FIGURE 3 | (A) Massive coarse-grained anhydrite from chimney in the Steinahóll field. **(B)** Massive pyrite-marcasite collected from underneath siliceous slabs indicating reduced conditions in the immediate subseafloor. The sample is upside down, the overlying, white siliceous and barite-rich cap can be seen. **(C)** Brecciated hydrothermal crusts colored dark from fine-grained sulfides. **(D)** Large siliceous slab showing Fe-oxyhydroxide staining and remnants of bacterial mats. Sampling card is 4 cm across.

ind.) deployments. These specimens were assigned to a wide range of phyla, spanning 41 taxonomic groupings used further for comparison of faunal community in this study (**Table 2**), with taxonomic composition of each sampling effort visible in **Figure 4**. Full tables of sampled Polychaeta, Amphipoda, Isopoda, Mollusca, and harpacticoid Copepoda to family level are provided in the **Supplementary Tables 1–5**, respectively.

Observations made during ROV deployment also showed large numbers of fish in the area, as well as a number of cold-water corals, which were unable to be physically sampled during our efforts. However, as the area of study was located within Icelandic territorial waters, we observed evidence of fishing pressure through discarded long-line and gill-net equipment (**Figure 5**).

Vent-Associated Fauna

Steinahóll was categorized biologically by two distinct habitats, rocky areas with relatively low densities of visible megafauna (except large quantities of various fish species) and hydrothermally active sites, containing wide coverages of bacterial mats. The megafaunal composition comprised crustaceans, sponges, echinoderms, corals, reef building polychaetes, molluscs, fish, and ascidians.

Video-based observations

Porifera. The sponge fauna on this section on the Reykjanes Ridge appears to be very rich with several types of sponge communities existing side by side. By applying a very conservative approach, 39 taxa (ranging from species level to class) were identified from the ROV footage (**Supplementary Table 6**). ROV 14 contained the highest number of taxa as well as most dense sponge communities (31 out of the total of 39), while in the ROV dives 212, 213, 221, and 228, only 2–6 sponge taxa were observed. The high sponge richness and abundance were confined to areas outside of the active venting, and the transition zones between soft sediments and various cold-water corals. Only one species, *Lycopodina cupressiformis* (Carter, 1874), was found within the area of active venting, while *Asbestopluma (Asbestopluma) furcata* (Lundbeck, 1905), Cladorhiza Sars, 1872 sp., unidentified Axinellidae Carter, 1875, and unidentified encrusting sponges were found in areas with more diffuse venting and bacterial mats or filaments.

Hard and soft substrates in the close surroundings of the vents hosted sponge faunas of both boreal and more temperate affinities. The most abundant boreal species included *Geodia atlantica* (Stephens, 1915), *G. barretti* Bowerbank, 1858, *G. macandrewii* Bowerbank 1858, *G. phlegraei* (Sollas, 1880), *Stelletta* Schmidt, 1862 sp., *Mycale (Mycale) lingua* (Bowerbank, 1866), *Petrosia crassa* (Carter, 1876) and *Asconema* cf. *foliatum* (Fristedt, 1887). The more temperate fauna was highly dominated by glass sponges, with *Euplectella suberea* Thomson, 1876, *Hyalonema (Cyliconema) thomsonis* Marshall, 1875, *Pheronema carpenteri* (Thomson, 1869), *Aphrocallistes* cf. *beatrix* Gray, 1858, Euretidae Zittel, 1877 indet., and *Asconema* Kent, 1870 spp. being the most abundant species. In addition, *Geodia megastrella*

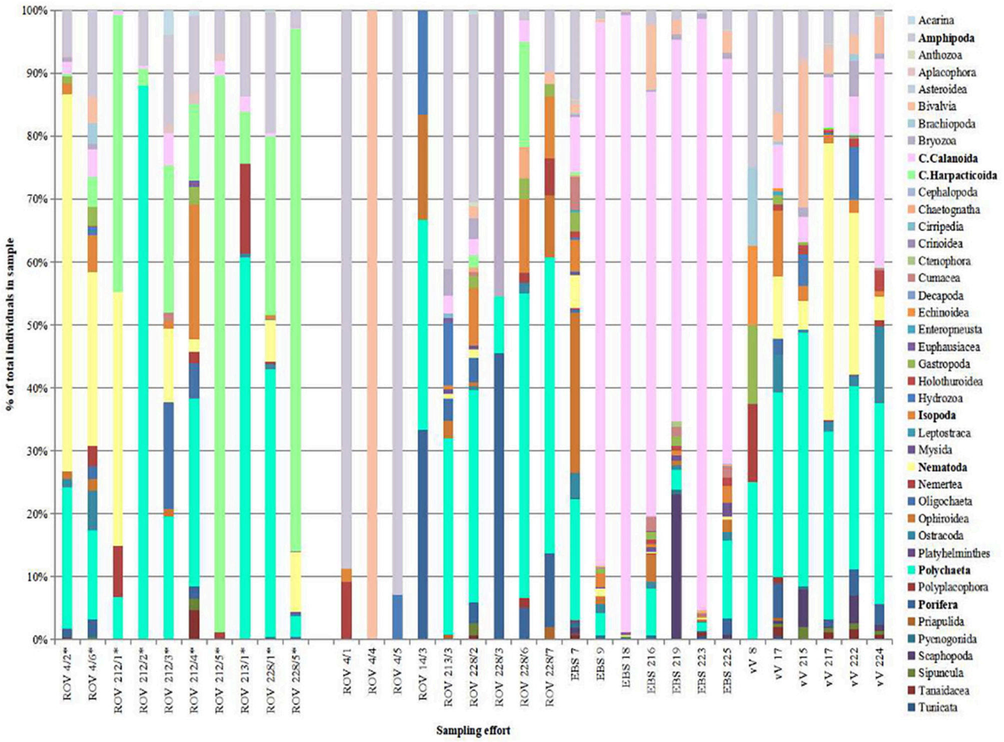

FIGURE 4 | Total percentage composition of taxonomic groups from biological samples taken in the Steinahóll region. *Denotes hydrothermally influenced sampling effort. Bold taxonomic names discussed in results/discussion.

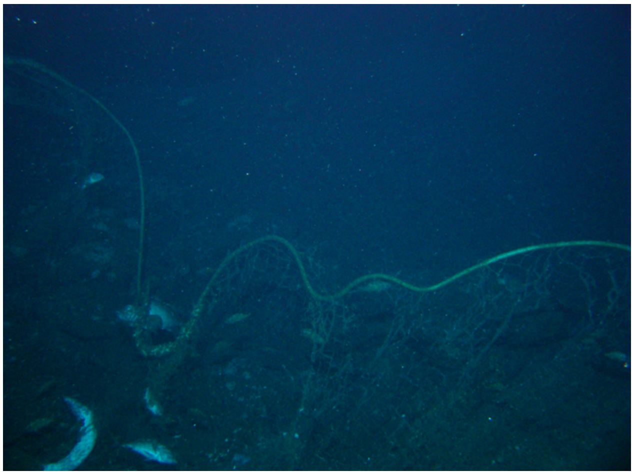

FIGURE 5 | Photo demonstrating fishing pressure example showing a discarded gill-net that has caught fresh fish, located near the Hafgufa hydrothermal vent field.

Carter, 1876, *Geodia* cf. *hentscheli* Cárdenas et al. (2010) and a species tentatively identified as *Cinachyrella* Wilson, 1925 sp. were highly present (**Supplementary Table 6**).

Hydrothermal fauna from Steinahóll vents

This section concentrates on the taxa where we have clear indications that they occur in the hydrothermal vent affected samples, namely the ROV deployments where bacterial mats or active venting were visible, as defined in **Table 1**, rather than those that can be considered usual Icelandic shelf fauna.

Copepoda, Harpacticoida. During the dive ROV 228, there were seven sampling stations, with almost all individuals coming from a net sample taken of bacterial mats (ROV 228/1) and a chimney top sampled with the sampling arm of the ROV (228/5). ROV 228/1 sampled 1,109 individuals, 6.4 times more than the next highest quantity, 173 individuals during ROV 212 (212/2 - Net: Vent field with chimneys). Both locations were under the direct influence of hydrothermal activity. A total of 27 morphospecies could be identified. The two species, *Tisbe* Lilljeborg, 1853 sp. nov. and *Amphiascus* Sars G.O., 1905 sp. nov., (**Figure 6**) occurred very abundantly at hydrothermally active sites and in less abundance at non-hydrothermal sites (228/1 – Net: Bacterial mats: total Harpacticoida = 334; *Tisbe* sp. nov. = 222, *Amphiascus* sp. nov. = 111; 228/5 – Arm: Chimney top: total Harpacticoida = 575; *Tisbe* sp. nov. = 568; **Figure 7**). These two samples were the only examples where we observed large quantities of Harpacticoida, with these two species almost encompassing the entirety of individuals sampled.

Out of 963 *Tisbe* specimens, only 24 were encountered at non-hydrothermal sites. Out of 153 *Amphiascus* specimens, only 1 was detected at a non-hydrothermal site. All non-hydrothermal sites with *Tisbe* and *Amphiascus* were located in the vicinity of vents and not in more distant samples taken by EBS and van Veen grab. Five additional copepod species (six *Ameira* Boeck, 1865 sp.1 specimens, one Tegastidae Sars G.O., 1904 sp.1 specimen, three additional singletons) were only detected at active venting sites. 20 copepod species were only encountered at non-hydrothermal sites, including 13 singletons and 3 doubletons.

Peracarida. At the Steinahóll region (vent and non-vent samples together), 3802 peracarids were sampled in total between 157 and 363 m depth. Of this 59.9% were Amphipoda, 19.2% Isopoda, 15.0% Cumacea, 3.6% Mysida, and 2.3% Tanaidacea. Peracarids occurred in all ROV samples except ROV 14. Most of the peracarids were provided by the EBS samples (2775 ind.), mainly from station EBS 7 (2341 individuals). Amphipods and isopods were determined on family level (**Supplementary Tables 1, 2**, respectively). Here, we observed a high taxonomic richness with at least 33 different amphipod families and 15 isopod families. The preliminary findings suggested that hydrothermal activity did not significantly affect the overall peracarid family composition.

Five hundred and nine amphipods were determined from the vent-influenced ROV-samples (**Supplementary Table 1**). 15.1% of these are Stenothoidae Boeck, 1871, with Amphilochidae Boeck, 1871 (3.9%) also represented in numbers that can be considered as non-stray specimens. Compared with ROV samples from areas not influenced by vents, there are more amphipods in general present, represented by fewer families. Families dominating the non-vent samples are Lysianassoidea Dana, 1849 (33%) Stenothoidae (15.2%) Pleustidae Buchholz, 1874 (14.7%), and Calliopiidae G.O. Sars, 1893 (6.9%) (**Figure 8**). Examples of Ampithoidae, Stenthoidae, and Calliopiidae can be seen in **Figure 9**.

The 15 isopod families sampled at Steinahóll have all been reported earlier from Icelandic waters (Brix et al., 2018b). In ROV samples with venting activity, isopods were collected only at two sampling sites (ROV212/2 – Net: Vent field with chimneys and ROV228/1 – Net: Bacterial mats). The families collected at hydrothermal vent sites, i.e., the Janiridae G.O. Sars, 1897 and the Gnathiidae Leach, 1814, were reported also outside the vent sites. Thus, no "stand out" Isopoda families were recorded from the vent-related samples.

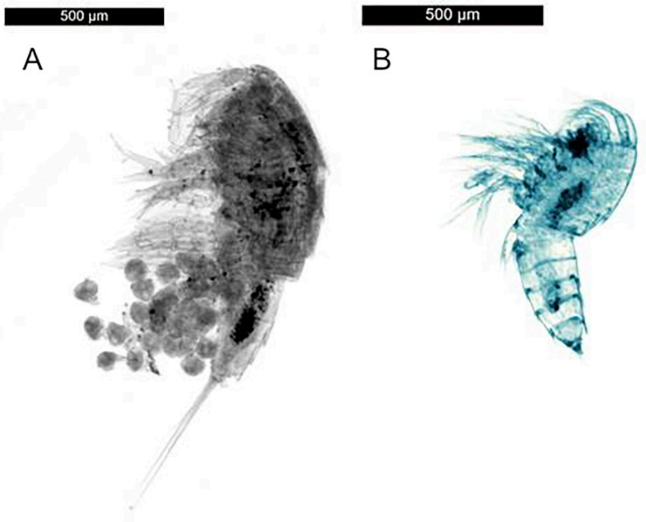

FIGURE 6 | Microscope images of **(A)** *Tisbe* sp. nov. (with nauplii), and **(B)** *Amphiascus* sp. nov.

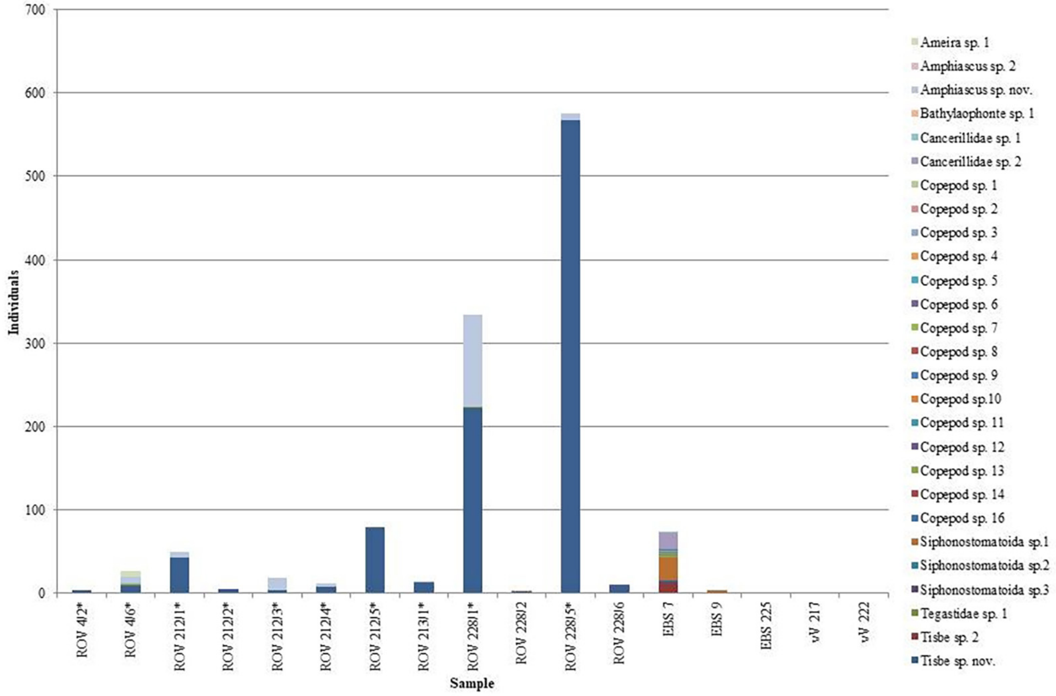

FIGURE 7 | Total individuals of Copepoda, Harpacticoida species taken during biological sampling during ROV, EBS, and vV deployments.

Polychaeta. A total of 4328 specimens of polychaetes representing 40 families were recorded in the samples from the Steinahóll area (**Supplementary Table 3**). About 60% of the specimens were collected by use of EBS, 25% by ROV and 15% by van Veen. The ROV samples taken from hydrothermal influenced sediments (9 samples) contained 1284 specimens representing 20 families of polychaetes, of which two, Dorvilleidae (530 specimens) and Capitellidae (466 specimens), accounted for more than 75% of the total number of specimens from these samples. Both families were also recorded from ROV, EBS and vV samples regarded as not hydrothermally influenced, but in far less quantities. Identification of specimens belonging to the two dominating families in hydrothermally influenced samples indicates that both families were represented by only a single species each, *Capitella* Blainville, 1828 sp. (Capitellidae) and *Mammiphitime* Orensanz, 1990 sp. (Dorvilleidae), both putative new to science (**Figure 10**).

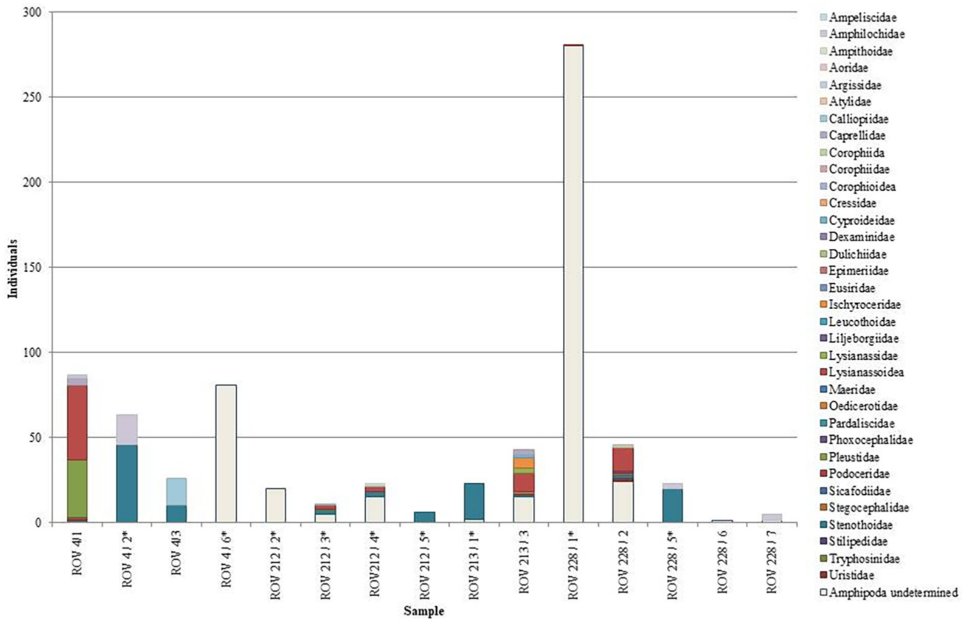

FIGURE 8 | Total individuals described to family level for Amphipoda during biological sampling of hydrothermally and non-hydrothermally influenced sites using ROV Phoca.

FIGURE 9 | Photographic plate demonstrating examples of the Amphipoda **(a)** Ampithoidae sp. (5 mm scale bar), **(b)** Stenothoidae sp. (1 mm scale bar), and **(c)** Calliopiidae sp. (5 mm scale bar) from ROV 212/4*.

Mollusca. A total of 1135 molluscs were present in sediment samples collected by ROV, EBS, and vV grab. Identification to morphospecies level yielded 27 bivalve species, 24 gastropod species, one polyplacophoran, and five scaphopod species. The majority of species were represented by a low number of specimens or by juveniles. No molluscs were recorded from vent-influenced ROV samples, except for two specimens recovered from bacterial mats at a diffuse flow site (ROV 228/1), representing one specimen each of the cimid *Cima inconspicua* Warén, 1993 and a juvenile buccinid *Colus* Röding, 1798 species.

Microbiology. The preliminary results of the microbial diversity show some accordance with other deep-sea hydrothermal vents (Dick, 2019), especially to the high-temperature vent field east of Grímsey, North of Iceland (Hannington et al., 2001; Marteinsson et al., 2013).

Cultivation results show high diversity of thermophilic, heterotrophic, and chemoautotrophic microorganisms belonging to bacterial and archaeal domains. These thermophilic taxa were cultivated from bacterial mats and chimney pieces stored anaerobically at 4°C before enrichments and isolation of strains performed at 65°C and above. Taxonomic identification was performed by sequencing the 16S rRNA genes from the isolates.

Preliminary results revealed bacterial strains belonging to different taxa such as *Thermotogales*, *Proteobacteria*, *Bacteroidetes,* and *Deinococcus*. Archaeal strains belonged mainly to the members of *Thermococcales, Archaeoglobales,* and *Thermoproteales* to some extent.

DISCUSSION

The presence of anhydrite chimneys, siliceous, and barite-bearing slabs from Steinahóll also resembles that of shallow-water vent sites further south along the Mid-Atlantic Ridge (MAR). Albeit

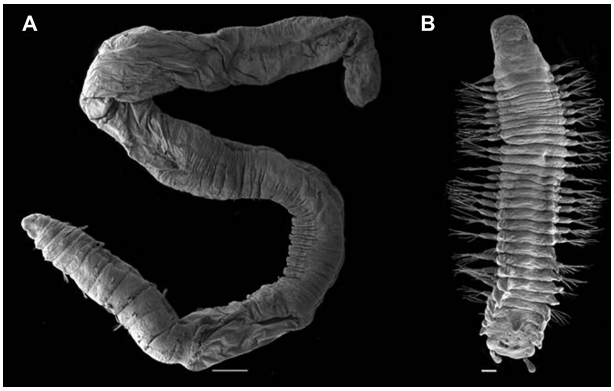

FIGURE 10 | Photographic plate demonstrating examples of the Polychaeta **(A)** *Capitella* sp. (500 μm scale bar) and **(B)** *Mammiphitime* sp. (100 μm scale bar).

at greater depth than Steinahóll, similar chimneys and slabs have been documented from the Menez Gwen and Bubbylon vent fields near 37°50′N in water depths between 800 and 1000 m (Colaço et al., 1998; Bogdanov et al., 2005; Marcon et al., 2013). Additionally, clear fluids have also been reported from the Grímsey vent field, north of Iceland (Hannington et al., 2001). Here, 250°C hot, boiling, and metal-depleted fluids are venting at a water depth of 400 m and form anhydrite chimneys, barite-rich slabs, and clay-rich mounds. The venting style at Steinahóll resembles both, Menez Gwen and Grímsey, with respect to venting of clear fluids and the presence of visible boiling.

Despite the (biological) limitation of working with higher taxon level at present state, the discovery of the vent sites is based on an exploratory expedition. Sampling, particularly with the ROV, was limited by the multidisciplinary character of each dive. The non-uniform sampling of the ROV in combination with the other gears led to limited options for community comparisons between the samples. ROV sampling focused on the lava pillows and ridge structures, whereas EBS and vV deployments had to be conducted in plain and/or soft-bottom areas. As expected, the use of different sampling gears was accompanied by distinctly different faunal elements. The deployment of the EBS and vV equipment in the detected vent sites was avoided to prevent any potential damage to the fragile structures.

Vent Fauna at Steinahóll Vent Sites

The present study describes a lower total number of taxonomic groups initially discovered in vent areas, compared with the fauna present in close proximity to the Steinahóll vent field, with *Lycopodina cupressiformis* (Porifera), *Capitella* sp. and *Mammiphitime* sp. (Polychaeta), *Tisbe* sp. nov., *Amphiascus* sp. nov. and a species of Stenothoidae (Crustacea) having a notable presence in vent-influenced samples. All apart from *L. cupressiformis* in this list await careful taxonomic checks as they may be new to science. Almost no sponges were found within the active venting and/or the surrounding area with diffuse seepage and bacterial growth, barring *L. cupressiformis*. This difference falls well within what has also been found on the Mohns Ridge further to the north, where also the cladorhizids *Asbestopluma furcata* and *L. cupressiformis* were among the very few thriving at hydrothermal vents, or in the very close enrichment zone surrounding the vents (Schander et al., 2010; Hestetun et al., 2017), potentially benefiting from the enhanced food availability (Hestetun et al., 2016).

The two stand-out polychaete species in the hydrothermally influenced samples, *Capitella* sp. and *Mammiphitime* sp., represent taxa well known from reduced shallow water environments (Oug, 1990; Blake et al., 2009). *Capitella* sp. was also recorded from the Kolbeinsey Ridge (Fricke et al., 1989), and may be the same species as our records of these taxa from Steinahóll. Polychaetes of the genus *Capitella* are considered to be opportunistic, typically occurring in high abundance in reduced environments (Blake et al., 2009; Silva et al., 2017) including shallow water hydrothermal vents (Gamenick et al., 1998; Sweetman et al., 2013). Specimens identified as *Mammiphitime* sp. from Steinahóll are morphologically similar to *Mammiphitime cosmetandra* (Oug, 1990) described from benthic algal-deposits at shallow water near Tromsø, northern Norway. However, the specimens differ in details related to morphology of the jaws as well as the number of segments, and is therefore regarded to constitute a separate, undescribed species.

The copepod species *Tisbe* sp. nov. and *Amphiascus* sp. nov., were extremely abundant in the bacterial mats at Steinahóll. The absence of these species in further distance to the ridge as well as the low abundance of these species at non-hydrothermal sites in the vicinity of vents, suggests that they have adapted to a life under extreme vent conditions. Since they are putative new species [only one formally described *Tisbe* species by Ivanenko et al. (2011), no description from *Amphiascus*], it is not possible yet to discuss distribution patterns and potential vent endemism of these species. *Tisbe* and *Amphiascus* are genera that often occur at deep-sea hydrothermal vents, in the direct vent vicinity (Gollner et al., 2010, 2016; Plum et al., 2017) as well as in the intertidal (Steinarsdóttir et al., 2003).

The amphipod-family Stenothoidae can be considered to be having at least one vent-associated species in the Steinahóll area. In the hydrothermally influenced samples, stenothoid amphipods were a dominant family, but they were also present out of the active areas. Similar opportunist behavior has been already pointed out for other stenothoids in the Lucky Strike vent fields, where the same species was collected at 1–2 m from the hydrothermal fluid emissions, among sponges, dead mussels, or gorgonians outside of the active hydrothermal areas (Bellan-Santini, 2005). Comparing that we observe only the family Stenothoidae as being vent influenced, with the observations of 20 families being vent-influenced along the entire Mid-Atlantic Ridge (Vinogradov, 1995; Bellan-Santini and Thurston, 1996; Desbruyères et al., 2001; Myers and Cunha, 2004; Bellan-Santini, 2005, 2006, 2007; Schander et al., 2010; Tandberg et al., 2012; Corbari and Sorbe, 2018), Steinahóll seems very limited in vent-influenced amphipods. However, most vent-influenced observations of amphipods tend to be one species to one vent, all seemingly endemic (e.g., Schander et al., 2010; Tandberg et al., 2012; Corbari and Sorbe, 2018 and references therein). Further identification to species level will show us if, and how many, vent-adapted species are amongst the stenothoid Amphipoda of the Reykjanes Ridge. The composition of the isopod families collected in the Steinahóll area resembles the fauna collected at the Mohns Ridge (Schander et al., 2010), with members of the families Janiridae and Gnathiidae being present in the bacterial mats.

Non-vent Fauna at Steinahóll Vent Sites

The non-vent sponge fauna is a peculiar mix of typically boreal and temperate sponge species. The species *Geodia atlantica*, *G. barretti*, *G. macandrewii,* and *G. phlegraei* are all characteristic components of boreal tetractinellid sponge grounds (Klitgaard and Tendal, 2004; Cárdenas et al., 2013; Maldonado et al., 2017), while the hexactinellids *Pheronema carpenteri*, *Euplectella suberea*, *Hyalonema thomsoni*, *Aphrocallistes* cf. *beatrix, Asconema* spp., and Euretidae indet. are typical for more temperate grounds (e.g., Maldonado et al., 2017). In addition, there are also a number of temperate demosponges, e.g., *Geodia megastrella* and a tentative *Cinachyrella* species. The presence of *Geodia* cf. *hentscheli* is interesting as it is a very common component of arctic sponge grounds (normally found at negative temperatures) (Roberts et al., 2018; Meyer et al., 2019). However, Cárdenas and Rapp (2015) reported *G. hentscheli* and *G.* cf. *hentscheli* from further south on the Mid-Atlantic Ridge, and already then it was noted that the records were far outside the normal distribution and temperature range for the species. Most likely these southern records, as well as the numerous specimens observed in the Steinahóll area, represent a different and hereto undescribed species.

The molluscan fauna in Steinahóll is typical to that of southern Iceland (Madsen, 1949; Warén, 1989, 1991, 1993, 1996; Dijkstra et al., 2009) and western Norway (Bouchet and Warén, 1979, 1980, 1985, 1986, 1993; Warén, 1989, 1991, 1993, 1996; Høisæter, 2010). In fact, all live-collected species that have been determined to species level (34 species) are known to live in western Norway. Most species of this set have large distribution ranges, typically including the continental margins of western Europe.

The comparison of the Steinahóll molluscan fauna (57 live-collected species) with the one reported from the Mohns Ridge hydrothermal vent sites (28 reported species; Schander et al., 2010) highlights both differences and similarities. Typical vent fauna, such as the genera described by Warén and Bouchet (2001), have been found at neither the Mohns Ridge nor in Steinahóll; with both sites displaying a species set characteristic of lower shelf, upper bathyal species with large distribution areas. At species level, only the bivalves *Bathyarca frielei* (Friele, 1877) and *Lyonsiella abyssicola* Sars G.O., 1878 are present in both areas. The malacofauna of the Mohns Ridge are characteristic of those found on the continental margins off northern Iceland, Norway, and Russia.

Non-vent samples in this study observe similar peracarid crustacean family composition described of the background Icelandic fauna in Brix et al. (2018a,b). For peracarid crustaceans, the shelf may function as a pathway from Norway to Iceland and farther on to Greenland or vice versa. While for amphipods, the differences between north and south of the Greenland-Iceland-Faroe (GIF) Ridge can already be observed on family level, for isopods depth gradients are more important. There are typical shallow-water families and typical deep-sea families, with the exception being Munnopsidae. They are the only asellote isopods with clearly proven swimming abilities (Schnurr et al., 2014, 2018; Bober et al., 2018; Malyutina et al., 2018) crossing the MAR and the GIF Ridge.

Comparisons to Hydrothermal Vents in the North Atlantic and Arctic

Marine hydrothermally active sites in Icelandic waters have been reported from around 350 m water depth on the northern end of the Reykjanes Ridge (Olafsson et al., 1991), around 100 m water depth on the Kolbeinsey Ridge (Fricke et al., 1989), and at 20–60 m depth in the fjord Eyjafjörður (Marteinsson et al., 2001; Eythorsdottir et al., 2016). Similar to the Steinahóll vent field, no vent-endemic, chemosynthetic taxa have been reported from these shallow water vents (Fricke et al., 1989). Absence of vent-endemic species was also reported from the Arctic Jan Mayen vent fields at 550–720 m depth at the AMOR ridge (Schander et al., 2010).

In comparison, the macrofauna of the deeper MAR vent fields is characterized by the presence of a high abundance of vent-endemic and chemosynthetic taxa, such as the shrimps *Miricaris* and *Rimicaris*, the gastropod *Peltospira* (Warén and Bouchet, 2001), or the bivalve *Bathymodiolus* (e.g., Desbruyères et al., 2006; Wheeler et al., 2013). The Arctic Loki's Castle vent field on the Knipovich Ridge in 2350 m also supports an endemic fauna (Pedersen et al., 2010; Kongsrud and Rapp, 2012; Tandberg et al., 2012; Sweetman et al., 2013; Kongsrud et al., 2017). In general, these Arctic deep sea vents support a completely different fauna from the deep Atlantic vents south of Iceland (Bellan-Santini, 2005).

Shallow water vents are typically colonized by a subset of local background fauna (Dando, 2010). Species diversity commonly declines along a transect toward the vent due to increasing temperatures, sulfide concentration and decreasing pH (Dando, 2010). Whilst we were unable to test this, we observed the presence of only a few species occurring in high abundance in the vent-influenced samples. Further, the absence, or sporadic presence, of those taxa we found within vent-influenced samples in the surrounding areas, is also observed from other shallow water vents (Fricke et al., 1989; Dando, 2010; Sweetman et al., 2013).

Amphipoda as vent-associated fauna has been proven by *Exitomelita sigynae* from Loki's Castle north of Iceland (Tandberg et al., 2012) and *Dulichiopsis dianae* from the TAG hydrothermal vent field along the MAR (Corbari and Sorbe, 2018), with each species being restricted to a single vent site. The amphipod species found in the bacterial mats at Steinahóll belongs to different families than the species described from the North (Loki) and requires further taxonomic attention to confirm the theory of a vent-associated species new to science. The two reported vent-associated isopod families Janiridae G.O. Sars, 1897 and Gnathiidae Leach, 1814 were also reported as present by Schander et al. (2010) from the Mohns Ridge.

For harpacticoid copepods preliminary results based on COI data and morphological identification (Eva Paulus and Sabine

Gollner, unpublished data) show that the same harpacticoid *Tisbe* species can be found at Steinahóll as at the shallow water vent in the fjord Eyjafjörðður. This connectivity could suggest more undiscovered shallow-water vents between the two sites and supports the hypothesis of the shelf as a pathway of fauna and linking the north and south of Iceland.

At present, the knowledge about organisms associated with hydrothermal vents and other reduced environments in Icelandic waters is essentially limited to the literature discussed here and the present study of Steinahóll. Additional sampling of vent communities in Icelandic waters is fundamental in order to understand biodiversity, species composition and distribution of species associated with these extreme habitats. Along the Reykjanes Ridge, potential hydrothermal activity was detected in deeper areas during the MSM75 expedition. Exploration of fauna from these potential deeper, hydrothermally active sites may provide new insight into bathymetric distributions of different vent and seep species, as well as uncover the potential presence of a specialized chemosynthetic fauna at greater depth, similar to what is described from deep-sea vents at the MAR and AMOR.

How Vulnerable Is Steinahóll?

Meeting many of the criteria when asking "what constitutes a VME?" such as uniqueness, functional significance, fragility, structural complexity, and certain life history traits, the Steinahóll vent sites should be protected accordingly. Despite a ban in the area of bottom and midwater trawling by the Icelandic government (Reg. No. 310/2007) the area is still under stress from fishing, with numerous observed occasions of abandoned long-line and gill-net fishing equipment. The picture of the faunal composition is presently limited to higher taxon level and family level, but the species determination for several taxa is in progress and will bring more light into the macrofauna associated with the vent sites, as well as other VMEs in the close vicinity.

CONCLUSION

Although Steinahóll is known as a geological active area since the 1990s, the published materials remain sparse. Through future cross-institute collaborations, more work is to be expected on species level based on the samples presented from IceAGE_RR (MSM75), as well as analysis of recent and previous photo/video material. As a first impression, we conclude that shallow vent sites north and south of Iceland are comparable. The vent sites themselves show little to no megafauna, but meio- and macrofauna taxa associated with reduced environments in North Atlantic are visible in the microscopic view, mainly harpacticoid copepods occurring with species new to science, and dorvelleid worms hiding in bacterial mats not visible on video material, only in physical samples. We do not observe the characteristic chemosynthetic fauna seen in deep-sea hydrothermal vents, but rather species belonging to genera typically associated with shallow-water reduced environments. The bacterial mats and chimneys house unique fauna not observed in the surrounding environment. As more results on species level will be expected in the future, we may conclude here that the microscopic view already reveals a vulnerable unique environment.

DATA AVAILABILITY STATEMENT

All datasets generated for this study are included in the article/**Supplementary Material**.

AUTHOR CONTRIBUTIONS

CD and SB organized the expedition MSM75. JT, CD, and SB contributed conception and design of the study. SB and JT organized the database. SB, IF, AHT, KL, and JT collected and processed the specimens on board. HR determined the Porifera presence and absence during ROV deployments based on video analysis. TK performed 3D reconstruction of vent. JT, SB, SP, and DP wrote the first draft of the manuscript. JT, SB, KL, A-NL, AHT, IF, SP, ML, LH, DP, SG, EP, JK, TK, and HR wrote sections of the manuscript. ML, SP, and JT created the figures. All the authors contributed to manuscript revision, read and approved the submitted version.

FUNDING

The biological part of cruise MSM75 and the follow-up sorting workshop was financed by the German Science Foundation under grant BR3843/5-1 (SB). The costs for the geological dives of ROV and AUV on the cruise were provided by GEOMAR/Helmholtz-Foundation (to CD). JT was completely supported by the German Science Foundation under contract no. BR 3843/5-1. HR and AT received funding from the European Union's Horizon 2020 research and innovation programme through the SponGES project (grant agreement No 679849). AT payed in part by Norwegian Species Initiative project 16_18-NorAmph2. This document reflects only the authors' view and the Executive Agency for Small and Medium-sized Enterprises (EASME) is not responsible for any use that may be made of the information it contains.

ACKNOWLEDGMENTS

We would like to dedicate this manuscript to the memory of HR, a dear friend and colleague who passed away during the review phase of this manuscript. We miss him and would like to use this paragraph here to thank him for his enthusiastic support of the IceAGE project and his highly valuable scientific contributions. We would like to thank the following people for their key contributions to our manuscript: the crew of *MS Merian* during IceAGE_RR (MSM75). Antje Fischer (TA DZMB HH), Karen Jeskulke (TA DZMB HH), Sarah Menke (TA DZMB WHV), and Franziska Iwan (TA WHV) for their support in logistics and organization of the sorting workshop at the University of Iceland's Research Centre in Sandgerði and all necessary database entries in the whole progress. Steinunn Hilma Ólafsdóttir for sample storage of all coral pieces and Icelandic fishing regulation consultation. Guðmundur Guðmundsson for helping with sample storage at the Natural History Museum Iceland. The late Guðmundur V. Helgason for his efforts into sample sorting. Hanna María Kristjánsdóttir for her assistance in setting up the sorting workshop in Sandgerði. Jon Tomas Magnusson, Anna Huras, and Carolin Uhlir for their assistance in sorting physical specimens and finally Thorge von Bosse and the ROV team from GEOMAR for their contributions in helping us obtain high quality video and image material.

SUPPLEMENTARY MATERIAL

The Supplementary Material for this article can be found online at: https://www.frontiersin.org/articles/10.3389/fmars.2021.520713/full#supplementary-material

Supplementary Figure 1 | Interactive 3D model of the Steinahóll largest venting field, Hafgufa.

Supplementary Table 1 | Amphipoda family composition at Steinahóll vent fields. *: Hydrothermally influenced sample.

Supplementary Table 2 | Isopoda family composition at Steinahóll vent fields. *: Hydrothermally influenced sample.

Supplementary Table 3 | Polychaeta family composition at Steinahóll vent fields. *: Hydrothermally influenced sample.

Supplementary Table 4 | Mollusca family composition at Steinahóll vent fields. *: Hydrothermally influenced sample.

Supplementary Table 5 | Copepoda Harpacticoida family composition at Steinahóll vent fields. *: Hydrothermally influenced sample.

Supplementary Table 6 | Porifera presence/absence during ROV deployments based on video analysis at Steinahóll vent fields.

REFERENCES

Bani-Hassan, N., Iyer, K., Rüpke, L. H., and Borgia, A. (2012). Controls of bathymetric relief on hydrothermal fluid flow at mid-ocean ridges. *Geochem. Geophys. Geosystems* 13:Q05002. doi: 10.1029/2012GC004041

Bellan-Santini, D. (2005). Stenothoidae (Crustacea, Amphipoda) of hydrothermal vents and surroundings on the mid-atlantic ridge, azores triple junction zone. *J. Nat. History* 39, 3435–3452. doi: 10.1080/00222930500345749

Bellan-Santini, D. (2006). Rhachotropis species (Crustacea: Amphipoda: Eusiridae) of hydrothermal vents and surroundings on the Mid-Atlantic Ridge, Azores Triple Junction Jone. *J. Nat. History* 40, 1407–1424.

Bellan-Santini, D. (2007). New amphipods from hydrothermal vent environments on the mid-atlantic ridge, azores triple junction zone. *J. Nat. History* 41, 567–596. doi: 10.1080/00222930701262537

Bellan-Santini, D., and Thurston, M. (1996). Amphipoda of the hydrothermal vents along the mid-Atlantic Ridge. *J. Nat. History* 30, 685–702. doi: 10.1080/00222939600770381

Bianchi, G. G., Hall, I. R., McCave, I. N., and Joseph, L. (1999). Measurement of the sortable silt current speed proxy using the sedigraph 5100 and coulter multisizer IIe: precision and accuracy. *Sedimentology* 46, 1001–1014. doi: 10.1046/j.1365-3091.1999.00256.x

Blake, J. A., Grassle, J. P., and Eckelbarger, K. J. (2009). Capitella teleta, a new species designation for the opportunistic and experimental *Capitella sp.* I, with a review of the literature for confirmed records. *Zoosymposia* 2, 25–53. doi: 10.11646/zoosymposia.2.1.6

Bober, S., Brix, S., Riehl, T., Schwentner, M., and Brandt, A. (2018). Does the midatlantic ridge affect the distribution of benthic crustaceans across the atlantic ocean? *Deep-Sea Res. Part II.* 148, 91–104. doi: 10.1016/j.dsr2.2018.02.007

Bogdanov, Y. A., Lein, A. Y., and Sagalevich, A. M. (2005). Chemical composition of the hydrothermal deposits of the Menez Gwen vent field (Mid-Atlantic Ridge). *Oceanology* 45, 849–856.

Bouchet, P., and Warén, A. (1979). The abyssal molluscan fauna of the Norwegian Sea and its relation to other faunas. *Sarsia* 64, 211–243. doi: 10.1080/00364827.1979.10411383

Bouchet, P., and Warén, A. (1980). Revision of the northeast Atlantic bathyal and abyssal turridae (Mollusca, Gastropoda). Milano, Italy. *J. Molluscan Stud.* 8, 1–119. doi: 10.1093/mollus/46.Supplement_8.1

Bouchet, P., and Warén, A. (1985). Revision of the northeast Atlantic bathyal and abyssal neogastropoda excluding turridae (Mollusca, Gastropoda). *J. Molluscan Stud.* 8, 124–296. doi: 10.5962/bhl.title.140763

Bouchet, P., and Warén, A. (1986). Revision of the northeast atlantic bathyal and abyssal aclididae, eulimidae, epitoniidae. *Bollettino Malacol. Suppl.* 2, 297–576. doi: 10.5962/bhl.title.140762

Bouchet, P., and Warén, A. (1993). Revision of the northeast Atlantic bathyal and abyssal *Mesogastropoda. Bollettino Malacologico. Suppl.* 3, 577–840. doi: 10.5962/bhl.title.140732

Brenke, N. (2005). An epibenthic sledge for operations on marine soft bottom and bedrock. *Mar. Technol. Soc. J.* 39, 10–21. doi: 10.4031/002533205787444015

Brix, S., Lörz, A.-N., Jażdżewska, A. M., Hughes, L., Tandberg, A. H. S., Pabis, K., et al. (2018a). Amphipod family distributions around Iceland. *ZooKeys* 731, 1–53. doi: 10.3897/zookeys.731.19854

Brix, S., Stransky, B., Malyutina, M., Pabis, K., Svavarsson, J., and Riehl, T. (2018b). Distributional patterns of isopods (Crustacea) in Icelandic and adjacent waters. *Mar. Biodiversity* 48, 783–811. doi: 10.1007/s12526-018-0871-z

Brix, S., Meißner, K., Stransky, B., Halanych, K. M., Jennings, R. M., Kocot, K. M., et al. (2014a). The IceAGE project – a follow up of BIOICE. *Polish Polar Res.* 35, 141–150. doi: 10.2478/popore-2014-0010

Brix, S., Svavarsson, J., and Leese, F. (2014b). A multi-gene analysis reveals multiple highly divergent lineages of the isopod Chelator insignis (Hansen, 1916) south of Iceland. *Polish Polar Res.* 35, 225–242. doi: 10.2478/popore-2014-0015

Brix, S., and Svavarsson, J. (2010). Distribution and diversity of desmosomatid and nannoniscid isopods (Asellota) on the Greenland-Iceland-Faeroe Ridge. *Polar Biol.* 33, 515–530.

Brix, S., and Devey, C. W. (2019). Stationlist of the IceAGE project (Icelandic marine Animals: Genetics and Ecology) expeditions. *Mar. Data Arch.* doi: 10.14284/349

Cárdenas, P., and Rapp, H. T. (2015). Demosponges from the northern mid-atlantic ridge shed more light on the diversity and biogeography of North Atlantic deep-sea sponges. *J. Mar. Biol. Assoc. UK* 95, 1475–1517. doi: 10.1017/S0025315415000983

Cárdenas, P., Rapp, H. T., Klitgaard, A. B., Best, M., Thollesson, M., and Tendal, O. S. (2013). Taxonomy, biogeography and DNA barcodes for Geodia species (Porifera, Demospongiae, Astrophorida) in the Atlantic Boreo-Arctic region. *Zool. J. Linnean Soc.* 169, 251–311. doi: 10.1111/zoj.12056

Cárdenas, P., Rapp, H. T., Schander, C., and Tendal, O. S. (2010). Molecular taxonomy and phylogeny of the Geodiidae (Porifera, Demospongiae, Astrophorida) – combining phylogenetic and Linnaean classification. *Zool. Scripta* 39, 89–106. doi: 10.1111/j.1463-6409.2009.00402.x

Colaço, A., Desbruyères, D., Comtet, T., and Alayse, A.-M. (1998). Ecology of the menez gwen hydrothermal vent field (Mid-Atlantic Ridge/Azores Triple Junction). *Cahiers Biol. Mar.* 39, 237–240.

Copley, J. T. P., Tyler, P. A., Sheader, M., Murton, B. J., and German, C. R. (1996). Megafauna from sublittoral to abyssal depth along the Mid-Atlantic Ridge south of Iceland. *Oceanol. Acta* 19, 549–559.

Corbari, L., and Sorbe, J. C. (2018). First observation of the behaviour of the deep-sea amphipod *Dulichiopsis dianae* sp. nov. (Senticaudata, Dulichiidae) in the TAG hydrothermal vent field) Mid-Atlantic Ridge). *Mar. Biodiversity* 48, 631–645. doi: 10.1007/s12526-017-0788-y

Dando, P. R. (2010). "Biological communities at marine shallow-water vent and seep sites," in *The Vent and Seep Biota. Topics in Geobiology*, ed. S. Kiel (Dordrecht: Springer), doi: 10.1007/978-90-481-9572-5_11

Dauvin, J.-C., Alizier, S., Weppe, A., and Gudmundsson, G. (2012). Diversity and zoogeography of Icelandic deep-sea Ampeliscidae (Crustacea: Amphipoda).

Deep-Sea Res. Part I: Oceanographic Res. Papers 68, 12–23. doi: 10.1016/j.dsr.2012.04.013

DeMets, C., Gordon, R. G., Argus, D. F., and Stein, S. (1990). Current plate motions. *Geophys. J. Int.* 101, 425–478. doi: 10.1111/j.1365-246X.1990.tb06579.x

Desbruyères, D., Almeida, A., Biscoito, A., Comtet, T., Khripounoff, A., LeBris, N., et al. (2000). A review of the distribution of hydrothermal vent communities along the northern Mid-Atlantic Ridge: dispersal vs. environmental controls. *Hydrobiologia* 440, 201–216.

Desbruyères, D., Biscoito, T., Caprais, J. C., Colaço, A., Comtet, T., Crassous, P., et al. (2001). Variations in deep-sea hydrothermal vent communities on the Mid-Atlantic Ridge near the Azores plateau. *Deep-Sea Res. Part I* 48, 1325–1346. doi: 10.1016/S0967-0637(00)00083-2

Desbruyères, D., Segonzac, M., and Bright, M. (2006). *Handbook of Deep-Sea Hydrothermal Vent Fauna*, 2ed Edn. Linz: Biologiezentrum der Oberosterreichische Landesmuseen.

Dick, G. J. (2019). The microbiomes of deep-sea hydrothermal vents: distributed globally, shaped locally. *Nat. Rev. Microbiol.* 17, 271–283. doi: 10.1038/s41579-019-0160-2

Dijkstra, H. H., Warén, A., and Guðmunsson, G. (2009). Pectinoidea (Mollusca: Bivalvia) from Iceland. *Mar. Biol. Res.* 5, 207–243. doi: 10.1080/17451000802425643

Eythorsdottir, A., Omarsdottir, S., and Einarsson, H. (2016). Antimicrobial activity of marine bacterial symbionts retrieved from shallow water hydrothermal vents. *Mar. Biotechnol.* 18, 293–300. doi: 10.1007/s10126-016-9695-7

Foulger, G. R., and Anderson, D. L. (2005). A cool model for the Iceland hotspot. *J. Volcanol. Geothermal Res.* 141, 1–22. doi: 10.1016/j.jvolgeores.2004.10.007

Fricke, H., Giere, O., Stetter, K., Alfredsson, G. A., Kristjansson, J. K., Stoffers, P., et al. (1989). Hydrothermal vent communities at the shallow subpolar Mid-Atlantic Ridge. *Mar. Biol.* 102, 425–429. doi: 10.1007/BF00428495

Gamenick, I., Abbiati, M., and Giere, O. (1998). Field distribution and sulphide tolerance of Capitella capitata (Annelida: Polychaeta) around shallow water hydrothermal vents off Milos (Aegean Sea). a new sibling species? *Mar. Biol.* 130, 447–453. doi: 10.1007/s002270050265

German, C. R., Briem, J., Chin, C., Danielsen, M., Holland, S., James, R., et al. (1994). Hydrothermal activity on the Reykjanes ridge: the steinahóll vent-field at 63°06'N. *Earth Plan. Sci. Lett.* 121, 647–654. doi: 10.1016/0012-821X(94)90098-1

Gollner, S., Riemer, B., Martinez Arbizu, P., Le Bris, N., and Bright, M. (2010). Diversity of meiofauna from the 9u50'N East Pacific Rise across a gradient of hydrothermal fluid emissions. *PLoS One* 5:e12321. doi: 10.1371/journal.pone.0012321

Gollner, S., Stuckas, H., Kihara, T. C., Laurent, S., Kodami, S., and Martinez Arbizu, P. (2016). Mitochondrial DNA analyses indicate high diversity, expansive population growth and high genetic connectivity of vent copepods (Dirivultidae) across different Oceans. *PLoS One* 11:e0163776. doi: 10.1371/journal.pone.0163776

Hannington, M., Herzig, P., Stoffers, P., Scholten, J., Botz, R., Jonasson, I. R., et al. (2001). First observations of high-temperature submarine hydrothermal vents and massive anhydrite deposits off the north coast of Iceland. *Mar. Geol.* 177, 199–220. doi: 10.1016/S0025-3227(01)00172-4

Hestetun, J. T., Jørgensen, S. L., Dahle, H., Olsen, B. R., and Rapp, H. T. (2016). The microbiome and occurrence of methanotrophy in carnivorous sponges. *Front. Microbiol.* 7:1781. doi: 10.3389/fmicb.2016.01781

Hestetun, J. T., Tompkins-MacDonald, G., and Rapp, H. T. (2017). A review of carnivorous sponges from the boreal North Atlantic and Arctic Oceans. *Zool. J. Linnean Soc.* 181, 1–69. doi: 10.1093/zoolinnean/zlw022

Høisæter, T. (2010). The shell-bearing, benthic gastropods on the southern part of the continental slope off Norway. *J. Molluscan Stud.* 76, 234–244. doi: 10.1093/mollus/eyq003

Höskuldsson, Á, Hey, R., Kjartansson, E., and Guðmundsson, G. B. (2007). The reykjanes ridge between 63°10'N and Iceland. *J. Geodynam.* 43, 73–86. doi: 10.1016/j.jog.2006.09.003

Humphris, S. E., Herzig, P. M., Miller, D. J., Alt, J. C., Becker, K., Brown, D., et al. (1995). The Internal structure of an active sea-floor massive sulphide deposit. *Nature* 377, 713–716. doi: 10.1038/377713a0

Ivanenko, V. N., Ferrari, F. D., Defaye, D., Sarradin, P.-M., and Sarrazin, J. (2011). Description, distribution and microhabitats of a new species of Tisbe (Copepoda: Harpacticoida: Tisbidae) from a deep-sea hydrothermal vent field at the Mid-Atlantic Ridge (37°N, Lucky Strike). *Cahiers de Biol. Mar.* 52, 89–106.

Jakobsson, S. P., Jonsson, J., and Shido, F. (1978). Petrology of the Western Reykjanes Peninsula, Iceland. *J. Petrol.* 19, 669–705. doi: 10.1093/petrology/19.4.669

Jochumsen, K., Schnurr, S. M., and Quadfasel, D. (2016). Bottom temperature and salinity distribution and its variability around Iceland. *Deep-Sea Res. Part I: Oceanographic Res. Papers* 111, 79–90. doi: 10.1016/j.dsr.2016.02.009

Johnsson, G. L., and Jakobsson, S. P. (1985). Structure and peterology of the Reykjanes Ridge between 62°55'N and 63°48'N. *J. Geophys. Res.* 90, 10073–10083. doi: 10.1029/JB090iB12p10073

Keeton, J. A., Searle, R. C., Parsons, B., White, R. S., Murton, B. J., Parson, L. M., et al. (1997). Bathymetry of the Reykjanes Ridge. *Mar. Geophys. Res.* 19, 55–64. doi: 10.1023/A:1004266721393

Klitgaard, A. B., and Tendal, O. S. (2004). Distribution and species composition of mass occurrences of large-sized sponges in the northeast Atlantic. *Prog. Oceanography* 61, 57–98. doi: 10.1016/j.pocean.2004.06.002

Kongsrud, J. A., Eilertsen, M. H., Alvestad, T., Kongshavn, K., and Rapp, H. T. (2017). New species of Ampharetidae (Annelida: Polychaeta) from the Arctic Loki Castle vent field. *Deep Sea Res. Part II: Top. Stud. Oceanography* 137, 232–245. doi: 10.1016/j.dsr2.2016.08.015

Kongsrud, J. A., and Rapp, H. T. (2012). Nicomache (Loxochona) lokii sp. nov. (Annelida: Polychaeta: Maldanidae) from the Loki's Castle vent field—an important structure builder in an Arctic vent system. *Pol. Biol.* 35, 161–170.

Kwasnitschka, T., Koeser, K., Sticklus, J., Rothenbeck, M., Weiss, T., Wenzlaff, E., et al. (2016). DeepSurveyCam – a deep ocean optical mapping system. *Sensors* 16:164. doi: 10.3390/s16020164

LeBris, N., Arnaud-Haond, S., Beaulieu, S., Cordes, E., Hilario, A., Rogers, A., et al. (2016). "Hydrothermal vents and cold seeps," in *World Ocean Assess*, eds S. van de Gaever, and H. Watanabe (Cambridge: Cambridge University Press), 1–18.

Madsen, F. J. (1949). Marine bivalvia". *Zool. Iceland* 4, 1–166.

Maldonado, M., Aguilar, R., Bannister, R. J., Bell, J., Conway, K. W., Dayton, P. K., et al. (2017). "Sponge grounds as key marine habitats: a synthetic review of types, structure, functional roles and conservation concerns," in *Marine Animal Forests – The Ecology of Benthic Biodiversity Hotspots*, eds S. Rossi, L. Bramanti, A. Gori, and C. Orejas (Berlin: MeteorSpringer).

Malyutina, M., Frutos, I., and Brandt, A. (2018). Diversity and distribution of the deep-sea Atlantic *Acanthocope* (Crustacea, Isopoda, Munnopsidae), with description of two new species. *Deep-Sea Res. I.* 148, 130–150. doi: 10.1016/j.dsr2.2017.11.003

Marcon, Y., Sahling, H., Borowski, C., Santos Ferreira, dos, C., Thal, J., et al. (2013). Megafaunal distribution and assessment of total methane and sulfide consumption by mussel beds at Menez Gwen hydrothermal vent, based on geo-referenced photomosaics. *Deep-Sea Res. I.* 75, 93–109. doi: 10.1016/j.dsr.2013.01.008

Marteinsson, V. T., Kristjánsson, J. K., Kristmannsdóttir, H., Sæmundsson, K., Hannignton, M., Petursdottir, S. K., et al. (2001). Discovery and description of giant submarine smectite cones on the seafloor in eyjafjordur, northern iceland, and a novel thermal microbial habitat. *Appl. Eviron. Microbiol.* 67, 827–833. doi: 10.1128/AEM.67.2.827-833.2001

Marteinsson, V. T., Rúnarsson, Á, Stefánsson, A., Thorsteinsson, T., Jóhannesson, T., Magnússon, S. H., et al. (2013). Microbial communities in the subglacial waters of the Vatnajökull ice cap, Iceland. *ISME J.* 7, 427–437. doi: 10.1038/ismej.2012.97

Martin, E., Paquette, J. L., Bosse, V., Ruffet, G., Tiepolo, M., Sigmarsson, O., et al. (2011). Geodynamics of rift-plume interaction in Iceland as constrained by new 40Ar/39Ar and in situ U-Pb zircon ages. *Earth Planetary Sci. Lett.* 311, 28–38. doi: 10.1016/j.epsl.2011.08.036

Meißner, K., Fiorentino, D., Schnurr, S., Martinez Arbizu, P., Huettmann, F., Holst, S., et al. (2014). Distribution of benthic marine invertebrates at northern latitudes — an evaluation applying multi-algorithm species distribution models. *J. Sea Res.* 85, 241–254. doi: 10.1016/j.seares.2013.05.007

Meyer, H. K., Roberts, E. M., Rapp, H. T., and Davies, A. J. (2019). Spatial patterns of arctic sponge ground fauna and demersal fish are detectable in autonomous underwater vehicle (AUV) imagery. *Deep-Sea Res. I* 153:103137. doi: 10.1016/j.dsr.2019.103137

Murton, B. J., and Parson, L. M. (1993). Segmentation, volcanism and deformation of oblique spreading centres: a quantitative study of the

Reykjanes Ridge. *Tecto* 222, 237–257. doi: 10.1016/0040-1951(93)90051-K

Myers, A. A., and Cunha, M. R. (2004). New and little known corophiidean amphipods from the Lucky Strike hydrothermal vent, Mid-Atlantic Ridge. *J. Mar. Biol. Assoc. UK* 84, 1019–1025. doi: 10.1017/S0025315404010343h

Olafsson, J., Thors, K., and Cann, J. R. (1991). A sudden cruise off Iceland. *RIDGE Events* 2, 35–38.

OSPAR (2008). *). Agreement 2008–07. Description of habitats on the OSPAR list of threatened and/or declining species and habitats, 2008*. Available online at: https://www.ospar.org/convention/agreements/ (Accessed 10 September, 2017)

OSPAR (2014). *OSPAR Recommendation 2014/11 on Furthering the Protection and Conservation of Hydrothermal Vents/fields Occurring on Oceanic Ridge in Region V of the OSPAR Maritime Area, Annex 16, 2014*. Available online at: https://www.ospar.org/convention/agreements/, https://www.ospar.org/meetings/archive?Q=&a=&y=1993&s= (accessed 10 September, 2017)

Oug, E. (1990). Morphology, reproduction, and development of a new species of Ophryotrocha (Polychaeta: Dorvilleidae) with strong sexual dimorphism. *Sarsia* 75, 19–201. doi: 10.1080/00364827.1990.10413447

Pałgan, D., Devey, C. W., and Yeo, I. A. (2017). Volcanism and hydrothermalism on a hotspot–influenced ridge: comparing Reykjanes Peninsula and Reykjanes Ridge. Iceland. *J. Volcanol. Geothermal Res.* 348, 62–81. doi: 10.1016/j.jvolgeores.2017.10.017

Palmer, M., Kasper, K., van Benthem, K. J., Arni, M., Berg, C. W., Anders, N., et al. (1995). Dissolved methane and hydrogen in the Steinahóll hydrothermal plume, 63°N, Reykjanes Ridge. *Geol. Soc. London Special Publications* 87, 111–120. doi: 10.1144/GSL.SP.1995.087.01.10

Pedersen, G. B. M., and Grosse, P. (2014). Morphometry of subaerial shield volcanoes and glaciovolcanoes from Reykjanes Peninsula, Iceland: effects of eruption environment. *J. Volcanol. Geothermal Res.* 282, 115–133. doi: 10.1016/j.jvolgeores.2014.06.008

Pedersen, R. B., Rapp, H. T., Thorseth, I. H., Lilley, M. D., Barriga, F. J. A. S., Baumberger, T., et al. (2010). Discovery of a black smoker vent field and vent fauna at the Arctic Mid-Ocean Ridge. *Nat. Commun.* 1:126. doi: 10.1038/ncomms1124

Petersen, S., Kuhn, K., Kuhn, T., Augustin, N., Hékinian, R., Franz, L., et al. (2009). The geological setting of the ultramafic-hosted Logatchev hydrothermal field (14°45'N, Mid-Atlantic Ridge) and its influence on massive sulfide formation. *Lithos* 112, 40–56. doi: 10.1016/j.lithos.2009.02.008

Plum, C., Pradillon, F., Fujiwara, Y., and Sarrazin, J. (2017). Copepod colonization of organic and inorganic substrata at a deep-sea hydrothermal vent site on the Mid-Atlantic Ridge. *Deep Sea Res. II* 137, 335–348. doi: 10.1016/j.drs2.2016.06.008

Riehl, T., Brenke, N., Brix, S., Driskell, A., Kaiser, S., and Brandt, A. (2014). Field and laboratory methods for DNA studies on deep-sea isopod crustaceans. *Polish Pol. Res.* 35, 203–224. doi: 10.2478/popore-2014-0018

Roberts, E. M., Mienis, F., Rapp, H. T., Hanz, U., Meyer, H. K., and Davies, A. J. (2018). Oceanographic setting and short-timescale environmental variability at an Arctic seamount sponge ground. *Deep-Sea Res. I.* 138, 98–113. doi: 10.1016/j.dsr.2018.06.007

Sandwell, D. T., Müller, R. D., Smith, W. H. F., Garcia, E., and Francis, R. (2014). New global marine gravity model from CryoSat-2 and Jason-1 reveals buried tectonic structure. *Science* 346, 65–67. doi: 10.1126/science.1258213

Schander, C., Rapp, H. T., Kongsrud, J. A., Bakken, T., Berge, J., Cochrane, S., et al. (2010). The fauna of hydrothermal vents on the Mohn Ridge (North Atlantic). *Mar. Biol. Res.* 6, 155–171. doi: 10.1080/17451000903147450

Schnurr, S., Brandt, A., Brix, S., Fiorentino, D., Malyutina, M., and Svavarsson, J. (2014). Composition and distribution of selected munnopsid genera (Crustacea, Isopoda, Asellota) in Icelandic waters. *Deep-Sea Res. Part II* 84, 142–155. doi: 10.1016/j.dsr.2013.11.004

Schnurr, S., Osborn, K. J., Malyutina, M., Jennings, R. M., Brix, S., Svavarsson, J., et al. (2018). Hidden diversity in two species complexes of munnopsid isopods (Crustacea) at the transition between the northernmost North Atlantic and the Nordic Seas. *Mar. Biodiversity* 48, 813–843. doi: 10.1007/s12526-018-0877-6

Searle, R. C., Keeton, J. A., Owens, R. B., White, R. S., Mecklenburgh, R., and Parsons, B. (1998). The Reykjanes Ridge: structure and tectonics of a hot-spot-influenced, slow-spreading ridge, from multibeam bathymetry, gravity and magnetic investigations. *Earth Plan. Sci. Lett.* 160, 463–478. doi: 10.1016/S0012-821X(98)00104-6

Silva, C. F., Seixas, V. C., Barroso, R., Di Domenico, M., Amaral, A. C. Z., and Paiva, P. C. (2017). Demystifying the Capitella capitata complex (Annelida, Capitellidae) diversity by morphological and molecular data along the Brazilian coast. *PLoS One* 12:e0177760. doi: 10.1371/journal.pone.0177760

Steinarsdóttir, M. B., Ingólfsson, A., and Ólafsson, E. (2003). Seasonality of harpacticoids (Crustacea, Copepoda) in a tidal pool in subarctic south-western Iceland. *Hydrobiologia* 503, 211–221. doi: 10.1007/978-94-017-2276-6_22

Sweetman, A. K., Levin, L. A., Rapp, H. T., and Schander, C. (2013). Faunal trophic structure at hydrothermal vents on the southern Mohn's Ridge, Arctic Ocean. *Mar. Ecol. Prog. Ser.* 473, 115–131. doi: 10.3354/meps10050

Sæmundsson, K. (1979). Outline of the geology of Iceland. *Jökull* 29, 7–28.

Talwani, M., Windisch, C. C., and Langseth, M. G. (1971). Reykjanes Ridge crest: a detailed geophysical study. *J. Geophys. Res.* 76, 473–577. doi: 10.1029/JB076i002p00473

Tandberg, A. H. S., Rapp, H. T., Schander, C., Vader, W., Sweetman, A. K., and Berge, J. (2012). Exitomelita sigynae gen. et sp. nov.: a new amphipod from the Arctic Loki Castle vent field with potential gill ectosymbionts. *Pol. Biol.* 35, 705–716. doi: 10.1007/s.00300-011-1115-x

Tarasov, V. G., Gebruk, A. V., Mironov, A. N., and Moskalev, L. I. (2005). Deep-sea and shallow-water hydrothermal vent communities: two different phenomena? *Chem. Geol.* 224, 5–39. doi: 10.1016/j.chemgeo.2005.07.021

Thorarinsson, S. (1969). The lakagigar eruption of 1783. *Bull. Volcanol.* 33, 910–929. doi: 10.1007/BF02596756

Van Dover, C. L., Arnaud-Haond, S., Gianni, M., Helmreich, S., Huber, J. A., Jaeckel, A. L., et al. (2018). Scientific rationale and international obligations for protection of active hydrothermal vent ecosystems from deep-sea mining. *Mar. Policy* 90, 20–28. doi: 10.1016/j.marpol.2018.01.020

van Veen, J. (1933). Onderzoek naar het zandtransport von rivieren. *De Ingenieur* 48, 151–159.

Vinogradov, G. M. (1995). Amphipods from hydrothermal vents and cold seepings on the ocean bottom. *Oceanol. Russ. Acad. Sci.* 35, 69–74.

Warén, A. (1989). New and little known Mollusca from Iceland. *Sarsia* 74, 1–28. doi: 10.1080/00364827.1989.10413419

Warén, A. (1991). New and little known mollusca from Iceland and Scandinavia. *Sarsia* 76, 53–124. doi: 10.1080/00364827.1991.10413466

Warén, A. (1993). New and little known mollusca from Iceland and Scandinavia. Part 2. *Sarsia* 78, 159–201. doi: 10.1080/00364827.1993.10413534

Warén, A. (1996). New and little known mollusca from Iceland and Scandinavia. Part 3. *Sarsia* 81, 197–245. doi: 10.1080/00364827.1996.10413622

Warén, A., and Bouchet, P. (2001). Gastropoda and Monoplacophora from hydrothermal vents and seeps; new taxa and records. *Veliger* 44, 116–231.

Wheeler, A. J., Murton, B., Copley, J., Lim, A., Carlsson, J., Collins, P., et al. (2013). Moytirra: discovery of the first known deep-sea hydrothermal vent field on the slow-spreading Mid-Atlantic Ridge north of the Azores. *Geochem. Geophys. Geosystems* 14, 4170–4184. doi: 10.1002/ggge.20243

Conflict of Interest: PV and VM are employed by Matis Ltd.

The remaining authors declare that the research was conducted in the absence of any commercial or financial relationships that could be construed as a potential conflict of interest.